Investigating the Mechanism of Clonal Expansion of Deleted mtDNA Species.

Georgia Elizabeth Campbell

BSc (Hons)

This thesis is submitted for the degree of Doctor of Philosophy at Newcastle University.

Wellcome Trust Centre for Mitochondrial Research

Institute for Ageing and Health

Newcastle University

September 2013

Author's Declaration

This thesis is submitted for the degree of Doctor of Philosophy at Newcastle University. The research was conducted in the Wellcome Trust Centre for Mitochondrial Research, Institute for Ageing and Health, Newcastle University under the supervision of Prof D M Turnbull, Prof R W Taylor and Dr K J Krishnan and all work is my own unless otherwise stated.

I certify that none of the material offered in this thesis has been previously submitted by me for a degree or qualification at this or any other university.

For my Mam and Dad

Abstract

Mitochondrial DNA deletions are a primary cause of inherited and sporadic mitochondrial disease, whilst somatic mtDNA deletions contribute to the focal respiratory chain deficiency observed in post-mitotic cells associated with ageing and neurodegenerative disorders. As mtDNA deletions only cause cellular pathology at high levels of heteroplasmy, an mtDNA deletion formed within a cell must accumulate by a process known as clonal expansion to levels which result in biochemical dysfunction. The mechanism driving clonal expansion remains uncertain; this research aimed to investigate clonally expanded mtDNA deletions in sporadic and inherited mitochondrial myopathies in order to elucidate this mechanism.

A number of different approaches were taken to assess the mechanism driving accumulation of mtDNA deletions. The effect of the mtDNA deletion size on clonal expansion was first investigated by assessing the longitudinal spread of mtDNA deletions in single muscle fibres isolated from patients presenting with mtDNA maintenance disorders; no relationship was found to exist between mtDNA deletion size and the area over which the mutation has accumulated. A longitudinal study was carried out using tissue acquired over a 13-year period from a single patient with a sporadic mtDNA deletion, to identify whether the mtDNA deletion heteroplasmy level continued to increase over time, as would be expected if the mutation displayed a selective advantage over wildtype mtDNA – however, both the genetic and biochemical defect were found to be stable over time in this patient. A subsequent study aimed to identify a correlation between mtDNA deletion size and heteroplasmy levels at the whole tissue level in a cohort of patients with sporadic single mtDNA deletions, but no evidence was found to suggest that larger mtDNA deletions accumulate to higher levels of heteroplasmy. Finally, single cytochrome *c* oxidase-deficient muscle fibres were investigated using single-molecule PCR to assess whether clonal expansion of multiple mtDNA deletions could be observed in single cells. Evidence of multiple clonally expanded mtDNA species was found in approximately 40% of all examined fibres, with no correlation between mtDNA deletion size and level of accumulation.

Each of these four studies has highlighted accumulation by random genetic drift to be the most likely mechanism for clonal expansion of mtDNA deletions in human muscle; no evidence has been found to support the presence of a selective advantage for mtDNA deletion species over wildtype mtDNA.

Acknowledgements

First and foremost I owe my sincere thanks to my supervisors, Professor Doug Turnbull and Professor Robert Taylor, for the opportunity to undertake this PhD. Your guidance and support have been invaluable to the completion of this thesis. I would also like to thank Dr Kim Krishnan for supervising the early days of my PhD; finding my feet in the lab would have been much more difficult without your knowledge and patience.

I have had the privilege of carrying out my PhD in a wonderful working environment, and so have many people to thank for contributing to the completion of this work! I'd particularly like to thank the staff of the Newcastle Mitochondrial Diagnostics Group for providing access to the many patient samples involved in this body of work, Miss Charlotte Alston for all of her expert help with sequencing, and Dr John Grady for his statistical wizardry. Other star awards go to Dr Amy Reeve and Dr Karolina Rygiel, who have both been an unwavering source of support throughout my PhD. I hope they both already know how grateful I am to them for their excellent advice over the years.

Over my time at the MRG I've had the good fortune to share laughs, tears, countless cups of tea and almost as many post-work drinks with so many great friends. Sharing an office with Eve, Ollie, Tilly, Laura and Sally at various times has made coming to work that little bit easier every morning, but I'd especially like to thank Adya Misra and John Yarham for their friendship through good times and bad – you are both amazing!

My final thanks go to the family and friends who have supported me throughout this work, and believed in me even at times when I didn't believe in myself; I love you all. I promise I will try to stress out a bit less now! My friends at Coalfields Race Team - there are too many to mention you all, but you know who you are. You have kept me sane while writing up (no mean feat, and I'm sure I've driven you all a little crazy along the way), and you are all such an inspiration to me. We've had an amazing time since the team was put together, and things are only going to keep getting better! Finally, and most importantly, my wonderful family – I wouldn't be here without you. You've supported and encouraged me since day one, and I love you all so much. This thesis is for you.

Table of Contents

Chapter 2 - Materials and Methods

Chapter 5 - Investigating the impact of molecular mtDNA deletion characteristics on disease presentation and progression in single mtDNA deletion patients.

List of Figures

List of Tables

Publications

Grady, J.P.*, **Campbell, G**.*, Ratnaike, T.*, Blakely, E.L., Falkous, G., Nesbitt, V., Schaefer, A.M., McNally, R.J., Gorman, G.S., Taylor, R.W., Turnbull, D.M. and McFarland, R. (2014) 'Disease progression in patients with single, large-scale mitochondrial DNA deletions', *Brain*, 137(2), pp. 323-334.

*These authors contributed equally to this work.

Spendiff, S., Reza, M., Murphy, J.L., Gorman, G., Blakely, E.L., Taylor, R.W., Horvath, R., **Campbell, G**., Newman, J., Lochmüller, H. and Turnbull, D.M. (2013) 'Mitochondrial DNA deletions in muscle satellite cells: implications for therapies', *Human Molecular Genetics*, 22(23), pp. 4739-4747.

Abbreviations

A	adenine
ADP	adenosine diphosphate
AGE	agarose gel electrophoresis
ATP	adenosine 5’-triphosphate
ATPase	ATP synthase
BAX	bcl-2-like protein 4
BER	base excision repair
Bp	base pair
BpB	bromophenol blue
Ca^{2+}	calcium ion
CO_2	carbon dioxide
CoA	coenzyme A
CO1	complex IV subunit 1
CO2	complex IV subunit 2
CO3	complex IV subunit 3
COX	cytochrome *c* oxidase
CPEO	chronic progressive external ophthalmoplegia
CRS	Cambridge Reference Sequence
Ct	threshold cycle
Cu	copper
Cyb	cytochrome b
D-loop	displacement loop
Da	Dalton
DAB	3.3’diaminobenzidine
dH_2O	deionised water
DNA	deoxyribonucleic acid
Dnm1	Dynamin 1
dNTP	2’-deoxynucleotide 5’triphosphate
DRP	dynamin related protein
ETC	electron transport chain
FAD	flavin adenine dinucleotide

$FADH_2$	reduced flavin dinucleotide
FMN	flavin mononucleotide
$FMNH_2$	reduced flavin mononucleotide
Fe-S	iron-sulphur
G	guanine
g	grams
GABA	gamma-aminobutyric acid (neurotransmitter)
Glu	glutamate
GTP	guanosine triphosphate
H^+	proton
H_2O	water
H_2O_2	hydrogen peroxide
HCl	hydrochloric acid
H strand	heavy strand
HSP	heavy strand promoter
HSP-2	second heavy strand promoter
HVR	hypervariable region
IMM	inner mitochondrial membrane
IT_{H1}	H strand transcription initiation site
IT_{H2}	second H strand transcription initiation site
IT_{L1}	L strand transcription initiation site
Kb	kilobase pair
KDa	kilo Dalton
KSS	Kearns Sayre Syndrome
L strand	light strand
LC3	Microtubule-associated protein 1A/1B-light chain 3
Leu	leucine
LHON	Leber's hereditary optic neuropathy
LSP	light strand promoter
LSP-2	second light strand promoter
M	molar
MAP1	microtubule-associated protein 1
MCU	mitochondrial Ca^{2+} uniporter

MELAS	Mitochondrial encephalomyopathy with lactic acidosis and stroke like episodes
MERRF	myoclonic epilepsy with ragged-red fibres
Mfn	mitofusin
Mg	magnesium
$MgCl_2$	magnesium chloride
ml	millilitre
MIB1	E3 ubiquitin-protein ligase
MNGIE	mitochondrial neurogastrointestinal encephalopathy
mRNA	messenger RNA
mRyR	mitochondrial ryanodine receptor
mtDNA	mitochondrial DNA
mtSSB	mitochondrial single-stranded DNA-binding protein
mTERF	mitochondrial transcription termination factor
mt-tRNA	mitochondrial tRNA
Na^+	sodium ion
NAD+	nicotinamide adenine dinucleotide
NADH	reduced nicotinamide adenine dinucleotide
NARP	neuropathy, ataxia and pigmentary retinopathy
NaOH	sodium hydroxide
NBT	nitro blue tetrazolium
NCLX	Na^+/Ca^{2+} exchanger
NER	nucleotide excision repair
ND	NADH dehydrogenase
nDNA	nuclear DNA
NDUFS	NADH dehydrogenase ubiquinone iron-sulphur
NDUFV	NADH dehydrogenase ubiquinone flavoprotein
NIP3	proapoptotic member of the Bcl-2 family of cell death factors
NMDAS	Newcastle mitochondrial disease adult scale
O_2^-	superoxide anion
OH^-	hydroxyl radical
O_2	oxygen
O_H	origin of heavy strand replication

O_L	origin of light strand replication
OMM	outer mitochondrial membrane
OPA1	optic atrophy 1
OXPHOS	oxidative phosphorylation
PARK1	Parkinson disease, familial 1
PBS	phosphate buffered saline
PCR	polymerase chain reaction
PEO	progressive external ophthalmoplegia
PGC	primordial germ cells
PGD	pre-implantation genetic diagnosis
PINK1	PTEN-induced putative kinase 1
PND	prenatal diagnosis
POLG	polymerase γ
POLRMT	mitochondrial RNA polymerase
PTEN	Phosphatase and tensin homolog
PTP	permeability transition pore
Q	ubiquinone
QH^2	ubiquinol
rCRS	revised Cambridge Reference Sequence
RITOLS	ribonucleotide incorporation throughout the lagging strand
ROS	reactive oxygen species
RRF	ragged red fibres
RNA	ribonucleic acid
ROS	reactive oxygen species
Rpm	revolutions per minute
rRNA	ribosomal ribonucleic acids
S^{2-}	Sulphide ions
SDH	succinate dehydrogenase
SKM	skeletal muscle
T	thymidine
TAE	tris-acetate EDTA
TCA cycle	tricarboxylic acid cycle / citric acid cycle
TFAM	mitochondrial transcription factor

TFB1M	mitochondrial transcription factors B1
TFB2M	mitochondrial transcription factors B2
TIMS	translocases of the inner membrane
TOMS	translocases of the outer membrane
tRNA	transfer RNA
T_m	melting temperature
VDAC	voltage dependant anion channel
YME1L	YME1-like 1 ATPase
Zn	zinc
2D-NAGE	neutral/neutral 2D agarose gel electrophoresis
µm	micrometre
µl	microlitre

Chapter One

Chapter 1

Introduction

1.1 Mitochondrial Origins

Mitochondria are widely believed to be the evolutionary result of an endosymbiosis event, the engulfment of a primitive bacteria-like organism by a eukaryotic cell, as proposed by Lynn Margulis in 1970 (Margulis, 1970). This key event in early eukaryote evolution would have provided a safer and more stable intracellular environment for the bacteria-like organism, while the eukaryotic cell would have thrived on a constant supply of energy in the form of ATP-production, making this a mutually beneficial relationship for both organisms.

While phylogenetic analyses have pinpointed the time of this endosymbiotic event to approximately 1500 million years ago, some of the same studies have created debate as to whether the primitive bacteria was engulfed by a nucleated a-mitochondrial cell, or a prokaryote which developed a nucleus after the development of this symbiotic relationship (Embley and Martin, 2006). Evidence is now possibly weighted more strongly for the endosymbiotic event occurring before the development of a nucleus, as the existence of true archezoa has been brought into question. The archezoa were an amitochondrial eukaryote group believed to have diverged from the eukaryote evolutionary tree prior to the symbiosis event, serving as evidence of the evolution of a nucleus prior to the symbiosis which led to mitochondria. However, the discovery of mitochondrial genes in the nuclear DNA of members of this eukaryote group has provided evidence of the ancestral presence of mitochondria in these species (Clark and Roger, 1995; Roger, 1999). Subsequently, the presence of hydrogenosomes and mitosomes – double-membrane bound organelles evolutionarily derived from mitochondria - in these species has provided evidence beyond all doubt that mitochondria must have been present in the ancestors of the so-called archezoa (Embley and Martin, 2006). In light of the lack of evidence for any eukaryotes which may have diverged before the symbiosis that led to the development of mitochondria, it now seems more likely that endosymbiosis occurred between a primitive bacteria and a prokaryote which later developed a nucleus.

While opinions are still divided over the eukaryote or prokaryote cell involved in endosymbiosis, the bacterial origins of mitochondria have proved easier to trace. Sequencing of the genome of α-proteobacteria *Rickettsia prowazekii*, an aerobic intracellular parasitic bacteria which causes epidemic typhus, revealed a set of genes encoding elements of the tricarboxylic acid cycle and respiratory chain complexes similar to that found in mitochondria (Andersson et al., 1998). Subsequent phylogenetic analysis of the cytochrome b and cytochrome c oxidase I genes from *Rickettsia prowazekii* was then used to confirm that the evolutionary ancestor of the mitochondria must have been an α-proteobacteria, specifically from within the Rickettsiaceae family (Sicheritz-Ponten *et al.*, 1998).

Prior to the endosymbiosis event, the free-living α-protobacterial ancestors of mitochondria must have contained all of the genetic information required for independence. Over time as the symbiosis between host and mitochondria has increased much of this genetic material has been lost, leaving only a small vestigial genome present in mitochondria. This decrease in genome size will have occurred due to multiple pressures, including the mutational degradation of genes made redundant by the sharing of the host's metabolites and the transfer of genes to the host nucleus (Kurland and Andersson, 2000). Gene transfer has been possible in instances where encoded proteins have a targeting sequence, allowing translation in the cytoplasm prior to movement into the mitochondria. This gene transfer is believed to be a neutral, multistage process, beginning with the movement of an inactive copy of the gene to the nucleus while an active copy is still present and functional in the mitochondria. A tagging process can then occur, activating the gene copy now present in the nucleus and leaving the mitochondrial gene copy is essentially redundant. The mitochondrial gene can therefore be harmlessly subjected to mutational degradation, leaving the mitochondrial gene present only in the nucleus (Berg and Kurland, 2000). For each gene lost from the intracellular symbiont by mutation in favour of a nuclear copy, reliance on the host cell becomes greater and the bond of symbiosis between becomes stronger; this has caused the evolution of mitochondria from intracellular α-proteobacteria into the organelles we see present in the majority of modern eukaryotes.

1.2 Mitochondrial Structure

Mitochondria are typically present throughout the cytoplasm of eukaryotic cells, though notable exceptions such as erythrocytes do not contain any mitochondria at all. The mitochondrial content of cells - including size, shape and number – all vary depending on the energy requirements of each specific cell and tissue type; a highly metabolically active cell type would be expected to have a higher level of mitochondria to supply its energy demands than would be seen in a less energy-demanding tissue.

Mitochondria are typically depicted as single oval-shaped organelles, as shown in Figure 1.1, though morphology within the tissue can vary from spherical to rod-like structures and the mitochondria actually interact dynamically with each other. While variable, mitochondrial size is usually within a spectrum of 1 – 4µm in length and 0.3 – 0.7µm in diameter.

Early visualisations of mitochondria were obtained through light microscopy, where only basic morphology could be investigated; here the smooth outline of the organelle was noted, as was the presence of an outer membrane and an inner matrix. Lamellae were also seen protruding from the inner surface of the mitochondrial membrane, reaching into the matrix but not reaching the opposite side of the organelle. These 'folds' in the membrane were called 'cristae mitochondriales' (Palade, 1952). Further work with electron microscopy revealed further details of mitochondrial structure, including the outer double plasma membrane consisting of a smooth outer membrane (OM) and highly folded inner membrane (IM) (Palade, 1953).

The outer membrane has the simplest structure of the two mitochondrial membranes, forming a smooth structure around the mitochondrial periphery. The shape given to the mitochondria by the OM conformation can change depending upon tissue type; the OM typically displays a tubular shape when adhered to the cytoskeleton, and forms an ellipsoid or sphere in isolated suspension. Though the OM does partly serve as a barrier to prevent free movement of molecules between the mitochondrial interior and the cytoplasm, ions <10kDa in size are able to freely diffuse across the OM through the voltage dependant anion channel (VDAC) known as porin. Proteins, too large to be imported into the organelle in this fashion, must pass through the translocases of the outer membrane (TOMS) and translocases of the inner membrane (TIMS) (Truscott *et al.*, 2003; Ahmed and Fisher, 2009).

The inner membrane is responsible for forming a scaffold upon which the respiratory chain complexes can be assembled and can operate, as well as providing a permeable barrier which the complexes can subsequently use to generate an electrochemical gradient (Munn, 1974). The IM can be separated into two distinct regions – the cristae, which serve to create a much larger surface area for assembly of the respiratory complexes, and the peripheral regions – which are joined by tubular connections known as cristae junctions (Perkins *et al.*, 1997). The proportion of each of these two areas can change, resulting in greater amounts of cristae or larger smooth peripheral regions, as a result of fission and fusion of the inner membrane (Mannella *et al.*, 2001). It has been suggested that this varied morphology displayed by the IM could be part of a functional regulatory system (Mannella, 2006), as some mitochondrial functions can be affected by changes to the IM topology (Mannella *et al.*, 1997; Mannella *et al.*, 2001).

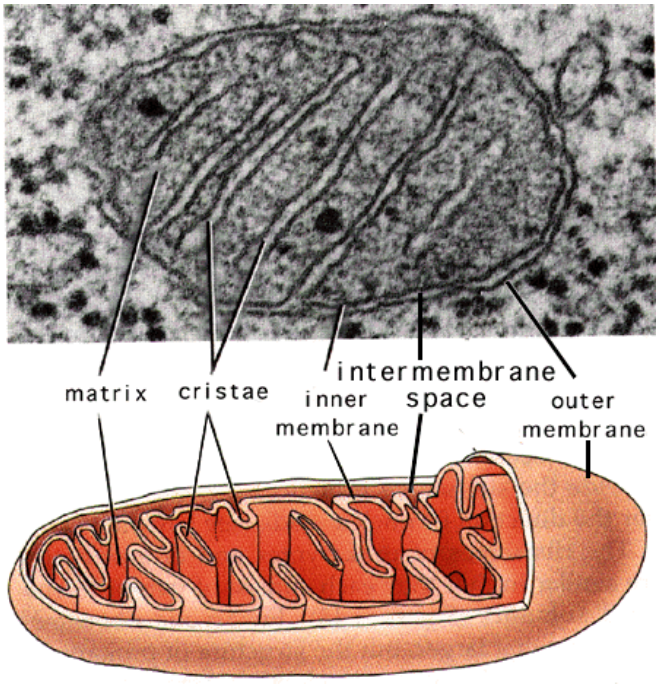

Figure 1.1 – Mitochondrial structure

An electron microscopy image of a single mitochondria aligned to a classical 3D representation of mitochondrial structure. Taken from *http://academic.brooklyn.cuny.edu/biology/bio4fv/page/mito.htm*

1.3 Mitochondrial Functions

1.3.1 Iron-sulphur cluster formation

Fe-S clusters are formed by the interaction of iron cations ($Fe^{2+/3+}$) and sulphide (S^{2+}) anions, most commonly in a rhombic (2Fe-2S) or cubane (4Fe-4S) formation. These inorganic compounds are able to act as protein cofactors, participating in electron transfer, catalysis and regulatory processes (Beinert *et al.*, 1997). Historically, Fe-S clusters were believed to assemble spontaneously on proteins (Malkin and Rabinowitz, 1966), but later evidence confirmed that synthesis of these compounds is in fact a catalysed process (Johnson *et al.*, 2005). Fe-S clusters are formed through 2 pathways in eukaryotic cells, though a third pathway has been identified in bacteria; mitochondria are the major site of iron-sulphur (Fe-S) cluster formation in eukaryotic cells (Lill *et al.*, 1999). The system for Fe-S biosynthesis in the mitochondria involves the ISC assembly machinery, a major source of Fe-S cluster generation in bacteria and likely inherited during the endosymbiotic event which led to mitochondria. This is a two-step process, involving Fe-S assembly on scaffold proteins Isu1 and Isu2 by a currently unknown mechanism prior to trafficking of Fe-S clusters from Isu1 to the apoprotein for assembly into a functional protein (Lill, 2009). There are many assisting proteins involved in this complex mechanism, as outlined in Figure 1.2.

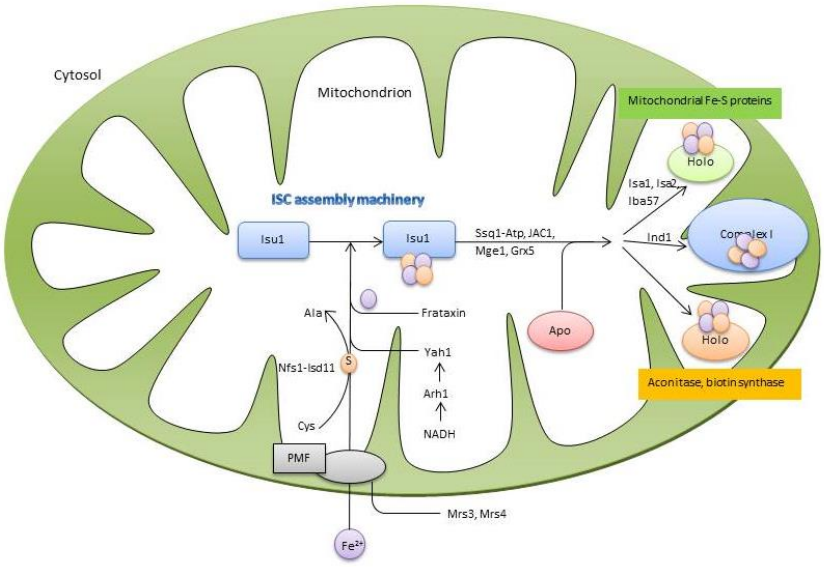

Figure 1.2 - **Fe-S biosynthesis**

A schematic representation of Fe-S cluster assembly on the Isu protein scaffolding, prior to inclusion into apoproteins to form functional proteins.

1.3.2 Calcium handling

Calcium (Ca^{2+}) is an important signalling molecule in eukaryotes, involved in major cell events including differentiation, cell signalling, apoptosis, and cellular proliferation. Different signals can be identified by the cell according to different intensities, frequencies, localisation or durations of Ca^{2+} signalling (Berridge *et al.*, 2000). At rest, cytosolic concentrations of Ca^{2+} are maintained at a steady level by import into and export out of the cell through the plasma membrane (Rizzuto and Pozzan, 2006). Cytoplasmic Ca^{2+} signals can then be created in the cell through an influx of Ca^{2+} through the plasma membrane from the extracellular matrix, or a release of Ca^{2+} from intracellular stores. Ca^{2+} is stored in most organelles within the cell, though the endoplasmic reticulum is often the largest store of Ca^{2+}(Saris and Carafoli, 2005).

The ability of mitochondria to accumulate and store Ca^{2+} has been well documented since the 1960s (Chance, 1965), though investigations to elucidate the molecular mechanisms involved in mitochondrial Ca^{2+} handling continue to this day. Mitochondria are able to buffer cellular Ca^{2+} levels by uptaking potentially vast quantities of Ca^{2+} when levels in the cell peak too high - preventing potential cell damage from Ca^{2+} overload – or releasing Ca^{2+} into the cytoplasm when cellular levels drop (Collins and Meyer, 2010).

Ca^{2+} was originally believed to move freely cross the mitochondrial outer membrane through the voltage dependent anion channel (VDAC), when this channel was shown to conduct Ca^{2+} in addition to its known role in conducting monovalent ions (Gincel *et al.*, 2001). However, more recent data has shown VDAC to provide a barrier to free diffusion of $Ca^{2+,}$ allowing for very tight regulation of Ca^{2+} movement across the OM (Rapizzi *et al.*, 2002). Once across the OM, Ca^{2+} can then be imported across the mitochondrial IM by the mitochondrial Ca^{2+} uniporter (MCU), a non-MCU Ca^{2+} channel or a mitochondrial ryanodine receptor (mRyR) (Gunter and Sheu, 2009).

Three separate mechanisms serve to efflux Ca^{2+} from the mitochondrial matrix. In excitable cells, including neurons and cardiomyocytes, efflux is Na^{+} dependent; the Na^{+}/Ca^{2+} exchanger NCLX is responsible for the electrogenic exchange of $3Na^{+}$ with $1Ca2^{+}$ (Palty *et al.*, 2010). A Na^{+} independent mechanism for Ca^{2+} efflux exists predominantly in non-excitable cells, coupling Ca^{2+} export to the import of H^{+}(Puskin *et*

al., 1976). Finally, the permeability transition pore (PTP) allows Ca^{2+} to pass out of the mitochondria under conditions of Ca^{2+} overload. In this case, mitochondrial stress - caused by excessive levels of Ca^{2+} in conjunction with other factors such as oxidative stress – can cause the PTP to open, allowing free movement of Ca^{2+} across the mitochondrial membranes into the less saturated cellular cytoplasm (Halestrap, 2009).

1.3.3 The TCA cycle

The tricarboxylic acid (TCA) cycle - also known as the citric acid cycle or the Krebs cycle - was discovered by Sir Hans Krebs, who won the Nobel prize "for his discovery of the citric acid cycle" in 1953 (Krebs, 1953). The TCA cycle is the first stage in cellular respiration, where NADH and $FADH_2$ are generated through the processing of carbon fuels. Both NADH and $FADH_2$ are important downstream of the TCA cycle in oxidative phosphorylation (see 1.3.5), to reduce O2 in order to generate the proton gradient used in ATP synthesis.

Under aerobic conditions in the cell, pyruvate - generated from glucose by glycolysis - is transported into the mitochondrial matrix, where it forms acetyl CoA under the action of the pyruvate dehydrogenase complex:

$$\text{Pyruvate} + \text{CoA} + NAD^+ \rightarrow \text{acetyl CoA} + CO_2 + \text{NADH} + H^+$$

Acetyl CoA can then enter the citric acid cycle, where it reacts with oxaloacetate under catalysis by citrate synthase to form citrate; the by-product of this reaction is CoA, which is then free to react with a new molecule of pyruvate to initiate a new beginning to the citric acid cycle. The citric acid cycle then continues, with seven further enzymatic steps bringing the set of reactions full circle back to oxaloacetate (Thauer, 1988), as outlined in Figure 1.3. Importantly for downstream ATP production by oxidative phosphorylation, NADH is produced as a by-product from 3 stages of the TCA cycle and $FADH_2$ is produced as the by-product of a further reaction, as outlined below:

- Isocitrate + NAD^+ → α-ketoglutarate + **NADH** + CO^2

(catalysed by isocitrate dehydrogenase)

- α-ketoglutarate + NAD^+ + CoA → succinyl CoA + **NADH** + CO^2

(catalysed by α-ketoglutarate dehydrogenase complex)

- Malate + NAD^+ → oxaloacetate + **NADH** + H^+

(catalysed by malate dehydrogenase)

- Succinate + FAD → fumerate + **$FADH_2$**

(catalysed by succinate dehydrogenase)

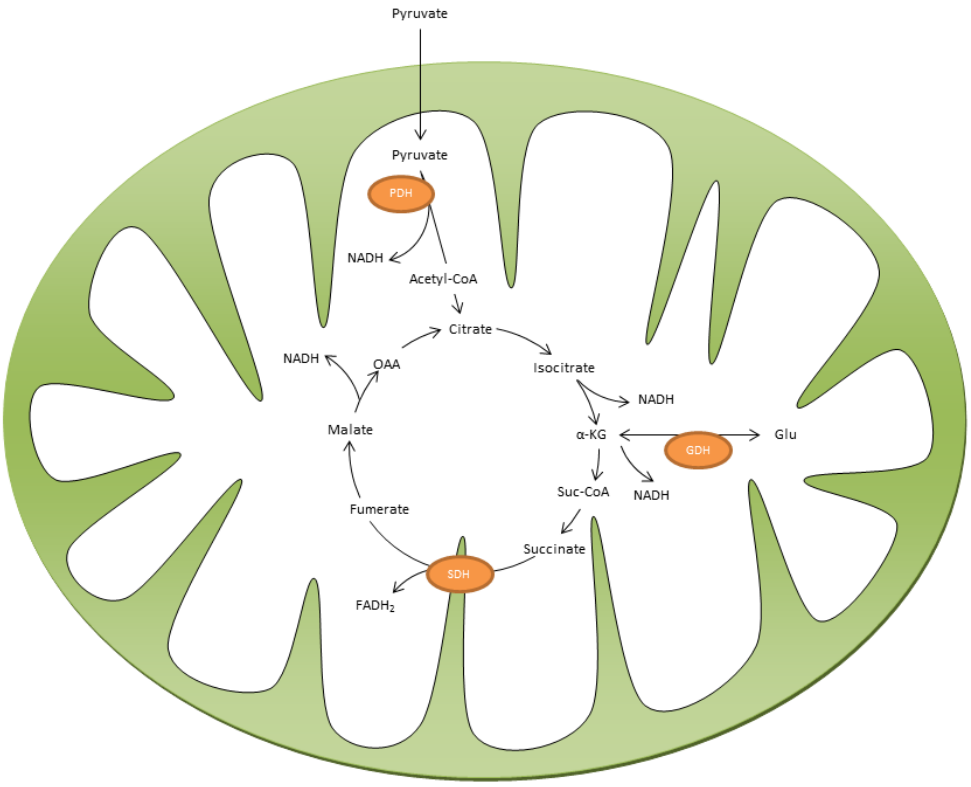

Figure 1.3 Outline of the TCA cycle

A brief overview of the citric acid cycle within the mitochondrial matrix; this process is the first stage of cellular respiration, generating NADH and $FADH_2$, both of which play important roles in oxidative phosphorylation.

1.3.4 Apoptosis

Programmed cell death, a highly regulated process distinct from cellular necrosis, was first investigated in the 1960's, and given the term apoptosis (Kerr *et al.*, 1972). Apoptosis is identified by a consistent pattern of changes to cell morphology prior to death, including cell shrinkage, nuclear fragmentation and condensation of chromatin, as opposed the characteristic cellular swelling and lysis of necrosis (Pollack and Leeuwenburgh, 2001). Unlike necrosis, which occurs following cellular insult such as infection or acute injury, apoptosis is an advantageous cellular mechanism for multicellular eukaryotic organisms, allowing fine control of cell numbers, tissue remodelling, homeostasis and disposal of dysfunctional cells.

Two major apoptotic pathways exist in eukaryotic cells - the extrinsic and the intrinsic pathways - both of which respond to different cellular signals. The extrinsic apoptosis pathway is activated by extracellular, proapoptotic ligands binding to and hence activating transmembrane death receptors. When active, the death receptors form a cell death inducing signalling complex, which in turn activates caspases 8 and 10. These active caspases then stimulate the activity of caspases 3, 6 and 7, which carry out apoptosis (Ashkenazi, 2008).

The intrinsic pathway, which is also referred to as the mitochondrial pathway due to heavy involvement of mitochondria in this signalling pathway, acts in response to cell death stimuli including DNA damage and UV radiation. This pathway is activated by the BH3 family of proteins (a heterogeneous group of proteins, including Puma, Bmf and Bad, which share a BH3 motif), which are capable of binding to and inhibiting anti-apoptotic Bcl-2 proteins and hence acting as pro-apoptotic proteins (Youle and Strasser, 2008). The inhibition of the anti-apoptotic Bcl-2 proteins allows the pro-apoptotic proteins Bak and Bax to permeabilise the outer mitochondrial membrane, releasing cytochrome *c* (Suen *et al.*, 2008). As apoptosis is initiated, Bax is translocated from the cytosol to the mitochondria, where it forms oligomers that appear as foci on the mitochondria (Antonsson *et al.*, 2001); Bak is already located at the mitochondria, but undergoes conformational changes to form oligomers during apoptosis (Griffiths *et al.*, 1999). The three-dimensional structures of Bcl-2 family proteins, including Bax, have been shown to resemble the structure of bacterial toxins capable of creating holes in cellular membranes (Muchmore *et al.*, 1996). It is now widely believed that

the oligomerisation of Bax is fundamental to the release of cytochrome *c* (Eskes et al., 2000), following the demonstration of Bax involvement in the formation of openings in the OMM in cell-free systems (Kuwana *et al.*, 2002).

When released from the mitochondria, cytochrome *c* binds to Apaf-1; until this point, Apaf-1 exists is autoinhibited by the closed, compact state it exists in (Bao *et al.*, 2005). Binding of cytochrome *c* causes Apaf-1 to undergo a conformational change, moving into an open formation and freeing the N-terminal caspase recruitment domain (CARD). This allows for seven molecules of Apaf-1 to bind together in a wheel-like structure to form the apoptosome (Acehan *et al.*, 2002), which can then recruit, bind and activate procaspase 9 (Shi, 2006). The now active caspase 9 remains associated with the Apaf-1 apoptosome, forming a complex known as a holoenzyme (Rodriguez and Lazebnik, 1999) , increasing the activity of the apoptosome and initiating apoptosis by stimulating the activity of caspases 3, 6 and 7 (Wang and Youle, 2009).

1.3.5 Oxidative Phosphorylation

The oxidative phosphorylation (OXPHOS) system is regarded as one of the most essential mitochondrial functions, being responsible for the majority of ATP synthesis within a eukaryotic cell. The OXPHOS system is made up of five multi-subunit protein complexes and two electron carriers (coenzyme Q and cytochrome *c*); together, this group of proteins link together cellular respiration and ATP synthesis. The electron transport chain (ETC) is made up from four protein complexes: Complex I (NADH dehydrogenase), complex II (succinate dehydrogenase), complex III (cytochrome *c* reductase) and complex IV (cytochrome *c* oxidase). Electrons flow through the ETC from NADH or $FADH_2$ to O_2 during a series of oxidoreductase reactions, releasing energy at each stage; the energy released from this electron transfer is used to sustain a proton (H^+) gradient across the IMM (Smeitink *et al.*, 2001). This H^+ gradient, which is generated by the pumping of H^+ from the mitochondrial matrix into the inter-membrane space through complexes I, III and IV, is then utilised by ATP synthase to catalyse the production of ATP from ADP and inorganic phosphate (Mitchell, 1961).

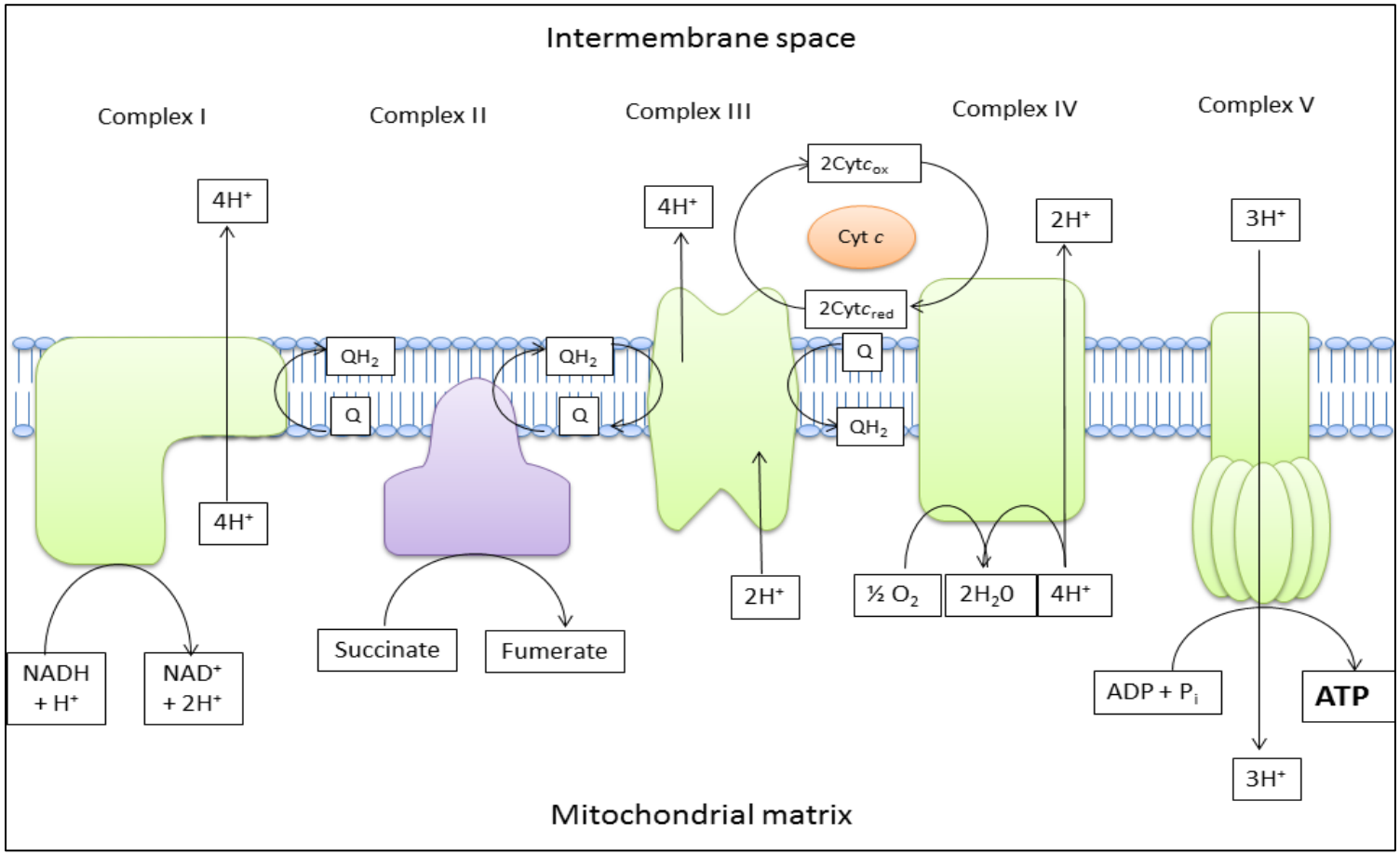

Figure 1.4 - The mitochondrial oxidative phosphorylation system.

A schematic of the five major protein complexes embedded in the inner mitochondrial membrane involved in oxidative phosphorylation. Electron transport is coupled to proton translocation across the membrane at complexes I, III and IV, while the conversion of succinate to fumerate at complex II also releases two electrons. Complex V is able to utilise the electrochemical gradient generated across the inner membrane by complexes I, II, III and IV to synthesise ATP.

1.3.5.1 Complex I

Complex I, also known as NADH or ubiquinone oxidoreductase, is the first complex of the ETC and oxidative phosphorylation; this is one of two entrances to the OXPHOS system, the other being Complex II. Complex I is also the largest and most complicated protein complex of the OXPHOS system, consisting of forty-five subunits with a combined mass of 980kDa in mammals (as assed in *Bos Taurus* heart mitochondria – closely related to human mitochondria for modelling purposes) (Carroll *et al.*, 2006). Of these subunits, seven are encoded within the mitochondrial DNA (ND1, ND2, ND3, ND4, ND4L, ND5 and ND6), while the remaining thirty-eight are nuclear encoded (Hirst *et al.*, 2003). In bacteria, Complex I (NDH-1) consists of fourteen subunits, all of which are evolutionarily conserved from bacteria to mammals; these fourteen subunits of mammalian Complex I are known as the 'core subunits', and are essential to the enzymatic activity of the complex. The other thirty-one subunits are known as 'accessory subunits' (Friedrich and Scheide, 2000) or 'supernumerary subunits' (Hirst, 2013) – though these are not required for catalysis, they are known to be involved in normal Complex I function due to the pathogenic nature of mutations in these subunits (Valsecchi *et al.*, 2010; Koene *et al.*, 2012).

Mitochondrial Complex I is believed, based upon structural and phylogenetic studies, to structurally consist of three sectors – the peripheral arm which protrudes into the matrix is comprised of a dehydrogenase domain and a hydrogenase-like domain, while the H+ transporter is embedded in the IMM (Mathiesen and Hägerhäll, 2002). An alternative interpretation of Complex I structure, based upon analysis of the intact complex and it's subunit composition from bovine heart mitochondria, defines four subcomplexes of Complex I (Iα, Iβ, Iγ, and Iλ) (Carroll *et al.*, 2003). Subcomplex Iλ consists of 15 subunits, including the seven nuclear-encoded 'core' subunits, the flavin mononucleotide (FMN, the primary electron acceptor of Complex I), and nine Fe-S clusters. Subcomplex Iλ forms the hydrophilic peripheral arm of Complex I, with only one of its constituent eight subunits containing a transmembrane helix. Subcomplex Iα consists of all of the subunits which comprise subcomplex Iλ, plus eight more subunits which serve to anchor the subcomplex to the IMM. Subcomplex Iβ predominantly consists of twelve subunits, with a thirteenth present at a sub-stoichiometric level, and has a high level of transmembrane helices spread across its constituent subunits; this

subcomplex makes up the majority of the IMM embedded arm of Complex I. The five remaining subunits not involved in subcomplexes Iα or Iβ are collectively regarded as subcomplex Iγ (Janssen *et al.*, 2006).

Complex I catalyses the oxidation of NADH to $NAD^+ + H^+$ releasing two electrons that are transferred to FMN, the primary electron acceptor of Complex I, reducing FMN to $FMNH_2$. These two electrons are then transferred through a series of seven of the total nine Fe-S clusters present in Complex I to a membrane bound ubiquinone molecule (Sazanov and Hinchliffe, 2006) (Figure 1.5)- the remaining two Fe-S clusters are believed to be an anti-oxidant centre (Yagi and Matsuno-Yagi, 2003) and a functionless evolutionary remnant (Sazanov and Hinchliffe, 2006). Cluster N2 (4Fe-4S) acts as the terminal electron donor; this iron sulphur cluster transfers both electrons to a single molecule of ubiquinone, reducing Q to QH_2.

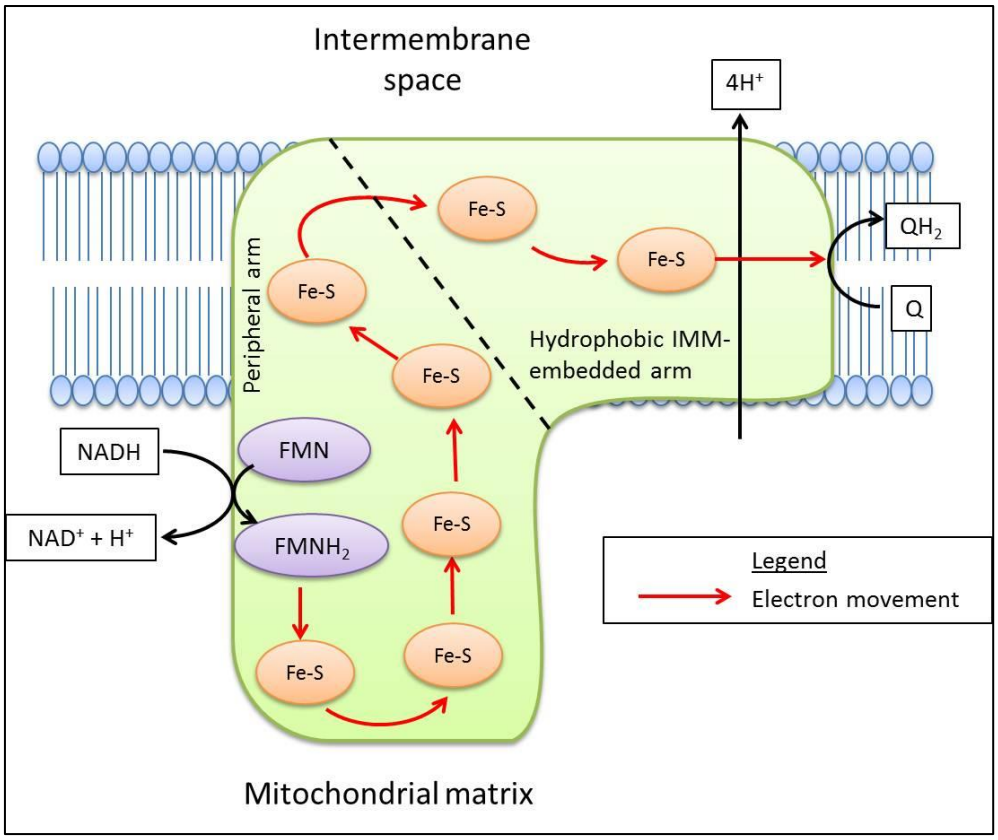

Figure 1.5 - Transport of electrons through Complex I.

Complex I is also known as NADH-ubiquinone oxidoreductase or NADH dehydrogenase I. This protein complex catalyses the reaction $NADH + Q + 5H^+ \rightarrow NAD^+ + QH_2 + 5H^+$, releasing two electrons which are collected by FMN, the primary electron acceptor of Complex I. The electrons are passed through seven Fe-S clusters to a membrane-bound ubiquinone molecule, catalysing its reduction to ubiquinol. Four protons are translocated across the mitochondrial inner membrane during this process.

1.3.5.2 Complex II

Mitochondrial complex II – succinate dehydrogenase, SDH – is the smallest protein complex of the OXPHOS system, consisting of only four subunits with a total mass of 124kDa which make up a catalytic heterodimer and an integral membrane region (Hägerhäll, 1997). Uniquely within the respiratory chain, complex II is entirely nuclear encoded, with no subunits encoded by mitochondrial DNA.

Complex II can also be classified within a family of proteins known as succinate: ubiquinone oxidoreductases; these proteins are classified into five types (A-E) according to their structural and biochemical properties. Mitochondrial complex II falls into category C, with one heme molecule and two transmembrane proteins (Lemos *et al.*, 2002). Among mitochondrial succinate: ubiquinone oxidoreductases, two subunits are highly conserved among bacteria, archaea and eukaryotic, known as the two 'core' subunits. These two subunits – A and B – form the hydrophilic domain of the protein complex.

Subunits A and B of Complex II form a catalytic heterodimer, located on the matrix side of the IMM. Subunit A contains a covalently bound flavin adenine dinucleotide (FAD) cofactor (an electron acceptor), while subunit B contains 3 Fe-s clusters, 2Fe-2S, 4Fe-4S, 3Fe-4S (Hägerhäll, 1997). FAD is responsible for catalysing the succinate to fumerate step of the Krebs cycle, transferring the two electrons released from this reaction into the respiratory chain via the Fe-S clusters of subunit B and the membrane domain of the complex, where electron acceptor coenzyme Q is located (Lancaster *et al.*, 1999). This is the second and final access point for electrons to enter the respiratory chain.

The remaining two subunits of Complex II are transmembrane proteins responsible for anchoring the complex to the IMM; the large cytochrome b binding protein (CybL, subunit C), and the small cytochrome b binding subunit (CybS, subunit D). Both of these hydrophobic subunits form α-helices (subunit C forms 5, while subunit D forms four); a heme group is located between the helices of the heterodimer formed by these two subunits (Sun *et al.*, 2005).

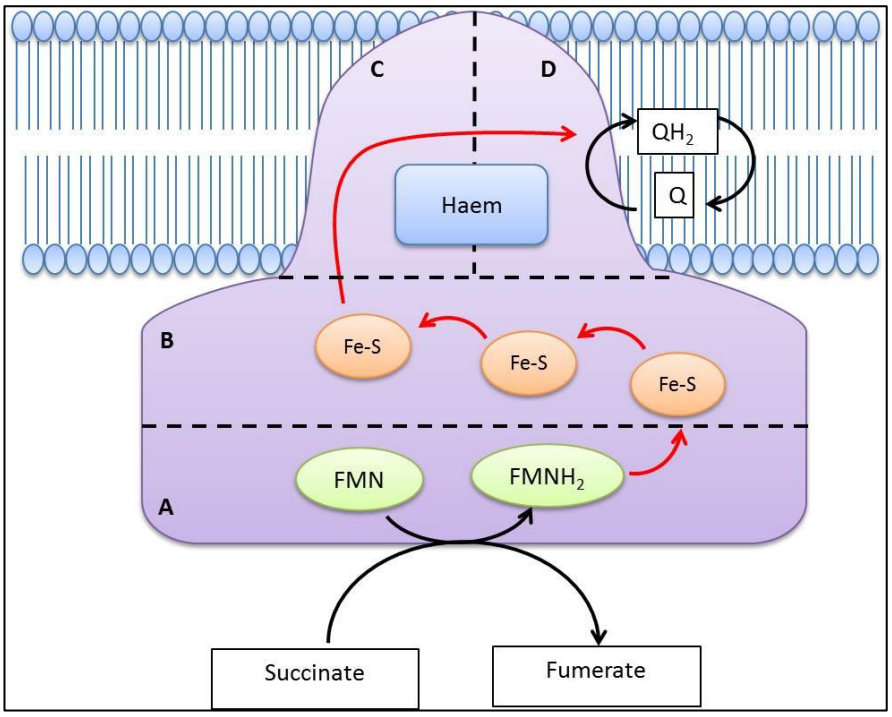

Figure 1.6 - Transport of electrons through Complex II.

Complex II is also known as succinate : ubiquinone oxidoreductase. This protein complex is unique in the oxidative phosphorylation system in being entirely nuclear encoded. Complex II is a second entrance point to the oxidative phosphorylation system, the alternative entry point being Complex I; Complex II catalyses the reaction succinate + Q → fumerate + QH_2, releasing two electrons into the respiratory chain via electron acceptor coenzyme Q.

1.3.5.3 Complex III

Mitochondrial Complex III, also known as ubiquinone-cytochrome *c* oxidoreductase or the bc_1 complex, was initially discovered in 1961 by Hafterfi *et al* (Hatefi *et al.*, 1961) from work in bovine heart. Mammalian Complex III consists of eleven subunits (Hatefi, 1985)and four prosthetic groups]), at a total mass of approximately 240kDa. The prosthetic groups are made up of one 2Fe-2S Rieske centre in subunit V and a total of three heme groups; two heme groups within cytochrome *b* - b_L (low affinity) and b_H (high affinity) - and a heme in cytochrome c_1. The heme groups present in cytochromes *b* (subunit III) and c_1 (subunit IV) are iron-protoporphyrin IX – the same heme group present in myoglobin and haemoglobin (Berry *et al.*, 2000). The three subunits containing these prosthetic groups (subunits III, IV and V) are the essential subunits, conserved across all species and constituting the minimal functional core of the

complex (Xia *et al.*, 1997), while the remaining eight subunits are termed the supernumerary subunits.

With the exception of cytochrome *b*, which is mitochondrially-encoded, Complex III is entirely encoded by the nuclear genome. The ten nuclear-encoded subunits of Complex III interact together with cytochrome *b* to form a bc_1 monomer; these eleven subunit structures dimerise symmetrically into a pear-shaped structure to form a complete Complex III (Berry *et al.*, 2000).

Complex III can be split into three functional regions; the intermembrane space region, the matrix region and the transmembrane helix region. Each bc_1 monomer contains thirteen membrane-spanning helices in the transmembrane domain, with eight of these belonging to cytochrome *b* and one more belonging to cytochrome c_1, Fe-S, and subunits VII, X, XI respectively. Over half of the molecular mass of Complex III is located in the matrix region, consisting of subunits I, II, VI, and IX, as well as part of subunit VII, the N-terminal region of the Fe-S cluster, and the C-terminal region of cytochrome c_1. The transmembrane domain, containing the transmembrane region of cytochrome *b*, also house heme groups b_L and b_H, and the Q_i and Q_o pockets. The intermembrane space region of Complex III houses the functional domains of cytochrome c_1, the 2Fe-2S Rieske centre and subunit VIII. The extramembrane regions of the Fe-S clusters in the two bc_1 monomers of Complex III interact when a dimer is formed. (Yu *et al.*, 1999).

As the third complex in the electron transport chain, ubiquinone-cytochrome *c* oxidoreductase, serves to transfer electrons from the pool of QH_2 produced by Complexes I and II to oxidised cytochrome *c*, and to pump protons from the mitochondrial matrix into the intermembrane space. These processes are believed to occur via the Q cycle, as first proposed by Peter Mitchell in 1976 (Mitchell, 1976), which involves the oxidation of ubiquinol at the Q_o site and the reduction of ubiquinone at the Q_i site. First, two QH_2 molecules consecutively bind to Complex III, each donating two electrons to the complex and releasing two H^+ into the intermembrane space. The first QH_2 molecule to binds to the Q_o site; the electrons released here travel through the complex via two distinct pathways. One electron travels, via the 2Fe-2S Rieske centre and cytochrome c_1, to a molecule of oxidised cytochrome *c*, which is then converted to its reduced form. A second electron travels to the second Q binding site (Q_i) via b_L and b_H; this reduces the oxidised ubiquinone present at this site to a

semi-quinone radical anion ($Q\cdot^-$). Now fully oxidised, the Q molecule at the initial Q_o site re-enters the Q pool, leaving the Q_o site free for a second molecule of QH_2 to bind. This molecule of QH_2 reacts in the same manner as the first molecule, transferring one electron to cytochrome *c* and one electron to fully reduce the partly reduced ubiquinone at Q_i. This quinone radical anion then takes up two protons from the mitochondrial matrix to form a molecule of QH_2. In total during this cycle, two protons are taken from the mitochondrial matrix and four are released into the inner membrane space - contributing to the proton gradient across the IMM – two molecules of QH_2 are oxidised to Q molecules, and one Q molecule is reduced to QH_2 (Yu *et al.*, 1999; Gao *et al.*, 2003; Papa *et al.*, 2012).

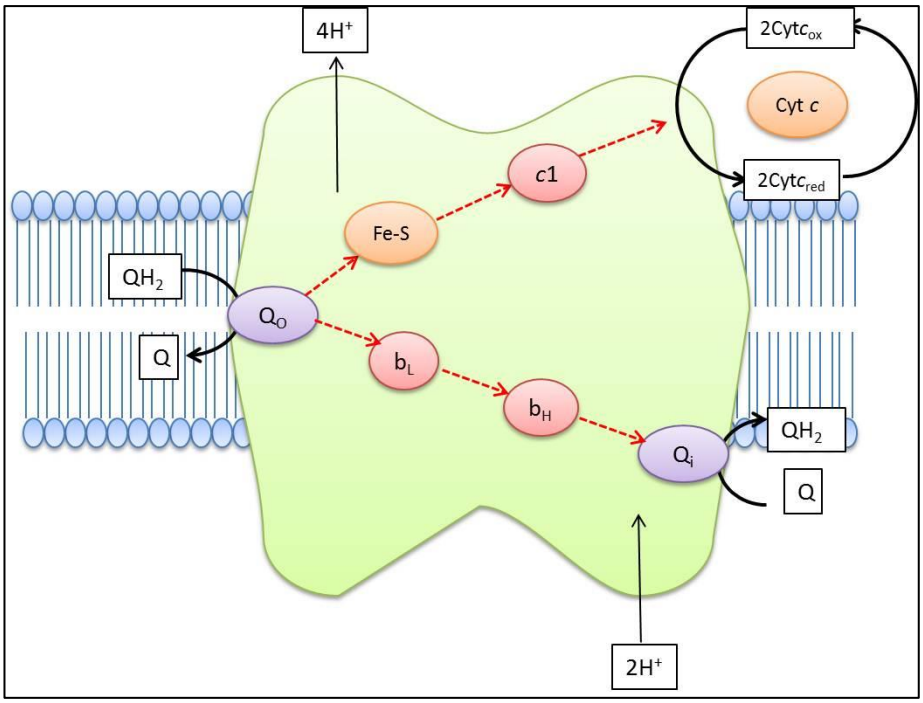

Figure 1.7 - Electron transport system of Complex III.

Complex III is also known as ubiquinone-cytochrome *c* oxidoreductase or the bc_1 complex. This protein complex transfers electrons from the pool of QH_2 produced by Complexes I and II to oxidised cytochrome *c*, and to pump protons from the mitochondrial matrix into the intermembrane space. These processes occur via the Q cycle, which involves the oxidation of ubiquinol at the Q_o site and the reduction of ubiquinone at the Q_i site.

1.3.5.4 Complex IV

Mitochondrial Complex IV, also known as cytochrome *c* oxidase, is the final complex of the electron transport chain, and the third proton pump involved in OXPHOS. The final step of the electron transport chain – the transfer of electrons from reduced cytochrome *c* to molecular oxygen, the final electron acceptor – is catalysed by Complex IV.

Mammalian Complex IV is made up of thirteen subunits and six prosthetic groups, with a total molecular mass of ~200kDa; ten of these subunits are nuclear encoded, with the remaining three being encoded by the mitochondrial genome. The three highly conserved mitochondrial subunits (CO1, CO2 and CO3) are the largest and most hydrophobic of the subunits, and form the catalytic core of the complex (Lazarou *et al.*, 2009), while the nuclear-encoded subunits serve structural and regulatory roles. The crystal structure of bovine Complex IV was resolved in 1996 by Tsukihara *et al,* showing that the active enzyme exists as a dimer (Tsukihara *et al.*, 1996).

The six prosthetic groups of cytochrome c oxidase consist of two heme groups, two copper centres, and additional metal centres of Zn and Mg. The copper centres present in the complex are able to act as electron acceptors/donors by alternating between the reduced Cu^{+} and oxidised Cu^{2+} form. Copper centre A (Cu_A), containing two copper ions linked by cysteine residues, is the entry point for electrons into Complex IV – electrons are initially passed here following the reduction of cytochrome *c* at the outer membrane of the complex. This copper centre is located in the extramembrane domain of subunit II. Copper centre B (Cu_B) consists of a single copper ion coordinated by three histidine residues. Cu_B is located at the transmembrane region of subunit I, as are heme groups *a* and a_3. Heme a_3 is located directly adjacent to Cu_B, together forming the active centre for reduction of O_2 to H_2O (Tsukihara *et al.*, 1996).

The initial step at Complex IV involves the consecutive binding of four individual molecules of cytochrome *c* to the enzyme, each releasing a single electron as the molecule is reduced. Electrons from two molecules of cytochrome *c* are sequentially passed through Cu_A and heme *a*, one electron then stopping at heme a_3 while the second electron continues on to Cu_B. The reduced heme a_3 and Cu_B centres are then

capable of recruiting and binding a molecule of O_2, which takes an electron from each of the ions present in the active centre to form a peroxide (O_2^{2-}) bridge between Fe^{3+} and Cu^{2+}. This process is repeated with 2 more electrons donated by the remaining two molecules of cytochrome *c* involved in this process, resulting in the addition of an electron and an H^+ ion from the mitochondrial matrix to each oxygen atom present at the active centre. This reduction of the peroxide bridge forms Fe^{3+} -OH and Cu^{2+} -OH. The reaction of each of these molecules with a further H^+ ion from the mitochondrial matrix allows the release of two molecules of H_2O, oxidising the a_3 and Cu_B centres back to their original state.

In addition to the uptake of four H^+ ions from the mitochondrial matrix to reduce O_2 to two molecules of H_2O, four further H^+ ions are directly transported through Complex IV from the mitochondrial matrix out into the intermembrane space. The energy for this translocation comes from the reduction of O_2 to H_2O. This proton pump is believed to work simultaneously with H^+ uptake to the active site of Complex IV (Faxen *et al.*, 2005).

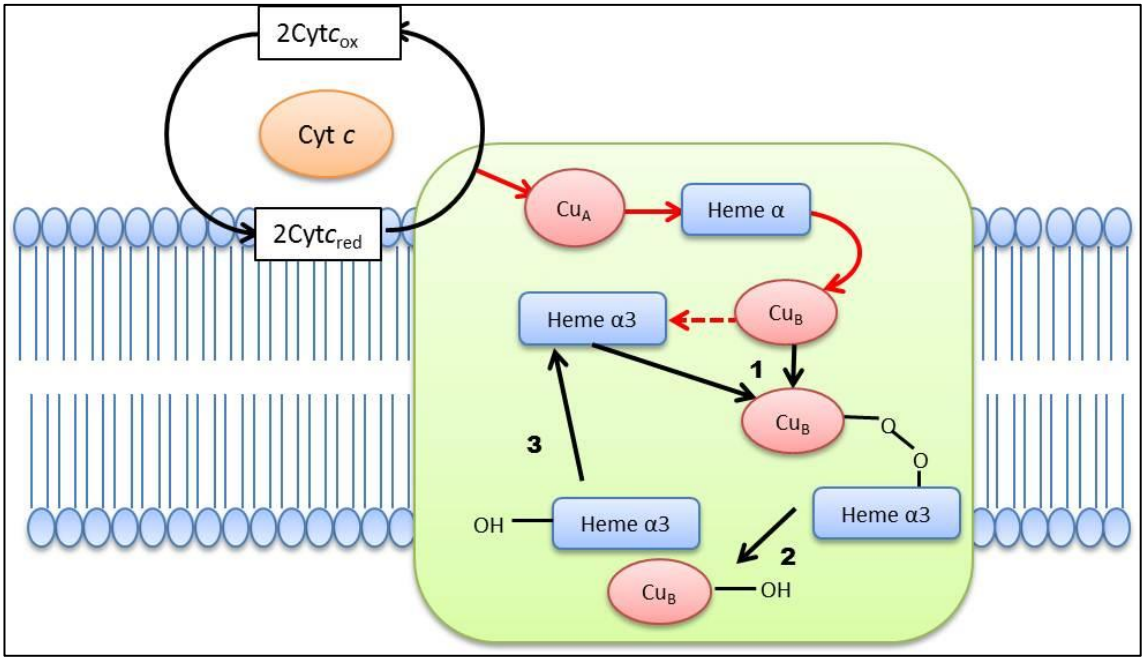

Figure 1.8 - Electron transport in Complex IV.

Complex IV is also known as cytochrome *c* oxidase; as the fourth and final respiratory chain complex, Complex IV is responsible for the transfer of electrons from reduced cytochrome *c* to molecular oxygen, the final electron acceptor. Complex IV takes up four H^+ ions from the matrix to reduce O_2 to H_2O, as well as transporting four more H^+ ions from the mitochondrial matrix out into the intermembrane space.

1.3.5.5 ATP Synthase

Mitochondrial ATP synthase, also referred to as F_OF_1-ATPase, catalyses the final step of oxidative phosphorylation – the synthesis of ATP from ADP and inorganic phosphate (P_i). This reaction is fuelled by the energy released by the transport of H^+ ions through ATP synthase down the electrochemical gradient across the IMM (Mitchell, 1961); this electrochemical gradient is produced by the movement of H^+ from the mitochondrial matrix into the intermembrane space by Complex I, III and IV. Mammalian ATP synthase is comprised of sixteen subunits, two of which are mitochondrially encoded (ATPase 6 and 8), at a total molecular weight of approximately 550kDa (Boyer, 1997).

Fourteen of the sixteen ATP synthase subunits form the two domains of the complex; the hydrophobic F_O transmembrane domain, and the hydrophilic F_1 domain which protrudes into the mitochondrial matrix. The remaining two subunits of ATP synthase are the oligomycin-sensitivity-conferring protein (OSCP), and the IF_2 inhibitor protein which plays a key role in ATP hydrolase regulation (Gaballo and Papa, 2007). The F_1 domain is made up from five subunits, in the following proportions: 3α subunits, 3β subunits, and 1 each of subunits γ, δ and ε (Abrahams *et al.*, 1994). The α and β subunits directly interact with one another, forming a hexameric ring, while the γ and ε subunits form the central stalk of the subunit. A long helical coiled coil domain of the γ subunit protrudes into the centre of the $\alpha_3\beta_3$ hexamer, linking it to the γε stalk. The area of the γ subunit bound to each of the β subunits serves to distinguish these otherwise identical molecules. Finally, the δ subunit forms part of the exterior column of the molecule; the δ subunit is bound to the $\alpha_3\beta_3$ hexamer, while two b subunits form the long stretch of the column bound at one end to the δ subunit, and at the other end bound to an a subunit on the periphery of the F_O domain.

The mitochondrial F_O has three highly conserved 'core' subunits – a, b and c, which are present in a ratio of 1:1:10-12 – plus six additional subunits with currently unknown function (d, e, f, g, F6 and 8). Ten to fourteen c subunits form a ring embedded in the IMM; the single a subunit is bound to the outside of this ring, while two b subunits form the exterior column attaching the a subunit of the F_O domain to the δ subunit of the F_1 domain (Collinson *et al.*, 1994).

The proton gradient established by complexes I, III and IV of the electron transport chain allows for the movement of H^+ protons through the F_O proton channel, causing the rotation of the ring of c subunits in the F_O domain (Cox *et al.*, 1984). The rotation of the c-ring subsequently causes the rotation of the F_1 domain subunits γ, δ and ε, providing energy for the production of ATP by a mechanism known as rotary catalysis (Devenish *et al.*, 2008). This energy is utilised by the β subunits, which act as the catalytic sites for the synthesis of ATP. At any one time, each β subunit exists in one of three states; the β subunits cycle through these three states, moving from one to the next with each 120° turn of the γ subunit. In the 'loose state', ADP and P_i are bound to the subunit, ATP synthesised from is ADP and P_i but remains bound to the subunit in the 'tight' state, and in the 'open' state of a β subunit ATP is released, allowing ADP and P_i to bind (Jonckheere *et al.*, 2012). This is known as the 'binding-change' mechanism, as was first proposed by Boyer in 1975 (Boyer, 1975).

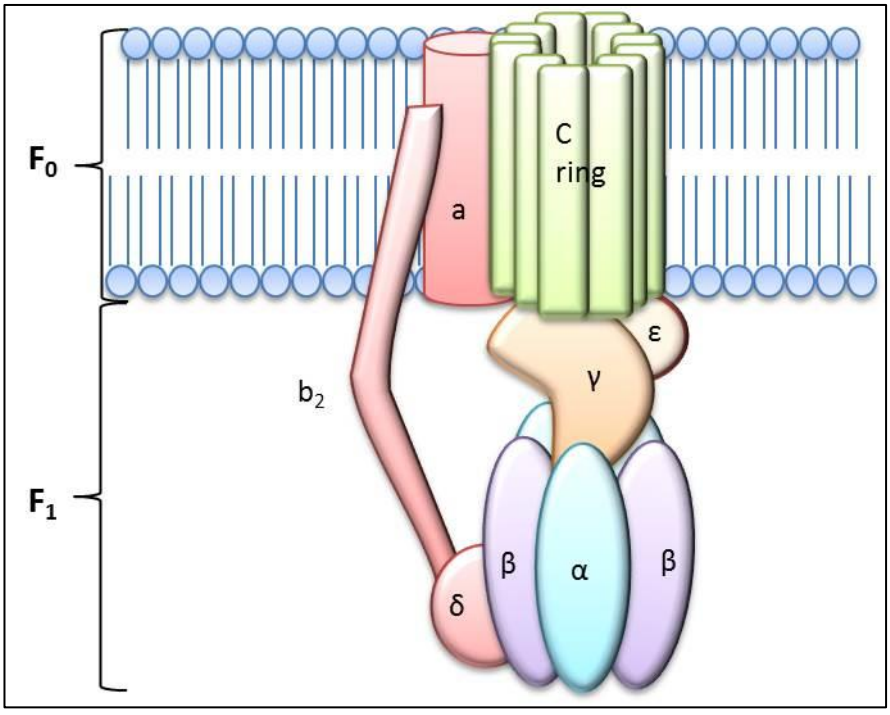

Figure 1.9 - ATP synthase structure.

ATP synthase, also known as F_OF_1-ATPase, is the final protein complex involved in oxidative phosphorylation. ATP synthase catalyses the ATP synthesis from ADP and inorganic phosphate. This reaction is fuelled by the energy released from the transport of H^+ ions through ATP synthase, down the electrochemical gradient across the inner mitochondrial membrane generated by the other protein complexes involved in oxidative phosphorylation.

1.4 Mitochondrial DNA

1.4.1 Human Mitochondrial Genome

Mitochondrial are unique organelles within eukaryotic cells in that they contain their own DNA, separate from the nuclear DNA of the cell – the only other organelles containing their own genetic material are chloroplasts (Borst, 1977). This genetic material results from the ancestral history of the mitochondria as a free-living primitive bacteria-like organism, prior to the symbiosis event with a eukaryotic cell (Kurland and Andersson, 2000).

The mitochondrial genome was first discovered in chick embryos in 1966, later being confirmed to exist in chick liver cells (Borst and Ruttenberg, 1966). The mitochondrial genome is comprised of double stranded DNA – the two strands being identified as the guanine-rich heavy (H) strand and cytosine-rich light (L) stand – and a short three-strand region of the genome known as the displacement loop (D-loop) (Kasamats.H *et al.*, 1971). In humans, the mitochondrial genome has been confirmed as a circular 16,569 base pair molecule, with the first complete sequence being published in 1981 (Anderson *et al.*, 1981b). This sequence - derived from the genetic information from a single human, bovine cells and HeLa cells - became known as the Cambridge Reference Sequence, though further work which widened the resources used to best sequence the mitochondrial genome has led to the formation of the Revised Cambridge Reference Sequence (Andrews *et al.*, 1999).

The mitochondrial DNA is very condensed, with no introns within the DNA and very few non-coding regions – the only lengthy non-coding region contains control elements for mtDNA transcription and translation (Shadel and Clayton, 1997). The 16,569bp human mitochondrial genome encodes thirty-nine genes; 22tRNAs, 2 rRNAs, and 13 proteins essential for the respiratory chain and ATP production, including 7 subunits of complex I (NADH dehydrogenase-ubiquinone oxidoreductase), 1 subunit of complex III (ubiquinone cytochrome *c* oxidoreductase), 3 subunits of complex IV (cytochrome *c* oxidase), and 2 subunits of complex V (ATP synthetase) (Schon *et al.*, 1997). The remaining proteins required for normal mitochondrial function are encoded for by the nuclear DNA, and are imported into the mitochondria from the cytoplasm. Many of these protein encoding genes are proposed to have originally been present in

the mitochondrial genome, but have since been transferred to the 'host' nuclear genome during early eukaryote evolution (Sagan, 1967).

The mitochondrial genome is organised within the cell into structures known as nucleoids; stable protein-DNA complexes within the mitochondria, each containing 5-7 mitochondrial genomes (Gilkerson *et al.*, 2008). Studies of nucleoid dynamics suggest these structures to be immobile within the mitochondria, with no interaction between individual nucleoids. Investigation into the segregation of mitochondrial DNA (mtDNA) between nucleoids was carried out in a cybrid cell line created by the fusion of two homoplasmic cell lines carrying non-overlapping mitochondrial DNA deletions. Probes specific to each mtDNA deletion type were developed, and used to visualise the presence of the two deletion species in nucleoids within the cybrid cell line, but no fusion of separate nucleoids or exchange of genomic information was observed (Gilkerson *et al.*, 2008).

Most proteins known to be involved in mtDNA maintenance (including TFAM, POLG, mtSSB and TWINKLE) have been found to be contained within the nucleoids (Wang and Bogenhagen, 2006; Bogenhagen *et al.*, 2008). A layered model of nucleoid structure has been proposed following extensive analysis of the proteins involved in nucleoid formation and structure, suggesting that a core central region of the nucleoid is responsible for the replication and transcription of the mtDNA, while mtDNA translation and assembly of the mitochondrial complexes takes place in a peripheral outer region of the nucleoid structure (Bogenhagen *et al.*, 2008). This proposed model demonstrates the importance of nucleoid structure to mtDNA replication and processing, as indicated by the presence of many mitochondrial DNA maintenance proteins, but could also support a previous hypothesis put forward by Capaldi *et al* that nucleoid formation may play an important role in cellular respiration. This hypothesis suggests that binding several mtDNA molecules together may facilitate the pooling of the peptide products from each genome, supporting efficient assembly of the respiratory complexes (Capaldi *et al.*, 2002).

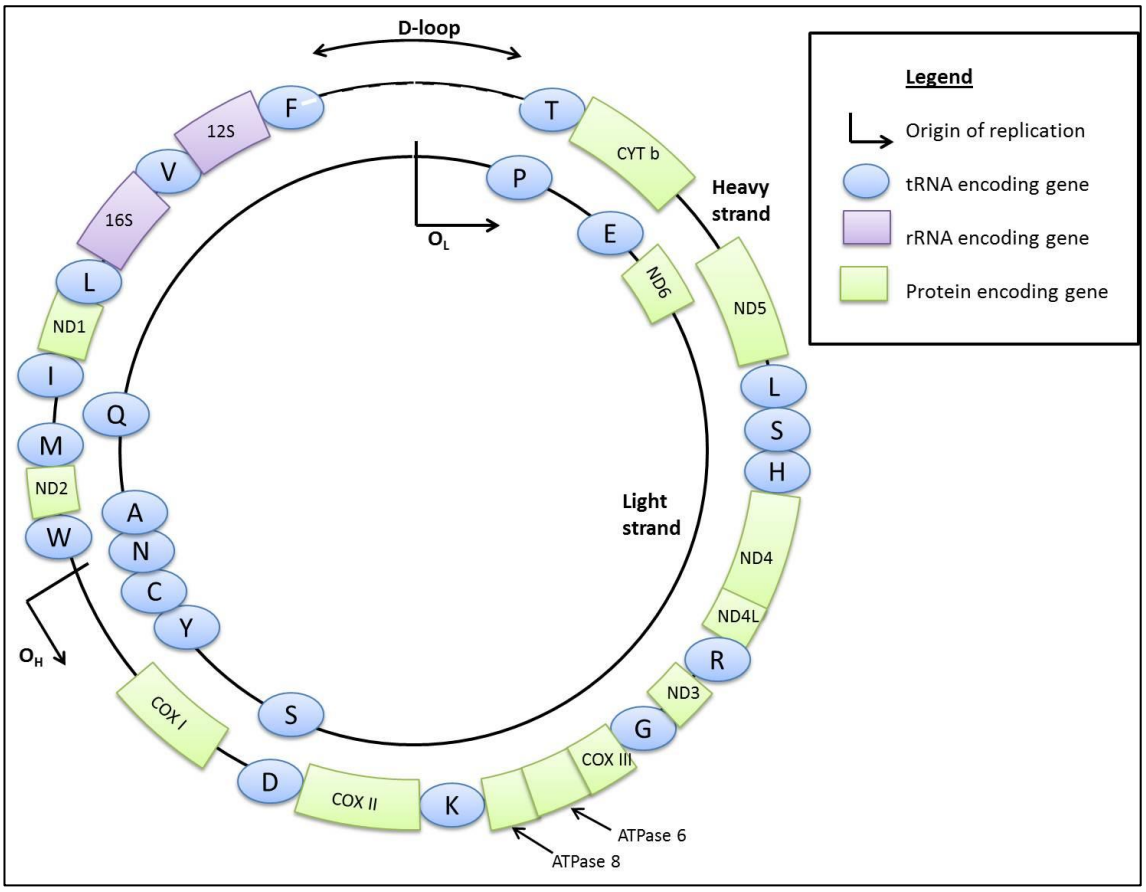

Figure 1.10 – The mitochondrial genome.

The mitochondrial genome is comprised of double stranded DNA – the two strands being identified as the guanine-rich heavy (H) strand and cytosine-rich light (L) stand – and a short three-strand region of the genome known as the displacement loop (D-loop). In humans, the mitochondrial genome has been confirmed as a circular 16,569 base pair molecule. The human mitochondrial genome encodes thirty-nine genes; 22tRNAs, 2 rRNAs, and 13 proteins essential for the respiratory chain and ATP production.

1.4.2 Transcription

The two major transcription initiation sites in the mitochondrial genome, IT_{H1} and IT_L, are both located within the D-loop, within a 150bp region. Surrounding both of these initiation site is a promoter with a 15bp consensus sequence, 5'-CANACC(G)CC(A)AAAGAYA-3', crucial to transcription. The adenine positioned 7 bases from the 3' end of this promoter sequence represents the transcription initiation site (Hixson and Clayton, 1985). IT_{H1}, at nucleotide position 561 within the heavy strand promoter, is where the majority of H-strand transcription begins, while L-strand transcription begins at nucleotide position 407 at IT_L within the light strand promoter.

Upstream enhancer elements, including binding sites for mitochondrial transcription activator A TFAM, are required for optimal transcription from these sites. A second heavy strand site for transcription initiation, IT_{H2} is located at nucleotide position 638 in the gene for $tRNA^{Phe}$, though the promoter for this initiation site shows little similarity to the 15bp consensus sequence; this initiation site is less frequently used than IT_{H1} (Chang and Clayton, 1984).

Mitochondrial RNA polymerase (POLRMT), mitochondrial transcription factors B1 and B2 (TFB1M and 2M), and TFAM are all required for successful mitochondrial transcription in mammals. POLRMT, a single-subunit RNA polymerase, is responsible for the transcription of DNA to RNA, but is unable to initiate transcription without the aid of TFAM and one of TFB1M or 2M. Prior to transcription initiation, either TFB1M or 2M forms a heterodimeric complex with POLRMT; this heterodimer has the capacity to recognise mitochondrial promoters, allowing the heterodimer to bind to the mtDNA and begin the process of transcription. TFAM, a 25kDa protein containing two High Mobility Group (HMG) box domains, is responsible for regulating the activity of the POLRMT-TFB1M/2M heterodimers, and hence regulates mtDNA transcription *in vitro*. TFAM binds directly to mtDNA in a sequence-specific manner, upstream of the light and heavy-strand promoters. This causes structural alterations to the mtDNA at the region, partially unwinding the transcription initiation sites to allow for binding of POLRMT-TFB1M/2M (Falkenberg *et al.*, 2007).

Once transcription of the L-strand has begun, the whole light strand is transcribed as a single polycistronic RNA (Aloni and Attardi, 1971). H-strand replication may occur in the same way, although an alternative mechanism has been proposed to account for the two initiation sites, and the different transcription rates of rRNAs and mRNAs encoded on the heavy strand (Gelfand and Attardi, 1981). This 'dual H-strand transcription model' proposes that most transcription begins at IT_{H1} and terminates just after the 16S rRNA; the model proposes that this is responsible for most of the transcription of the 2 rRNA genes contained on the heavy strand, and as this accounts for the majority of H-strand replication, this explains the higher rates of rRNA transcription seen in HeLa cells (Gelfand and Attardi, 1981). Transcription initiation at IT_{H2}, conversely, occurs much less frequently but leads to the transcription of polycistronic molecules almost the entire length of the heavy strand, including all of

the mRNAs and tRNAs encoded on the heavy strand. Evidence for both heavy chain transcripts have been found in vivo, supporting this method of transcription (Gelfand and Attardi, 1981).

Of the three mitochondrial transcripts produced - from transcription beginning at HSP2, HSP2, and LSP – the termination site for transcription has only been identified for the H1 transcript. This termination site is a tridecamer DNA sequence (5'-TGGCAGAGCCCGG-3') located at the 3' end of the 16S rRNA gene (Christianson and Clayton, 1988). Termination at this site is dependent upon the binding of mitochondrial transcription termination factor (mTERF), a 39kDa protein known to bind specifically to a 28-bp sequence at the 3' end of $tRNA^{Leu(UUR)}$ (Falkenberg *et al.*, 2007). Due to the evidence that mTERF functions bi-directionally, and exhibits increased activity during POLRMT transcription of the light strand, it is believed that mTERF is key to the termination of transcripts from all three initiation sites (Guja and Garcia-Diaz, 2012).

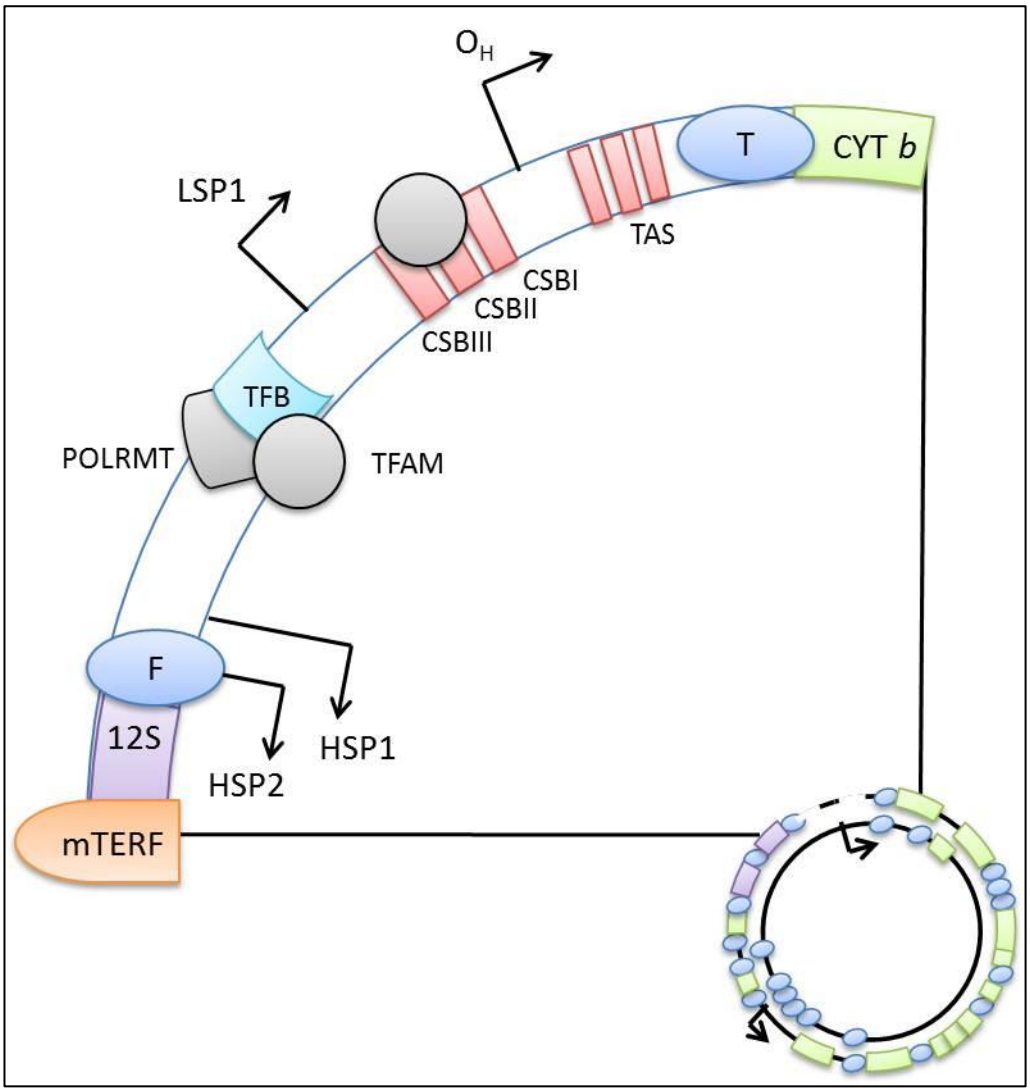

Figure 1.11 - mtDNA transcription.

MtDNA transcription is initiated from three promoters in the D-loop; one of these promoters is on the light strand (LSP1), while two are on the heavy strand (HSP1 and HSP2). The light strand of the mtDNA is transcribed as a single polycistronic RNA transcript; the heavy strand may also be transcribed this way from HSP1, while initiation from HSP2 results in transcription of only 2rRNAs and 2 tRNAs. TFAM is responsible for mtDNA transcription, but requires interaction with a POLRMT-TFBM1 or 2 heterodimer to initiate transcription. mTERF is responsible for the termination of transcription from all three initiation sites.

1.4.3 Translation

Mitochondrial translation displays a number of significant differences from the very well-characterised nuclear translation of both eukaryotes and prokaryotes. The most distinctive difference is perhaps the divergence in coding; in mitochondria arginine codons AGG and AGA serve as markers for termination, while UGA codes for tryptophan rather than termination, and AUA codes for methionine as opposed to isoleucine (Osawa *et al.*, 1992). The mRNAs also display some unusual characteristics; they either do not contain a 5' untranslated region or it is very small (Montoya *et al.*, 1981), they are uncapped (Grohmann *et al.*, 1978), and the poly(A)-tail immediately follows or even forms part of the stop codon (Ojala *et al.*, 1981). Also unusual is the translation mechanism itself, using only 22 tRNAs to translate all codons rather than 31 (Barrell *et al.*, 1980).

Mechanistically, mitochondrial translation takes place following the same three steps familiar from nuclear translation –initiation, elongation and termination. Mitochondrial translation factor IF3 initiates the separation of the two subunits – 28S and 39S – of the mitoribosome, before helping correctly orient the mRNA to bind the small subunit of the mitoribosome by placing the AUG start codon adjacent to the peptidyl site (P-site) of the mitoribosome (Liao and Spremulli, 1989). fMet-$tRNA_{Met}$ binds to the 28S small subunit with the aid of mitochondrial translation factor IF2 (Ma and Spremulli, 1996). The two mitoribosome subunits subsequently recombine, causing the dissociation of mtIF3 (Haque *et al.*, 2008), while GTP-hydrolysis of mtIF2 stimulates its dissociation from the complex (Ma and Spremulli, 1996); elongation can now begin.

Elongation factor mtEFTu is the main protein involved with the elongation process; mtEFTu forms a complex with a molecule of GTP and an aminoacylated tRNA, protecting the tRNA from hydrolysis (Nagao and Suzuki, 2007). MtEFTu carries the tRNA to the acceptor site (A-site) of the mitoribosome, where codon-anticodon recognition causes binding of the tRNA; mtEFTu is released as mtEFTu-GDP following the hydrolysis of the GTP molecule in the complex. The 3' end of the aminoacyl-tRA is then moved into the peptidyl transferase centre of the mitoribosome, adding the amino acid carried by the tRNA to the peptide being formed; this reaction is catalysed conformational changes in the mitoribosome induced by mtEFG1. This also causes tRNAs to move along one site within the mitoribosome. After amino transferral, tRNA

leaves the mitoribosome via an exit site allowing a new cycle of elongation to begin (Van Den Heuvel *et al.*, 2010).

Termination of the translation process begins when a stop codon binds to the mitoribosome. The stop codon is recognised by a mitochondrial release factor mtRF1/mtRF1a, causing the protein attached to the last tRNA in the P site to be released by hydrolysis of the ester bond between the tRNA and polypeptide. MtRF1 and mtEFG2 are then responsible for dissociation of all translational components in readiness for a new round of synthesis to begin (Van Den Heuvel *et al.*, 2010).

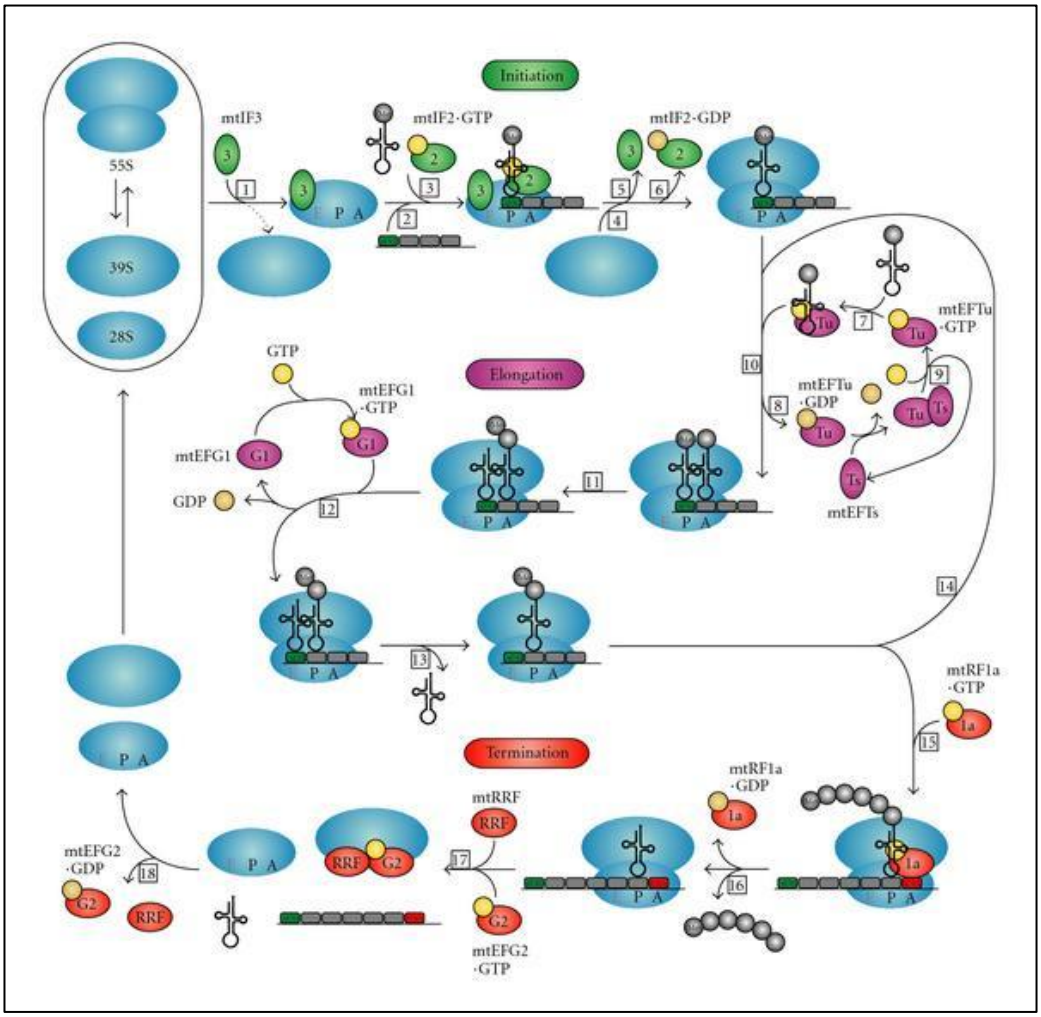

Figure 1.12 - mtDNA translation.

Schematic representation of the three stages of mtDNA translation - initiation, elongation and termination - taken with permission from (Smits *et al.*, 2010).

1.4.4 Replication

Mitochondria use their own unique DNA replication machinery, completely separate from that of the nuclear DNA. Each component of this machinery is encoded by the nuclear DNA, translated in the cytoplasm and transported into the mitochondria across the OMM and IMM (Wanrooij and Falkenberg, 2010). The mitochondrial replication machinery is much simpler than that contained in the nucleus, being much more closely related to the replication machinery of bacteriophages (Shutt and Gray, 2006).

Mitochondrial DNA replication has been shown to occur independently of the cell cycle; this work was originally carried out in mouse L cells, where mtDNA molecules were labelled with ^{3}H-thymidine for two hours prior to incubation with 5-bromodeoxyuridine after varying time periods. The results following mtDNA isolation showed that the mtDNA molecules originally labelled with ^{3}H-thymidine began to incorporate 5-bromodeoxyuridine during replication after only 1.5 – 2 hours, demonstrating that replication of the mtDNA continues to occur throughout the cell cycle (Bogenhagen and Clayton, 1977).

Mitochondrial DNA replication is carried out by a single DNA polymerase, POLγ. *In vitro* construction of the mitochondrial replication machinery requires only five proteins: the DNA polymerase gamma catalytic subunit (POLγA) and processivity subunit (POLγB), the DNA helicase TWINKLE, mitochondrial single-stranded DNA-binding protein (mtSSB), and mitochondrial RNA polymerase (POLRMT) (Gray and Tai Wai, 1992). POLRMT is required to initiate replication of the mtDNA, which it does by providing a primer at the origin sites. Following this initiation step, mtSSB stimulates the helicase activity of TWINKLE, allowing the enzyme to unwind short sections of double stranded DNA in a 5’-3’ direction. POLγ and TWINKLE together form the main body of the replication machinery, which is capable of using double-stranded DNA to synthesise DNA molecules of around 2kb in length. MtSSB also stimulates greater exonuclease activity from POLγ, allowing the generation of full mitochondrial genome length products (Falkenberg *et al.*, 2007). At the observed replication rate of 180 base pairs per minute, a genome would be replicated in ~90 minutes (Korhonen *et al.*, 2004).

Although the mitochondrial replication machinery has been well characterised, the mechanism by which replication occurs is still highly debated. Two main models have been proposed to characterise mitochondrial DNA replication; the strand a-synchronous replication model (Robberso.Dl and Clayton, 1972; Clayton, 1982), and the coupled leading-lagging strand DNA replication model (Holt *et al.*, 2000).

1.4.4.1 Strand asynchronous model of mtDNA replication

The strand a-synchronous model of replication, also known as the strand displacement model, was considered to be the method of mtDNA replication for decades after being originally put forward in 1972. This model, based upon the visualisation of replicating mtDNA molecules by electron microscopy, proposes that the leading and lagging strands are synthesised asynchronously from their respective origins O_H and O_L (Clayton, 1982), in a manner similar to plasmid replication (Masukata and Tomizawa, 1990). According to this model, mtDNA replication begins at O_H in the only large non-coding region of the mitochondrial genome, and proceeds uni-directionally in a clockwise manner (SEE FIGURE). Replication of the heavy strand of the mtDNA progresses until O_L is exposed on the heavy strand, allowing light strand replication to be initiated in the opposite direction. Both strands of replication are continuous, proceeding to completion of two daughter mtDNA molecules; these molecules are closed to form circular molecules, and undergo dissociation to form two distinct new copies of the genome. This model is characterised by a lack of short Okazaki lagging strand fragments, and the presence of single strand regions in all replicating mtDNA molecules (Clayton, 1982).

1.4.4.2 Coupled leading-lagging strand model of mtDNA replication

The long-held acceptance of the strand asynchronous model of mtDNA replication was challenged in 2000 by the emergence of a new model put forward by Holt, Lorimer and Jacobs (Holt *et al.*, 2000). As opposed to the microscopy techniques used in the development of the strand asynchronous model, the new coupled leading-lagging strand model was proposed based upon replication studies using neutral/neutral 2D agarose gel electrophoresis (2D-NAGE). 2D-NAGE is used to separate DNA molecules

based upon both size and shape, and as such is a useful method by which to analyse the quantity and structure of replication intermediates (Brewer and Fangman, 1987; Brewer and Fangman, 1988). 2D-NAGE was used to compare replication intermediates from two distinct scenarios; cultured human cells undergoing mtDNA amplification due to induced mtDNA depletion, and human cells undergoing low levels of mtDNA synthesis to maintain mtDNA copy number. Interestingly, different types of replication intermediates were observed in these two cell types; this implies that there is more than one mode of mtDNA replication which can occur in different cell conditions. Partially single-stranded replication intermediates were observed where DNA synthesis was exclusively responsible for mtDNA maintenance, in keeping with Clayton's asynchronous strand replication model, but where large levels of mtDNA amplification was necessary the replication intermediates observed were double stranded. These double-stranded intermediates were proposed to be the product of leading-lagging strand replication, suggesting that amplification of high levels of mtDNA are carried out by a similar mode of replication to that of nuclear DNA (Holt *et al.*, 2000).

As in the asynchronous model of replication, DNA synthesis is believed to be initiated at O_H in coupled strand mtDNA replication. Again, the synthesis of the leading strand proceeds in a clockwise direction around the genome. Shortly after synthesis of the heavy strand begins, replication of the light lagging strand begins in the opposite direction. Short sections of the light strand known as Okazaki fragments are generated as sections of the heavy strand become displaced – these fragments must be ligated to form a complete DNA strand. Two daughter molecules are produced by this method of replication, but as light strand synthesis begins much closer to the initiation of heavy strand synthesis than in asynchronous replication, all observed replication intermediates are double stranded (Holt *et al.*, 2000).

Additional to the coupled strand replication model, it has since been proposed that the lagging strand fragments generated during replication are initially composed of RNA – this is known as the RITOLS model (RNA incorporation throughout the lagging strand) (Yasukawa *et al.*, 2006). These RNA intermediates are later converted to DNA, starting at defined loci including the OL. This model is based upon 2D-NAGE evidence that mtDNA replication intermediates often contain RNA as well as DNA. The RITOLS model

is in all other ways consistent with the coupled strand model of replication (Yasukawa *et al.*, 2006).

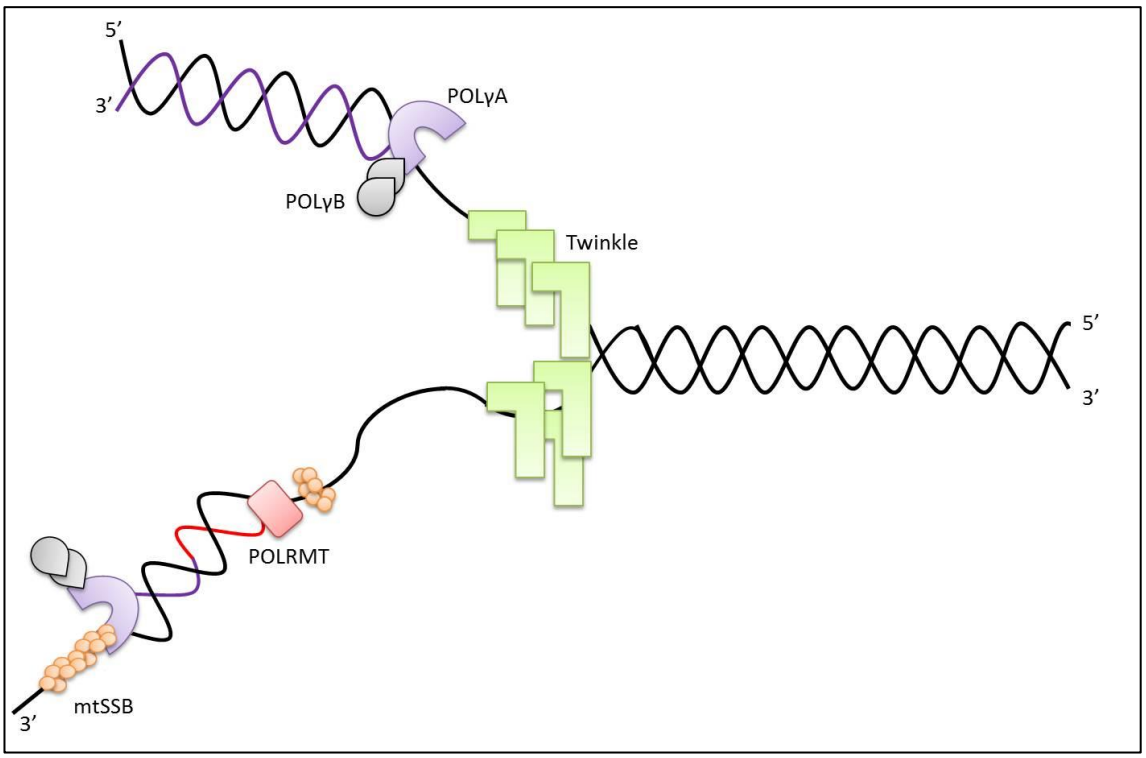

Figure 1.13 - mtDNA replication machinery.

The mtDNA replication machinery is made up of five proteins; the DNA polymerase gamma catalytic subunit (POLγA) and processivity subunit (POLγB), the DNA helicase TWINKLE, mitochondrial single-stranded DNA-binding protein (mtSSB), and mitochondrial RNA polymerase (POLRMT). POLRMT initiates replication, while mtSSB stimulates the helicase activity of TWINKLE, allowing the enzyme to unwind short sections of double stranded DNA in a 5'-3' direction. POLγ and TWINKLE together form the main body of the replication machinery, which uses double stranded DNA as a template to synthesise daughter DNA.

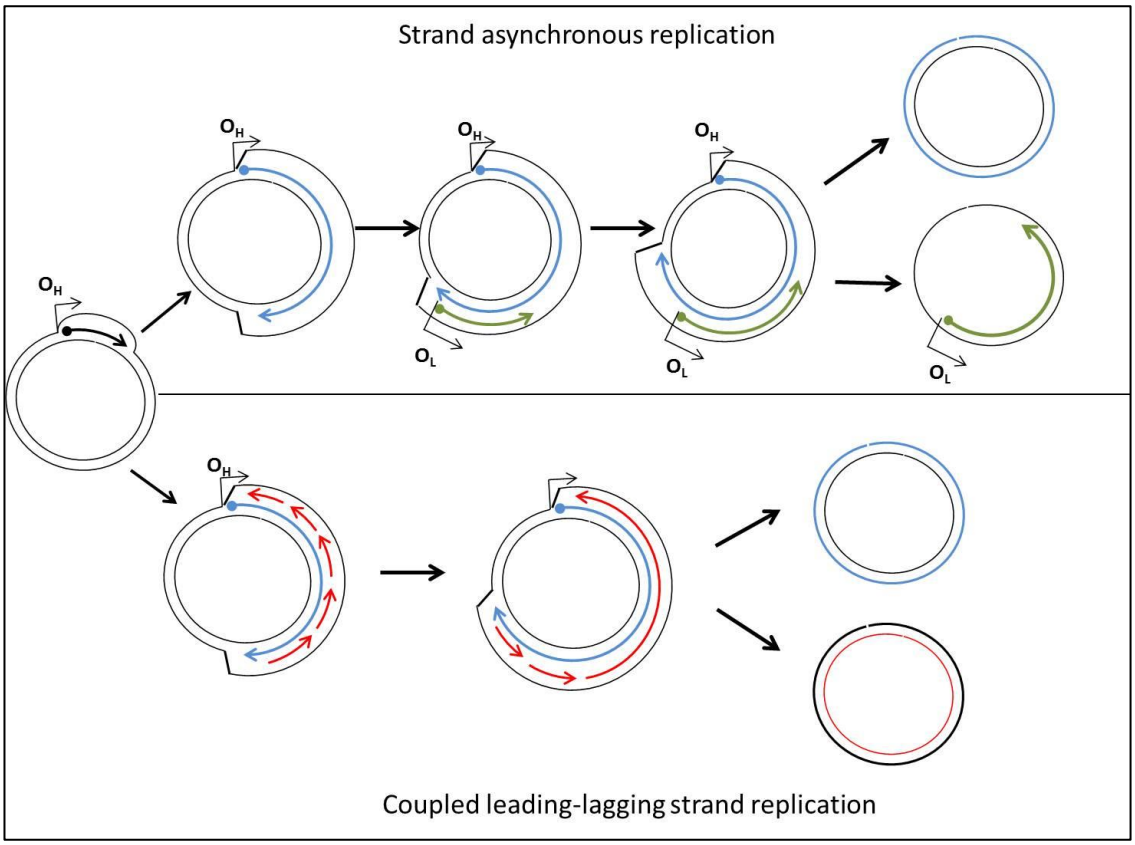

Figure 1.14 – Two proposed mtDNA replication models.

Both proposed models of mtDNA replication begin with strand displacement of the mtDNA beginning at the origin of heavy strand replication (O_H), but the models diverge from this point.

a) Strand asynchronous replication

Replication begins at the O_H, proceeding until the origin of light chain replication, O_L, is exposed. From this point, replication commences in the other direction, with replication of both strands continuing to completion.

b) Coupled leading-lagging strand replication

Replication also begins from O_H, but replication of the light strand begins soon after this initiation event. Sections of the light strand known as Okazaki fragments are generated as sections of the heavy strand become displaced – these fragments must be ligated to form a complete DNA strand.

1.4.5 Mitochondrial DNA Repair

Mitochondria were long believed to have no mechanism of DNA repair, following evidence presented in 1974 that no pyrimidine dimer repair mechanism existed in mammalian mitochondria (Clayton *et al.*, 1974). However, later worked showed that mitochondria were indeed capable of repairing some types of DNA damage, despite having no mechanism for the removal of large DNA lesions (Bogenhagen, 1999). The first evidence of mtDNA repair was put forward in 1991, showing that DNA lesions formed by exposure to an alkylating antibiotic, streptozotocin (Pettepher et al., 1991). Soon after this, a study carried out in Chinese hamster ovary cells compared repair of a variety of DNA lesions in nuclear and mitochondrial DNA, conclusively showing that the capacity for repair of mtDNA is lesion type dependant (LeDoux *et al.*, 1992). As well as being lesion-specific, mtDNA repair also seems to be cell type dependant, being much less effective in certain cell types such as glia and neurons (LeDoux *et al.*, 1999).

Base excision repair (BER) has been confirmed to occur in mitochondria in a very similar fashion to BER in the nucleus, to repair alkylation and oxidative DNA lesions, although the mitochondria do have BER machinery independent to that of the nucleus. Most importantly, BER is used to repair damage caused by reactive oxygen species (ROS), including 8-oxoguanine (8-oxoG) and thymine glycol (TG) lesions. BER is initiated by DNA glycosylases, which recognises and removes the damaged base by cleaving the N-glycolytic bond, leaving behind an abasic (AP) site. The lysate activity of the glycosylase then creates a single strand break 3' to the AP site, and an apurinic or apyramidic endonuclease cleaves the phosphodiester backbone of the DNA 5' to the AP site; together these activities cause excision of the single baseless sugar, creating a gap in the DNA. POLγ is recruited to fill the space left by the base excision mechanism, before the final step of repair – the ligation of the new base into the DNA by DNA ligase III – is carried out. (Bohr, 2002).

While BER is now relatively well characterised in mitochondria, other repair mechanisms are still undergoing study. Mismatch repair has been clearly identified in yeast (Reenan and Kolodner, 1992), but has yet to be identified in eukaryotic cells. The ability of mitochondria to repair mtDNA cross-linking by recombinational repair is an area of heated debate, with much contradictory evidence having been put forward regarding its existence. Recombination intermediates thought to be formed by

homologous recombination have been identified in Kearns-Sayre syndrome (KSS) and chronic external ophthalmoplegia (CPEO) patients (Poulton *et al.*, 1993) and *in vitro* studies have provided some evidence for the presence of homologous recombination activity in mammalian mitochondrial extracts (Thyagarajan *et al.*, 1996). However, no evidence of homologous recombination has been found in cell lines taken from patients with KSS or CPEO, where homologous recombination is thought to occur (Poulton *et al.*, 1993). Finally, while it has been conclusively shown that no nucleotide excision repair (NER) occurs to remove UV-induced pyrimidine dimers from mtDNA (Clayton *et al.*, 1974), evidence has emerged to support the involvement of NER in removing 4NQO (Snyderwine and Bohr, 1992) and possibly interstrand (but not intrastrand) cisplatin adducts (LeDoux *et al.*, 1992).

1.5 mtDNA Mutations

The mitochondrial genome is known to be very prone to mutagenesis, with a mutation rate approximately ten times that of nuclear DNA (Brown *et al.*, 1979). This high mutation rate can be contributed to a combination of factors, but is often primarily associated with the close proximity of mtDNA and the respiratory complexes within the mitochondria. mtDNA is therefore highly exposed to reactive oxygen species (ROS) such as superoxide (O_2^-) produced during OXPHOS, which are highly mutagenic. The high level of ROS exposure is made more problematic by the lack of protective histones in mtDNA – the naked DNA is much more susceptible to mutation.

A secondary probable cause of the high mutation rate of mtDNA is the accuracy of the mitochondrial DNA polymerase – POLγ is has been shown to have a much lower level of accuracy than its nuclear counterpart polymerase α (Kunkel and Loeb, 1981). This issue of lower polymerase fidelity is compounded by a high rate of turnover of mtDNA compared to nuclear DNA (Rabinowi.M and Swift, 1970).

The issues associated with a high mutation rate are exacerbated by the gene-dense nature of the mtDNA (as discussed in section *1.4.1*), which means that any mtDNA mutation is highly likely to occur within a coding region of the genome and so has a high probability of becoming pathogenic.

1.5.1 Point mutations

Point mutations in DNA are the substitution of one base pair for another in the genetic code. Point mutations in tRNA genes are the most common mitochondrial defects, with over 50% of mitochondrial disease cases with a known genetic defect accounted for by this mutation type (Schaefer *et al.*, 2008). Point mutations in mtDNA can be harmless or pathogenic, depending upon where in a three-base amino acid codon they fall; if an amino acid change is caused – known as a non-synonymous base change - downstream disruption in the production of the gene's encoded protein is caused, and the mutation becomes pathogenic. Non-pathogenic point mutations occur in unconserved base positions – if no gene disruption is caused by the base change, no further effects are caused by the point mutation – known as a synonymous base change. Due to the complexity of determining how a point mutation will affect the protein product of the gene that the mutation has arisen in, scoring systems have been proposed to determine the likely pathogenicity of newly discovered point mutations, to aid in diagnosis of mitochondrial disease and predicting patient outcome (Montoya *et al.*, 2009; Yarham *et al.*, 2012).

Pathogenic point mutations are known to cause mitochondrial encephalomyopathy, lactic acidosis and stroke-like episodes (MELAS), myoclonic epilepsy with ragged-red fibres (MERRF), Leigh syndrome, and Leber's hereditary optic neuropathy (LHON) (Wu *et al.*, 2010). The first identified pathogenic point mutation was the m.11778G>A modification – this base change in codon 340 in the ND4 gene changes a highly conserved amino acid (converting an arginine to a histidine), and was associated with LHON. This finding, as well as demonstrating that mtDNA mutations could be pathogenic, created a Diagnostic test for LHON, as the m.11778G>A mutation knocks out an Sfa NI restriction site (Wallace *et al.*, 1988).

The most common, and hence best characterised point mutations are the 8344 A to G substitution in the $tRNA^{Lys}$ gene, and the 3243 A to G substitution in the $tRNA^{Leu}$ gene in the mitochondrial genome – which has been estimated to have a carrier rate of 1 in 400 in the general population (Manwaring *et al.*, 2007). The m.8344A>G point mutation is known to cause 80 -90% of all known cases of MERRF, a mitochondrial disease characterised by muscle weakness and exercise intolerance, myoclonic twitches, cerebellar ataxia, heart conduction block, deafness and dementia (Wu *et al.*,

2010). Studies conducted in skin fibroblasts have shown a strong correlation between m.8344A>G and reduced function of Complex I and IV of the OXPHOS chain, meaning a much lower ATP-production in individuals with this mutation and hence organ dysfunction where tissues have a high energy demand (James *et al.*, 1996). More recent studies have shown, by microarray comparison of DNA expression in MERRF patients and age matched controls, the up-regulation of ~350 genes and the down-regulation of ~300 more in MERRF patients (Ma *et al.*, 2005).

The m.3243A>G transition is the mutation most commonly associated with MELAS, accounting for ~80% of all MELAS cases (Urata *et al.*, 2004), though patients with this mutation can present at different ages with an array of phenotypes ranging from MELAS to other multisystem syndromes (maternally inherited deafness and diabetes (MIDD), progressive external ophthalmoplegia (PEO), and Leigh syndrome) or isolated symptoms such as myopathy, cardiomyopathy, seizures, migraine, ataxia, cognitive impairment, bowel dysmotility or short stature. (Manwaring *et al.*, 2007; Nesbitt *et al.*, 2013). It is thought that severity of disease presentation with the m.3243A>G point mutation is dependent upon heteroplasmy levels – the highest percentages of mutation causing the most severe disease phenotypes, and vice versa (Koga *et al.*, 2000).

Point mutations, as well as being inherited, occur naturally within the cell with progressing age. A fibroblast study found high copy numbers of point mutations are in the control region (D-loop) of mtDNA in older individuals, with some high copy number point mutations not present at all in younger individuals, even at low level. Of particular interest was the study of the T414G transversion, present in no younger individuals, but with a heteroplasmy level of over 50% in 8/14 aging controls over 65 years of age (Michikawa *et al.*, 1999).

1.5.2 Large-scale Duplications

Large-scale duplications have been found to occur in mtDNA but there is some uncertainty over their pathogenicity. Duplications have been identified in some cases of sporadic Kearns-Sayre syndrome (KSS), though not as frequently as mtDNA deletions. KSS is a mitochondrial disease with an age of onset below 20, with a

presentation of chronic progressive external ophthalmoplegia (CPEO) and pigmentary retinopathy, with additional symptoms including cerebellar ataxia, cardiac conduction block hearing loss, endocrinopathies, muscle weakness and renal tube dysfunction. Duplicated mtDNA molecules can be found in tandem with deleted molecules, and these are structurally related (i.e. the duplicated mtDNA could be viewed as a wild-type mtDNA molecule into which a deleted mtDNA genome has been inserted). It is possible that a sizable number of KSS patients thought only to have mtDNA deletion may contain the equivalent duplicated mtDNA also, as duplications are detectable only by Southern blot and PCR specifically designed to amplify a duplication and these are not routine tests. (Schon *et al.*, 1997)

It is not currently clear whether duplications are pathogenic as no genes are missing in mtDNA molecules with duplicated sections, though it is possible that by duplicating only some genes, unbalanced levels of tRNA could affect turnover or translation as a whole. Alternatively, the expression of a fusion gene created by insertion of a duplicated section of the mitochondrial genome could be included into the respiratory complexes, having a detrimental effect on OXPHOS function. (Schon *et al.*, 1997)

Duplications have also been proposed to exist as an intermediate step in the formation of mtDNA deletions (Poulton *et al.*, 1993). This hypothesis was proposed following a molecular study carried out on three patients with KSS and diabetes mellitus or hypoparathyroidism who had previously been identified as carrying identified mtDNA duplications. Upon investigation, four mtDNA types were found to be present in each of these patients; one of these represents the wildtype DNA, while the remaining three were rearranged mtDNA forms. Of these three rearrangements, a large molecule was identified as carrying the previously characterised duplication in each patient, while two other molecule types represented an mtDNA deletion monomer and dimer. In each case, the deletion breakpoints were found to correspond to the junction regions of the duplication. In muscle sections taken ten years apart, a noticeable drop in duplication levels and rise in deletion monomer and dimer levels was found; this final piece of evidence led to the proposal that the two deletion rearrangement types arose from an original duplication rearrangement (Poulton *et al.*, 1993).

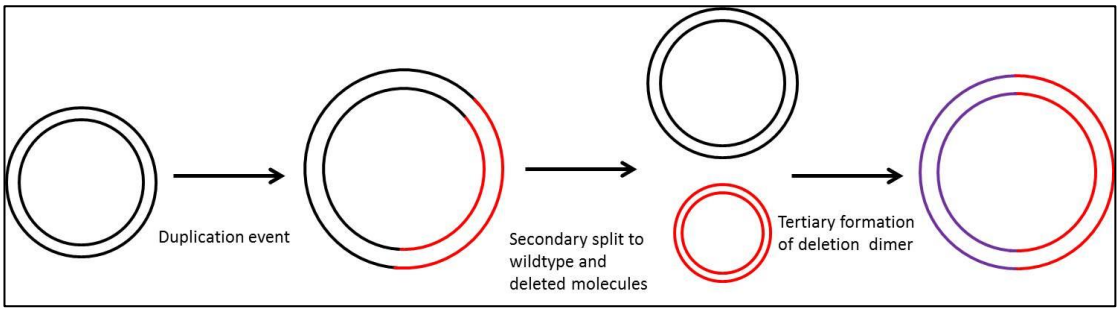

Figure 1.15 - Mitochondrial DNA duplications as a precursor to mtDNA deletions and further rearrangements.

A molecular study carried out on three mitochondrial disease patients, each carrying four mtDNA types - one representing the wildtype DNA, and three rearranged mtDNA forms comprised of an mtDNA duplication as well as a deletion monomer and dimer – found that in each patient the deletion breakpoints were found to correspond to the junction regions of the duplication. This led to the proposal that mtDNA duplications exist as a precursor to mtDNA deletions and further rearrangements, following the scheme depicted above.

1.5.3 Large-scale Deletions

Large-scale deletions occur when a portion of the mitochondrial genome is lost, causing the loss of protein-encoding genes. These re-arrangements have been documented to be disease causing for many years, with the first evidence of mtDNA deletion pathogenicity coming to light in 1988 (Holt *et al.*, 1988). Deletions most often occur within the major arc of the mitochondrial genome, between the light and heavy strand origins of replication and are usually - in approximately 85% of cases - flanked by short repeat regions (Bua *et al.*, 2006) (Samuels *et al.*, 2004). The highest levels of mtDNA deletions are often seen in post-mitotic tissues, including neurons and muscle fibres, in cases of mitochondrial disease and in aging individuals (Wang *et al.*, 1997); this accounts for the predominant neuromuscular symptoms of mitochondrial disease, and the onset of sarcopenia and neurodegeneration with progressing age. The size of mtDNA deletions, occurrence of repeat regions and length of repeats appears to be unrelated to disease type, with no significant differences found between neurons from individuals with Parkinson's disease or multiple mtDNA deletion disorders, or indeed from aging brain, suggesting the same mechanism for mtDNA deletion formation occurs in all cases (Reeve *et al.*, 2008a).

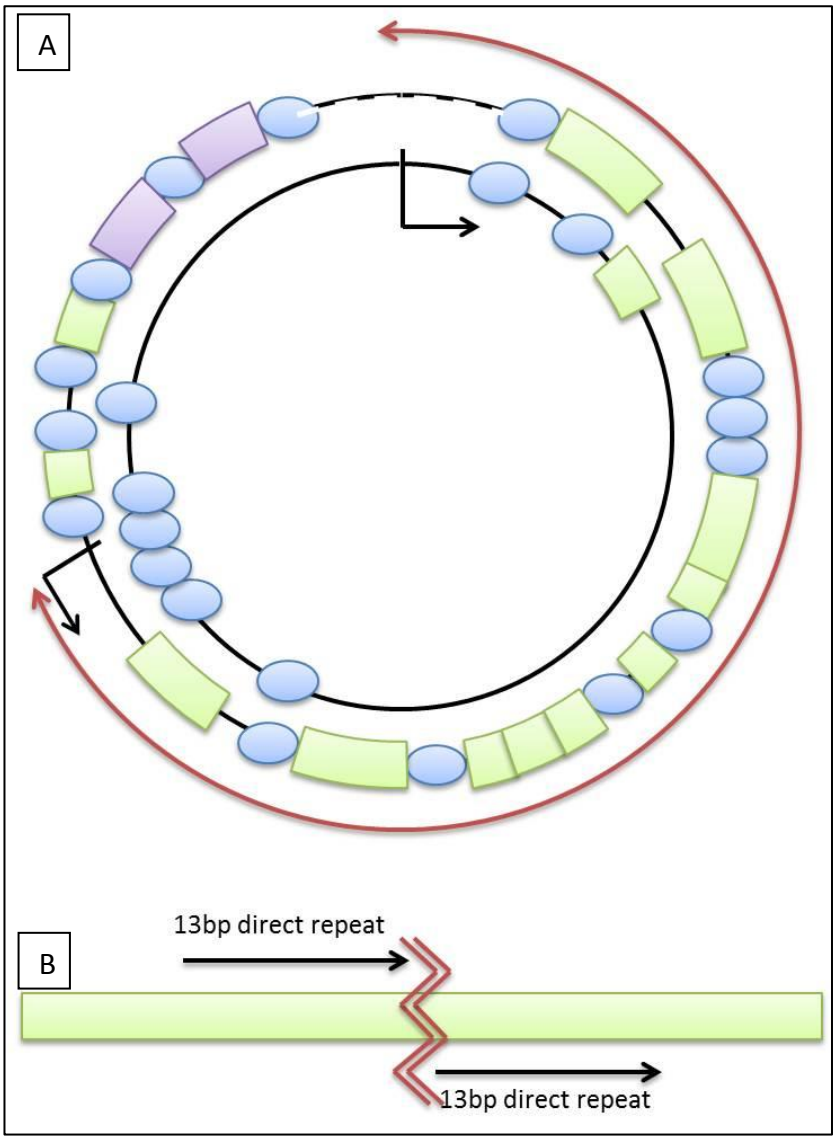

Figure 1.16 - Location of mtDNA deletions within the mitochondrial genome.

The majority of mtDNA deletions have been found to lie within the so-called 'major arc' of the mitochondrial genome, between the heavy and light strand origins of replication as depicted above (A). Example B depicts the 13bp direct repeat, typical of the 4977bp common deletion.

1.5.4 Mitochondrial DNA Deletions, Disease and Aging

Large-scale deletions within mitochondrial DNA are a primary cause of mitochondrial disease, accounting for ~18% of all mitochondrial disease cases (Schaefer *et al.*, 2008). However, the group of patients presenting with mitochondrial disease caused by mtDNA deletions is highly heterogeneous; mtDNA deletion patients display a large spectrum of phenotypes and disease severities, but can broadly be separated into two major categories. One group of patients present with sporadic single mtDNA deletions; in these cases, a single mitochondrial DNA deletion is present in all affected cells throughout the tissues of a patient causing a disease phenotype (Schaefer *et al.*, 2008). A second group of patients present with multiple mtDNA deletions, due to a primary defect in a nuclear gene involved in mtDNA maintenance. Nuclear genes involved in mtDNA maintenance include those for mitochondrial DNA replication and repair, or mitochondrial nucleotide metabolism; a prime example of this is seen in patients with defects in the POLG or POLG2 nuclear genes, which encode the single mitochondrial polymerase used in mtDNA replication (Hudson and Chinnery, 2006). In this patient group, multiple mtDNA deletions are seen in all affected cells, particularly in the post-mitotic muscle and CNS system tissues.

Patients presenting with multiple mtDNA deletions often present with CPEO, while sporadic single mtDNA deletions are primarily responsible for KSS (as outlined for duplications), CPEO and Pearson's syndrome, an early-onset disorder presenting with pancreatic dysfunction and anaemia (Schon *et al.*, 1997). Few patients survive Pearson's syndrome; those who do go on to develop KSS (McShane *et al.*, 1991). With a high enough level of heteroplasmy, mtDNA deletions can go on to be responsible for two scenarios in which the cell's respiratory function is altered. The deleted region itself may be the cause of the mutant cellular phenotype (i.e. too few copies of a protein-encoding gene may prevent one of the respiratory complexes being formed correctly), or alternatively none of the polypeptide-encoding mRNAs may be translated if an essential tRNA gene is located within the deleted genome region. (Nakase *et al.*, 1990b; Hayashi *et al.*, 1991).

MtDNA deletions are found in aged post-mitotic tissues in normal ageing and in patients with neurodegenerative diseases as well as in cases of mitochondrial disease, however the mtDNA deletion levels are often much lower (Bender *et al.*, 2006;

Kraytsberg *et al.*, 2006). Until a 2006 study of the substantia nigra, mtDNA deletions identified in aging and neurodegeneration were only detected at low levels, and certainly not approaching a heteroplasmy threshold level that could cause clinical significance (Cortopassi and Arnheim, 1990). However, two independent studies carried out in 2006 shed new light on the accumulation of mtDNA deletions in aging.

In one study, carried out by Bender *et al,* COX-normal neurons of patients with Parkinson disease and age matched controls were found to contain high levels of mtDNA deletions (an average of 52.3% and 43.3% respectively). As a comparison, COX-normal neurons of the hippocampus from the same experimental subjects were investigated, but similarly high levels of mtDNA deletion were not found (17.8% and 14.3% respectively) (Bender *et al.*, 2006). In substantia nigra COX-deficient neurons of aged controls, the mutation load was measured at 66.9% (compared to 47.7% in normal neurons), demonstrating that the COX-deficiency is due to increased mtDNA deletion levels. The results of this study led the authors to propose that high levels of neuronal loss in the substantia nigra with age (Fearnley and Lees, 1991) are due to the levels of deleted mtDNA within the neurons – this being much higher than in other investigated areas of the brain – and the resultant respiratory deficiency (Bender *et al.*, 2006).

A similar study carried out independently by Kraytsberg *et al* in Boston showed very similar results to those obtained by Bender *et al*, confirming a high level of mtDNA deletion in neurons of the substantia nigra (Kraytsberg *et al.*, 2006). These observations of high mtDNA deletion levels in substantia nigra neurons were very much in keeping with a previous study carried out in 2004 by Trifunovic *et al*, where real-time PCR investigations revealed a linear increase of mtDNA deletion levels in the substantia nigra with age, in a similar manner to increasing mutation load over time in an animal model of aging (Trifunovic *et al.*, 2004). This has led to speculation that, as well as respiratory dysfunction, the accumulation of mitochondrial DNA deletions may influence cell loss, primarily of muscle fibres, and neurons from the substantia nigra (Bender *et al.*, 2006; Herbst *et al.*, 2007).

Fibre loss can be as pronounced in muscle as neuronal loss in the substantia nigra with age - loss of muscle fibres and fibre atrophy are major contributing factors to the loss of muscle seen in aging adults and in sarcopenia (Evans, 1997), while muscle weakness

and atrophy are major clinical features seen in mitochondrial disease. MtDNA deletions were strongly linked to fibre loss by single fibre analysis in a study of aged rat muscle, comparing mitochondrial genotype to cellular phenotype (Herbst *et al.*, 2007). COX-deficient fibre areas were identified by histochemistry, with a selection of fibres containing respiratory abnormal areas being shown to display normal morphology, atrophy or fibre splitting. Subsequent analysis of mtDNA by breakpoint and real-time PCR analysis of mtDNA deletion level in multiple areas of each fibre showed the broken ends of atrophic fibres to have the highest measured levels of mtDNA deletions, $3x10^5$ mutant genomes, with a strong COX-deficient phenotype (Herbst *et al.*, 2007). Also, even in areas where fibre splitting did not overlap with COX-deficiency in fibres, deletion levels were higher in split fibre areas - though not high enough to cause COX-deficiency. It is postulated that fibre splitting may be a precursor to fibre atrophy as mtDNA deletion levels rise (Herbst *et al.*, 2007). In conjunction with previous studies showing 25% of COX-deficient fibres to be associated with fibre atrophy and 7% with fibre breakage (Wanagat *et al.*, 2001), these results implicate expansion of mtDNA deletions as the cause of fibre dysfunction and atrophy.

1.5.5 Common mtDNA deletions

In the majority of cases, the breakpoints of the mtDNA deletions found to be disease-causing in single mtDNA deletion patients are unique to each patient; however, there are exceptions to this trend. There are two mtDNA deletion types seen relatively often, the most prominent being the 4977bp 'common deletion' which removes 6 protein encoding genes and five genes for tRNAs between nucleotides 8470 and 13447, with 13bp sequence repeats on either side of the breakpoint. The common deletion is estimated to occur in ~25% of single mtDNA deletion patients, and ~33% of KSS patients, as well as commonly accumulating with age (Taylor, 2005). Another commonly occurring mutation often found in CPEO and KSS patients is the larger 7435bp deletion, which occurs between nucleotides 8649 and 16084 of the mitochondrial genome removing genes from ATPase6 to tRNA proline (Taylor 2005).

1.5.6 Mitochondrial DNA Deletion Formation

Mitochondrial DNA deletions are very well characterised in terms of deletion location and pathogenicity, but the mechanism by which these deletions arise is still unknown. Two main methods have been proposed to be involved in the formation of mtDNA deletions, with replication being the most long-standing and widely accepted hypothetical model. The 'slipped-strand' replication mechanism of mtDNA deletion formation relies upon replication occurring by a strand-asynchronous mechanism (see *1.4.4.1*), with a slipped strand between two direct repeats during replication causing the loss of a large section of the genome (Shoffner *et al.*, 1989). If strand slippage were to occur between two direct repeats, the displaced single stranded light strand DNA could misalign so that the 3' repeat of the light strand would anneal to the 5' repeat of the heavy strand. This would cause a single stranded loop to form downstream in the light chain, susceptible to strand breaks and so damaged and degraded, forming the mtDNA deletion in the light strand. Replication continues from here, creating a mtDNA wildtype molecule from the undamaged heavy chain and a deleted mtDNA molecule type from the light chain, where part of the genome was degraded during replication (Shoffner *et al.*, 1989).

Concerns have been raised about the replicative mechanism for mtDNA deletion formation, such as the need for mtDNA to be replicating at the point that the 3' and 5' repeats anneal to form a single strand loop that can be degraded (Krishnan *et al.*, 2008). However, the biggest question mark left hanging over the replicative mechanism is mitochondrial turnover; in both diseased tissue and aged controls, some of the highest mtDNA deletions levels are seen in post-mitotic tissues such as muscle and the CNS where the rate of turnover is thought to be very low (Wang *et al.*, 1997). If deletions do occur during replication, it would be expected that mtDNA deletion levels would be higher in cells with a rapid mitochondrial turnover where there would be a greater chance of an mtDNA deletion occurring. A study to this effect was carried out on human colonic tissue, but though no suggestion was found of selection against deleted mtDNA molecules in these rapidly dividing cells, no deleted molecules have been detected in this tissue (Taylor *et al.*, 2003). The high turnover of mitochondria in these cells with no evidence of deleted mtDNA molecules, and the high mtDNA deletion levels in post-mitotic tissue, would suggest that a mechanism other than

replication may be responsible for the formation of mtDNA deletions in human tissues (Krishnan *et al.*, 2008).

Such a mechanism was proposed by Krishnan *et al* in 2008, suggesting that mtDNA deletions may be formed during repair of damaged mtDNA molecules. This mechanism proposes that double stranded breaks occurring between direct repeats are responsible for mtDNA deletion generation; the DNA on either side of the break is susceptible to 3' to 5' exonuclease activity, creating single stranded DNA on either side of the break (Krishnan *et al.*, 2008). The single strands then anneal, the 3' repeat on one strand annealing to the 5' repeat of the other strand; the unbound single strands are then degraded, leaving an mtDNA molecule with a large deletion (Haber, 2000).

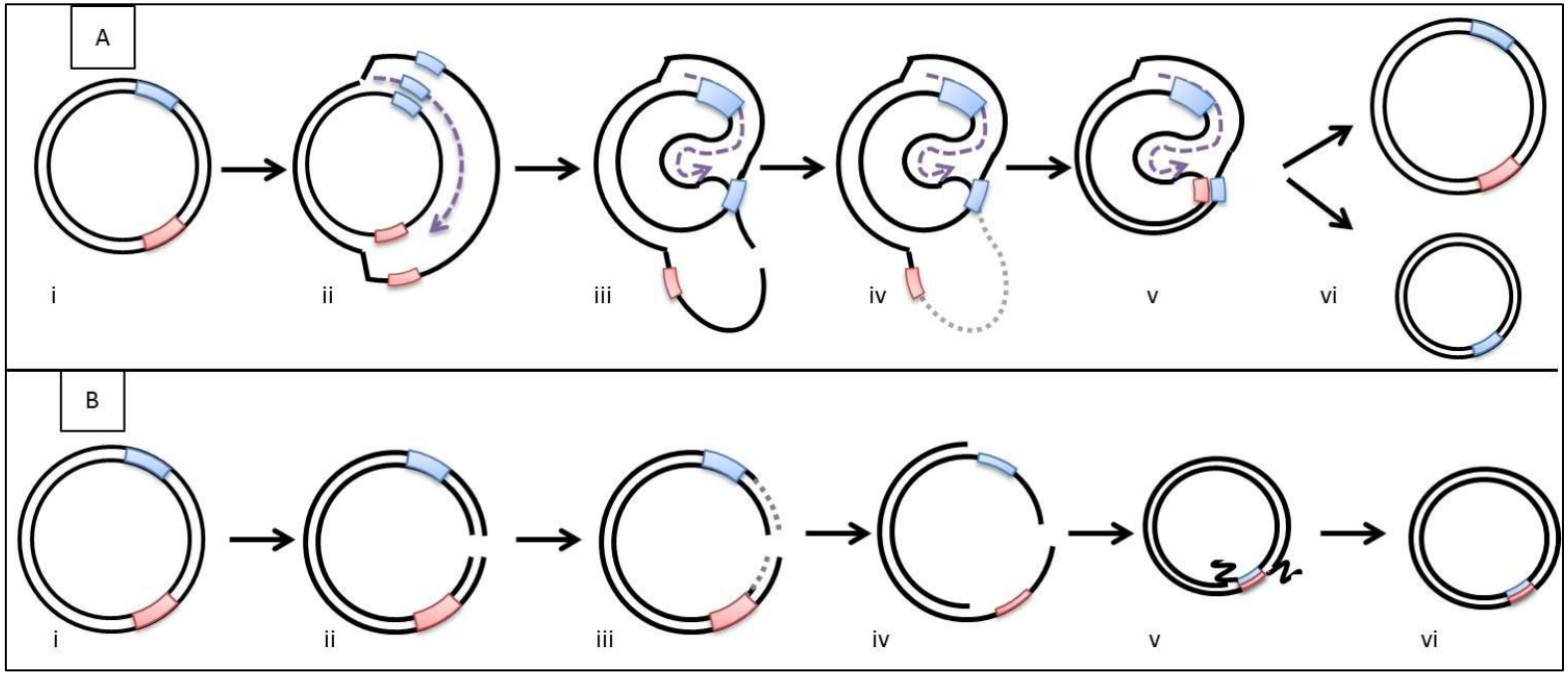

Figure 1.17 - mtDNA deletion formation by replication or repair.

A) Deletion formation by slipped-strand replication. This mechanism relies upon replication occurring by a strand-asynchronous mechanism (ii). If strand slippage were to occur between two direct repeats (indicated as pink and blue regions), the displaced light strand DNA could misalign so that the 3' repeat of the light strand would anneal to the 5' repeat of the heavy strand (iii). This would cause a single stranded loop to form downstream in the light chain, susceptible to strand breaks, damage and degradation (iii – iv), forming the mtDNA deletion in the light strand (v). This would lead to the production of 2 distinct daughter molecules – one wildtype and one deleted mtDNA species (vi).

B) Deletion formation during double-strand break (DSB) repair. When a DSB occurs (ii), the exposed 3' and 5' ends of the break are susceptible to exonuclease activity, forming single-stranded DNA on each side of the break (iii). If a DSB occurs between direct repeats (indicated as pink and blue regions), and the newly-formed single strands anneal (v), unbound single stranded DNA may be degraded leaving only an mtDNA molecule with a deletion (vi).

1.6 Mitochondrial DNA copy number

1.6.1 Copy number regulation

Studies of mouse and of human cells *in vitro* have shown that most cells contain 1000 – 5000 copies of the mitochondrial genome; this number is made up from the multiple copies of mtDNA in each of the hundreds of mitochondria present in most cell types (Bogenhagen and Clayton, 1974; Shmookler Reis and Goldstein, 1983). Interestingly, control of mtDNA copy number seems to be regulated by total mtDNA mass within the cell rather than genome copy, as first proposed by Tang *et al* in 2000 (Tang *et al.*, 2000a). This group carried out an analysis of mtDNA copy number in cybrids created by the fusion of ρ^0 cells (human cells lacking in mtDNA) and cytoplasts derived from KSS patient fibroblasts with 10% duplicated mtDNA, 20% deleted mtDNA and 70% wild type mtDNA. 27 resultant clones contained a mixture of wild type and rearranged mtDNA; ethidium bromide treatment was used to generate 3 cell lines which were homoplasmic for wild type mtDNA, deleted mtDNA or duplicated mtDNA. The mtDNA mass was found to be identical in each of these three cell lines, despite the presence of different numbers of replication origins and large variances in genome size in each cell line (Tang *et al.*, 2000a).

Though it seems clear from this evidence that mtDNA regulation occurs via control of total mtDNA mass, the actual mechanism for mtDNA copy number regulation remains unknown. Following their discovery that a constant total mtDNA mass seems to be maintained within the cell, rather than a specific number of mtDNA copies, Tang *et al* hypothesised that copy number may be regulated by controlling the size of the mitochondrial dNTP pools (Tang *et al.*, 2000a). However, a number of other hypotheses have also been proposed to explain mtDNA copy number regulation (Clay Montier *et al.*, 2009). These proposed mechanisms include regulation of mtDNA copy number by number of replication origins, where genomes with multiple replication origins are preferentially amplified regardless of molecule size (Tang *et al.*, 2000b); TFAM mediated copy number control, where the mode of mtDNA replication can be influenced by TFAM to change mtDNA copy number, as evidenced by mtDNA depletion in instances of TFAM knockdown (Pohjoismaki *et al.*, 2006). Although no data has been put forward to support this model, another widely accepted model is that the current

ATP requirements of a cell can influence the mtDNA copy number (Clay Montier *et al.*, 2009).

1.6.2 Mitochondrial DNA Heteroplasmy, Homoplasmy and Threshold

Due to the multi-copy nature of mtDNA in all cells with mitochondria, the mtDNA is able to exist in a number of states with regards to the presence of mutations. In healthy cells which harbour no mtDNA mutations, the mitochondrial DNA exists in a state where each copy is wildtype –each mtDNA molecule is therefore identical, and this state is known as homoplasmy. When mutations of the mtDNA do occur, if the mutation affects each copy of the genome within the cell, this too is known as homoplasmy – so a cell can be wildtype homoplasmic (0% mutation level) or mutant homoplasmic (100% mutation level). If a mutation co-exists within a cell with copies of wildtype DNA – as was observed with the first finding of a mitochondrial DNA mutation (Holt *et al.*, 1988) – the cell is known as heteroplasmic. Heteroplasmy can refer to any level of mutation above 0% and below 100%, and also includes scenarios where more than one mtDNA mutation is present within a single cell (Figure 1.18).

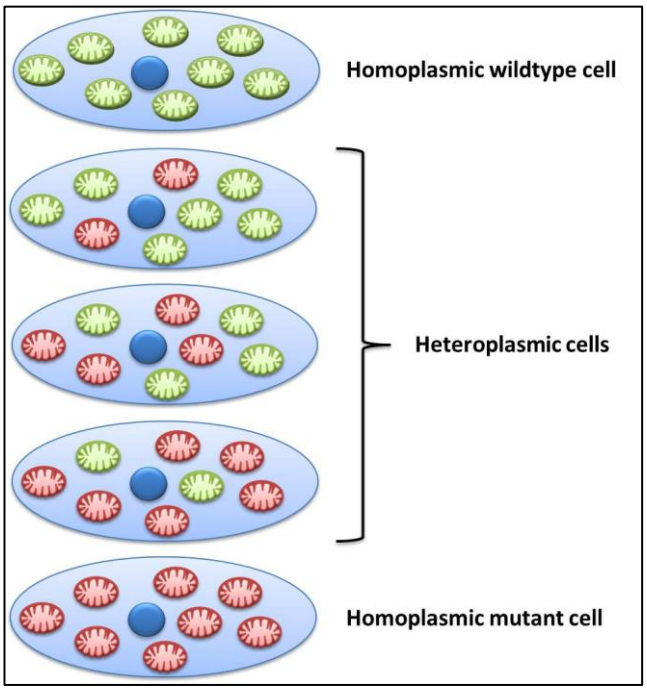

Figure 1.18 - Heteroplasmy and homoplasmy of mitochondria in single cells.

Cells containing mitochondria may be homoplasmic in two distinct scenarios, containing 100% wildtype or mutant mtDNA, or may be heteroplasmic, containing a mixture of wildtype and mutated mtDNA.

The potential for mitochondrial DNA mutations to exist in a heteroplasmic state gives rise to the mitochondrial 'threshold effect' (Rossignol *et al.*, 2004). Low level heteroplasmy, particularly in cases where mtDNA deletion heteroplasmy is so low as to be undetectable, does not affect the cell's phenotype due to the compensatory effect of the remaining wild-type molecules functioning normally within the cell. To affect the cell's respiratory chain function a significant level of mtDNA heteroplasmy must be established within the cell; i.e. the balance of mutant and wildtype mitochondrial DNA molecules must shift significantly in favour of the deleted genome type. The 'phenotypic threshold level' is the point at which the mtDNA mutation can no longer be compensated for by the remaining wildtype DNA, causing a functional defect and respiratory deficiency of the cell (Rossignol *et al.*, 2004).

The threshold level at which a biochemical defect is caused in the cell varies between different tissues and different mutation types. Mitochondrial DNA deletions in muscle have been reported to have phenotypic threshold values varying from 50% (Porteous *et al.*, 1998) to 90% (Sciacco *et al.*, 1994), though the average threshold level for mtDNA deletions has been determined to be approximately 60% (Hayashi *et al.*, 1991) (Figure 1.19). Point mutations of mtDNA show huge variations in phenotypic threshold level between mutation types; the $tRNA^{Lys}$ 8344 A to G substitution associated with MERRF has been shown to have a very high threshold level, as high as 97% in muscle fibres in some patients (Moslemi *et al.*, 1997), while other point mutations such as the 3243 A to G substitution show much lower phenotypic threshold levels – a mutation load above 50% was shown to be associated with abnormal VO2 max and muscle morphology, while mutation loads of 65% or higher were also associated with symptoms in other tissues, such as diabetes mellitus and hearing impairment (Jeppesen *et al.*, 2006).

Following the proposal of the phenotypic threshold effect (Howell *et al.*, 1983) two further mitochondrial threshold limits have been proposed; a biochemical threshold level, and a translational threshold level. The biochemical threshold limit is the level to which a single mitochondrial complex can be inhibited or decreased before a decrease is total respiratory activity of the cell is observed. This was initially observed in relation to cytochrome *c* oxidase (Complex IV) (Letellier *et al.*, 1994), but has since been investigated in other mitochondrial proteins and complexes; biochemical threshold

levels have been found for respiratory Complexes I, III and IV as well as the adenine nucleotide translocator, phosphate carrier and pyruvate carrier (Rossignol *et al.*, 2004). A translational threshold effect is observed when a threshold percentage of mutant mRNA or tRNA is exceeded, causing a decrease in the rate of mitochondrial protein synthesis. This translational threshold can be reached by increased RNA instability, meaning insufficient total RNA amounts are maintained within the mitochondria. Secondarily, the level of mtDNA mutation may rise to such a level that sufficient wildtype RNA cannot be produced to meet cellular requirements (Helm *et al.*, 1999).

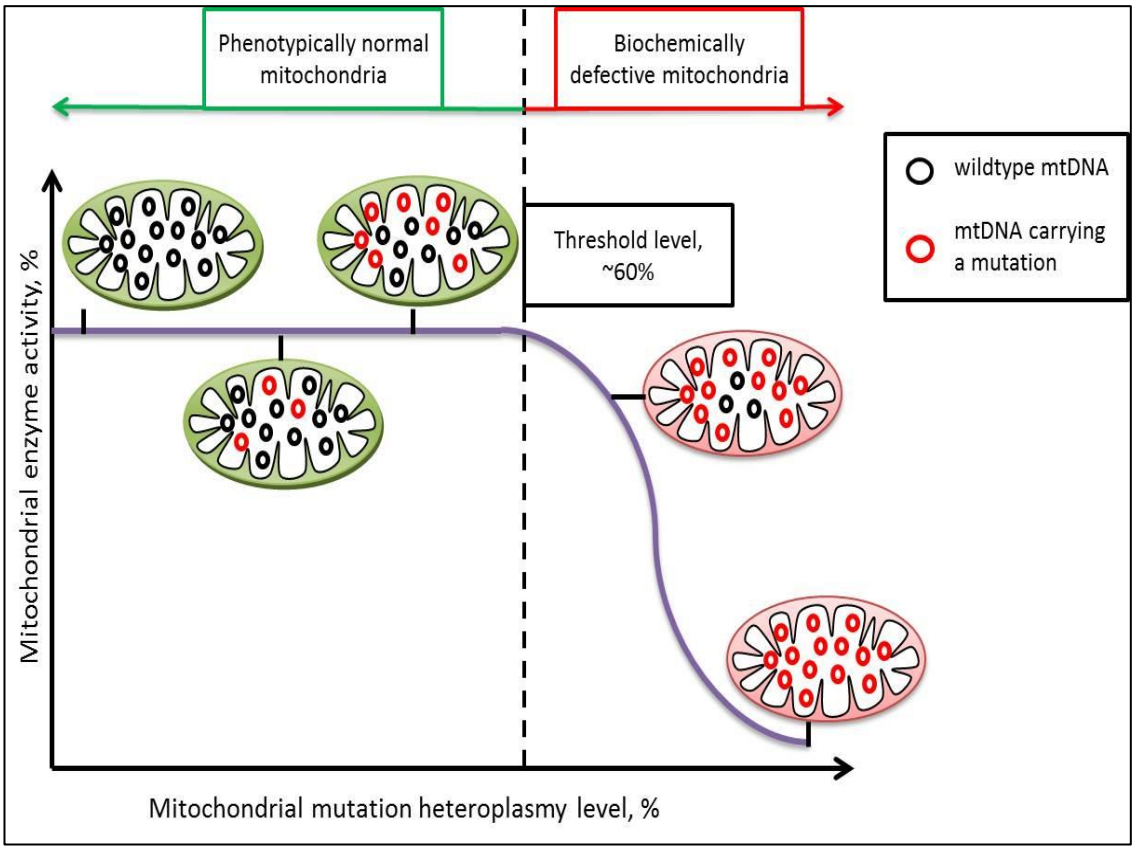

Figure 1.19 - Threshold of mitochondrial mutations

The potential for mitochondrial DNA mutations to exist in a heteroplasmic state gives rise to the mitochondrial threshold effect. Low levels of heteroplasmy can be tolerated within a cell due to wildtype compensation, but increasing levels of heteroplasmy can lead to reduced mitochondrial enzyme activity. As heteroplasmy levels rise, more mitochondria contain a level of mutant DNA incompatible with normal mitochondrial function, and insufficient ATP is produced for normal cellular function. The threshold level, which varies between different mutations and tissue types, is the point at which the mtDNA mutation can no longer be compensated for by the remaining wildtype DNA, causing a functional defect and respiratory deficiency of the cell.

Interestingly, it has been shown that mtDNA mutation heteroplasmy levels alone may not account for the severity of patient phenotypes, with no direct correlation between patient phenotype and genotype having been found (Morgan-Hughes *et al.*, 1995; Chinnery *et al.*, 2001). Not only is there no link between disease severity and mutation load, but identical mutations can cause vastly different patient phenotypes – the common deletion, for example, is present is a spectrum of patients with mtDNA deletion disorders ranging from PEO and KSS through to the much more severe Pearson's syndrome in children (Bernes *et al.*, 1993) – and mutations present homoplasmically in all tissues may still phenotypically present in a tissue-specific manner (Fischel-Ghodsian, 2000).

1.7 Clonal Expansion

Mitochondrial DNA mutations only become detrimental to the cell once a specific mutation threshold level has been passed (see *1.6.2*); a mutation must originally be formed in only a single mtDNA molecule, and so this mutation must accumulate within the cell in order to reach a detrimental level. This increase in mutant mtDNA heteroplasmy over time, and the associated decline in mitochondrial function, was first proposed to be a major cause of mitochondrial disease and human aging in 1989 (Linnane *et al.*, 1989). This 'ageing mitochondria' hypothesis was supported by experimental evidence that mitochondrial respiratory activity declined with age (Trounce *et al.*, 1989). Originally, the accumulation of mutant mtDNA with time was attributed to high mutation levels of mtDNA paired with a perceived lack of mtDNA repair mechanisms (Linnane *et al.*, 1989), but later evidence of mitochondrial DNA repair mechanisms (see

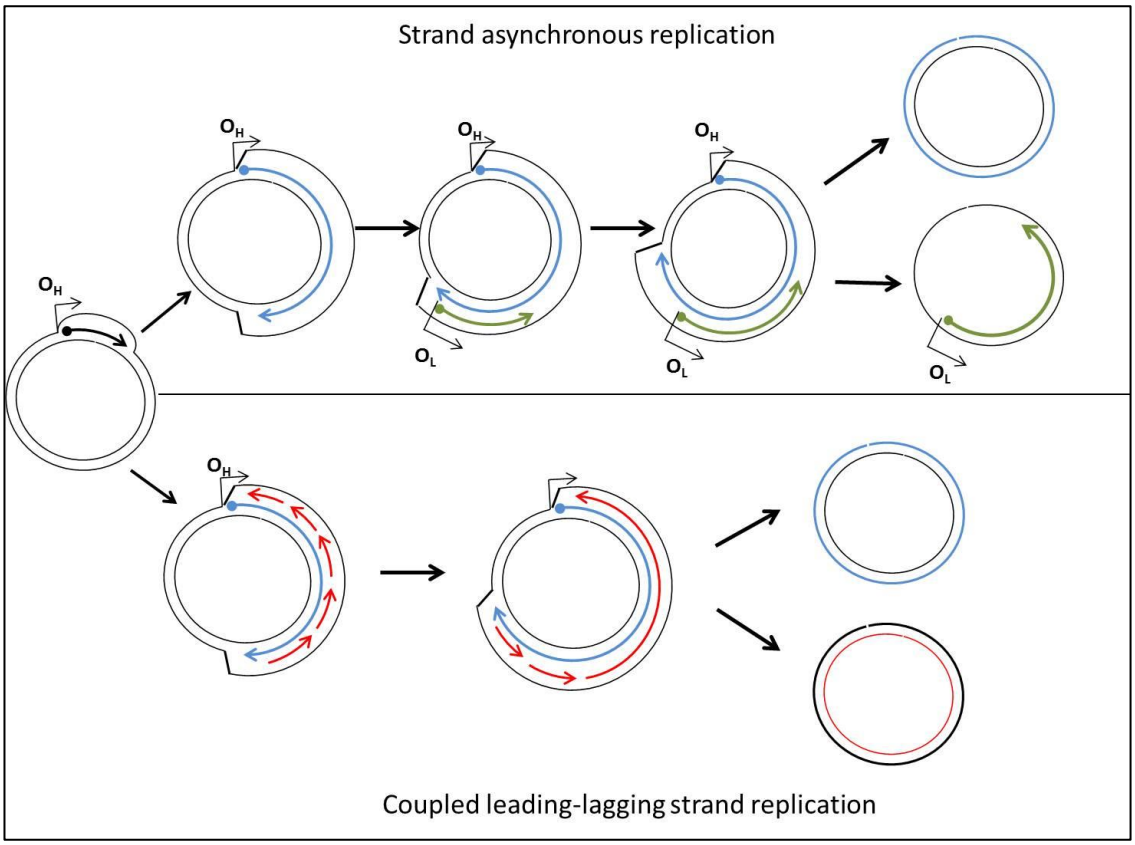

Figure 1.14 – Two proposed mtDNA replication models.

Both proposed models of mtDNA replication begin with strand displacement of the mtDNA beginning at the origin of heavy strand replication (OH), but the models diverge from this point.

c) Strand asynchronous replication

Replication begins at the OH, proceeding until the origin of light chain replication, OL, is exposed. From this point, replication commences in the other direction, with replication of both strands continuing to completion.

d) Coupled leading-lagging strand replication

Replication also begins from OH, but replication of the light strand begins soon after this initiation event. Sections of the light strand known as Okazaki fragments are generated as sections of the heavy strand become displaced – these fragments must be ligated to form a complete DNA strand.

1.4.5 Mitochondrial DNA Repair) is in strong opposition to this hypothesis. Since this first proposal of mutant mtDNA accumulation contributing to disease and aging, much work has been carried out in this field to try to understand how a single point mutation or mtDNA deletion could accumulate within the cell to cause pathology. This process of increasing heteroplasmy levels of a specific mutation has become known as clonal expansion.

For a considerable period of time, the only evidence of clonal expansion was found for mtDNA deletions. In the same year that Linnane *et al* first proposed the importance of the accumulation of mtDNA mutations, research began to show that at the cellular level, high deletion heteroplasmy levels were associated specifically with areas of muscle fibres showing evidence of respiratory deficiency in mitochondrial disease – specifically KSS in this first study (Mita *et al.*, 1989). More recent work has successfully linked the accumulation of mtDNA deletions to human aging - PCR amplification of whole mitochondrial genomes from single cells has shown high levels of single mtDNA deletions in individual cardiomyocytes, with each different cell carrying a different deletion (Khrapko *et al.*, 1999), while high levels of mtDNA deletions have been found in substantia nigra neurons in aged subjects (Trifunovic *et al.*, 2004; Bender *et al.*, 2006; Kraytsberg *et al.*, 2006) (see 1.5.3 for further details). Interestingly, identical sets of deletion types were found to be present in the substantia nigra neurons of Parkinson disease patients, multiple mtDNA deletion patients and aging controls, suggesting that a similar mechanism for clonal expansion of mtDNA deletions is present in each of these cases (Reeve *et al.*, 2008a).

Evidence for the clonal expansion of mtDNA point mutations began to emerge much later than for large-scale mtDNA deletions. The first identification of the accumulation of point mutations came from work in tumours, where it was suggested that clonal expansion was the cause of high levels of point mutations of the mitochondrial genome found in colorectal and gastric tumours (Alonso *et al.*, 1997). The investigation into whether clonal expansion is indeed responsible for high heteroplasmy levels of point mutations has since been carried over into healthy human tissue, where a cell-by-cell analysis of buccal epithelium and cardiomyocytes has revealed that approximately one third of cells (13 cells from 36 for both buccal epithelium cells and cardiomyocytes) in aged individuals (over 76 in this particular study) has clonally expanded point mutations at a high level of heteroplasmy. In most cases a single

mutation has undergone clonal expansion to accumulate to a high degree within the cell, though in rare cases two separate point mutations have both gone on to clonally expand (Nekhaeva *et al.*, 2002).

Though strong evidence has now been put forward for the clonal expansion of large-scale mtDNA deletions and pathogenic mtDNA point mutations, the mechanism by which these mutations accumulate within the cell has yet to be discovered. However, three main hypotheses have been put forward, as described below.

1.7.1 Survival of the smallest

The 'survival of the smallest' mechanism was first proposed by Wallace *et al* (Wallace, 1992), suggesting that deleted mtDNA molecules are clonally expanded due to a selective advantage of smaller mtDNA molecules. It was proposed that replication of mitochondrial DNA molecules harbouring mtDNA deletions occurs faster due to the smaller size of the molecules. This would allow for more frequent replication, causing the deleted mtDNA to outcompete wildtype DNA within the cell and the percentage of mutant DNA to rise within the cell to exceed the threshold level (Figure 1.20).

Since the initial proposition of the 'survival of the smallest' mechanism a number of papers have since questioned its validity, one of the main arguments being that an accumulation of point mutations is also seen in patients with mitochondrial disease; as point mutations do not change the mitochondrial genome size there can be no selective advantage for these molecules based on the length of time taken for replication, which brings into question whether a selective advantage is seen based on size in deleted molecules (Weber et al., 1997). Also, a 1997 study of replicative dynamics showed that all mitochondrial molecules, including wildtype molecules, replicate in under 90 minutes – a much shorter period of time than that between replications – meaning the time taken to replicate the mitochondrial genome is not rate-limiting for mitochondrial turnover (Shadel and Clayton, 1997). The shorter time span for replication of deleted mtDNA molecules, taking this into account, should not influence the individual turnover rates of wildtype and deleted mtDNA molecules and so percentage heteroplasmy should not change.

Despite these criticisms of the 'survival of the smallest' model of clonal expansion, a study of cell repopulation was performed to investigate whether smaller, deleted mtDNA molecules do have a replicative advantage in cells in 2002 (Diaz et al., 2002). Under tight copy number control – i.e. during normal, non-selective cell conditions – it was demonstrated that over time deleted molecules actually show a small decrease (10 – 20%), believed to be due to better growth of cells containing higher levels of wildtype DNA. This is in keeping with other studies that have shown cells with the highest percentage of deleted mtDNA molecules to have the longest population doubling time (Hayashi et al., 1991). Significantly different results, however, were seen under relaxed copy number control following mitochondrial DNA depletion by treatment with ethidium bromide. Seven days after treatment, cell lines undergoing repopulation displayed a higher percentage deleted mtDNA molecules – deleted mtDNA molecules repopulated the cell 2-3 times faster than the wildtype molecules (Diaz et al., 2002). This suggests that deleted molecules may have a replicative advantage within the cell, which could be the cause of clonal expansion of deleted mtDNA molecules. Experimental evidence with regards to the 'survival of the smallest' hypothesis is therefore inconclusive, with different cellular conditions yielding very different results in terms of a replicative advantage for mitochondrial genomes with large-scale DNA deletions. Further work has been done to try to further elucidate the likelihood of a replicative advantage for mtDNA deletions, as discussed in further detail in Chapter 3, but no conclusive evidence has yet proven whether or not this hypothesis is correct.

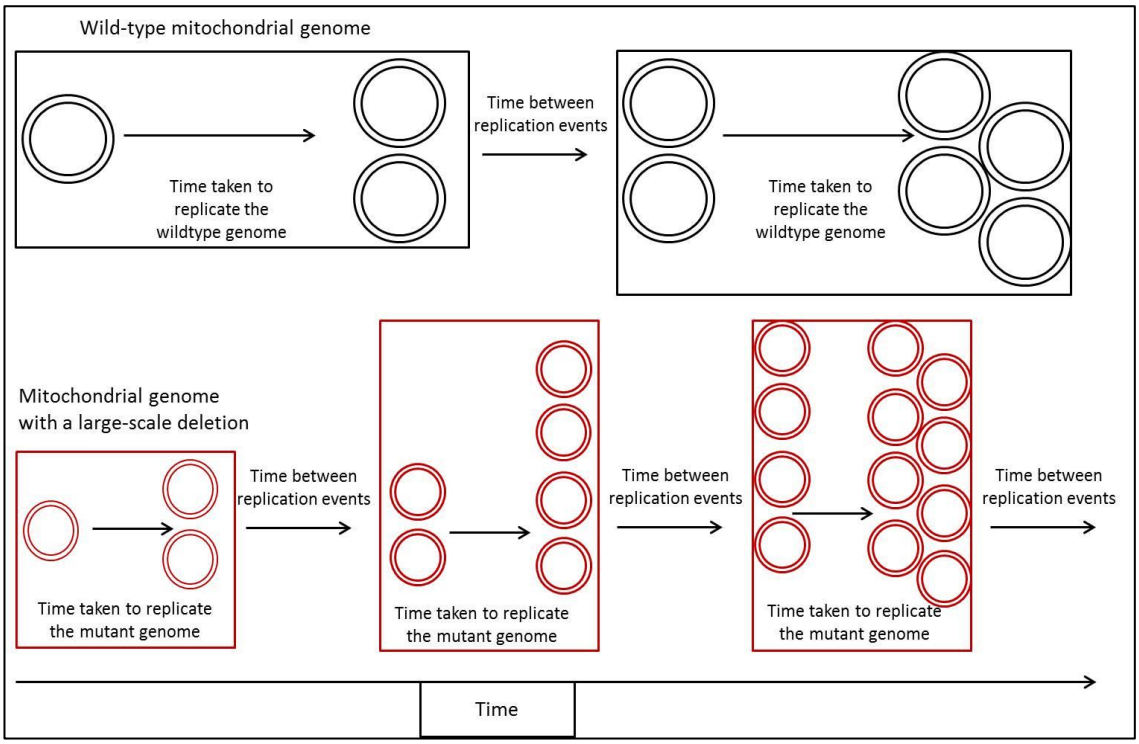

Figure 1.20 - Survival of the smallest mechanism for the clonal expansion of mtDNA deletions.

This proposed mechanism for the clonal expansion of mtDNA deletions suggests that the smaller size of mitochondrial genomes with DNA deletions confers a selective advantage over wildtype genomes due to a faster rate of replication. It was proposed that replication of the smaller mitochondrial DNA molecules harbouring mtDNA deletions occurs faster than that of wildtype genomes, allowing for more frequent replication. This would result in the deleted mtDNA outcompeting wildtype mtDNA within the cell, leading to a rise in the percentage of mutant mtDNA.

1.7.2 Survival of the slowest

An alternative model proposing an advantage for mtDNA mutations within the cell, the 'survival of the slowest' mechanism, was proposed by De Grey (1997). This hypothetical model for clonal expansion stated that the inherent dysfunction of mutated mitochondrial DNA molecules gave them a selective advantage in the cell, proposing that mitochondrial genomes within dysfunctional mitochondria (i.e. mitochondria with no, or limited, respiratory function) would be preferentially amplified within a cell. The main rationalisation of this hypothesis was that mitochondria with no respiratory function do not produce as great a level of damaging free radicals as normally functioning mitochondria (reactive oxygen species being a common by-product of oxidative phosphorylation), meaning the mitochondrial membranes undergo less damage. As a result of this, non-functional mitochondria are

less likely to be targeted for mitophagy, as mitochondrial membrane damage by ROS in otherwise healthy mitochondria causes membrane depolarisation, leading to selective mitophagy (Kim *et al.*, 2007). If normally functioning mitochondria with predominantly wildtype DNA are targeted for mitophagy more often than dysfunctional mitochondria carrying mtDNA mutations then wildtype mtDNA molecules must be destroyed more often, increasing the percentage of deleted molecules within the cell and making it more likely that deleted mtDNA molecules will be replicated to a higher level of heteroplasmy (De Grey, 1997) (Figure 1.21).

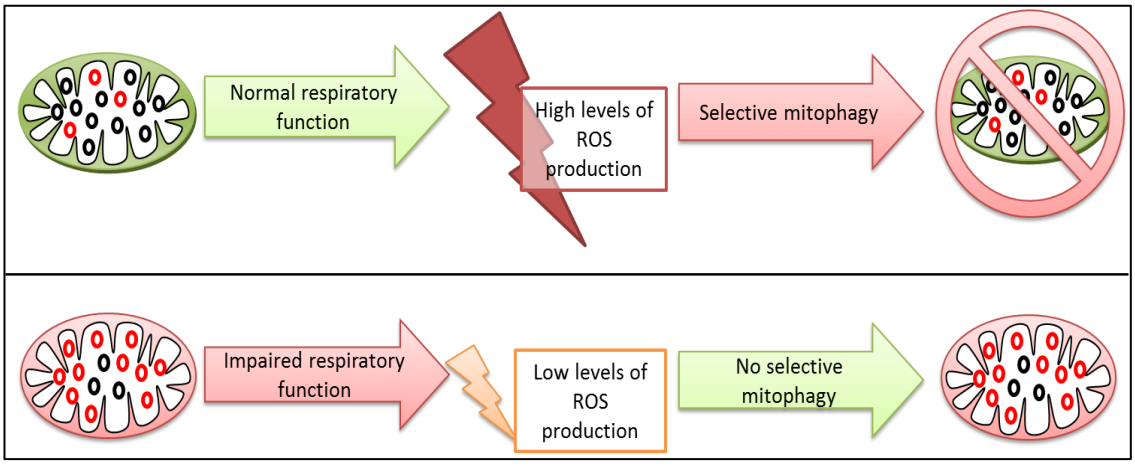

Figure 1.21 - Survival of the slowest mechanism for clonal expansion of mtDNA deletions.

This proposed mechanism for the clonal expansion of mtDNA deletions suggests that the inherent dysfunction of mutated mitochondrial DNA molecules provides a selective advantage in the cell, as a reduced capacity to carry out oxidative phosphorylation reduces the quantity of ROS produced by the mitochondria. The reduced level of damage to the mitochondrial membrane by harmful free radicals in this case could reduce the potential for dysfunctional mitochondria to be targeted by mitophagy, increasing the chances of mutant DNA within the dysfunction mitochondria being replicated.

1.7.3 Random Drift

Both of the mechanisms discussed above suggest that deleted mitochondrial DNA molecules are preferentially amplified due to an inherent selective advantage, but another school of thought suggests that this may not be the case, and that clonal

expansion can occur by random genetic drift - as proposed by Elson *et al* (2001). This mechanism of clonal expansion is based on the theory of relaxed replication within cells, which explains the constant turnover of mtDNA independent of the cell cycle and replication of nuclear DNA (Bogenhagen and Clayton, 1977). Elson *et al* set up a model based on mitochondrial replicative dynamics demonstrated previously (Shadel and Clayton, 1997), and showed that relaxed replication alone can cause the clonal expansion of deleted mtDNA molecules without any necessary replicative advantage in post mitotic tissue (Figure 1.22). However, large clonal expansions were shown to be the result of a lengthy process; results for simulated cells equivalent to 80 years old showed that 78% of the original mtDNA deletion formation events occurred before 30 years, and 46% before 15 years. The model showed that mutations acquired later in life would not have sufficient time to reach significant levels of heteroplasmy by random genetic drift alone (Elson et al., 2001), suggesting that any mtDNA deletions observed to have clonally expanded to a significant level of heteroplasmy in aged tissue (Bender *et al.*, 2006; Bua *et al.*, 2006; Kraytsberg *et al.*, 2006) must have formed early in development. This raises the question of how early-onset disease phenotypes such as Leigh syndrome could arise if clonal expansion occurs by this mechanism alone as, by extension of this finding, there would have been insufficient time for clonal expansion of an mtDNA mutation to have occurred to a degree that could cause pathology. A further question raised by the 'random drift' mechanism of clonal expansion is the number of cells predicted to become COX-deficient within a human lifespan. The prediction by Elson et al was that ~4% of post-mitotic cells would become COX-deficient over the course of 80 years, but this does not correlate with the high levels of mtDNA deletions observed in aged substantia nigra neurons (Reeve et al., 2008).

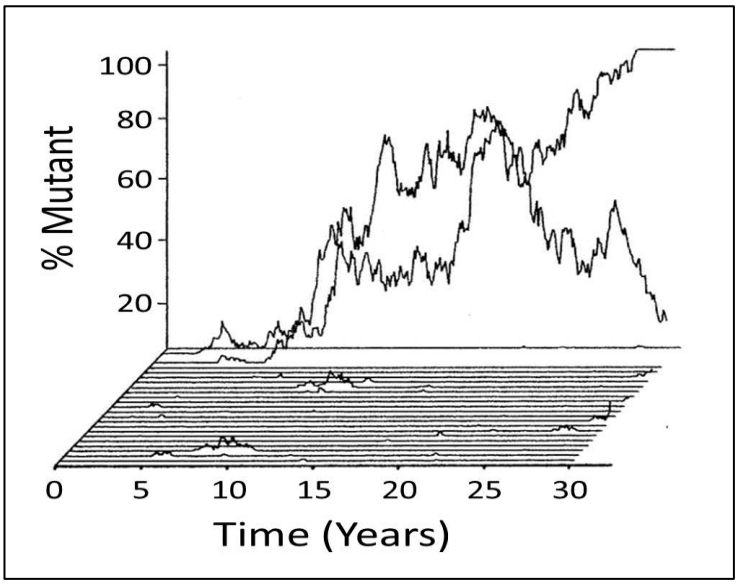

Figure 1.22 – Random drift mechanism for the clonal expansion of mtDNA deletions.

Taken with permission from (Elson *et al.*, 2001). Proportion of mutant mtDNA in single simulated cells. Each simulated cell contained 1,000 mtDNAs and had a half-life, $T_{1/2}$, of 10 d and a copy-error (mutation) probability of 10^{-5} (measurements taken monthly for 30 years). For illustration, we have shown the results of 24 simulations from a total of 600. In the 600 cells, one mutant event went to fixation (trace at the back) and three others showed a significant expansion (one shown), but, in most, the mutations were rapidly lost. When these simulations were continued for a full 120 years (not shown on the graph), a mean of only 31.27 mutations occurred per cell, corresponding to the value predicted by the equation $N_{mut}=[N_{mtDNA}P_{mut}t\ \ln(2)]/T_{1/2}$, where N_{mut} is the number of mutation events and t is the duration of the simulation in d. Many of these mutations were lost almost instantaneously (41% were lost within one $T_{1/2}$, and 88% were lost within 10 $T_{1/2}$), but, in some cells, the proportion of mutant mtDNA increased.

1.8 Mitochondrial inheritance

Mitochondrial DNA is inherited in a non-Mendelian fashion, being inherited from only one parent. In humans, the mother is the only parent to pass on mtDNA to the offspring; this was first demonstrated by screening for single nucleotide polymorphisms (SNPs) in blood platelets from individuals across three generations of several families. Of these families, seven were found to have informative, easily traceable polymorphisms – 5 families with a polymorphism disrupting the *Hae II* restriction enzyme cleavage site, a family with a polymorphism disrupting the *Hae III* restriction site and a family with a polymorphism disrupting the *Hine II* restriction site – all of which were found to segregate maternally (Giles *et al.*, 1980).

Despite discovering the maternal mode of mtDNA inheritance over three decades ago, the mechanism by which paternal mtDNA is prevented from being passed on to the offspring in humans remains unclear. One method by which the paternal mtDNA may be destroyed was discovered in fertilized cow and monkey eggs by Sutovsky *et al* in 1999. This group found that the sperm mitochondria donated to an egg following fertilisation – which can number up to approximately 100 – are ubiquitin-tagged, and are therefore targeted for degradation within the embryo. It was proposed that this degradation may occur at the embryo pre-implantation stage (Sutovsky *et al.*, 1999). Recent work carried out in *Drosophila melanogaster* has revealed an alternative method by which paternal mitochondrial DNA transmission may be prevented, as mature *Drosophila* sperm contain little to no mtDNA due to the loss of mitochondrial genetic material during spermatogenesis. This removal of mtDNA from the sperm is carried out in two ways - mitochondrial endonuclease EndoG is responsible for the removal of mtDNA nucleoids from spermatids, while any remaining nucleoids are removed along with any other debris by cellular remodelling. This remodelling occurs after the accumulation of any remaining nucleoids and cellular debris into a structure known as the 'cystic bulge', which travels the length of the spermatid before being extruded from the end of the tail (Chan and Schon, 2012; DeLuca and O'Farrell, 2012). A third method preventing the paternal transmission of mtDNA has been identified in mice (Al Rawi *et al.*, 2011) and in *Caenorhabditis elegans* (Sato and Sato, 2011), where autophagy has been shown to destroy paternal mitochondria in the zygote. In both *C elegans* and mouse embryos, LC3-dependent autophagy markers were detected; it was found that sperm mitochondria could be selectively degraded by this mechanism with no detriment to the cytoplasmic major sperm proteins (Al Rawi *et al.*, 2011; Sato and Sato, 2011).

Only one isolated case of paternal mtDNA transmission has been discovered in humans. A male patient, 28 years of age at the time of investigation, presented with extreme exercise intolerance due to severe lactic acidosis, suspected to be due to a mitochondrial defect. This patient was indeed found to have a short, pathogenic 2 base pair deletion (5132delAA) in the mitochondrial *ND2* gene at approximately 90% heteroplasmy in muscle. This discovery of this deletion and a 1303G-A point mutation led to extensive sequencing analysis of mtDNA from the patient's skeletal muscle tissue blood and hair, as well as cultured fibroblasts; this revealed the presence of two

distinct mtDNA sequences present in the patient's skeletal muscle. These two mtDNA sequences, which showed variations at 18 different nucleotide positions, were assigned to different European haplogroups. Subsequent sequencing analysis of mtDNA from the blood of the patient's parents and paternal uncle revealed that the patient's 2bp deletion had occurred in a mitochondrial DNA sequence identical to the paternal line – i.e. the patient had inherited paternal DNA which had segregated to a high proportion in skeletal muscle. Maternal mtDNA only was present in the patient's blood, hair and fibroblast samples (Schwartz and Vissing, 2002).

1.8.1 The mtDNA Bottleneck

The mtDNA bottleneck theory pertains to the transmission of mtDNA from mother to offspring; at a currently undetermined point during oogenesis, a small number of maternal mtDNA molecules undergo a high level of amplification to form the total mtDNA pool to be passed on to an offspring. Evolutionarily, this mechanism is believed to function to limit the inheritance of mutations by offspring – limiting the number of mtDNA molecules involved in transmission limits the chances of passing on a maternal mutation. The rapid genetic drift then created by the amplification of a small number of mitochondrial genomes to a full oocyte complement of mtDNA is also likely to cause either the loss or fixation of an mtDNA mutation, which has been said to allow for natural selection at the level of the individual organism to come into effect (Bergstrom and Pritchard, 1998; Chinnery *et al.*, 2000b).

The mtDNA bottleneck does serve to limit the transmission of mtDNA mutations and to preserve genome integrity in the healthy population, but there are complications in the case of mitochondrial disease – specifically for point mutations, as cases of transmitted rearrangements are much rarer (risk of transmission is approximately 1 in 24 according to a cohort study of 226 families, (Chinnery *et al.*)). Due to the effects of the genetic bottleneck there is no link between the level of mutation heteroplasmy of a mother and her offspring, and siblings sharing a mother may have vastly different heteroplasmy levels (Figure 1.23).

Evidence for the existence of an mtDNA bottleneck first emerged in a 1982 study of maternal transmission of an mtDNA polymorphism in cows. One maternal lineage of

Holstein cows was found to carry two distinct mitochondrial genotypes which could be tracked through consecutive generations – a wildtype genome, and a genome carrying a polymorphism in the form of an A to G transition which created a new *HaeIII* restriction site. Large genotype shifts were observed in this maternal lineage between generations, leading to the suggestion that large levels of mtDNA amplification from a small starting pool of mtDNA in oocytes may be responsible for rapid, inter-generational variations in mtDNA (Hauswirth and Laipis, 1982). Since then, the presence of a bottleneck in mtDNA transmission has become widely accepted, though at what point the bottleneck lies is still a point of contention.

In 2007, it was proposed by Cao *et al* that an mtDNA bottleneck could exist without any overall changes to mtDNA copy number in the developing oocyte; a study carried out in the C57BL/6 mouse model by this group showed no decrease in mtDNA copy number in primordial germ cells (PGCs) during development. With no mass decline in mtDNA copy numbers at this point in oogenesis, the genetic bottleneck cannot purely be due to amplification from very small number of starting mtDNA molecules. Instead, Cao *et al* hypothesised that the mtDNA aggregates into a small number of homoplasmic nucleoids, which then act as the segregation units in the germ cells (Cao *et al.*, 2007).

This finding was almost immediately thrown into contention, as the following year Cree *et al* presented evidence that the alkaline phosphatase staining of PGCs used by Cao *et al* disrupts the detection of mtDNA copy number, due to the sensitivity of qPCR. The data put forward in the mouse study completed by this group showed that mtDNA copy number is in fact reduced in mouse PGCs, backing the original hypothesis of Hauswirth and Laipis that a reduced number of mitochondrial genomes during oogenesis is responsible for the genetic bottleneck (Cree *et al.*, 2008).

The same finding – a reduction in mtDNA copy number in the PGCs of mice – was also presented in 2008 by Wai *et al*, though this study was extended with a follow-up analysis of mtDNA heteroplasmy in the PGCs. Interestingly, in direct contrast to the expected results if reduced mtDNA levels were responsible for the genetic bottleneck, no great variation in heteroplasmy levels was found in the PGCs immediately following copy number reduction. This led the group to hypothesise that, although mtDNA copy number is indeed reduced in the PGCs, this is not necessarily where the genetic

bottleneck lies. An alternative mechanism was proposed to explain the genetic bottleneck, involving the selective replication of a subpopulation of mtDNA genomes at the later developmental stage of postnatal folliculogenesis (Wai *et al.*, 2008).

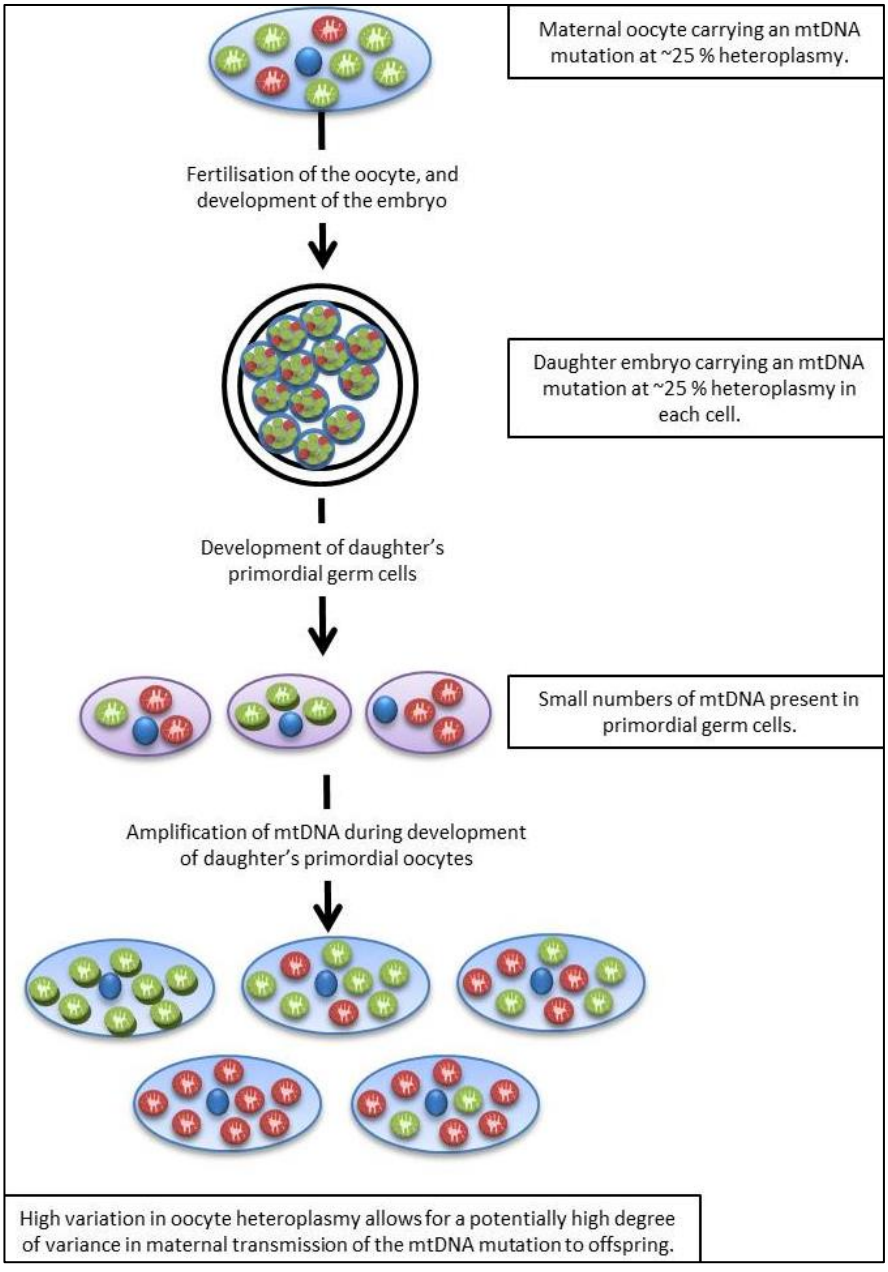

Figure 1.23 - The mtDNA bottleneck

The mtDNA bottleneck theory pertains to the transmission of mtDNA from mother to offspring; at a currently undetermined point during oogenesis, a small number of maternal mtDNA molecules undergo a high level of amplification to form the total mtDNA pool to be passed on to an offspring. This bottleneck is designed to limit the inheritance of mutations by offspring – limiting the number of mtDNA molecules involved in transmission limits the chances of passing on a maternal mutation. A rapid accumulation of mtDNA follows this bottleneck stage. However, in instances where an oocyte is heteroplasmic for a mutation following the bottleneck stage, the rapid genetic drift then created by the amplification of a small number of mitochondrial genomes to a full oocyte complement of mtDNA is also likely to cause either the loss or fixation of an mtDNA mutation.

1.9 Mitochondrial Dynamics

Mitochondrial structure has been well characterised since the original electron microscopy work carried out by Palade *et al* uncovered the presence of the double mitochondrial membrane (Palade, 1953). However, mitochondria are still typically depicted as single, oval-shaped organelles when in fact they exist in a much more dynamic state. The size and shape of individual mitochondria are dynamic, varying in different cellular conditions, while the internal mitochondrial structure can change from a characteristic morphology of narrow cristae and few cristae junctions in low ADP conditions to large cristae with many more cristae junctions in the presence of high levels of ADP (Detmer and Chan, 2007). The dynamic interactions between individual mitochondria are perhaps the most important for maintenance of normal mitochondrial function. Mitochondria are now known to exist within a dynamic network undergoing fusion, where two mitochondria merge to become a single organelle and fission events where individual mitochondria divide into two separate structures. This allows for the exchanging of mitochondrial contents, as well as regulating mitochondrial size, number and morphology. Fission and fusion are also integral in maintaining the correct mitochondrial membrane potential in healthy organelles, and decreasing membrane potential in organelles to be targeted for mitophagy (Chan, 2006).

1.9.1 Mitochondrial Fusion

Membrane fusion is an important cellular event in many circumstances - including the merging of gametes during fertilisation, the fusion of transport vesicles with other

organelles, or the fusion of lysosomes with vacuoles to facilitate the digestion of the enclosed cellular debris – but is particularly complex in the case of mitochondrial fusion, requiring the simultaneous management of four membranes due to the mitochondrial double membrane. Outer membrane fusion is coordinated with inner membrane fusion, as opposed to occurring as separate sequential events, although outer membrane fusion can still occur normally in instances where inner membrane fusion is impaired (Westermann, 2010).

Mitochondrial fusion is carried out by mitofusins, a subset of dynamin-related proteins (DRPs), which are a specific class of GTPases conserved across yeast, worms, flies and mammals (Escobar-Henriques and Anton, 2012). The first protein found to be involved in mitochondrial fusion was fuzzy onions (FZO), discovered in *Drosophila melanogaster* in 1997, which is expressed during spermatogenesis (Hales and Fuller, 1997). FZO is unusual in being expressed so specifically; in all other known cases, mitochondrial fusion proteins are expressed constitutively. In mammals, the DRPs known to mediate outer membrane fusion are mitofusin 1 and 2 (Mfn1 and Mfn2), which are both nuclear encoded proteins. Mfn1 and Mfn2 each contain two hydrophobic coiled coil heptad repeat region - HR1 and 2 - which sit on either side of two transmembrane domains, and an N terminal GTPase domain (Escobar-Henriques and Anton, 2012). These two large GTPases are arranged with the two hydrophobic transmembrane regions located in the OMM, a short loop in the intermembrane space, and the large functional portions of the protein protruding into the cytosol. Both Mfn1 and Mfn2 are involved in mitochondrial docking, as the cytosolic regions of the proteins from adjacent mitochondria interact with each other, allowing for lipid bilayer mixing. GTPase activity then provides the biomechanical energy required for full outer membrane fusion (Figure 1.24) (Westermann, 2010).

Fusion of the IMM is controlled separately from the OMM, mediated by nuclear encoded DRP protein OPA1 in mammals (Cipolat *et al.*, 2004). OPA1 is present in the IMM in multiple forms; several long, membrane-anchored isoforms are formed by alternate splicing, and these are processed to form several shorter, soluble isoforms. Each OPA1 isoform contains a mitochondrial targeting sequence, which is cleaved after import into the mitochondria. Long OPA1 isoforms contain a transmembrane region to anchor the protein to the IMM, while the rest of the protein protrudes into the

intermembrane space. Not all of the long OPA1 isoforms undergo cleavage – only some of these proteins undergo processing at the S2 cleavage site to create equimolar quantities of each long and short isoform; both types of OPA1 are required for fusion to proceed normally. Long isoforms of OPA1 promote the tethering of the two inner mitochondrial membranes following OMM fusion, promoting the direct contact of the two inner membranes, while the GTPase activity which is believed to trigger membrane conformational changes and lead to membrane fusion is provided by the short OPA1 isoforms (Figure 1.24) (Escobar-Henriques and Anton, 2012).

Though the Mfn1, Mfn2 and OPA1 are the main proteins directly responsible for mitochondrial fusion in mammals, accessory proteins are also involved in the regulation of this process. These accessory proteins include YME1L, which is responsible for the cleavage of the long OPA1 isoform, MitoPLD for OMM fusion promotion, the pro-apoptotic protein BAX for both positive and negative regulation of mitochondrial fusion, and MIB1, which negatively regulates mitochondrial fusion through physical interaction with Mfn1 and Mfn2 (Westermann, 2010).

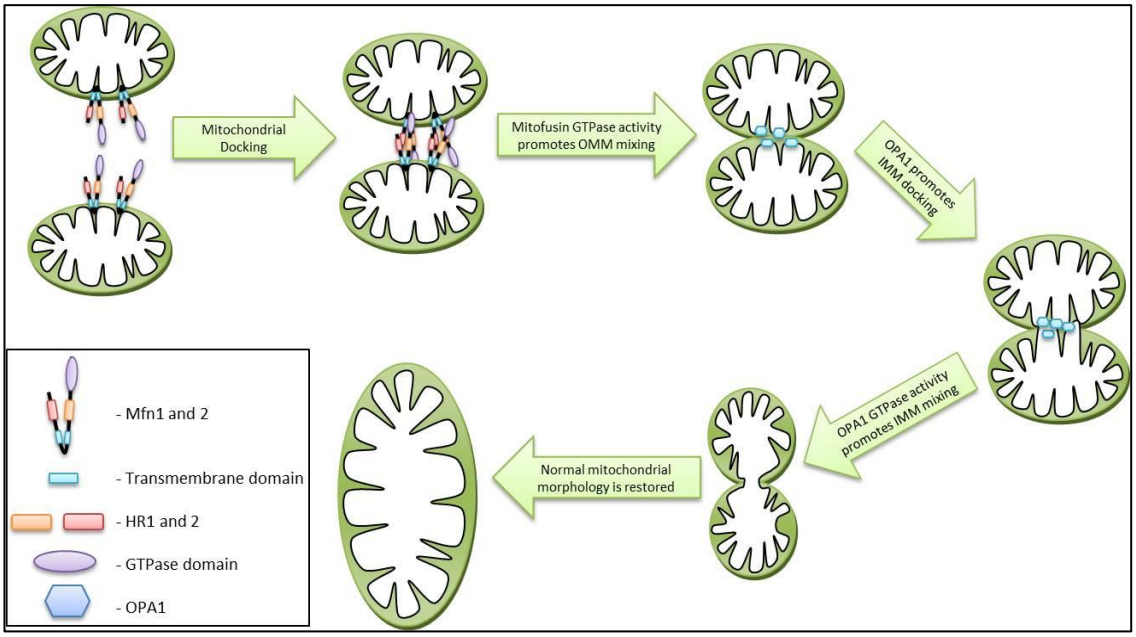

Figure 1.24 – Mitochondrial Fusion

Mitochondrial fusion is a complex process, requiring the coordination of inner and outer mitochondrial membrane fusion. This process allows for the dynamic interaction of individual mitochondria, permitting the free exchange of mitochondrial matrix components as well as playing a role in the regulation of mitochondrial size, number and morphology In mammals, mitochondrial fusion is regulated by three

major dynamin-related proteins – Mitofusin 1 and 2 are responsible for mitochondrial docking and outer mitochondrial membrane fusion, while OPA1 is the key component of inner mitochondrial membrane tethering and fusion.

1.9.2 Mitochondrial Fission

The first identification of a protein involved in mitochondrial fission was that of Dnm1 in yeast - a dynamin-related GTPase similar to those involved in mitochondrial fusion (as discussed above in section *1.9.1*). Dnm1 was initially discovered through yeast genetic screens, and was subsequently found to be localised to the OMM; its importance in mitochondrial dynamics is highlighted in Dnm1-knockout strains of yeast, where the mitochondria are observed to form a single interconnected web of tubules in each cell due to normal mitochondrial fusion but a lack of fission events (Bleazard *et al.*, 1999). A study in the same year in *C elegans* found a protein called Drp1 to be responsible for a similar role in OMM fission. Studies carried out in a *C elegans* Drp1 knockout model demonstrated separation of the mitochondrial matrix into distinct blebs contained within a single tubular network, indicating that IMM fission can still occur in the absence of Drp1 and that Drp1 must therefore responsible only for OMM fission events in C elegans (Labrousse *et al.*, 1999). Subsequent studies in mammalian cells have identified the two major components of the fission machinery as dynamin-related protein 1 (Drp1, the mammalian homolog of C elegans Drp1) (Smirnova *et al.*, 2001) and Fis1 (James *et al.*, 2003).

Drp1 is a classic dynamin related protein, with a structure comprised of a GTPase domain, a central domain and a GTPase effector domain (Chan, 2006). A second isoform of Drp1 is present specifically in human brain; this tissue-specific isoform has a insertion between the central domain and GTPase effector domain caused by alternative splicing (Westermann, 2010). Drp1 resides primarily in the cytoplasm in mammalian cells, but a proportion of this protein is recruited to the mitochondrial outer membrane by Fis1 to carry out fission. It is still unclear at this point whether

Drp1 directly interacts with the OMM following recruitment.

Fis1 is a small protein anchored to the OMM by a C-terminal transmembrane domain; the remainder of the protein, which is comprised of six antiparallel helices, protrudes into the cytoplasm (Chan, 2006). The importance of Fis1 in Drp1 recruitment to the OMM has been demonstrated in overexpression models, where fission rates are greatly increased leading to a fragmented mitochondrial network, and in instances of Fis1 depletion where tubular networks deficient in mitochondrial fission are observed (Westermann, 2010).

Following recruitment to the OMM, Drp1 is believed to behave in a manner similar to dynamin during the mediation of endocytic vesicle membrane scission. Multiple Drp1 molecules are thought to self-assemble to form a helical oligomer capable of wrapping around the mitochondrial membrane. The Drp1 oligomer is then believed to constrict around specific mitochondrial fission sites, this process being driven by the energy released during GTP hydrolysis (Westermann, 2011). The constriction of Drp1 at these regions is thought to sever both the inner and outer mitochondrial membranes, leading to a complete fission event (Youle and van der Bliek, 2012), though this differs from the OMM-only fission events mediated by Drp1 in C elegans (Labrousse *et al.*, 1999).

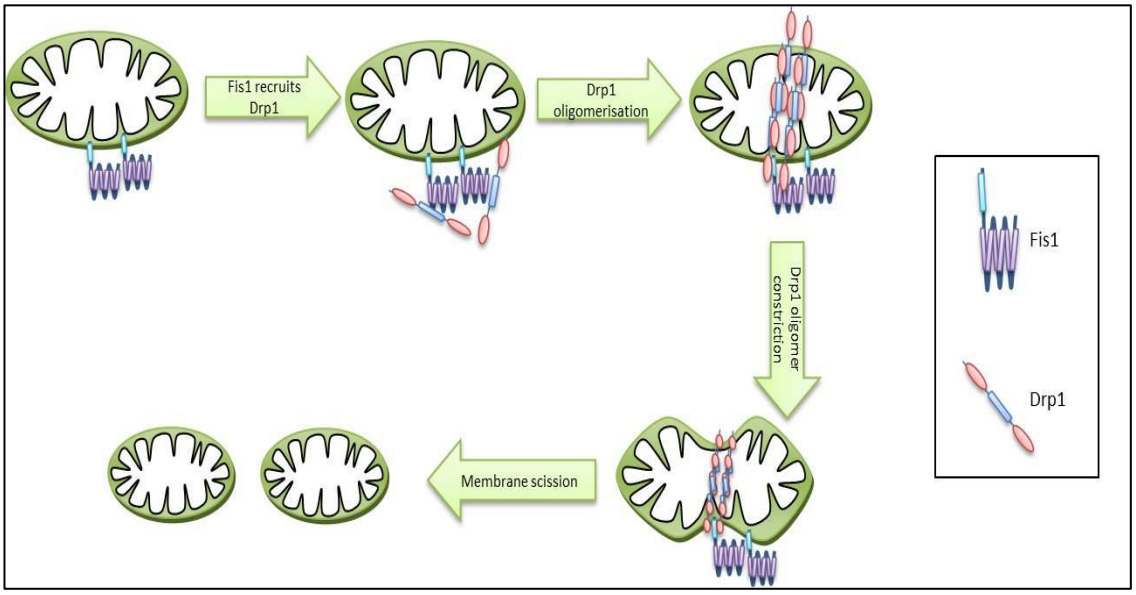

Figure 1.25 – Mitochondrial Fission

Mitochondrial fission, as well as being involved in the regulation of mitochondrial size, number and morphology, is key in maintaining the correct mitochondrial membrane potential in healthy organelles,

and decreasing membrane potential in organelles to be segregated from the mitochondrial network and targeted for mitophagy. This process is regulated by a dynamin-related GTPase, Drp1, which is recruited to the mitochondria by a small protein located at the outer mitochondrial membrane, Fis1. Following recruitment, Drp1 self-assembles to form a helical oligomer which then restricts around a specific fission site to cause membrane scission, creating two separate daughter mitochondria.

1.9.3 Mitophagy

Mitophagy is a type of cargo-specific autophagy employed to remove selected mitochondria from the cell. More specifically, mitophagy refers to the engulfment of mitochondria by vesicles coated with MAP1 light chain 3, an autophagosome marker. The ability to remove selected mitochondria is important in mitochondrial quality control, preventing an accumulation of dysfunctional mitochondria damaged by oxidative stress, but is also crucial in the degradation of mitochondria during erythrocyte development, steady-state turnover of mitochondria, and the adjustment of mitochondrial numbers in response to cellular energetic demands (Youle and Narendra, 2011). The sequestration of mitochondria into lysosomes was first observed in early electron microscopy studies of mitochondria, though the term mitophagy was not coined until many years later following the study of selective mitochondrial degradation in instances of cellular stress induced by starvation and UV damage (Kim *et al.*, 2007).

More than one mechanism for mitophagy exists in mammalian cells, allowing for a distinction to be made between mitophagy of undamaged and damaged mitochondria. Undamaged mitochondria may be selected for degradation during key developmental processes such as red blood cell maturation – mature erythrocytes contain no mitochondria – or to control the number of individual mitochondria in relation to changing metabolic demands. In these scenarios, a protein located on the OMM known as NIP3-like protein X (NIX) is believed to mediate mitophagy. It is thought that the WXXL-like motif located in the cytosolic region of NIX directly binds LC3 (a ubiquitin-like protein required for the formation of autophagosomal membranes) and the LC3 homolog GABA receptor-associated protein (GABARAP). This binding allows

mitophagy induction via the direct recruitment of isolation membranes (Youle and Narendra, 2011).

An alternate pathway for the selective degradation of damaged mitochondria during normal aging or in disease relies upon the segregation of dysfunctional mitochondria from the dynamic network before the induction of mitophagy by two main proteins – PTEN-induced putative kinase 1 (PINK1) and Parkin. Damaged mitochondria become isolated from the mitochondrial network via a fission event which leaves the damaged daughter mitochondria with a reduced membrane potential. This depolarisation event prevents the damaged mitochondria from re-entering the network, as a reduced membrane potential inhibits the capacity of mitochondria to undergo fusion, in addition to initiating mitophagy (Twig *et al.*, 2008). Under normal conditions PINK1 is a constitutively expressed kinase which is constantly imported into all mitochondria, but is subjected to high rate of proteolysis and so maintained at a very low level in the mitochondria. However, the depolarisation of the mitochondrial membrane allows the stabilisation of PINK1 at the OMM, with its kinase domain facing into the cytosol. This increase in expression at the OMM allows PINK1 to recruit Parkin, cytosolic E3 ubiquitin ligase, to the mitochondria via a direct physical interaction between the two proteins. Parkin is bound and phosphorylated by PARK1 at the OMM before beginning to mediate the ubiquitination of Mfn1, Mfn2 and voltage-dependent anion-selective channel protein 1 (VDAC1), all of which are embedded in the OMM (Youle and Narendra, 2011). Following Parkin-mediated ubiquitination, p62 has been found to accumulate on the mitochondria; this ubiquitin-binding adapter is able to recruit autophagosomes to the mitochondria through its capacity to bind LC3 (Pankiv *et al.*, 2007; Youle and Narendra, 2011) (Figure 1.26).

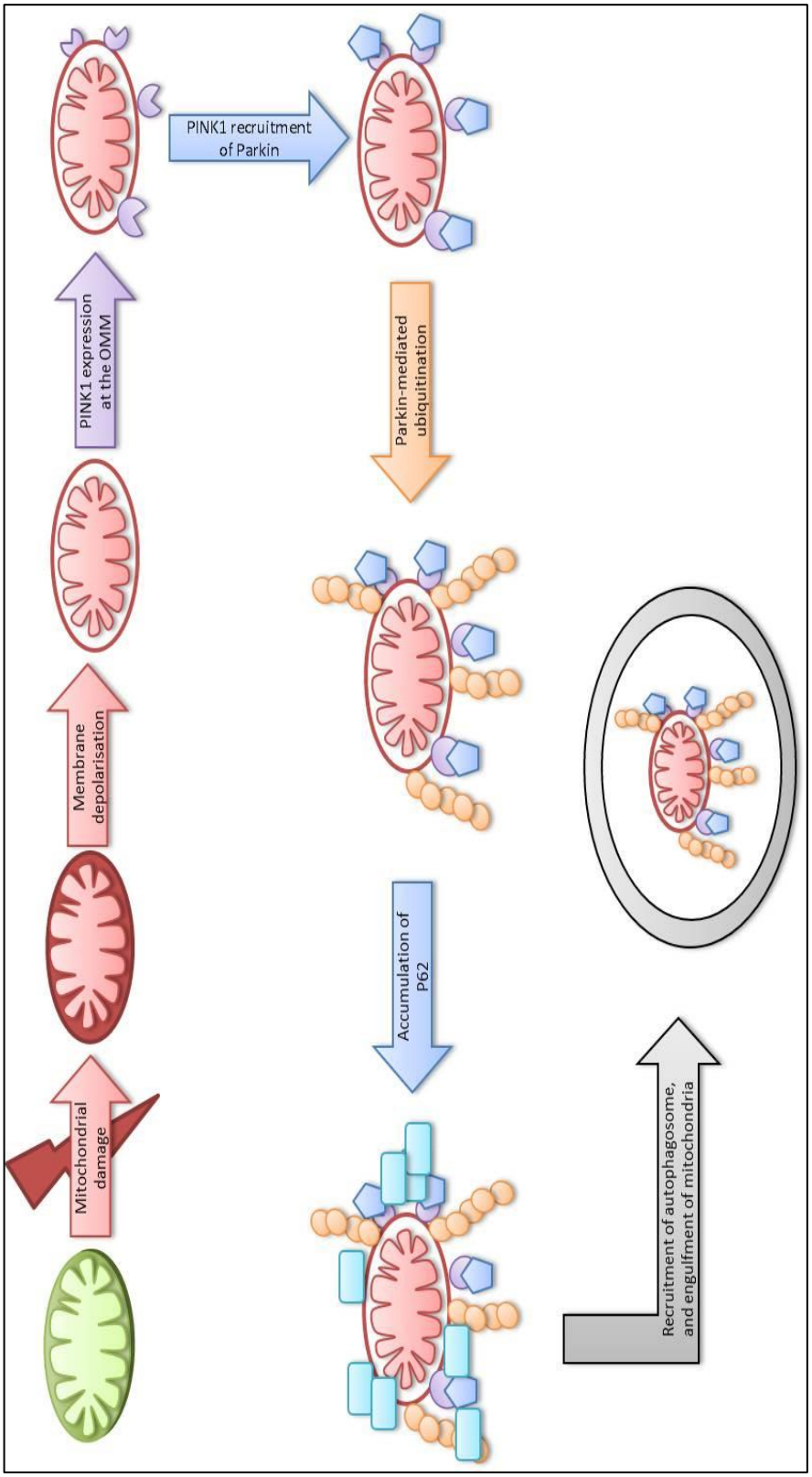

Figure 1.26 – PINK1 and Parkin mediated selective mitophagy
In cellular circumstances requiring the selective degradation of damaged mitochondria, PINK1 and Parkin are the two main proteins involved in regulating mitophagy. The mitochondrial membrane becomes depolarisation following the segregation of the damaged mitochondria from the mitochondrial network through a fission event; this disrupts the normal proteolysis of PINK1, allowing this protein to be expressed at the outer mitochondrial membrane. PINK1 is then able to recruit Parkin, an E3 ubiquitin ligase, which mediates the ubiquitination of Mfn1, Mfn2 and VDAC1 at the OMM. Following Parkin-mediated ubiquitination, p62 has been found to accumulate on the mitochondria; this ubiquitin-binding adapter is able to recruit autophagosomes to the mitochondria through its capacity to bind LC3.

1.10 Mitochondrial Disease

Many diseases are known to be associated with mitochondrial abnormalities and dysfunction of the oxidative phosphorylation system; these disorders are grouped together under the umbrella term of ‘mitochondrial disorders’. This range of disorders

can present at any age, and can clinically affect almost any tissue due to the universal need for ATP production throughout the body and the presence of mitochondria in almost every cell type to fulfil this energy demand. Due to the wide variety of potential symptoms of mitochondrial diseases, patients can present in a number of ways – with a single organ or tissue type being clinically affected (a tissue specific disorder), with clinical symptoms spread throughout the nervous system and skeletal muscle (a neuromuscular disorder), or with neuromuscular symptoms alongside further clinical pathology (multisystem disorders) (Di Donato, 2009).

1.10.1 Prevalence of mitochondrial disease

Correctly diagnosing patients with mitochondrial disease presents difficulties for clinicians, with the diverse symptoms of the mitochondrial disorder spectrum making it difficult to establish a diagnosis for many patients; this has consistently led to an under-estimation of mitochondrial disease prevalence. However, as understanding of mitochondrial disease continues to improve, more patients are receiving the correct diagnosis, care and advice, leading to an ever-increasing estimation of the prevalence of the disease in the general population (Schaefer *et al.*, 2004; Schaefer *et al.*, 2008).

A study by Elliot *et al* in 2008 set out to determine the prevalence of ten separate mtDNA point mutations in the general population, through the analysis of neonatal-cord blood samples from 3168 live births in Cumbria, England. This study, determined to be representative of the whole of the UK through haplotype analysis, found point mutations to be present in 0.54% of samples (Elliott *et al.*, 2008) – a huge increase from previous estimates of 12.48 in 100,000 (Chinnery *et al.*, 2000a) or 13.1in 100,000 live births (Skladal *et al.*, 2003). Fortunately, though this study determined that point mutations may be present in up to 1 of every 200 members of the general population, these mutations do not seem in be pathogenic in every case, meaning the prevalence of mitochondrial disease remains much lower than this.

A study in 2008 carried out in the North East of England followed the diagnosis of adults with suspected mitochondrial disease at a single specialised neurology centre, and found that 9.2 of every 100,000 people had clinical symptoms of mitochondrial disease. This high level in the general population makes mitochondrial disease one of

the most common inherited neuromuscular disorders; correctly diagnosing mitochondrial disease, in order to best advise patients on potential disease progression paths and the risks of disease transmission to children, is therefore of paramount importance (Schaefer *et al.*, 2008). As our understanding of mitochondrial disease progresses and more pathogenic mutations are discovered, it seems likely that the prevalence of mitochondrial disease will continue to rise.

1.10.2 Mitochondrial disorders

Though the spectrum of mitochondrial disorder presentation is wide, certain symptoms are strongly linked to specific mutations, and some sets of symptoms often segregate together. On this basis, mitochondrial disorders can be considered as a number of different conditions.

1.10.2.1 Chronic Progressive External Ophthalmoplegia (CPEO)

Chronic progressive external ophthalmoplegia is a progressive eye movement disorder, typically involving ptosis (a characteristic drooping of the eyelids) and weakness of the extraocular muscles. Patients are often found to move the entire head to compensate for the loss of peripheral vision caused by the inability to correctly move the eye. Both eyes are usually affected in CPEO, though it is common for symptoms to occur only on one side before eventually affecting both. CPEO is one of the most common symptoms of mitochondrial disease and is a relatively mild disorder, though can be a secondary symptom of some multisystem syndromes such as KSS. As a stand-alone syndrome CPEO can present at any age, though it usually presents in the third or fourth decade of a patient's life (Laforêt *et al.*, 1995; McFarland *et al.*, 2002). In later life, some CPEO patients may begin to suffer from more general muscle weakness and/or wasting, and exercise intolerance as symptoms of more general myopathy (Zeviani and Di Donato, 2004). CPEO is most commonly caused by sporadic single mtDNA deletions, but has also been linked by multiple mtDNA deletions resulting from nuclear mutations and mtDNA point mutations.

1.10.2.2 Kearns-Sayre Syndrome (KSS)

Kearns-Sayre syndrome (MIM 530000) is a multisystem disorder typically caused by sporadic single mtDNA deletions but, as for CPEO, this disorder has also been linked to mtDNA point mutations and nuclear mutations. Onset of KSS typically occurs before 20 years of age, and is clinically characterised by the presence of CPEO and pigmentary retinopathy (Kearns and Sayre, 1958) – these symptoms may be combined with one or more of cerebellar syndrome, diabetes, short stature, increased cerebrospinal fluid protein levels, and heart block (Zeviani and Di Donato, 2004). Histochemically ,this syndrome is associated with high levels of COX-deficiency and ragged red fibres in the muscle (Mita *et al.*, 1989). Interestingly, though the same large-scale mtDNA deletions are capable of causing either CPEO or KSS, evidence has recently come to light that the time at which the deletion is formed may determine the final clinical outcome and which tissues are affected by affecting the final deletion load and tissue distribution of the mtDNA deletion (López-Gallardo *et al.*, 2009).

1.10.2.3 Pearson Syndrome

Pearson marrow-pancreas syndrome (MIM 557000) is the most severe of the three syndromes associated with sporadic single mtDNA deletions, with onset commonly occurring in early infancy. First described in 1979 in four children in the USA by Pearson *et al*, this mitochondrial disorder is characterised by the presence of transfusion-dependent sideroblastic anaemia and exocrine pancreatic dysfunction (Pearson *et al.*, 1979). These two characteristic symptoms are often combined with lactic acidosis, poor growth and neutropaenia, thrombocytopaenia, or pancytopaenia. Clinical symptoms may also include enteropathy and severe renal tubulopathy. Pearson syndrome is often fatal - a combination of early childhood onset and high risks of liver failure or overwhelming lactic acidosis gives a poor patient prognosis – but in cases where patients survive early infancy, a much milder KSS phenotype is often developed (Pitceathly *et al.*, 2012).

1.10.2.4 Myoclonic Epilepsy with Ragged Red Fibres (MERRF)

MERRF is a multisystem disorder brought about by the presence of an mtDNA point mutation. MERRF usually presents in the 2nd or 3rd decade of a patient's life, characteristically developing a combination of symptoms including myoclonic epilepsy, and ragged red fibres in muscle. Additional symptoms include dementia, the development of lipomas, neuropathy, cardiomyopathy, optic nerve atrophy and deafness. The mutation most commonly associated with MERRF, present heteroplasmically in approximately 80 to 90% of all clinical cases, is the A to G transversion at nucleotide 8344 in the $tRNA^{Lys}$ gene (Wu *et al.*, 2010). The remaining clinical cases of MERRF are made up of cases of the much rarer m.8356T>C (Silvestri *et al.*, 1992) and m.8363G>A (Ozawa *et al.*, 1997) point mutations. These tRNA mutations cause multiple complex deficiency of the respiratory chain, most strongly affecting complexes I and IV, due to defective mtDNA translation (Bindoff *et al.*, 1991) .

1.10.2.5 Mitochondrial myopathy, encephalomyopathy, lactic acidosis and stroke-like episodes (MELAS)

MELAS is one of the most commonly occurring mitochondrial diseases, caused by the m.3243A>G point mutation in the $tRNA^{Leu(UUR)}$ gene. First described in 1984 in two children, MELAS was characterised by the presence of ragged red fibres in a muscle biopsy, short stature, seizures, hemiparesis or hemiplegia, visual impairment and lactic acidosis (Pavlakis *et al.*, 1984). Later in the study of this syndrome – following the discovery of the m.3243A>G mutation in 1990 (Goto *et al.*, 1990b) – it was found that the stroke-like episodes which are a prominent feature of MELAS are often preceded by a mild clinical prodrome and are associated with good recovery (Sue *et al.*, 1998). Early in the study of MELAS, prevalence was estimated to be as low as 0.06% (Gerbitz *et al.*, 1995), but more recent studies have shown this to be a much more commons syndrome, present in 0.24% of the Caucasian population (Manwaring *et al.*, 2007). Molecular analyses following the discovery of the m.3243A>G point mutation have also shown that clinical symptoms due to this nucleotide transition may present at any age, and can be responsible for a range of syndromes beyond MELAS, including CPEO, diabetes and deafness, diabetes mellitus or isolated hearing loss . A recent overview of

the clinical phenotypes in 129 patients (from 83 families) suggested that the classical MELAS phenotype associated with the m.3243A>G transition is not actually the most common clinical phenotype to result from this point mutation; 10% of patients exhibited a classical MELAS phenotype, while 30% had MIDD, 6% MELAS/MIDD, 2% MELAS/chronic PEO (CPEO) and 5% MIDD/CPEO overlap syndromes. 6% had PEO and other features of mitochondrial disease not consistent with another recognised syndrome. Isolated sensorineural hearing loss occurred in 3%. Interestingly, 28% of patients presented with clinical features that were not consistent with any of the classical syndromes associated with the m.3243A>G mutation, while 9% of individuals harbouring the mutation were clinically asymptomatic (Nesbitt *et al.*, 2013).

1.10.2.6 MERRF/MELAS overlap syndrome

In rare cases, members of a family can be affected with a syndrome featuring characteristics of both MERRF and MELAS , as first described in 1993 in a three-generation Sardinian family (Zeviani *et al.*, 1993). This disease was found to be caused by a heteroplasmic T to C transition at nucleotide 8356 in the $tRNA^{Lys}$ gene – a mutation which had previously been associated purely with MERRF (Silvestri *et al.*, 1992). Other cases have been identified where two distinct point mutations have been carried by a single family with mitochondrial encephalopathy where symptoms of both MERRF and MELAS may be displayed in individual family members. One notable case followed a family carrying both the common MERRF and MELAS mutations (the 8344 and 3243 point mutations), where the MERRF/MELAS overlap syndrome was clearly displayed (Nakamura *et al.*, 2010).

1.10.2.7 Leber's Hereditary Optic Neuropathy (LHON)

LHON, first described by German ophthalmologist Theodor Leber in 1871 (Leber, 1871a), is a syndrome characterised by severe visual loss, most frequently presenting between the ages of 15 and 55 – though the average age of onset is slightly higher in females (31.3) than males (24.3) (Huoponen, 2001). LHON presents with a marked gender bias, with over 80% of patients being male (Newman *et al.*, 1991), though the reason for this pattern of male predominance remains unknown (Abu-Amero, 2011).

with acute visual loss in one eye. Vision in the second eye is most often affected within one year of the initial presentation, though this can occur within weeks, with most patients progressing to a visual acuity lower than 20/200 in both eyes. In some cases, there may be some visual recovery within a year of the onset of LHON symptoms, and in some rare cases a profound improvement in vision has occurred after many years of impaired vision. While visual loss is the only symptom in most LHON cases, some patients may have cardiac defects or major neurological defects; this more severe clinical presentation is called Leber Plus. Leber Plus may present with basal ganglionic degeneration, spasticity, movement disorders, psychiatric disturbances or encephalopathy (Fraser *et al.*, 2010). First described in 1871, LHON was originally thought to be an X-linked disease (Leber, 1871b), but became linked to mitochondrial dysfunction following the discovery that a point mutation at nucleotide 11778 in the mitochondrial genome resulting in a change of a histidine to an arginine in the ND4 subunit of Complex I was a primary cause of LHON (Wallace *et al.*, 1988). Subsequently, point mutations at nucleotide 3460 in the ND1 gene and nucleotide 14484 in the ND6 gene were also found to cause LHON (Howell *et al.*, 1991; Johns *et al.*, 1992). These three mutations are involved in approximately 90 - 95% of clinical LHON cases, with many other mutations responsible for one or two cases each in the remaining 5 - 10% of cases (Yu-Wai-Man *et al.*, 2009; Fraser *et al.*, 2010). In most cases, individuals with LHON are homoplasmic for the pathogenic mutation, though 10 -15% are heteroplasmic – in these cases, level of heteroplasmy and variances in tissue segregation may be responsible for some of the phenotypic variation between patients. Interestingly, the three primary LHON mutations which usually cause optic atrophy have been found to be responsible for Leber Plus syndrome in some families, demonstrating that specific mutations are not necessarily associated with disease severity (Fraser *et al.*, 2010).

1.10.2.8 Leigh Syndrome

Leigh syndrome was first described in 1951 as a subacute necrotizing encephalopathy – a neurological disorder with striking neuropathological features including necrotic lesions in the basal ganglia, cerebellum or cerebral white matter causing demyelination, vascular proliferation and gliosis (Leigh, 1951). Leigh syndrome presents in a particularly varied clinical manner; while necrotic neural lesions are the

neuropathological hallmark of Leigh disease, clinical symptoms often include – but are not restricted to - psychomotor delay, weakness, hypotonia, truncal ataxia, intention tremor and lactic acidosis (Finsterer, 2008). While Leigh syndrome usually occurs in the first two years of life, rare cases with presentation in youth or young adulthood have been found (Arii and Tanabe, 2000). Leigh syndrome was first linked to mitochondrial dysfunction through an association with COX-deficiency 26 years after its initial discovery (Willems *et al.*, 1977), prior to being associated with a the T to G point mutation at nucleotide 8993 of the ATPase6 gene in maternally inherited cases of Leigh syndrome (Tatuch *et al.*, 1992). Many more pathogenic mutations have since been discovered to cause Leigh syndrome – both in mitochondrial and nuclear genes – with point mutations in the genes coding for subunits of the respiratory chain or assembly factors of respiratory chain complexes being the most common cause of Leigh syndrome or Leigh-like syndrome (a condition which presents with neurological problems atypical of Leigh syndrome) (Finsterer, 2008).

1.10.2.9 Neuropathy, ataxia and Pigmentary Retinopathy (NARP)

Axonal neuropathy characterised by cerebellar and olivopontocerebellar atrophy, gait and limb ataxia and pigmentary retinopathy are the classic hallmarks of NARP, though additional symptoms may include dementia and seizures. As with Leigh syndrome, lactic acid is also found to be elevated in the blood and cerebrospinal fluid. NARP typically manifests in the 2nd decade of life, with slow progression throughout the patient's life. Though NARP is a much less severe syndrome than Leigh disease, these two disorders have been shown to share the same common point mutation, the m.8993T>G transversion in the ATPase 6 gene. Mutation loads of over 90% result in Leigh syndrome, while mutation heteroplasmy levels between 70 and 90% tend to lead to the development of NARP; an individual with less than 70% heteroplasmy for the m.8993T>G point mutation tends to be asymptomatic (Schmiedel *et al.*, 2003).

1.10.2.10 Mitochondrial neurogastrointestinal encephalopathy (MNGIE)

MNGIE is caused by a recessive mutation in the nuclear *TYMP* gene, encoding thymidine phosphorylase – for MNGIE to occur in an individual, both parents must be

heterozygous for the *TYMP* mutation and each parent must pass on the mutated gene copy to the offspring. *TYMP* mutations are known to knock out thymidine kinase activity, allowing a build-up of thymidine to occur in the body, which is disruptive to the normal maintenance and repair of mtDNA. This creates a cellular environment conducive to a build-up of harmful mtDNA mutations, and can also result in mtDNA depletion. MNGIE is characterised by severe gastrointestinal dysmotility and cachexia, ptosis, PEO, sensorimotor neuropathy and asymptomatic leukoencephalopathy, though other symptoms may include hearing loss and demyelinating peripheral neuropathy. Age of onset is very variable in MNGIE, typically occurring between the 2nd and 5th decades of life, and the order in which symptoms manifest and speed at which they progress may also vary between patients (Nishino *et al.*, 2000).

1.10.3 Diagnosis of Mitochondrial Disease

The wide range of symptoms with which mitochondrial disease can present complicates the diagnosis process for patients. Patients with suspected mitochondrial disease first undergo an extensive clinical assessment, discussing family history and the extent of any clinical symptoms with a clinician. If it does seem that mitochondrial disease could fit the patient's symptoms, diagnostic tests can be performed to measure blood levels of creatine kinase, lactate and glucose – all potential indicators of mitochondrial function – and blood counts. At this stage, a positive diagnosis of mitochondrial disease may be made, though negative results do not necessarily exclude the possibility of a mitochondrial disorder (Munnich and Rustin, 2001).

Following these initial tests, if a definitive diagnosis of mitochondrial disease has not been found, a muscle biopsy must be taken for analysis. This 'gold standard' of diagnosis allows for histological, biochemical and molecular analyses to be carried out to diagnose respiratory chain deficiency (Taylor *et al.*, 2004). Two major histochemical protocols have been established as a starting point to determine the presence of any mitochondrial dysfunction. The modified Gomori one-step trichrome stain (Engel and Cunningham, 1963) is used to visualise any accumulation of mitochondria at the outer edges of the cell; the red component of the trichrome stain is selectively taken up by these subsarcollemal mitochondria, which gave rise to the term 'ragged red fibres' as

in MERRF. Possibly the most important histochemical diagnostic test is the dual-stain for cytochrome *c* oxidase (COX) and succinate dehydrogenase (SDH) (Old and Johnson, 1989a) – *COX*/*SDH* dual staining is explained in full in chapter 2. This two-part histochemical protocol begins with the application of the COX reagent solution, which creates a brown precipitate where cytochrome *c* (a subunit of complex IV in the electron transport chain, involved in ATP production) is active within the muscle fibres, and therefore where the mitochondria are functional. A secondary histochemical assay for SDH (succinate dehydrogenase subunits A and B - fully nuclear-encoded subunits of complex II of the electron transport chain unaffected by mitochondrial DNA mutations) activity is then applied, highlighting any COX-deficient areas with a blue precipitate where they have previously remained unstained for cytochrome *c* activity. When muscle fibres are affected by respiratory chain deficiency, a characteristic mosaic pattern will often be observed throughout the tissue section – there will be COX-deficient and COX-positive fibres present, as well as some fibres classed as 'COX-intermediate', where partial respiratory activity remains (Murphy *et al.*, 2008). The results from the *COX/SDH* histochemistry, particularly in cases which demonstrate low levels of COX-deficiency, must be interpreted with consideration to the patient's age, as low levels of COX-deficient fibres are known to accumulate with age (Brierley *et al.*, 1998; Bodyak *et al.*, 2001). However, a lack of COX-deficient fibres does not necessarily rule out respiratory chain dysfunction, as only defects affecting Complex IV activity will be picked up by this assay.

Biochemical assessment of mitochondrial function can be carried out following the isolation of mitochondria from biopsy tissue. A fresh muscle biopsy sample is preferable to frozen - where the IMM will be damaged, meaning no information regarding overall OXPHOS capacity can be obtained - as a wider series of assays can be carried out using functionally intact mitochondria isolated from fresh tissue (Janssen *et al.*, 2003). In this case, levels of enzyme activity, oxidation, ATP production and flux rates can all be measured; this is of particular use in the diagnosis of paediatric cases, though can narrow down the diagnosis of a specific mitochondrial syndrome for many patients (Taylor *et al.*, 2004; Rodenburg, 2011). However, measurement of PDH complex and individual respiratory chain enzyme activities can still be carried out using mitochondria isolated from frozen tissue (Janssen *et al.*, 2003).

Once a diagnosis of mitochondrial disease has been confirmed, and the potential range of conditions has been narrowed down based upon clinical presentation, family history, and histochemical and biochemical findings, molecular work can begin in order to determine a specific genetic defect. Rearrangements of the mitochondrial genome may be identified via Southern blotting or long-range PCR of the mtDNA, while genetic sequencing may be used to identify point mutations of the mtDNA or nuclear defects (Chinnery and Turnbull, 1997).

1.10.4 Mitochondrial Disease Therapy

Despite huge recent advances in understanding the pathological mechanisms underlying mitochondrial disease and in diagnosing these syndromes, the availability of therapy for these disorders remains small. A cure is yet to be found for any mitochondrial disorder, while therapy has retained a focus upon symptomatic relief (DiMauro *et al.*, 2006). However, opportunities for prevention of transmission are now becoming available to patients, and research is still continuing into potential treatments and further therapies to offer to patients.

1.10.4.1 Early Therapies for Mitochondrial Disease

Early therapies for mitochondrial disease focussed on attempting to restore respiratory function through the application of patient supplementation with substrates, vitamins or electron carriers. These supplements included carnitine, coenzyme Q_{10}, thiamine, succinate, folate and methylene blue (Schon *et al.*, 2010). L-arginine has been used in the treatment of MELAS due to its vasodilatory effects, and treatment of the thymidine phosphorylase defect in MNGIE may be treated temporarily with platelet infusions or permanently with a bone marrow transplant (Schapira, 2012).

1.10.4.2 Symptomatic Relief of Mitochondrial Disease Symptoms

In many cases of mitochondrial disease, surgical intervention is one option which may be considered to alleviate a patient's symptoms. Ptosis, which may be obstructive to vision, can be managed through brow suspension surgery or a levator resection, while cochlear implants have been deemed appropriate for implantation in cases of hearing loss. Tendon release surgery can be used to improve joint mobility in children suffering from progressive neuromuscular disorders, and a tracheotomy or mechanical ventilation may be considered in cases of chronic respiratory failure. In patients displaying a failure to thrive, a gastrostomy tube may be necessary to ensure the intake of a sufficient number of calories (Edmonds, 2004). In patients with MERRF, lipomas may be surgically excised due to patient discomfort but in many cases these will grow back following surgery, often to such a degree that further excisions may be deemed necessary (Holme *et al.*, 1993). With more severe complications, such as acute cardiomyopathy, organ transplant may be considered – this is becoming more accepted in cases of individual organ failure, but remains controversial in cases of multisystem disorder (DiMauro *et al.*, 2006). Other, non-invasive methods of symptomatic relief are available for different manifestations of mitochondrial disease. Examples include diabetes mellitus commonly occurs in patients with MELAS and KSS, and can be managed with dietary intervention and insulin, while anticonvulsants are effective in most cases in controlling the seizures associated with many mitochondrial disorders (DiMauro *et al.*, 2006).

1.10.4.3 Genetic Manipulation

A number of possible approaches to influence the level of mutant mtDNA heteroplasmy have been investigated as potential treatments for mitochondrial disease. In terms of gene therapy, a variety of methods to import wildtype mtDNA into the mitochondria are under investigation; allotopic expression of mitochondrial genes introduced to the nucleus has shown some promise in cultured cells, while xenotopic expression of single subunit enzymes from other species shows some promise in rescuing phenotypes caused by OXPHOS complex defects. Some success has also been had in targeting mtDNA molecules harbouring a mutation with restriction

endonucleases, following nuclear transfection with a specific restriction endonuclease gene. However, these gene therapy treatments are all in very early stages of development, and require research to be carried out in animal models in order to scale up the treatment from single cells in culture to the tissue level in living organisms (Kyriakouli *et al.*, 2008).

Aside from gene therapy approaches, attempts to combat mitochondrial disease via genetic manipulation have focussed upon affecting heteroplasmy, in an attempt to shift the balance of mtDNA in favour of wildtype over mutant copies. Methods to achieve this heteroplasmy shift include inhibiting the replication of mutant mtDNA with peptide nucleic acids without affecting wildtype mtDNA replication, importing RNAs into mitochondria to restore normal function, importing polypeptides into the mitochondria, or selecting for respiratory function by selectively placing pharmacological or metabolic stress on mitochondria with high mutation levels (DiMauro *et al.*, 2006). The induction of muscle regeneration is thought to be a potential method to decrease mutant heteroplasmy specifically in patient muscle. This can be achieved through the recruitment of muscle satellite cells due to stress placed on the muscle via resistance training (Gardner *et al.*, 2007). Finally, the induction of increased amounts of mitochondrial fusion is thought to be one more way of addressing the issue of heteroplasmy. This should encourage a more even distribution of mutant mtDNA molecules, rather than discreet populations of normally functioning mitochondria with low levels of mutation and dysfunctional mitochondria with high levels of mutation. A more even mutation load distribution should ensure that more organelles within the cell remain below the mutation threshold, maintaining normal function, despite no overall decrease in mitochondrial mutation load (DiMauro *et al.*, 2006).

1.10.4.4 Genetic Counselling

Genetic counselling is an important option for mitochondrial disease patients considering having children, as well as providing important information regarding disease progression and prognosis to all affected individuals. However, as mitochondrial disorders are so heterogeneous, giving accurate advice to all patients

concerning the risk of disease for any offspring remains challenging (DiMauro *et al.*, 2006). It has been proposed that, for the purposes of counselling, patients are split into three groups; patients with identified nuclear gene mutations, patients with a respiratory chain defect but no identified mutation, and patients with a known pathogenic mutation in a mitochondrial gene. Counselling is most straightforward in the case of patients with known nuclear mutations, though this group only represent approximately 10% of mitochondrial disease diagnoses (Thorburn and Dahl, 2001; Zhu *et al.*, 2009), as there is a clear pattern of Mendelian inheritance for nuclear mutations. Prenatal diagnosis (PND) can be reliably carried out in the case of known nuclear mutations, reducing the risk of having an affected child (Thorburn and Dahl, 2001). Where a genetic defect has not been identified but a respiratory gene defect has, genetic counselling becomes more difficult. In these cases, family history may imply a mode of inheritance, or risk of transmission may be inferred from a specific clinical presentation or enzymatic defect, but prenatal diagnosis is less likely to be an option, and may be unreliable (Thorburn and Dahl, 2001). Genetic counselling is most difficult for the final patient group, where a pathogenic mutation has been identified in the mitochondrial DNA. Patients with single large-scale deletions can be advised that it is unlikely that this defect will be transmitted to an offspring as these defects tend to be sporadic rather than maternally inherited, though they should be made aware that there are rare circumstances where the mtDNA deletion may still be passed on (DiMauro *et al.*, 2006). Advice is harder to give in the case of mtDNA point mutations; the mutation load in each of the patient's oocytes may be different, and the level of heteroplasmy passed on to a child need bear no relation to the mother's mutation load because of the genetic bottleneck (as discussed in *1.8.1*), so the disease severity with which any offspring may be affected is hard to predict. It is also important to stress to families that having had one unaffected child does not necessarily mean that that mutation may not be passed onto a second child at a much higher level (Thorburn and Dahl, 2001).

1.10.4.5 Prevention of Transmission

Though a cure for mitochondrial disease remains elusive, much progress has been made in preventing the transmission of pathogenic mutations from generation to generation. Prenatal diagnosis can be safely carried out where a nuclear defect is

known to be the cause of disease but is less informative for other causes of mitochondrial disorders, where the lack of correlation between mtDNA deletion heteroplasmy and disease severity restricts predictions of disease presentation or clinical severity (Sallevelt *et al.*, 2013). A more recent alternative, pre-implantation genetic diagnosis (PGD) can now safely be carried out for many mitochondrial disease patients. PGD involves patients undergoing a round of IVF and removing one or two single cells from each successful embryo to test for the genetic defect before selecting embryos with the lowest mutation loads for implantation. Though there is no guarantee that offspring with low levels of mutation will be unaffected, this does reduce the risk of parents having a severely affected child (Bredenoord *et al.*, 2008). The most recent method under investigation to prevent the transmission of mtDNA mutations is pronuclear transfer (Craven *et al.*, 2010). This technique involves the transfer of the pronucleus from a fertilised zygote into an enucleated donor zygote with normally functioning mitochondria. This prevents transmission of maternal mtDNA mutations to the offspring, as only wildtype donor mtDNA will be present in the reconstituted zygote. This technique does however require further research to ensure that the zygote manipulations cause no chromosomal or epigenetic abnormalities, and that the resultant embryo is able to develop normally (Craven *et al.*, 2010).

Chapter Two

Chapter 2

Materials and Methods

2.1 Reagents, equipment, solutions and consumables

2.1.1 Equipment and consumables

2.1.1.1 Equipment

ABI 3130xl genetic analyser	Applied Biosystems
ABI Gene Amp 9700 Thermal Cycler	Applied Biosystems
ABI Veriti 96 well Thermal Cycler	Applied Biosystems
ABI Step-one Plus Real Time PCR system	Applied Biosystems
ABI Prism 7000 sequence detection system	Applied Biosystems
ABI Step one software v2.0	Applied Biosystems
Autoclave	Astell
Balance EK-120A	Salter
Balance: Sartorius Basic	Sartorius
Bench-top Microcentrifuge	Sigma
Bench-top Centrifuge 3-15	Sigma
Binder General Purpose Incubator	Phillip Harris
Cryostat (Cryostar HM 560M)	Microm International
Dry Heat Block	Techne
Electrophoresis power supply model 250EX	Life Technologies
Horizontal Agarose Gel Electrophoresis Systems	Amersham
Laminar Flow hood	Jencons-PLS
Leica Laser-microdissection system	Leica
Nanodrop ND-1000 Spectrophotometer	Labtech International
ND-1000 Software	Labtech International
NANOpureII Water Purification System	Barnstead
OFT 5000 Cryostat	Bright
PALM MicroBeam	Zeiss
PURELAB flex	Elga

UV Gel Documentation System	Flowgen
with AlphaImage series 2200 Software	Flowgen
Vortex Genie 1 Touch Mixer	Wolf Laboratories
Vortex Genie	Scientific Industries

2.1.1.2 Consumables

0.2ml Thin-walled PCR tubes	Biogene
0.5ml Thin-walled PCR tubes	Biogene
1.5ml Eppendorph tubes	Biogene
2.0ml Eppendorf tubes	Biogene
96 Well semi-skirted Plate, with Raised Rim	Starlabs
96 Well Fast Optical Reaction Plates	Applied Biosystems
Aerosol Resistant Pipette Tips	Starlabs
Bioclean Pipette Tips	Rainin
Capstrips, domed	Eppendorph
Coverslips (37 x 58m)	Cellpath
Destaining Bags	Amresco
Electronic Pipettes	Rainin
Expand Long Template PCR system kit	Roche
Falcon Tubes (15ml ad 50ml)	Costar
Gel Extraction Kit	Qiagen
Gilson Pipetteman (P2, P20, P200, P1000)	Anachem
Gloves	Ultrasense
Medical Wipes	Kimberly Clarke
MicroAmp Fast Optical 96 Well Reaction plates	ABI
Microscope Slides (76x26x1.0-1.2mm)	Cellpath
Parafilm	Pechiney plastic packaging
Polyethylenenaphthalate (PEN) Slides	Leica
QIAamp DNA micro kit	Qiagen
Scalpels	Swann Morton
SlideRite 5 Mailer	Cellpath
Slide tray and box	Thermo Scientific

Starseal Advanced Polylefin Film	Thermo Scientific
Superfrost microscope slides	Starlabs
Tissue Extraction Kit	Qiagen
Thermo-Fast 96 Well Plates, Non-skirted	Thermo Scientific
Weigh boats	Heathrow Scientific
Whatman Grade IV filter	Merck

2.1.2 Solutions and Chemicals

2.1.2.1 Solutions

Buffers and solutions were prepared with NANOpure (18 Mega Ohms activity) water.

DNA loading buffer:

0.25% (w/v) Bromophenol Blue

0.25% (w/v) Xylene Cyanol

30% (v/v) Glucerol

Gel Buffer (1l)

100ml 10x TAE

900ml NANOpure water

Electrophoresis buffer (1l)

100ml 10x TAE

900ml NANOpure water

Lysis buffer for single molecule PCR (1ml)

5ml SDS

945ml 10mM EDTA

50µl proteinase K

Lysis buffer (standard, 500µl)

250µl 1% Tween 20

50µl 0.5M TrisHCl pH8.5

195µl dH_2O

5µl proteinase K

0.5M TrisHCl pH8.5

30.275g Trisma base in 500ml dH_20

Phosphate Buffered Saline

Prepared from tablets; 1 tablet in 100ml dH_20

2.1.2.2 Chemicals

2.1.2.2.1 Tissue Preparation

Iso-pentane	Merck
Liquid Nitrogen	BOC
OCT-embedding matrix	Raymond Lamb

2.1.2.2.2 Histological and histochemical reagents

Catalase	Sigma
Cytochrome *c*	*Sigma*
3.3’ Diaminobenzidine Tetrahydrochloride	Sigma
DPX™ Mount	BDH
Ethanol Analar	Merck
Histoclear™	National Diagnostics
Nitro Blue Tetrazolium	Sigma
Phenazine Methosulphate	Sigma
Phosphate Buffered Saline Tablets	Sigma
Sodium Dodecyl Sulohate (SDS)	BDH
Sodium Azide	Sigma
Sodium Succinate	Sigma
Trizma base	Sigma
Tween-20	Sigma

2.1.2.2.3 DNA extraction, amplification and sequencing reagents

Betaine	Sigma
BigDye Terminator v3.1 cycle sequencing kit	Applied Biosystems
DNA Oligonuleotide synthesis	MWG BioTech UK Ltd
DNA Oligonuleotide synthesis	IDT
Dioxynucleotide triphosphates	Roche
dNTPs (pre-prepared, for use with LA Taq)	TaKaRa
ExoSAP-IT	GE Healthcare
Expand Long Template PCR system	Roche
HiDi	Applied Biosystems
LA Taq	TaKaRa
LA buffer	TaKaRa
Phusion polymerase with HF buffer	Fisher Scientific
Primers for real time PCR	Applied Biosystems
Proteinase K solution	Fisher Scientific
Restriction Enzymes (XhoI, BamHI, XcmI, DraI)	New England Biolabs
Tamra labelled probes (18S, ND1, ND4)	Applied Biosystems
Taqman mastermix	Applied Biosystems

2.1.2.2.4 Gel Electrophoresis reagents

1kb DNA ladder	New England BioLabs
Agarose MP	Roche
Bromophenol Blue	Sigma
Ethidium bromide	Merck
GelRed nucleic acid stain	Biotium
Glycerol	Sigma
Tris acetate EDTA (TAE:10X)	Sigma
Xylene cyanol	Sigma

2.1.2.3 Histochemical Solutions

COX stock solutions

Diaminobenzidine

5mM DAB in 0.2M phosphate buffer pH 7.0

Stored in 800µl aliquots

Cytochorome c

500µM cytochrome c in 0.2M phosphate buffer pH 7.0

Stored in 200µl aliquots

SDH stock solutions

Sodium succinate

1.3M sodium succinate in 0.2M phosphate buffer pH 7.0

Stored in 300µl aliquots

NitroBlue Tetrazolium

1.875mM NBT in 0.2M phosphate buffer pH 7.0

Stored in 800µl aliquots

Phenazine methosulphate

2mM PMS in 0.2M phosphate buffer pH 7.0

Stored in 150µl aliquots

Sodium azide

100mM sodium azide in 0.2M phosphate buffer pH 7.0

Stored in 50µl aliquots

2.2 Methods

2.2.1 Patient samples

The majority of patient samples used are from patients referred to the NCG Mitochondrial Diagnostic Laboratory, Newcastle Upon Tyne. All samples were taken with informed consent, and patient anonymity was maintained at all times.

2.2.1.1 Patient DNA samples

Patient DNA samples were extracted from tissue by the NCG Mitochondrial Diagnostic Laboratory, Newcastle Upon Tyne. The majority of patient DNA samples were extracted from skeletal muscle samples, though a small proportion of DNA samples were extracted from blood or urine. Samples were requested in volumes of 5 – 10µl and stored at -20^{o}C until needed.

2.2.1.2 Patient tissue samples

All tissue used in this study was skeletal muscle tissue, isolated from the mid-portion of the *Vastus Lateralis*, apart from patients 2 and 3 in Chapter 3 (see *3.3.3*), where skeletal muscle tissue was isolated by open biopsy from the biceps brachii muscle. Tissue blocks were mounted onto Whatmen grade IV filter paper using OCR adhesive and snap-frozen by immersion into iso-pentane which had been pre-cooled to -160^{o}C in liquid nitrogen. Mounted tissue blocks were stored at -80^{o}C.

Tissue was sectioned at -19^{o}C using the OFT 5000 Cryostat or the Cryo-star HM 560M cryostat, with the blade set at -21^{o}C. Muscle sections were taken at a thickness of 20µm and mounted on SuperFrost glass slides or Polyethylenenaphthalate (PEN) membrane slides. Sections were air-dried for an hour before being stored in airtight containers at -20^{o}C until required.

2.2.2 Dual cytochrome c oxidase (COX) and succinate dehydrogenase (SDH) histochemistry

COX/SDH histochemistry (Old and Johnson, 1989b) was performed on frozen muscle sections to assess complex II and IV activity. Muscle sections were defrosted in slide mailers for 30 minutes, then air dried for one hour. The COX incubation medium was prepared by adding 200µl of 500µM cytochrome c to 800µl of 5mM diaminobenzidine and approximately 20µg of catalase. This solution was mixed well using a bench-top vortex, and then applied in sufficient volume (approximately 200µl) to each section to ensure the entire tissue section is covered. The slides were incubated for 45 minutes at 37^{o}C in a humidified chamber, and then washed twice with PBS to remove any excess COX incubation medium.

The SDH incubation medium was prepared by adding 100µl of sodium succinate, 100µl of PMS and 10µl of sodium azide to 800µl of NBT. This solution was mixed well using a bench-top vortex, and then applied in sufficient volume (approximately 200µl) to each section to ensure the entire tissue section is covered. Again, the slides were incubated for 45 minutes at 37^{o}C in a humidified chamber, and then washed twice with PBS to remove any excess COX incubation medium.

The sections were dehydrated by passing the slides through a graded ethanol series – 75%, 95%, 2 x 100% - and were left in the final 100% ethanol bath for 10 minutes. PEN-membrane slides were left at this stage to air-dry for 1 hour before being stored in an airtight container at -20^{o}C until required for use. Glass slides were cleared through two stages of Histoclear™ and then mounted in DPX™ before the addition of a coverslip.

2.2.2.1. Dual cytochrome c oxidase (COX) and succinate dehydrogenase (SDH) histochemistry in serial sections

Where single muscle fibres were to be isolated from tissue sections for mtDNA analysis, a minimum of 3 slides of serial sections would be cut and stained as below (Table 2.1).

Slide type	Number of tissue sections	Histochemical stain
Glass, Superfrost	1	COX/SDH
PEN-membrane	3	SDH only
Glass, Superfrost	1	COX/SDH

Table 2.1 – Histochemical assessment of COX/SDH activity in serial sections

Evidence suggests that the COX histochemical stain may affect mtDNA copy number, while the SDH histochemical stain has no such effect, so sections from which single muscle fibres were to be isolated for mtDNA analysis were assessed for SDH activity only (Murphy *et al.*, 2012). Sections which had been assessed for dual COX/SDH histochemistry were then used as maps of biochemical activity for serial sections treated only with the SDH histochemical stain in order to allow an assessment of COX-activity in individual fibres.

2.2.3 DNA extraction

2.2.3.1 Extraction of DNA from homogenate tissue.

DNA was extracted from homogenate muscle tissue samples using the QIAGEN DNeasy blood and tissue extraction kit. Samples of frozen tissue were added to 180µl Buffer ATL and equilibrated to room temperature. 20µl proteinase K was then added, and mixed thoroughly by vortexing for 15 seconds. This mixture was then incubated at 56°C, with occasional agitation, until the tissue was completely lysed. (Lysis was usually complete in 1–3 hours.) The sample was then mixed thoroughly by vortexing for 15 seconds, before adding 200µl Buffer AL to the sample and thoroughly vortexing again. 200µl of 100% ethanol was added to the sample next, before mixing again thoroughly by vortexing. The resulting lysate, including any precipitate, was then transferred by

pipette into a DNeasy Mini spin column which was placed in a 2 ml collection tube. The lysate was passed through the spin column membrane by centrifugation 6000 x g; the collection tube and any flow-through it contained was discarded after this step. The DNeasy Mini spin column was subsequently placed in a new 2 ml collection tube. 500µl Buffer AW1 was added to the spin column membrane, and this underwent centrifugation for 1 minute at 6000 x g. The collection tube and any flow-through were again discarded at this point, and the DNeasy Mini spin column was placed in another new 2 ml collection tube. 500µl Buffer AW2 was added to the spin column membrane, and this underwent centrifugation for 3 minutes at 20,000 x g to dry the DNeasy spin column membrane. Discard flow-through and collection tube. The collection tube and flow-through were again discarded at this point, and the DNeasy Mini spin column placed in a clean 1.5 ml or 2 ml microcentrifuge tube. 200µl Buffer AE was added onto the DNeasy membrane, and the spin column allowed to incubate at room temperature for 1 minute before undergoing centrifugation for 1 minute at 6000 x g to elute the DNA into the microcentrifuge tube. This was then stored at -20^{o}C until required.

2.2.3.2 Single fibre isolation and lysis

2.2.3.2.1 Single cell isolation and lysis, standard method

Individual cells were captured by laser microdissection into the caps of 0.5ml eppendorph tubes. 15µl of lysis buffer containing 1%Tween-20, 0.5M Tris-HCl pH8.5 and proteinase K was then added to the cap of each tube, before mixing vigorously for 20 to 30 seconds using a bench-top vortex. In a bench-top centrifuge, these single cells were then spun at 16,000 x g for 5 minutes to accumulate the isolated cell and lysis buffer at the bottom of the eppendorph tube. The isolated cells were incubated at 55°C in a humidified chamber for 2 hour to complete cell lysis, before denaturing the proteinase K with a single 10 minute incubation at 95^{o}C.

2.2.3.2.2 Single cell isolation and lysis for smPCR, using Leica AS-LMD

Individual cells were captured by laser microdissection into the caps of 0.5ml eppendorph tubes. 5µl of lysis buffer (0.5% SDS, 10mM EDTA, 5% proteinase K) was

then added to the cap of each tube, before mixing vigorously for 20 to 30 seconds using a bench-top vortex. In a bench-top centrifuge, these single cells were then spun at 16,000 x g for 5 minutes to accumulate the isolated cell and lysis buffer at the bottom of the eppendorph tube. The isolated cells were incubated at 37°C in a humidified chamber for 1 hour, prior to the addition of 5µl of dH2O; this was gently mixed into the lysate solution by pipetting up and down. The fibres were then returned to 37°C in a humidified chamber for 1 further hour, before the addition of 10µl of TE. This was the 10^-1 dilution. This was mixed well using a bench-top vortex, and stored at -80°C until needed.

2.2.3.2.3 Single cell isolation and lysis for smPCR, using Zeiss PALM LMD

Individual cells were captured by laser microdissection into 20µl of lysis buffer (0.5% SDS, 10mM EDTA, 5% proteinase K) in the cap of a 0.5ml eppendorph tube. In a bench-top centrifuge, these single cells were spun at 16,000 x g for 5 minutes to accumulate the isolated cell and lysis buffer at the bottom of the eppendorph tube. The isolated cells were incubated at 37°C in a humidified chamber for 2 hours. Due to capture into a larger volume of lysis buffer, no further dilution was required at this stage. The cell lysate was mixed well using a bench-top vortex, and stored at -80°C until needed.

2.2.4 Polymerase Chain Reaction (PCR) based methods

Polymerase chain reactions (PCRs) were used to amplify target areas of the mitochondrial genome. Specific primers were designed to flank each area of interest; cycling conditions were then designed to be appropriate for the oligonucleotides, length of template DNA required to be amplified, and the polymerase used. Long range and single molecule PCRs used a Gene Amp 9700 Thermal Cycler or a Veriti 96 well Thermal Cycler, while real-time PCR was carried out using a Step-one Plus Real Time PCR system.

2.2.4.1 Primer design

All primers were designed according to the revised Cambridge Reference Sequence (rCRS- GenBank No. NC_012920), and were obtained from MWG BioTech or Integrated DNA technologies. Primers were designed to avoid hairpin structures and dimer formation, as these could limit PCR efficiency, and primer pairs were designed together to limit T_m differences. All primers were re-suspended in sterile water to a stock concentration of 200µl, and stored at -20^{o}C until required.

2.2.4.2 Long range PCR

2.2.4.2.1 TaKaRa LATaq long range PCR

Homogenate DNA isolated from tissue, by myself or the NCG Mitochondrial Diagnostic Laboratory, was amplified using this technique. All reactions were set-up on the bench-top, as the assay is relatively insensitive to contamination. The primers were situated approximately 10kb apart (NC_012920.1, 5875 – 15896bp), and were designed to flank a majority of the major arc of the mitochondrial genome. For the PCR reaction ~100ng of DNA was added to PCR mastermix (dH2O, LA Taq buffer (TaKaRa), 10mM dNTPs, 20mM forward and reverse primers and LA Taq enzyme (TaKaRa), to a total volume of 50µl. Amplifications were carried out using a thermal cycler (GeneAmp® PCR System 9600, Applied Biosystems) with the following cycling conditions: 94°C for 1 minute; 35 cycles of 94°C for 30 seconds, 58°C for 30 seconds and 68°C for 11 minutes; final extension of 72°C for 10 minutes.

2.2.4.2.2 Roche expand long template PCR

Long range PCR of mtDNA extracted from single fibres was accomplished using a two-step protocol (Expand Long Template PCR system®) to amplify regions of the major arc of the mitochondrial genome. A two-step protocol is used to increase the efficiency of the assay when using only small amounts of DNA. All reactions were set up in a UV hood and a prior 20 minute UV exposure to materials was carried out to prevent contamination. The first round amplification used 1µl of DNA as a template, and the reaction mix comprised 1x reaction buffer (Roche), 0.35mM dNTPs, 1mg/ml BSA 0.75µl enzyme mix and 30pmol of each primer set in a total volume of 50µl. Amplifications

were carried out using a thermal cycler (GeneAmp® PCR System 9600, Applied Biosystems) with the following cycling conditions: 3 minutes as 93˚C; 10 cycles of 93˚C for 30 seconds, 58˚C for 30 seconds and 68˚C for 12 minutes; 20 cycles of 93˚C for 30 seconds, 58˚C for 30 seconds and 68˚C for 12 minutes + 5 seconds per additional cycle; and a final extension of 11 minutes at 68˚C.

The PCR product was then diluted 1:20 and 1µl was used as a template in the second round PCR which again, was set up in the UV hood. Identical reaction buffer mix was used as in the first round PCR with identical cycle conditions.

2.2.4.2.3 AmpliTaq Gold PCR

Standard PCR reactions using AmpliTaq Gold were carried out to amplify mtDNA fragments for sequencing, and to generate ND1 and ND4 templates for copy number analysis with real-time PCR. The two-step protocol, used to increase the efficiency of the assay, was carried out on the bench-top. Each reaction was performed in a volume of 25µl.

The first round amplification used 1µl of DNA as a template, and the reaction mix consisted of 16.87µl of autoclaved water, 2.5µl of 10 x dNTP's (ROVALAB), 2.5µl of 10 x PCR buffer (10mM Tris-HCl pH8.3 15mM MgCl2, 50mM KCL, 0.001% w/v gelatine), 0.13µl of AmpliTaq Gold® DNA polymerase (Applied Biosystems), and 1µl of both forward and reverse primer at 20µM (Table 2.2, Table 2.3). 1µl of wild type (WT) blood DNA was used as a positive control, while 1µl of dH2O was used as a negative control. Reactions were carried out using a thermal cycler (GeneAmp® PCR System 9600, Applied Biosystems) with the following cycling conditions: 95^{o}C for ten minutes, thirty cycles of: 94^{o}C for forty five seconds (denaturing), 58^{o}C for forty five seconds (annealing), and 72^{o}C for one minute (extension), with a final extension of 72^{o}C for eight minutes.

1µl of the first round PCR product was then used as a template in the second round PCR. An almost identical reaction buffer mix was used as in the first round PCR, with only adjustment being a different primer pair nested inside the first pair(Table 2.4, Table 2.5), with identical cycle conditions.

First round primers			
Primers	**Primer position**		**Size (incl primer)**
	Forward	**Reverse**	
A	627-646	3087-3068	2460
B	2395-2415	4653-4633	2258
C	4489-4508	6468-6450	1979
D	6113-6133	8437-8417	2324
E	8128-8147	10516-10487	2388
F	9821-9841	12101-12080	2280
G	11866-11887	13924-13904	2038
H	13721-13742	15997-15978	2276
I	15659-15680	868-847	1778

Table 2.2 - First round primer positions

First round primers	
Primer	**Sequence**
A Forward A Reverse	GCTCACATCACCCCATAAAC GATTACTCCGGTCTGAACTC
B Forward B Reverse	ACCAACAAGTCATTATTACCC TGAGGAAATACTTGATGGCAG
C Forward C Reverse	CCGTCATCTACTCTACCATC GGACGGATCAGACGAAGAG
D Forward D Reverse	AATACCCATCATAATCGGAGG GGTGATGAGGAATAGTGTAAG
E Forward E Reverse	AACCACTTTCACCGCTACAC AGTGAGATGGTAAATGCTAG
F Forward F Reverse	ACTTCACGTCATTATTGGCTC ATAGGAGGAGAATGGGGGATAG
G Forward G Reverse	ACCCCCCACTATTAACCTACTG GGTAGAATCCGAGTATGTTGG
H Forward H Reverse	TATTCGCAGGATTTCTCATTAC AGCTTTGGGTGCTAATGGTG
I Forward I Reverse	CCCATCCTCCATATATCCAAAC GGTTAGTATAGCTTAGTTAAAC

Table 2.3 - First round primer sequences

Second Round Primers			
Primers	**Primer Position**		**Size (incl primer)**
	Forward	**Reverse**	
1	721-740	1268-1248	548
2	1157-1177	1709-1689	553
3	1650-1671	2193-2175	544
4	2091-2111	2644-2625	536
5	2549-2569	3087-3068	539
6	3017-3036	3374- 3356	558
7	3533-3351	4057-4037	558
8	4005-4025	4577-4556	573
9	4518-4537	5003-4983	486
10	4950-4969	5481-5462	532
11	5367-5386	5924-5906	558
12	5875-5895	6430-6410	556
13	6378-6398	6944-6924	567
14	6863-6882	7396-7376	534
15	7272-7293	7791-7773	520
16	7744-7763	8301-8283	558
17	8196-8215	8740-8720	545
18	8656-8676	9201-9183	546
19	9127-9146	9661-9641	535
20	9607-9627	10147-10128	541
21	10085-10104	10649-10629	565
22	10534-10553	11109-11089	576
23	11054-11074	11605-11586	552
24	11541-11561	12054-12034	514
25	12001-12019	12545-12527	545
26	12498-12517	13009-12991	538
27	12940-12959	13453-13435	514
28	13365-13383	13859-13839	495
29	13790-13809	14374-14356	585
30	14331-14350	14857-14838	527
31	14797-14815	15368-15349	572
32	15316-15334	15896-15877	581
D1	15758-15777	16294-16274	537
D2	16223-16244	129-110	476
D3	15-34	389-370	375
D4	323-343	771-752	449

Table 2.4 - Second round primer positions

Second Round Primers	
Primer	**Sequence**
1 Forward	TGTAAAACGACGGCCAGTTCACCCTCTAAATCACCAG
1 Reverse	CAGGAAACAGCTATGACCGATGGCGGTATATAGGCTGAG
2 Forward	TGTAAAACGACGGCCAGTTTAAAACTCAAAGGACCTGGC
2 Reverse	CAGGAAACAGCTATGACCCTGGTAGTAAGGTGGAGTGGG
3 Forward	TGTAAAACGACGGCCAGTAACTTAACTTGACCGCTCTGAG
3 Reverse	TGTAAAACGACGGCCAGTAACTTAACTTGACCGCTCTGAG
4 Forward	TGTAAAACGACGGCCAGTACTGTTAGTCCAAAGAGGAAC
4 Reverse	CAGGAAACAGCTATGACCTCGTGGAGCCATTCATACAG
5 Forward	TGTAAAACGACGGCCAGTCAGTGACACATGTTTAACGGC
5 Reverse	CAGGAAACAGCTATGACCGATTACTCCGGTCTGAACTC
6 Forward	TGTAAAACGACGGCCAGTCAGCCGCTATTAAAGGTTCG
6 Reverse	CAGGAAACAGCTATGACCGGAGGGGGGTTCATAGTAG
7 Forward	TGTAAAACGACGGCCAGTCCTTAGCTCTCACCATCGC
7 Reverse	CAGGAAACAGCTATGACCAGAGTGCGTCATATGTTGTTC
8 Forward	TGTAAAACGACGGCCAGTAATAAACACCCTCACCACTAC
8 Reverse	CAGGAAACAGCTATGACCGTTTATTTCTAGGCCTACTCAG
9 Forward	TGTAAAACGACGGCCAGTACACTCATCACAGCGCTAAG
9 Reverse	CAGGAAACAGCTATGACCGATTTTGCGTAGCTGGGTTTG
10 Forward	TGTAAAACGACGGCCAGTTCCATCATAGCAGGCAGTTG
10 Reverse	CAGGAAACAGCTATGACCTGTAGGAGTAGCGTGGTAAGG
11 Forward	TGTAAAACGACGGCCAGTACCTCAATCACACTACTCCC
11 Reverse	CAGGAAACAGCTATGACCTAGTCAACGGTCGGCGAAC
12 Forward	TGTAAAACGACGGCCAGTCACTCAGCCATTTTACCTCAC
12 Reverse	CAGGAAACAGCTATGACCATGGCAGGGGGTTTTATATTG
13 Forward	TGTAAAACGACGGCCAGTTTAGGGGCCATCAATTTCATC
13 Reverse	CAGGAAACAGCTATGACCAAGAAAGATGAATCCTAGGGC
14 Forward	TGTAAAACGACGGCCAGTATTTAGCTGACTCGCCACAC
14 Reverse	CAGGAAACAGCTATGACCCATCCATATAGTCACTCCAGG
15 Forward	TGTAAAACGACGGCCAGTGGCTCATTCATTTCTCTAACAG
15 Reverse	CAGGAAACAGCTATGACCGGCAGGATAGTTCAGACGG
16 Forward	TGTAAAACGACGGCCAGTTAACATCTCAGACGCTCAGG
16 Reverse	CAGGAAACAGCTATGACCTACAGTGGGCTCTAGAGGG
17 Forward	TGTAAAACGACGGCCAGTACAGTTTCATGCCCATCGTC
17 Reverse	CAGGAAACAGCTATGACCGTATAAGAGATCAGGTTCGTC
18 Forward	TGTAAAACGACGGCCAGTACCACCCAACAATGACTAATC
18 Reverse	CAGGAAACAGCTATGACCGTTGTCGTGCAGGTAGAGG
19 Forward	TGTAAAACGACGGCCAGTATCCTAGAAATCGCTGTCGC
19 Reverse	CAGGAAACAGCTATGACCATTAGACTATGGTGAGCTCAG
20 Forward	TGTAAAACGACGGCCAGTCATCCGTATTACTCGCATCAG
20 Reverse	CAGGAAACAGCTATGACCTAGCCGTTGAGTTGTGGTAG
21 Forward	TGTAAAACGACGGCCAGTCAACACCCTCCTAGCCTTAC
21 Reverse	CAGGAAACAGCTATGACCAGGCACAATATTGGCTAAGAG
22 Forward	TGTAAAACGACGGCCAGTATCGCTCACACCTCATATCC
22 Reverse	CAGGAAACAGCTATGACCATGATTAGTTCTGTGGCTGTG
23 Forward	TGTAAAACGACGGCCAGTCTAATCTCCCTACAAATCTCC
23 Reverse	CAGGAAACAGCTATGACCTAGGTCTGTTTGTCGTAGGC
24 Forward	TGTAAAACGACGGCCAGTTCCTTGTACTATCCCTATGAG
24 Reverse	CAGGAAACAGCTATGACCCGTGTGAATGAGGGTTTTATG
25 Forward	TGTAAAACGACGGCCAGTACAATGGGGCTCACTCACC
25 Reverse	CAGGAAACAGCTATGACCGTGGCTCAGTGTCAGTTCG
26 Forward	TGTAAAACGACGGCCAGTCATGTGCCTAGACCAAGAAG

26 Reverse	CAGGAAACAGCTATGACCCTGATTTGCCTGCTGCTGC
27 Forward	TGTAAAACGACGGCCAGTGCCCTTCTAAACGCTAATCC
27 Reverse	CAGGAAACAGCTATGACCGGGAGGTTGAAGTGAGAGG
28 Forward	TGTAAAACGACGGCCAGTCGGGTCCATCATCCACAAC
28 Reverse	CAGGAAACAGCTATGACCGTTAGGTAGTTGAGGTCTAGG
29 Forward	TGTAAAACGACGGCCAGTACCTAAAACTCACAGCCCTC
29 Reverse	CAGGAAACAGCTATGACCAGGATTGGTGCTGTGGGTG
30 Forward	TGTAAAACGACGGCCAGTCAACCACCACCCCATCATAC
30 Reverse	CAGGAAACAGCTATGACCAAGGAGTGAGCCGAAGTTTC
31 Forward	TGTAAAACGACGGCCAGTATTCATCGACCTCCCCACC
31 Reverse	CAGGAAACAGCTATGACCGGTTGTTTGATCCCGTTTCG
32 Forward	TGTAAAACGACGGCCAGTAGCCCTAGCAACACTCCAC
32 Reverse	CAGGAAACAGCTATGACCTACAAGGACAGGCCCATTTG
D1 Forward	TGTAAAACGACGGCCAGTATCGGAGGACAACCAGTAAG
D1 Reverse	CAGGAAACAGCTATGACCGTGGGTAGGTTTGTTGGTATC
D2 Forward	TGTAAAACGACGGCCAGTCTCAACTATCACACATCAACTG
D2 Reverse	CAGGAAACAGCTATGACCAGATACTGCGACATAGGGTG
D3 Forward	TGTAAAACGACGGCCAGTCACCCTATTAACCACTCACG
D3 Reverse	CAGGAAACAGCTATGACCCTGGTTAGGCTGGTGTTAGG
D4 Forward	TGTAAAACGACGGCCAGTGCCACAGCACTTAAACACATC
D4 Reverse	CAGGAAACAGCTATGACCTGCTGCGTGCTTGATGCTTG

Table 2.5 - Second round primer sequences

2.2.4.3 Agarose gel electrophoresis

Agarose was dissolved in a 1x TAE buffer by heating in a microwave until boiling – the concentration of agarose was varied according to the level of PCR product separation that was required. 4µl of GelRed per 100mls agarose gel was then added to the solution, for DNA visualisation. The solution was poured into a cast, with a 20-prong comb insert to form loading wells, and allowed to set before use.

Approximately 1µl loading dye was added to each PCR product and mixed thoroughly by pipetting. 5µl of each PCR product/loading dye solution was then subsequently loaded into an agarose gel well. An appropriate commercially available base pair ladder was also loaded onto the gel to allow for sizing of the separated PCR products. Gels were electrophoresed in a tank containing 1x TAE buffer at 70 volts until products were sufficiently separated. PCR products were visualised using UV light.

2.2.4.4 Single molecule PCR

2.2.4.4.1 First round PCR

For single molecule PCR, the cell lysates from the above stage needed to be diluted – initial dilutions of 1:10 and 1:100 were made, to give concentrations of 10^{-2} and 10^{-3}. Dilutions were made in Tris-EDTA (TE) buffer - 5µl template: 45µl TE for 1:10, and 5µl (1:10): 45µl TE for 1:100.

Once the serial dilutions of template mtDNA had been performed, the first round PCR mastermix was made up (100x master-mix for a 96 well plate - 200µl buffer, 200µl betaine, 150µl dNTPs, 50µl primer 2999F, 50µl primer 2949R, 10µl bromophenol blue, 4µl Phusion™ polymerase, and 243.6µl dH_20) (Table 2.6). This mastermix was split into aliquots of 150µl in six 0.5ml eppendorph tubes. 14.4µl of 10^{-2} template DNA was added to into each 'mini-mix' and mixed well using a bench-top vortex giving a template DNA concentration of 9 x 10^{-2} for the first round of smPCR. 10µl of mini-mix/template DNA solution was then distributed into each well of a 96-well plate, touching the bottom of each well with the pipette tip (2 x 8-well-rows per sample, 6 samples per plate). A drop of oil was then added to each well. The plate was sealed, pulse spun down using a centrifuge, and then kept on ice until a PCR machine was up to temperature to start the first-round PCR run. First round smPCR cycle conditions were: 94°C for 1 minute, then 35 cycles of 94°C for 20 seconds, 68°C for 16 minutes; hold at 4°C.

2.2.4.4.2 Second round PCR

Using a multi-channel pipette, 1.6µl first round smPCR product from each well was transferred to a clean 96-well plate; a drop of oil was then added on top of the PCR product in each well of the new plate while the second round master-mix was made. The plate was pulse spun down the plate using a centrifuge. The plate was kept on ice while the second round smPCR master-mix was made up (100x master-mix for a 96 well plate – 530µl dH20, 100µl LA Buffer, 150µl dNTPs, 100µl primer 3160F, 100µl primer 2494R, 10µl bromophenol blue, 10µl LA Taq)(Table 2.6). 10µl second round smPCR master-mix was added into each well, on top of the oil, and then the plate was

pulse spun down using a centrifuge. The plate was kept on ice until a PCR machine was up to temperature to start the second-round PCR run. Second round smPCR cycle conditions were: 94°C for 1 minute, then 20 cycles of 94°C for 20 seconds, 68°C for 16 minutes; hold at 4°C.

	Single molecule PCR primers		
Primer	**Primer position**	**Sequence**	**Size (inc. primers)**
2999F	2999 – 3028	GTCCTGTAGGGCTACCACGTCGGCGATAAT	16,519
2949R	2918 - 2949	GGATTGCGCTGTTATCCCTAGGGTAACTTGTT	
3160F	3160 - 3191	TCGCGGAAGGGGGCATTTACTATAGTAGAGTT	15,903
2494R	2462 - 2494	GCGGGGTAAGATTTGCCGAGTTCCTTTTACTT	

Table 2.6 - Single molecule PCR primer positions and sequences

2.2.4.4.3 Agarose gel electrophoresis

Agarose was dissolved in a 1x TAE buffer by heating in a microwave until boiling – the concentration of agarose was varied according to the level of PCR product separation that was required. 4µl of GelRed per 100mls agarose gel was then added to the solution, for DNA visualisation. The solution was poured into a cast, with a 20-prong comb insert to form loading wells, and allowed to set before use.

Using a multi-channel pipette, approximately 1µl loading dye was added to each well of the smPCR plate and mixed with the PCR products. 5µl of this mixture from each well was then subsequently loaded into an agarose gel well. An appropriate commercially available base pair ladder was also loaded onto the gel to allow for sizing of the separated PCR products. Gels were electrophoresed in a tank containing 1x TAE buffer at 70 volts until products were sufficiently separated. PCR products were visualised using UV light.

2.2.4.4.4 Result interpretation

To ensure that there were enough smPCR product bands to analyse, while at a low enough quantity to be sure that each well started with s single mtDNA molecule to amplify, the aim was to have ~¼ wells successfully amplify a PCR product. If no bands, or too few product bands were obtained, the DNA concentration per well for first round PCR needed to be increased, 2 rows total per DNA sample as below:

4 wells of 5 x 10^{-2}/well, + 15µl MM (total 20µl/well)

4 wells of 3 x 10^{-2}/well, + 17µl MM (total 20µl/well)

8 wells of 1 x 10^{-2}/well; make a 90µl MM + 9µl of 10^{-2} template, aliquot 10µl/well (total 10µl/well)

If a higher proportion of wells produced product bands, the starting DNA concentration needed to be diluted according to calculations from the Poisson distribution table (Table 2.7) and the smPCR protocol repeated. The level of dilution required involved working out the fraction of positive well results from a sample (e.g. 8 wells out of 16 would be 0.5), and from this obtain the 'true number' of copies per sample from Table 2.7 (working fraction of 0.5 would gave a 'true number' of copies of 0.69). To ensure that the PCR is being run at single molecule level, 1/4 successful gel lanes should be aimed for (i.e. a 0.25 success rate, with a 'true' success rate of 0.29). This gives the ratio of observed to desired success rate (0.69/0.29, or 2.4, in this example). The original quantity of template DNA per well was then divided by the observed: desired ratio, to calculate the optimal concentration to run smPCR with this sample.

Fraction of positives 1-p(0)	True no of copies per sample	fraction of doublets p(2)	fraction of multiplets 1-p(0)-p(1)
0	-	-	-
0.05	0.05	0	0
0.1	0.11	0	0.01
0.15	0.16	0.01	0.01
0.2	0.22	0.02	0.02
0.25	0.29	0.03	0.03
0.3	0.36	0.04	0.05
0.35	0.43	0.06	0.07
0.4	0.51	0.08	0.09
0.45	0.6	0.1	0.12
0.5	0.69	0.12	0.15
0.55	0.8	0.14	0.19
0.6	0.92	0.17	0.23
0.65	1.05	0.19	0.28
0.7	1.2	0.22	0.34
0.74	1.35	0.24	0.39
0.75	1.39	0.24	0.4
0.8	1.61	0.26	0.48
0.85	1.9	0.27	0.57
0.9	2.3	0.27	0.67
0.925	2.59	0.25	0.73
0.9333	2.71	0.24	0.75
0.95	3	0.22	0.8

Table 2.7 – Poisson distribution table

2.2.4.5 Real-time PCR (qPCR)

2.2.4.5.1 Detection of mtDNA deletions by real-time PCR

Deletions in the mitochondrial genome were detected and quantified using a multiplex real-time PCR method, *MTND1/MTND4* qPCR, as described by Krishnan *et al.* (Krishnan *et al.*, 2007). The ND1 gene (*MTND1*) lies within the minor arc of the mitochondrial genome, an area rarely involved in deletions, while the ND4 gene (*MTND4*) is encoded within an area of the major arc of the mitochondrial genome taken out in almost every large-scale mtDNA deletion. The difference in the relative proportions of these genes, as measured by quantitative PCR, can then be used as an accurate indication of mtDNA deletions present in tissue samples or lysed single cells.

Primers were designed to flank the *MTND1* and *MTND4* regions of the genome, in order to specifically amplify these two regions. Fluorescently-tagged (VIC and FAM) probes were also designed to bind to these specific areas (Table 2.8, Table 2.9); the fluorescent dye was inactivated using a TAMRA quencher. The quencher is removed from the fluorescently-tagged probe by the 5'nuclease of the DNA polymerase once the probe has annealed, allowing a fluorescent signal to be emitted to indicate specific amplification. The intensity of this fluorescent signal was measured throughout the real-time PCR run to quantify levels of DNA amplification, and was compared to the fluorescent signal of a passive reference dye for normalization.

Real-time PCR reactions were all set up in the UV-hood in 96-well plates, and all samples were run in triplicate. Each plate was run with 6 wells of no-template control, and triplicates of a blood sample and 3 deletion standards. No-template control wells were to ensure that there was no DNA contamination in any reagents or consumables, and the deletion standards were to check that the deletion levels calculated from the relative levels of ND1 and ND4 were accurate on each run. Any deletion level detected in the blood sample was subtracted from all other sample results. Each well contained 1µl of template DNA and 24µl of reaction mastermix containing 12.5µl TaqMan Universal mastermix, 0.5µl ND1 probe (5µM stock), 0.5µl ND4 probe (5µM stock), 0.75 ND1 forward primer (10µM working stock), 0.75 ND1 reverse primer (10µM working stock), 0.75 ND4 forward primer (10µM working stock), 0.75 ND4 reverse primer (10µM working stock) and 7.5µl dH20. The plate was sealed using a MicroAmp™

Optical Adhesive Film and centrifuged down. Real-time PCR plates were run on an ABI Step-one Plus Real Time PCR system. Reaction cycle conditions were: 2 minutes at 50^{o}C, 10 minutes at 95^{o}C, and then 40 cycles of 15 seconds at 95^{o}C and 1 minute at 60^{o}C.

When the plate had been completely processed by the ABI Step-one Plus Real Time PCR system, results were exported from the machine into a spread sheet format, and analysed using Microsoft Excel. Average Ct values were calculated from the triplicate runs of each sample, where Ct is the cycle threshold (the cycle number at which the level of DNA amplification exceeded a pre-determined threshold), and a ΔCt was calculated by subtracting the average ND1 Ct value from the average ND4 Ct value. The ΔCt is indicative of the difference between wildtype (ND4) and total (ND1) mtDNA levels, and so mtDNA deletion heteroplasmy can be calculated from this value. First, the ΔCt of the blood sample was subtracted from all other data sets, to increase accuracy of calculated deletion levels. The percentage mtDNA deletion heteroplasmy level was then calculated with the equation:

%deletion = (1-(2^-ΔCt))*100.

2.2.4.5.2 Detection of relative mtDNA copy number by real-time PCR

The multiplex qPCR assay outlined above can be run in conjunction with one further assay, to amplify and detect 18S rRNA, to measure depletion of mitochondrial DNA. 18S rRNA is a nuclear gene, so amplification of *MTND1* alongside this allows for calculation of the number of mtDNA copies relative to nuclear DNA. As 18S rRNA is a multi-copy gene present in an unknown quantity in each sample, it is not possible to accurately quantify absolute mtDNA copy number using this method. However, relative copy number can be compared to an appropriate control to determine whether there is evidence of mtDNA depletion. This assay is only appropriate for use with tissue samples, as 18S rRNA is not present in a sufficient quantity for detection by qPCR in single lysed cells.

Amplification of 18S rRNA was run alongside the ND1/ND4 assay to allow for simultaneous screening of mtDNA deletion level and depletion in a single real-time

PCR run. Primers were designed to specifically flank to 18S rRNA region, and a fluorescent FAM-tagged probe – inactivated by a TAMRA quencher until bound - was designed to specifically bind to amplified 18S rRNA (Table 2.8, Table 2.9). 3 extra standards with known mtDNA copy number were run in triplicate alongside samples when running the 18S rRNA assay, to ensure that all results were as accurate as possible.

As for the ND1/ND4 qPCR assay, all 18S rRNA real-time PCR reactions were all set up in the UV-hood in 96-well plates, and all samples were run in triplicate. Each well for the 18S rRNA qPCR assay contained 1µl of template DNA and 24µl of reaction mastermix containing 12.5µl TaqMan Universal mastermix, 0.75µl 18S rRNA probe (5µM stock), 0.13 18S rRNA forward primer (10µM working stock), 0.75 18S rRNA reverse primer (10µM working stock) and 9.87µl dH20. The plate was sealed using a MicroAmp™ Optical Adhesive Film and centrifuged down. Real-time PCR plates were run on an ABI Step-one Plus Real Time PCR system. Reaction cycle conditions were: 2 minutes at 50^{o}C, 10 minutes at 95^{o}C, and then 40 cycles of 15 seconds at 95^{o}C and 1 minute at 60^{o}C.

To quantify the amount of *MTND1* present in a sample compared to 18S rRNA, average Ct values were first calculated from the triplicate runs of each sample. A ΔCt for each sample was then calculated by subtracting the average 18S rRNA Ct value from the average ND1 Ct value. The samples were normalised to the blood control by subtracting the blood ΔCt from all other sample ΔCt values. Relative mtDNA copy number could then be calculated using the equation $R = 2^{-\Delta Ct}$. The ΔCt is indicative of the difference between wildtype (ND4) and total (ND1) mtDNA levels, and so mtDNA deletion heteroplasmy can be calculated from this value. First, the ΔCt of the blood sample was subtracted from all other data sets, to increase accuracy of calculated deletion levels. The percentage mtDNA deletion heteroplasmy level was then calculated with the equation %deletion = (1-(2^-ΔCt))*100.

Real time PCR primers		
Primer	**Primer position**	
	Forward	**Reverse**
ND1	L 3485 – 3504	H 3506 – 3553
ND4	L 12087 - 12109	H 12170 - 12140
18S	L 1050 - 1071	H 1115 - 1135

Table 2.8 - Real time PCR primer and probe positions

Real time PCR primers and probes	
Primer	**Sequence**
ND1 F	CCCTAAAACCCGCCACATCT
ND1 R	GAGCGATGGTGAGAGCTAAGGT
ND1 VIC probe	VIC-5'-CCATCACCCTCTACATCACCGCCC-3'-TAMRA
ND4 F	CCATTCTCCTCCTATCCCTCAAC
ND4 R	CACAATCTGATGTTTTGGTTAAACTATATTT
ND4 FAM probe	FAM-5'-CCGACATCATTACCGGGTTTTCCTCTTG-3'-TAMRA
18S F	GCCGCTAGAGGTGAAATTCTTG
18S R	CATTCTTGGCAAATGCTTTCG
18S FAM probe	FAM-5'-CCGGCGCAAGACGGACCAGA-3'-TAMRA

Table 2.9 - Real time PCR primer and probe sequences

2.2.4.5.3 Generation of DNA templates for copy number standard curves

ND1 and ND4 template DNA was isolated from wildtype DNA using standard long range PCR (primers 6F and 7R for ND1, 25F and 26R for ND4) to give approximately 1kb PCR products. PCR products were run out on a 0.7% agarose gel at 70 volts for 1 hour; products were then excised from the gel with a scalpel, and collected into a 1.5ml eppendorph tube. The amplified DNA templates were then extracted from the gel using a QIAGEN gel extraction kit (quick spin protocol). The gel slice was weighed by comparing the weight of the eppendorph containing the excised gel to an empty

eppendorph; 3 volumes of Buffer QG were then added to one volume of gel (i.e. 300µl of Buffer QG to each 100mg of gel. The eppendorph containing the gel slice and buffer was then incubated at 50^{o}C for 10 minutes, and mixed by vortexing every 2-3 minutes during the incubation. After the gel slice was completely dissolved, the gel slice should have been yellow, indicating that the solution is at pH7.5 and appropriate for use with the QIAquick membrane. If orange or violet, indicating a higher pH, 10µl of 3M sodium acetate pH 5 was added and mixed thoroughly by vortexing, to correct the pH.

When an appropriate pH was achieved, 1 gel volume of isopropanol was added to the sample and mixed. The sample was then applied to a QIAquick column, placed in a 2ml collection tube, and centrifuged for 1 min at 16,000 x g. Flow through was discarded from the collection tube, and the spin column placed back into the same 2ml collection tube. 0.5ml of Buffer QG was then applied to the QIAquick column and centrifuged for 1 minute at 16,000 x g, to remove all traces of agarose from the solution. 0.75ml of Buffer PE was then added to the QIAquick column and centrifuged at 16,000 x g for 1 minute to wash the membrane. All flow-through was then discarded, and the QIAquick spin column was placed back into the same 2ml collection tube. The QIAquick column was then centrifuged for an additional minute at 17.900 x g to remove all residual ethanol from buffer PE. The collection tube and any flow through were then discarded, and the QIAquick column was placed into a clean 1.5ml microcentrifuge tube. To elute the DNA from the membrane in the QIAquick spin column, 50µl of Buffer EB (10mM Tris-Cl, pH 8.5) was added to the QIAquick membrane, and the column was centrifuged for 1 minute at 16,000 x g. DNA is collected in approximately 48µl of elution in the 1.5ml microcentrifuge tube; the spin column was discarded after this step.

The DNA content of the purified DNA was measured using the Nanodrop ND-1000 Spectrophotometer. Isolated template DNA was then sequentially diluted 1 in 10 a total of ten times to create a serially diluted standard curve with known DNA content. The two sets of serial dilutions were then run on a plate of real time PCR, using ND1 or ND4 primers and probe respectively, to assess the levels of template DNA present in each dilution. The resulting Ct values were plotted against log known copy number to obtain a standard curve, from which copy number (total copy number from ND1, wildtype copy number from ND4) for single cells could be estimated.

2.2.4.5.4 Quantification of mtDNA copy number by standard curve in single cells

The ND1/ND4 multiplex qPCR is carried out as standard (*2.2.4.5.1*), including wells for both sets of serial dilutions (*2.2.4.5.3*) to obtain ND1 and ND4 Ct values for all samples. Average Ct values were then calculated for both ND1 and ND4 from each sample. A standard curve was then plotted from each serial dilution - Ct values were plotted against log known copy number - and the equation for this standard curve was calculated. The equation for this standard curve was determined to be $y = x * (Ct + z)$, where y represents $\log_{10}$ of absolute copy number (ND1 Ct value) or absolute wildtype mtDNA copy number (ND4 Ct value) present in 1µl of cell lysate, x is the slope of the standard curve, and z is the value at which the standard curve crosses the y axis. Copy number per unit area of the cell could then be calculated using the equation $cu = (y \times 15)/\text{cell area}$, where *cu* is the copy number per unit area of the cell, and 15 is the total quantity of lysate obtained per cell. Copy number per unit area of the cell, as derived from these two equations, is then a value comparable across all copy number results from single fibres on this ND1/ND4 qPCR run.

2.2.4.5.5 Generation of a universal standard curve for ND1 and ND4 copy number

Through the method outlined above, a new standard curve was required to be generated and run with the samples through the ND1/ND4 qPCR assay for each new set of samples. This was both time-consuming and inefficient, and meant that samples from different batches (i.e. run with separately generated standard curves) did not have comparable results. To resolve this, a universal standard curve needed to be generated. A set of serial dilutions of wildtype mtDNA of known concentration and copy number was prepared by Dr Kim Krishnan. This was run through the ND1/ND4 qPCR assay, as standard (*2.2.4.5.1*) to obtain Ct values for both ND1 and ND4 from each lysed fibre. Average Ct values were calculated for both ND1 and ND4 from each sample. The resulting Ct values were plotted against log known copy number to obtain a standard curve. The equation for this standard curve was determined to be $y = -3.0024 \times (Ct + 40)$, where y represents $\log_{10}$ absolute copy number (ND1 Ct value) or absolute wildtype mtDNA copy number (ND4 Ct value) present in 1µl of cell lysate. Copy number per unit area of the cell could then be calculated using the equation *cu* =

(*y* x 15)/cell area, where *cu* is the copy number per unit area of the cell, and 15 is the total quantity of lysate obtained per cell. Copy number per unit area of the cell, as derived from these two equations, is then a value comparable across all copy number results from single fibres analysed through the ND1/ND4 qPCR assay. Three samples from the original set of serial dilutions, stored in aliquots at -80^{o}C, were then included as copy number standard controls with every plate of real-time PCR for copy number analysis, to ensure that the results from each plate were accurate.

2.2.5 Cycle Sequencing

2.2.5.1 Generation of DNA templates for sequencing

Samples for sequencing were primarily amplified using TaKaRa LA Taq, as outlined in *2.2.4.2.1*. This generated 50µl of PCR product from which to work from throughout the rest of this protocol, and almost every mtDNA deletion for which sequencing was required was captured in the 10kb region of the mitochondrial genome that was amplified by this technique. PCR products were separated by gel electrophoresis, as outlined in *2.2.4.3*, alongside a suitable DNA ladder. As the size of the wildtype PCR product was known to be 10kb, the size of the PCR product obtained from each sample was indicative of the expected mtDNA deletion size (i.e. a 6kb PCR product would indicate a 4kb mtDNA deletion).

2.2.5.2 Restriction endonuclease digest

To more accurately determine where in the amplified 10kb region of the mitochondrial genome the mtDNA deletion was located, a restriction endonuclease digest was performed. In a 200µl thin-walled PCR tube, 5µl ddH_20, 2µl NE Buffer2, 1µl 10 x BSA, 0.25µl Xho1, 0.25µl Bam H1, 0.25µl Xcm1, and 0.25µl Dra1 were mixed thoroughly by vortexing. 2µl of PCR product were then added to the restriction digest buffer, and mixed thoroughly by vortexing. The restriction digest was incubated in a humidified chamber for 1 hour at 37^{o}C. The products from this digest were then separated by gel electrophoresis (*2.2.4.3*), to assess fragment size.

There were predicted sizes for each of the 6 fragments created from this digest of a wildtype mtDNA molecule, and each of these fragment sizes was associated with a section of the mitochondrial genome (Table 2.10, Table 2.11). By determining which of these fragments were present or absent, a predication could be made as to where the mtDNA deletion lay in the genome. A table was consulted, based upon which of these restriction fragments were successfully identified when separated by gel electrophoresis, in order to identify which reverse primer would be most likely to amplify across the mtDNA deletion breakpoint for identification by sequencing (Table 2.11). If this primer was then unsuccessful, a nested primer would then be used, continuing until the deletion breakpoints were identified.

2.2.5.3 Purification of PCR products

Before cycle sequencing, 5µl of each PCR product was transferred to a 96-well plate on ice; 2µl ExoSAP-IT was then added to each sample. ExoSAP-IT, which contains alkaline phosphatase and Exonuclease I, removes any excess primers or deoxynucleotides from the PCR product to prevent interference with downstream sequencing. The plate was then sealed with capstrips, and placed in a GenAmp PCR system 9700. The plate was incubated at 37^{o}C for 15 minutes, to digest primers and dNTPs, followed by 15 minutes at 80^{o}C to denature the components of ExoSAP-IT. The plate was then removed from the thermal cycler and placed back on ice.

2.2.5.4 Cycle Sequencing

BigDye amplification of the purified PCR products was carried out next; 7µl of dH_20, 3µl of 5 x sequencing buffer, 1µl of an appropriate primer (10mM) and 2µl of BigDye® v3.1 were added to each well of the 96-well plate that contained a sample. The plate was re-sealed with capstrips after this step. The plate was then placed back into a GenAmp PCR system 9700 under the following conditions: 1 minute at 96^{o}C, then 25 cycles of 96^{o}C for 10 seconds, 50^{o}C for 5 seconds and 60^{o}C for 4 minutes. At this point the plate could be carried forward straight into the precipitation step, or stored at -20^{o}C until required.

2.2.5.5 Precipitation and sequencing

For the precipitation step, 2µl of 3M sodium acetate, 2µl of 125mM of EDTA and 50µl of 100% Analar ethanol were added to each sample in the 96-well plate. The plate was then sealed with capstrips, inverted 4 times to mix the contents of each individual well, and allowed to incubate for 15 minutes at room temperature. Following this, the plate was spun in a centrifuge at 2090g for 30 minutes, before being unsealed, inverted onto white tissue paper and spun in a centrifuge at 100g for 2 minutes to remove supernatants. 70µl of 70% Analar ethanol was added to each well to wash the sample, and the plate was then sealed and spun at 1650g for 15 minutes. The supernatant was then removed from each well by unsealing the plate, inverting it onto white tissue paper and spinning in a centrifuge at 100g for 2 minutes. The plate was then left to air-dry in the dark for 15 minutes.

Once the plate of samples had been left to dry, 10µl of HiDi formamide was added to each sample, and the plate was heated to 95^{o}C for 2 minutes in a GenAmp PCR system 9700. This incubation was designed to separate the DNA strands for each sample, and HiDi aids this process by lowering the melting point of the DNA. The plate was then placed in an ABI 3130xl Automated DNA Sequencer to run. Using SeqScape software, the fragments were aligned and compared to the Cambridge Reference Sequence (Anderson *et al.*, 1981a).

Position	Expected band size
10416 – 12270	1854
12270 – 135700	1430
13700 – 14257	557
14257 – 14954	697
14954 – 16009	1055
16009 - 16450	441

Table 2.10 - Predicted bands from restriction digest of wildtype mtDNA

441bp	1055bp	697bp	557bp	1430bp	1854bp	Primer
√						16450R
X	√					PINK25R
X	X	√				31R
X	X	X	√			29R
X	X	X	X	√		28R
X	X	X	X	X	√	25R

Table 2.11 - Sequencing primer to use, as predicted by restiction digest

2.2.6 Statistical analysis

Unless stated otherwise, all statistical analysis was carried out using GraphPad Prism v.4 statistical software. Both parametric and non-parametric tests were used and individual tests are stated in the relevant chapters.

Chapter Three

Chapter 3

Analysis of the accumulation of mtDNA deletions longitudinally through skeletal muscle fibres.

3.1 Introduction

3.1.1 Proposed mechanisms of clonal expansion of mtDNA deletions

Elucidating the mechanism by which mtDNA deletions clonally expand is key to understanding how these DNA defects reach pathogenic levels to cause biochemical defects in mitochondrial disease and in aging; a number of hypothetical mechanisms have been proposed. These can be split broadly into three categories. Firstly, hypothetical "mtDNA structure" mechanisms suggest that an advantage is gained by the direct change to the mtDNA imparted by a mutation; this advantage is not necessarily associated with any functional change to mtDNA encoded proteins. The most prominent and widely studied of these is the 'survival of the smallest' mechanism, as discussed section *1.7.1*, (Figure 1.20). An alternative mtDNA structure-based mechanism, proposed by Shoubridge *et al* in 1990, suggests that mutations which go on to clonally expand may eliminate or inactivate negative *cis*-acting proliferative control elements (Shoubridge *et al.*, 1990). This would provide a proliferative advantage over wild-type mtDNA, allowing mutant mtDNA to replicate independent of metabolic demands and resulting in an accumulation of higher levels of mutant mtDNA. This particular mechanism is attractive in that it is able to simultaneously account for the accumulation of both mtDNA deletions and mtDNA point mutations over time; both of these mutation types have the capacity to affect a control sequence, while mtDNA point mutations do not alter mtDNA size in the same manner as mtDNA deletions.

The second group of proposed mechanisms for clonal expansion can be described as "phenotype-based" hypotheses, due to their assertion that the propagative advantage which allows for the accumulation of mutant mtDNA over wildtype is due to the mutation's downstream effect on mitochondrial enzyme activity rather than the primary change to the mtDNA molecule. The 'survival of the slowest' hypothesis (see section *1.7.2*, Figure 1.21), is the most well-known example of a phenotype-based hypothesis, though an earlier phenotype-based hypothesis had been proposed by

Shoubridge *et al* as an alternative to the inactivated *cis*-acting control elements model – also suggesting that the impaired ability of mitochondria carrying mtDNA mutations to synthesise cellular ATP is the driving force behind the accumulation of mutant mtDNA (Shoubridge *et al.*, 1990). The decline in ATP production could trigger a metabolic feedback loop where declining levels of ATP drive increased mitochondrial biogenesis, potentially increasing the level of mutant mtDNA and dysfunctional mitochondria. This hypothesis was based on earlier evidence in skeletal muscle that increased oxidative demand leads to an increase in mitochondria proliferation (Salmons and Henriksson, 1981; Williams *et al.*, 1986). This hypothesis was later adopted by another research group as a mechanism that could drive the clonal expansion of both mtDNA point mutations and deletions, being applicable to known mtDNA point mutations which affected no known proliferative control sequence, and was dubbed the 'crippled mitochondria' theory (Yoneda *et al.*, 1992).

More recently, it was proposed that a selective advantage may not be required for the clonal expansion of mtDNA deletions – proposed mechanisms which fall under this category can be widely termed "random segregation" hypotheses. These suggest that random genetic drift during mtDNA replication could be sufficient to allow clonal expansion of a single mtDNA mutation within a cell (Chinnery and Samuels, 1999; Elson *et al.*, 2001) due to relaxed mtDNA replication (Bogenhagen and Clayton, 1977) (see section *1.7.3*, Figure 1.22) . Random genetic drift is supported by mathematical models based on previously demonstrated principles of mitochondrial replicative dynamics (Shadel and Clayton, 1997), but the presence of high levels of deleted mtDNA in all substantia nigra neurons from aged individuals (Bender *et al.*, 2006; Reeve *et al.*, 2008a) is challenging to explain based on an accumulation of mtDNA deletions by random genetic drift.

3.1.2 Recent amendment to the 'survival of the smallest' theory of clonal expansion

In the same year that the 'survival of the slowest' mechanism for the clonal expansion of mtDNA deletions was put forward, the identification of pathogenic point mutations able to accumulate over time in patient cells caused the 'survival of the smallest' hypothesis to fall out of favour within the scientific community. Point mutations

maintain an identical genome size to wild-type mtDNA molecules, meaning that the accumulation of pathogenic mtDNA point mutations over time cannot be driven by a replicative advantage based on size (Weber *et al.*, 1997). Furthermore, a study of replicative dynamics found that all mitochondrial DNA molecules are replicated in under two hours (Davis and Clayton, 1996); this fast rate of replication is much quicker than the rate of mitochondrial turnover in any cell types in which the clonal expansion of mtDNA deletions normally occurs. This would suggest that replication of the DNA is not a rate-limiting step during mitochondrial biogenesis, making it unlikely that the smaller genome size of mitochondrial genomes with deletions confers a selective advantage (Weber *et al.*, 1997).

An amendment to the 'survival of the smallest' mechanism was proposed in 2001, suggesting that the shorter size of mtDNA deletions may confer a selective advantage without influencing the speed at which the genome is replicated (Birky, 2001). This hypothesis, which was designed to address the issues that had been raised in opposition to the 'survival of the smallest' mechanism, was heavily influenced by the finding that mtDNA copy number control is based upon total mtDNA content within the cell in terms of mass as opposed to control of the number of individual mtDNA molecules (Tang *et al.*, 2000a). Based upon this finding, Birky suggested that short deleted genomes would have to undergo more rounds of replication than longer wild-type genomes to reach a prescribed mtDNA mass within the cell, leading to an increase in the proportion of short genomes (Birky, 2001). However, further analysis of this model determined that equilibrium would be reached when the ratio of deleted mtDNA:wildtype molecules was equal to the reciprocal ratio of the genome lengths. In this case, the common deletion would not rise above 60%, which is not in keeping with the high heteroplasmy levels seen in patient cells. While this mechanism may therefore not play a role in the clonal expansion of mtDNA deletions - due to the predicted slow accumulation of mutant mtDNA and the inability of the mechanism to account for high heteroplasmy levels for most mtDNA deletions - it has been suggested that this copy number control mechanism may stabilise mtDNA deletion heteroplasmy levels (De Grey, 2003).

3.1.3 Recent evidence supporting the 'survival of the smallest' theory of clonal expansion.

New evidence in support of the 'survival of the smallest' mechanism of clonal expansion emerged from a 2002 study of cellular mtDNA, contradicting the evidence which had been amassing in opposition to this hypothesis in previous years. This work was carried out in cytoplasts derived from fibroblasts of patients with mtDNA disease to investigate whether smaller, deleted mtDNA molecules do have a replicative advantage in cells (Diaz *et al.*, 2002). Two groups of cytoplasts were derived – one group with heteroplasmic large-scale mtDNA deletions and a second group with heteroplasmic mtDNA point mutations – both of which were first investigated during normal, non-selective cell conditions under the exertion of tight copy number control. After 45 days in culture, mtDNA deletion levels had dropped by 10 to 20% in the heteroplasmic deletion cybrids lines, while mtDNA point mutations had also shown a small decrease in mutation heteroplasmy levels in the cybrids carrying point mutations (Diaz *et al.*, 2002). This initial finding was in keeping with previous work which has shown cells with the highest percentage of deleted mtDNA molecules to have the longest population doubling time (Hayashi *et al.*, 1991).

Following analysis in normal cellular conditions, both sets of cytoplasts underwent treatment with ethidium bromide (EtBr) to deplete the mtDNA, inducing mtDNA repopulation and hence allowing the investigation of mtDNA replication under relaxed copy number control. Following the EtBr treatment, no increase in point mutation heteroplasmy levels was observed in the set of cytoplasts harbouring pathogenic point mutations, showing no difference in repopulation rate compared to wild-type mtDNA. However, a much greater mtDNA deletion heteroplasmy was observed following EtBr mitochondrial depletion and repopulation in the cytoplast lines containing deleted mtDNA molecules – in these lines, deleted mtDNA molecules were shown to repopulate the cell 2-3 times faster than wild-type molecules. These results clearly demonstrated a replicative advantage for deleted mtDNA over wild-type molecules in the same cell under relaxed copy number control conditions; the authors concluded that the stimulation of defective mitochondria to proliferate in muscle may relax copy number control, allowing for a replicative advantage for deleted mtDNA molecules as witnessed in the cytoplasts cell lines (Diaz *et al.*, 2002).

In addition to the cytoplast-based evidence for the existence of a replicative advantage for deleted mtDNA molecules, a 2009 study by Fukui and Moraes presented evidence that smaller mitochondrial genomes accumulate more rapidly *in vivo* in a mito*Pst1* mouse model (Fukui and Moraes, 2009). This mouse model was developed to express an inducible mitochondria-targeted restriction endonuclease (mito*Pst1*), causing the generation of double-strand breaks in adult neurons and the subsequent formation of deleted mtDNA molecules which mimicked as closely as possible the range of naturally-occurring mtDNA deletions found in aging neurons. Mito*Pst1* was regulated by the presence of doxycycline (Dox) in the diet of the mice, and was induced for a short time period by removal of Dox from the diet for 3 days at four weeks of age; DNA from cortical tissues of the mito*Pst1* induced mice was then analysed alongside age-matched controls at 5 and 14 weeks of age. DNA analysis by semi-quantitative PCR found mtDNA deletions to be present in tissue from 5 week old mito*Pst1* induced mice, but present at a much greater level at 14 weeks, demonstrating the accumulation of mtDNA deletions over time. It was inferred that, if the smaller size of deleted mtDNA molecules compared to wild-type mtDNA conferred a replicative advantage, small mitochondrial genomes carrying large mtDNA deletions should also have a replicative advantage within the cell over larger mtDNA molecules with small deletions.

The combined evidence from the cytoplast and mito*Pst1* mouse models strongly support the 'survival of the smallest' mechanism of clonal expansion, with a replicative advantage for smaller mtDNA molecules having been observed in both cases. However, it is important to take into consideration that both of these studies modelling clonal expansion of mtDNA deletions have been carried out in modified systems; no conclusive evidence has yet been presented to suggest that mtDNA deletions species have a replicative advantage in human tissue.

3.2 Aims and hypothesis

The aim of this study was to investigate the presence of a replicative advantage for mtDNA deletions in human tissue, following on from evidence presented in cytoplast and mouse model studies in favour if the 'survival of the smallest' theory.

The 'survival of the smallest' hypothesis that mtDNA deletions have a replicative advantage over wild-type mtDNA molecules due to a smaller genome size was further extrapolated, suggesting that the largest mtDNA deletions would also display a replicative advantage over smaller mtDNA deletions due to a smaller genome size. In this case, the most sizeable mtDNA deletions would be subject to the greatest rate of replication and rate of accumulation within the cell. Due to this replicative advantage, it would be reasonable to expect that in muscle fibres, the largest mtDNA deletions would spread more quickly and generate larger segments of COX-deficiency than smaller mtDNA deletions.

Based upon the above hypotheses, it was decided to focus this study on determining whether the largest mtDNA deletions spread the furthest longitudinally through muscle fibres, demonstrating a greater rate of accumulation within the muscle than smaller mtDNA deletion species. Previous assessments of COX-deficiency in muscle fibres have identified a large range in the length of COX-deficient fibre segments from just 10µm to in excess of 1.2mm within single patients (Elson *et al.*, 2002), in keeping with previous observations of COX-deficient muscle fibre segments in excess of 1.6mm in model organisms (Lopez *et al.*, 2000). A large spectrum of COX-deficient fibre segment lengths should be available within individual biopsies from multiple mtDNA deletion patients to allow the identification of any correlation with mtDNA deletion size. Interestingly, prior studies have identified a strong relationship between the length of COX-deficient segments of muscle and disease severity (Elson *et al.*, 2002), though no work has so far been carried out to identify a link between mtDNA deletion size and COX-deficient fibre segment length. The presence of a positive relationship between these two variables would demonstrate that a smaller genome size does confer a replicative advantage within the cell, fulfilling the project aim of determining whether mtDNA deletions display a replicative advantage based upon genome size in human tissue.

3.3 Methods

3.3.1 Patient Biopsies

Skeletal muscle samples (vastus lateralis) were obtained by open muscle biopsy from 6 patients with multiple mtDNA deletions. All patients presented with chronic progressive external ophthalmoplegia and had a mosaic pattern of respiratory chain deficiency in muscle. These biopsies were taken either for diagnostic purposes (patients 2 and 3) or at post-mortem. Five patients harboured pathogenic mutations in the *POLG* gene, as outlined in *3.3.2*, while the underlying nuclear genetic defect remains unknown in one patient (screened for mutations in *POLG*, *POLG2*, *PEO1*, *SLC25A4*, *RRM2B* and *TK2* with no mutations identified). Large muscle biopsies were available from each of these patients, allowing longitudinal sections to be cut for analysis along the length of each skeletal muscle fibre. Samples were frozen in isopentane cooled by liquid nitrogen for histological and histochemical analysis. Ethical approval was obtained from Newcastle and North Tyneside LREC.

3.3.2 Mitochondrial enzyme histochemistry

20µm thick skeletal muscle sections were taken from each of the biopsies outlined above. Dual cytochrome c oxidase (COX) and succinate dehydrogenase (SDH) histochemistry was carried out to identify muscle fibres areas displaying a biochemical defect. Due to the nature of the patients from which tissue was obtained, all biochemically deficient fibre areas could be attributed to the presence of high levels of mtDNA deletions. An initial stain for COX activity creates a brown precipitate where cytochrome *c* is active within the muscle fibres, and therefore where the mitochondria are functional. The application of a second histochemical stain for SDH activity creates a blue precipitate in the presence of succinate dehydrogenase subunits SDHA and SDHB, both of which are entirely nuclear encoded and are therefore unaffected by the presence of mtDNA deletions. This creates a stain which is only visible in areas unstained, or weakly stained, for COX activity, highlighting COX-deficient muscle fibre areas in blue (Figure 3.27).

Patient	Age at biopsy	Gene defect	Clinical presentation	Histochemical defect	mtDNA deletion detection	Biopsy type
1	59	POLG – p.G848S and p.S1104C (Betts-Henderson et al., 2009)	CPEO, myopathy, ataxia and Parkinsonism.	15% COX-deficient fibres, 5% RRF	Long-range PCR	PM
2	74	POLG – p.T251I/p.P587L and p.R627Q	CPEO	5% COX-deficient fibres	Southern blotting	Diagnostic
3	55	POLG – p.A467T and p.W748S	SANDO	7% COX-deficient fibres, 1% RRF	Southern blotting	Diagnostic
4	50	POLG – p.A467T and p.X1240Q (Cottrell et al., 2000; Lax et al., 2012)	CPEO, ataxia, parkinsonism and neuropathy	20% COX-deficient fibres,	Long-range PCR	PM
5	63	Undiagnosed nuclear defect, POLG, POLG2, PEO1, SLC25A4, RRM2B and TK2 all excluded	CPEO	20% COX-deficient fibres, 5% RRF	Long-range PCR	PM
6	80	POLG – p.T251I/p.P587L and p.A467T	CPEO	15% COX-deficient fibres, 3% RRF	Long-range PCR	PM

Table 3.12 – Histochemical and molecular genetic characterisation of patients with multiple mtDNA deletions in muscle.

COX – cytochrome *c* oxidase; RRF – ragged-red fibres.

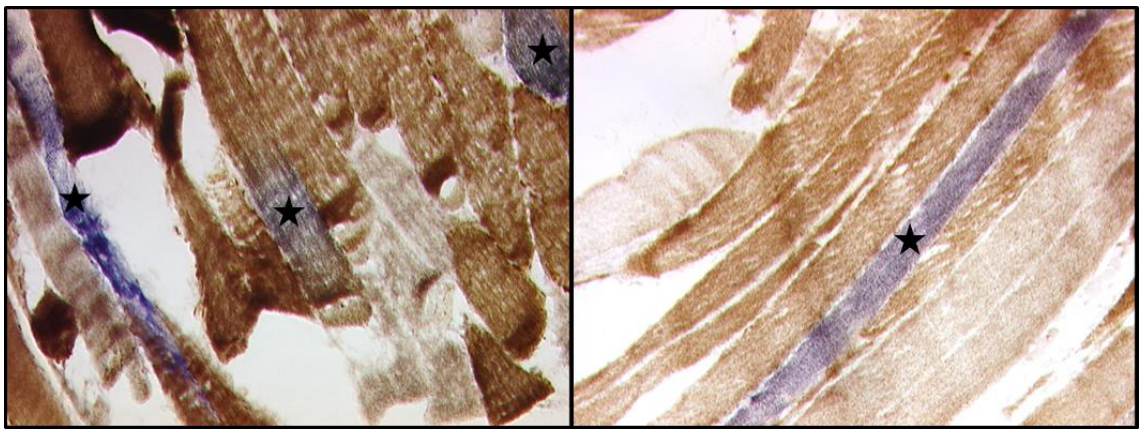

Figure 3.27 – 20µm thick longitudinal sections of *vastus lateralis* skeletal muscle tissue dual-stained for COX and SDH histochemistry.

Starred fibres demonstrate COX-deficiency, with no detectable brown precipitate from the applied COX histochemical assay present, but very visible blue precipitate from the SDH histochemical assay which was subsequently applied.

All other fibres positively demonstrate normal COX activity, with visible brown precipitate forming following the application of the COX histochemical assay.

3.3.3 Single fibre isolation

Two categories of fibres were selected for investigation from the COX/SDH stained longitudinal muscle biopsy sections; for the purposes of this study, they were termed 'long' and 'short' regions of COX-deficiency. Short COX-deficient regions were those under 200µm in length, while long COX-deficient regions were over 500µm in length. These values were chosen based upon the maximum cutting length on our microscope/LMD system of 650µm.

It was initially decided to compare two discrete groups of fibres in order to maximise the power of the statistical tests available to determine whether any relationship existed between mtDNA deletion size and COX-deficient fibre area. Selecting only fibres >500µm or <200µm in length ensured that there was no overlap between the two fibre groups, with a buffer of 300µm in length of COX-deficient fibre area separating the two data sets.

3.3.4 Long-extension PCR, gel electrophoresis and mtDNA deletion detection

To detect mtDNA deletions in individual COX-deficient muscle fibres, long-extension PCR was performed on DNA from isolated single COX-deficient fibre regions alongside wild-type homogenate DNA. Over the course of the study two sets of primer pairs were used; one set amplified a 13.5kb region of the major arc of the mitochondrial genome (NC_012920.1, 2999 – 16450bp), while the other set amplified a smaller 10kb region within the same section of the major arc (NC_012920.1, 6240 – 16132bp). After running the 13.5kb long-range PCR on ~30 isolated muscle fibres with few successful DNA amplifications, a more efficient 10kb primer pair was designed for the long-range assay to increase the PCR success rate. Both sets of data were used. PCR product sizes were read from agarose gels following gel electrophoresis using the accompanying DNA ladder; the size of the mtDNA deletion present in a sample was determined by the difference in size between sample and wild-type DNA products.

3.3.5 Restriction endonuclease digest and sequencing analysis

A restriction endonuclease digest using 4 restriction enzymes - *Xho1*, *BamH1*, *Xcm1* and *Dra1* - was used to fine map the location of the mtDNA deletion breakpoints (Khrapko *et al.*, 1999). The restriction sites for these enzymes in wild-type mtDNA produce a pattern of restriction fragments, ranging between 441 and 4474bp in length, which can be clearly visualised following separation by gel electrophoresis in 2% agarose gel (Figure 3.28, Table 3.14). The mtDNA deletion present in sample DNA from individual isolated COX-deficient muscle fibre regions could then be roughly mapped by identifying which restriction fragments were missing following the restriction endonuclease digest. PCR products were then sequenced using appropriate PCR primers close to the predicted mtDNA deletion breakpoint to identify the mtDNA deletion breakpoint sequences (Figure 3.29), and accurately determine the size of the deleted region of mtDNA.

3.3.6 Statistical Analysis

All statistical analysis was carried out using GraphPad Prism v.4 statistical software. Relevant t-tests we chosen to carry out dataset comparisons according to whether data was paired, and whether the data followed a normal distribution (Table 3.13). Similarly, data correlation was assessed using a 2-tailed Spearman or Pearson correlation test at 95% confidence, dependent upon data distribution (these are non-parametric and parametric tests, respectively). To assess data distribution a battery of normality tests were carried out: the Kolmogorov-Smirnov test, where samples are standardized and compared with a standard normal distribution; the Shapiro-Wilk normality test, which compares low sample numbers (<50) to a standard normal distribution with higher accuracy; and the D'Agostino and Pearson omnibus normality test, which identifies data skewness and kurtosis. Normality was assumed when at least two of these three tests identified a normal distribution.

	Normal data distribution	**Non-normal data distribution**
Paired data	Paired t-test	Wilcoxon matched pairs test
Unpaired data	Unpaired t-test	Mann-Whitney u-test

Table 3.13 Selection of appropriate tests to carry out data group comparisons.

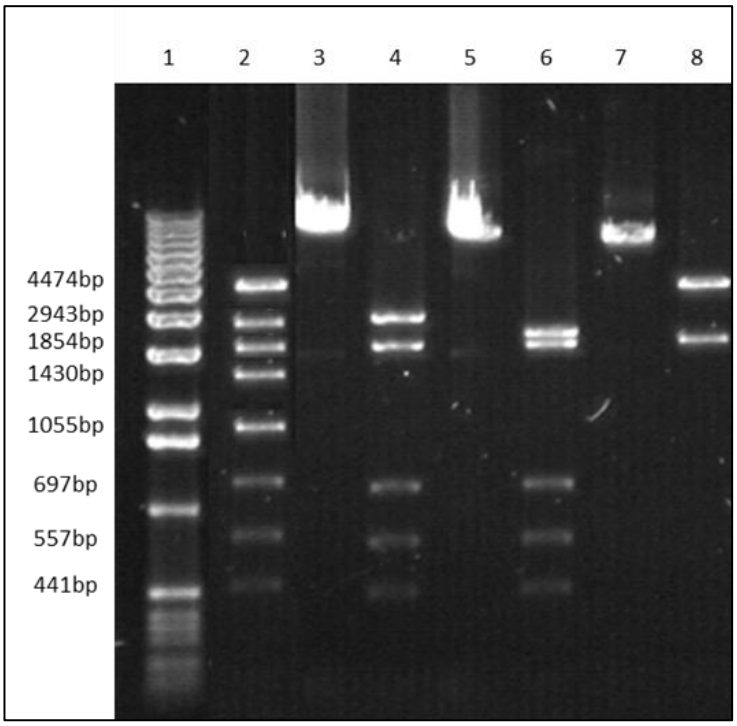

Figure 3.28 – Restriction digest products from one wildtype mtDNA sample and 3 long-range PCR amplimers from single COX-deficient fibre DNA samples; products separated on a 2% agarose gel by gel elctrophoresis.

1 - 1kb ladder; **2** - Digested wildtype mtDNA, all 8 expected digest bands present; **3** - Long-range PCR amplimer 1; 5kb deletion (8kb product from a 13kb long-range PCR); **4** - Digested products of long-range PCR amplimer 1; expected bands present at 441bp, 557bp, 697bp, 1854bp and 2943bp; expected bands at 4474bp, 1430bp and 1055bp missing. Sequencing initiated with primers 28R and 21F; **5** - Long-range PCR amplimer 2; 5kb deletion (8kb product from a 13kb long-range PCR); **6** - Digested products of long-range PCR amplimer 2; expected bands present at 441bp, 557bp, 697bp and 1854bp; expected bands at 2943bp, 4474bp, 1430bp and 1055bp missing, unexpected band at approximately 2kb. Sequencing initiated with primers 28R and 19F; **7** - Long-range PCR amplimer 3; 6kb deletion (7kb product from a 13kb long-range PCR); **8** - Digested products of long-range PCR amplimer 1; expected bands present at 4447bp and 1854bp only. Sequencing initiated with primers 16540R and 23F.
All relevant primer locations and sequences are listed in section *2.2.4.2.2*, Tables 2.4 and 2.5 respectively.

441bp	1854bp	697bp	557bp	1055bp	1430bp	4474bp	2943bp
Absent: 16450R	Present: 32F						
Present	Absent: 32R	Present: 31F					
Present	Present	Absent: 31R	Present: 29F				
Present	Present	Present	Absent: 29R	Present: 28F			
Present	Present	Present	Present	Absent: 28R	Present: 25F		
Present	Present	Present	Present	Present	Absent: 25R	Present: 23F	
Present	Present	Present	Present	Present	Present	Absent: 23R	Present: 21F
Present	Present	Present	Present	Present	Present	Present	Absent: 21R

Table 3.14- Predicted sequencing primers to use, as determined by restiction endonuclease digest.

The presence of expected restriction digest bands, of a range of sizes from 441bp to 4474bp, was assessed following separation of restriction di gest products by gel electrophoresis (Figure 3.28). The most appropriate reverse primer to utilise for breakpoint sequencing was determined by the first missing band from the restriction digest, reading left-to-right from the above table; i.e. if the 441bp and 1845bp bands were present, but the 697bp band was found to be absent, primer 31R was used for breakpoint sequencing analysis. The most appropriate forward primer to use as a starting point for breakpoint sequencing was determined either by the first band to appear after a break in the restriction digest sequence (i.e. if the 441bp band is present, 1854bp, 697bp and 557bp bands are absent, but the 1055bp bands is present, forward primer 25F would be used), or by the estimated deletion size (i.e. using a forward primer located *x*kb after the determined reverse primer, where *x* is the deletion size predicted by long-range PCR).

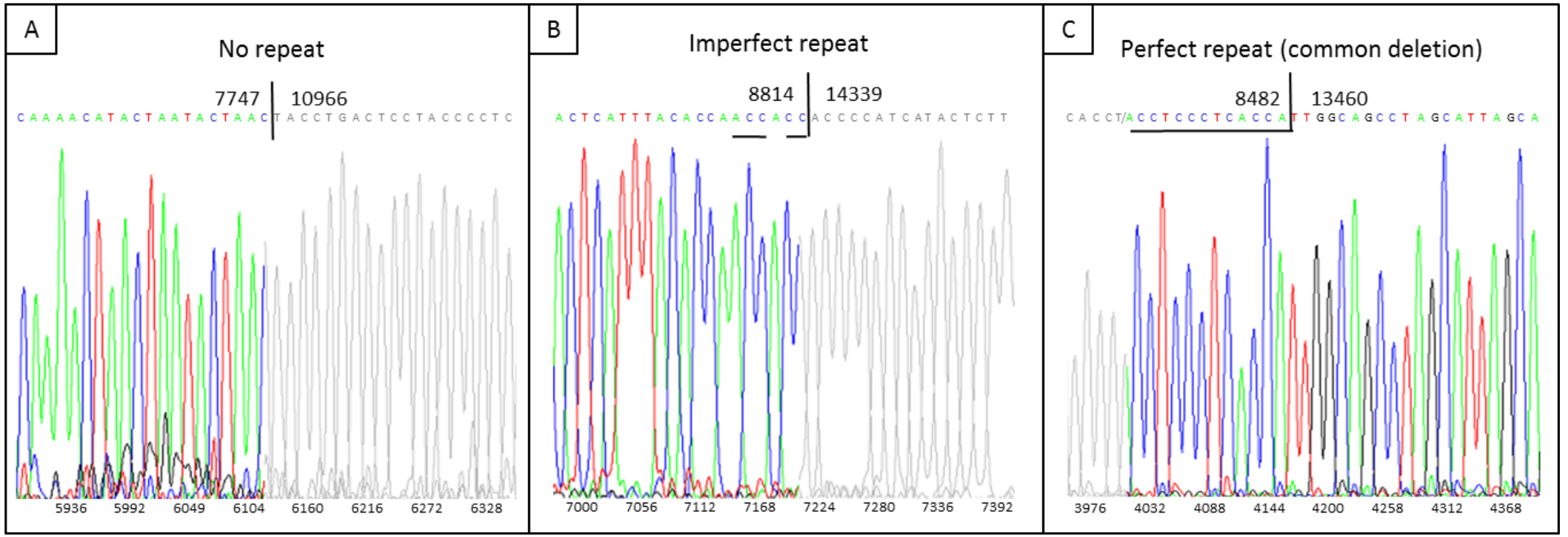

Figure 3.29 – Representative breakpoint analysis output from ABI PRISM SeqScape Software Version 2.6

Breakpoints were categorised into 3 types: **A** – No repeat; the mtDNA sequences surrounding the identified mtDNA deletion breakpoints (10bp in this study) contains no repeated bases. **B** – Imperfect repeat; the 10bp mtDNA sequences either side of the identified mtDNA deletions breakpoints contain 4 or more repeated bases, but are not identical. **C** – Perfect repeat; the mtDNA sequences (10bp in this study) found 3' and 5' of the identified mtDNA breakpoints are identical. This is demonstrated by the common deletion, which displays a 13bp prefect repeat

3.4 Results

3.4.1 COX-deficient fibre segment length.

Two categories of fibres were selected for investigation from longitudinal sections of skeletal muscle biopsy, identified as 'long' and 'short' regions of COX-deficiency. Short fibres were under 200µm in length and long fibres over 500µm in length; these values were chosen based on a maximum cutting length of our microscope/LMD system of 650µm (Figure 3.30). Previous measurements of COX-deficient fibre segments found regions of biochemical defect to range in length from 10µm to over 1.2mm (Shadel and Clayton, 1997), meaning the categories of <200µm and >500µm in length fell within an acceptable range. The area (μm^2) of individual muscle fibre regions isolated by laser microdissection was determined and was found to be a more variable measurement than fibre length when extracting fibres, but analysis showed no overlap between the two groups of COX-deficient fibre areas, with a maximum area of 12800μm^2 for short COX-deficient fibre regions, and a minimum area of 19412μm^2 for long COX-deficient fibre regions.

The mean fibre area for short COX-deficient regions under 200µm in length was 5725μm^2, with a standard deviation in area of 3194μm^2 and a total range in size of 11498μm^2, from 1302μm^2 to 12800μm^2. The mean fibre area for long COX-deficient regions over 500µm in length was 32120μm^2, with a standard deviation in area of 10536μm^2 and a total range in size of 45800μm^2, from 19412μm^2 to 57289μm^2 (Figure 3.31). A Mann-Whitney u-test, chosen because the spread of data did not follow a normal distribution, performed on the 2 fibre area data sets gave a p-value <0.0001, showing a significant difference in area of COX-deficiency between the long and short fibres.

Although long and short COX-deficient muscle fibre regions were selected based upon the length of the fibre region affected by the biochemical defect, it became apparent that total fibre area (μm^2) isolated by laser microdissection would be a more appropriate measure for any statistical analyses within this study. The area affected by the biochemical defect is a better measure of the spread and accumulation of the mtDNA deletion species responsible for the COX-deficiency, as basing measurements

purely on the length over which the biochemical defect has spread fails to take into consideration variable fibre width.

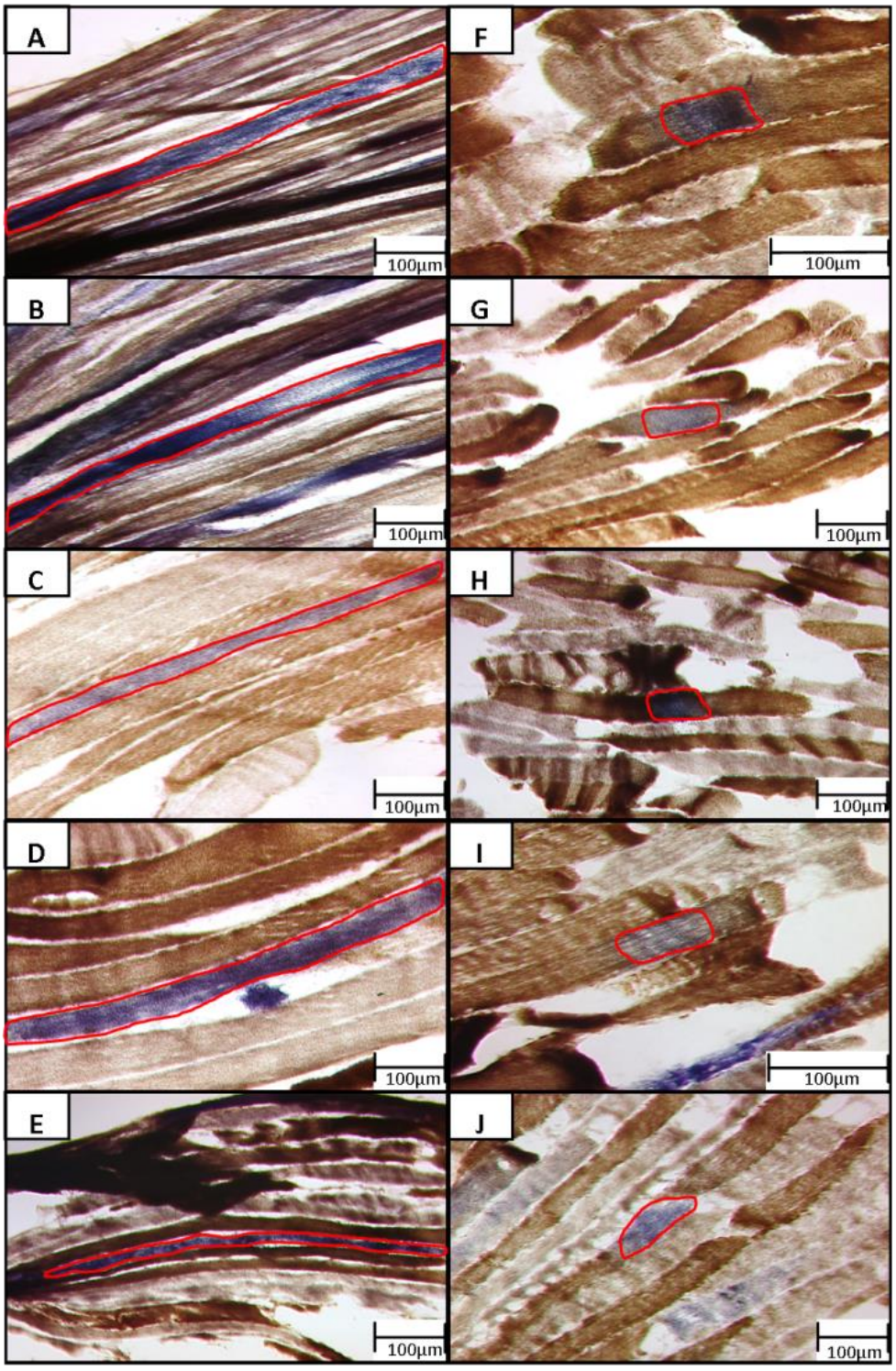

Figure 3.30 - Example images of COX-deficient skeletal muscle fibre areas to be extracted by laser capture micro-dissection.

A – E: Long COX-deficient regions, over 500µm in length.

F – J: Short COX-deficient regions, under 200µm in length.

COX-deficient fibres region to be captured by laser microdissection in each example is outlined in red.

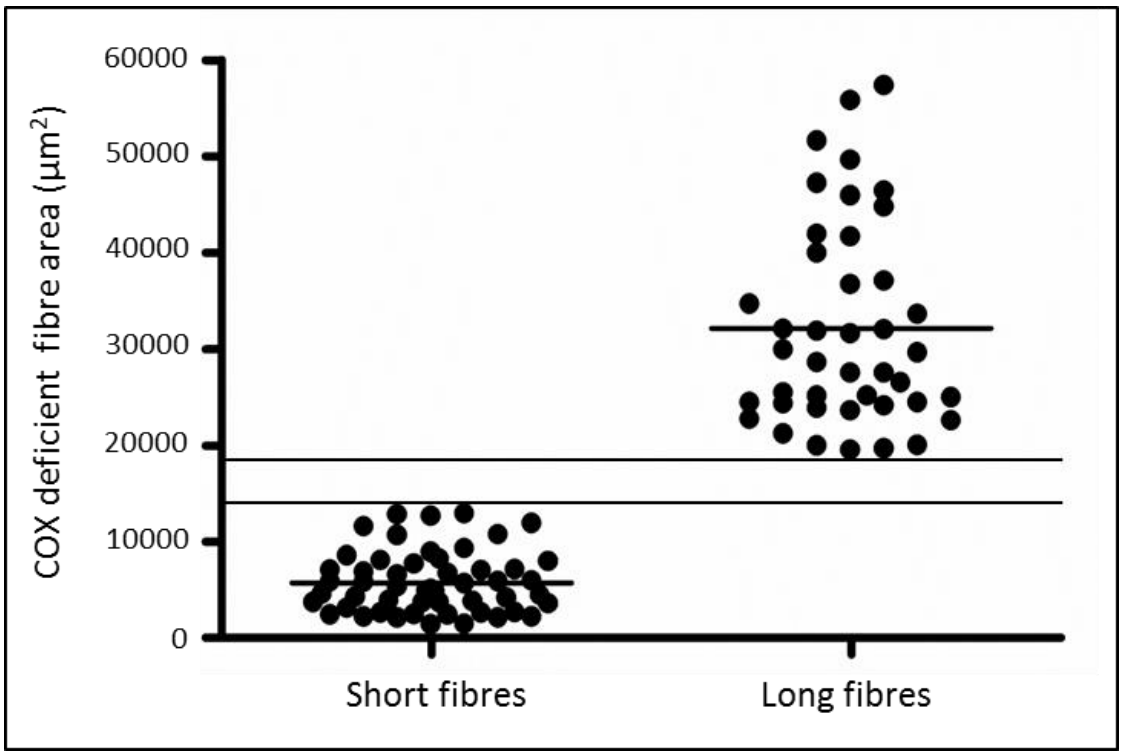

Figure 3.31 – COX-deficient fibre areas, measured in µm^2, captured by laser microdissection.

'Short fibres' are short COX-deficient fibre regions isolated by laser microdissection, and 'long fibres' are long COX-deficient fibre regions isolated by laser microdissection.

The mean fibre area for short COX-deficient regions under 200µm in length was 5725µm^2, with a standard deviation in area of 3194µm^2 and a total range in size of 11498µm^2, from 1302µm^2 to 12800µm^2.

The mean fibre area for long COX-deficient regions over 500µm in length was 32120µm^2, with a standard deviation in area of 10536µm^2 and a total range in size of 45800µm^2, from 19412µm^2 to 57289µm^2.

The two groups of COX-deficient muscle fibre areas were found to be significantly different using a Mann-Whitney u-test ($P<0.0001$).

3.4.2 Assessing mtDNA deletion size in individual COX-deficient SKM fibre regions

Long range TaKaRa LA Taq PCR was successfully performed on total cell lysate from 62 short COX-deficient fibres (under 200µm in length) and 60 individual long (over 500µm in length) COX-deficient fibre regions, from a total of 6 patients with multiple mtDNA deletion disorders. Following amplification of the mtDNA, PCR products were separated and analysed by gel electrophoresis – the size of the amplified PCR product from each sample could then be compared to the product size from wild-type mtDNA, allowing an assessment of mtDNA deletion size. In most cases, a single PCR product representing one mtDNA deletion was seen per muscle fibre – these were the successful samples, which were then used for analysis of the relationship between mtDNA deletion size and the length of the COX-deficient fibre area (Figure 3.32). Interestingly, multiple mtDNA deletion bands were evident in mtDNA samples from approximately 20% of successfully amplified COX-deficient fibre regions. While this in itself was a thought-provoking finding, as clonal expansion is usually considered in terms of the accumulation of a single mtDNA deletion species, these results could not be included in this particular study; there was no way of distinguishing how the multiple mtDNA deletions were distributed through the biochemically affected muscle fibre area, and so no length of COX-deficiency could be attributed to a specific mtDNA deletions size. The presence of multiple mtDNA deletions in single COX-deficient muscle fibre areas was, however, investigated in a later study (see Chapter 7).

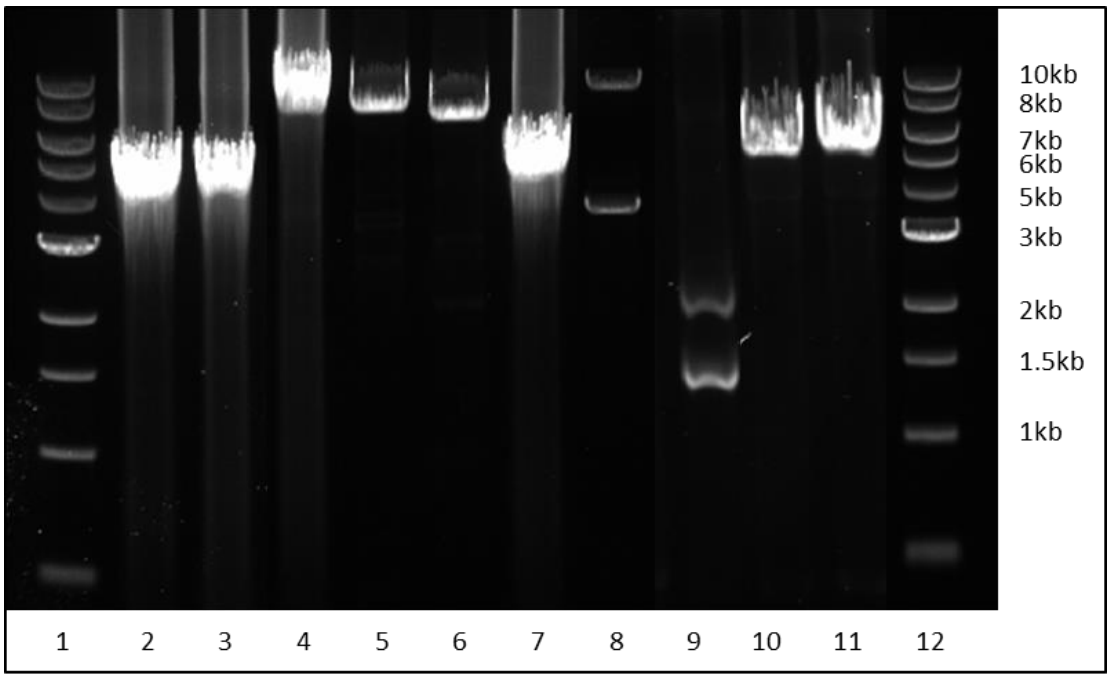

Figure 3.32 - Example gel: mtDNA deletions amplified by a 10kb long-range PCR from 6 'short' and 6 'long' COX-deficient fibres.

10kb PCR, using primer pair 1, of 5 short and 5 long COX-deficient fibre regions, bands separated by gel electrophoresis on a 0.7% agarose gel.

1 – 1 kb ladder; 2 – short fibre, 6kb PCR product, 4kb deletion; 3 - short fibre, 6kb PCR product, 4kb deletion; 4 – short fibre, 9kb PCR product band, 1kb deletion; 5 - short fibre, 9kb PCR product band, 1kb deletion; 6 – short fibre, 8kb PCR product band, 2kb deletion; 7 - long fibre, 7kb PCR product band, 3kb deletion; 8 - long fibre, 10kb wildtype PCR product plus 4.5kb PCR product, 5.5kb deletion; 9 – 2kb and 1.25kb PCR products, multiple deletions of 8kb and 8.75kb, discarded from study; 10 - long fibre, 6.5kb PCR product band, 3.5kb deletion; 11 - long fibre, 6.5kb PCR product band, 3.5kb deletion; 12 – 1kb ladder.

3.4.3 Validation of long-range PCR analysis of mtDNA deletion size

In total, mtDNA deletion sizes from 122 COX-deficient muscle fibre regions were analysed by long-range PCR, as described above. To ensure that the mtDNA deletion sizes estimated by this method were accurate to the true mtDNA deletion size, a stratified sample of 10 random short and 10 random long COX-deficient fibre regions were also analysed through mtDNA deletions breakpoint sequencing. All sequenced samples revealed a deletion size within a 0.5kb range of accuracy of the mtDNA deletion size predicted by the long-range PCR products. The mean deviation from mtDNA deletion size as estimated by long-range PCR analysis to true mtDNA deletion size as measured by breakpoint sequencing was only 229bp, ±191bp, demonstrating that long-rage PCR can be used to assess mtDNA deletion size to a high degree of accuracy (Table 3.15). The 20 mtDNA deletions analysed by both long-range PCR and breakpoint sequencing were determined to be normally distributed in terms of deletion size following analysis by a battery of normality tests (see section *3.3.6*). Due to the normal distribution of these data, a two-tailed paired t test at 95% confidence was carried out to determine how tight the relationship between the two measurements of deletion size was; there was found to be no significant difference between the paired measurements of mtDNA deletion size ($P= 0.3792$), and the pairing was determined to be significantly effective ($r = 0.9922$, $P<0.0001$). This allowed the confident use of data from long-range PCR analysis to compare mtDNA deletion sizes between long and short COX-deficient muscle fibre regions.

Table 3.15 – Table of results for the validation of long-range PCR as an appropriate method to investigate mtDNA deletion size.

A stratified sample of 10 short (COX-deficient fibres 1 – 10) and 10 short (COX-deficient fibres 11 – 20) muscle fibre areas displaying COX-deficiency were fully analysed for mtDNA deletion size; first by long-range PCR, and subsequently by breakpoint sequencing. mtDNA deletion size estimated by long-range PCR differed from actual deletion size, as determined by successful breakpoint sequencing, by no more than 0.5kb (mean difference of 229bp ± 191bp between results). A paired t-test at 95% confidence was used to assess the similarity of the two readings of mtDNA deletion size; there was found to be no significant difference between mtDNA deletion size as determined by long-range PCR or by breakpoint sequencing ($P = 0.3792$), with a correlation coefficient (r) of 0.9922 demonstrating the similarity of the reading for each individual fibre.

COX deficient fibre	Estimated mtDNA deletion length (kb)	Verified mtDNA deletion length (bp)	Size difference (bp)	5' deletion breakpoint	5' breakpoint sequence	3' deletion breakpoint	3' breakpoint sequence	Breakpoint repeat type
1	3.5	3715	215	9576	***a***tc***a***cc***c***gc	13291	***a***ca***a***t***c***ggca	No repeat
2	3.5	3904	404	10265	tctagaaatt	14269	atcctcccga	No repeat
3	5	4977	23	8482	***tccctcacca***	13459	***tccctcacca***	Direct repeat
4	6.5	6994	444	9075	***aa***tatcaac***c***	16069	***aa***gtattga***c***	No repeat
5	7	7479	479	7939	***a***ctaat***c***t***tc***	15436	***a***gacgc***c***c***tc***	Imperfect repeat (***4/10***)
6	7.5	7648	148	6341	aga***cctaa***cc***c***	13989	gcc***cctaa***ct***c***	Imperfect repeat (***5/10***)
7	8.5	8493	7	5438	***a***aaacccacc	13931	***a***ccctagcat	No repeat
8	9	9033	33	6558	a***a***cacc***a***c***c***t	15591	c***a***att***c***t***cc***g	Imperfect repeat (***4/10***)
9	9	9026	26	6634	***c***tga***a***g***t***tta	15660	***c***aat***a***a***t***ccc	No repeat
10	9	9120	120	6468	tg***a***tccg***tc***c	15588	ac***a***caat***tc***t	No repeat
11	2.5	2880	120	7236	gac***tacc***c***c***g	9516	ttt***tacc***a***c***t	Imperfect repeat (***5/10***)
12	5	4977	23	8482	***tccctcacca***	13459	***tccctcacca***	Direct repeat
13	6	5647	353	7406	***c***cccccc***a***cc***c***	13053	***c***ataga***a***gg***c***	No repeat
14	6.5	6175	325	7947	***t***caac***t***c***t***a	14122	***t***tcc***c***a***c***tc***a***	Imperfect repeat (***4/10***)
15	7.5	7046	464	5787	***a***a***gc***tgctt***c***	12833	***atgc***caaca***c***	Imperfect repeat (***4/10***)
16	9.5	9044	556	6105	a***t***aa***tc***ttc***t***	15149	g***t***cc***tc***c***c***g***t***	Imperfect repeat (***4/10***)
17	10	9846	154	5341	tta***a***cc***t***ct***a***	15187	agt***a***at***t***ac***a***	No repeat
18	6.5	6927	427	8734	***a***cctgat***c***t***c***	15661	***a***ataatc***c***c***c***	No repeat
19	8	8026	26	7634	tcccctat***c***a	15660	caataatc***c***c	No repeat
20	3	3250	250	12140	t***c***ct***c***ttg***t***a	15390	c***c***tc***c***cat***t***c	No repeat

3.4.4 Assessing differences in mtDNA deletion size between long and short COX-deficient skeletal muscle fibre areas.

A total of 62 short and 60 long COX-deficient muscle fibre areas were successfully isolated, lysed and analysed by long-range PCR to assess the size of the mtDNA to which the biochemical defect is attributable. mtDNA deletions detected in short skm fibre areas of COX-deficiency ranged in size from 0.5kb to 12kb, with a mean mtDNA deletion size of 6589bp (±2788bp), while mtDNA deletions detected in long muscle fibre areas of COX-deficiency ranged in size from 1kb to 12kb, with a mean mtDNA deletion size of 6508bp (±2478bp). A comparison of the two groups of deletion size data showed a similar data spread, with a difference in mean deletion size of only 81bp. As the battery of normality tests used to assess the data (see section *3.3.*6) found this dataset not to adhere to a normal distribution, a Mann-Whitney u-test was deemed the most appropriate test to determine if the two groups of deletion size data were significantly different. This 2-tailed Mann-Whitney u-test, carried out at a 95% confidence level, showed the set of mtDNA deletion sizes found in long and in short COX-deficient muscle fibre areas were not significantly different (P = 0.5506) (Figure 3.33).

In order to ensure that no trends linking mtDNA deletion size and affected COX-deficient muscle fibre area in individual patients being masked by inclusion into the total dataset, data from individual cases were also independently analysed. No significant difference between mtDNA deletion sizes in long and in short COX-deficient muscle fibre areas was identified in any of the 6 cases included in this study (Figure 3.34, Table 3.16), in keeping with the total dataset.

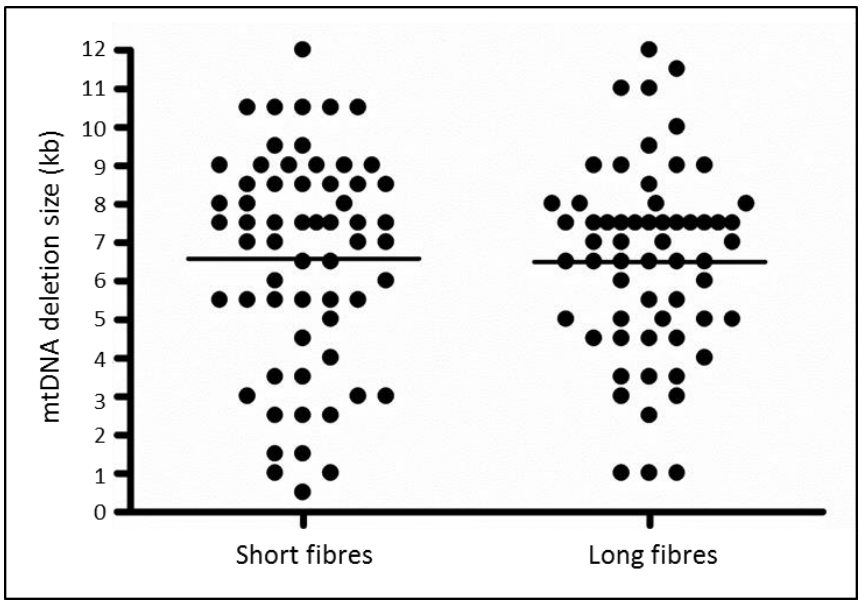

Figure 3.33 - mtDNA deletion sizes present in the total investigated long and short COX-deficient skeletal muscle fibre areas.

A total of 62 short muscle fibre areas displaying COX-deficiency were investigated, with a mean mtDNA deletion size of 6589bp (±2788bp). The mtDNA deletion size range was 11.5kb, with a data spread between 0.5kb and 12kb.

A total of 60 long muscle fibre areas displaying COX-deficiency were investigated, with a mean mtDNA deletion size of 6508bp (±2478bp). The mtDNA deletion size range was 11kb, with a data spread between 1kb and 12kb.

Both long and short regions of COX-deficiency displayed a similar range of mtDNA deletion sizes, with mean mtDNA deletions size values differing by only 81bp. No significant difference was found to exist between the two data sets by Mann-Whitney u-test (P = 0.5506).

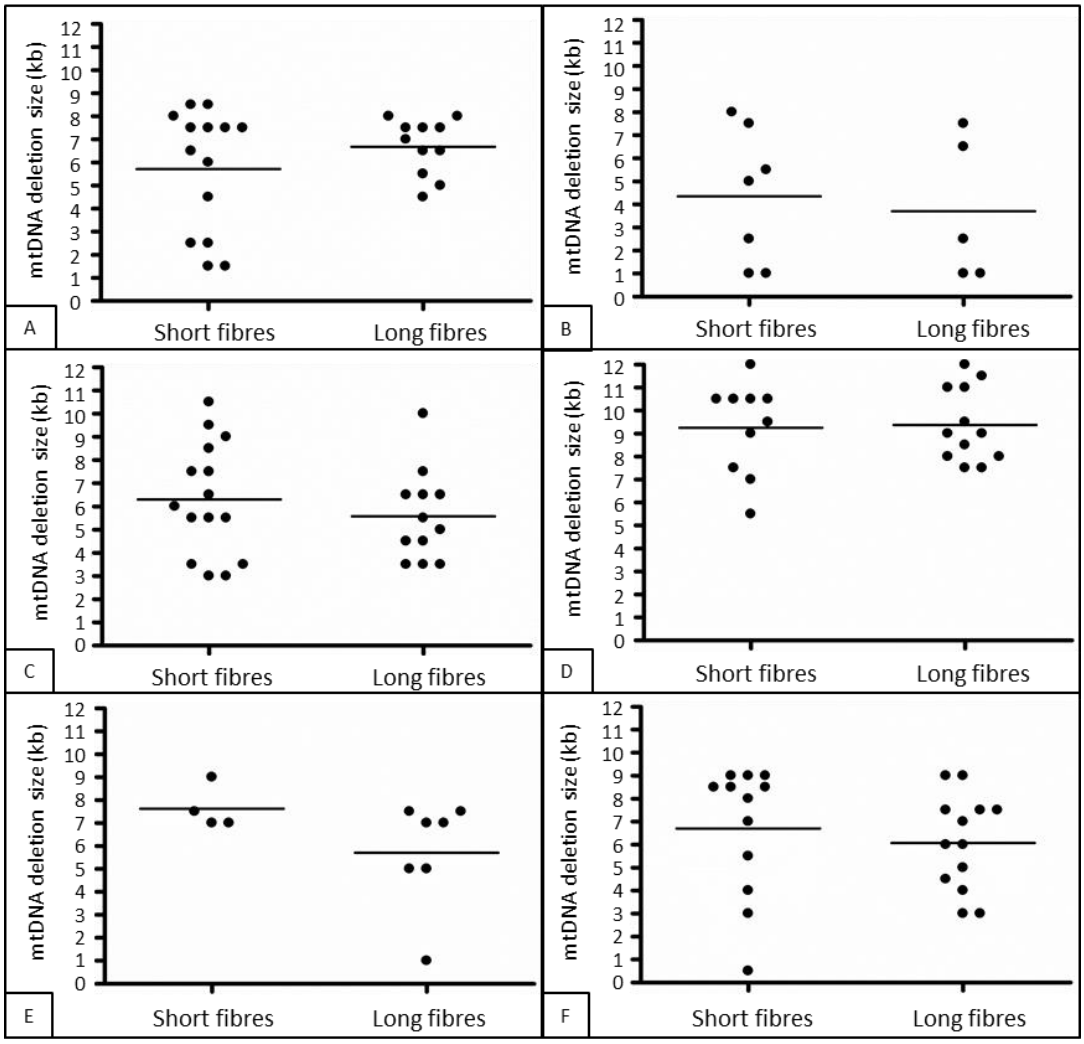

Figure 3.34 - mtDNA deletions sizes in long and short COX-deficient skm fibre regions from 6 investigated patients.

A (Patient 1) - Mean mtDNA deletion size of 5714bp (±2658bp, N = 14) in short fibres and 6682bp (±1210bp, n = 11) in long fibres (no significant difference, P = 0.7009). **B** (Patient 2) – Mean mtDNA deletion size of 4357bp (±2911bp, N = 7) in short fibres and 3700bp (±3094bp, N = 5) in long fibres (no significant difference, P = 0.7751). **C** (Patient 3) – Mean mtDNA deletion size of 6300bp (±2462bpN = 15) in short fibres and 5583bp (±1940bp, N = 12) in long fibres (no significant difference, P = 0.4136). **D** (Patient 4) – Mean mtDNA deletion size of 9250bp (±2003bp, N = 10) in short a fibres and 9375bp (±1611bp, N = 12) in long fibres, (no significant difference, P = 0.8727). **E** (Patient 5) – Mean mtDNA deletion size of 7625bp (±946bp, N = 4) in short fibres and 6714bp (±2343bp, N = 7) in long fibres (no significant difference, P = 0.2303). **F** (Patient 6) – Mean mtDNA deletion size of 6708bp (±2832bp, N = 12) in short fibres and 6077bp (±2060bp, N = 13) in long fibres (no significant difference, P = 0.3406). Data comparisons were carried out by Mann-Whitney u-test for A, B, E and F; C and D were assessed by unpaired t test.

Patient	Short fibre, average mtDNA deletion size (kb)	Long fibre, average mtDNA deletion size (kb)	Fibre type carrying larger mtDNA deletions	Average difference in mtDNA deletion size (kb)	Significant difference?
1	5.71±2.66	6.68±1.21	Long	0.97±0.86	No (P=0.7009)
2	4.36±2.30	3.70±3.09	Short	0.66±1.75	No (P=0.7751)
3	6.30±2.43	5.58±1.94	Short	0.72±0.86	No (P=0.4136)
4	9.25±2.02	9.34±1.61	Long	0.13±0.77	No (P=0.8727)
5	7.63±0.97	5.71±2.34	Short	1.91±1.25	No (P=0.2303)
6	6.71±2.83	6.08±2.06	Short	0.63±0.98	No (P=0.3406)

Table 3.16 – Average mtDNA deletion sizes in long and short COX-deficient fibres in 6 patients with multiple mtDNA deletions in muscle.

The average mtDNA deletion size and standard deviation were calculated for both long and short COX-deficient fibres from each individual patient dataset. From this information, it was determined which COX-deficient fibre category the largest deletion species tended to be associated with; the average difference in mtDNA deletion size between the two fibre types was also calculated. Statistical tests were carried out to see if any of these associations were significant (Mann-Whitney u-test for patients 1, 2, 5 and 6; unpaired t test for patients 3 and 4; all tests at 95% confidence intervals); mtDNA deletion sizes were not found to be significantly associated with long or short COX-deficient fibre regions in any of the 6 individual datasets.

3.4.5 Correlating mtDNA deletion size with COX-deficient skeletal muscle fibre area

Although no difference was found between mtDNA deletion size in long and short areas of COX-deficiency in muscle fibres, there was still potential for a correlation to exist between mtDNA deletion size and area (μm^2) of biochemical defect; a trend could have existed within each of the two groups for the smallest deletion size to result in the smallest area of COX-deficiency. To ensure that this was not the case – i.e. that the smallest area of COX-deficiency in both the long and short muscle fibre groups did not contain the smallest mtDNA deletions, and vice versa – correlation analyses were carried out between mtDNA deletion size and resultant area (μm^2) of muscle fibre COX-deficiency.

Total data for mtDNA deletion size and COX-deficient skeletal muscle fibre area were not normally distributed (analysis by a Kolmogorov-Smirnov normality test, a D'Agostino & Pearson omnibus normality test and a Shapiro-Wilk normality test), making a Spearman correlation analysis the most appropriate for this data set. No significant correlation was found to exist between mtDNA deletion size and COX-deficient skm fibre area in the total 122 biochemically affected fibre regions successfully analysed for this study (P = 0.7792) (Figure 3.35). Individual analyses of the data for the short and the long regions of skm fibre COX-deficiency similarly revealed no significant correlation between mtDNA deletion size and area (μm^2) of skm fibre biochemical defect (P = 0.8845 and 0.5827 respectively) (Figure 3.35).

As for the assessment of differences in mtDNA deletion size between long and short COX-deficient skeletal muscle fibre areas (Section *3.4.4*, page 138), data sets from individual patients were individually analysed in order to prevent any trend in a single patient becoming obscured when combined into the total data set. The spread of mtDNA deletion sizes and area (μm^2) of COX-deficiency were analysed in each case to determine whether they followed a normal distribution, in order to carry out the most appropriate statistical analyses. Data were normally distributed for patients 3 and 4, making a Pearson correlation test the most appropriate, but data from patients 1, 2, 5 or 6 did not follow a normal distribution, meaning the highest degree of statistical power would be gained by using a Spearman correlation test. No significant correlation was found to link mtDNA deletion size to the size of the area of COX-deficiency in muscle fibres in any of the 6 investigated cases (Figure 3.36).

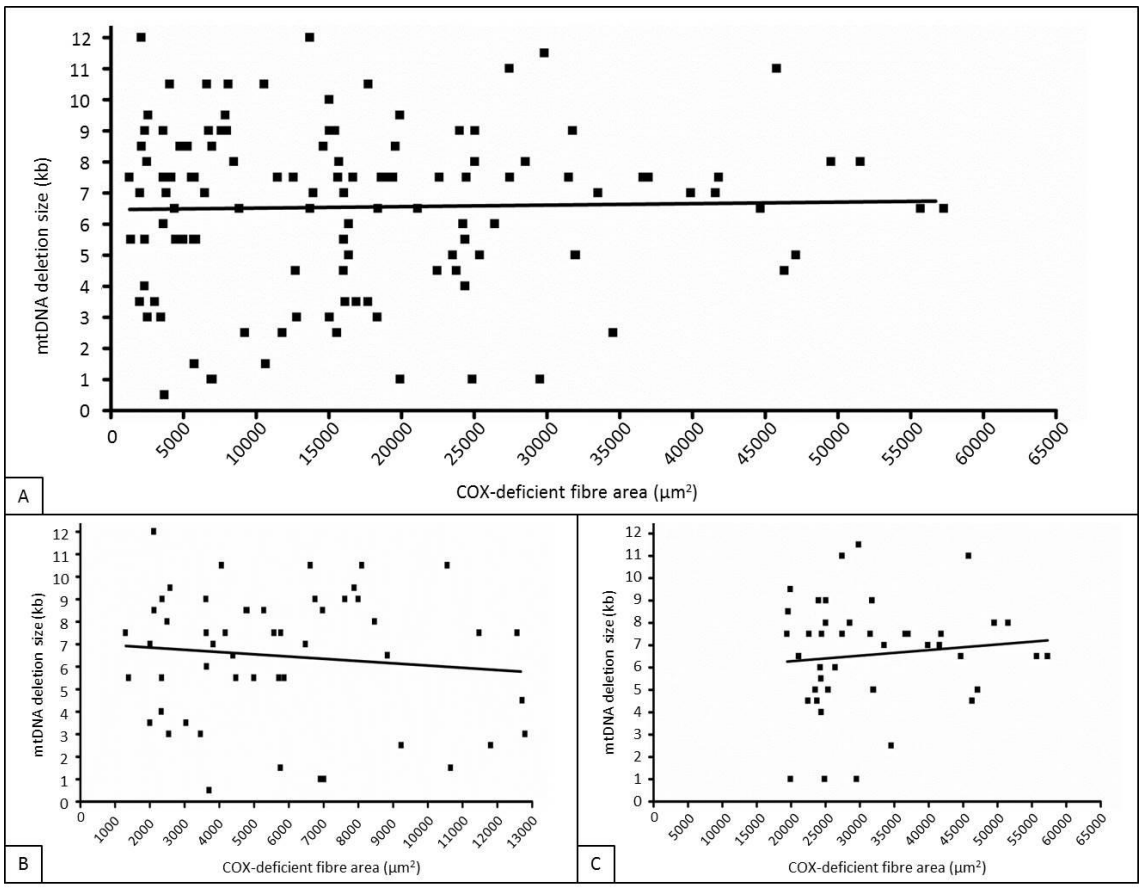

Figure 3.35 - Correlation between the biochemically deficient skm fibre area and mtDNA deletion size.

A - Spearman correlation analysis carried out on the total data set of 122 COX-deficient skeletal muscle fibre regions, to determine if any relationship exists between mtDNA deletion size and the size of the resulting area of biochemical deficiency. No significant correlation was found to exist between these two parameters (P = 0.7792).

Subsequent Spearman correlation analyses carried out on the separate short (**B**) and long (**C**) COX-deficient fibre area groups also revealed no significant correlation between mtDNA deletion size and area (μm^2) of muscle fibre COX-deficiency (P = 0.8845 and 0.5827 respectively).

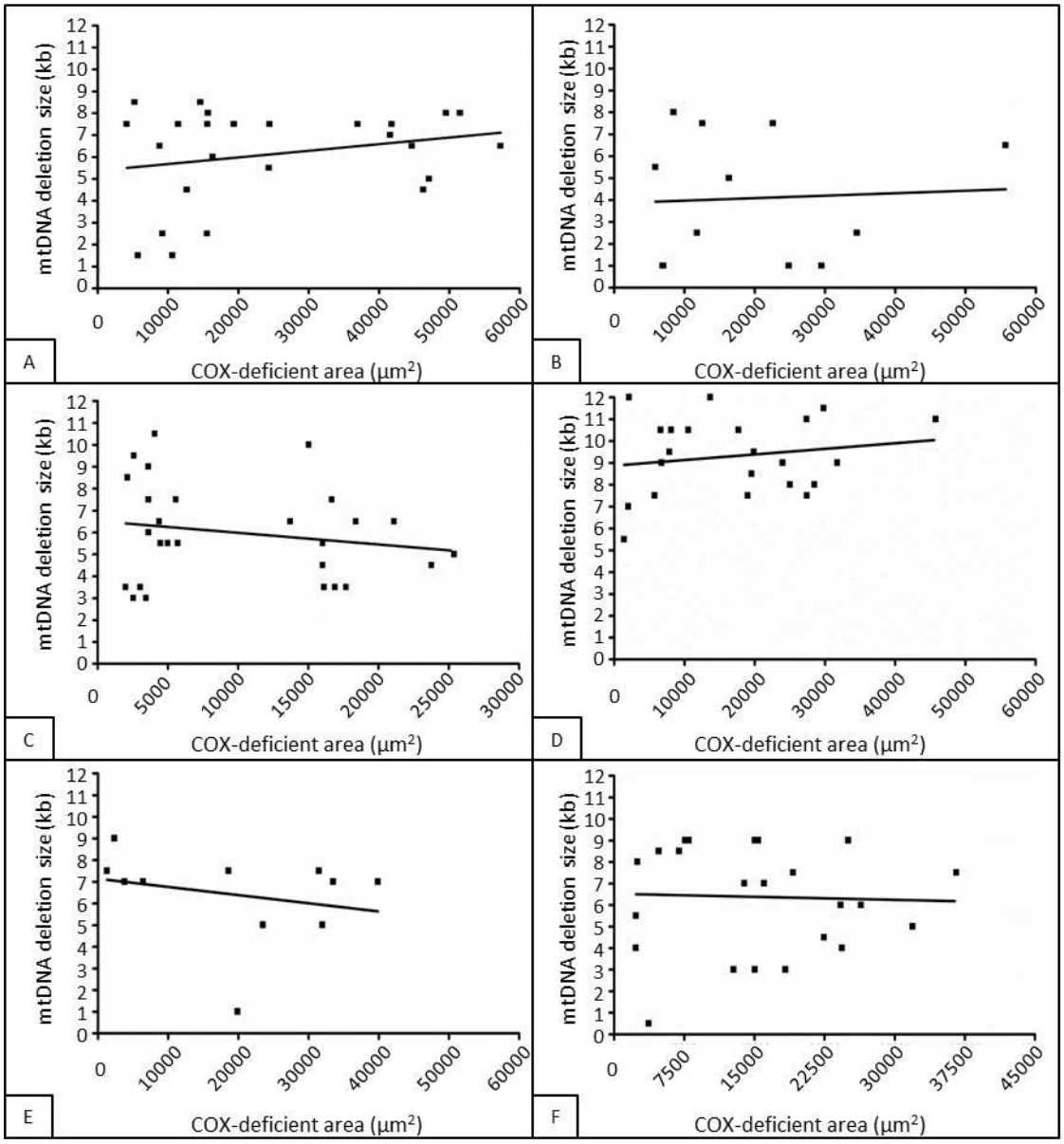

Figure 3.36 - Correlation between mtDNA deletion size and area of COX-deficiency from 6 investigated patients.

A (Patient 1) – No significant correlation between mtDNA deletion size and COX-deficient fibre area identified in COX-deficient fibres (P = 0.2477, N = 25). **B** (Patient 2) – No significant correlation between mtDNA deletion size and COX-deficient fibre area identified in COX-deficient fibres (P = 0.8572, N = 12). **C** (Patient 3) – No significant correlation between mtDNA deletion size and COX-deficient fibre area identified in COX-deficient fibres (P = 0.2477, N = 27). **D** (Patient 4) - No significant correlation between mtDNA deletion size and COX-deficient fibre area identified in COX-deficient fibres (P = 0.4438, N = 22). **E** (Patient 5) – No significant correlation between mtDNA deletion size and COX-deficient fibre area identified in COX-deficient fibres (P = 0.4590, N = 11). **F** (Patient 6) – No significant correlation between mtDNA deletion size and COX-deficient fibre area identified in COX-deficient fibres (P = 0.8599, N = 25).

3.5 Discussion

Previous studies carried out to assess the length of COX-deficient segments in skeletal muscle fibres have identified a range from 10µm to in excess of 1.2mm. While longer sections of COX-deficiency have been linked with more severe disease cases (Elson *et al.*, 2002), no work has been carried out prior to this study to identify any link between the length of COX-deficient fibre segments and the size of mtDNA deletions. Following the hypothesis that the largest mtDNA deletions accumulate at the greatest rate in muscle, we would expect to see a strong correlation between COX-deficient segment length and mtDNA deletion size. However, in this study we see no significant difference in size of mtDNA deletion between 'long' and 'short' COX-deficient fibre areas, and no evidence of a correlation between mtDNA deletion size and the size of the resulting area of skm fibre COX-deficiency. The results from this study therefore do not support the hypothesis that a smaller genome size creates a replicative advantage that drives the clonal expansion of mtDNA deletions.

The results of this study do not agree with the 'survival of the smallest' mechanism for the clonal expansion of mtDNA deletions, despite the emergence of strong evidence in support of this theory from studies carried out over the last decade in mouse models and cytoplasts. As discussed in the introduction to this chapter (see section 3.1.3, page 120), the 2002 study of mtDNA deletion cytoplasts carried out by Diaz *et al* demonstrated a replicative advantage for deleted mtDNA over wildtype molecules under relaxed mtDNA copy number conditions (Diaz *et al.*, 2002). Further evidence in favour of a replicative advantage for mtDNA deletions was gathered in the study of the mito*Pst1* mouse model, where it was observed that smaller mitochondrial genomes accumulate more rapidly *in vivo* following the induction of a range of mtDNA deletions comparable to those found in ageing neurons. (Fukui and Moraes, 2009).

The differences in experimental findings between this work and the studies carried out in the mtDNA deletion cytoplasts and the mito*Pst1* mouse model could be due to the different models used. Firstly, it is possible that different mechanisms may be driving clonal expansion of mtDNA deletions in humans and in mice. While a strong similarity between mtDNA deletion accumulation in human and murine muscle has been documented in a number of independent studies (Bua *et al.*, 2006; Herbst *et al.*, 2007), more recent research has shown that mtDNA do not accumulate within mouse

neurons in a manner comparable to human neurons (Guo *et al.*, 2010). When this is taken into considerations alongside other age-related differences, such as a reduced accumulation of neuromelanin in murine compared to human substantia nigra (Kim *et al.*, 2006), it becomes clear that there are some significant and fundamental differences in ageing between humans and mice. This highlights the importance of choosing models carefully, as the relevance of age-related changes in mice to human cases seems to vary between tissue types. It is therefore plausible that mtDNA deletions have a replicative advantage in neurons from the mito*Pst1* mouse but not necessarily in other tissue types from the same model; there is also no guarantee that comparable results would be observed in human cases.

In comparing our findings to the reported observations in the mtDNA deletion cytoplasts, it is important to note that a replicative advantage for mtDNA deletions was only found under relaxed copy number control in the mtDNA deletion cytoplast study. In fact, Diaz *et al* reported no accumulation of or selective advantage for mtDNA deletions under normal cellular conditions (Diaz *et al.*, 2002), in agreement with our own findings in patient tissue. The observation of a an accumulation of mtDNA deletions under relaxed copy number conditions has since been confirmed in human muscle, in a study of changes to the mitochondria following HIV treatment with nucleoside analog reverse transcriptase inhibitor anti-retroviral drugs (NRTIs) (Payne *et al.*, 2011). NRTIs were known to inhibit the function of mitochondrial POLγ (Lim and Copeland, 2001), to cause a temporary but severe level of mtDNA depletion (Cote *et al.*, 2002), and were reported to be associated with mtDNA deletions(Maagaard *et al.*, 2006); the study carried out by Payne *et al* successfully demonstrated an accelerated accumulation of mtDNA deletions associated with an increase in mtDNA turnover following the mtDNA depletion induced by the application of NRTIs (Payne *et al.*, 2011). The findings reported by Diaz *et al* in mtDNA deletion cytoplasts therefore seem to mimic current findings in human tissue remarkably well; no replicative advantage for mtDNA deletions is reported under normal cellular conditions (as in this study), but a selective advantage leading to accumulation of mtDNA deletions seems to be present under relaxed copy number control (as in the NRTI study carried out by Payne *et al*, 2011).

A subtle difference between the research aims of this study and those of the mito*Pst1* mouse study could also contribute to explaining the contradictory results we have gathered. While the mito*Pst1* mouse study aimed to identify whether mtDNA deletion size affected the likelihood of the mutation undergoing clonal expansion, our work focussed upon how mtDNA deletion size affected the area through which the mutation spread by clonal expansion – with the implication that a greater spread of mtDNA deletion accumulation could be due to a more rapid rate of accumulation. Though no indication was found to suggest that larger mtDNA deletions were more prone to clonal expansion over greater distances through muscle fibres, with no distinction between the deletion sizes in 'long' and 'short' COX-deficient regions, the overall results are still in keeping with the mito*Pst1* mouse model study. Analysis of the total 122 mtDNA deletions in our study showed that larger mtDNA deletions were more prevalent than small (75% were >5kb and 50% were >6.75kb) which could either suggest that larger mtDNA deletions are formed more frequently, or that increasing mtDNA deletion size correlates with an increase in likelihood for clonal expansion to be initiated. In either scenario, our results would suggest that there is no further advantage for large mtDNA deletions sizes once clonal expansion of an mtDNA deletion has begun, as no observed correlation was found to exist between mtDNA deletion size and area of accumulation by clonal expansion.

A potential drawback to the use of patient tissue for this study was the examination of each mtDNA deletion at only a single time point during clonal expansion, with no information on how much time has passed since the deletion formation event (i.e. how long each deletion has been accumulating for). As area of COX-deficiency caused by the clonal expansion of a specific mtDNA was being used as an indicator of clonal expansion rate – as rate could not be directly determined from examination of tissue from a single time point – this prompted a concern that we may simply observe the deletions which formed first accumulating the most to cause the largest regions of COX-deficiency. However, having carried out an *a priori* power analysis to calculate the minimum sample size required to observe a significant difference in deletion size between 'long' and 'short' COX-deficient regions, we are confident that sufficient analysis has been done to pick up any trend between mtDNA deletion size and rate of accumulation. The *a priori* power analysis was carried out using the highest standard

deviation seen experimentally (2.74kb), demonstrating a need for a minimum of 36 samples per group to observe a difference in mtDNA deletion size of at least 2kb; our analysis of 60 'short' and 62 'long' COX-deficient muscle fibre regions would be more than sufficient to pick up any significant difference in mtDNA deletion size.

The importance of clonal expansion in causing cellular pathology in ageing and disease is highlighted by the ability of cells to maintain normal function in the presence of low level mtDNA deletions; the initial deletion formation event could therefore never lead to a biochemical defect without the intercession of clonal expansion. It is consequently of paramount importance to understand the mechanism by which clonal expansion functions, in order to be able to intervene in the clinical progression of diseases involving mtDNA deletions. We have observed no variation in the ability of mtDNA deletions of different sizes to accumulate longitudinally through skeletal muscle fibres, leading us to the conclusion that smaller mtDNA molecules do not possess a replicative advantage to drive forward clonal expansion. While we have focussed upon the finding that smaller genome size is not an advantage, it is important to note that we have seen no trend toward a greater rate of clonal expansion for the smallest mtDNA deletions either, implying that there is no disadvantage associated with losing larger sections of the genome through a deletion event. However, it remains possible that there may be an advantage for large mtDNA deletions at an early stage of clonal expansion. Though smaller mtDNA molecules do not seem to display an elevated rate of clonal expansion, the high proportion of large mtDNA deletions in the overall set of investigated deletions may indicate a preferential initiation of clonal expansion for large mtDNA deletions, as reported in the miso*Pst1* mouse model study (Fukui and Moraes, 2009). In short, our results suggest that, at least in terms of mtDNA deletion size, there is no selection taking place once the deletion has formed. In addition, if deleted mtDNA had a marked replication advantage over wild-type mtDNA then we would expect patients with large-scale single mtDNA deletions to show a marked increase in deletion levels over time. Whilst studies are limited in this area, there is little evidence that mtDNA deletion level changes over time; further evidence against the selective replication of smaller mtDNA species. Our results therefore indirectly support the hypothesis that random genetic drift is the likely mechanism driving the clonal expansion of mtDNA deletions in ageing and disease (Elson *et al.*, 2001).

Chapter Four

Chapter 4:

Does the mtDNA deletion load increase over time in single mtDNA deletion patients?

4.1 Introduction – Progression of mtDNA disease over time

Mitochondrial disease is known to be highly heterogeneous in terms of disease presentation and progression, and single large-scale mtDNA deletion disease is no exception. Little is known about the disease progression, and research into this area is obfuscated by the different phenotypic presentations and rates of progression observed in patients. This creates a need for longitudinal studies of individual patients to study the phenotypic course of disease progression, as it is currently not possible for clinicians to predict a patient's disease course - a topic explored further in Chapter 5.

At a molecular level, there is an awareness of many changes which occur during progression in single mtDNA deletion disease, but not which factors actually drive progression. Respiratory chain dysfunction has clearly been shown to increase over time in cases of muscle myopathy, with decreasing respiratory function directly related to worsening muscle myopathy (Chinnery *et al.*, 2003). MtDNA copy number has also been found to decrease over time in patients with single mtDNA deletions, with a reduction in absolute wildtype mtDNA number in single cells suggested as a cause for increasing levels of dysfunction over time in skeletal muscle (Durham *et al.*, 2006). A marked reduction in wildtype mtDNA in COX-deficient fibres in extraocular muscle has also been identified in cases of CPEO (Greaves *et al.*, 2010), suggesting similar tissue-specific mechanisms of disease progression in extraocular and skeletal muscle.

Due to decreasing levels of wildtype mtDNA copy number, an assumed accumulation of mtDNA deletion levels over time has been attributed to the progression of single mtDNA deletion disease over time. Findings that mtDNA deletions also accumulate in normal aging have strengthened this assumption, with a number of groups establishing a role for the formation and accumulation of mtDNA deletions in neuronal loss (Bender *et al.*, 2006; Kraytsberg *et al.*, 2006), COX-deficient muscle fibres occurring in normal aging (Bua *et al.*, 2006), muscle fibre loss (Herbst *et al.*, 2007) and many other hallmarks of ageing. Despite the mounting evidence in accumulation of age-related mtDNA deletions over time in the healthy population, little work has been undertaken

to investigate changing heteroplasmy levels over time in single mtDNA deletion patients. Evidence of a continuous increase in mtDNA levels over time in this patient group would strongly support the presence of an inherent advantage for mtDNA deletions driving clonal expansion.

4.2 Aims and Hypotheses

The aims of this case study of a patient with a single large-scale mtDNA deletion were twofold; to identify potential causes of patient progression at a molecular level, and to investigate the presence of a replicative advantage for mtDNA deletions in human tissue. This investigation was based upon a thorough genetic analysis of two muscle biopsies from a single patient, these samples having been acquired thirteen years apart.

This study was driven primarily by the long-standing hypothesis of a replicative advantage for mtDNA deletions over wildtype mitochondrial genomes (Wallace, 1992), due to their smaller size and an inferred decrease in replication time. If this hypothesis were to hold true in cases of single large-scale mtDNA disease, we would expect to see a continuous increase in mtDNA deletion heteroplasmy levels, until homoplasmy was reached for the deleted mtDNA species. We therefore hypothesised that, where samples were available for analysis from different time-points in a single patient's life-course, the later sample(s) would display a higher level of mtDNA deletion heteroplasmy.

At a cellular level, if the 'survival of the smallest' theory of a replicative advantage for deleted mtDNA species over wildtype mtDNA holds true, it would be predicted that individual COX-deficient fibres would also demonstrate an increase in deletion heteroplasmy levels over time, tending towards mutant homoplasmy. Other cellular developments which would hold true with the 'survival of the smallest' theory would be increasing levels of COX-deficient fibres; specifically where increased COX-deficiency has been driven by increased mtDNA deletion levels (i.e. the single mtDNA deletion present in the muscle of this patient has increased above a threshold for normal biochemical activity in an increasing number of muscle fibres over time). Therefore it can be suggested that increased COX-deficiency, linked with a rise in mtDNA deletion heteroplasmy levels, should be apparent over time if deleted mtDNA

deletion species do display a replicative advantage over wildtype mtDNA molecules. If this is found to be the case, this would be indicative of rising mtDNA deletion levels over time driving phenotypic progression of single large-scale mtDNA deletion disease over time in patients.

4.3 Methods

4.3.1 Patient history

The patient involved in this study had a classic presentation with CPEO and muscle weakness. He first presented with CPEO at 28 years of age; with was confirmed as a case of single large-scale mtDNA deletion disease following analysis of an initial diagnostic muscle biopsy. 35% of muscle fibres in this biopsy were reported to be COX-deficient, while the mtDNA deletion heteroplasmy load in this biopsy was measured at 75%. Despite this high mtDNA deletion load, disease progression was found to be slow in this patient, with an average increase of 1.2 NMDAS points per year. However, much of this progression is was due to increasing severity of the patient's epileptic seizures - thought to be unrelated to his single deletion disease as epilepsy is not a common phenotype in patients with large-scale single mtDNA deletions, and the patient's epileptic seizures were long-standing prior to onset of CPEO. Symptom progression was seen in exercise tolerance, gait stability, myopathy and ataxia, as well as vision and migraine.

4.3.2 Patient biopsies, tissue sections and histochemistry

Two skeletal muscle samples (vastus lateralis) were obtained by open biopsy from the single deletion patient discussed above; these were obtained from the same leg, but a different biopsy site. The initial biopsy was taken for diagnostic purposes, while a second biopsy was taken thirteen year later as part of an exercise trial (Exercise testing in patients with mitochondrial myopathy, 2003/21) and was consented for research use. These are henceforth to be referred to as Biopsy 1 (diagnostic) and Biopsy 2 (after 13 years, exercise trial). Unfortunately, no information is available regarding changes

to the patient's muscle mass over the 13 years between biopsies, these having been carried out at different hospitals.

Multiple 20µm-thick sections were taken from each biopsy; an initial set of three sections were cut onto glass slides for total DNA extraction, while all further sections were mounted onto PEN-membrane slides for subsequent histochemical analysis and single fibre isolation.

4.3.3 Histochemical analysis and tissue DNA extraction

Sequential tissue sections of 20µm thickness mounted onto PEN-membrane slides were alternately assessed for dual COX and SDH histochemistry or SDH histochemistry only. The dual histochemical assay was carried out in order to identify muscle fibres displaying a biochemical defect, and served as a map of histochemical activity for sections assayed for only SDH activity from which individual muscle fibres were isolated for genetic analysis, as discussed in section *2.2.2.1*.

Tissue sections mounted onto glass slides were scraped into 1.5ml microcentrifuge tubes using a single-use scalpel, in preparation for DNA extraction. The DNA extraction was carried out using a Qiagen DNeasy blood and tissue kit, following the standard protocol for purification of total DNA from animal tissues (as described in *2.2.3.1*). DNA was eluted into the minimum recommended amount of 100µl buffer AE (supplied with Qiagen DNeasy blood and tissue kit) to maximise DNA concentration; this was done twice per sample in order to maximise the total DNA yield from each sample.

4.3.4 Individual muscle fibre isolation and lysis

Individual muscle fibres were identified as being deficient in COX activity, biochemically normal in terms of COX activity or COX-intermediate (Murphy *et al.*, 2012) from sections upon which the dual COX/SDH histochemical assay had been carried out. These sections were then used as a map of biochemical activity for serial sections assayed only for SDH activity, allowing accurate identification of COX-normal and COX-deficient fibres without the use of the histochemical assay for COX activity.

Individual muscle fibre isolation and DNA extraction were carried out as standard, following the method outlined in section *2.2.3.2.1*.

4.3.5 Real-time PCR analyses

Quantitative assessments of mitochondrial DNA, including mtDNA copy number analysis and measurement of the mtDNA deletion heteroplasmy level, were carried our using real-time PCR. Total mtDNA copy number was determined by comparison of the number of mtDNA copies relative to nuclear DNA marker *18S* (see section *2.2.4.5.2*), while both wildtype and total mtDNA copy numbers were assessed in single cell DNA samples using an established standard curve protocol (*2.2.4.5.3-5*); mtDNA deletion levels in both tissue homogenate and single cell DNA samples were determined by *MTND1*/*MTND4* quantification (see section *2.2.4.5.1*).

4.3.6 Statistical Analysis

All statistical analysis was carried out using GraphPad Prism v.4 statistical software. Group comparisons were made using unpaired t tests or Mann Whitney tests, and data correlation was assessed using a 2-tailed Spearman test at 95% confidence and simple (linear or non-linear) regression. In some cases, data transformation was required to allow for appropriate analysis by linear regression; a Box-Cox power transformation (Box and Cox, 1964) was carried out in each of these cases to identify the most appropriate data transformation to use. Relevant tests, as detailed in section *2.2.6*, were chosen based upon data distribution (i.e. depending upon whether or not the spread of data followed a normal distribution, in order to maximise the power of each statistical analysis).

4.4 Results

4.4.1 Initial repeat biopsy investigations

Initial histochemical analysis of two *vastus lateralis* biopsies, taken either side of a thirteen year interval from a single large-scale mtDNA deletion disease patient, was carried out by the Newcastle Mitochondrial NCG Diagnostic Laboratory. COX, SDH, and COX/SDH histological stains were performed on serial sections of each biopsy, revealing a clear histological progression and large increase in COX-deficient muscle fibres in the patient tissue (Figure 4.37).

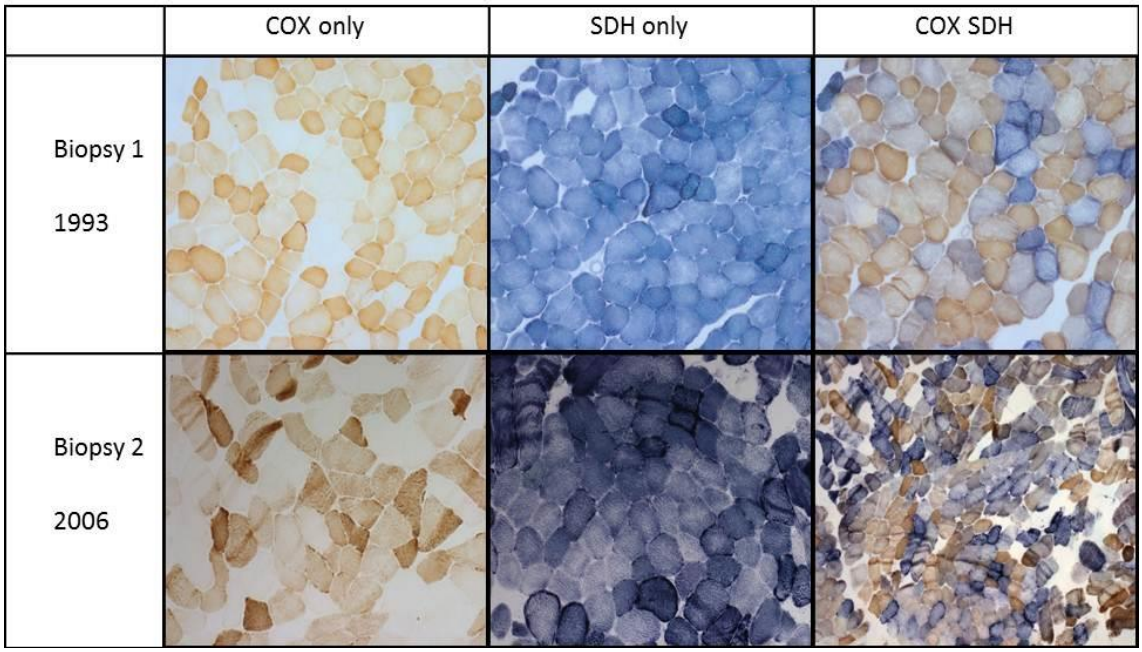

Figure 4.37 - Histochemical activity assays.

COX only, SDH only and dual COX/SDH histochemical assays carried out on serial 10µm thick sections of available patient tissue. Images courtesy of the Newcastle Mitochondrial NCG Diagnostics service.

Initial estimates of COX-deficiency levels were carried out by the Newcastle Mitochondrial NCG Diagnostics service based upon these histochemical assays; approximately 35% of muscle fibres were reported to be COX-deficient in biopsy 1, compared to 80% of muscle fibres in biopsy 2. This constitutes a 2.28-fold rise in COX-deficiency over the thirteen year period between these biopsies, or an increase of – on average – an extra 3.5% of muscle fibres becoming COX-deficient each year. The

presence of COX-intermediate fibres was not reported, not being part of the standard diagnostic assessment of patient samples.

Following the reported increase in COX-deficiency over the 13 year period between these 2 muscle biopsies, in keeping with increasing severity of muscular symptoms, it was expected that a rise in mtDNA deletion heteroplasmy levels would be observed. However, Southern blot analysis carried out by the Newcastle Mitochondrial NCG Diagnostics service revealed no change to the mutation level in homogenate mtDNA; mtDNA deletion heteroplasmy remained stable at approximately 75%.

4.4.2 Analysis of homogenate tissue DNA samples

For each of the two biopsies, homogenate DNA extracted from biopsy tissue was available for analysis from the NCG Diagnostics Laboratory.

To ensure that the previous deletion level analysis carried out by Southern blot was accurate, real-time PCR was used to measure mtDNA deletion heteroplasmy in DNA samples from both biopsies. The ND1/ND4 assay (He *et al.*, 2002) was used to compare the ratios of total and wild-type mtDNA species present in each sample, as described in *2.2.4.5.1*, in order to quantify the level of mtDNA deletion present. Biopsy 1 was found to have an mtDNA deletion heteroplasmy level of 75.1%, while Biopsy 2 had an mtDNA deletion level of 76.6% – a rise of only 1.5% over thirteen years. This was very much in keeping with the previous Southern blot results, though these results were surprising given the reported drastic increase in COX-deficiency from Biopsy 1 to 2.

As it was found that increasing deletion levels could not be the cause of the histological progression between the two biopsies, mitochondrial DNA copy number was next investigated by real-time PCR. For these homogenate tissue DNA samples the 18S/ND1 assay was employed to establish total mtDNA copy number relative to nuclear DNA copy number, determined by the measurement of *18S* rRNA copy number, as described in *2.2.4.5.1*. Biopsy 1 was found to have approximately 385 copies of the mitochondrial genome per copy of nuclear marker 18S rRNA, while Biopsy 2 had approximately 190. This shows a decrease in total mtDNA copy number of ~50% over the thirteen year period between biopsies.

Biopsy	Year taken	COX-deficiency level	mtDNA deletion heteroplasmy level	Total mtDNA copy number
1	1993	35%	75.1%	385
2	2006	80%	76.6%	190
	13 year interval	55% increase in COX-deficiency	No significant increase in deletion level	50% reduction in total mtDNA copy number

Table 4.17 - Summary of initial repeat biopsy findings.

Total mtDNA copy number is expressed as number of mitochondrial genome copies per copy of nuclear marker gene *18S* rRNA. Results from the initial analysis of homogenate tissue DNA from Biopsy 1 and 2, taken thirteen years apart from the same single large-scale mtDNA deletion patient. No increase in mtDNA deletion level was observed over this time period, despite a large increase in observed COX-deficient muscle fibres. However, mtDNA copy number was found to half - suggesting reduced copy number may be responsible for the observed biochemical progression.

4.4.3 Single muscle fibre extraction

The results from molecular analysis of homogenate tissue mtDNA from Biopsies 1 and 2 were not in keeping with the reported histochemistry, making further investigation vital. A minimum of 25 individual COX-deficient muscle fibres, 25 individual COX-positive muscle fibres and 25 COX-intermediate individual fibres were extracted from tissue sections assessed only for SDH histochemistry (as discussed in *2.2.2.1*), from each biopsy. It was decided that it was as important to look for molecular changes in COX-normal and COX-intermediate fibres as in COX-deficient fibres, in order to identify on-going molecular changes. All fibres were lysed using the same single cell lysis method, as described in *2.2.3.2.1*.

Individual fibres were extracted by laser microdissection from sections upon which only the SDH histochemical assay had been carried out, using a serial section assessed for both COX and SDH activity as a map of COX-deficiency. In the examples demonstrated in Figure 4.38, 5 COX-deficient - highlighted with stars on a COX/SDH map - were selected for laser microdissection. Fibres are shown, having been drawn around, pre- and post- extraction.

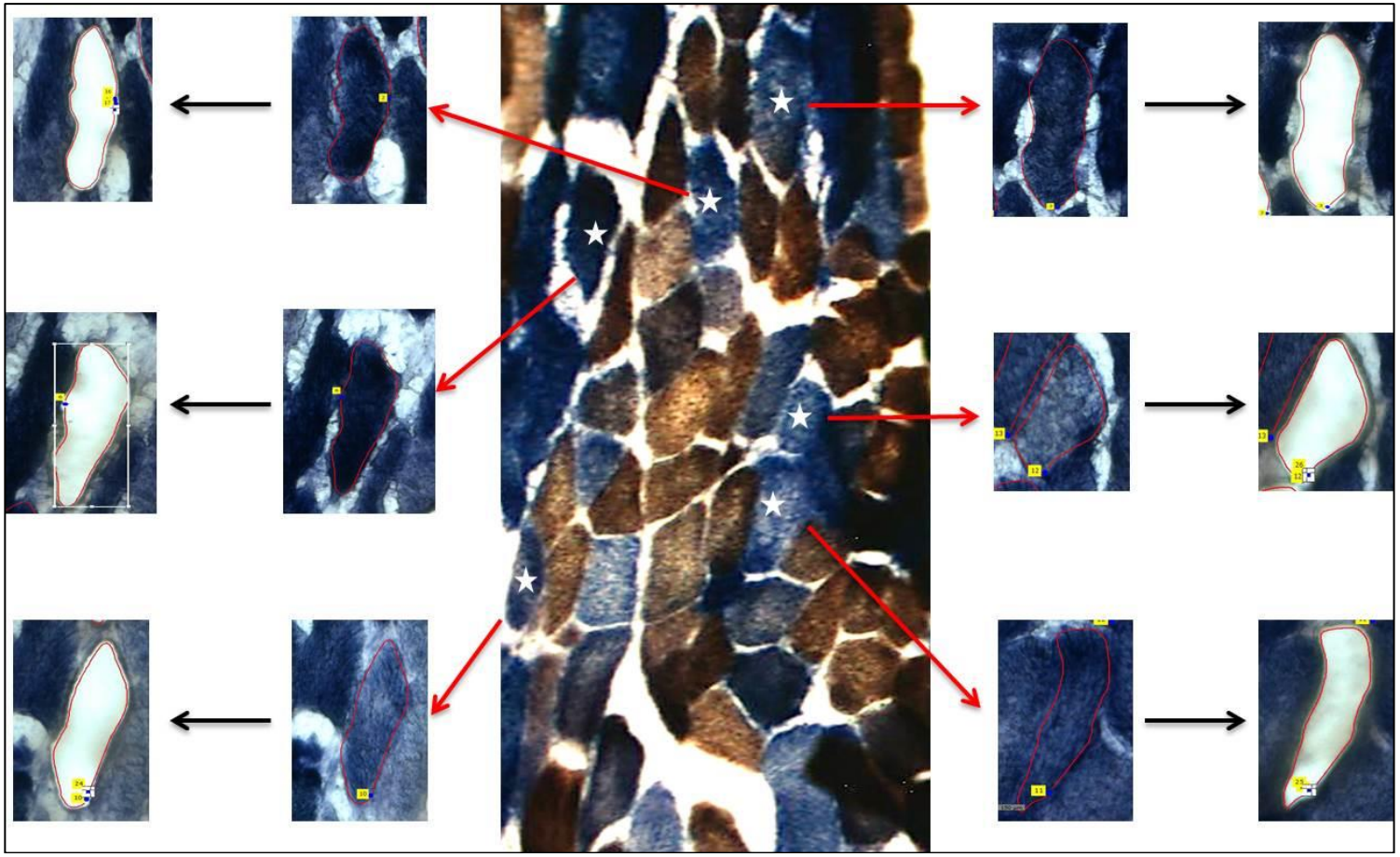

Figure 4.38 - Extraction of individual COX-deficient fibres from SDH only stained tissue.

Individual COX-deficient fibres were identified from a single COX/SDH muscle section; using this section as a map, these fibres were then identified on an SDH-only serial section mounted on a PEN-membrane slide. These fibres were selected for laser microdissection – the edge of the fibre was traced around using the Zeiss PALM software, allowing measurement of fibre area and providing a guideline for the laser to cut around. 5 fibres are highlighted above on a COX/SDH section map, and subsequently located on an SDH-only section before extraction by laser microdissection.

4.4.4 Individual muscle fibre mtDNA deletion level analysis

As for DNA extracted from homogenate tissue, the ND1/ND4 quantitative PCR assay (He *et al.*, 2002) was carried out to determine deletion level for all isolated individual muscle fibres. As in the homogenate tissue DNA study, mtDNA deletion levels were found to be stable at the single cell level between the two biopsies (Figure 4.39).

In Biopsy 1, COX-positive fibres (N = 27) were found to have a low average mtDNA deletion load of 32% (± 22%), though the total range in mtDNA deletion heteroplasmy levels was high – from 0% up to a maximum observed mtDNA deletion load of 76%. COX-deficient fibres isolated from Biopsy 1 (N = 29) had, as would be expected, a much higher average mtDNA deletion level than that found in COX-normal fibres. In the COX-deficient fibres, a mean mtDNA deletion load of 91% (± 14%) was found. For 28 of the total 29 COX-deficient fibres isolated from Biopsy 1 the spread of deletion load was quite small – particularly in comparison to the wide range of mtDNA deletion heteroplasmy found in COX-positive fibres – ranging from 83% to 98%. A single outlier had an unusually low deletion level of just 21% - this is discussed later, in *4.4.6*. COX-intermediate fibres (N = 28) isolated from Biopsy 1 were found to contain the largest range of mtDNA deletion levels, from 0% up to 84% deletion load, with a mean mtDNA deletion heteroplasmy level of 57% (±23%). An impairment of COX activity was observed in some fibres despite a low level of mtDNA deletion heteroplasmy where mtDNA copy number was subsequently found to be depleted (intermediate fibres with deletion levels 0, 11 and 23% had wildtype copy numbers of 13, 17 and 14 respectively, compared to an average of 42 in wildtype fibres, see section 4.4.5.2).

Similar results were found in individual fibres extracted from Biopsy 2. COX-positive fibres (N = 26) were again found to have a low average deletion load (28% ± 29%) but a high degree of spread, with a minimum deletion level of 0% and a maximum observed deletion level of 85%. COX-intermediate fibres extracted from Biopsy 2 were also found to display a large spread of mtDNA deletion heteroplasmy level, ranging from 0% to 87% deletion load (intermediate fibres with deletion levels 3, 14 and 16% had wildtype copy numbers of 19, 13 and 18 respectively, compared to an average of 42 in wildtype fibres, see section 4.4.5.2). However, the average heteroplasmy level was higher than that observed in COX-positive fibres, with a mean deletion level of 58% (+28%). COX-deficient muscle fibres isolated from Biopsy 2 (N = 25) displayed a smaller

range of spread than COX-normal fibres – ranging from 65% to 97%, excluding two outliers with mtDNA deletion loads of 0% and 13% (to be discussed in *4.4.6*) – and a much higher average mtDNA deletion level (81% ± 25%).

Mann-Whitney tests, chosen as the data sets do not follow a normal distribution, were carried out at a 95% confidence interval to assess whether any significant differences were apparent between the 6 assessed groups of mtDNA deletion levels. As would be expected, mtDNA deletion heteroplasmy was significantly higher in COX-deficient than in COX-normal muscle fibres in both biopsies ($P < 0.0001$ in both cases). Also observed in both biopsies were the expected intermediary mtDNA deletion levels present in COX-intermediate fibres – significantly higher than the levels present in COX-positive fibres, but significantly lower than the observed mtDNA deletions loads in COX-deficient fibres (Biopsy 1 COX-intermediate fibres vs COX-positive and vs COX-deficient $P < 0.0001$, Biopsy 2 COX-intermediate fibres vs COX-positive $P = 0.0007$, vs COX-deficient $P = 0.0003$). No change in mtDNA deletion load was found to have occurred between the two biopsies in COX-positive muscle fibres ($P = 0.3732$) or in COX-intermediate fibres ($P = 0.3307$), though the small decrease in average mtDNA deletion level in COX-deficient muscle fibres from Biopsy 1 to 2 was found to be significant ($P = 0.0480$). However, when the outliers mentioned above (mtDNA deletion levels more than 2 standard deviation's outside of the mean heteroplasmy levels observed in that fibre group) were excluded, no significant difference was found to exist between the deletion levels in COX-deficient muscle fibres from the two biopsies ($P = 0.0678$).

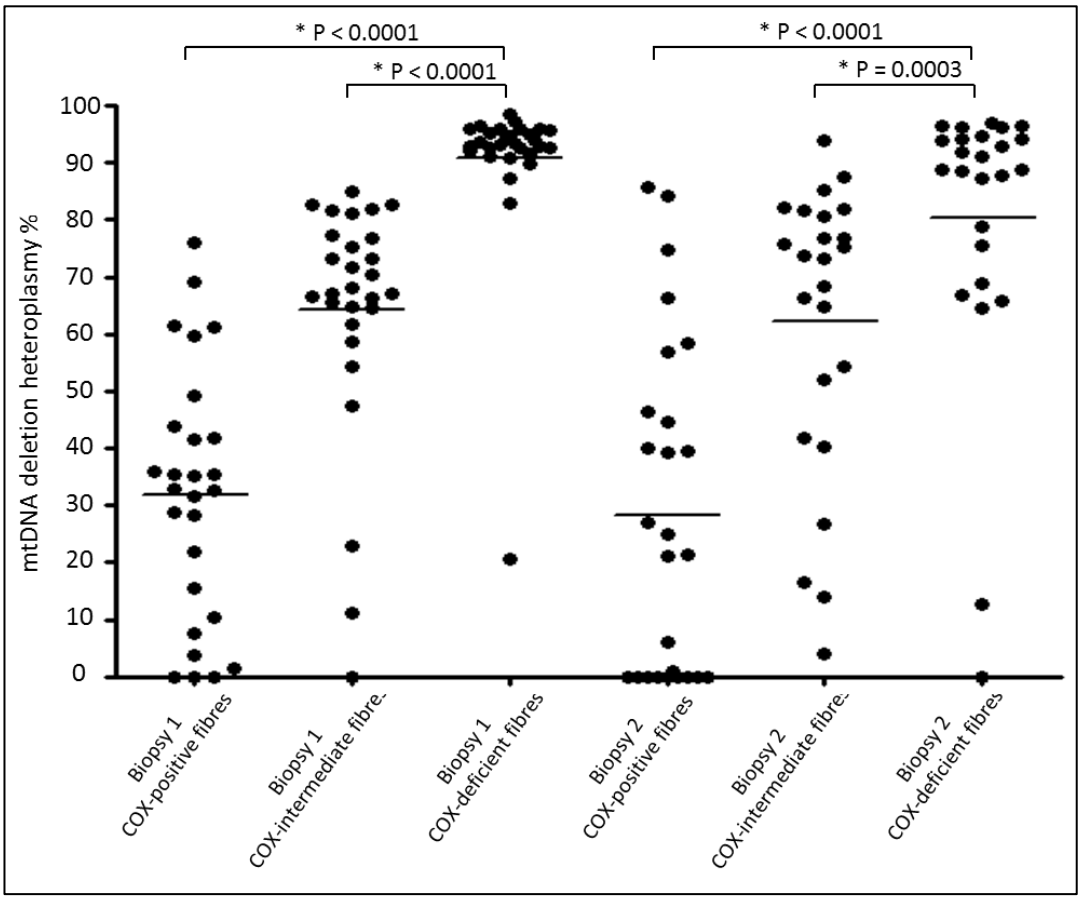

Figure 4.39 - mtDNA deletion heteroplasmy % measured in individual COX-positive, intermediate and deficient muscle fibres isolated from Biopsy 1 and 2.

Individual COX-positive, intermediate and deficient fibres were isolated from each of two biopsies taken from a single large-scale deletion patient either side of a 13-year interval, and were assessed for mtDNA deletion heteroplasmy level (%) using the *ND1/ND4* quantitative PCR assay. mtDNA deletion level was found to be significantly higher in COX-deficient fibres than in COX-positive fibres in both patient biopsies, with COX-intermediate fibres typically displaying an intermediate level of heteroplasmy. Mann-Whitney t-tests were carried out to assess the similarity in mtDNA deletion heteroplasmy levels between groups; statistically significant differences in mtDNA deletion level are indicated with an asterisk, with relevant P values supplied.

4.4.5 Individual muscle fibre mtDNA total copy number analysis

Following the mtDNA deletion analysis, mitochondrial DNA copy number was assessed for each of the isolated individual COX-positive, intermediate or deficient muscle fibres. This was carried out using the universal standard curve method of absolute mtDNA copy number analysis, as described in *2.2.4.5.5*. A universal standard curve was generated to allow results to be comparable between separate real-time PCR runs, and

validated by the inclusion of 3 copy number standards on each real-time run to ensure that the standard curve was generating accurate results. Copy number was, in all cases, expressed as copy number/μm^2 to allow an accurate comparison of relative copy number between all extracted muscle fibres of different areas (Figure 4.40).

4.4.5.1 Individual muscle fibre mtDNA total copy number analysis

In Biopsy 1, COX-positive muscle fibres were found to have the lowest total mtDNA copy numbers, as measured by the quantity of *MTND1* present by quantitative PCR. COX-positive fibres had a mean mtDNA copy number of 59 ± 53 copies/μm^2, with a range from 6 to 197 copies/μm^2. Both COX-intermediate and COX-deficient fibres displayed significantly higher levels of mtDNA (P = 0.0003 and 0.0022 respectively), with no significant difference existing in terms of total mtDNA copy number between these two groups (P = 0.8419). COX-deficient fibres displayed a much larger range of mtDNA copy number than that observed in COX-positive fibres, and a higher average total mtDNA copy number (range 6 – 399 copies/μm^2, mean 142 ± 109 copies/μm^2). The range in total mtDNA copy number observed in COX-intermediate fibres was slightly smaller than in COX-deficient fibres (range 36 – 314 copies/μm^2, mean 121 ± 73 copies/μm^2).

No significant differences were observed in any cell type between the 2 biopsies. A rise in total mtDNA copy number was observed in COX-positive fibres (from 59 ± 53 copies/μm^2 to 96 ± 95 copies/μm^2), though this was found not to be a significant change (P = 0.1910). Total mtDNA copy number remained more clearly stable in both the COX-intermediate (from 121 ± 73 copies/μm^2 in Biopsy 1 to 129 ± 109 copies/μm^2 in Biopsy 2) and COX-deficient fibre types (from 142 ± 109 copies/μm^2 in Biopsy 1 to 119 ± 106 copies/μm^2 in Biopsy 2), with no significant change in total mtDNA copy number over time identified in either group (P = 0.5945 and 0.3144 respectively). However, no significant difference was found to exist between COX-positive and deficient fibres (P = 0.5529) or COX-intermediate and COX-positive or deficient fibres (P = 0.1481 and 0.5157 respectively) in Biopsy 2; the loss of significant difference between COX-positive and COX-intermediate or deficient fibres may be explained by the small rise of copy number in COX-positive fibres. The lower levels of total mtDNA

copy number observed remain static in all 3 fibre types (7 copies/µm2 for COX-positive, 31 copies/µm^2 for COX-intermediate fibres and 6 copies/µm2 for deficient fibres), while the range of copy numbers is increased in Biopsy 2 in both COX-positive and COX-intermediate fibres (7 – 409 copies/µm^2 in COX-positive fibres, and 31 – 432 copies/µm^2 in COX-intermediate fibres). The range of total mtDNA copy numbers observed in COX-deficient fibres was found to remain similar from Biopsy 1 to 2 (6 – 377 copies/µm^2).

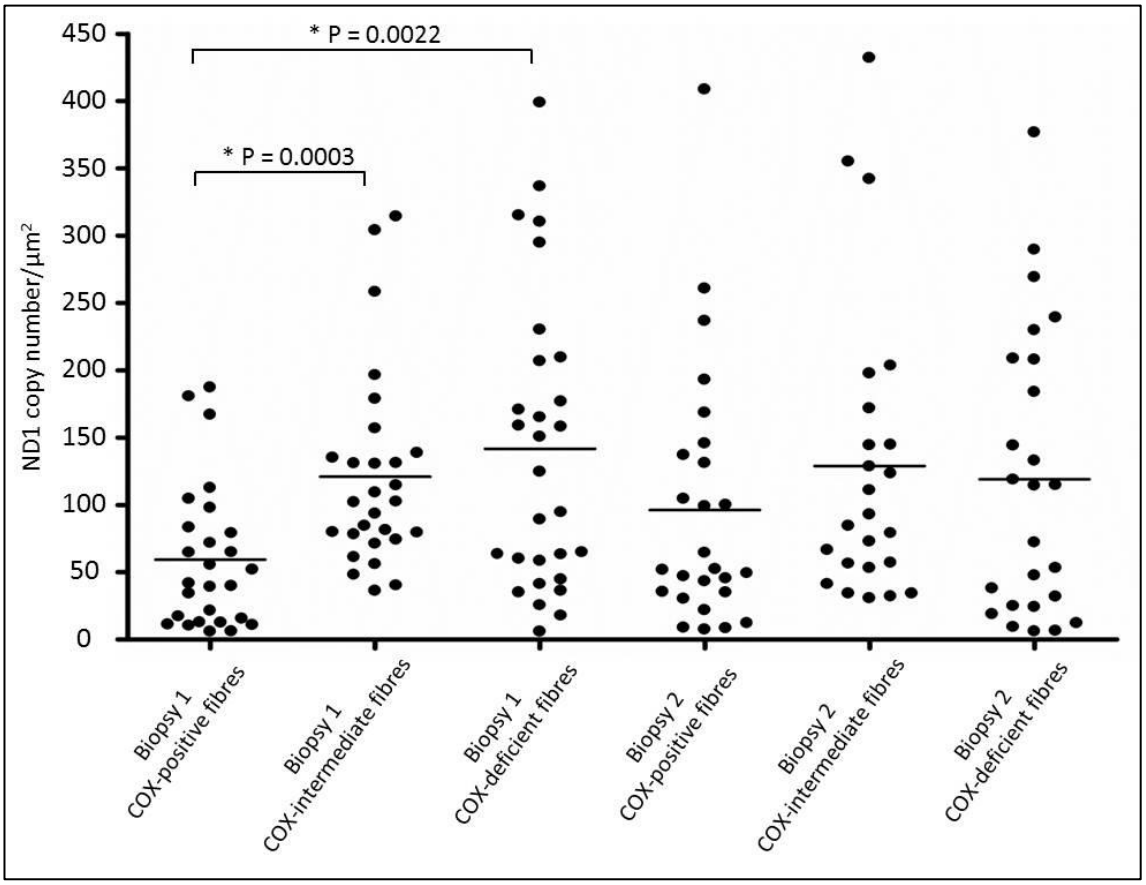

Figure 4.40 - Total copy number/µm^2 assessed in individual COX-positive, intermediate and deficient fibres from Biopsies 1 and 2.

Individual COX-positive, intermediate and deficient fibres were isolated from each of two biopsies taken from a single large-scale deletion patient either side of a 13-year interval, and were assessed for total mtDNA deletion heteroplasmy level using *MTND1* as a marker. Mann-Whitney t-tests were carried out to assess the similarity in mtDNA deletion heteroplasmy levels between groups; statistically significant differences in mtDNA deletion level are indicated with an asterisk, with relevant P values supplied. The only significant differences observed were between COX-positive and COX-intermediate and COX-deficient fibres in patient biopsy 1; the similarity in total mtDNA copy number between most fibre categories may be due to the high degree of data spread.

4.4.5.2 Individual muscle fibre mtDNA wildtype copy number analysis

Wildtype copy number, as measured using *ND4* as a marker of wildtype mtDNA, was found to be exceptionally stable in all three investigated fibre types between the two biopsies, despite a thirteen year gap between biopsies and a drastic reported histological progression in the assessed tissue. COX-positive fibres from Biopsy 1 had a mean wildtype mtDNA copy number of 42 ± 37 copies/μm^2, with a range of 5 - 155 copies/μm^2, while individual COX-positive fibres examined from Biopsy 2 were found to have a mean wildtype copy number of 43 ± 33 copies/μm^2, with a range of 3 - 135 copies/μm^2. In both biopsies, COX-positive fibres had the highest observed range of wildtype mtDNA copy number. These two fibre sets were found to have no significant difference in wildtype copy number (2-tailed Mann-Whitney test at 95% confidence interval, P = 0.7827).

COX-intermediate fibres also displayed a stable copy number over the 13 year period between the two patient biopsies. Individual COX-intermediate fibres extracted from Biopsy 1 had a mean wildtype copy number of 47 ± 21 copies/μm^2, with a range from 13 – 102, while those isolated from Biopsy 2 had a mean wildtype copy number of 46 ± 25 copies/μm^2, with a range from 9 – 97 copies/μm^2. These two fibre sets were found to have no significant difference in wildtype copy number (2-tailed Mann-Whitney test at 95% confidence interval, P = 0.5210). COX-intermediate fibres seemed to have a higher average wildtype mtDNA copy number than COX-positive fibres in both biopsies, but this difference was found not to be statistically significant in either of the sample sets (2-tailed Mann-Whitney test at 95% confidence interval, P = 0.0786 in Biopsy 1, p = 0.4316 in Biopsy 2).

COX-deficient fibres were found to display the same lack of variation in terms of wildtype mtDNA copy number between the 2 biopsies as was observed in both COX-positive and intermediate fibres. COX-deficient fibres isolated from Biopsy 1 had a mean wildtype copy number of 9 ± 6 copies/μm^2, with a range of 2 - 31 copies/μm^2, while individual COX-deficient fibres examined from Biopsy 2 were found to have a mean wildtype copy number of 10 ± 7 copies/μm^2, with a range of 3 - 34 copies/μm^2. Both groups of COX-deficient fibres investigated were found to display the smallest range in wildtype mtDNA copy number. No significant difference in wildtype mtDNA copy number was found to exist between the two sets of COX-deficient fibre data (2-

tailed Mann-Whitney test at 95% confidence interval, P = 0.8043). COX-deficient fibres were consistently found to contain the lowest levels of wildtype mtDNA. In Biopsy 1, wildtype mtDNA copy number was significantly lower in COX-deficient fibres than in COX-positive or intermediate fibres (2-tailed Mann-Whitney test at 95% confidence interval, P < 0.0001 for both comparisons); the same trend was found to exist in Biopsy 2 (COX-deficient fibres found to have significantly lower wildtype mtDNA than COX-positive or intermediate fibres by 2-tailed Mann-Whitney test at 95% confidence interval, P < 0.0001 for both comparisons).

The high wildtype mtDNA copy number levels observed in COX-intermediate fibres was unexpected, especially in the light of reports highlighting the importance of absolute wildtype mtDNA copy number in determining cellular biochemical function (Durham *et al.*, 2005). These high mtDNA copy levels were maintained due to a strong correlation between total mtDNA copy number and mtDNA deletion heteroplasmy level (see *4.4.6.3*, Figure 4.46 C - assessed by Spearman's rho at 95% confidence, r = 0.5165, P = 0.0001). This means that the fibres with the lowest total mtDNA copy number also tend to have the lowest mtDNA deletion heteroplasmy levels, hence maintaining a high wildtype mtDNA copy number. However, while this data makes sense in the context of the total mtDNA copy number and mtDNA deletion heteroplasmy data, the similarity of the observed wildtype mtDNA levels in COX-positive and intermediate fibres does not seem to fit with the difference in cellular biochemistry. One possibility is that we see a COX-intermediate phenotype in more energy demanding cells (i.e. a high proportion of COX-intermediate fibres not be Type IIa as opposed to Type I fibres) where a higher than average wildtype mtDNA copy number would be require to meet the cell's ATP demands. This is something that could be investigated with further histochemical analysis of muscle tissue in the future, as muscle fibre type was not assessed as part of this study.

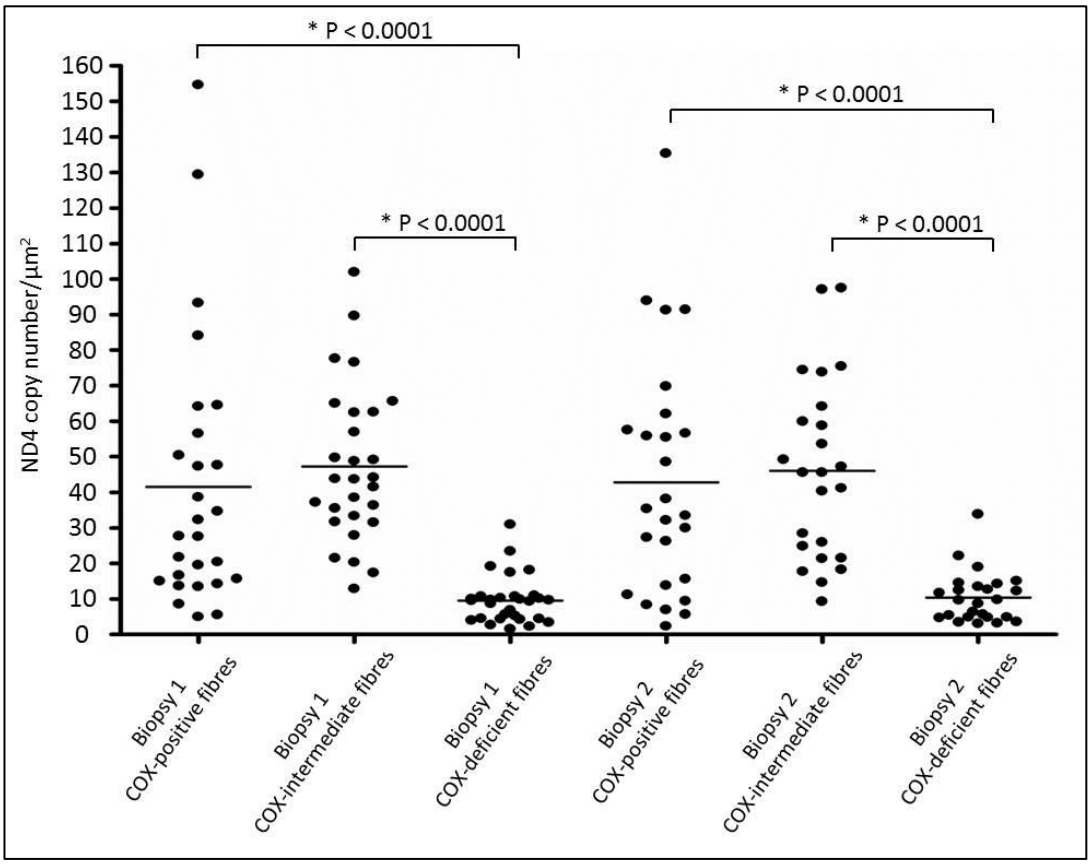

Figure 4.41 - Wildtype copy number/µm2 assessed in individual COX-positive, intermediate and deficient fibres from Biopsies 1 and 2.

Individual COX-positive, intermediate and deficient fibres were isolated from each of two biopsies taken from a single large-scale deletion patient either side of a 13-year interval, and were assessed for total mtDNA deletion heteroplasmy level using *MTND4* as a marker. Mann-Whitney t-tests were carried out to assess the similarity in mtDNA deletion heteroplasmy levels between groups; statistically significant differences in mtDNA deletion level are indicated with an asterisk, with relevant P values supplied. Wildtype mtDNA copy number was shown to be significantly lower in COX-deficient fibres than either COX-positive or COX-intermediate fibres in both patient biopsies, while COX-intermediate and positive fibres were found to be very similar in terms of wildtype mtDNA copy number.

4.4.6 Correlating mtDNA deletion level and copy number

4.4.6.1 Analysis of total mtDNA and mtDNA deletion heteroplasmy level in total dataset.

Total data from both biopsies was combined in order to assess whether deletion level tends to correlate with mtDNA copy number. Total mtDNA copy number was investigated first; correlation analysis by Spearman's rank correlation identified a significant positive relationship between mtDNA deletion level and total mtDNA copy number/μm^2 ($P < 0.0001$, $r = 0.4732$). The relationship between total mtDNA copy number and mtDNA deletion heteroplasmy was assessed for linearity – it was determined that this relationship could be better described by an exponential curve than by linear regression. The following curve was generated to fit the data:

$$\gamma = 46.04 \times 2^{\left(\frac{x}{51.14}\right)}$$

where γ = ND1 copy number/μm^2 and χ = mtDNA heteroplasmy level (Figure 4.42). This relationship indicates that total copy number is likely to be higher where mtDNA deletion levels are also high, suggesting a compensatory increase in mtDNA copy number is triggered by rising levels of mtDNA deletion heteroplasmy. The exponential relationship between these two variables also indicates that any change at high heteroplasmy levels is likely to have more effect than at low levels. For example, following the exponential curve fitted to the data, total copy number at 20% heteroplasmy is likely to lie around 60 copies/μm^2, increasing to 69 copies/μm^2 at 30% heteroplasmy (a small increase of 15% in mtDNA copy number when mtDNA deletion heteroplasmy increases from 20% to 30%); however total copy number of 93 copies/μm^2 at 80% heteroplasmy is predicted to increase to 156 copies/μm^2 following a 10% increase in mtDNA heteroplasmy level, to 90% (a large increase of 69% in mtDNA copy number when mtDNA deletion heteroplasmy increases from 80% to 90%).

Although this curve seemed to fit the data quite well, analysis of the residuals showed a skew for data-points to lie further above than below the best-fit curve. To rectify this issue, a Box-Cox transformation was carried out to identify the best data form for analysis. This transformation gave a rounded λ-value of 0.246801, meaning that the

best linear relationship can be generated between mtDNA deletion level and (total mtDNA copy number/μm^2)$^{0.246801}$, or approximately $\sqrt[4]{\text{total mtDNA copy number}/\mu m^2}$. The linear regression between these variables can then be described by the equation:

$$\gamma = 0.0103\chi + 2.4127$$

where γ = $\sqrt[4]{\text{ND1 copy number}/\mu m^2}$ and χ = mtDNA heteroplasmy level (Figure 4.43). This analysis confirmed the presence of a strong positive relationship between mtDNA copy number and mtDNA deletion heteroplasmy level, accounting for approximately 47% of variation in total mtDNA copy/μm^2 ($P < 0.0001$, $r = 0.4688$).

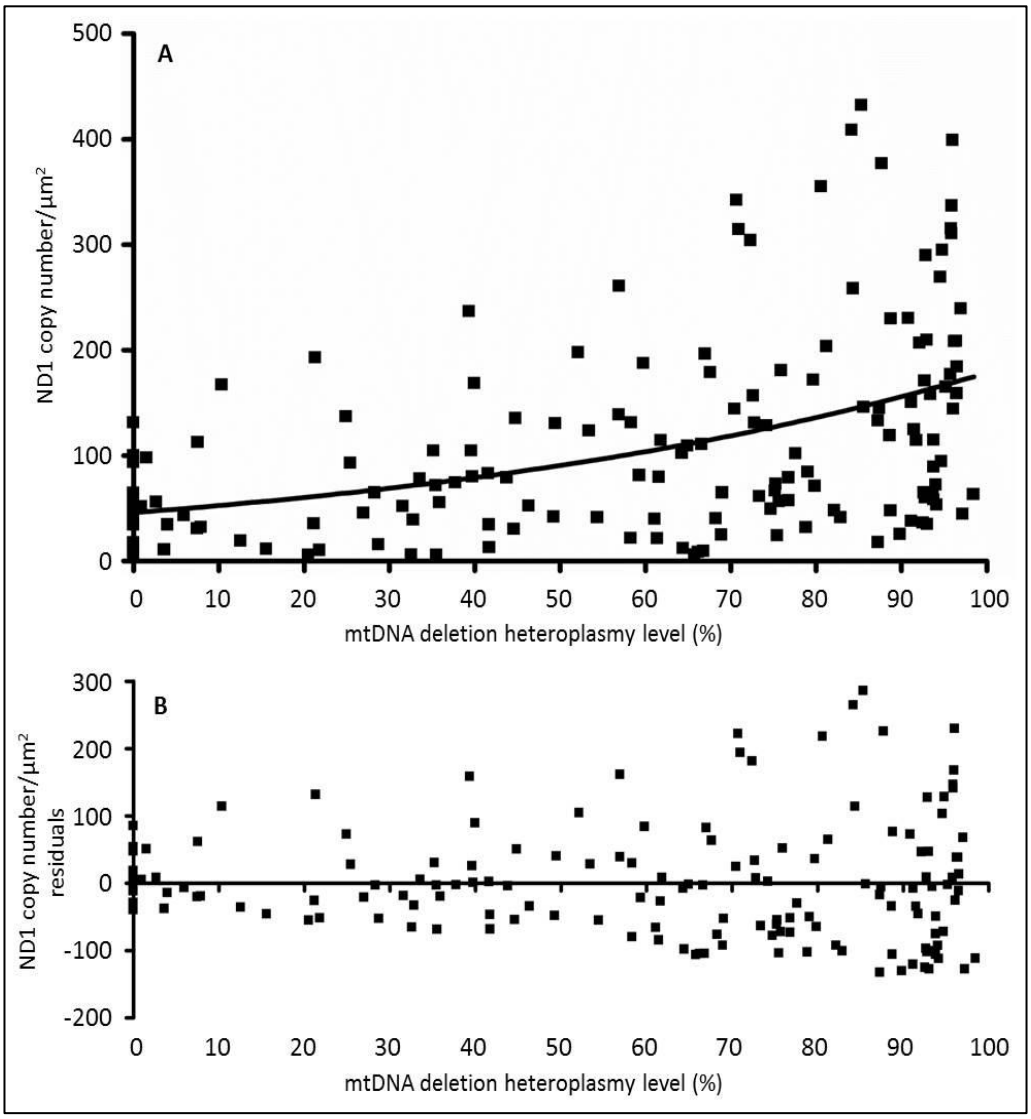

Figure 4.42 – Exponential non-linear regression of mtDNA heteroplasmy level with total mtDNA copy number/µm^2.

A – The relationship between mtDNA deletion heteroplasmy level (%) and total (*ND1*) mtDNA copy number was assessed by non-linear regression, revealing the presence of an exponential relationship between these two variables. The trend line generated by this analysis is described by the equation y = 46.04 x 2^(x/51.14), where y is total mtDNA copy number and x is mtDNA deletion heteroplasmy level. The positive, exponential relationship between mtDNA deletion level and total copy number was found to account for approximately 45% of the data spread (r = 0.4484) in this dataset. **B** – The residuals created by this data analysis were plotted and assessed for normality. The residuals were not found to follow a Gaussian distribution, meaning further analyses were required in order to accurately assess the relationship between total (*ND1*) copy number and mtDNA deletion heteroplasmy level in the most appropriate manner.

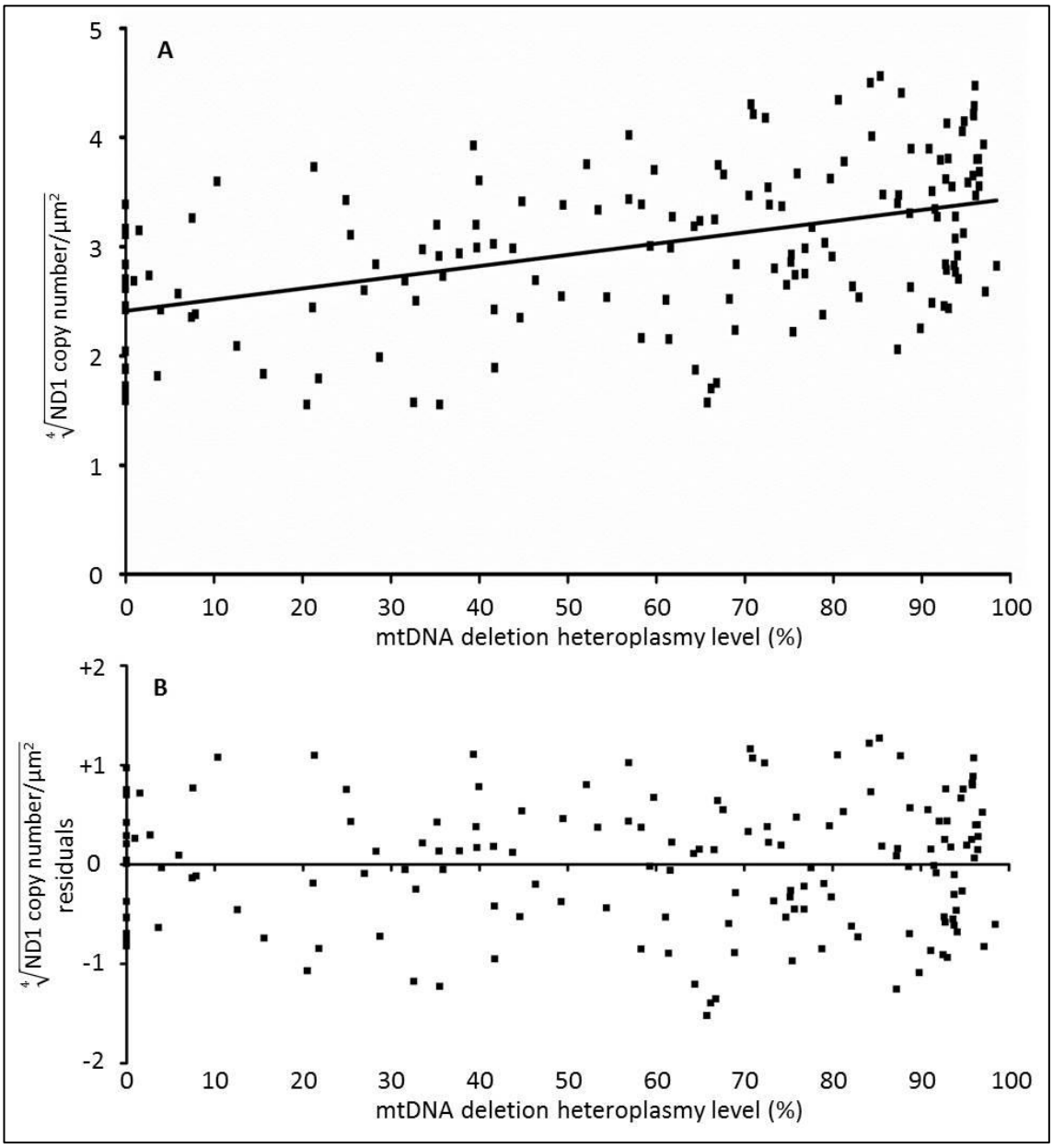

Figure 4.43 - Linear regression of the 4th root total mtDNA copy number/µm² and mtDNA deletion heteroplasmy level in total dataset.

A - A Box-Cox data transformation gave a rounded λ-value of 0.246801, suggesting the most appropriate data transformation to use to investigate a linear relationship is the 4th root of the total mtDNA copy number/µm². Linear regression was carried out to assess the relationship between the 4th root of the total mtDNA copy number and mtDNA deletion heteroplasmy level, and identified a strong positive relationship between these variables ($r^2 = 0.2198$, $P < 0.0001$). This relationship can be described by the equation $y = -0.0103x + 2.4127$, where y is the 4th root total mtDNA copy number/µm² and x is mtDNA deletion heteroplasmy level. **B –** Analysis of the residuals generated by this linear regression were found to follow a normal distribution, confirming that linear regression is an appropriate assessment of the relationship between mtDNA deletion heteroplasmy levels and the transformed total (*ND1*) mtDNA copy number dataset.

4.4.6.2 Analysis of wildtype mtDNA and mtDNA deletion heteroplasmy level in total dataset.

Following identification of a positive relationship between mtDNA deletion heteroplasmy levels and total mtDNA copy number, heteroplasmy was similarly investigated with wildtype mtDNA copy number. Correlation analysis by Spearman's rank correlation identified a significant negative relationship between mtDNA deletion level and wildtype mtDNA copy number/μm^2 ($P < 0.0001$, $r = -0.4985$). This is a stronger correlation than that with total copy number, and accounts for a greater level of data variance; this is to be expected, given that increasing deletion heteroplasmy by definition correlates to lower levels of wildtype mtDNA copy number.

The relationship between wildtype mtDNA copy number and mtDNA deletion heteroplasmy was assessed first by linear regression, but this generated an uneven spread of residuals and was therefore an inappropriate analysis; however, the following non-linear, exponential regression generated a worse spread of data, suggesting this was a worse model to use (Figure 4.44). To rectify this issue, a Box-Cox transformation was carried out to identify the best model to use for analysis. This transformation gave a rounded λ-value of 0.165495, meaning that the best linear relationship can be generated between mtDNA deletion level and (wildtype mtDNA copy number/μm^2) 0.165495, or approximately $\sqrt[6]{\text{wildtype mtDNA copy number}/\mu m^2}$. The linear regression between these variables can then be described by the equation:

$$\gamma = -0.0038\chi + 1.895$$

where $\gamma = \sqrt[6]{\text{ND4 copy number}/\mu m^2}$ and χ = mtDNA heteroplasmy level (Figure 4.45). This analysis confirmed the presence of a strong negative relationship between wildtype mtDNA copy number and mtDNA deletion heteroplasmy level, accounting for approximately 45% of variation in total mtDNA copy/μm^2 ($P < 0.0001$, $r = 0.4473$). The residuals generated by this analysis were found to follow a Gaussian distribution, confirming this as the most appropriate data transformation to carry out. The most dramatic effects of heteroplasmy are, as for the relationship between total mtDNA copy number and mtDNA deletion heteroplasmy level, seen at higher levels of mtDNA deletion heteroplasmy.

For example, following the best fit of linear regression of the transformed data, wildtype copy number at 20% heteroplasmy is likely to lie around 36 copies/μm^2, decreasing to 32 copies/μm^2 at 30% heteroplasmy; however wildtype copy number of 16 copies/μm^2 at 80% heteroplasmy is predicted to decrease to 2 copies/μm^2 following a 10% increase in mtDNA heteroplasmy level, to 90%.

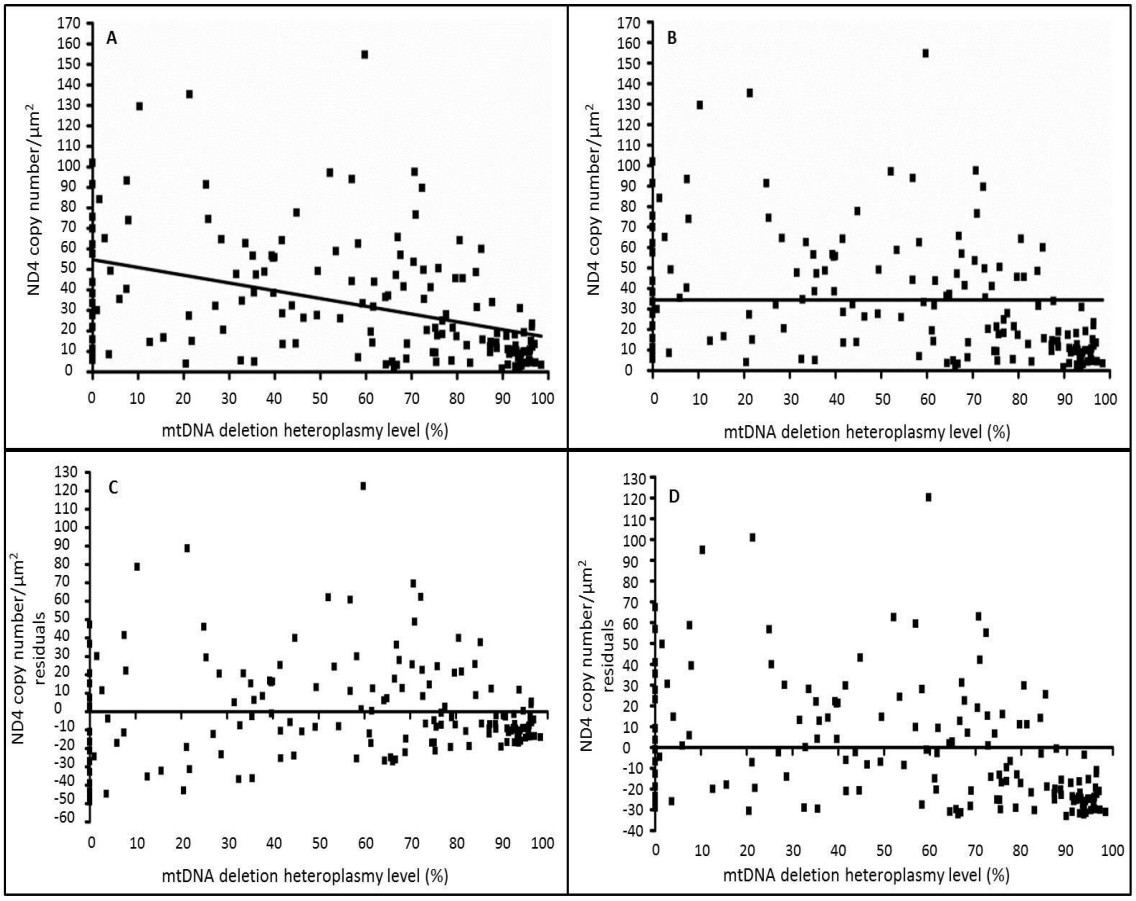

Figure 4.44 - Analysis of the relationship between wildtype mtDNA copy number and mtDNA deletion heteroplasmy level by linear and by non-linear regression.

Neither linear regression analysis (**A**) nor non-linear regression analysis (**B**) were able to generate a model suitable to analyse the relationship between wildtype (ND4) mtDNA copy number and mtDNA deletion heteroplasmy level. This is demonstrated by the non-Gaussian distribution of the residuals generated by both of these models (**C** and **D** respectively). This identified a need for further analyses to accurately assess the relationship between total (*ND1*) copy number and mtDNA deletion heteroplasmy level in the most appropriate manner.

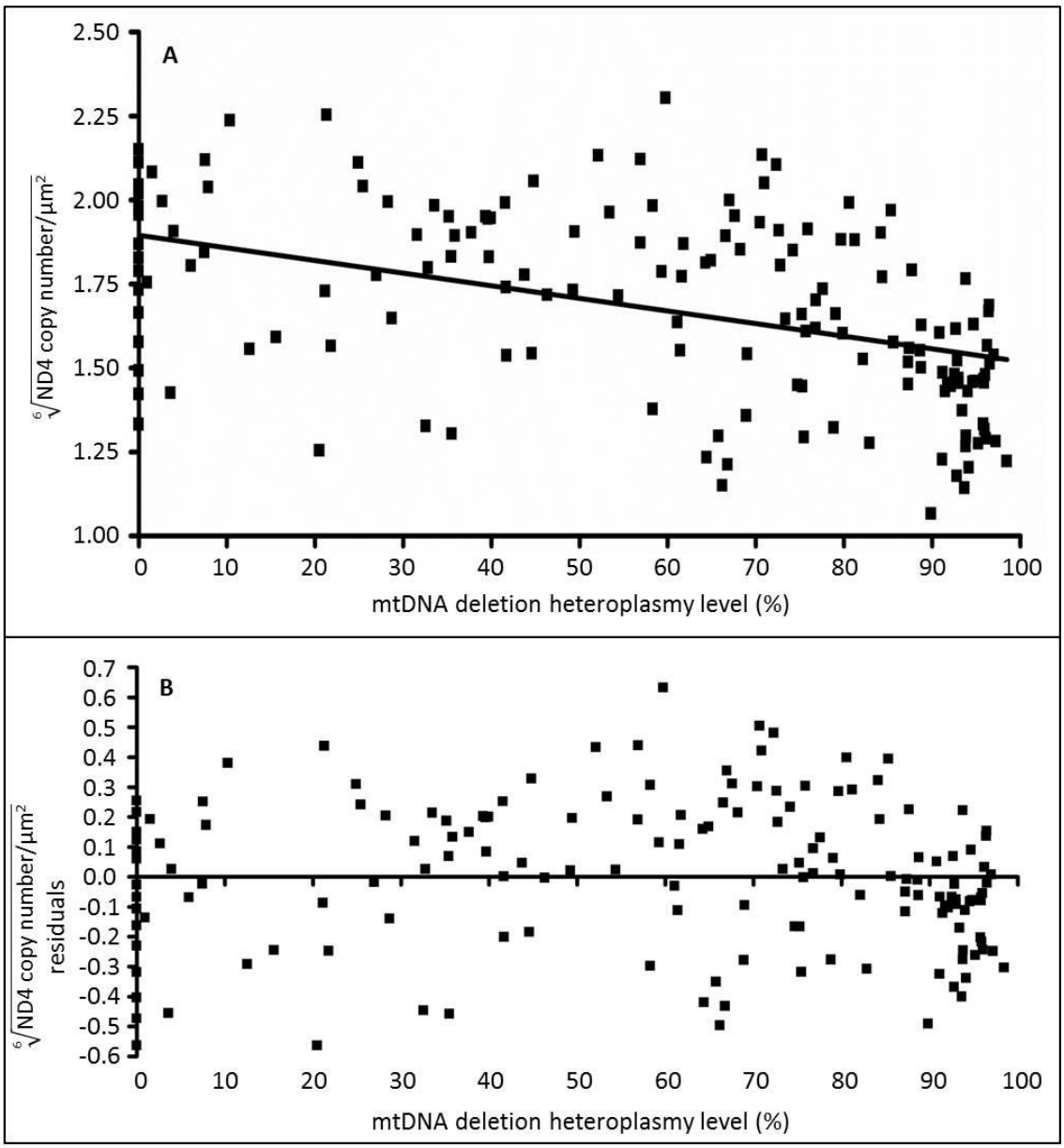

Figure 4.45 - Linear regression of 6th root wildtype mtDNA copy number/µm² and mtDNA deletion heteroplasmy level in total dataset.

A - A Box-Cox data transformation gave a rounded λ-value of 0.165495, suggesting the most appropriate data transformation to use to investigate a linear relationship is the 6th root of the wildtype (*ND4*) mtDNA copy number/µm². Linear regression was carried out to assess the relationship between the 6th root of the total mtDNA copy number and mtDNA deletion heteroplasmy level, and identified a strong negative relationship between these variables ($P < 0.0001$, $r^2 = 0.1995$). This relationship can be described by the equation $y = -0.0038x + 1.895$, where y is the 6th root wildtype mtDNA copy number/µm² and x is mtDNA deletion heteroplasmy level. **B –** Analysis of the residuals generated by this linear regression were found to follow a normal distribution, confirming that linear regression is an appropriate assessment of the relationship between mtDNA deletion heteroplasmy levels and the transformed wildtype (*ND1*) mtDNA copy number dataset.

4.4.6.3 Relationship between mtDNA deletion heteroplasmy level and total mtDNA copy number in individual cell categories.

Following the identification of a significant positive relationship between total mtDNA copy number and mtDNA deletion heteroplasmy in the total dataset (*4.4.6.1*, Figure 4.43), this relationship was assessed in the three separate cell categories. This was done to determine whether the same positive relationship between total mtDNA copy number and mtDNA deletion heteroplasmy could be observed in COX-positive, COX-intermediate and COX-deficient fibres; this would indicate a true relationship between these two variables. If this relationship was not observed in the individual data groups, the observed trend in the total dataset would be due to the concurrence, on average, of the lowest total mtDNA copy numbers and heteroplasmy levels in COX-positive fibres, and the highest total mtDNA copy numbers and heteroplasmy levels, on average, in COX-deficient fibres.

Total mtDNA copy number (as measured by the presence of *MTND1* by quantitative PCR) was found to correlate significantly with mtDNA deletion heteroplasmy level in all three investigated cell types – COX-positive, intermediate and deficient muscle fibres. Total mtDNA copy number and mtDNA deletion level were found to have a linear relationship in COX-positive fibres, meaning the data required no transformation to be appropriately analysed. As this data followed a Gaussian distribution, correlation of these 2 variables was first assessed using Pearson's correlation coefficient; a significant positive correlation was found to exist (Pearson r = 0.4765, P = 0.0090). Linear regression was then used to further assess the relationship between mtDNA deletion heteroplasmy level and total mtDNA copy number (Figure 4.46A), again showing a significant positive relationship to exist (P = 0.0090). This relationship can be described using the equation $y = 1.087x + 44.54$, where *y* represents total mtDNA copy number and *x* represents percentage mtDNA deletion heteroplasmy. However, the low r^2 value associated with this best fit for the data suggests that this is quite a weak relationship, accounting for only 35% of the data spread.

In COX-intermediate and COX-deficient fibres, where the highest levels of mtDNA deletion heteroplasmy tended to be detected, the total copy number data needed to be transformed in order to linearize the relationships between total copy number and

mtDNA heteroplasmy level for analysis. In both cases a Box-Cox analysis generated a λ-value of 0, recommending a transformation of the data by L_n for analysis by linear regression. L_n total mtDNA copy number was therefore plotted against measured mtDNA deletion heteroplasmy level for both datasets (Figure 4.46 C & E). The total dataset from COX-intermediate fibres was first assessed using Spearman's rank correlation coefficient, which indicated a significant positive relationship to exist between total copy number and mtDNA deletion heteroplasmy level (Spearman's r = 0.5165, P = 0.0001). The subsequent linear regression carried out on the transformed data set revealed a much stronger trend between the natural log of the total copy number and mtDNA deletion heteroplasmy levels than was observed in the linear regression analysis carried out in COX-positive fibres (Figure 4.46 C). This relationship is best described by the equation $\log_n y = 0.01046x + 4.535$ where *y* represents total mtDNA copy number and *x* represents percentage mtDNA deletion heteroplasmy. The r^2 value of 0.3216 suggests that the relationship between copy number and deletion level is likely to account for approximately 57% of the total data spread. Finally, Spearman's rho was carried out on the dataset from COX-deficient fibres, revealing a strong positive relationship to exist between total mtDNA copy number and mtDNA deletion level (Spearman's r = 0.6023, P <0.0001). A linear regression analysis of the natural log of total copy number against mtDNA deletion load revealed the strongest positive relationship between these two variables in any of the three fibres categories (P < 0.0001), accounting for approximately 68% of the data variability (r^2 = 0.4688). This relationship is best described by the equation $\log_n y = 0.03865x + 1.080$ where *y* represents total mtDNA copy number and *x* represents percentage mtDNA deletion heteroplasmy.

4.4.6.4 Relationship between mtDNA deletion heteroplasmy level and wildtype mtDNA copy number in individual cell categories.

Following the analysis above of total wildtype mtDNA copy number in relation to mtDNA heteroplasmy levels, wildtype mtDNA copy number was also investigated in the separate cell category data groups. A significant negative relationship between total mtDNA copy number and mtDNA deletion heteroplasmy was observed in the

total dataset (*4.4.6.2*, Figure 4.43); the presence of this relationship was therefore assessed in the three separate cell categories. This was done to determine whether the same negative relationship between wildtype mtDNA copy number and mtDNA deletion heteroplasmy could be observed in COX-positive, COX-intermediate and COX-deficient fibres; this would indicate a true relationship between these two variables. If this relationship was not observed in the individual data groups, the observed trend in the total dataset would be due to the concurrence, on average, of the highest wildtype mtDNA copy numbers and lowest mtDNA heteroplasmy levels in COX-positive fibres, and vice versa in COX-deficient fibres.

No relationship was found to exist between wildtype mtDNA copy number and mtDNA deletion levels, regardless of the biochemical fibre profile. This was confirmed by both correlation analysis (Pearson's correlation assessment for COX-positive fibres, P = 0.4765, Spearman's correlation assessment of COX-intermediate and deficient fibres, P = 0.1188 and 0.3165 respectively) and linear regression (COX-positive, intermediate and deficient fibres, P = 0.4765, 0.9491 and 0.2793 respectively) (Figure 4.46 B, D and F). These analyses strongly suggest that the presence of either an mtDNA deletion, or the subsequent biochemical defect caused by the presence of an mtDNA deletion, may stimulate an increase in mtDNA copy number; however, this does not necessarily correlate to an increase in wildtype mtDNA and therefore may not be sufficient to rescue a biochemical phenotype.

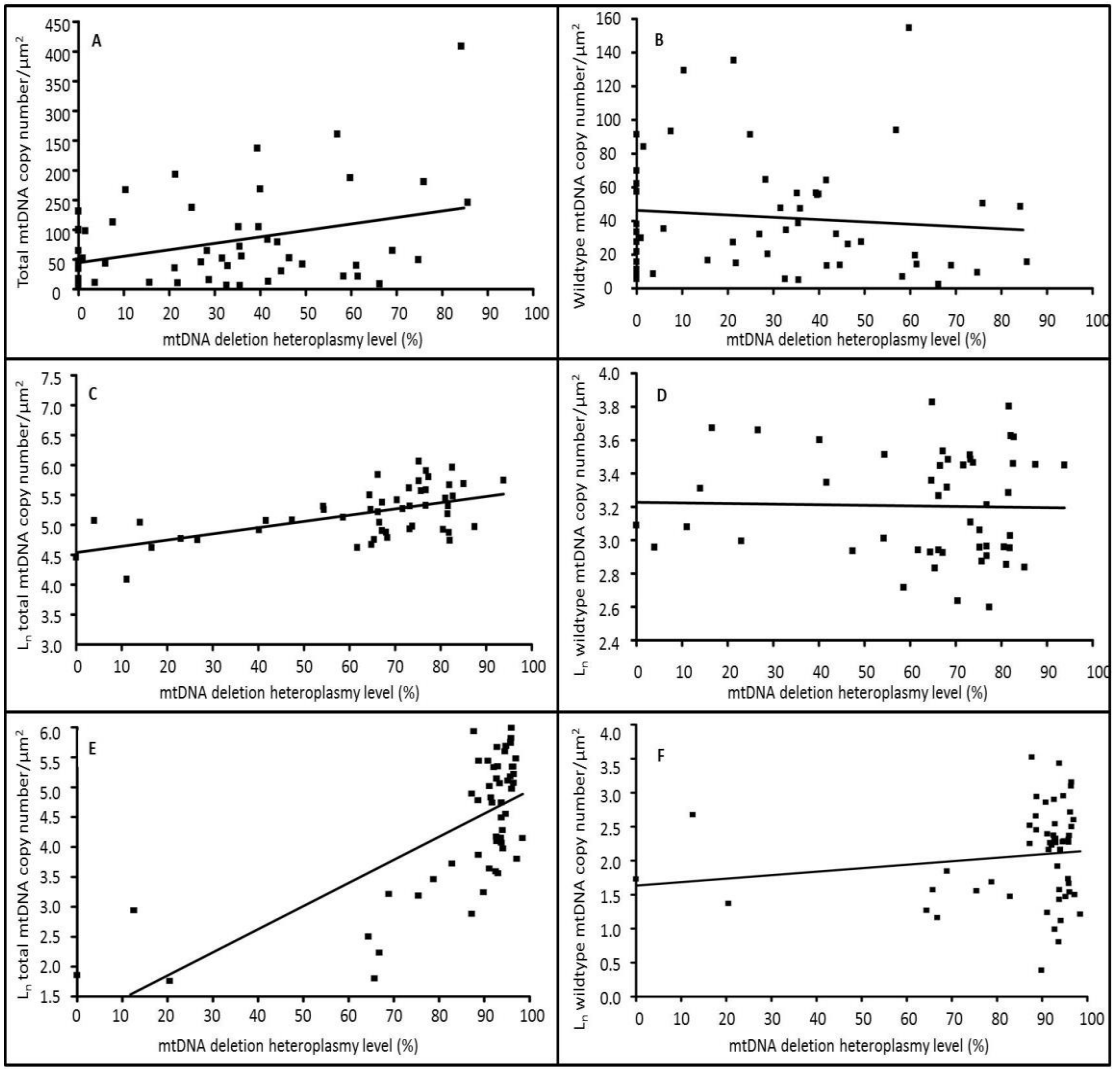

Figure 4.46 – Relationship between mtDNA deletion heteroplasmy levels and total/wildtype mtDNA copy number in individual COX-positive, intermediate and deficient fibres.

Linear regression was carried out on all datasets – to ensure that this analysis was appropriate, copy number data was transformed by Ln for the COX-intermediate and deficient fibre datasets, as recommended by a Box-Cox analysis. No significant correlation was found between mtDNA deletion heteroplasmy levels and wildtype mtDNA copy number in COX-positive (B), intermediate (D) or deficient (F) fibres. However, strong positive correlations were identified between mtDNA deletion heteroplasmy level and total mtDNA copy number in all 3 fibre types; this was stronger in COX-intermediate (C) than COX-positive (A) fibres, with the strongest relationship being identified in COX-deficient fibres (E).

4.4.6.5 Analysis of outlying data points.

A selection of outlying data points were individually analysed for deletion level and both total and wildtype mtDNA copy number; these included COX-deficient fibres with unusually low levels of mtDNA deletion, and COX-positive fibres with high mtDNA heteroplasmy levels (Table 4.18). Three COX-deficient fibres were identified as potential outliers in the mtDNA deletion heteroplasmy level analysis (section *4.4.4*), with low mtDNA deletion levels more than 2 standard deviations from the mean mtDNA deletion heteroplasmy in the remaining 51 COX-deficient fibres analysed from the two patient biopsies available. These were confirmed as outliers using Dixon's Q test, as demonstrated here for 21% heteroplasmy:

$$Q = \frac{gap}{range} = \frac{65 - 21}{98 - 21} = 0.5714$$

The Q-test limits for sample sizes of 10+ are 0.412, 0.466 and 0.568 for 90, 95 and 99% confidence intervals respectively; 0.5714>0.568, meaning we can be 99% sure that the 21% heteroplasmy level is an outlier. Though these levels could have been due to experimental error, analysis was conducted to assess whether COX-deficiency in these cells may be attributable to something other than a high heteroplasmy level – i.e. low wildtype copy numbers or overall mtDNA depletion. In all 3 cases, these COX-deficient fibres were found to have low total and wildtype copy number – these were in fact some of the lowest copy numbers identified in the whole study. This suggests that low mtDNA copy number – and particularly low wildtype copy number – may be responsible for the cellular biochemical defect rather than the specific mtDNA deletion. With 94% of all assessed COX-deficient fibres presenting with a heteroplasmy level of >65%, it is possible that the only reason no COX-deficient fibres were detected with a deletion level between 21 and 65% is due to a small sample size.

Conversely, 8 fibres identified as having normal COX biochemical activity were found to have mtDNA deletion levels exceeding 60%. In these cases, total mtDNA copy number tended to be high, while wildtype mtDNA copy number was higher than the range that was identified in COX-deficient fibres in either biopsy (Table 4.18). This again suggests that wildtype mtDNA copy number is playing a greater role in cellular function than mtDNA deletion heteroplasmy levels.

Following on from the outlier analysis, a further selection of individual COX-deficient fibres taken from Biopsy 2 were individually assessed. These 6 fibres were selected for further analysis due to their spectrum of mtDNA deletion heteroplasmy levels – above 60%, the generally accepted mtDNA deletion threshold for skeletal muscle, but below 80%, the lowest observed mtDNA deletion level in COX-deficient fibres isolated from Biopsy 1 (excluding 1 outlier). Sorting the M158 COX-deficient fibre data (N = 23, excluding 2 deletion level outliers) by total copy number revealed that the 6 COX-deficient muscle fibres with mid-range mtDNA deletion heteroplasmy levels had the lowest levels of total mtDNA copy number (Table 4.19). In keeping with this, these fibres also displayed very low levels of wildtype mtDNA – 6 wildtype copies/μm^2 at the highest, which still lies at the lower end of the normal range of wildtype mtDNA copy number found in COX-deficient fibres. This suggests that low levels of wildtype mtDNA alone may have been sufficient to cause a biochemical defect in these muscle fibres; however, a combination of a moderate level of mtDNA deletion heteroplasmy and a low mtDNA copy number is certainly sufficient to cause a state of COX-deficiency in an individual muscle fibre.

Muscle fibre identifier	Deletion level (%)	Total mtDNA copy number/μm^2	Wildtype mtDNA copy number/μm^2
1 - COX-deficient 29	21	41	6
2 - COX-deficient 24	13	18	12
2 - COX-deficient 25	0	6	6
1 - COX-positive 1	80	180	50
1 - COX-positive 2	69	105	36
1 - COX-positive 3	62	210	79
1 - COX-positive 4	61	79	34
2 - COX-positive 1	85	145	21
2 - COX-positive 2	84	408	49
2 - COX-positive 3	74	149	48
2 - COX-positive 4	66	80	27
Mean COX-positive values (median and interquartile range)	30 1 – 45	55 19 – 104	42 14 - 57
Mean COX-deficient values (median and interquartile range)	86 88 – 96	101 37 - 208	9 4 - 12

Table 4.18 - mtDNA deletion level and copy number analysis for outlier data points.

3 COX-deficient fibres were found to have deletion levels much lower than the norm for biochemically deficient fibres in the patient, while 8 COX-positive fibres contained relatively high deletion levels of more than 60%. The data for these samples were individually analysed, looking at mtDNA deletion load alongside total and wildtype mtDNA copy number. Total mtDNA copy number/μm^2 and wildtype mtDNA copy number/μm^2 were compared to the normal range of values for both COX-positive and deficient fibres (the normal range being defined between the 25% and 75% quartile of the total data). All 3 COX-deficient fibres with low deletion levels were found to have low levels of wildtype mtDNA, in keeping with a COX-deficient fibre profile. Conversely, COX-positive fibres with higher than normal mtDNA deletion levels were found to have higher levels of wildtype mtDNA, in keeping with a COX-positive fibre profile.

Muscle fibre identifier	Deletion level (%)	Total mtDNA copy number/μm^2	Wildtype mtDNA copy number/μm^2
2 - COX-deficient 1	65.77456	6.049481	4.809915
2 - COX-deficient 2	66.81219	9.308882	3.193685
2 - COX-deficient 3	64.42739	12.19774	3.554521
2 - COX-deficient 4	75.46981	24.15154	4.733096
2 - COX-deficient 5	68.92391	24.85533	6.328166
2 - COX-deficient 6	78.83015	31.74704	5.399714
2 - COX-deficient 7	91.16354	37.92714	3.445369
2 - COX-deficient 8	88.74969	47.62401	11.60864
2 - COX-deficient 9	94.15784	53.16965	3.055765
2 - COX-deficient 10	94.05193	72.19366	8.693602
2 - COX-deficient 11	91.77197	114.3179	9.596667
2 - COX-deficient 12	93.82996	114.7862	4.814649
2 - COX-deficient 13	88.65739	118.8834	14.2358
2 - COX-deficient 14	87.2738	132.7548	12.40535
2 - COX-deficient 15	96.10166	144.0944	4.651978
2 - COX-deficient 16	96.53834	183.9715	12.17113
2 - COX-deficient 17	96.2478	207.9941	15.06114
2 - COX-deficient 18	96.43901	208.6513	22.08622
2 - COX-deficient 19	88.79622	229.7572	18.91965
2 - COX-deficient 20	97.00394	239.1385	13.48394
2 - COX-deficient 21	94.60243	269.2664	9.740551
2 - COX-deficient 22	92.86837	289.5642	12.66709
2 - COX-deficient 23	87.71744	376.6842	33.84432
Mean COX-positive values (median 50 percentile)	30 1 – 45	55 19 – 104	42 14 - 57
Mean COX-deficient values (median 50 percentile)	86 88 – 96	101 37 - 208	9 4 - 12

Table 4.19 - mtDNA deletion level and copy number analysis for COX-deficient fibres extracted from biopsy 2.

Total data for all COX-deficient fibres extracted from Biopsy 2 (excluding 2 outliers, 2 - COX-deficient24 and 2 - COX-deficient25, Table 4.18). All data is sorted from lowest to highest total mtDNA copy number/μm^2. Mean values and the median range (between the 25% and 75% data quartiles) for mtDNA deletion level, total copy number and wildtype copy number are also displayed for COX-positive and COX-deficient fibres, as a point of reference.

4.4.7 Further investigations of histochemistry and homogenate DNA genetics.

Following the individual fibre investigations discussed in *4.4.3 – 4.4.6*, it became evident that the two biopsies needed to be re-assessed; the initial report of a large increase in COX-deficiency and decrease in total mtDNA copy number between the two investigated biopsies did not tally with the observed lack of change in either mtDNA deletion heteroplasmy level or mtDNA copy number in individual muscle fibres.

First, fresh tissue sections were taken from each of the two muscle biopsies for histochemical analysis. The initial analyses carried out by the NCG Mitochondrial Diagnostics Service were carried out independently as the samples arrived for assessment- it was thought that this may have contributed to skewing the COX-deficiency data – so care was taken to investigate the set of freshly cut sections simultaneously, using the same batch of reagents. A new analysis also allowed for histochemical analysis to take into account the presence of COX-intermediate fibres, which are not assessed as part of the current diagnostic process with the NCG mitochondrial disease diagnostics service.

Tissue sections of 20µm thickness from each biopsy were simultaneously investigated for COX and SDH activity, following the standard COX/SDH dual-histochemistry protocol. 6 tissue areas were chosen by random sampling from sections from each of the two biopsies for investigation (Figure 4.47); fibre counts were carried out in each of these areas in order to establish with as much accuracy as possible the level of biochemical deficiency in each biopsy. Individual fibres were assigned as being COX-positive where the fibre was fully brown, as being COX-deficient where the fibre appeared fully blue, and COX-intermediate where a dull grey or purple colour was observed. The range of colours seen in COX-intermediate fibres is due to the presence of products from both the COX and SDH histochemical assays, where a low level biochemical deficiency has allowed some brown precipitate to be produced from the COX activity assay, but an insufficient amount to inhibit the SDH histochemical assay. Fibre counts in the 6 assessed areas from each biopsy were averaged to give an estimate of the percentage of each fibre type present in the whole biopsy (Table 4.20). These counts revealed no overall change in the level of biochemical deficiency from the first biopsy to the second biopsy taken 13 years later. Biopsy 1 gave observed

average values of 38.3% COX-positive fibres, 33.2% COX-intermediate fibres and 28.5% COX-deficient fibres, compared to 33.5% COX-positive fibres, 38.1% COX-intermediate fibres and 28.4% COX-deficient fibres observed in Biopsy 2. Although this was not the result we may have originally expected, this lack of histochemical progression over the 13 year period between biopsies is in keeping with the stable genetics observed at the individual fibre level between the two biopsies. This finding also highlights the importance of maintaining identical experimental conditions to allow for comparable results, as the initial reported increase in COX-deficiency from biopsy 1 to 2 is likely to have been an artefact of a stronger reaction in the SDH histochemical assay in biopsy 2 (due to different reagent batches, or different incubation conditions).

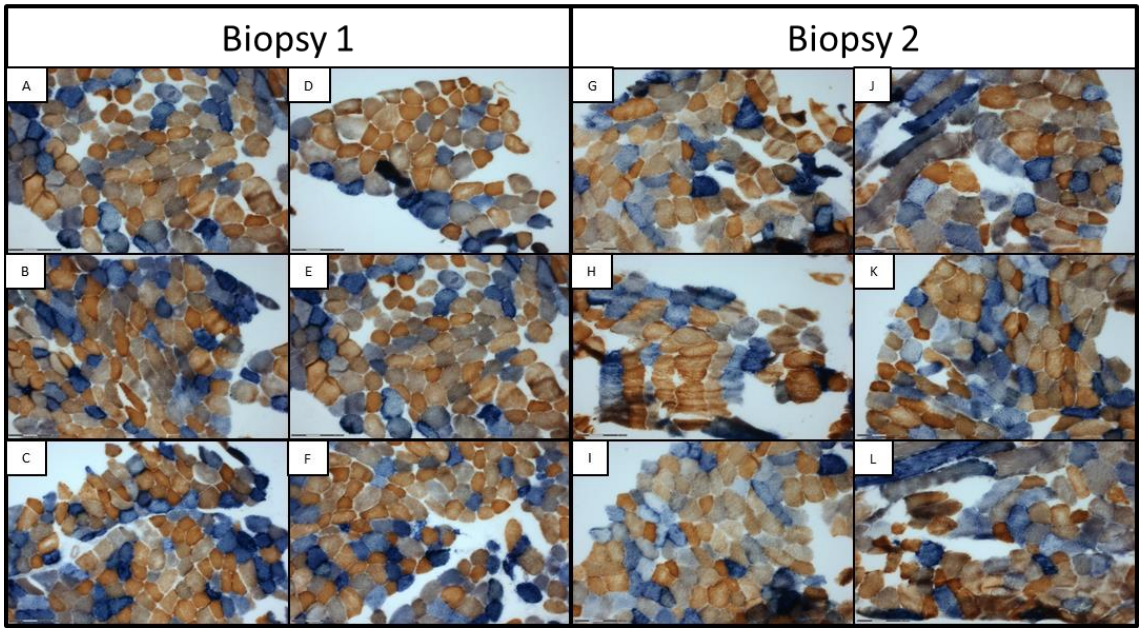

Figure 4.47 - Images of 6 areas from each of two biopsies from a single patient, assessed by dual histochemical assays for COX and SDH activity.

Tissue sections of 20µm thickness were taken from each biopsy and assessed for biochemical activity using a standard protocol for dual COX and SDH histochemistry. Images were taken at x10 magnification of 6 randomly sampled section areas from each biopsy for fibre counts and assessment of biochemical activity.

	Biopsy 1				Biopsy 2		
Area	COX-pos	COX-int	COX-def	Area	COX-pos	COX-int	COX-def
A	42	41	40	G	34	43	27
B	28	12	14	H	26	46	23
C	21	36	17	I	30	35	35
D	29	27	16	J	27	22	11
E	48	29	36	K	36	32	34
F	45	40	36	L	36	37	30
	Average number	%			Average number	%	
COX-pos	35.5	38.3		COX-pos	31.5	33.5	No change in fibre %
COX-int	30.83	33.2		COX-int	35.8	38.1	
COX-def	26.5	28.5		COX-def	26.7	28.4	

Table 4.20 - Tallied fibre count of COX-positive, COX-intermediate and COX-deficient fibres in 6 areas from each of two biopsies.

Numbers of COX-positive, COX-intermediate and COX-deficient fibres were tallied in 6 randomly sampled section areas from each biopsy (Figure 4.47). The values from each of these sample areas were averaged for each biopsy, giving an estimate of the percentage of each fibre type present in the muscle as a whole. No significant change was observed between the two biopsies.

Finally, to establish whether total mtDNA copy number from homogenate tissue DNA could be found to fit with the rest of the consistent data. To this end, fresh homogenate DNA was extracted from each biopsy. This was done in two ways: firstly, total DNA was extracted from a single unstained section from each biopsy; secondly, 4 randomly sampled areas of known size (each contained ~20 muscle fibres) were extracted from a section from each biopsy assessed for SDH histochemistry only, and DNA was extracted from these. In both cases, the *18S/ND1* quantitative PCR assay was used to assess the quantity of total mtDNA present. As the mtDNA deletion levels from the first assessment were consistent with the Southern blot analysis carried out by the NGC Mitochondrial Disease Diagnostics service, it was decided that no further investigation of mtDNA deletion heteroplasmy was required.

Each of the DNA samples extracted from isolated regions of SDH-only assessed sections were run together on a single plate of *ND1/18S* quantitative PCR for analysis (3 wells per sample), while the two homogenate DNA samples extracted from a whole biopsy section were run as a pair (3 wells per sample) on 3 separate plates; average values were then taken for analysis. Both sets of analyses revealed no change in total copy number between the two biopsies (Table 4.21). The isolated section areas from Biopsy 1 had a large range in total mtDNA copy number from 149 – 756 copies/*18S*, demonstrating the heterogeneity of the tissue as a whole, with an average mtDNA copy number per *18S* rRNA of 342. A similar spread of copy number was observed in the areas extracted from Biopsy 2 sections, with a data spread of 127 – 601 copies/*18S* rRNA. This gave an average total mtDNA copy number of 331, with no significant difference observed between the two sets of data by Mann-Whitney test (P = 0.9814). Similarly, no difference was observed in total mtDNA copy number between the DNA samples extracted from whole tissue sections from Biopsies 1 and 2; the three runs for Biopsy 1 gave values of 235, 161 and 169 copies/*18S* rRNA (mean value 195 copies/*18S* rRNA) compared to 224, 198 and 241 copies/*18S* rRNA (mean value 221 copies/*18S* rRNA) in Biopsy 2. Again, no significant difference was observed in total mtDNA copy number between Biopsies 1 and 2 in this dataset Mann-Whitney test, P = 0.4001). Though no difference was found between the two biopsies in either analysis, total mtDNA copy numbers were, on average, higher in the analysis of laser micro-dissected sections areas. This may be due to the heterogeneity of the tissue in the whole tissue section – i.e. the presence of factors such as collagen and fatty infiltrate between muscle fibres in the tissue as a whole, which were not included in the small areas extracted by laser microdissection for copy number analysis.

	Sample	Copy number/18S rRNA	Average values	
Isolated section areas from Biopsy 1	Area 1	156	342	No significant difference
	Area 2	307		
	Area 3	756		
	Area 4	149		
Isolated section areas from Biopsy 2	Area 5	326	331	
	Area 6	601		
	Area 7	270		
	Area 8	127		
Biopsy 1 section homogenate DNA	Run 1	235	195	No significant difference
	Run 2	161		
	Run 3	169		
Biopsy 2 section homogenate DNA	Run 1	224	221	
	Run 2	198		
	Run 3	241		

Table 4.21 - Total mtDNA copy number in homogenate DNA extracted from each biopsy.

4 randomly selected areas from sections assessed for SDH activity only were isolated by laser microdissection from each biopsy; homogenate DNA was extracted from each of these areas for copy number analysis. A single unstained section from each biopsy was also used for total homogenate DNA extraction. All DNA samples were assessed for total mtDNA copy number, using the *18S/ND1* quantitative PCR assay. No significant difference was found to exist between the two biopsies in terms of total mtDNA copy number. Lower measured copy numbers in the whole sections are likely to be an artefact; isolated section areas contained almost exclusively muscle fibre tissue, while sections are likely to have included a greater proportion of inter-fibre space/fatty infiltrate/etc .

4.5 Discussion

Early work investigating mtDNA deletion disease suggested that the defect continued to accumulate over time (Larsson *et al.*, 1990), which led to the initial proposal of a replicative advantage for deleted mtDNA species over wildtype mtDNA (Wallace, 1992). More recent work in the field suggests that in single mtDNA deletion diseases the mtDNA deletion is amplified rapidly following formation in early development (Pitceathly *et al.*, 2012); however, very little comment has been made in recent literature to suggest whether the level of mtDNA defect continues to change throughout a patient's lifespan. Work carried out in a mouse model of single mtDNA deletion disease in 2007 has been proposed to support continuous accumulation of mtDNA deletion species in a tissue-specific manner. mtDNA deletion heteroplasmy was measured in a variety of tissues (tail, heart, skeletal muscle, kidney, liver, testis and ovaries) at set time-points throughout the lifespan. Heteroplasmy levels of the mtDNA deletion were found to rise over time in the tail, heart, skeletal muscle, kidney, liver, testis and ovaries, but not the pancreas, spleen, brain or blood (Sato *et al.*, 2007).

To determine if an increase in mtDNA deletion levels is seen in human tissue – specifically in muscle, this being a primary affected tissue in patients with single large – scale mtDNA deletions, a case study was undertaken where two muscle biopsies taken thirteen years apart were available from a single patient, allowing analysis of molecular changes in this patient's tissue over time. Initial histochemical and quantitative PCR analyses undertaken by the Newcastle Mitochondrial NCG Diagnostics service indicated a histochemical progression over the thirteen year period between these two biopsies and a dramatic loss of mtDNA (a drop in total mtDNA copy number of almost 50%). However, subsequent analysis was found to be required in order to ensure the results were accurate – histochemical analysis of the biopsies needed to be carried out simultaneously for comparisons to be appropriate, and homogenate DNA samples were extracted from fresh biopsy sections to ensure the best DNA quality possible for analysis. Following these safeguards, it became clear from the new analyses that there was no change in muscle histochemistry over the 13 years between the two biopsies taken from this patient (Figure 4.47) and no change in total mtDNA copy number over time (Table 4.21). In stark disagreement with our

hypothesis, no increase in mtDNA deletion level was observed in the homogenate tissue DNA over the thirteen year period between the two biopsies. Southern blot analysis showed no change in deletion level between the two biopsies; this was subsequently confirmed by quantitative PCR, which showed stable mtDNA deletion heteroplasmy levels of approximately 75% between the two biopsies.

Following the assessment of any molecular changes at the whole tissue level, investigations were carried out at the single cell level to identify any progression of molecular defects that may have taken place over the thirteen year period between these two biopsies. A minimum of 25 COX-positive, 25 COX-intermediate and 25 COX-deficient fibres were isolated from tissue sections taken from each of the available muscle biopsies, and lysed to extract single muscle fibre DNA for genetic analysis. First, a deletion level analysis was carried out using the *ND1*/*ND4* quantitative PCR assay. Deletion level was found, on average, to stay stable across the two biopsies in COX-positive fibres (32% ± 22% for Biopsy 1 and 28% ± 29% for Biopsy 2) and COX-intermediate fibres (57% ± 23% for Biopsy 1 and 58% ± 28% for Biopsy 2), although average deletion load dropped a small but statistically significant amount in COX-deficient fibres over time (91% ± 14% for Biopsy 1 and 85% ± 21% for Biopsy 2). However, the significance of this drop in average COX-deficient fibre deletion load can be attributed to a small number of outlying data points, suggesting that no true difference exists in mtDNA deletion level between COX-deficient fibres from Biopsy 1 and from Biopsy 2. These outlying fibres are likely to be muscle fibres which were normally functioning at the time of the 1st muscle biopsy but have gone on to develop a biochemical deficiency by the time the 2nd muscle biopsy was taken from this patient. Either deletion load has risen in these muscle fibres to just above the threshold level up to which the cell can successfully tolerate the presence of the mtDNA deletion (Rossignol *et al.*, 2004), or a drop in copy number has occurred in fibres with an already reasonably high level of mtDNA deletion heteroplasmy, these two parameters combining to deplete wildtype mtDNA below a functional threshold (Durham *et al.*, 2005; Durham *et al.*, 2007). If this is the case, this would suggest that some of the worst affected fibres have been lost over time in order for the proportion of COX-positive, intermediate and deficient fibres to remain stable over time (Herbst *et al.*, 2007). These results fit with the findings in homogenate tissue; a stable level of

mtDNA deletion heteroplasmy in each of the three designated fibre types is consistent with a stable mtDNA deletion level and stable level of biochemical deficiency in the tissue as a whole.

Following mtDNA heteroplasmy level analysis, wildtype and total mtDNA copy number were assessed in each of the individual isolated muscle fibres. Total wildtype copy number was found to be significantly higher in COX-deficient and intermediate fibres than COX-positive fibres in Biopsy 1 (P = 0.0022 and 0.0003 respectively), but this was no longer the case in Biopsy 2 (P = 0.5529 and 0.1481 respectively). Mean total copy number has remained very consistent in COX-intermediate fibres (121 copies/μm^2 in Biopsy 1 and 129 copies/μm^2 in Biopsy 2), while it has slightly risen over the 13 year period in COX-positive fibres (from 59 to 96 copies/μm^2) and it has slightly decreased in COX-deficient fibres (from 142 to 119 copies/μm^2). However, neither of these observed changes were statistically significant (P = 0.1910 and 0.3144 respectively).

Wildtype mtDNA copy number was found to be even more consistent between the two biopsies than total copy number; no change was observed over time in COX-positive (42 copies/μm^2 in Biopsy 1 compared to 41 copies/μm^2 in Biopsy 2, P = 0.7827), intermediate (47 copies/μm^2 in Biopsy 1 compared to 46 copies/μm^2 in Biopsy 2, P = 0.5210) or deficient fibres (9 copies/μm^2 in Biopsy 1 compared to 10 copies/μm^2 in Biopsy 2, P = 0.8043). The difference between wildtype mtDNA copy number in COX-positive and COX-deficient fibres was found to be highly statistically significant in both biopsies (P < 0.0001 in both cases), as was the difference between wildtype mtDNA copy number in COX-intermediate and COX-deficient fibres (P < 0.0001 in both cases). No significant difference was observed between COX-intermediate and COX-positive fibres in terms of wildtype mtDNA copy number in either biopsy (P = 0.0786 Biopsy 1, P = 0.4316 Biopsy 2).

An investigation of the relationship between total mtDNA copy number and mtDNA deletion heteroplasmy levels revealed a strong positive trend between these two variables in the total dataset (P < 0.0001), as well as in each of the three defined fibre types. Interestingly, this relationship was found to be strongest in COX-deficient fibres (P < 0.0001), while COX-intermediate fibres (P = 0.0001) displayed a stronger positive trend than COX-positive fibres (P = 0.0090). The presence of higher mtDNA copy

numbers where high mtDNA deletion heteroplasmy levels are observed is indicative of a compensatory amplification of mtDNA in the presence of mtDNA deletion species in order to preserve a functional quantity of wildtype mtDNA (Wong and Bai, 2002; Bai *et al.*, 2004).

Wildtype mtDNA copy number was subsequently assessed against mtDNA deletion level in the same manner, revealing a significant negative correlation in the total dataset ($P < 0.0001$); this was expected given that increasing mtDNA deletion heteroplasmy is synonymous with a decreasing proportion of wildtype mtDNA in the cell. This correlation may have confounded previous studies in this area, many of which agreed that increasing levels of mtDNA deletion heteroplasmy above a determined threshold level (~60% in muscle (Hayashi *et al.*, 1991)) was ultimately responsible for causing cellular biochemical defects (Porteous *et al.*, 1998; Rossignol *et al.*, 2004). However, the importance of mtDNA deletion heteroplasmy level, and indeed the presence of a deletion threshold in skeletal muscle, has previously been brought into question in studies of single mtDNA deletion disease patients (Schroder *et al.*, 2000). This is perhaps reinforced by the lack of a relationship between wildtype mtDNA copy number and mtDNA deletion heteroplasmy levels in any of the three defined fibre types (Figure 4.46), which suggests that the combination of absolute wildtype mtDNA copy number and mtDNA deletion level is most likely to be responsible for defining the cell's biochemical profile.

The importance of absolute wildtype mtDNA copy number is further highlighted by the analysis of outliers in the individual cell study. 3 COX-deficient fibres found to have low deletion levels (21, 13 and 0% mtDNA deletion heteroplasmy) were all found to have unusually low wildtype copy numbers, suggesting that depletion of wildtype mtDNA past a functional threshold is responsible for the biochemical deficiency in these cells rather than the mtDNA deletion heteroplasmy level. Conversely, a number of COX-positive fibres were found to have relatively high deletion levels – above the 60% mutation threshold for skeletal muscle proposed by Hayashi *et al*. However, these fibres all maintained a level of wildtype mtDNA within the normal range for COX-positive muscle fibres, suggesting that the presence of sufficient wildtype genome copies is adequate to maintain normal biochemical function.

One of the most interesting subset of cells in the analysis were the COX-deficient fibres from Biopsy 2 which displayed a deletion level above the proposed skeletal muscle mtDNA deletion threshold of 60% but lower than 80%, the lowest level of heteroplasmy observed in COX-deficient fibres taken from Biopsy 1. This subset of COX-deficient fibres had the lowest total mtDNA copy numbers observed in any fibres extracted from Biopsy 2, and lay among the lowest levels of wildtype mtDNA observed. This indicates that increasing mtDNA deletion level and mtDNA depletion have had a combined effect to cause a biochemical defect to occur in these muscle fibres – again suggesting that absolute wildtype mtDNA copy number is at least as important, if not more so, than mtDNA deletion heteroplasmy level.

Overall, no evidence in support of the 'survival of the smallest' model for the clonal expansion of mtDNA deletions (Wallace, 1992) has been uncovered in this study. The presence of a replicative advantage for the mtDNA deletion species over wildtype mtDNA would lead to a continued increase in deletion heteroplasmy throughout the patient's lifespan, until homoplasmy is reached; instead, we have observed a steady level of mtDNA deletion across the two biopsies and therefore across a thirteen year time-span. If a replicative advantage for mtDNA deletions over wildtype did exist, we would also expect to see an increase in COX-deficiency in a patient's muscle over time driven by mtDNA deletion accumulation within single fibres. However, we have found the molecular defects present in this patient's muscle to be exceptionally stable – the lack of change in mtDNA deletion levels or in total or wildtype mtDNA copy numbers have led to the maintenance of a similar level of biochemical deficiency over the thirteen years between these two biopsies.

Results obtained from individual COX-positive fibres taken from each biopsy are arguably the most comparable datasets – all COX-positive fibres taken from biopsy 2 must have been biochemically functional at the time of Biopsy 1, but COX-deficient fibres taken from the 2nd Biopsy could have become biochemically deficient at any time prior to the 2006 biopsy. In these fibre groups, there is no observed change in mtDNA deletion level or wildtype mtDNA copy number over time, and only a modest increase in total mtDNA copy number which was shown not to be statistically significant. This suggests no replicative advantage for mtDNA deletion species in these fibres, and lends no support to the 'survival of the smallest' hypothesis of clonal

expansion. As no advantage seems to be driving a continuous accumulation of mtDNA deletions over time, this work supports the hypothesis that random genetic drift is the likely mechanism driving the accumulation of mtDNA deletions by clonal expansion in aging and disease (Elson *et al.*, 2001).

A secondary aim of this study was to investigate the molecular changes that drive disease progression in single mtDNA deletions disease patients over time. This case has turned out to be a particularly interesting one, with no change in either molecular defects or biochemical deficiency in the muscle over the thirteen years between the two biopsies. This suggests that – at least in some patients – the mtDNA deletion accumulation responsible for disease symptoms may occur early in life before a plateau is reached. However, a wide patient cohort would have to be investigated to determine whether there are cases where mtDNA deletion level may continue to increase through a patient's lifespan; this is perhaps the case where disease progression is more severe. The investigation of individual COX-deficient, COX-intermediate and COX-normal fibres undertaken in this patient does suggest that wildtype mtDNA copy number as at least as important in determining cellular health as mtDNA deletion heteroplasmy – this was particularly evident in outlying data points from COX-positive and deficient fibres, where the effects of unusual mtDNA deletion levels were modified by more typical mtDNA wildtype copy numbers (see *4.4.6.5*). This highlights the importance of mtDNA maintenance in the muscle, and lends support to the hypothesis that absolute wildtype copy number may be vital for maintaining normal biochemical function, superseding mtDNA deletion heteroplasmy level in determining cellular health (Durham *et al.*, 2005). The results of the individual fibre studies, if extrapolated to whole tissue level, therefore indicate that decreasing levels of wildtype mtDNA below a threshold level may be the primary cause of patient progression in single mtDNA deletion disease. However, it is as yet unclear how strong a regulatory role mtDNA deletion heteroplasmy level has in modifying the effect of wildtype mtDNA copy number on cell fate.

The variability in both the histochemical *COX*/*SDH* assay and the *MTND1*/*18S* quantitative PCR assay observed during the course of this study has led to an unexpected outcome for this study in the form of recommendations for future experimental design. Issues with both of these current experimental techniques have

been identified and, though these assays are both currently the best available techniques to assess COX-deficiency and mtDNA copy number respectively, this study highlights a need for improvement. Variability with the histochemical *COX*/*SDH* assay was shown to increase when samples were processed at different times – this could be due to unavoidable differences in reagent batches or experimental conditions such as room temperature. Consistency in measurements of biochemical deficiency can therefore be maximized by assessing relevant tissue sections concurrently, regardless of any previous analyses which may have taken place; any future studies involving the assessment of COX-deficiency levels in tissue should be designed to take this into account. Identifying an approach to increase the accuracy of mtDNA copy number measurements is more complicated. A need for a more reliable technique than the *MTND1*/*18S* TaqMan assay has been identified, though this technique remains best practice until an alternative measure can be established. The current assay is flawed due to the multi-copy nature of nuclear marker *18S* rRNA, which can vary not only between individuals, but from cell to cell in any one individual. Ideally mtDNA copy number should be normalised to a single copy nuclear marker, but these are difficult to detect by quantitative PCR and, if detected, are likely to be read at an unreliably high C_t value. *18S* rRNA therefore currently remains the most appropriate nuclear marker to use in real-time PCR quantification of mtDNA copy number, but the limitations in terms of accuracy of the *18S*/*ND1* assay should be taken into account in all future studies and research must be undertaken to identify a more reliable alternative.

Chapter Five

Chapter 5:

Investigating the impact of molecular mtDNA deletion characteristics on disease presentation and progression in single mtDNA deletion patients.

5.1 Introduction

5.1.1 Correlation of mtDNA deletion breakpoints/level/progression/phenotype

Although the three main syndromes associated with single, large-scale mtDNA deletions – CPEO, KSS and Pearson syndrome – seem to be quite clearly defined, the reality is that a wide spectrum of disorders exists, from patients who may not be diagnosed until late in life with CPEO to onset of Pearson syndrome in very early infancy. The mid-range of this spectrum presents a serious problem for clinicians in that no genetic markers have been found to conclusively identify how severe a patient's symptoms may become, or how quickly they will progress. In order to provide the best possible patient care and support, it is vital that we are able to better understand disease severity and progression. To date, many studies have been carried out with the aim of uncovering a link between the genetic defect present in cases of single large-scale mtDNA deletion disease, the resultant biochemical defect and the presented clinical phenotype – these have, however, met with mixed success, and many of the research findings have been contradictory.

Early investigative efforts from a number of independent research groups uncovered no link between the mitochondrial genetics, biochemical defect and patient phenotype in heterogeneous groups of mitochondrial disease (Holt *et al.*, 1988), a group of only KSS patients (Zeviani *et al.*, 1988), a group of CPEO and KSS patients (Moraes *et al.*, 1989), or in a group of patients with Pearson syndrome (Rotig *et al.*, 1995). No evidence was found in any of these studies to suggest a link between mtDNA deletion size and location, the resultant biochemical defect or clinical presentation. Further studies also brought mtDNA deletion heteroplasmy levels under scrutiny – findings from separate studies began to diverge at this point. Moraes *et al* had initially suggested that no link existed between heteroplasmy levels and clinical presentation (Moraes *et al.*, 1989) – in keeping with contemporary work by Holt *et al* (Holt et al., 1989) – but later found a strong relationship to exist between heteroplasmy levels and levels of COX-deficiency in muscle (Moraes *et al.*, 1995). A similar relationship had

previously been identified by two other groups (Mita *et al.*, 1989; Goto *et al.*, 1990a), confirming a link between COX-deficiency and mtDNA deletion heteroplasmy levels. However, these papers were contradictory in many other aspects, leaving the field open to further study and interpretation.

To date, controversy remains rife in this field of research. The most consistent indicator of disease severity and progression has been found to be age of symptom onset, with earlier symptom onset being indicative of a more severe and rapidly progressing clinical presentation (Goto *et al.*, 1990a; Aure *et al.*, 2007; Yamashita *et al.*, 2008). The presence and proportion of the mtDNA deletion in blood has also been associated with a more severe disease presentation (Aure *et al.*, 2007), while assessment of urothelial cells has shown the presence of mtDNA deletions at higher levels in younger, more severely affected patients (though mtDNA deletion levels tend not to be representative of those seen in a clinically affected tissue) (Blackwood *et al.*, 2010). Interestingly, mtDNA deletion size has been found to be predicative of age of onset (Yamashita *et al.*, 2008; López-Gallardo *et al.*, 2009), but has not been consistently found to correlate with disease phenotype or progression despite the predictive role of age of onset in determining these factors. Two studies of large groups of single large-scale mtDNA deletion disease patients presented conflicting evidence to suggest that mtDNA deletion size can (Yamashita *et al.*, 2008) or cannot (López-Gallardo *et al.*, 2009) be used to predict disease course.

Some consistency has been achieved in that both the Yamashita and Lopez-Gallardo study have agreed that mtDNA deletion location is predictive of phenotype/age of onset. However, the studies disagree on which region of the mitochondrial genome plays the most vital role of determining the pathogenicity of the mtDNA deletion. Yamashita et al. found that deletions including *COX* (and *ATP*) subunit genes had significantly earlier onset, therefore correlating with a worse predicted disease phenotype and rate of disease progression (Bua *et al.*, 2006); contradictorily, López-Gallardo et al. found deletion of *Cyt b* to be associated with a severe KSS phenotype, and did not corroborate the findings of Yamashita *et al*. (López-Gallardo *et al.*, 2009). A recent overview has suggested that the pathogenicity of mtDNA deletions is based upon the deletion of one or more tRNA genes (Schon *et al.*, 2012) , on the basis that the loss of a single tRNA gene may have a global effect on the translation of all

mitochondrial-encoded genes (Nakase *et al.*, 1990a). This review refutes the importance of mtDNA deletion size or location in determining pathogenicity.

Overall, outside of the established relationship age of symptom onset shares with disease severity and rate of clinical progression, the presence of any relationships between the three major areas of mitochondrial genetics, biochemical defects and clinical presentation in cases of single large-scale mtDNA disease remains contentious. This area of research must become a focus for research in order to better understand the whole spectrum of mtDNA deletion disease, to allow for the most accurate diagnoses and most specialised care to be provided to patients.

5.2 Aims and Hypothesis

This study aimed to investigate and thoroughly characterise mtDNA deletions in a large cohort of patients with single large-scale mtDNA deletions. Following assessment of mtDNA deletion heteroplasmy levels and mapping of mtDNA deletion breakpoints, we aimed to assess the presence of any correlation between deletion size and heteroplasmy levels, and evaluate the impact that specific deletion sites may have upon mtDNA heteroplasmy levels.

The working hypothesis for this study once again rests upon the proposed 'survival of the smallest' mechanism of clonal expansion. The larger the mtDNA deletion, the smaller the remaining mtDNA genome and the greater its replicative advantage will therefore be. It would be reasonable to expect that a greater replicative advantage would lead to higher levels of mtDNA deletion heteroplasmy, due to a more rapid accumulation of the smaller mitochondrial genomes harbouring mtDNA deletions. Therefore, the hypothesis for this study is that a strong positive correlation will exist between mtDNA deletions size and heteroplasmy level in our patient cohort if a replicative advantage for smaller mtDNA molecules is driving the clonal expansion of mtDNA deletions.

A secondary aim for this study was to identify if any correlation existed in this patient cohort between the mitochondrial genetic defect (including mtDNA deletion size, location and heteroplasmy level), cellular biochemical defect (COX-deficiency) and clinical presentation (NMDAS score). Due to the lack of consistent results so far in this field of study, it was also important to assess where results from this study lay in relation to previous investigations, and to assess whether any genetic markers could be identified to predict disease severity and/or rate of disease progression.

5.3 Methods

5.3.1 Patient cohort

All patients identified as having mitochondrial DNA disease caused by a single large-scale mtDNA deletion within the MRC Mitochondrial Disease Patient Cohort Study (UK) were originally included in this study; a number of research-consented samples from patients with single, large-scale mtDNA deletion disease available through the NCG Mitochondrial Diagnostics Service were also included in this study. All DNA samples were accessed with appropriate consent through the NCG Mitochondrial Diagnostics service. From a total cohort of 150 patients, appropriate DNA samples were available from 113 individuals. These patients presented with varying degrees of disease severity and a spectrum of phenotypic presentations ranging from CPEO, through CPEO with muscular or multi-system involvement, to KSS. Samples included in this study are from patients from 2 main groups: those who have been clinically assessed at Newcastle (these patients have extensive clinical data available, including NMDAS rating scale data), and those assessed clinically elsewhere (DNA or muscle biopsy samples having subsequently been sent to the NCG Mitochondrial Diagnostics service; clinical information has been obtained from hospital records).

5.3.2 Muscle biopsy and DNA extraction

Information regarding muscle biopsy procedure and DNA extraction relates primarily to patients seen clinically at Newcastle – procedures may vary at other centres. Skeletal muscle samples (*vastus lateralis*) were obtained by muscle biopsy from all adult patients involved in this study – procedure varied between patients depending upon the required diagnostic analyses, with either a needle or open muscle biopsy being performed. Total homogenate DNA was extracted from a small quantity of biopsied muscle tissue by the NCG Mitochondrial Diagnostic Service. 3 paediatric cases presenting with Pearson Syndrome or KSS were included in this study; blood samples were taken from these patients rather than muscle biopsies due to the young age of clinical presentation. Genetic analysis was carried out on total extracted DNA from blood in these 3 cases only; mtDNA deletion heteroplasmy levels in blood have been

reported to accurately mirror deletion heteroplasmy in muscle in paediatric cases (McShane *et al.*, 1991).

5.3.3 Detection of mtDNA deletion level by quantitative PCR.

Quantitative PCR analysis was used to assess the level of mtDNA deletion present in each homogenate DNA sample, employing the *MTND1/MTND4* assay as discussed in section *4.3.5.*1.

5.3.4 Long-extension PCR, gel electrophoresis and mtDNA deletion detection

Long-extension PCR was carried out on homogenate patient DNA samples alongside a homogenate wildtype DNA control sample, primarily to assess the size of mtDNA deletion present, but also to amplify sufficient mtDNA for breakpoint sequencing. MtDNA amplification was carried out as outlined in section *2.2.4.2.1*, using primers approximately 10kb apart (NC_012920.1, 5875 – 15896bp) (primers 12F and 32R, section *2.2.4.2.*3, Table 2.4), while mtDNA deletion detection and sizing were carried out as discussed in section *3.3.4.*

5.3.5 Restriction endonuclease digest and breakpoint sequencing

A restriction endonuclease digest using 4 restriction enzymes - *Xho1*, *BamH1*, *Xcm1* and *Dra1* - was used to fine map the location of the mtDNA deletion breakpoints (Khrapko *et al.*, 1999), as outlined in section *2.2.5.2*. A standard cycle sequencing protocol was then followed by determine mtDNA deletion breakpoint location, as outlined in sections *2.2.5.2 – 2.2.5.5*.

5.3.6 Statistical analyses and modelling

All basic statistical analysis was carried out using GraphPad Prism v.4 statistical software. Relevant tests were chosen based upon data distribution; each data set was analysed using a battery of tests (Kolmogorov-Smirnov, D'Agostino and Pearson, and Shapiro-Wilk normality tests) in order to assess whether the data conformed to a Gaussian distribution. This allowed the most appropriate analysis to be carried out for each dataset in order to maximise the power of each statistical test. Mann-Whitney u-tests were carried out to compare data sets where data was non-parametric, while unpaired t-tests were utilised where data followed a parametric distribution; in both cases, two-tailed tests were carried out at 95% confidence. Correlation assessments were carried out using Spearman's rho for non-parametric data and Pearson's *r* for parametric data. All relationships were modelled using simple linear regression; in cases where the relationship between variables was not linear, Box-Cox analysis was used (through MiniTab 16 Statistical Software) to identify optimal transformations of data to enable parametric tests to be used (Box and Cox, 1964). All statistical modelling work was carried out by Dr John Grady.

5.4 Results

5.4.1 Relationship between mtDNA deletion size and heteroplasmy level.

A detailed genetic analysis was undertaken for all available DNA samples (total extracted DNA from blood in 3 paediatric cases, and from SKM in all other cases) from patients identified as having mitochondrial DNA disease caused by a single large-scale mtDNA deletion. In total, samples from 97 single mtDNA deletion patients were successfully analysed for mtDNA deletion heteroplasmy level, deletion size and breakpoint location. However, samples with a measured heteroplasmy percentage of 20% or below could not be included in the final analysis; the ND1/ND4 mtDNA deletion level assay is not sufficiently accurate at low levels of heteroplasmy to include any measurements ≤20%. This led to the exclusion of data obtained from 11 patient samples, leading to a final sample number of 86. Future investigations could utilise Southern blotting in order to ensure accurate measurement of any samples with low levels of mtDNA deletion heteroplasmy.

In the total dataset, a range of deletion sizes between 2300bp and 9123bp was identified, with the majority of deletion breakpoints occurring in only one individual patient. However, a small number of deletions occurred in 2 (NC_012920, 9486 – 13723, 9349 – 11419, 7128 – 13992, 7128 – 13992, 7540 - 14012) or 4 (NC_012920, 12112 – 14422) individuals, with the 'common' 4977bp deletion picked up in 22 cases – approximately a quarter of the total number of fully assessed patient samples, in keeping with earlier reports of 'common deletion' prevalence (Taylor and Turnbull, 2005).

Linear regression was used to identify whether a correlation existed between mtDNA deletion size and heteroplasmy level. This revealed a trend for lower heteroplasmy levels to be associated with larger deletions, and vice-versa; the best-fit given by linear regression was found to be $y = -0.0041x + 77.679$, where y is mtDNA deletion heteroplasmy level (%) and x is deletion size (bp). This negative correlation between deletion size and heteroplasmy was found to be statistically significant, with a P value of 0.0034 (Figure 5.48). Although this trend was shown to be significant, further analysis was required to ensure that the high level of data spread had not skewed the result in any way. A comparison was therefore made between the 10 largest and 10

smallest mtDNA deletion size found within this study, and the 10 highest and 10 lowest mtDNA heteroplasmy levels identified within this patient cohort (Table 5.22, Figure 5.49). mtDNA deletion heteroplasmy levels were found to be significantly lower in the samples with the largest deletion sizes as compared to the 10 samples containing the smallest mtDNA deletion sizes (P = 0.0359), in keeping with the predicted inverse correlation between mtDNA deletion size and heteroplasmy predicted by analysis of the total dataset. Assessment of the mtDNA deletion heteroplasmy levels found for each of the 22 patients with the 4977bp common deletion was also carried out (Figure 5.49) – this revealed the largest spread of heteroplasmy data, suggesting that mid-sized deletions show the greatest spread of heteroplasmy levels.

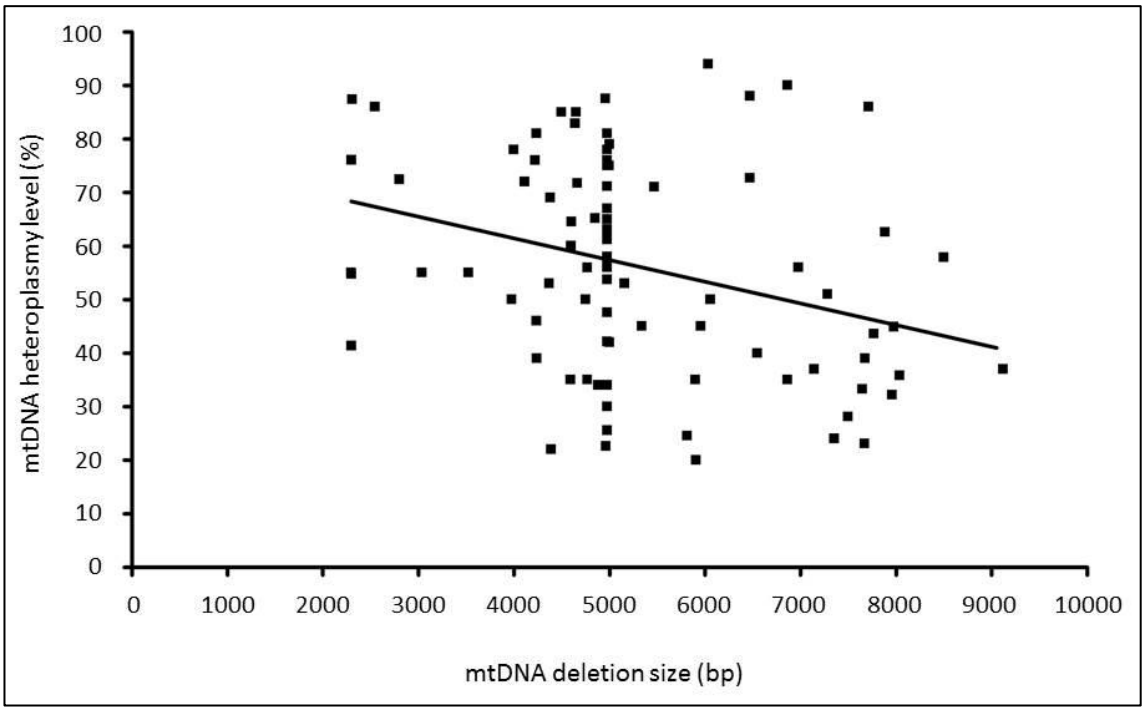

Figure 5.48 – Assessing the relationship between mtDNA deletion size and heteroplasmy level.

Correlation between mtDNA deletion size (as determined by breakpoint sequencing analysis) and heteroplasmy level (as determined by *ND1/ND4* quantitative PCR analysis) revealed a negative correlation between these two factors. Linear regression carried out on this data found this correlation to be statistically significant (P = 0.0034) despite a high level of data spread. The trend between these two genetic measures is expressed by the equation y = -0.0041x + 77.679, where y is mtDNA deletion heteroplasmy level (%) and x is deletion size (bp).

The limitations of the relationship found to exist between mtDNA deletions size and heteroplasmy level is highlighted by the analysis of the 10 samples with the highest and lowest heteroplasmy levels assessed in this study (Table 5.22, Figure 5.49); no significant difference was found to exist between these two groups (P = 0.1395). This demonstrates the detrimental effect of the high level of data spread on the strength of the inverse relationship between mtDNA deletion size and heteroplasmy level, meaning one cannot necessarily be used as an accurate predictor of the other. Indeed, the inverse relationship observed between mtDNA deletion size and heteroplasmy levels may well simply be due to patient sampling bias – as discussed in section 5.5.

10 smallest mtDNA deletions		10 largest mtDNA deletion		10 lowest mtDNA heteroplasmy levels		10 highest mtDNA heteroplasmy levels	
Size (bp)	Heteroplasmy (%)	Size (bp)	Heteroplasmy (%)	Heteroplasmy (%)	Size (bp)	Heteroplasmy (%)	Size (bp)
2297	55	7714	23	20	5906	83	4641
2300	41	7768	39	22	4392	85	4500
2300	55	7886	86	23	4963	85	4652
2300	76	7958	44	23	7671	86	2549
2308	87	7977	62	24	7355	86	7714
2549	86	8039	32	25	5813	87	2308
2803	72	8500	45	26	4978	88	4959
3039	55	8560	36	28	7498	88	6472
3527	55	8704	56	30	4978	90	6864
3979	50	9120	37	32	7958	94	6036
Average values:							
2740.2	63.2	8030.9	46	25.3	6151.2	87.2	5069.5
Significantly higher het % in smallest deletions.				No significant difference in average deletion size.			

Table 5.22 - Comparisons of 10 largest and smallest deletion sizes, and 10 highest and lowest heteroplasmy levels.

Data from all patient samples with full genetic data were organised first by mtDNA deletion size, and secondly by heteroplasmy level; the 10 top and bottom data points were selected from each of these data-sets. A Mann-Whitney test carried out on the measured heteroplasmy levels of the 10 largest and smallest mtDNA deletions showed a significant difference, with larger deletions having a significantly lower heteroplasmy level (P = 0.0359). However, no significant difference in deletion size was observed between the samples with the 10 highest and 10 lowest heteroplasmy levels (P = 0.1395), highlighting the weakness of the deletion size/heteroplasmy relationship caused by the wide spread of data.

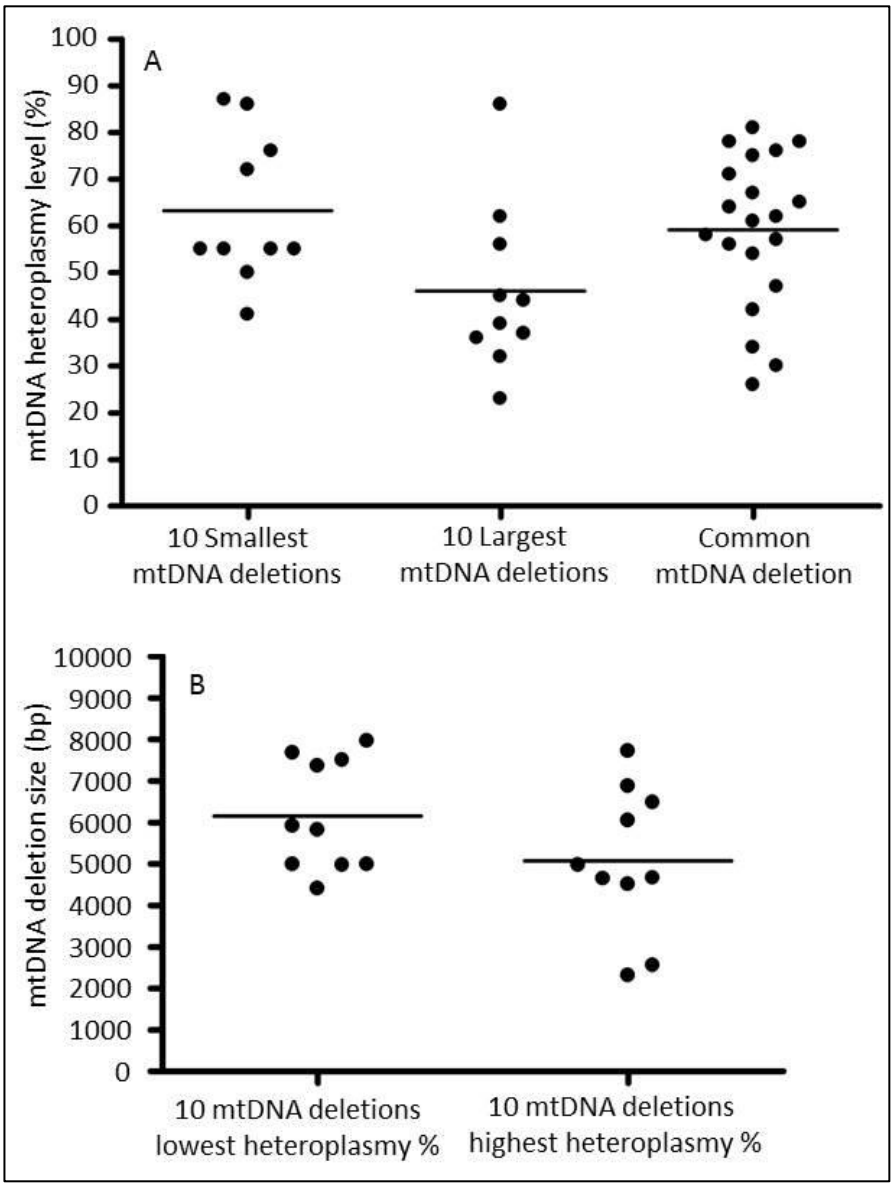

Figure 5.49 - Comparisons of heteroplasmy levels on the extreme mtDNA deletion sizes and the common deletion, and variance of deletion size in the extreme heteroplasmy level data.

Representation of the heteroplasmy levels for the 10 largest and smallest mtDNA deletions, and deletion size for the 10 highest and lowest heteroplasmy levels (as described in Table 5.22). All 22 instances of the 4977bp 'common deletion' were also assessed, and shown to have the highest spread of mtDNA deletion levels - implying that mid-sized deletions display the widest range of heteroplasmy %.

5.4.2 Relationship between mtDNA deletion breakpoints and heteroplasmy

Breakpoint analysis was carried out on data from each of the 86 samples which had successfully undergone breakpoint sequencing as well as *ND1/ND4* quantitative PCR analysis of mtDNA deletion heteroplasmy level. 3' and 5' breakpoint locations were both found to correlate well with mtDNA deletion size, with a high degree of significance and a reasonably low level of data spread. Correlation between breakpoint location and deletion size was in both cases determined using Spearman's rank correlation coefficient, as the data does not follow a Gaussian distribution. 5' mtDNA deletion breakpoint location was found to strongly correlate negatively with deletion size (Spearman $r = -0.7679$, $P < 0.0001$) – i.e. the further through the genome the mtDNA deletion begins, the smaller the total deletion size is likely to be. The opposite trend was observed for the 3' deletion breakpoints, which correlated positively with deletion size, though this correlation was neither as strong nor as significant (Spearman $r = 0.2083$, $P = 0.0463$) (Figure 5.50). These results were expected, and make sense in the context that larger mtDNA deletions must cover a larger area of the mitochondrial genome; due to the tendency for mtDNA deletions to occur in the major arc of the genome, centred around the ND4 gene (rCRS 10760 – 12137), larger deletions are likely to have a 5' breakpoint occurring further upstream and a 3' breakpoint further downstream in the genome.

Breakpoint location was assessed alongside mtDNA deletion heteroplasmy levels as well as deletion size. Correlation analysis using Spearman's rank correlation coefficient showed that 5' breakpoint location was found to correlate positively with mtDNA deletion level (Spearman $r = 0.3029$, $P = 0.0035$) – as would be expected, given that later 5' breakpoints correlate with a smaller deletion size, and smaller deletion sizes have shown a trend for higher heteroplasmy levels of mtDNA deletions. However, 3' breakpoint location was not found to have any significant relationship with heteroplasmy levels (Spearman $r = -0.04084$, $P = 0.7007$), despite the observed relationship between 3' breakpoint location and deletion size, and the trend for larger deletions to accumulate to lower levels of mtDNA deletion heteroplasmy (Figure 5.50). This suggests that 5' breakpoint location may be more important than deletion size in determining mtDNA heteroplasmy, while the trend for early 5' deletion breakpoints to

lead to larger deletion sizes (and vice versa) creates the basis of the relationship between mtDNA deletion size and heteroplasmy.

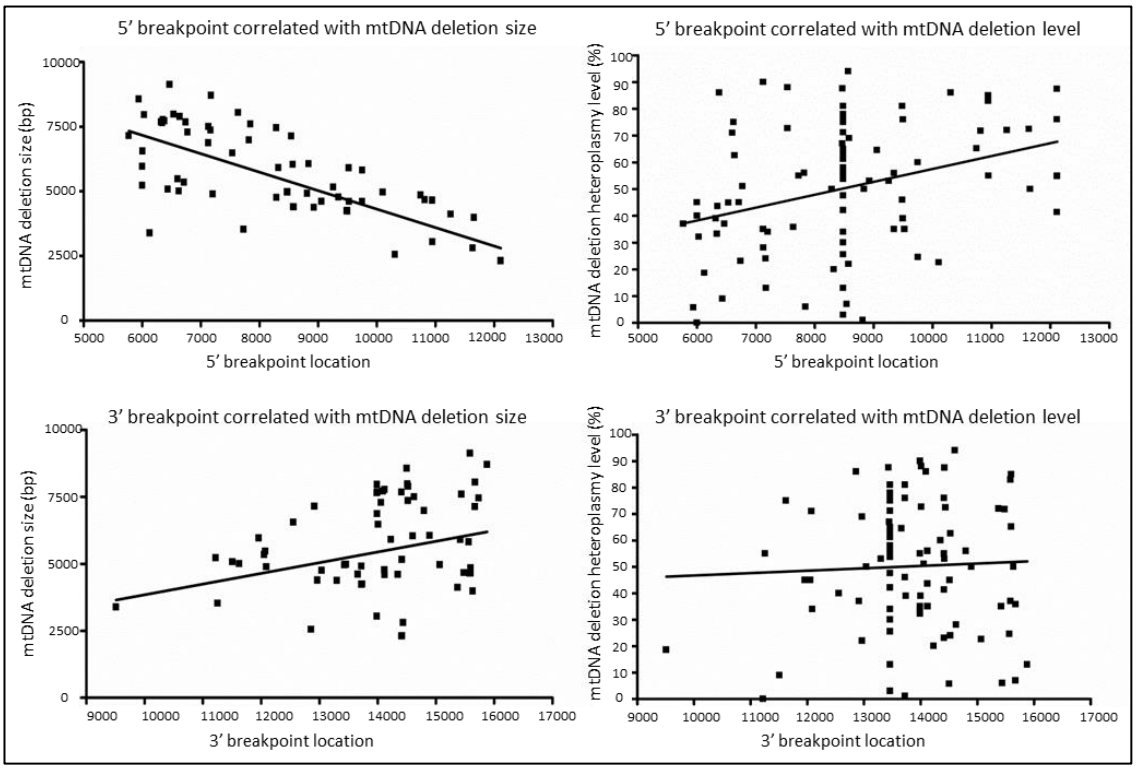

Figure 5.50 – Assessing the relationships between mtDNA deletion breakpoint and mtDNA deletion size and heteroplasmy level.

Breakpoint location, as determined by breakpoint sequencing, was assessed for correlation with mtDNA deletion size and heteroplasmy level. Correlation analyses were carried out in all cases using Spearman's rho, due to the non-Gaussian data spread. 5' breakpoint location was found to have a very strong relationship with deletion size (Spearman $r = -0.7679$, $P < 0.0001$), and to correlate significantly with mtDNA deletion heteroplasmy levels (Spearman $r = 0.3029$, $P = 0.0035$). This correlation was stronger than that of deletion size with heteroplasmy. 3' breakpoint location also correlated well with deletion size, though not as tightly as 5' breakpoint location (Spearman $r = 0.2083$, $P = 0.0463$); however, 3' breakpoint location showed no relationship with deletion heteroplasmy levels (Spearman $r = -0.04084$, $P = 0.7007$).

5.4.3.1 mtDNA deletion breakpoint distribution assessment

The distribution of mtDNA deletion 3' and 5' breakpoints was investigated using information from all 92 cases where full breakpoint data was available. Breakpoint locations were grouped into 1000bp bins (based on the revised Cambridge reference sequence (Anderson *et al.*, 1981a)) to assess breakpoint location frequency. 5' breakpoint location was found to be bimodal, with a main peak of mtDNA breakpoint location frequency at 8-9kb and a minor peak at 6 – 7kb. The 5' breakpoint location distribution was skewed in a 5' direction, with a majority of 5' breakpoints falling in the first 4 bin categories (5 – 9kb) compared to a lower level of mtDNA deletions with a 5' breakpoint situated in the second 4 bin categories (9kb – 13kb). 3' breakpoint location was found to follow a unimodal distribution, peaking at 13 – 14kb. The 3' breakpoint location distribution was skewed in a 3' direction, with almost all 3' mtDNA deletion breakpoint falling in the last 3 bin categories (13kb – 16kb) (Figure 5.51 A). A further investigation of mtDNA deletion breakpoint location was carried out using the same dataset minus the 22 occurrences of the 4977bp common deletion (5' breakpoint at 8482bp, 5' breakpoint at 13447bp)m to ensure that the common deletion was not skewing the mtDNA deletion breakpoint distribution (Figure 5.51B). In this case the 5' breakpoint location distribution skews further in the 5' direction, with a major peak at 6 -7kb and a minor peak at 9 – 10kb, while the 3' breakpoint location distribution skews further in the 3' direction with a single peak occurring at 14 – 15kb.

The mtDNA deletion breakpoint distributions observed in this study, when the weighting of the common mtDNA deletion is removed (Figure 5.51Figure 5.51B), do not quite match up with those previously reported by Samuels *et al* (2004). The major site of 5' breakpoint locations in our dataset is shifted in a 5' direction to 7 – 8kb (compared to 8 – 9kb in in the 2004 study by Samuels *et al*), while the majority of 3' breakpoint lie in the 14 – 15kb region in our dataset (compared to 13 – 14kb in in the 2004 study by Samuels *et al*). These distinctions suggest that the common mtDNA deletion breakpoints may not play as central a role in mtDNA deletion formation as previously thought, though further work would be required to clarify this issue. A limitation of our study compared to that of Samuel's *et al* lies in the molecular techniques employed; we were unable to assess whether a peak occurred in 3' breakpoint location in the genome 3' of 16kb, as was shown by Samuels *et al* (2004).

Unfortunately, the assay used to detect mtDNA deletion in this patient cohort was not designed to detect mtDNA deletions occurring in this area. However, breakpoints were successfully identified in the majority of our patient cohort (92/113), suggesting it is unlikely that many 3' mtDNA deletion breakpoints would fall in the 16000 – 16569bp region.

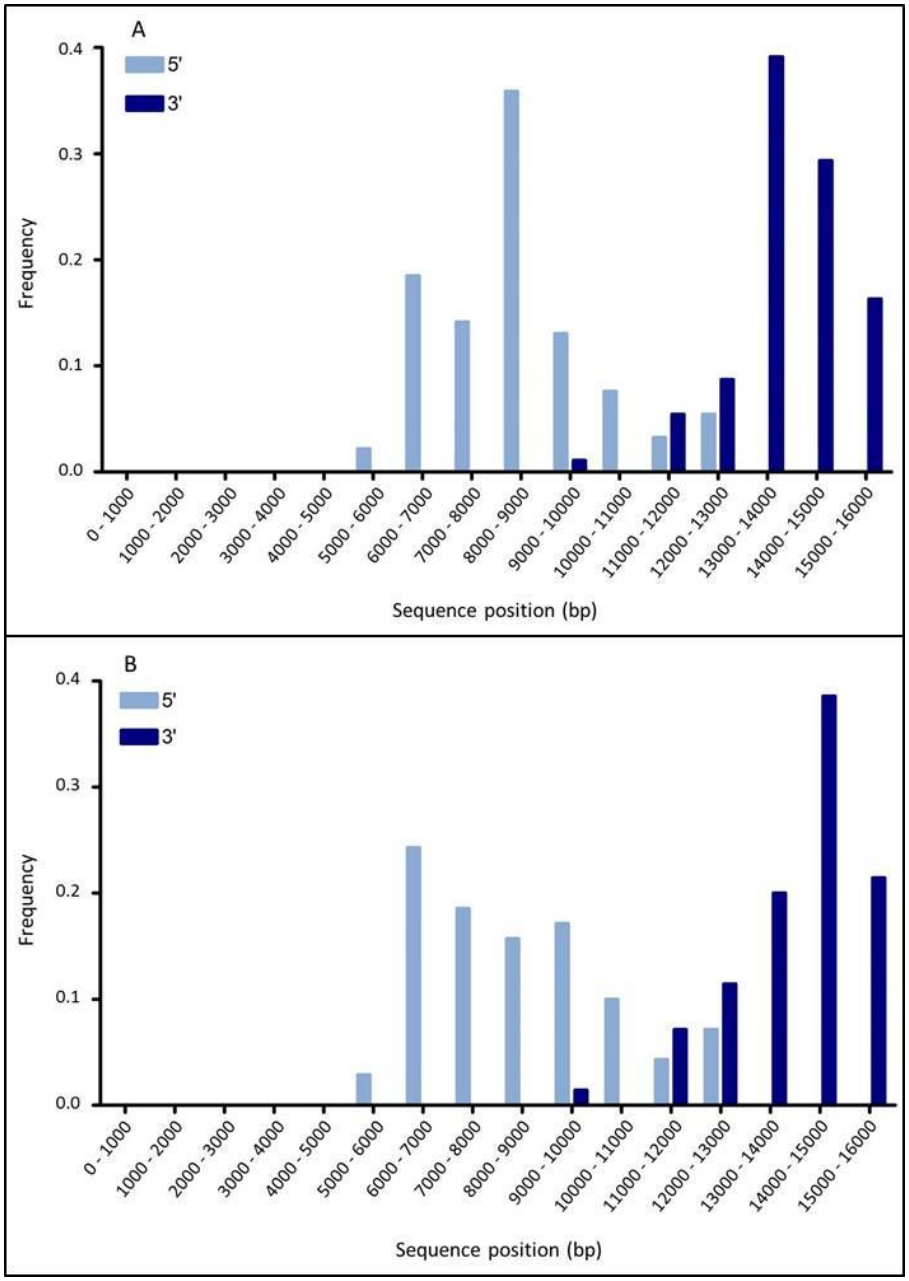

Figure 5.51 – mtDNA deletion breakpoint distribution

mtDNA deletion breakpoint position frequency calculated for **A** – all 96 successfully sequenced patient samples; **B** – 84 successfully sequenced patient samples (total dataset minus the 22 cases of the mtDNA 'common deletion'). Values were calculated based on a 1000bp bin size. Distributions are independently shown for 5' and for 3' breakpoint locations; all assessed distributions are non-uniform.

5.4.3.2 mtDNA deletion breakpoint sequence analysis

Following the analysis of mtDNA deletion breakpoint distribution, an assessment of sequence homology at the 5' and 3' breakpoint locations of each mtDNA deletion was carried out. This assessment was carried out for all 92 cases where full breakpoint data was available, as outlined in section *5.4.3.*1, following the protocol outlined by Sadikovic *et al* (2010) - involving the analysis of a total of 49 nucleotides surrounding the deletion junction (24 nucleotides either side of the breakpoint nucleotide, as recommended by McVey and Lee (2008)) at both the 5' and 3' end of the mtDNA deletion region. Sequence homology was evaluated using ClustalW software with default parameters (Thompson *et al.*, 1994), and the presence of a Class I, or 'direct' repeat of 3 or more nucleotides was assessed. All relevant mtDNA deletion breakpoint data is presented in Chapter 8, Appendix B.

A number of research questions were to be addressed by this analysis in order to best assess the potential impact of mtDNA deletion breakpoint sequences on deletion formation or propagation. Early reports suggested that different deletion formation mechanisms may account for mtDNA deletions displaying different breakpoint motifs (i.e. the presence or absence of a direct repeat) (Degoul *et al.*, 1991); subsequent studies have found that a majority of mtDNA deletions (approximately 70%) are Class I, being flanked by two short direct repeats (Mita *et al.*, 1990). However, these studies were undertaken with small numbers of patients, a high proportion of whom carried the common mtDNA deletion (known to be flanked by a 13bp direct repeat), meaning these results require verification. More recently, the mtDNA deletion breakpoint study conducted by Samuels *et al* reported that of 263 different human mtDNA deletions, 143 were found to involve direct repeat sequences of 2bp or more (54%). Most recently, a study was conducted by Sadikovic *et al* to investigate the relationship between mtDNA deletion breakpoint sequences and clinical presentation in a group of 67 patients; low levels of sequence homology at breakpoint regions were found, along with high mtDNA deletion heteroplasmy levels, to correlate with early symptom onset and more severe clinical presentations (Sadikovic *et al.*, 2010).

5.4.3.2.1 mtDNA deletion breakpoint repeat sequence analysis

The first stage of our breakpoint analysis involved assessing the presence of direct repeats of 2 or more base pairs at the 5' and 3' breakpoint regions of each mtDNA deletion (in keeping with the methods used by Sadikovic *et al* (2010)), to identify the number of Type I mtDNA deletions. 63 mtDNA deletions were found to present with direct repeat sequences at the 5' and 3' breakpoint regions – 68% of the total cohort of 92 mtDNA deletions with fully characterised breakpoints (Appendix B). When the influence reoccurring mtDNA deletions was taken into consideration – with 22 incidences of the common deletion, five mtDNA deletions picked up in two patients (NC_012920, 9486 – 13723, 9349 – 11419, 7128 – 13992, 7128 – 13992, 7540 - 14012) and a 2.3kb deletion occurring in four patients (NC_012920, 12112 – 14422) - 63 unique mtDNA deletions were found to be appropriate for inclusion in this analysis. Of these, 34 were found to present with direct repeat sequences of a minimum of 2 nucleotides – a total of 54% (Appendix B). An occurrence of direct repeats in 54% of unique mtDNA deletions is precisely in keeping with the findings of Samuels *et al* (2004), confirming this as an accurate representation of repeat sequences around mtDNA deletion breakpoints. Additionally, the study carried out by Sadikovic *et* al (2010) reported that approximately 70% of deletions presented with a direct repeat at the 3' and 5' breakpoints; when the re-occurrence of the common deletion (present in 25 patients) and a 7436bp deletion (present in 6 patients) are taken into account, 20 unique mtDNA deletions present with direct breakpoint repeats from a total of 40 unique mtDNA deletions (50%). These findings are again consistent with the results of this study and the report by Samuels *et al* (2004), confirming that approximately 50% of mtDNA deletions occur with direct repeats at the 5' and 3' breakpoint regions, and suggesting that direct repeats may not be responsible for a common mtDNA deletion formation mechanism.

5.4.3.2.2 mtDNA deletion breakpoint repeat sequences; correlation with other molecular markers and with clinical presentation

Following the analysis of repeat sequences at the 5' and 3' breakpoint regions of mtDNA deletions, the relationship between mtDNA deletion breakpoint characteristics and clinical presentation was investigates, following the assertion by Sadikovic *et al* (Sadikovic *et al.*, 2010) that low levels of sequence homology at breakpoint regions correlate with high mtDNA deletion heteroplasmy levels, early symptom onset and more severe clinical presentation.

Full sets of appropriate data – breakpoint characterisation, mtDNA deletion heteroplasmy levels and clinical onset age – were available for a total of 48 patients. This dataset was divided into four age-at-symptom-onset categories for analysis following the methodology used by Sadikovic *et al* (2010), though the 10-year age ranges for our four groups (1 – 10, 11 – 20, 21 – 30 and 31+) differed from those used in the Sadikovic study in order to best reflect our spread of data (Table 5.23). The number of patients which fell into each of the onset-age brackets was recorded alongside mtDNA deletion size and heteroplasmy levels (mean, standard deviation and total range for both measurements), and the number of occurrences of type I breakpoints and the common mtDNA deletion (Table 5.23).

Age	Number	Heteroplasmy, % [mean (range, s.d.)]	mtDNA deletion size, kb [mean (range, s.d.)]	Type I breakpoints	Samples with common mtDNA deletion
0 -10	9	68.3 (13 - 94, 27.8)	6176 (2549 - 8704, 1844)	7/9 (78%)	2/9 (22%)
11 - 20	20	53.6 (6 - 85, 23.4)	5643 (4113 - 9122, 1263)	13/20 (65%)	5/20 (25%)
21 - 30	11	48.6 (22 - 75, 19.8)	5332 (4241 - 7498, 1377)	7/11 (67%)	3/11 (27%)
41 +	8	52.6 (1 - 78, 24.2)	4255 (2310 - 7891, 1850)	4/8 (50%)	1/8 (13%)

Table 5.23 – mtDNA deletion breakpoint characteristics.

A total of 48 patient datasets were available for analysis with mtDNA deletion size and heteroplasmy data in conjunction with complete breakpoint data; these were divided by patient age at symptom onset into four 10-year age categories for analysis. mtDNA deletion heteroplasmy levels were significantly higher in the youngest age group (0 – 10 years) than any other group, while Type I breakpoints were also most common in the youngest age category.

Significantly more mtDNA deletions were found to present with Type I breakpoints in the youngest age group, with a trend for lower numbers of Type I deletions as age at symptom onset increases, though no trend was found to exist in terms of incidence of the common mtDNA deletion. This contradicts the decrease in sequence homology reported in patients with earlier clinical onset ages by Sadikovic *et al* (2010), highlighting the need for a much larger dataset to clarify this relationship. Similarly, increased numbers of Type I breakpoints appear to correlate with higher levels of mtDNA deletions heteroplasmy in our dataset – in opposition to the inverse relationship between these two factors proposed by Sadikovic *et al* (2010).

Unfortunately, the correlation between decreased breakpoint sequence homology and increased severity of clinical presentation described by Sadikovic *et al* (2010) could not be assessed in our patient cohort due to low numbers of patients with Pearson syndrome or multisystem involvement for whom all appropriate data was available. This is certainly an issue to be addressed in the future, to assess whether breakpoint homology is a factor which could improve mtDNA deletion disease progression modelling (discussed in section *5.4.5*). The reduced range of clinical severity in this 48 patient cohort compared to that assessed by Sadikovic *et al* (2010) could also account for the different outcomes in terms of the relationship between mtDNA deletion breakpoint sequence homology and onset age. If reduced sequence homology is associated with more severe clinical onset, the inclusion of more data from severely affected patients with early disease onset (i.e. those with Pearson syndrome) would likely bring down the percentage of early-onset patients with Type I breakpoints/high sequence homology.

5.4.4 Investigating the effect of specific gene involvement on mtDNA deletion characteristics.

Following on from early indications that 5' mtDNA deletion breakpoint location may play a role in determining heteroplasmy levels, further analysis was carried out to identify whether any 5' specific genes could be linked to higher or lower levels of heteroplasmy.

First, each of the 86 mtDNA deletions fully characterised by breakpoint sequencing and *ND1/*ND4 quantitative PCR analysis were organised by the gene location of the 5' mtDNA deletion breakpoint (Figure 5.52, Table 5.24), with a view to identify whether any specific gene locations correlated with heteroplasmy. It became apparent that the 5' breakpoint positions were not distributed evenly throughout different genes; more 5' breakpoints tended to fall within genes of a larger size, while approximately a quarter of the total dataset has a 5' breakpoint falling within ATPase8 due to the location of the common mtDNA deletion. This distribution prevented any reliable analysis of the relationship between mtDNA deletion gene location and heteroplasmy, meaning an alternative method of data analysis needed to be utilised.

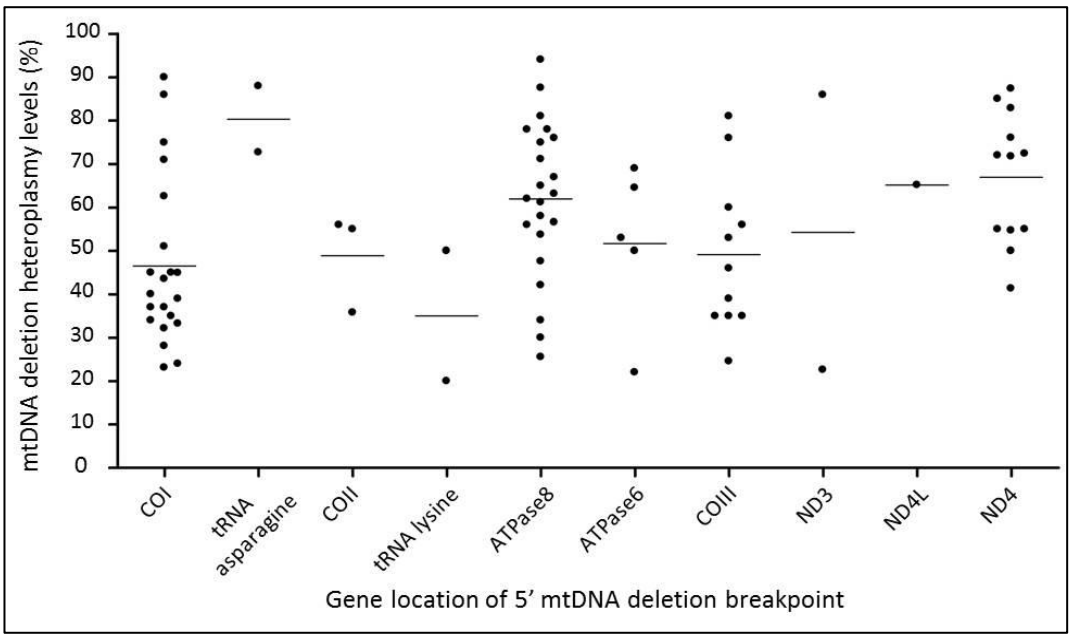

Figure 5.52 - mtDNA deletion heteroplasmy levels for deletions organised by gene location of 3' deletion breakpoint.

Representation of the spread of mtDNA deletion heteroplasmy levels for all 81 patient samples with fully characterised deletion breakpoints and heteroplasmy levels. All deletions were organised according which gene the 5' deletion breakpoint occurs within; the visibly uneven distribution of 5' breakpoint gene location prevented any further analysis based on this analysis.

Gene name	Gene location (rCRS)	Number of deletion with 5' breakpoints in this region	Average heteroplasmy level
CO1	5904 – 7445	21	46.51±19.36
TD	7518 – 7585	2	80.35±10.81
CO2	7586 – 8269	3	48.93±11.39
TK	8295 – 8364	2	35±21.21
ATP8	8366 – 8572	22	61.94±18.16
ATP6	8527 – 9207	5	51.71±18.38
CO3	9207 – 9990	11	49.14±17.98
ND3	10059 – 10404	2	54.30±44.83
ND4L	10470 – 10766	1	65.18
ND4	10760 – 12137	12	66.97±15.19

Table 5.24 - mtDNA deletion heteroplasmy levels for deletions organised by gene location of 5' deletion breakpoint.

All 81 mtDNA deletions with fully characterised deletion breakpoints and heteroplasmy data were organised according to which gene the 5' deletion breakpoint within. An uneven distribution of 5' breakpoint locations was observed, which can largely be attributed to the variance in gene length – less mutations happen to occur with a 5' breakpoint situated in the smallest genes. This distribution made it unreasonable to perform statistical analysis to assess the relationship between 5' breakpoint location and heteroplasmy.

As an alternative method of carrying out this analysis, and in order to ensure sufficient data points for statistical analysis to be reliably performed, gene locations of 3' breakpoints were grouped together (Figure 5.53, Table 5.25). This allowed a clearer analysis of whether a deletion of one area of the mitochondrial genome could be tolerated at a higher heteroplasmy level than another. A sequential set of groups were set up for analysis, following the pattern set out in Table 5.25; two-tailed unpaired t-tests were carried out at 95% confidence level, to determine if any significant difference existed between the two regions of 3' breakpoint locations. Significant variations in heteroplasmy were identified in a number of groups (Table 5.25). Firstly, deletions with 3' breakpoints occurring in *CO1* have significantly lower heteroplasmy values than mtDNA deletions which occur after rCRS base number 7445 and therefore do not affect *CO1* ($P = 0.0150$), suggesting that deletions which do not impact upon this complex 4 subunit can be tolerated at higher heteroplasmy levels. The next significant region appears to be the gene for tRNA lysine, as deletions occurring

between *CO1* and *TK* appear to accumulate to lower heteroplasmy levels than those with 3'breakpoints within or beyond *ATP8* (0.0179). However, few deletions in this study have been found to have 3' breakpoints in *TD*, *CO2* or *TK*, meaning this significance is likely to still depend on the apparent lower heteroplasmy levels of mtDNA deletions which affect *CO1*. The final gene region of interest highlighted by this analysis is *CO3* – deletion occurring with a 3' breakpoint within the region *CO1* to *CO3* were found to have significantly lower heteroplasmy levels than those with 3' breakpoint regions later in the genome (P = 0.0295) – again suggesting that deletions which affect *CO3* are less likely to accumulate to high heteroplasmy levels than those which don't.

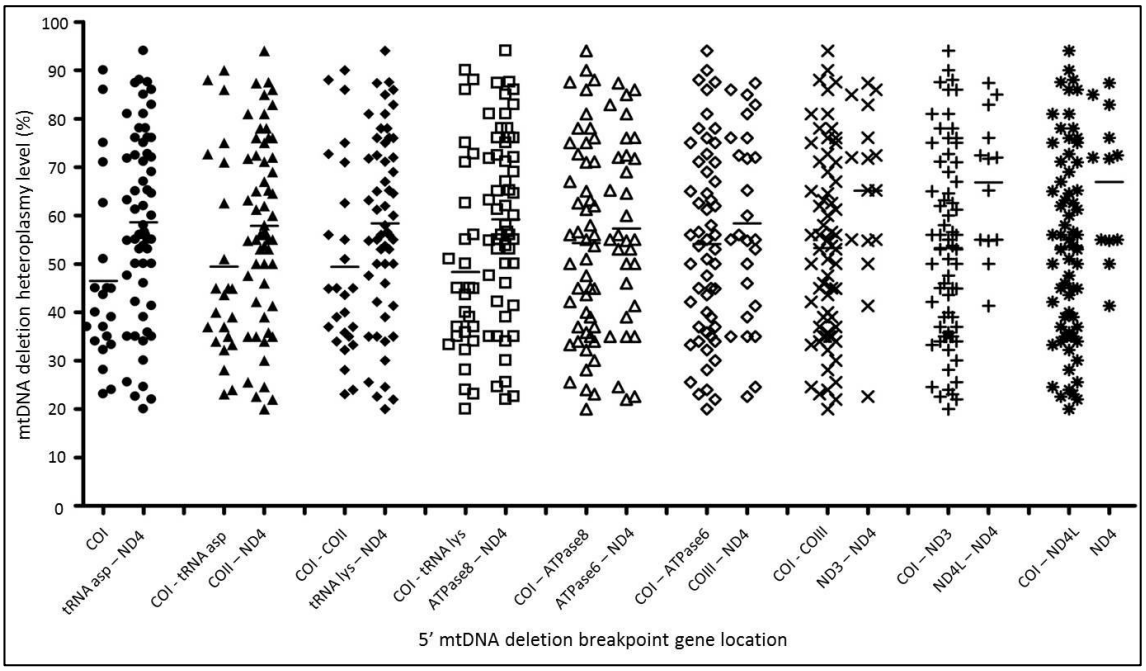

Figure 5.53 - mtDNA deletion heteroplasmy levels for deletions organised by grouped gene locations of 3' deletion breakpoints.

As the uneven distribution of 5' breakpoints made it unreasonable to analyse whether gene location of the 5' deletion breakpoint correlated with heteroplasmy levels, an alternative approach was required. To this end, genes were combined into a series of groups, to determine which locations may be most significant in determining deletion heteroplasmy levels (results presented in Table 5.24). *COI, TK* and *CO3* were highlighted by this analysis as areas with significant bearing on heteroplasmy.

3' deletion bp location group 1	Average het %	3' deletion bp location group 2	Average het %	Mann-Whitney test p-value	Group het levels sig different?
CO1	46.51±19.36	*TD-ND4*	58.61±19.14	0.0150	Yes
CO1-TD	49.45±21.01	*CO2-ND4*	57.86±18.97	0.0849	No
CO1-CO2	49.39±19.97	*TK-ND4*	58.35±19.25	0.0569	No
CO1-TK	49.37±20.00	*ATP8-ND4*	59.23±18.82	0.0179	Yes
CO1-ATP8	54.34±20.20	*ATP6-ND4*	57.31±19.34	0.5156	No
CO1-ATP6	54.10±19.90	*CO3-ND4*	58.38±19.68	0.3669	No
CO1-CO3	53.27±19.55	*ND3-ND4*	65.16±17.93	0.0295	Yes
CO1-ND3	53.30±20.02	*ND3-ND4L*	66.83±14.55	0.0231	Yes
CO1-ND4L	53.48±19,92	*ND4*	66.97±15.19	0.0285	Yes

Table 5.25 - average heteroplasmy levels for mtDNA deletions grouped by gene location of 3' breakpoint.

Average heteroplasmy data for mtDNA deletions grouped by 5' deletion breakpoint location. Mann-Whitney t-tests were carried out on appropriate groups (5' breakpoints occurring within *CO1* tested for significant difference from deletion occurring after *CO1* in the *TD – ND4* region, for example), in order to assess whether any regions appeared to have a significant impact on mtDNA deletion heteroplasmy levels. *CO1* and *CO3* were highlighted as being associated with lower mtDNA deletion levels, suggesting that deletion of these genes at a high level of heteroplasmy may not be tolerated. *TK* also appears to associate with lower levels of heteroplasmy, though it seems likely that this effect is maintained by *CO1* due to low levels of data with breakpoints occurring in TD, *CO2* and *TK*.

The analysis of the 5' mtDNA deletion breakpoint data has suggested that deletions affecting Complex IV subunit genes – particularly *CO1* and *CO3* – may be less well tolerated in the cell, and may be less likely to accumulate to high levels of mtDNA deletion heteroplasmy. Further analysis was therefore undertaken to establish if the mitochondrial Complex IV (COX) genes are a major determinant of deletion heteroplasmy levels. *COX* subunit-encoding genes have been previously established as regions of interest, with mtDNA deletions affecting these (or genes encoding ATPase subunits) being found to potentially correlate with an earlier symptom onset age (Yamashita *et al.*, 2008). Earlier symptom onset age has itself been found to correlate with a more severe disease phenotype (Aure *et al.*, 2007), so a correlation between *COX* gene involvement in an mtDNA deletion and symptom onset makes this an attractive gene set for analysis. However, it is worth noting that the link between *COX*

genes deletion and earlier symptom onset has not been consistently reported; a later meta-study carried out by an independent group found no correlation between these two factors (López-Gallardo *et al.*, 2009).

Firstly, the relationship between the number of *COX* subunit genes deleted and total mtDNA deletion size was assessed; this was carried out using Spearman's rho, due to the non-Gaussian data spread. As was expected, these were found to positively correlate ($r = 0.7609$, $P < 0.0001$); i.e. the bigger the mtDNA deletion, the more likely it is to affect more mitochondrial-encoded *COX* subunit genes (Figure 5.54 a). What was unexpected was the lack of any correlation found between the number of *COX* subunit genes disrupted by an mtDNA deletion and the respective mtDNA deletion heteroplasmy level (Figure 5.54 b & c). Following the grouping of deletion data into sets of mutations affecting 0, 1, 2 or all 3 of the mitochondrial *COX* genes, no significant difference was found in average heteroplasmy level between any groups. The biggest difference was found to exist between deletions disrupting 0 or 3 of these genes - average heteroplasmy levels of 61.07 ± 20.33 and 49.45 ± 21.01 respectively – but even this was not found to be significant ($P = 0.1005$ by Mann-Whitney test). Correlation analysis using Spearman's rho detected no significant relationship to exist between *COX* genes disrupted by an mtDNA deletion and the heteroplasmy level of the deletion ($r = -0.1931$, $P = 0.0841$). This was surprising given that the 5' breakpoint data suggested these gene locations to be important in determining heteroplasmy, but particularly interesting in that the number of disrupted *COX* genes correlates well with mtDNA deletion size. This relationship with mtDNA deletion size – which displays a negative correlation with mtDNA deletion heteroplasmy levels - had suggested that mtDNA deletion levels would be lower for deletions with the largest involvement of *COX* genes. The lack of a significant relationship between number of *COX* genes deleted and mtDNA deletion heteroplasmy level therefore led to the conclusion that another set of genes may be influential in terms of determining mtDNA deletion heteroplasmy levels; insufficient data may have been collected with breakpoints in these genes regions for identification in the 5' breakpoint analysis. The mitochondrial-encoded tRNA genes were therefore assessed in the same manner as the Complex IV subunit genes to assess the influence of this gene set on mtDNA deletion heteroplasmy levels.

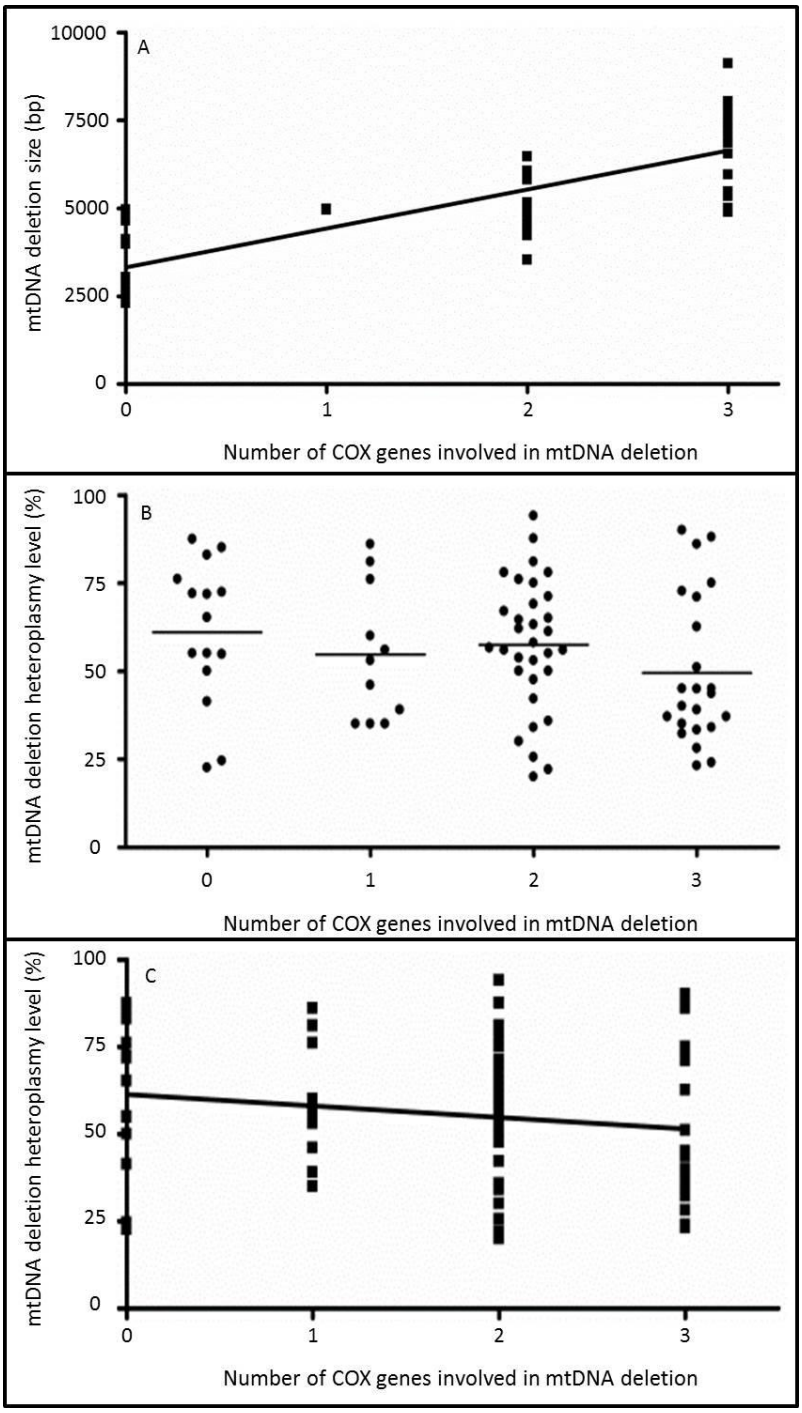

Figure 5.54 - Assessment of relationship of number of *COX* genes deleted with mtDNA deletion size and heteroplasmy level.

A – Demonstration of the positive relationship between the number of *COX* genes deleted (0 – 3) and total mtDNA deletion size (bp). This correlation was determined to be significant using Spearman's rank correlation coefficient ($r = 0.7609$, $P < 0.0001$). B – Average heteroplasmy levels demonstrated for deletions grouped by number of *COX* genes deleted. Average heteroplasmy levels: 0 = 61.07, 1 = 54.73, 2 = 57.44, 3 = 49.45. No significant difference was identified between any of these groups. C – Demonstration of the examined relationship between the number of *COX* genes affected by an mtDNA deletion and the deletion heteroplasmy level. No significant correlation was found to exist between these measures ($r = -0.1931$, $P = 0.0841$).

The tRNA genes were chosen for examination due to their potentially important role in causing mtDNA mutation pathogenicity, as specified by in a recent review by Schon, DiMauro and Hirano (Schon *et al.*, 2012). It was first noted that tRNA genes appeared to increase pathogenicity of mtDNA point mutations, with over 50% of total reported point mutations (over 270 since 1988, (Ruiz-Pesini, 2007)) occurring in tRNA genes, despite these comprising only approximately 10% of the coding regions of the mitochondrial genome. In comparison, only ~40% of point mutations occur in poly-peptide encoding regions of the mitochondrial genome, which take up almost 70% of the total coding genome area; this irregular distribution highlights the potential importance of gene location of point mutations. While it is possible that mutations in the tRNA genes are less efficiently selected against during embryogenesis than those in polypeptide-encoding genes, Schon *et al* suggest that this skewed distribution is due to the increased pathogenicity of mutations present in tRNA genes due to the downstream effects upon all mitochondrial-encoded respiratory subunits if mitochondrial translation is compromised (Schon *et al.*, 2012). This is then extrapolated to mtDNA deletions, where it is likely that at least one tRNA gene will be affected by any given mutation (in our study cohort alone, every mtDNA deletion affected 3 or more mitochondrial tRNA genes); reduced translation of all mt-mRNAs when an mtDNA deletion passes a threshold is therefore cited as a likely mechanism for mtDNA deletion pathogenicity (Schon *et al.*, 2012).

The number of tRNA genes disrupted by an mtDNA deletion was found to correlate strongly with deletion size ($r = 0.8816$, $P < 0.0001$) in a manner similar to the previously assessed *COX* genes; again, this is to be expected, with bigger deletions covering more of the genome and therefore being more likely to disrupt an increasing number of tRNA genes (Figure 5.55 a). An initial assessment of average heteroplasmy per number of tRNA genes disrupted by an mtDNA deletion revealed no single number of affected tRNAs to be significantly different to any other group (Figure 5.55 b). However, an overall trend for increasing numbers of deleted tRNAs to correlated with decreasing levels of mtDNA deletion heteroplasmy was found to be significant (Figure 5.55 c) ($r = -0.3797$, $P = 0.0005$). The strength of this relationship – stronger than that between deletion size and heteroplasmy level – suggests that the number of tRNA genes affected by a deletion may be one of the major determinants of heteroplasmy.

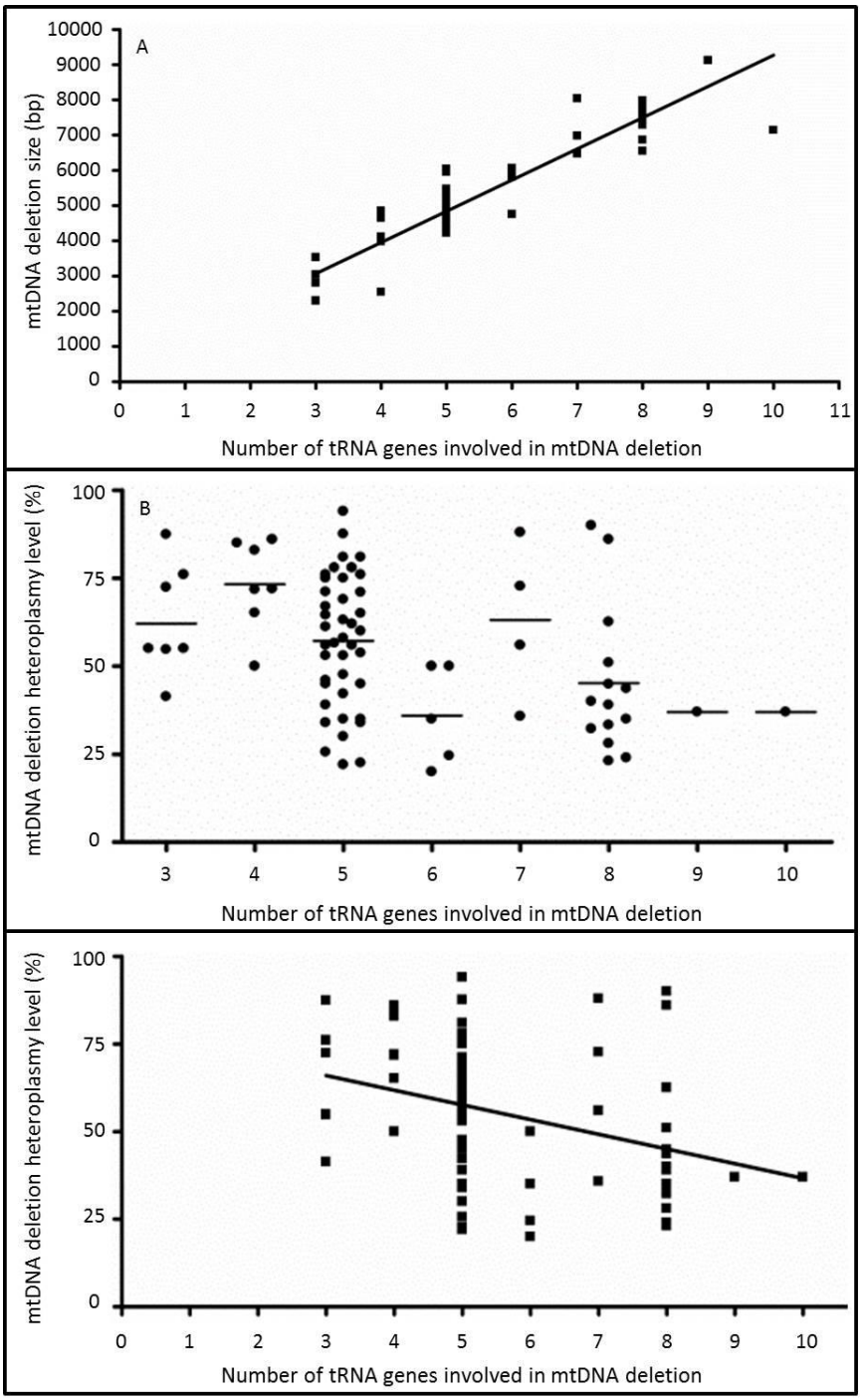

Figure 5.55 - Assessment of relationship of number of tRNA genes deleted with mtDNA deletion size and heteroplasmy level.

A – Demonstration of the strong positive relationship between the number of tRNA genes deleted (3 – 10) and total mtDNA deletion size (bp). This correlation was determined to be significant using Spearman's rank correlation coefficient ($r = 0.8816$, $P < 0.0001$). B – Average heteroplasmy levels demonstrated for deletions grouped by number of *COX* genes deleted. Average heteroplasmy levels ranged from 37% to 73%. C – Demonstration of the examined relationship between the number of *COX* genes affected by an mtDNA deletion and the deletion heteroplasmy level. A significant negative correlation was found to exist between these measures ($r = -0.3797$, $P = 0.0005$).

5.4.4.1 Limitations of assessing the effect of specific gene involvement on mtDNA deletion characteristics.

A major limitation of assessing the involvement of specific gene sets is the strong relationship between many of the molecular features of each mtDNA deletion. This is demonstrated by the strong positive correlation between number of COX-subunit or tRNA encoding genes involved in an mtDNA deletion, and the total size of that deletion ($r = 0.7609$ and 0.8816 respectively, $P < 0.0001$ in both cases), both of which demonstrate a negative correlation with mtDNA deletion heteroplasmy levels. It is therefore difficult to establish for these two datasets whether the observed relationship between an increased number of tRNA/COX-subunit genes involved in an mtDNA deletion and lower levels of heteroplasmy is an artefact induced by the correlation between mtDNA deletion size and heteroplasmy levels, or whether the observed relationship between mtDNA deletion size and level is in fact due to an increased chance of including specific genes at larger deletion sizes (i.e. the mtDNA deletion size is irrelevant other than altering the odds of the mtDNA deletion including more tRNA/COX-subunit genes). The difficulty of teasing out how the molecular characteristics of mtDNA deletions are linked, and the overlapping effects of many measures, is likely to be responsible for the contradictory nature of many reports published in this area (see Section 4.1.2, pages 193 - 5). It therefore became clear that a more sophisticated level of statistical analysis was necessary to interpret the molecular and clinical data in the best possible way, leading to the modelling work discussed in the remainder of this chapter.

5.4.5 Modelling progression: can we predict mtDNA disease progression using molecular data?

The initial analyses of the molecular data gathered for this study revealed a relationship to exist between mtDNA deletion size and level, and an observed potential importance for 5' deletion breakpoint location and the number of tRNAs involved in the deletion. In order to identify how this data relates to patients' clinical presentation, a modelling study was undertaken by Dr John Grady. This included the molecular profile for each patient, as examined in sections *4.4.1 – 3*, the level of COX-deficiency

in muscle as measured by the NCG Mitochondrial Diagnostics service, and clinical data accessed via patient records including age at symptom onset and NMDAS scores. NMDAS is the Newcastle Mitochondrial Disease Adult Scale is a clinically validated, semi-quantitative rating scale used to measure mitochondrial disease (Schaefer *et al.*, 2006). Use of the NMDAS scale to measure disease burden allowed for a much less subjective measure of disease severity than separation of patients into phenotype categories as in previous studies, with the additional bonus of creating a more continuous spectrum of disease severity. Where NMDAS measurements were available from more than one clinical assessment, a rate of progression was calculated, allowing assessment of the impact of genetic and biochemical features on disease progression as well as severity. Multiple regression analysis was carried out to determine the relationship between heteroplasmy, deletion size and location and either disease severity or biochemical defects; we propose that analysis by multiple regression, in order to separate the individual effects of otherwise related deletion characteristics, is necessary to properly understand these relationships. At each stage of analysis, the maximum number of patients for whom all appropriate data was available was included; a summary of the patient cohort numbers with available data is included below (Table 5.26).

	With NMDAS	Without NMDAS	Total
Patients with SKM heteroplasmy and deletion size	49	37	86
Of which have fully sequenced breakpoints	46	36	82
With onset age	42	12	54
With COX-deficient fibre %	46	30	76

Table 5.26 - Summary of patient cohort and available data at time of analysis.

5.4.5.1 mtDNA deletion heteroplasmy and deletion location predict level of COX deficiency.

The first stage of analysis was used to determine if the level of COX-deficiency in muscle was found to be related to any specific molecular features (Table 5.27). As in

previous studies (Mita *et al.*, 1989; Moraes *et al.*, 1989; Goto *et al.*, 1990a), heteroplasmy levels were found to display a strong positive correlation with the level of COX-deficient fibres observed in muscle (P = 0.0001). However, neither deletion size nor location was found to have any significant relationship with COX-deficiency.

Initial analysis of the deletion location showed no particular gene set to be predictive of COX-deficiency levels, with the presence of any *COX* genes within the deleted region coming the closest to showing any significant relationship with COX-deficiency (P = 0.2405). However, when assessed by co-regression with the mtDNA deletion heteroplasmy level, the involvement of *COX* genes in an mtDNA deletion does become predictive of a higher level of COX-deficiency (P = 0.0010). Though the presence of *COX* genes in the deleted region was found to be the most predictive of COX-deficiency, other gene loci including ND3, ND4L and ATP6 were also found to be predictive markers for COX-deficiency.

As *COX* genes tend to be involved in deletions of a larger size, it was expected that total mtDNA size would also be predictive of COX-deficiency. mtDNA deletion size was co-regressed with mtDNA deletion heteroplasmy level and the involvement of *COX* genes after finding that deletion size alone was not significantly predictive of COX-deficiency (P = 0.1160), though did show a slight trend towards larger deletions predicting lower levels of COX-deficiency. Following co-regression, mtDNA deletion size was found to correlate less well with COX-deficiency levels (P = 0.3959), suggesting that the trend towards a negative relationship between mtDNA deletion size and level of COX-deficiency was likely to be due to the inherent nature of larger deletions to involve *COX* genes and to correlate to lower heteroplasmy levels.

	Predictive of COX-deficiency?	Correlation with COX-deficiency?	P value
Heteroplasmy (%)	Yes	Positive	<0.0001
COX gene involvement	No	None	0.2405
COX gene involvement (co-regressed with het %)	Yes	Positive	0.0010
Heteroplasmy (co-regressed with *COX* gene involvement)	Yes	Positive	<0.0001
Deletion size	No	None	0.1160
Deletion size (co-regressed with *COX* gene involvement & het %)	No	None	0.3959

Table 5.27 - Regression analysis to determine the predictive effect of mtDNA deletion size, heteroplasmy level and location for level of COX-deficiency (%).

mtDNA deletion size and heteroplasmy level, as well as the involvement of *COX* genes in the deleted region, were selected as markers to check for potential correlation with COX-deficiency level. Each of these markers was assessed alone and subsequently co-regressed with other markers against COX-deficiency level, to identify if any of these markers is predictive of COX-deficiency level in muscle.

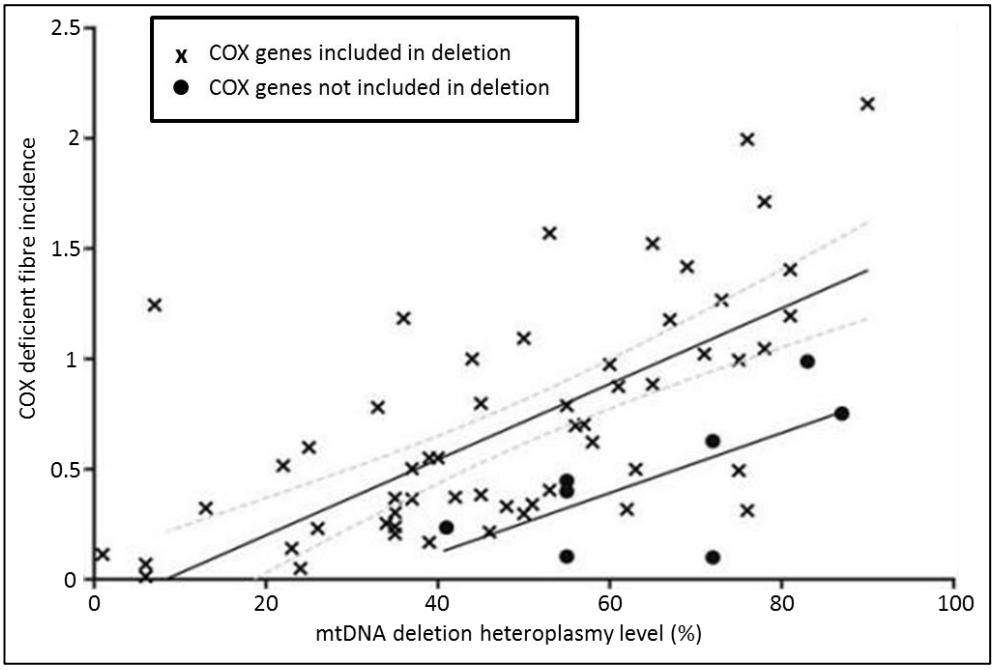

Figure 5.56 - Correlation of mtDNA deletion heteroplasmy and *COX* gene involvement with COX-deficiency level.

COX-deficient fibre incidence is dependent on skeletal muscle heteroplasmy and deletion of *COX* genes. The y axis shows COX-deficient fibre incidence (COX-deficient fibre prevalence divided by age at biopsy). Data are from our cohort, N=76, r = 0.66. Heteroplasmy ($p < 0.0001$) and deletion of *COX* genes ($p = 0.0011$) are both significant predictors. Separate regression lines are shown for those that delete one or more *COX* genes(N= 58, 95% confidence interval for regression line shown) and those that do not (N=8, gradient of regression line is not significantly non-zero, confidence interval not shown).

5.4.5.2 Clinical progression is determined by mtDNA deletion size and heteroplasmy.

Age of symptom onset and rate of clinical progression (measured as number of points increase on the NMDAS scale per year) have both been found to correlate well with mtDNA deletion size and heteroplasmy level. In the MRC Mitochondrial Disease Patient Cohort Study (UK), patients had carried out an average of 4.5 NMDAS assessments over a median of 5.4 years – an average progression of approximately 0.8 NMDAS points per year. Two sets of analyses carried out in this patient cohort have confirmed these findings, as outlined below.

First, all appropriate patient data sets were divided into four individual categories; mtDNA deletion size was determined to be 'large' or 'small' (above or below 5kb in size), while deletion heteroplasmy level was determined to be 'higher' or 'lower' (above or below 60%), leading to 4 data groups comprised of small deletions with low or high heteroplasmy levels and large deletions with low or high deletions levels. Statistical analysis of these data groups identified that small deletions lead to a significantly later age of onset and significantly slower rate of clinical progression, while lower heteroplasmy levels follow the same trend. No significant difference in age at onset of clinical symptoms and rate of clinical progression between large mtDNA deletions with low heteroplasmy levels and small mtDNA deletions with high levels of heteroplasmy (Figure 5.57).

A second analysis was undertaken, using both mtDNA deletion size and heteroplasmy level as continuous predictors; the regression analysis undertaken is summarised in Table 5.28. Both deletion size and heteroplasmy were found to be predictive of symptom onset age and rate of NMDAS progression, though in both cases the predictive power of these markers was strengthened by co-regression – the implication of this being that each predictor modulates the effect of the other.

Dependent Variable	N	Deletion size alone	Co-regressed with heteroplasmy level	Heteroplasmy level alone	Co-regressed with mtDNA deletion size	R^2 (co-regress)
Onset age	54	0.0056	$3x10^{-6}$	0.0113	$5x10^{-6}$	39.7%
NMDAS progression	49	0.0010	$1x10^{-6}$	$2x10^{-5}$	$2x10^{-9}$	66.3%

Table 5.28 - Prediction of age at onset and NMDAS progression by mtDNA deletion size and heteroplasmy level.

Table shows p-values for the regression of age of onset and progression of NMDAS score per year against predictors deletion size and SKM heteroplasmy. In all cases, co-regression of both predictors improves statistical significance.

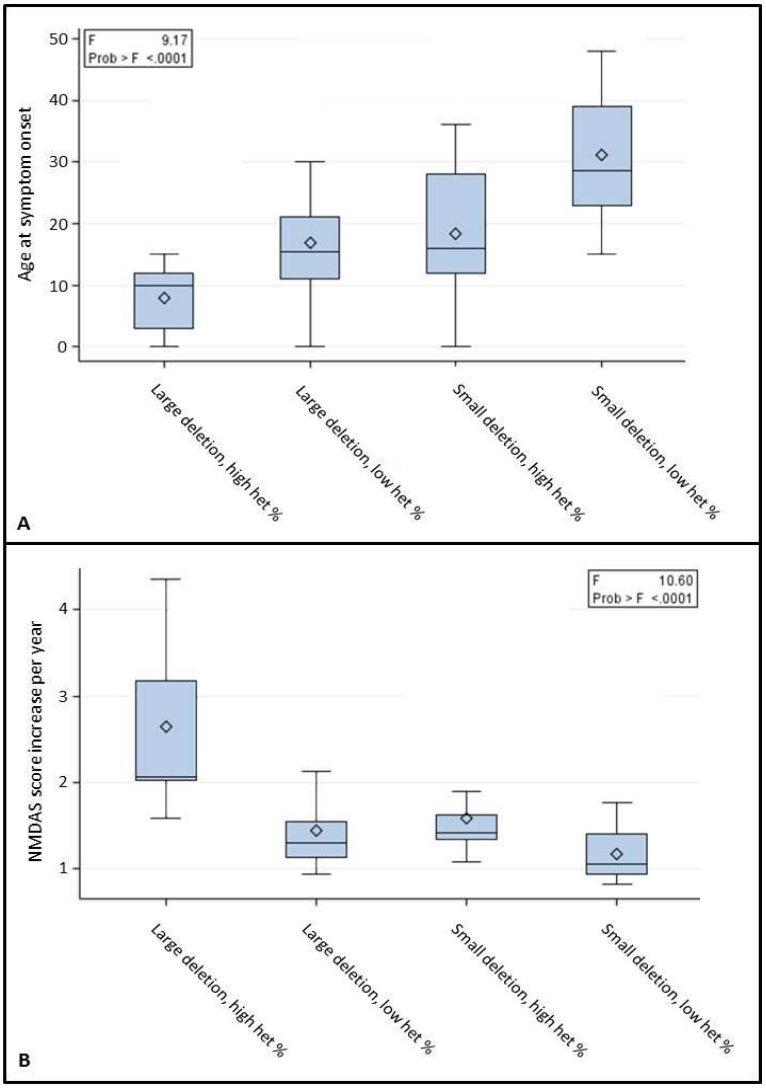

Figure 5.57 - Prediction of age at onset and NMDAS progression by mtDNA deletion size and heteroplasmy level.

In both panels, low heteroplasmy is considered < 60%, and small deletion < 5kb. A - Age at onset is found to be predicted by both molecular markers, with lower heteroplasmy levels and smaller deletion sizes both leading to later onset of clinical symptoms. B – Both molecular markers are indicative of rate of disease progression, with smaller deletion sizes and lower deletion heteroplasmy levels leading to a lower increase in NMDAS per year following symptom onset.

5.4.5.3 Longitudinal clinical progression is predicted by mtDNA deletion size, heteroplasmy level and location.

Longitudinal modelling has been carried out to determine the effect of mtDNA deletion size and heteroplasmy level on clinical progression; both of these molecular markers have been found to be strongly predictive of rate of NMDAS score increase (heteroplasmy, $P < 0.0001$; deletion size, $P < 0.0001$). A significant interaction between mtDNA deletion size and heteroplasmy level was also identified by longitudinal modelling ($P = 0.0002$) – a stronger relationship than was apparent when assessing deletion size and heteroplasmy level alone (see *5.4.1*). The effect of this is clearly visible when comparing panels A and C of Figure 5.58 – at low heteroplasmy levels, mtDNA deletion size has a negligible impact on disease progression, but is found to highly modulate rate of progression at high heteroplasmy levels. Interestingly, the location of the deletion in the mitochondrial genome has also proven to impact upon rate of clinical progression. The most predictive gene locus is ND6, inclusion of which predicts faster progression ($p = 0.0031$); conversely, genes below ND4, from ND4L down to COX3, predict faster progression ($p=0.0034$).

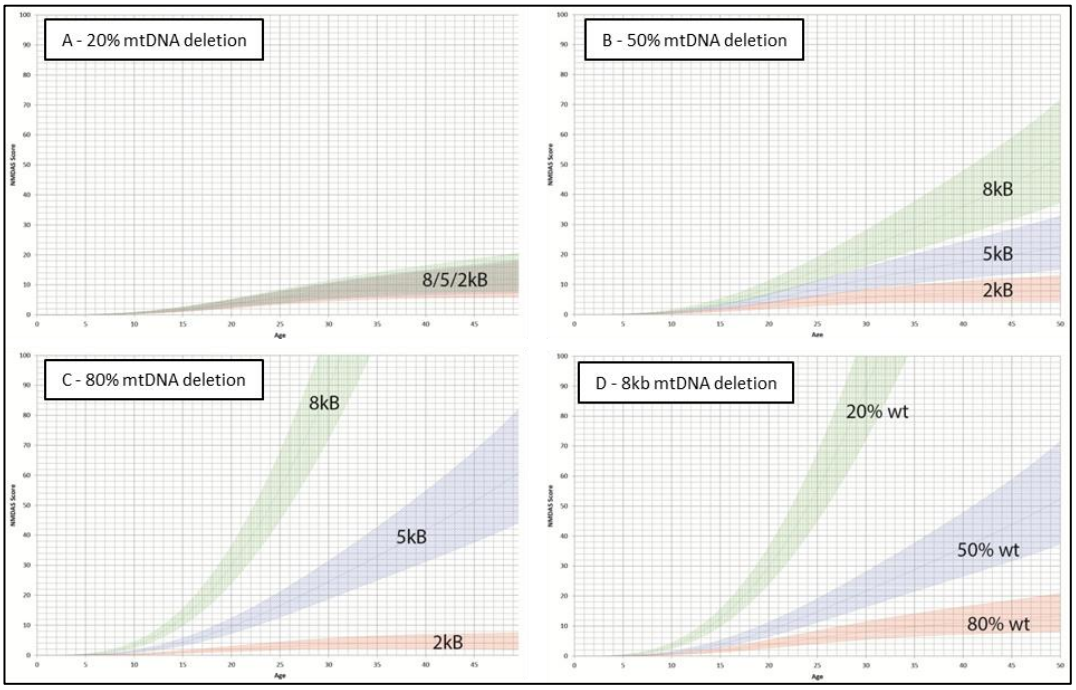

Figure 5.58 - Effect of mtDNA deletion size and level on NMDAS progression.

A: The effect of deletion size for 20% heteroplasmy. Note that the size of deletion at this low level of heteroplasmy is minimal. B: The effect of deletion size at 50% heteroplasmy. C: The effect of deletion size at 80% heteroplasmy. D: The effect of heteroplasmy for a large (8kB) deletion. Graphs courtesy of Dr John Grady.

5.5 Discussion

The primary aim of this study was to identify whether any evidence could be found to support the 'survival of the smallest' theory of clonal expansion in a large cohort of single large-scale mtDNA deletion patients. In order to test this hypothesis, a test for correlation between mtDNA deletion size and heteroplasmy levels was carried out. The expected positive correlation between mtDNA deletion size and heteroplasmy, which would have lent support to the replicative advantage model of mtDNA deletion clonal expansion, was not observed. This is in keeping with results from Chapters 3 and 4, suggesting that it is unlikely that a replicative advantage for mtDNA deletions species over wildtype mtDNA does exist.

Interestingly, the relationship between mtDNA deletion size and heteroplasmy was not found to be neutral – a negative correlation was in fact found to exist between these two factors. Though this negative trend was found to be significant (P = 0.0034), the large range of data spread did raise questions about the relevance of this finding. However, further analysis of separate deletion groups did show the largest deletions to have significantly lower heteroplasmy levels than the smallest deletions (P = 0.0359), and mid-range deletions to account for a large proportion of the data spread. This negative trend between mtDNA deletion size and heteroplasmy level was also identified in a recent report by Lopez-Gallardo *et al*, though at a non-significant level (P = 0.0601). The relevance of this finding is minimally discussed in this report, suggesting that this is simply due to a lack of replicative advantage for mtDNA deletions (López-Gallardo *et al.*, 2009) However, I would suggest that this should lead to a neutral relationship between deletion size and heteroplasmy level rather than a negative correlation. I therefore propose that this negative trend is a result of the clinically observed phenotypes of patients from whom samples are available to access; individuals with small deletions at low heteroplasmy levels would not be likely to present clinically with symptoms, and large deletions at high heteroplasmy levels may be so deleterious as to be lethal early in development. An important implication of this is that the heteroplasmy threshold for pathogenicity of a deletion is likely to be dependent on deletion size and location.

Following this observation, analysis of the role of mtDNA deletion breakpoint location was carried out. While breakpoint location was predictably found to dictate the

resulting mtDNA deletion size, it was interesting to observe that only 5' breakpoint location and not 3' deletion location forms a significant relationship with mtDNA deletion heteroplasmy level. It was proposed that this may be due to specific genes affected at the 3' mtDNA deletion breakpoint regions, so an analysis of affected genes was undertaken. Initial analyses suggested that the deletion of *COX* genes may ultimately affect mtDNA deletion heteroplasmy levels, but a more in depth study uncovered a closer link between the number of tRNA genes affected by an mtDNA deletion and the resultant heteroplasmy level. This is in keeping with the recent assertion by Schon *et al* that the pathogenicity of mtDNA deletions is based upon the disruption of tRNA genes and the downstream effects of this on translation of all of the mitochondrial genes (Schon *et al.*, 2012). The strong correlation between the total number of tRNA genes disrupted and mtDNA deletion size also observed therefore supports the importance of deletion size and location in determining the heteroplasmy threshold for pathogenicity of a deletion.

Additional investigations were carried out using the available mtDNA deletion breakpoint data to assess breakpoint distribution and breakpoint repeat sequences. 5' and 3' mtDNA deletion breakpoint in this patient cohort were found to follow a similar distribution to that reported by Samuels *et al* (2004); both breakpoint sites followed unimodal distributions, with 5' breakpoints most commonly occurring at 8 – 9kb and 3' breakpoints most commonly occurring at 13 – 14kb (Revised Cambridge Reference Sequence, NC_012920.1 (Andrews *et al.*, 1999)). However, when only unique mtDNA deletions were included in the analysis (removing the weighting of the 22 occurrences of the 4978bp common mtDNA deletion) the peaks of both the 5' and 3' breakpoint distributions shifted. In this re-analysis, the 5' breakpoint distribution peaked at 6 – 7kb while the 3' breakpoint distribution peaked at 14 – 15kb. This shift away from the common deletion breakpoint regions (bp 8482 and 13460, NC_012920.1) suggests that the 13bp direct repeat present at the common mtDNA deletion breakpoints may not play as crucial a role in mtDNA deletion formation as originally suggested by Samuels *et al* (2004), though work must be done to further consider this. An assessment of 5' and 3' mtDNA deletion breakpoint sequences revealed that 68% of our total mtDNA deletion cohort with available breakpoint data present with direct (Type I) repeats of 2 or more nucleotides. When only unique mtDNA deletions were included in this analysis, this figure reduced to 54%. These figures are consistent with previous findings

by both Samuels *et al.* (2004) and Sadikovic *et al.* (2010), confirming that direct breakpoint repeats are found at the 5' and 3' breakpoint sites of approximately half of all mtDNA deletions. Breakpoint homology was further investigated to determine whether any correlation could be found to exist with mtDNA deletion heteroplasmy levels or age at disease onset (a strong predictor of disease severity (Aure *et al.*, 2007)), as was reported in a preliminary study by Sadikovic *et al.* (2010). The cohort of 48 patient for whom all relevant information was available (breakpoint analysis, mtDNA deletion heteroplasmy levels and age at onset of clinical symptoms) was divided into four groups based upon age at symptom onset for analysis. High levels of breakpoint sequence homology were found to correlate with high mtDNA deletion heteroplasmy levels and an earlier age at onset; these results conflict with the original findings of Sadikovic *et al.* (2010), highlighting a need for further study in this area.

Following these analyses, the collected molecular data was combined with clinical information and biochemical defect measures to be used in a modelling study. This was divided into three main areas, with the first investigation assessing the impact of genetic markers on the biochemical defect caused by a deletion. mtDNA deletion heteroplasmy was found to be highly predicative of COX-deficiency in muscle, which is in line with previous research by a number of independent groups (Mita *et al.*, 1989; Moraes *et al.*, 1989; Goto *et al.*, 1990a). Initially, neither deletion size nor location showed any affinity with the level of observed biochemical defect in muscle. However a co-regression analysis with mtDNA deletion heteroplasmy level identified deletions involving *COX* genes to display a higher level of COX-deficiency than deletions located elsewhere in the genome. A correlation between the involvement of *COX* genes in an mtDNA deletion and the resulting level of cellular biochemical defect has been ruled out in previous studies (Goto *et al.*, 1990a), highlighting the importance of analysis by co-regression in order to factor in the close relationship between many molecular features of mitochondrial DNA deletions. Interestingly, no significant relationship was identified between mtDNA deletion size and COX-deficiency – the probability of these being related actually decreased following co-regression with heteroplasmy level and the involvement on *COX* genes. This lies in agreement with early studies which found no relationship to exist between mtDNA deletion size and enzyme activity (Moraes *et al.*, 1989; Goto *et al.*, 1990a).

The next analysis undertaken demonstrated a predictive role for mtDNA deletion size and heteroplasmy level for disease severity. Both deletion size and heteroplasmy were found to be predictive of symptom onset age and rate of NMDAS progression, though in both cases the predictive power of these markers was strengthened by co-regression – the implication of this is that each predictor modulates the effect of the other. In addition, deletion size is in all cases the stronger predictor. This finding ties together both the recent studies of single deletion disease (Yamashita et al., 2008; López-Gallardo et al., 2009) that found deletion size predictive (though these reports differed on the effect of heteroplasmy,) and the more seminal studies (Holt et al., 1990). It is possible that, due to the intrinsic relationship between mtDNA deletion size and heteroplasmy level identified earlier in this study, our ability to observe a relationship between heteroplasmy level and age at symptom onset is confounded.

Finally, a longitudinal modelling study was carried out, using change in NMDAS score over time as a measure of clinical progression. This is the first study of its kind and, though further verification of these results is required, is the first step towards providing clinicians with a better set of prognostic tools for patient analysis. Both mtDNA deletion size and location have been found to be highly predictive of patient progression, with larger deletion sizes and higher heteroplasmy levels indicating a more rapid disease course. These quantitative measures have the potential to be much more reliable indicators of a patient's likely disease course than just age of onset and current clinical severity. A number of gene loci have also been found to modulate disease progression – specifically ND6 involvement which predicts faster progression while the deletion of genes in the region ND4L to COX3 predict slower progression – though this analysis is currently at an early stage.

In conclusion, this study has identified no evidence to support a replicative advantage for mtDNA deletions over wildtype genomes. A negative relationship was observed between mtDNA deletion size and level, but this is believed to be due to a sample bias – suggesting a true neutral relationship between these molecular characteristics, and therefore supporting the hypothesis that the clonal expansion of mtDNA deletions occurs by random intracellular drift (Elson *et al.*, 2001). Evidence for a modulatory effect of deletion size and location on the heteroplasmy threshold for individual deletions has been presented, though a more comprehensive data set would be

required to fully determine the importance of specific tRNA and OXPHOS protein genes in regulating mtDNA heteroplasmy levels and the severity of any resulting biochemical defect. Statistical studies carries out by Dr John Grady have identified a role for mtDNA deletion heteroplasmy level and the involvement of *COX* genes in a deletion in determining the severity of the enzymatic defect caused by a deletion. Furthermore clinical severity can be predicted by mtDNA deletion size and heteroplasmy, while the combination of size, heteroplasmy and deletion location shows promise in predicting the course of disease progression over time.

Chapter Six

Chapter 6

Analysis of clonally-expanded mtDNA deletions in single muscle fibres by single molecule PCR.

6.1 Introduction

6.1.1 mtDNA deletions in ageing and disease

Mitochondrial dysfunction has been implicated in human ageing since a very early stage in the study of mitochondria, beginning with the hypothesis that ageing is due to the accumulation of damage from ROS and other free-radicals produced during normal metabolism (Harman, 1955). The idea of mitochondria acting as a kind of 'biological clock' in human ageing was later proposed in 1972 (Harman, 1972); this theory has been developed over time as more was discovered about mitochondrial biology, with an ever-increasing set of evidence being collected that mitochondria play an integral role in ageing and disease (Reeve *et al.*, 2008b). With free-radicals in the form of ROS being produced consistently during respiration – estimates suggesting that 0.1 to 4% of oxygen consumption leads to ROS production (Sanz and Stefanatos, 2008) – mitochondria are a primary source of free-radical generation in the cell, and were proposed to be the main target for their action (Harman, 1972). This proposition was refined to suggest that the respiratory complexes and mtDNA are the main targets for the harmful action of ROS produced during respiration, given the close proximity of the respiratory complexes to the mtDNA at the IMM (Fleming *et al.*, 1982). This formed the basis of the 'mitochondrial free radical theory of ageing' (Linnane *et al.*, 1989), which attributes ageing and age-related cellular pathology to a decline in mitochondrial ATP-production capacity over time due to an increase in mtDNA defects caused by free radicals. While debate continues to date regarding the accuracy of this hypothesis (De Grey, 1997; Sanz and Stefanatos, 2008) , it has certainly become accepted that accumulated mtDNA defects are an important contributor to the ageing process, and play an important role in age-related disease. mtDNA deletions are specifically associated with the ageing of post-mitotic tissues, and age-related neurodegenerative disorders (Taylor and Turnbull, 2005; Bender *et al.*, 2006; Kraytsberg *et al.*, 2006; Reeve *et al.*, 2008b; Larsson, 2010).

As well as contributing to human ageing and age-related disease, mtDNA deletions are also a primary cause of a range of inherited and sporadic mitochondrial disorders. The role of single sporadic large-scale mtDNA deletions is more fully discussed in section *4.1.1*, while multiple mtDNA deletion disorders caused by inherited nuclear genetic defects are examined in section *1.5.4*.

6.1.2 Clonal expansion of mtDNA deletions

The importance of clonal expansion was established early in the study of mtDNA deletions in human ageing (Brierley *et al.*, 1998). While the identification of mtDNA deletions in a range of human tissues (Cortopassi and Arnheim, 1990; Zhang *et al.*, 1992; Horton *et al.*, 1995; Melov *et al.*, 1995) and an observed decrease in mitochondrial enzymatic activity over time (Cooper *et al.*, 1992; Boffoli *et al.*, 1994) supported a likely role for mtDNA deletions in human ageing, heteroplasmy analysis found individual mtDNA deletions to be present only at low levels in aged tissue samples. This was problematic for the field, with low mtDNA deletion heteroplasmy levels being unlikely to impair tissue function (Ozawa *et al.*, 1990; Simonetti *et al.*, 1992) and complementation being likely to occur between different mtDNA deletion species as well as between mtDNA deletions and wildtype mtDNA (D'Aurelio *et al.*, 2006; Nakada *et al.*, 2009). The discovery that mtDNA deletions did not occur heterogeneously throughout a given tissue, but rather accumulate to high heteroplasmy levels to cause a biochemical defect in a subset of cells, went some way to explaining the low level of deletions detected in tissue samples (Brierley *et al.*, 1998). This investigation, carried out in aged human muscle tissue, found mtDNA deletions to be present at high heteroplasmy levels in all investigated COX-deficient muscle fibres, while no COX-normal fibres harboured mtDNA deletions at heteroplasmy levels sufficient to cause a biochemical defect. Of equal importance was the discovery that different mtDNA deletions were found to have reached high heteroplasmy levels in different cells. This served both to explain the low level of any given mtDNA deletion in total mtDNA from tissue, and to emphasise the importance of clonal expansion; each of these individual mtDNA deletions has accumulated to a high level within a single cell over time to create a cellular biochemical defect (Brierley *et al.*, 1998).

6.1.3 Single cell studies of mtDNA deletion mutants.

Since the identification of different clonally expanded mtDNA deletions in separate single cells (Brierley *et al.*, 1998), clonal expansion of mtDNA deletions has been considered to result in the accumulation of a single mtDNA deletion type within any given single cell. Early evidence did emerge that multiple mtDNA deletions may be present in biochemically deficient cells (Kopsidas *et al.*, 1998). This study, carried out in single fibres isolated from human skeletal muscle, found all COX-deficient or intermediate fibres to contain a heterogeneous population of mtDNA deletion species, with no detectable levels of wildtype mtDNA (Kopsidas *et al.*, 1998). The authors suggested that a degree of functional complementation was able to occur between the mtDNA deletion strains present in COX-intermediate fibres, while a lack of wildtype mtDNA with no complementation occurring between the remaining deleted strains of mtDNA was the cause of fully COX-deficient fibres (Kopsidas *et al.*, 1998). However, subsequent studies have failed to replicate this finding. A study carried out in human cardiomyocytes, published just one year after the apparent discovery of multiple mtDNA deletions in single cells by Kopsidas *et al*, confirmed the presence of a trend for single mtDNA deletions to be present in individual cells. Myocytes from human autopsy heart samples (donors aged 31 to 109 years of age) which contained mtDNA deletions each harboured only one clonally expanded mtDNA deletion species (Khrapko *et al.*, 1999). Of the 14 cells with detectable mtDNA deletions, 12 had unique breakpoints while 2 contained the same mtDNA deletion mutant. Interestingly, all mtDNA deletions were detected in centenarian samples while no mtDNA deletions were identified in samples from younger donors, highlighting the likely importance of increasing levels of mtDNA deletions in influencing the ageing of the heart. (Khrapko *et al.*, 1999).

In subsequent years, a number of single cell studies have been undertaken in model organisms, designed to characterise the distribution of mtDNA deletion mutants in tissues displaying mosaic COX-deficiency; these have served to confirm the presence of single, clonally expanded mtDNA deletions in post-mitotic cells displaying COX-deficiency. One of the earliest single cell studies of mtDNA deletions, undertaken in rectus femoral muscle from aged rats, looked to characterise the mtDNA deletions present in age-associated ragged-red fibres (Cao *et al.*, 2001). This investigation found

only one species of mtDNA deletion mutant to be present in each investigated ragged-red fibre, though breakpoint sequencing found the mtDNA deletion type to be different in each case. Each of these single mtDNA deletions were found to have accumulated to a high heteroplasmy level, while only wildtype mtDNA was found to be present at a detectable level in biochemically-normal fibre areas (Cao *et al.*, 2001). This was confirmed in aged muscle tissue in a 2007 study of rat quadriceps tissue, where single fibres were found to contain segmental, clonal expansions of unique mtDNA deletions (Herbst *et al.*, 2007). Following on from the work of Cao *et al*, a 2004 study of laser micro-dissected ETS abnormal muscle fibres from aged rhesus monkeys found a similar pattern of mtDNA deletions in single cells. The clonal accumulation of single mtDNA deletion species in each single muscle fibre was supported by not only the identification of a single mtDNA deletion species in each ETS abnormal muscle fibre, but also the identification of the same single mtDNA deletion in different regions of the same ETS abnormal fibre (Gokey *et al.*, 2004).

More recently, studies have been carried out in human neuronal tissue to assess whether mtDNA deletions accumulate in human tissue with age in the same manner as had been observed in murine substantia nigra neurons (Trifunovic *et al.*, 2004). mtDNA deletions were found to have accumulated in a clonal manner in individual substantia nigra neurons assessed in tissue from individuals with Parkinson disease and from healthy aged controls (Bender *et al.*, 2006; Kraytsberg *et al.*, 2006). Though substantia nigra neurons have been shown to display the highest observed levels of mtDNA deletions, and as such have been the most studied neuron type in terms of mtDNA deletions accumulation, other neurons have been shown to be susceptible to the accumulation of mtDNA deletions over time. A range of major-arc mtDNA deletions have been shown to be present in human cochlear spiral ganglion cells where COX-deficiency has resulted in presbycusis (age-related hearing loss) (Markaryan *et al.*, 2010); again, different mtDNA deletion species were found to have independently accumulated in separate COX-deficient cells (Markaryan *et al.*, 2010). Findings in the muscle of animal models (Cao *et al.*, 2001; Gokey *et al.*, 2004) were found to be reflective of the situation in aged human muscle, where unique mtDNA deletions were found to accumulate to detrimental levels (>90% of the total mtDNA) in a clonal manner within individual COX-deficient muscle fibres (Bua et al., 2006).

Barring one study in human skeletal muscle which identified multiple mtDNA deletions to have accumulated within a single muscle fibre (Kopsidas *et al.*, 1998), each study outlined above has observed the clonal accumulation of a single mtDNA deletions species within a single cell to be standard in both ageing and disease. This seems to suggest that the mtDNA deletion in each cell has accumulated due to some sort of selective pressure; if random drift was sufficient to allow for clonal expansion, it would be reasonable to expect the continuous state of flux within the cell's mtDNA content to result in the presence of multiple mtDNA deletions in at least a subset of cells.

6.2 Aims and Hypothesis

The aim of this study was to investigate the presence of multiple clonally expanded mtDNA deletions in single COX-deficient muscle fibres, following the amplification of multiple mtDNA deletion bands from approximately 20% of all investigated COX-deficient fibre regions in the longitudinal mtDNA deletion accumulation study discussed in Chapter 3 (see *3.4.2*). As these fibres had been studied using only long-range PCR, it was not possible to determine whether a single mtDNA species was dominant within the cell, or whether mtDNA deletions of different sizes had accumulated to similar levels within these single muscle fibres. This follow-up study was designed to establish whether multiple mtDNA deletion species can be seen to clonally accumulate to biologically significant levels in single human muscle fibres; this is of particular interest given that human skeletal muscle is the only tissue in which multiple mtDNA deletion species have previously been reported to exist in single cells (Kopsidas *et al.*, 1998).

As discussed in section *6.1.3* (page 232), the clonal accumulation of mtDNA deletions is typically considered to involve the accumulation of a single mtDNA deletions species; a logical starting point for this study was therefore to identify what proportion of COX-deficient skeletal muscle fibres contained more than one mtDNA deletion species. The level to which each of these mtDNA deletion types had accumulated within the cell was then to be examined using a specialised technique known as single molecule PCR (smPCR), developed specifically to examine samples containing multiple DNA species (Kraytsberg and Khrapko, 2005; Kraytsberg *et al.*, 2009). It would then be possible to

assess whether any pattern existed to determine a deletion type that would be most likely to accumulate to a high level within the cell; e.g. whether larger or smaller deletions tend to accumulate to higher heteroplasmy levels in instances where multiple mtDNA deletions. It would be expected that the largest mtDNA deletions would consistently accumulate to the highest levels of heteroplasmy if clonal expansion is driven by a replicative advantage due to a smaller genome size and shorter replication time; conversely, no relationship would be expected to exist between mtDNA deletion size and dominance in a single cell containing multiple mtDNA deletions if clonal expansion occurs due to random genetic drift.

6.3 Methods

6.3.1 Patient biopsies and mitochondrial enzyme histochemistry

Skeletal muscle samples (*vastus lateralis*) were obtained by open biopsy from 3 patients with multiple mtDNA deletions. The defect resulting in the formation of multiple mtDNA deletions was located in a different nuclear gene in each of these patients, as outlined below in Table 6.29.

Patient	Age at biopsy	Gene defect	COX-deficiency level	Biopsy type
1	80	*POLG* – p.T251I/p.P587L and p.A467T	15% COX-deficient fibres, 3% RRF	PM
2	31	*PEO1* - p.Arg374Gln	10% COX-deficient fibres, 1% RRF	Diagnostic
3	37	*RRM2B* – p.Thr144Ile and p.Gly273Ser	42% COX-deficient fibres, 6% RRF	Diagnostic

Table 6.29 - Histochemical and molecular genetic characterisation of patients with multiple mtDNA deletions in muscle.

COX, cytochrome *c* oxidase; RRF, ragged-red fibres.

Multiple 20µm thick transverse sections were taken from each of the biopsies and mounted onto PEN-membrane slides for subsequent histochemical analysis. Sequential tissue sections were alternately assessed for dual COX-SDH histochemistry or SDH histochemistry alone, as outlined in section *4.3.3*.

6.3.2 Single fibre isolation and DNA extraction

Individual COX-deficient muscle fibres were isolated by laser microdissection from tissue sections assessed only for SDH activity, using tissue sections assessed using the dual COX/SDH histochemical assay as a map of biochemical activity as discussed in section *2.2.2.1*.

Single cell lysis was performed following the protocols outlined in sections *2.2.3.2.2* or *2.2.3.2.3*; the appropriate protocol was selected based upon the laser microdissection system employed for single fibre isolation. DNA was purified from the cell lysate using a QIAamp DNA micro kit, following the standard spin protocol, in order to maximise the efficiency and success rate of single molecule PCR.

6.3.3 Single molecule PCR

Single molecule PCR (smPCR) is a molecular technique which was specifically designed to look at a range of DNA mutations present within a single sample (Kraytsberg and Khrapko, 2005). This variant of 'limiting dilution' long-range PCR was originally developed - following evidence that PCR can be performed using a single DNA template molecule (Jeffreys *et al.*, 1990; Vogelstein and Kinzler, 1999; Mitra *et al.*, 2003) - as a more reliable alternative to conventional PCR fragment cloning and as an alternative to some quantitative techniques, but has been shown to be particularly useful for mtDNA analysis in single cells (Kraytsberg *et al.*, 2009). This was therefore an ideal technique to employ to investigate the presence of multiple mtDNA deletions within a single cell.

Single molecule PCR was used to amplify whole, individual mtDNA molecules from a DNA sample extracted from a single muscle fibre, following the protocol outlined in section *2.2.4.4.1* - *2.2.4.4.4*. The amplification of a single mtDNA molecule in any one reaction removes the product-size bias observed in traditional long-range PCR, allowing mtDNA molecules with different deletion sizes to be amplified with equal efficiency. Running multiple smPCR reactions simultaneously allows the amplification of different mtDNA deletion species in separate reactions. Following an initial round of smPCR, optimal template DNA concentration was calculated based on the Poisson

distribution for a further round of smPCR analysis; it is important to ensure that a maximum of 30% of reactions result in a PCR product in order to ensure that each successful reaction can be confidently said to have resulted from a single template mtDNA molecule, as a 0.3 success rate correspond to an estimate of 0.05 reactions with multiple mtDNA templates.

By running sufficient reactions from a single cell – i.e. running a 96-well plate of smPCR with template DNA from the same single cell added to each reaction – the relative proportions of different deletion types can be calculated. At single molecule level, we would expect approximately 24 successful amplifications from a 96 well plate. Therefore, if a 4kb deletion is observed in 18 wells and a 6kb deletion has been amplified in 6 wells, we would say that these existed in the muscle fibre at a proportion of 0.75 to 0.25 respectively.

6.3.4 Real-time PCR mtDNA deletion level analysis

Following analysis by smPCR, mtDNA deletion heteroplasmy levels were assessed in total DNA extracted from single cells using the multiplex *ND1/ND4* TaqMan PCR assay (He *et al.*, 2002), as outlined in *4.3.6.3*. This allowed for an accurate measure of the total mtDNA deletion heteroplasmy in the cell, though this assay is unable to distinguish between any two mtDNA deletions affecting the *MTND4* region of the genome. However, this is a useful measure when assessed alongside results obtained by smPCR analysis; for example, in a single cell found to contain two mtDNA deletions of 4kb and 6kb at a 3:1 ratio, a total mtDNA deletion heteroplasmy level of 80% would dictate that the 4kb mtDNA deletion is present at a heteroplasmy of 60% within the cell, while the 6kb mtDNA deletion affects 20% of the cell's total mtDNA.

6.3.5 Statistical analysis

All statistical analysis was carried out using GraphPad Prism v.4 statistical software. Relevant tests were chosen based upon data distribution; each data set was analysed using a battery of tests (Kolmogorov-Smirnov, D'Agostino and Pearson, and Shapiro-Wilk normality tests), in order to assess whether or not the data conformed to a Gaussian distribution. This allowed the most appropriate tests to be utilised for each in

order to maximise the power of each statistical test. All data from this study was found to follow a non-parametric distribution, resulting in the use of Mann Whitney tests to compare unpaired datasets, Wilcoxon matched pairs tests to compare paired datasets and Spearman's rho for correlative assessments. All relationships were modelled using simple linear regression.

6.4 Results

6.4.1 Analysis of single COX-deficient fibres by single molecule PCR.

Each COX-deficient muscle fibre extracted from one of the three patient muscle biopsies was lysed in 15µl of lysis buffer optimised for use with smPCR. With 3µl required for accurate total mtDNA heteroplasmy analysis, this left 12µl of single cell lysate available for smPCR analysis; this was diluted in a 1:1 ratio with TE buffer, giving a total of 24µl of stock DNA to work from during smPCR analysis. In each case, an initial long-range PCR assessment was carried out following an identical protocol; this preliminary assessment was carried out with 1µ of template DNA - diluted to a 10^{-1} concentration from stock – per well. With a total of 10µl reaction mix/template DNA per well, this gave a final concentration of 1 x 10^{-2} template DNA per well. 16 wells of a 96-well PCR plate were allocated to each fibre for initial assessment, allowing 6 fibres to be screened per plate – the inclusion of a control sample on each plate reduced this to 5 investigative samples per plate. Typically, only 1 or two fibres would successfully amplify from each plate of 5 samples per initial PCR screen (Figure 6.59).

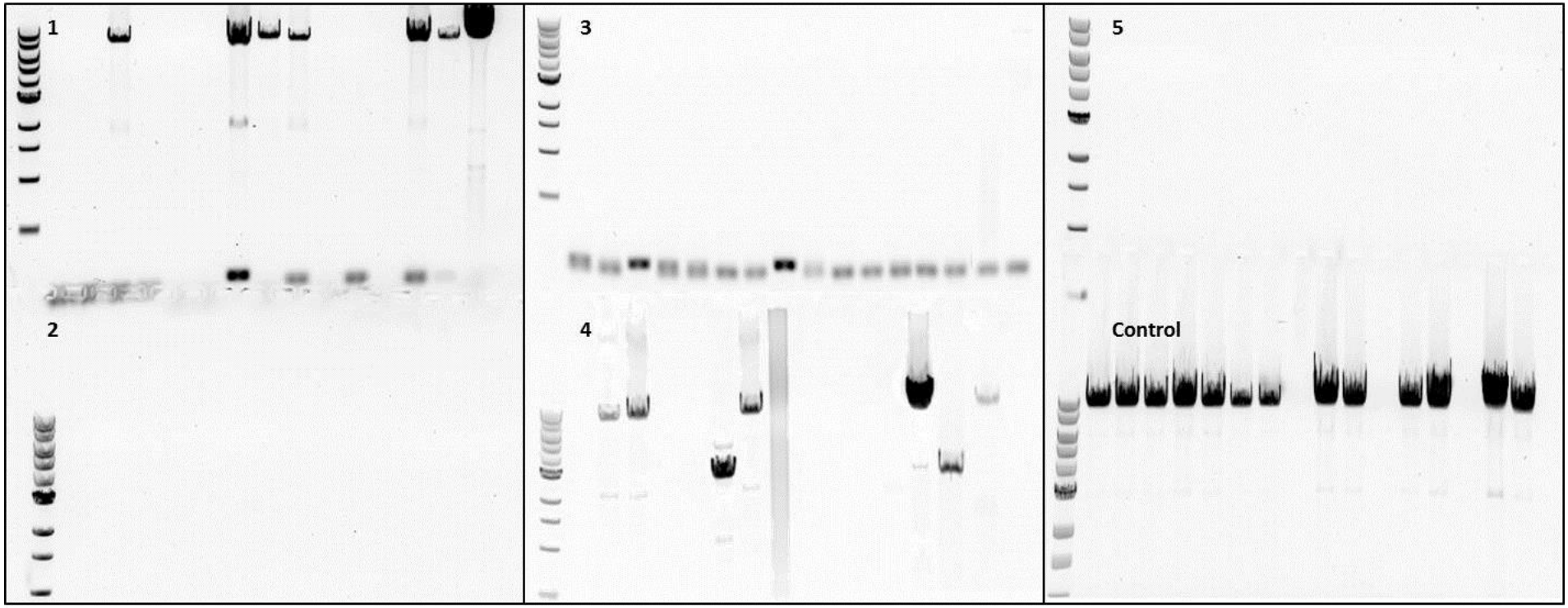

Figure 6.59 – first round smPCR screen of 5 individual COX-deficient muscle fibres.

Successful amplification of 2 fibres from 5 screened for smPCR analysis, plus control sample. 16 wells of smPCR were run for each of these 6 samples; these are represented by 16 gel lanes alongside 1 lane of 1kb DNA ladder for each sample. Each set of 17 lanes is labelled by sample number on this graphic. A wildtype smPCR product of 16kb would be seen to sit above the ladder – product size was measured against the 1kb ladder to determine mtDNA deletion size compared to the expected 16kb wildtype product size.

1 Amplification product visible in 7 wells from a total of 16; observed success rate of 0.43; 'true' success rate of approximately 0.6. Aiming for a 'true' success rate of 0.29. Ratio of observed to desired success of 0.6:0.29, which is expressed as a ratio of approximately 2:1. Optimal template DNA concentration of ($1x10^{-2}$) / 2 = 5 x 10^{-3}µl template DNA per well. **2**. No successful amplification product visible. **3**. No successful amplification product visible. **4**. Amplification product visible in 7 wells from a total of 16; observed success rate of 0.43; 'true' success rate of approximately 0.6. Aiming for a 'true' success rate of 0.29. Ratio of observed to desired success of 0.6:0.29, which is expressed as a ratio of approximately 2:1. Optimal template DNA concentration of ($1x10^{-2}$) / 2 = 5 x 10^{-3}µl template DNA per well. **5.** No successful amplification product visible. **Control**. High success rate of 13 wells from 16 – indicates a successful round of smPCR.

Following this initial PCR screen, the number of wells which result in a successful amplification could be used to calculate an optimal template DNA concentration per reaction, based on the Poisson distribution table (Table 6.30). An example is outlined below:

- Following product analysis by gel electrophoresis, 9/16 wells are found to have resulted in an amplimer during the initial PCR screen of 'fibre x'; this is a success rate of approximately 0.55.
- An observed success rate of 0.55, following the Poisson distribution table, translates to a 'true' success rate of 0.8.
- Aiming for an observed positive success rate of 0.25; this translates to a 'true' success rate of 0.29.
- This gives a ratio of observed to desired success of 0.8:0.29, which is expressed as a ratio of 2.75:1
- Therefore to calculate the optimal template DNA concentration:

$$(1x10^{-2}) / 2.75 = 3.63 \times 10^{-3}\mu l \text{ template DNA per well}$$

- $3.63 \times 10^{-3}\mu l$ template DNA per well in a 96 well plate results in a requirement for $3.49x10^{-2}\mu l$ template DNA from 'fibre x' for optimal smPCR analysis.

In cases where all 16 reactions were successful – i.e. where the observed success was 1.0, and no further information could be obtained – a second round of preliminary smPCR was undertaken, with template DNA concentration reduced tenfold to result in $1 \times 10^{-3}\mu l$ template DNA per reaction. Optimisation of template DNA concentration could then be carried out in any cases where observed success rates lay between 0.05 and 0.95.

Following optimisation of template DNA concentration smPCR was carried out using an entire 96-well PCR plate per fibre, to ensure sufficient amplimers could be observed at a success rate of approximately 0.25 to calculate mtDNA deletion proportions. In cells with one species of clonally expanded mtDNA deletion, the observed deletion band resulting from each successful reaction was an identical size (Figure 6.60). Multiple mtDNA deletions could therefore be detected by observing mtDNA deletion bands of different sizes resulting from independent amplifications from the same cell (Figure 6.61).

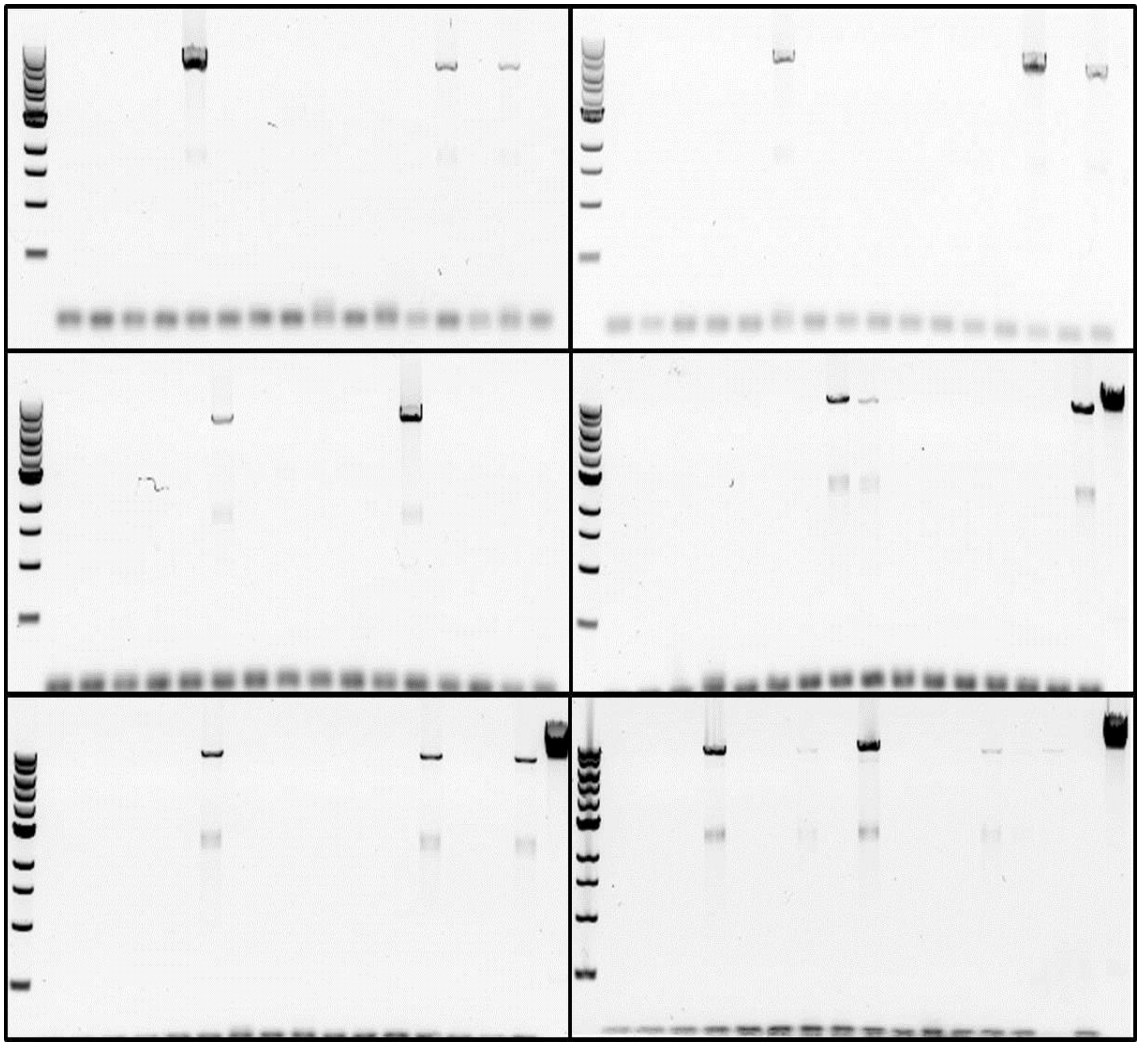

Figure 6.60 – smPCR carried out with an optimised template DNA concentration, for a single fibre containing one mtDNA deletion species.

Each gel depicted above shows 16 lanes of smPCR product – smPCR having been carried out with an optimised template DNA concentration – assessed by gel electrophoresis, for a single fibre containing one mtDNA deletion species, alongside a single lane of 1kb DNA ladder. Following the optimisation of template DNA concentration of fibre 1 (see Figure 6.59) for smPCR, it was confirmed that a single mtDNA deletion of 6kb was present in this fibre. A wildtype product would have been present at 16kb, while all observed PCR products from this sample ran at 10kb. Single molecule level was successfully achieved in the set of gels displayed above, with successful amplification of the mtDNA deletion in 19 wells from a total of 96 (one 96-well PCR plate). This mtDNA deletion was found to exist at 84% heteroplasmy by ND1/ND4 real-time PCR analysis.

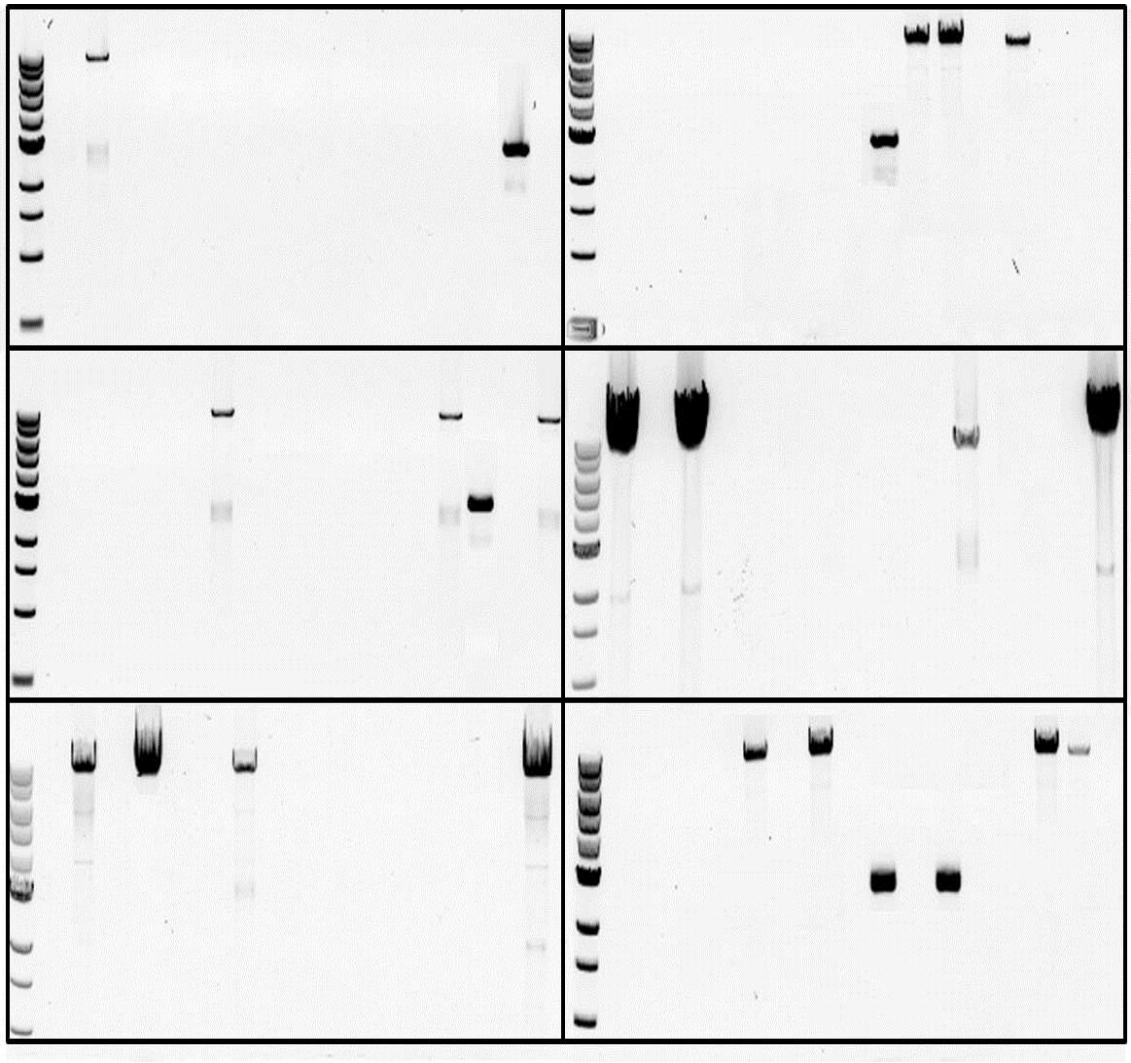

Figure 6.61 - smPCR carried out with an optimised template DNA concentration, for a single fibre containing two mtDNA deletion species.

Each gel depicted above shows 16 lanes of smPCR product – smPCR having been carried out with an optimised template DNA concentration – assessed by gel electrophoresis, for a single fibre containing two mtDNA deletion species, alongside a single lane of 1kb DNA ladder. Following the optimisation of template DNA concentration of fibre 4 (see Figure 6.59) for smPCR, it was confirmed that two mtDNA deletion of 6kb and 10kb were present in this fibre. Single molecule level was successfully achieved in the set of gels displayed above, with an overall successful amplification rate of 24 wells from a total of 96 (a 0.25 success rate from one 96-well PCR plate).
The 6kb and 10kb mtDNA deletions were present in 19 and 5 of the total 24 successful wells respectively; this was calculated to show that these two deletion species existed at relative proportions of 0.79 and 0.21 respectively. An overall cellular heteroplasmy level of 61% was ascertained by ND1/ND4 real-time PCR analysis; the two mtDNA deletion species were therefore estimated to account for approximately 48% (6kb mtDNA deletion species) and 13% (10kb mtDNA deletion species).

Observed level of positive reactions 1-p(0)	True level of positive reactions	Level of doublets p(2)	Level of multiplets 1-p(0)-p(1)
0	-	-	-
0.05	0.05	0	0
0.1	0.11	0	0.01
0.15	0.16	0.01	0.01
0.2	0.22	0.02	0.02
0.25	0.29	0.03	0.03
0.3	0.36	0.04	0.05
0.35	0.43	0.06	0.07
0.4	0.51	0.08	0.09
0.45	0.6	0.1	0.12
0.5	0.69	0.12	0.15
0.55	0.8	0.14	0.19
0.6	0.92	0.17	0.23
0.65	1.05	0.19	0.28
0.7	1.2	0.22	0.34
0.74	1.35	0.24	0.39
0.75	1.39	0.24	0.4
0.8	1.61	0.26	0.48
0.85	1.9	0.27	0.57
0.9	2.3	0.27	0.67
0.925	2.59	0.25	0.73
0.9333	2.71	0.24	0.75
0.95	3	0.22	0.8

Table 6.30 – Poisson distribution table.

P(x) = probability of a well resulting in (x) successful amplifications.
This distribution was employed to calculate the optimal template DNA concentration per smPCR reaction. An observed success rate of less than 0.3 was targeted for smPCR, as the probability of a single reaction resulting in amplification from more than one template copy of mtDNA became insignificant ($P < 0.05$) below this level.

6.4.2 Assessing the presence of multiple mtDNA deletions in single skeletal muscle fibres.

A total of 70 single, COX-deficient fibres were successfully isolated from 3 different patient muscle biopsies and assessed for total mtDNA deletion heteroplasmy level – using the *MTND1/MTND4* real-time PCR assay – and the presence of multiple mtDNA deletions using smPCR. In all 70 cases smPCR was carried out over 96 reactions, using an individually optimised level of mtDNA to ensure an appropriate success rate of approximately 25% (indicating that each successful amplification originates from a single template mtDNA copy, see *6.3.3,* page 238). While only one mtDNA deletion species was detected in many cases, 29 fibres – 41% of the assessed sample group – were found to contain mtDNA deletions of different sizes. This ratio was found to be maintained in sample groups from each patient biopsy; 7 of 17 COX-deficient fibres assessed from patient biopsy 1 (41%) (Table 6.31) were found to contain multiple mtDNA deletions, 10 of 26 assessed fibres from patient biopsy 2 (38%) contained multiple observed mtDNA deletions (Table 6.32), and multiple mtDNA deletion species were amplified from 12 of 27 fibres isolated from patient biopsy 3 (44%) (Table 6.33).

mtDNA deletion size was determined from amplimer size during gel electrophoresis for all 99 mtDNA deletions detected by smPCR (41 from fibres with single and 58 from fibres with multiple clonally expanded mtDNA deletions), this method having been validated by sequencing analysis in Chapter 3 (see section *3.4.3*). No difference was found to exist between mtDNA deletion sizes observed in fibres containing single or multiple clonally expanded mtDNA deletions (mean = 5.78 ± 1.51kb and 6.32 ± 1.55kb respectively, P = 0.1273). The range of mtDNA deletion sizes observed in these two fibre groups was also found to be consistent; mtDNA deletion sizes ranged from 2kb to 10 kb in single mtDNA deletion fibres and 4 to 10kb in multiple mtDNA deletion fibres, with all mtDNA deletions in the 2nd and 3rd quartiles of the data falling between 5 and 7 kb in both datasets (Figure 6.62).

The 58 mtDNA deletions observed in multiple mtDNA deletion fibres were also split into 2 separate groups – the larger and smaller mtDNA deletion observed in each individual fibre - for mtDNA deletion size analysis. For example, where two fibres each contain two mtDNA deletions – fibre 1; 3kb and 5kb, fibre 2; 6kb and 8kb – the 3kb and

6kb mtDNA deletions would be classified as the 'smallest' mtDNA deletions present in each fibre, while the 5kb and 8kb mtDNA deletions would be classified as the 'largest' mtDNA deletions present in each fibre. This is despite the smallest mtDNA deletion present in fibre 2 being larger than the largest mtDNA deletion in fibre 1 in this example, as the 'smallest' and 'largest' mtDNA deletion labels refer to the mtDNA deletions present in each individual fibre. Though these groups were significantly different in terms of size (mean = 7.31 ± 1.43kb and 5.36 ± 0.99kb respectively, $P < 0.0001$), it was interesting to observe a large degree of overlap between these two groups. All of the 'largest mtDNA deletion' group were 5kb or above, 89% of the 'smallest mtDNA deletion' group also fit this criterion. Similarly, all of the 'smallest mtDNA deletion' group were 8kb or smaller in size, while 79% of the 'largest mtDNA deletion' group fit into this size bracket (Figure 6.62). This overlap in data is indicative of a number of scenarios where the smaller mtDNA deletion in one fibre harbouring multiple clonally expanded mtDNA deletion is larger than the largest mtDNA deletion in another.

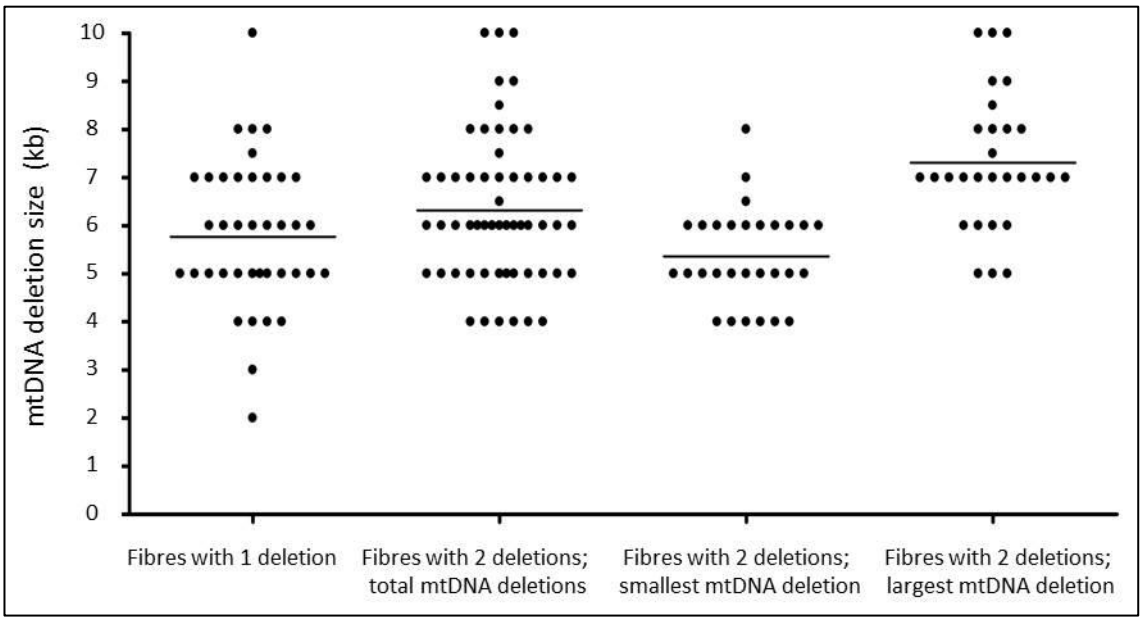

Figure 6.62 - mtDNA deletion sizes in all assessed fibre categories.

COX-deficient muscle fibres from which a single mtDNA deletion was detected had an average observed mtDNA deletion size of 5.78 ± 1.51kb; this was not found to differ significantly from the average mtDNA deletion size of 6.32 ± 1.55kb observed in fibres in which multiple clonally expanded mtDNA deletions were detected ($P = 0.1273$). As would be expected, the smaller of two mtDNA deletions present in a single fibre tend to be lower than average (mean 5.36 ± 0.99kb) while the larger mtDNA deletion present in a fibre with multiple deletions tends to be larger than average (mean 7.31 ± 1.34kb).

Table 6.31 – COX-deficient fibres from patient biopsy 1 assessed by real-time PCR heteroplasmy analysis and smPCR.

Heteroplasmy level was determined using the *MTND1/MTND4* TaqMan assay; where this is recorded as 'low level', it has been detected with an unreliable reading <10% heteroplasmy. Deletion numbers per fibre were assessed by smPCR. mtDNA deletion size was assessed by long-range PCR, as validated in Chapter 3 (see *3.4.3*). Where multiple mtDNA deletions were observed, the largest is recorded as 'Deletion 1' and the smallest is recorded as 'Deletion 2'. Deletion proportion was calculated by smPCR – i.e. if 2 deletions were detected in a 3:1 ratio, they would have a relative proportion of 0.75 and 0.25 – while deletion heteroplasmy was calculated by combining total mtDNA deletion heteroplasmy with deletion proportion.

Patient 1 (*POLG*, p.T251I/p.P587L and p.A467T)												
Fibre	Heteroplasmy level (%)	Deletions	Deletion 1			Deletion 2			wildtype mtDNA (%)	Difference in deletion size (kb)	Prevalent deletion	Difference in heteroplasmy (%)
			Size (kb)	Proportion	Heteroplasmy (%)	Size (kb)	Proportion	Heteroplasmy (%)				
1	14	1	4	1	14	n/a			86	n/a		
2	84	1	6	1	84	n/a			16	n/a		
3	91	1	7	1	91	n/a			9	n/a		
4	Low level	1	7	1	Low level	n/a			Undetermined	n/a		
5	82	2	5	0.75	61.5	8	0.25	20.5	18	3	5kb – smallest	41
6	95	1	5	1	95	n/a			5	n/a		
7	62	2	6	0.73	45.26	7	0.27	16.74	38	1	6kb – smallest	28.52
8	94	1	6	1	94	n/a			6	n/a		
9	67	2	6	0.37	24.79	7	0.63	42.21	33	1	7kb – largest	17.42
10	92	1	7.5	1	92	n/a			8	n/a		
11	57	2	6	0.17	9.69	8.5	0.83	47.31	43	2.5	8.5kb – largest	37.62
12	43	1	6	1	43	n/a			57	n/a		
13	38	2	6.5	0.43	16.34	7.5	0.57	21.66	62	1	7.5kb – largest	5.32
14	76	2	6	0.57	43.32	8	0.43	32.68	24	2	6kb – smallest	10.64
15	89	1	6	1	89	n/a			11	n/a		
16	Low level	1	2	1	Low level	n/a			Undetermined	n/a		
17	23	2	5	0.53	12.19	7	0.47	10.81	77	2	5kb – smallest	1.38

Table 6.32 – COX-deficient fibres from patient biopsy 2 assessed by real-time PCR heteroplasmy analysis and smPCR.

Heteroplasmy level was determined using the *MTND1/MTND4* TaqMan assay; where this is recorded as 'low level', it has been detected with an unreliable reading <10% heteroplasmy. Deletion numbers per fibre were assessed by smPCR. mtDNA deletion size was assessed by long-range PCR, as validated in Chapter 3 (see *3.4.3*). Where multiple mtDNA deletions were observed, the smallest is recorded as 'Deletion 1' and the largest is recorded as 'Deletion 2'. Deletion proportion was calculated by smPCR – i.e. if 2 deletions were detected in a 3:1 ratio, they would have a relative proportion of 0.75 and 0.25 – while deletion heteroplasmy was calculated by combining total mtDNA deletion heteroplasmy with deletion proportion.

Patient 2 (*PEO1*, p.Arg374Gln)

Fibre	Heteroplasmy level (%)	Deletions	Deletion 1			Deletion 2			wildtype mtDNA (%)	Difference in deletion size (kb)	Prevalent deletion	Difference in heteroplasmy (%)
			Size (kb)	Proportion	Heteroplasmy (%)	Size (kb)	Proportion	Heteroplasmy (%)				
1	72	2	4	0.23	16.56	5kb	0.77	55.44	28	1	5kb - largest	38.88
2	32	1	5	1	32	n/a			68	n/a	n/a	
3	73	2	6	0.69	50.37	7kb	0.31	22.63	27	1	6kb – smallest	27.74
4	85	2	5	0.86	73.1	7kb	0.14	11.9	15	2	5kb – smallest	61.2
5	69	1	7	1	69	n/a			31	n/a	n/a	
6	29	1	5	1	29	n/a			71	n/a	n/a	
7	84	2	4	0.28	23.52	5kb	0.72	60.48	16	1	5kb – largest	36.96
8	98	2	5	0.25	24.5	7kb	0.75	73.5	2	2	7kb – largest	49
9	83	1	7	1	83	n/a			17	n/a	n/a	
10	Low level	1	5	1	Low level	n/a			Undetermined	n/a	n/a	
11	28	1	5	1	28	n/a			72	n/a	n/a	
12	83	1	7	1	83	n/a			17	n/a	n/a	
13	82	2	6	0.42	34.44	7kb	0.58	47.56	18	1	7kb – largest	13.12
14	90	1	5	1	90	n/a			10	n/a	n/a	
15	30	1	6	1	30	n/a			70	n/a	n/a	
16	43	1	7	1	43	n/a			57	n/a	n/a	
17	81	1	8	1	81	n/a			19	n/a	n/a	
18	Low level	1	6	1	Low level	n/a			Undetermined	n/a	n/a	
19	47	2	5	0.67	31.49	10kb	0.33	15.51	53	5	5kb – smallest	15.98
20	86	1	6	1	86	n/a			14	n/a	n/a	
21	81	1	5	1	81	n/a			19	n/a	n/a	
22	95	1	5	1	95	n/a			5	n/a	n/a	
23	95	2	6	0.8	76	9kb	0.2	19	5	3	6kb – smallest	57
24	89	1	5	1	89	n/a			11	n/a	n/a	
25	61	2	6	0.79	48.19	10kb	0.21	12.81	39	4	6kb - smallest	35.38
26	77	2	6	0.86	66.22	10kb	0.14	10.78	23	4	6kb - smallest	55.44

Table 6.33 - COX-–deficient fibres from patient biopsy 2 assessed by real-time PCR heteroplasmy analysis and smPCR.

Heteroplasmy level was determined using the *MTND1/MTND4* TaqMan assay; where this is recorded as 'low level', it has been detected with an unreliable reading <10% heteroplasmy. Deletion numbers per fibre were assessed by smPCR. mtDNA deletion size was assessed by long-range PCR, as validated in Chapter 3 (see *3.4.3*). Where multiple mtDNA deletions were observed, the smallest is recorded as 'Deletion 1' and the smallest is recorded as 'Deletion 2'. Deletion proportion was calculated by smPCR – i.e. if 2 deletions were detected in a 3:1 ratio, they would have a relative proportion of 0.75 and 0.25 – while deletion heteroplasmy was calculated by combining total mtDNA deletion heteroplasmy with deletion proportion

Patient 3 (*RRMB2*, p.Thr144Ile and p.Gly273Ser)												
Fibre	Heteroplasmy level (%)	Deletions	Deletion 1			Deletion 2			wildtype mtDNA (%)	Difference in deletion size (kb)	Prevalent deletion	Difference in heteroplasmy (%)
			Size (kb)	Proportion	Heteroplasmy (%)	Size (kb)	Proportion	Heteroplasmy (%)				
1	17.00	2	4	0.6	10.2	5	0.4	9.8	83	1	4kb - smallest	3.4
2	67.00	2	8	0.2	13.4	9	0.8	53.6	33	1	9kb - largest	40.2
3	low level*	1	5	1	Low level	n/a			Undetermined	n/a		
4	low level*	1	4	1	Low level	n/a			Undetermined	n/a		
5	37.00	1	5	1	37	n/a			63	n/a		
6	59.00	1	3	1	59	n/a			41	n/a		
7	97.00	2	6	0.88	85.36	8	0.12	11.64	3	2	6kb – smallest	73.72
8	62.00	1	6	1	62	n/a			38	n/a		
9	96.00	1	5	1	96	n/a			4	n/a		
10	98.00	1	8	1	98	n/a			2	n/a		
11	37.00	2	5	0.33	12.21	6	0.67	24.79	63	1	6kb – largest	12.58
12	96.00	1	7	1	96	n/a			4	n/a		
13	80.00	1	7	1	80	n/a			20	n/a		
14	37.00	1	5	1	37	n/a			63	n/a		
15	59.00	2	4	0.57	33.63	6	0.43	25.37	41	2	4kb – smallest	8.26
16	low level*	1	4	1	Low level	n/a			Undetermined	n/a		
17	61.00	2	5	0.75	45.75	7	0.25	25	39	2	5kb – smallest	20.75
18	58.00	2	4	0.47	27.26	8	0.53	30.74	42	4	8kb – largest	3.48
19	46.00	1	5	1	46	n/a			54	n/a		
20	70.00	1	10	1	70	n/a			30	n/a		
21	98.00	2	5	0.29	28.42	7	0.71	69.58	2	2	7kb – largest	41.16
22	96.00	1	8	1	96	n/a			4	n/a		
23	80.00	2	4	0.27	21.6	6	0.73	58.4	20	2	6kb – largest	36.8
24	96.00	2	5	0.23	22.08	7	0.77	73.92	4	2	7kb – largest	51.84
25	98.00	1	4	1	98	n/a			2	n/a		
26	98.00	2	6	0.51	49.98	7	0.49	48.02	2	1	6kb - smallest	1.96
27	99.00	2	5	0.54	53.46	6	0.46	45.54	1	1	5kb - smallest	7.92

6.4.3 mtDNA deletion heteroplasmy assessments in COX-deficient muscle fibre with single or multiple mtDNA deletions.

Total mtDNA deletion heteroplasmy was assessed in each single COX-deficient fibre using the *MTND1/MTND4* TaqMan assay; this determined the total ratio of wildtype to deleted mtDNA within each fibre, regardless of the number of mtDNA deletions contributing to the total level of heteroplasmy. In fibres containing two clonally expanded mtDNA deletions, the heteroplasmy level of each mtDNA deletion species was calculated from the total heteroplasmy level and mtDNA deletion proportion. For example, in a single cell found to contain two mtDNA deletions of 4kb and 6kb at a 3:1 ratio, a total mtDNA deletion heteroplasmy level of 80% would dictate that the 4kb mtDNA deletion is present at a heteroplasmy of 60% within the cell, while the 6kb mtDNA deletion affects 20% of the cell's total mtDNA.

Single cell mtDNA deletion heteroplasmy levels in the total dataset covered a wide range – from a minimum of 14% to a maximum of 99% total cellular mtDNA content. It is possible that, a number of fibres may have mtDNA deletion heteroplasmy levels lower than this; the limitations of the assay employed to measure heteroplasmy mean that very low heteroplasmy levels cannot be accurately recorded. In the 7 cases where mtDNA deletion levels were measured at 10% or below, total mtDNA deletion heteroplasmy level was recorded as 'low level' (Table 6.31, Table 6.32, Table 6.33) – these fibres were not included in any further analyses involving mtDNA deletion heteroplasmy levels. Mean mtDNA deletion level was found to be 70.51 ± 24.45%, though the median mtDNA deletion was higher at 80% (25^{th} percentile 27% heteroplasmy, 75^{th} percentile 92% heteroplasmy).

Following this data overview, the total dataset was split into two categories – mtDNA deletion heteroplasmy levels in fibres with one and fibres with two observed clonally expanded mtDNA deletions. Both of these categories were found to be representative of the total dataset. mtDNA deletion heteroplasmy ranged from 14 to 98% with a mean mtDNA deletion level of 70.47 ± 26.18% in fibres containing a single clonally expanded mtDNA deletion, while fibres containing multiple clonally expanded mtDNA deletions had a mean mtDNA deletion level of 70.55 ± 22.72% with a range from 17 to 99% total mtDNA deletion heteroplasmy (Figure 6.63). Neither of these groups was

found to differ significantly from the total dataset (Mann Whitney test at 95% confidence, P = 0.9277 and 0.9197 respectively), and no significant difference was found to exist in terms of total mtDNA deletion heteroplasmy between fibres containing one or two clonally expanded mtDNA deletions (Mann Whitney test at 95% confidence, P = 0.8686) (Figure 6.63).

Next, mtDNA deletion heteroplasmy levels were separately assessed for the larger and smaller mtDNA deletions present in single fibres with two observed clonally expanded mtDNA deletions. Interestingly, these two groups of data were found to be very similar. The smaller of the two mtDNA deletions present in each of these cells covered an mtDNA deletion heteroplasmy range from 9.69 to 85.36 %, with a mean heteroplasmy level of 36.58 ± 21.38%, while the larger of the two mtDNA deletions present in each of these cells covered an mtDNA deletion heteroplasmy range from 6.80 to 73.92%, with a mean heteroplasmy level of 34.31 ± 20.83%. No significant difference was found between these two groups of data (Wilcoxon matched pairs test at 95% confidence, P = 0.8246) (Figure 6.63).

The similarities in mtDNA deletion heteroplasmy levels between the smallest and largest mtDNA deletions from each deletion pair observed in single cells suggested that it was unlikely that any correlation would exist between mtDNA deletion size and heteroplasmy level. This was first tested in the total dataset of 92 mtDNA deletions with complete deletion size and heteroplasmy data available. While no trend appeared to exist between mtDNA deletion size and heteroplasmy level following analysis by linear regression, correlation analysis using Spearman's rho was carried out to confirm this. No relationship was identified to exist between these two variables (P = 0.9442), confirming that larger deletion sizes are not linked to higher mtDNA deletion heteroplasmy levels in single cells (Figure 6.64A).

This correlation analysis was carried out in the same manner for the individual datasets from each of the 3 patients (Figure 6.64 B-D). Though each of the three cases appeared to display a different data trend by linear regression (neutral in patient 1, negative in patient 2 and positive in patient 3), no trend between mtDNA deletion size and heteroplasmy level was shown to be significant following Spearman's rank correlation

(for patients 1, 2 and 3, P = 0.8391, 0.2472 and 0.1149 respectively). The dataset available for each patient was therefore in keeping with the total dataset.

Similarly, no correlation was found to exist between mtDNA deletion size and heteroplasmy level where data is independently assessed for mtDNA deletions where a single or multiple mtDNA deletions have clonally expanded within a single fibre (Figure 6.65A). This is true for single fibres containing only a single clonally expanded mtDNA deletion (P = 0.1330), but is particularly noteworthy where two mtDNA deletions have clonally expanded within a single fibre (P = 0.4184) (Figure 6.65B), suggesting that the competition between two mtDNA deletions may not be affected by different mtDNA deletion sizes.

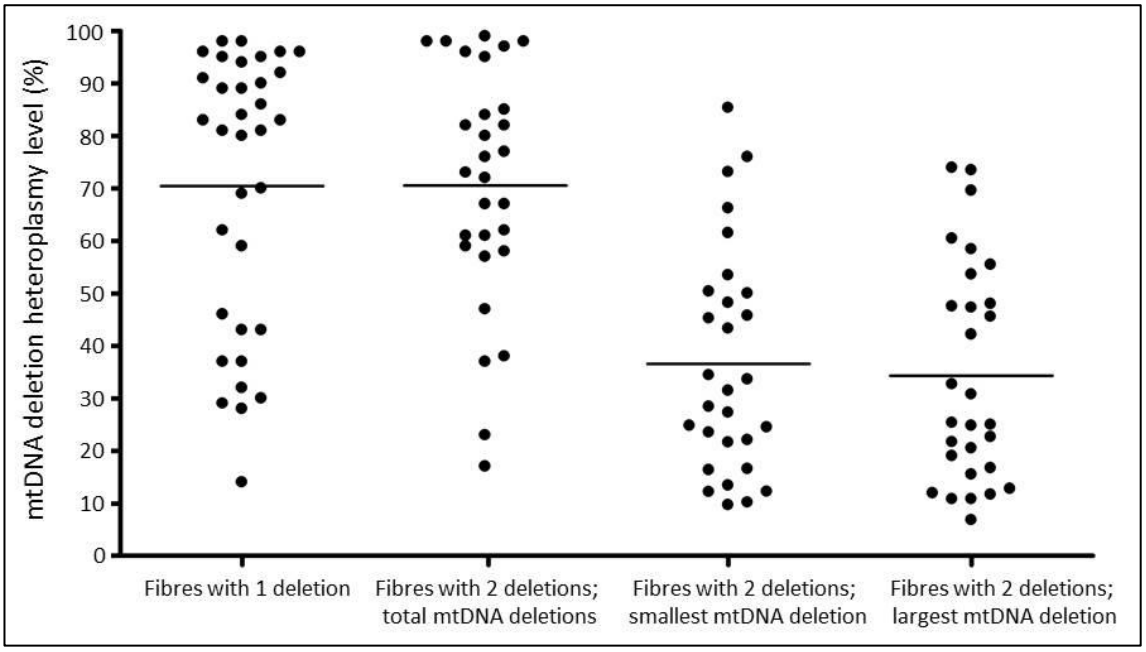

Figure 6.63 – mtDNA deletion heteroplasmy levels in all assessed fibres.

Muscle fibres with only 1 observed mtDNA deletion had an average mtDNA deletion heteroplasmy level of 70.47% (±26.18%); this was not found to vary significantly from the 70.55% (±22.72) average mtDNA deletion heteroplasmy level observed in fibres containing 2 mtDNA deletion species (Mann-Whitney u-test, P =0.8686). mtDNA deletion heteroplasmy levels were also differentially assessed in each fibre where multiple clonally expanded mtDNA deletions were observed; no significant difference was found to exist between the average deletion level for the smaller (36.58 ± 21.38%) and larger (34.31 ± 20.83%) mtDNA deletions present in these cells (Mann-Whitney u-test, P =0.6576). mtDNA deletion heteroplasmy levels were lower for both the larger and smaller mtDNA deletion size compared to the total mtDNA deletion heteroplasmy levels detected in single fibres harbouring either one or two mtDNA deletions (P < 0.0001 in all cases).

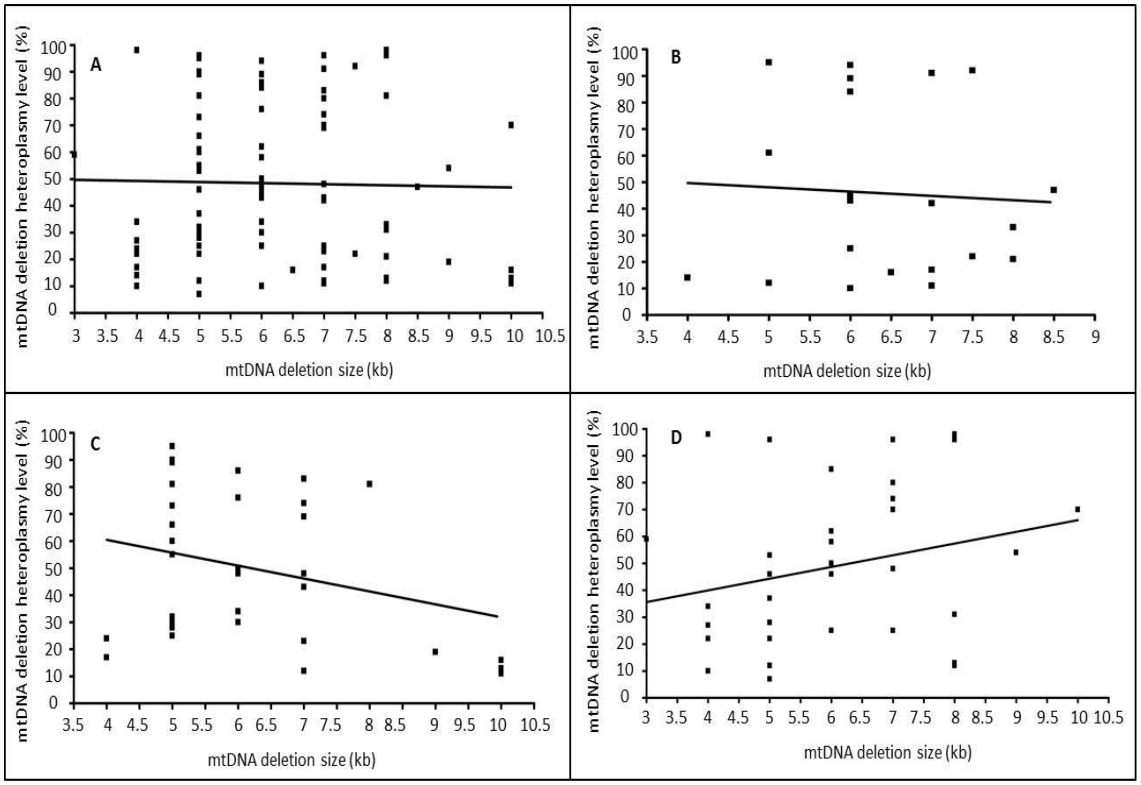

Figure 6.64 – Correlation of mtDNA deletion level and heteroplasmy level, with linear regression.

Linear regression carried out on the whole dataset of mtDNA deletion size, as determined by long-range smPCR, and heteroplasmy level, as determined by MT*ND1/MTND4* quantitative PCR analysis, revealed no relationship no exist between these two variables (P = 0.8400). This neutral relationship was further confirmed by Spearman's rank correlation analysis (0.9442).

Correlation analysis was carried out in the same manner for the individual datasets from each of the 3 patients (**B – D** representing patients 1 – 3 respectively). While linear regression indicated a neutral relationship between mtDNA deletion size and heteroplasmy level in patient 1, a potentially negative relationship was highlighted in patient 2 (**C**) and a potentially positive relationship in patient 3 (**D**). Further assessment by Spearman's rank correlation analysis showed none of these relationships to be significant (P = 0.8391, 0.2472 and 0.1149 respectively), in keeping with the neutral relationship in the total dataset.

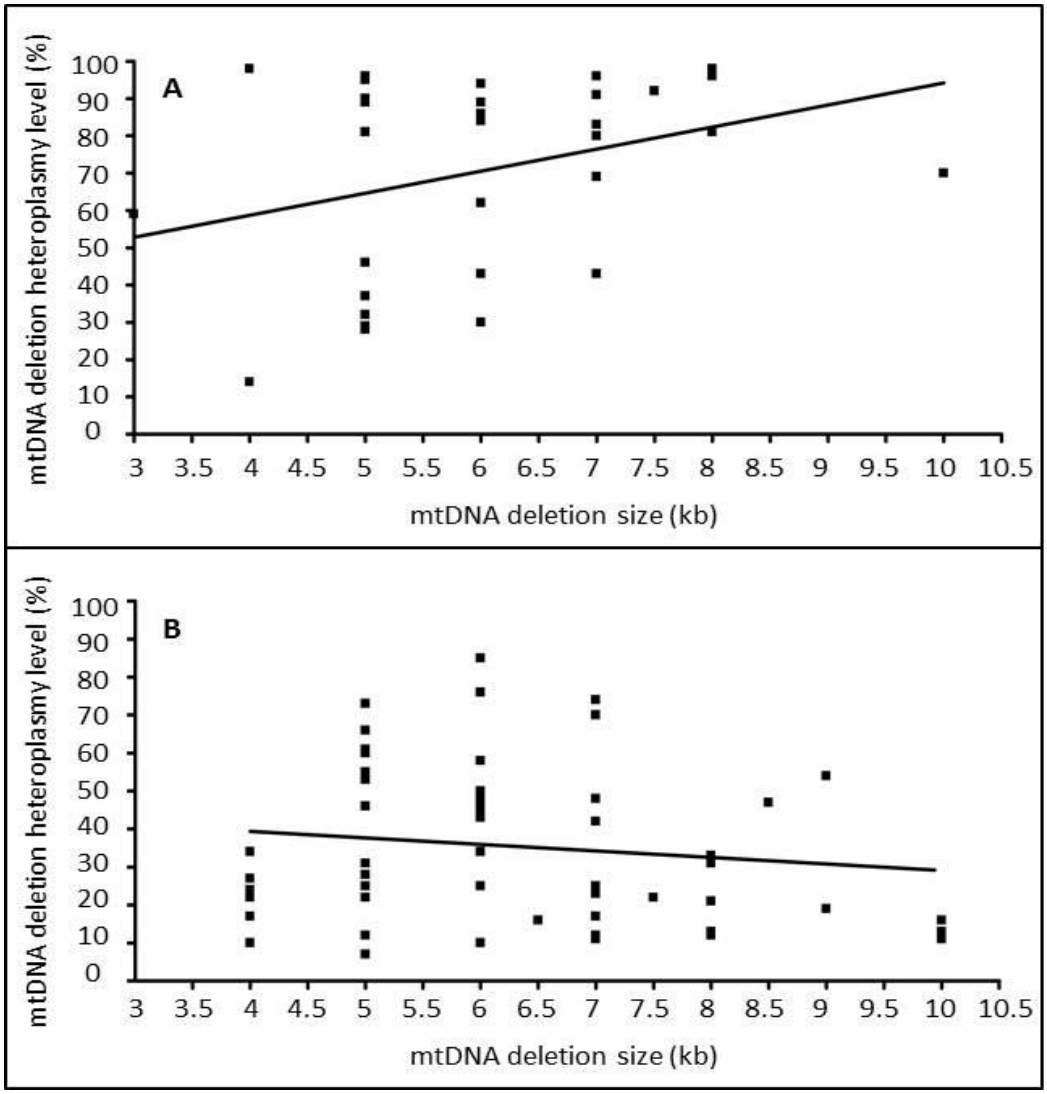

Figure 6.65 – Correlating mtDNA deletion heteroplasmy and deletion size in fibres containing single and multiple clonally expanded mtDNA deletions.

Correlation analysis between mtDNA deletion size, as determined by long-range smPCR, and heteroplasmy level, as determined by MT*ND1/MTND4* quantitative PCR analysis, revealed a no significant relationship to exist between these two factors in either fibres containing single (**A**) or multiple (**B**) clonally expanded mtDNA deletions. Though a positive trend was found to exist by linear regression between these two factors in single mtDNA deletion fibres, this was found not to be significant following Spearman's rank correlation analysis (P = 0.1330). Similarly, the slight negative trend found to exist between these two measures in multiple mtDNA deletion fibres by linear regression was found not to be significant by Spearman's rank correlation analysis (P = 0.4184). Single and multiple mtDNA deletion fibres were therefore independently representative of the total dataset (Figure 6.64).

6.4.4 Do larger mtDNA deletions accumulate to a higher proportion of heteroplasmy in multiple mtDNA deletion fibres?

An initial examination of the relative proportions of mtDNA deletion species in fibres containing more than one clonally expanded mtDNA deletion (Table 6.34) did not reveal any clear trend for either the larger or smaller of two mtDNA deletions present to reach a higher level of heteroplasmy. From a total of 29 single fibres found to contain two clonally expanded mtDNA deletion species, the larger of two mtDNA deletions was found to accumulate to the highest heteroplasmy level in 13 cases (45%), while the smaller of the two mtDNA deletions was found to have reached the higher level of heteroplasmy in 16 cases (55%) (Table 6.34). The mtDNA deletion heteroplasmy level of the most prevalent mtDNA deletion was assessed in these two groups of fibres (Figure 6.66). Where the smaller mtDNA deletion of two was found at a higher proportion of total deletion load, heteroplasmy for this mtDNA deletion was found to range from 10.2 to 85.4% with a mean heteroplasmy level of 49.1 ± 20.9% (N = 13). Similar statistics were found to describe the larger mtDNA deletion species in multiple mtDNA deletion fibres where the larger mtDNA deletion makes up the highest proportion of the total mtDNA deletion load; heteroplasmy ranged from 21.7 to 73.9% with a mean heteroplasmy level of 50.7 ± 17.3%. No significant difference was found to exist between these two groups by unpaired t-test (95% confidence, P = 0.8290).

Following this assessment of the mtDNA deletion heteroplasmy levels for the most prevalent mtDNA deletion in each multiple deletion fibre, the relative proportion of each of these mtDNA deletions was also examined. This was to ensure that the effects of total mtDNA deletion heteroplasmy for each assessed fibre had not skewed the data. The possibility that this could occur can be demonstrated by comparing two separate fibres, both containing two mtDNA deletions of 4kb and 6kb but at different levels of total mtDNA deletion heteroplasmy. Fibre 1 has a total mtDNA deletion heteroplasmy level of 98%, with two mtDNA deletions present at relative proportions of 0.45 (4kb) and 0.55 (6kb); these two mtDNA deletions would be present at heteroplasmy levels of 44% and 54% respectively. In comparison, fibre 2 has a total mtDNA deletion heteroplasmy level of 30%, with two mtDNA deletions present at relative proportions of 0.8 (4kb) and 0.2 (6kb); these two mtDNA deletions would be present at heteroplasmy levels of 24% and 6% respectively. The effect of total cellular

heteroplasmy therefore means that the 4kb mtDNA deletion present at a proportion of 0.8 in fibre 2 appears to be present at a lower level than the 6kb mtDNA deletion at a proportion of 0.55 in fibre 1. As for the mtDNA deletion heteroplasmy analysis, data was assessed for the most prevalent mtDNA deletion in each multiple mtDNA deletion fibre – this was the larger of two mtDNA deletions in 13 cases and the smaller of two mtDNA deletions in 16 cases. In instances where the smaller of two mtDNA deletions was found to be most prevalent, a range of relative mtDNA deletion proportion from 0.51 to 0.88 was observed, with a mean proportion of 0.69 ± 0.12 (N = 13). A similar range of relative mtDNA deletion proportion was observed in instances where the larger of two mtDNA deletions was found to be the most prevalent – from 0.53 to 0.83, with a mean mtDNA deletion proportion of 0.70 ±0.09 (N = 16) (Figure 6.66). No significant difference was found to exist between these two groups by unpaired t-test (95% confidence, P = 0.9410). It therefore seems clear that relative mtDNA deletion size does not affect the level to which an mtDNA deletion is able to accumulate within a single fibre.

Table 6.34 – Compiled data from all COX-deficient fibres containing multiple clonally expanded mtDNA deletions from all 3 patients.

Fibre number is expressed as 'N-X', where N refers to the appropriate patient number (1 – 3) and X refers to the fibre number cited in Tables 3 – 5. Heteroplasmy level was determined using the *MTND1/MTND4* TaqMan assay. Deletion numbers per fibre were assessed by smPCR. mtDNA deletion size was assessed by long-range PCR, as validated in Chapter 3 (see *3.4.3*). Where multiple mtDNA deletions were observed, the smallest is recorded as 'Deletion 1' and the smallest is recorded as 'Deletion 2'. Deletion proportion was calculated by smPCR – i.e. if 2 deletions were detected in a 3:1 ratio, they would have a relative proportion of 0.75 and 0.25 – while deletion heteroplasmy was calculated by combining total mtDNA

Fibre	Heteroplasmy level (%)	Deletions	Deletion 1			Deletion 2			wildtype mtDNA (%)	Difference in deletion size (kb)	Prevalent deletion	Difference in heteroplasmy (%)
			Size (kb)	Proportion	Heteroplasmy (%)	Size (kb)	Proportion	Heteroplasmy (%)				
1-5	82	2	5	0.75	61.5	8	0.25	20.5	18	3	5kb – smallest	41
1-7	62	2	6	0.73	45.26	7	0.27	16.74	38	1	6kb – smallest	28.52
1-9	67	2	6	0.37	24.79	7	0.63	42.21	33	1	7kb – largest	17.42
1-11	57	2	6	0.17	9.69	8.5	0.83	47.31	43	2.5	8.5kb – largest	37.62
1-13	38	2	6.5	0.43	16.34	7.5	0.57	21.66	62	1	7.5kb – largest	5.32
1-14	76	2	6	0.57	43.32	8	0.43	32.68	24	2	6kb – smallest	10.64
1-17	23	2	5	0.53	12.19	7	0.47	10.81	77	2	5kb – smallest	1.38
2-1	72	2	4	0.23	16.56	5kb	0.77	55.44	28	1	5kb - largest	38.88
2-3	73	2	6	0.69	50.37	7kb	0.31	22.63	27	1	6kb – smallest	27.74
2-4	85	2	5	0.86	73.1	7kb	0.14	11.9	15	2	5kb – smallest	61.2
2-7	84	2	4	0.28	23.52	5kb	0.72	60.48	16	1	5kb – largest	36.96
2-8	98	2	5	0.25	24.5	7kb	0.75	73.5	2	2	7kb – largest	49
2-13	82	2	6	0.42	34.44	7kb	0.58	47.56	18	1	7kb – largest	13.12
2-19	47	2	5	0.67	31.49	10kb	0.33	15.51	53	5	5kb – smallest	15.98
2-23	95	2	6	0.8	76	9kb	0.2	19	5	3	6kb – smallest	57
2-25	61	2	6	0.79	48.19	10kb	0.21	12.81	39	4	6kb - smallest	35.38
2-26	77	2	6	0.86	66.22	10kb	0.14	10.78	23	4	6kb - smallest	55.44
3-1	17.00	2	4	0.6	10.2	5	0.4	9.8	83	1	4kb - smallest	3.4
3-2	67.00	2	8	0.2	13.4	9	0.8	53.6	33	1	9kb - largest	40.2
3-7	97.00	2	6	0.88	85.36	8	0.12	11.64	3	2	6kb – smallest	73.72
3-11	37.00	2	5	0.33	12.21	6	0.67	24.79	63	1	6kb – largest	12.58
3-15	59.00	2	4	0.57	33.63	6	0.43	25.37	41	2	4kb – smallest	8.26
3-17	61.00	2	5	0.75	45.75	7	0.25	25	39	2	5kb – smallest	20.75
3-18	58.00	2	4	0.47	27.26	8	0.53	30.74	42	4	8kb – largest	3.48
3-21	98.00	2	5	0.29	28.42	7	0.71	69.58	2	2	7kb – largest	41.16
3-23	80.00	2	4	0.27	21.6	6	0.73	58.4	20	2	6kb – largest	36.8
3-24	96.00	2	5	0.23	22.08	7	0.77	73.92	4	2	7kb – largest	51.84
3-26	98.00	2	6	0.51	49.98	7	0.49	48.02	2	1	6kb - smallest	1.96
3-27	99.00	2	5	0.54	53.46	6	0.46	45.54	1	1	5kb - smallest	7.92

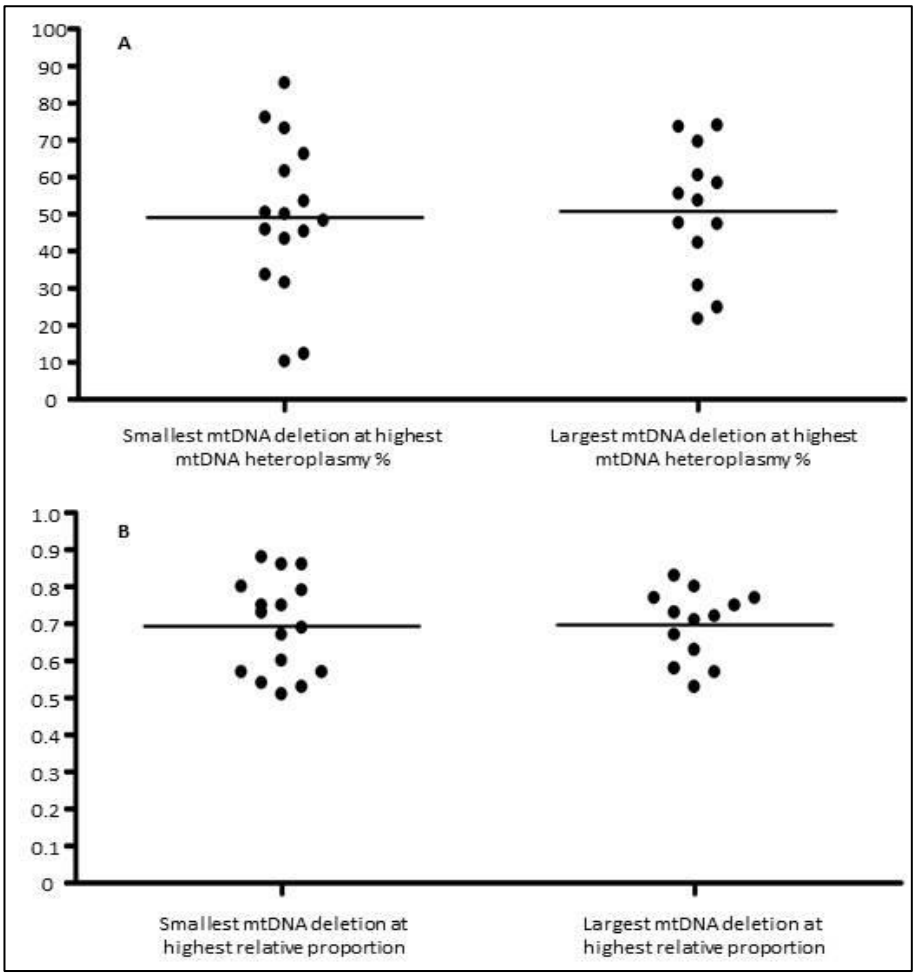

Figure 6.66 - Representation of the mtDNA deletion heteroplasmy level and relative mtDNA deletion proportion reached by the most common mtDNA deletion species in each fibre containing multiple clonally expanded mtDNA deletions.

A – The mtDNA deletion heteroplasmy level of the most prevalent deletion is depicted for each fibre containing multiple clonally expanded mtDNA deletions (N =29). This data has been split into two categories, dependent on whether the most prevalent deletion is the largest or smallest of the two mtDNA deletions present in each of these fibres. Where the smaller mtDNA deletion is most prevalent (N = 16), the average heteroplasmy level is 49.13 ± 20.93%; where the larger deletion is most prevalent (N = 13), the average heteroplasmy level is 50.71 ± 17.34%. No significant difference was observed between these two groups (P = 0.8290).
B – The same two fibre categories were assessed in terms of the 'relative deletion proportion' of the most prevalent deletion, to remove the influence of total mtDNA deletion heteroplasmy level – a potentially confounding factor. Where the smaller mtDNA deletion is most prevalent (N = 16), the smaller deletion makes up an average proportion of 0.69 ± 0.13 of the fibre's total mtDNA deletion load; where the larger deletion is most prevalent (N = 13), the larger deletion makes up an average proportion of 0.70 ± 0.09 of the fibre's total mtDNA deletion load. No significant difference was observed between these two groups (P = 0.9410).

6.4.5 Is a greater variance in mtDNA deletion heteroplasmy observed where a greater discrepancy in size exists between two mtDNA deletions in a single fibre?

As no significant difference was found to exist between the mtDNA deletions present at the highest level in multiple mtDNA deletion fibres where either the largest or smallest mtDNA deletion was most prevalent - in the assessed parameters of mtDNA deletion size (Figure 6.63), heteroplasmy level (Figure 6.66 A) and relative mtDNA deletion proportion (Figure 6.66 B) discussed above – the effect of different mtDNA deletion sizes within single fibres was investigated. The effect of increased variance of mtDNA deletion size on difference in mtDNA deletion heteroplasmy or relative mtDNA deletion proportion was investigated, to determine whether this was a more important factor than absolute mtDNA deletion size. The difference in size between the two mtDNA deletions present in each of the multiple mtDNA deletion fibres was calculated, and was first assessed in the total dataset (N =29) in correlation with the difference in mtDNA deletion heteroplasmy between the two mtDNA deletions (Figure 6.67A). Though a slight trend towards larger differences in mtDNA deletion size coinciding with larger differences in mtDNA deletion heteroplasmy was indicated by linear regression ($y = 3.794x + 21.26$, where y represents the difference in mtDNA deletion heteroplasmy levels and x represents the difference in mtDNA deletion size, $r^2 = 0.04351$), this relationship was found not to be significant using Spearman's rho (95% confidence, P = 0.3208).

As for absolute mtDNA deletion size, the difference in size between the two mtDNA deletions present in each of the multiple mtDNA deletion fibres was next assessed in the total dataset (N = 29) in correlation with relative mtDNA deletion proportion (Figure 6.67B). Again, a weak trend was observed between the difference in absolute mtDNA deletion size and relative mtDNA deletion proportion following linear regression ($y = 0.04952x + 0.2922$, where y represents the difference in relative mtDNA deletion proportion and x represents the difference in mtDNA deletion size, $r^2 = 0.06192$), but this relationship was found not to be significant by Spearman's rho (95% confidence, P = 0.3304). Overall, a larger variation in mtDNA deletion size between two species present in a single fibre does not appear to lead to a larger variance in mtDNA deletion accumulation.

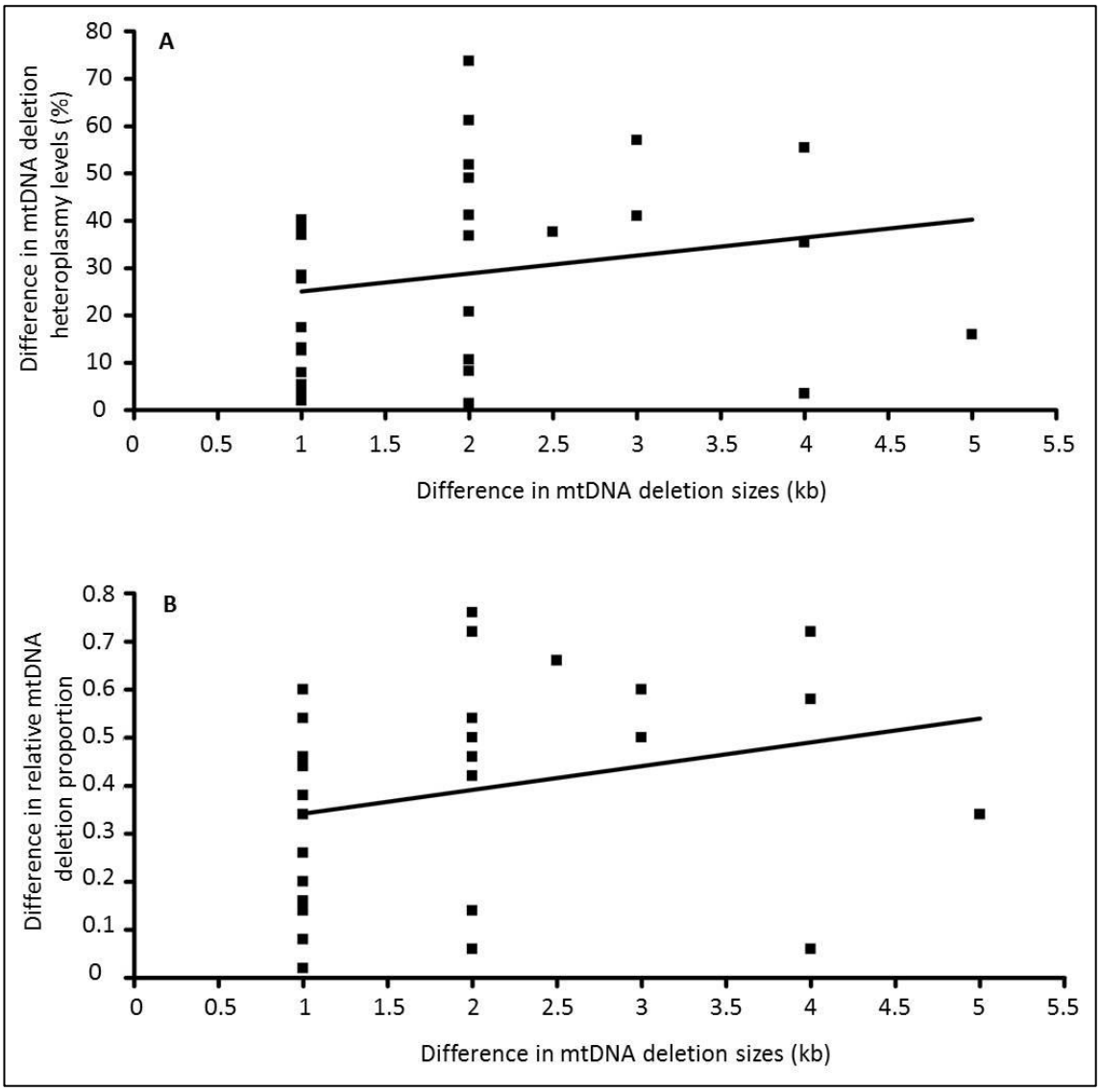

Figure 6.67 – Correlating the difference between mtDNA deletion size with the difference in (A) mtDNA deletion heteroplasmy, and (B) relative mtDNA deletion proportion in all multiple mtDNA deletion fibres.

A - Correlating variance in mtDNA deletion size and mtDNA deletion heteroplasmy levels in all multiple mtDNA deletion fibres. Visible trend for a larger discrepancy in deletion size to lead to a larger difference in heteroplasmy levels; however this trend was not found to be significant (Spearman's rho, 95% confidence, P = 0.3208). **B** - Correlating variance in mtDNA deletion size and relative mtDNA deletion proportion in all multiple mtDNA deletion fibres. Visible trend for a larger discrepancy in deletion size to lead to a larger difference in relative mtDNA deletion proportions; however this trend was not significant (Spearman's rho, 95% confidence, P = 0.3304).

The relationship between variance in mtDNA deletion size (between mtDNA deletions present in the same single fibre) and the variance in mtDNA deletion heteroplasmy levels/relative mtDNA deletion proportions was next examined separately in multiple mtDNA deletion fibres where either the smallest or largest mtDNA deletion was most prevalent (

Figure 6.68).

In instances where the smaller of two mtDNA deletions was found to be most prevalent, a positive trend was observed to exist - following linear regression - between the level of variance in mtDNA deletion size and the level of variance in both mtDNA deletion heteroplasmy levels and relative mtDNA deletion proportion (

Figure 6.68A and B). This suggests that where the smaller of two mtDNA deletions in a single fibre is smaller by a greater margin, it is more likely to a) accumulate to a higher level of heteroplasmy, and b) accumulate to a greater proportion of the overall mtDNA deletion load of the fibre. Correlation analysis by Spearman's rho unfortunately showed both of these trends to lie just outside of significance (P = 0.0802 and 0.0578 respectively); further work is required to assess whether this trend is real, or has been skewed by a low number of data-points (N = 13).

A similar analysis carried out where the larger of two mtDNA deletions was found to be most prevalent in a multiple mtDNA deletion fibre uncovered no trend between the level of variance in mtDNA deletion size and the level of variance in either mtDNA deletion heteroplasmy levels or relative mtDNA deletion proportion (

Figure 6.68 C and D). Analysis by Spearman's rho found no significant relationship to exist between variance in mtDNA deletion size and variance in either mtDNA deletion heteroplasmy levels or relative proportions (P = 0.5380 and 0.6307 respectively, N = 16). This suggests that, where the larger of two mtDNA deletions in a single cell is found to be more prevalent, the size of the smaller mtDNA deletion is irrelevant to the level of heteroplasmy either mtDNA deletion reaches.

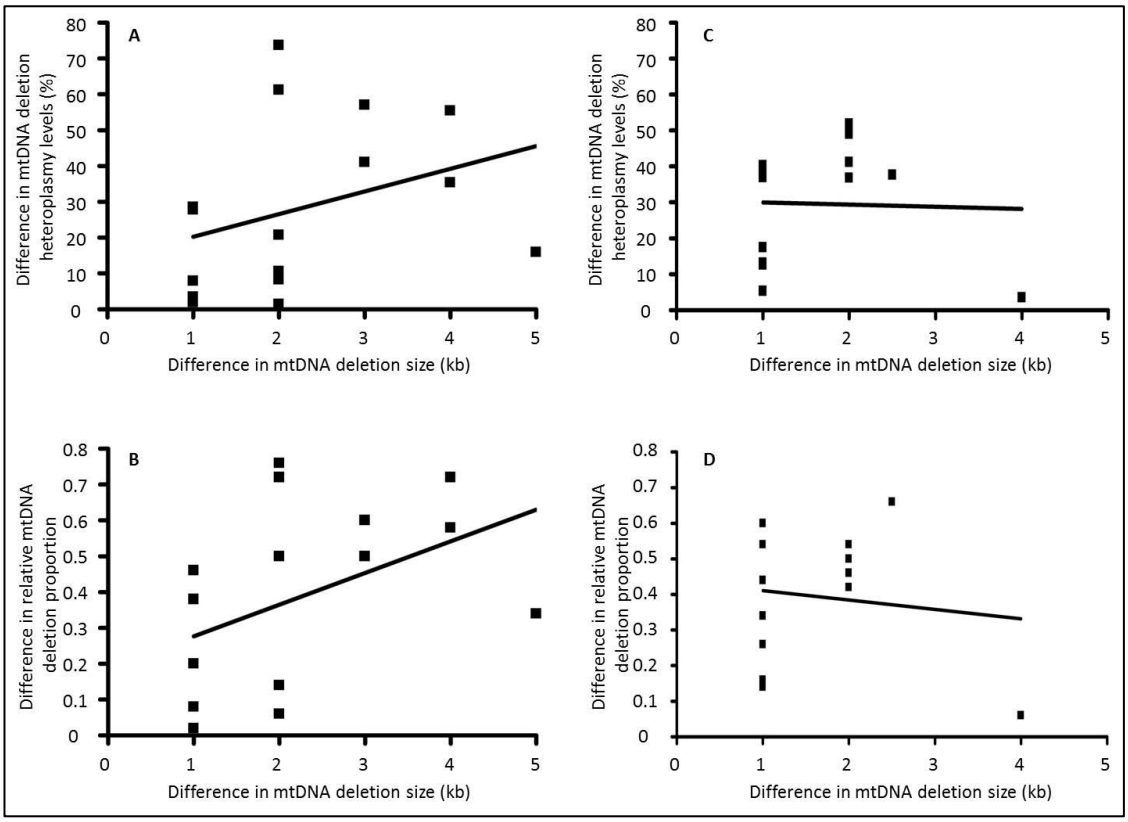

Figure 6.68 – Correlating the difference in mtDNA deletion size with the difference in mtDNA deletion heteroplasmy, and in relative mtDNA deletion proportion in multiple mtDNA deletion fibres where the smallest (A and B) or largest (C and D) mtDNA deletion species is most prevalent.

A – Correlating variance in mtDNA deletion size and mtDNA deletion heteroplasmy levels in multiple mtDNA deletion fibres where the smaller mtDNA deletion is most prevalent. Trend for a larger discrepancy in deletion size to lead to a larger difference in heteroplasmy levels; however this trend was not significant (Spearman's rho, 95% confidence, P = 0.0802). **B** - Correlating variance in mtDNA deletion size and mtDNA deletion proportions in multiple mtDNA deletion fibres where the smaller mtDNA deletion is most prevalent. Apparently strong trend for a larger discrepancy in deletion size to lead to a larger difference in relative mtDNA deletion proportions; however this trend was not significant (Spearman's rho, 95% confidence, P = 0.0578). **C** - Correlating variance in mtDNA deletion size and mtDNA deletion heteroplasmy levels in multiple mtDNA deletion fibres where the larger mtDNA deletion is most prevalent. No significant trend linking variance in deletion size to variance in heteroplasmy levels was found to exist (Spearman's rho, 95% confidence, P = 0.5380). **D** - Correlating variance in mtDNA deletion size and mtDNA deletion heteroplasmy levels in multiple mtDNA deletion fibres where the larger mtDNA deletion is most prevalent. No significant trend linking variance in deletion size to variance in relative mtDNA deletion proportions was found to exist (Spearman's rho, 95% confidence, P = 0.6307).

A final outcome of these assessments is the identification of the high level of variability in mtDNA deletion heteroplasmy levels in multiple mtDNA deletion fibres. While two mtDNA species exist at almost identical proportions in some fibres, a difference in relative mtDNA deletion proportions of up to 0.8 has been observed; similarly, two mtDNA deletions in a single fibre may exist at almost identical heteroplasmy levels, or differ by up to 80%. This high level of variability suggests that there is no evidence for a 'cut-off point' for the clonal expansion of these mtDNA deletions, where one mtDNA deletion has reached an end point of accumulation before clonal expansion of a second mtDNA deletion begins.

6.5 Discussion

The primary focus of this study was to investigate the presence of multiple clonally expanded mtDNA deletions in single COX-deficient muscle fibres, following the amplification of multiple mtDNA deletion bands from approximately 20% of all investigated COX-deficient fibre regions in the longitudinal mtDNA deletion accumulation study discussed in Chapter 3 (see *3.4.2*). Single COX-deficient muscle fibres were isolated from three multiple mtDNA deletion patients, each with a different nuclear gene defect – in *POLG*, *PEO*1 and *RRM2B* – and investigated by smPCR for the presence of mtDNA deletions and real time PCR for mtDNA deletions heteroplasmy levels.

Initial analysis focussed on identifying single fibres containing multiple clonally expanded mtDNA deletions. Of a total of 70 successfully assessed fibres, 29 (41%) were found to contain multiple clonally expanded mtDNA deletion species; of these, all contained mtDNA deletion sizes of two distinct sizes, differing by a minimum of 1kb. This proportion of fibres containing two clonally expanded mtDNA deletions was consistent across all 3 patients - 41% in patient 1 (*POLG* defect), 38% in patient 2 (*PEO1* defect), and 44% in patient 3 (*RRM2B* defect) – suggesting that this is typical for multiple mtDNA deletion patients regardless of the specific nuclear defect. This could in fact be an underestimate of the level of fibres containing multiple mtDNA deletions, as there are likely to be instances where two mtDNA deletions in the same fibre would be of a similar size; further analysis by breakpoint sequencing of the smPCR products from single fibres is required to distinguish mtDNA deletions of the same size from the same fibre.

As this has shown the possibility of multiple mtDNA deletions clonally expanding within a single muscle fibre, it is perhaps surprising that only 2 mtDNA deletions species were detected in these fibres, and not more. However, this is likely to be due to current low sample numbers – if mtDNA deletions are clonally expanded to a significant level in perhaps 40% of fibres from these patients, and ~40% of these contain 2 mtDNA deletions, that is approximately a 16% chance of 2 mtDNA deletion species clonally expanding within a single fibre. Assuming the risk of a 3rd mtDNA deletion becoming clonally expanded is also 40%, this would mean that only 6% of fibres would be likely to contain 3 mtDNA deletion species, within further decreasing

chances of 4 or 5 mutations clonally expanding in the same fibre – making it unlikely that a sample of only 70 fibres would detect this phenomenon, particularly as mtDNA deletions of a similar size are currently indistinguishable by this technique. Analysis of more samples, and subsequent breakpoint analysis of mtDNA deletion species, would be likely to identify a small number of fibres with more than 2 clonally expanded mtDNA deletion species in single fibres.

Prior to this study, only one research group has identified multiple mtDNA deletions to be present in single cells – interestingly, this study was also carried out in human muscle fibres (Kopsidas *et al.*, 1998), while much other research into the clonal expansion of mtDNA deletions has focussed on other tissue types (Khrapko *et al.*, 1999; Trifunovic *et al.*, 2004; Bender *et al.*, 2006; Kraytsberg *et al.*, 2006; Markaryan *et al.*, 2010) or model organisms (Cao *et al.*, 2001; Gokey *et al.*, 2004) (as discussed more fully in *6.1.3*). It is possible that this phenomenon is only observed in human muscle, though it seems unlikely that multiple mtDNA deletions would accumulate in such a high proportion of single cells in muscle but in no other tissue. The only likely explanation for this would be a different mechanism for the clonal expansion of mtDNA deletions in skeletal muscle compared to other tissue, which would be unlikely to lead to the similar spectrum of mtDNA deletions or the same common deletion types that have been observed across different tissue types.

It is important to note that, while these findings support those of Kopsidas *et al* in that multiple mtDNA deletions have been detected in single mtDNA deletion fibres, Kopsidas *et al* found up to 15 mtDNA deletions to be present in any one fibre, and in many cases there was no detection of wildtype mtDNA. In comparison, only 2 mtDNA deletion species were detected in single fibres by smPCR, with a maximum total heteroplasmy level of 98% identified in this study (i.e. the remaining wildtype mtDNA accounted for 2% of the total cellular mtDNA). These discrepancies highlight the need for a consistent molecular approach to investigate the presence of single cells containing mtDNA deletions in other tissue types in the future, as this will be necessary to determine whether the presence of multiple mtDNA deletion in single cells is tissue specific to skeletal muscle.

Following the identification of multiple mtDNA deletion in single muscle fibres, more in depth analyses of mtDNA deletion size and heteroplasmy levels were undertaken. No

significant difference was found to exist in terms of mtDNA deletion size between mtDNA deletion species present in single or multiple mtDNA deletion fibres (Mann Whitney test, P = 0.1273 at 95% confidence). This indicates that, in instances where multiple mtDNA deletions have accumulated within a single fibre, this is not due to an effect of unusually large or small mtDNA deletion size on the clonal expansion of these mtDNA species. Interestingly, total cellular mtDNA deletion heteroplasmy levels were also found to be consistent between fibres containing single or multiple mtDNA deletion fibres (Mann Whitney test, P =0.8686 at 95% confidence) – i.e. where two mtDNA deletion were found to exist in a single cell, the combined mtDNA deletion heteroplasmy for both deletions was, on average, a similar level to that of an mtDNA deletion present in a single mtDNA deletion fibre. This result was initially surprising, as it had been expected that higher total mtDNA deletion heteroplasmy levels would be observed where multiple mtDNA deletions had undergone clonal expansion in a single fibre. However, it is possible that the consistency of mtDNA deletion levels found between single and multiple mtDNA deletion fibres is indicative of a common method of wildtype mtDNA regulation - i.e. that each cell attempts to regulate the level of wildtype mtDNA rather than each mtDNA deletion species – making the number of mtDNA deletion species present irrelevant to the overall level of mtDNA deletion heteroplasmy. This would be in keeping with the importance of absolute wildtype mtDNA copy number in maintaining normal cellular biochemical function, as described by Durham *et al.* (2006) and Greaves *et al.* (2010), and as highlighted in the work discussed in Chapter 4.

In single fibres containing two distinct mtDNA deletion species, no significant difference was found to exist between the mtDNA heteroplasmy levels of the smaller or larger mtDNA deletions from each cell (Mann Whitney test, P =0.6676 at 95% confidence), despite a significant difference in mtDNA deletion size (Mann Whitney test, P < 0.0001 at 95% confidence), indicating that there may be no correlation between mtDNA deletion size and heteroplasmy level. This was confirmed by Spearman's rho correlation analyses carried out in the total dataset, which found the negative trend observed between mtDNA deletion size and heteroplasmy level not to be significant (P = 0.0838). This mirrors the weak negative trend between mtDNA deletion size and heteroplasmy levels observed at the whole tissue level in single mtDNA deletion patients in the study discussed in Chapter 5, confirming the

conclusion that no replicative advantage exists for larger mtDNA deletions. No correlation between mtDNA deletion size and level was found to exist in the separate datasets for single (P = 0.1033) or multiple mtDNA deletion fibres (P = 0.2870), in keeping with the total dataset. The difference in size between the two mtDNA deletions present in a multiple mtDNA deletion fibre had no impact on the difference in mtDNA heteroplasmy levels of relative mtDNA deletion proportion (Spearman's rho, P = 0.3208 and 0.3304 respectively at 95% confidence), further confirming that specific mtDNA deletion size does not impact upon the level to which an mtDNA deletion may clonally expand.

Overall, no evidence was found in this study to support the 'survival of the smallest' mechanism of clonal expansion (Wallace, 1992). As stated in the original project aims, it would be expected that the largest mtDNA deletions would consistently accumulate to the highest levels of heteroplasmy if clonal expansion is driven by a replicative advantage due to a smaller genome size and shorter replication time. In fact, no correlation was found to exist between mtDNA deletion size and heteroplasmy, indicating the presence of no selective advantage based on mtDNA deletion size. Of the current hypothetical mechanisms for the clonal expansion of mtDNA deletions, this best supports mtDNA deletion accumulation by random genetic drift (Elson *et al.*, 2001). When examining multiple mtDNA deletion fibres alone, if the 'survival of the smallest' mechanism were to hold true it would be expected that the largest DNA deletion in each fibre would clonally expand to the highest level of mtDNA deletion heteroplasmy; in fact, no pattern was determined to predict which mtDNA deletion would accumulate to the highest proportion in any given multiple mtDNA deletion fibre. Again, this seems to suggest that random genetic drift is the most likely driving force behind the clonal expansion of mtDNA deletions in these cells. Of particular interest is the lack of an apparent 'cut-off point' in terms of heteroplasmy level for one mtDNA deletion before another begins to clonally expand, as exemplified by the high level of variance in mtDNA deletion heteroplasmy levels in multiple mtDNA deletion fibres. While two mtDNA species exist at almost identical proportions in some fibres, a difference in relative mtDNA deletion proportions of up to 0.8 has been observed; similarly, two mtDNA deletions in a single fibre may exist at almost identical heteroplasmy levels, or differ by up to 80%. This is potentially the strongest evidence yet presented in favour of random genetic drift as a mechanism for the clonal

expansion of mtDNA deletions; this mechanism would likely result in a random flux of cellular mtDNA content, leading to variable heteroplasmy levels of different mtDNA deletions.

The similarity in the conclusions reached by this study at the single cell level and Chapters 4 and 5 at the whole tissue level in muscle – specifically the importance of wildtype mtDNA in determining the pathogenicity of an mtDNA deletion in a cell, and the lack of correlation between mtDNA deletion size and heteroplasmy level – strengthens the indication that random genetic drift is the most likely cause of mtDNA deletion accumulation in muscle. However, the discrepancies noted above between this study and previous work carried out in other tissues and in model organisms highlight the need for further work to be carried out to characterise mtDNA deletion accumulation in other tissue types to assess whether a common mechanism for the clonal expansion of mtDNA deletions exists or whether mtDNA deletion accumulation is tissue specific.

Chapter Seven

Chapter 7

Final Discussion

7.1 Introduction

Since the initial discovery of mtDNA deletion pathogenicity in 1988 (Holt *et al.*, 1988), large-scale mtDNA deletions have become widely recognised as a primary cause of genetic disease. mtDNA deletions are cited as a cause of approximately 18% of all mitochondrial disease cases (Schaefer *et al.*, 2008) and are implicated in the focal cellular dysfunction observed in both ageing and age-related neurodegenerative disease (Bender *et al.*, 2006; Kraytsberg *et al.*, 2006; Reeve *et al.*, 2008b; Larsson, 2010). Due to the multi-copy nature of mtDNA within the cell, an mtDNA deletion as a single entity is not thought to be harmful to the cell; all remaining wildtype mtDNA copies in a cell containing this deletion would be able to compensate for the presence of this mutation (Rossignol *et al.*, 2004). However, an accumulation of an mtDNA deletion species to a high level of heteroplasmy within a cell is known to cause mitochondrial dysfunction and result in cellular biochemical dysfunction. The process by which mtDNA deletion accumulate to a pathogenic level, known as clonal expansion, is key to causing mtDNA deletion related pathologies – in mtDNA deletion diseases, ageing and age-related diseases – due to the high mtDNA deletion heteroplasmy levels required for pathology to occur, but the mechanism by which clonal expansion occurs remains unknown. Though three main hypotheses have come to the fore in this field of research – propagation by replicative advantage (Wallace, 1992), accumulation over time due to selective advantage inherent to the dysfunction of mutated mtDNA deletions (De Grey, 1997), and accumulation by random genetic drift (Elson *et al.*, 2001) – no consensus has been reached as to how clonal expansion of mtDNA deletions may occur. The main focus of this work was to determine the mechanism by which clonal expansion of mtDNA deletions occurs, with a specific focus on human muscle as this is one of the main tissues affected by mtDNA deletions in disease and in ageing. Secondary aims were specific to each individual project within this body of work, including investigating how changes to a molecular defect over time influence a patient's clinical progression, whether any molecular markers could be

identified to determine clinical progression, and whether multiple clonally expanded mtDNA deletion species could be detected within single muscle fibres.

7.2 Major Findings and Further Work

7.2.1 Investigating the longitudinal spread of mtDNA deletions through muscle fibres.

The longitudinal spread of mtDNA deletions though muscle fibres, as visualised by the size of the COX-deficient region caused by the presence of an mtDNA deletion, was investigated to determine whether a relationship exists between mtDNA deletion size and the subsequent rate or range of accumulation of clonal expansion. Based on recent evidence supporting the 'survival of the smallest' hypothesis of clonal expansion (Diaz *et al.*, 2002; Fukui and Moraes, 2009), it was expected that the largest mtDNA deletions would have the greatest intra-cellular replicative advantage and so would accumulate at the greatest rate within a cell. It was therefore hypothesised that, if the 'survival of the smallest' mechanism was driving the clonal expansion of mtDNA deletions in muscle, a positive correlation would be found between mtDNA deletion size and COX-deficient fibre area.

Muscle samples from six patients with multiple mtDNA deletions caused by an underlying nuclear defect – a different mutation in each case – were investigated as part of this study. mtDNA deletion size was measured, using long-range PCR analysis as validated by breakpoint sequencing (section *3.4.3*), in isolated 'long' and 'short' fibre regions of COX-deficiency. While there was no overlap in terms of COX-deficient fibre length or area, the observed mtDNA deletion sizes were remarkably similar across these two groups; no evidence of a correlation between mtDNA deletion size and the size of the resulting area of skm fibre COX-deficiency was observed in either the dataset as a whole, or in data collected from each individual patient. Following the hypothesis that the largest mtDNA deletions accumulate at the greatest rate in muscle, we would expect to see a strong correlation between COX-deficient segment length and mtDNA deletion size. The results from this study therefore do not support the hypothesis that a smaller genome size creates a replicative advantage that drives the clonal expansion of mtDNA deletions.

A possible explanation for the discrepancies between our results and the findings from previous studies is that there are times when replication rate does become rate limiting. The data of Diaz and colleagues (Diaz *et al.*, 2002) would support this given that a replicative advantage for mtDNA deletions was only found under relaxed copy number control in the mtDNA deletion cytoplasts. No accumulation of, or selective advantage for, mtDNA deletions was reported under normal cellular conditions (Diaz *et al.*, 2002), in agreement with our own findings in patient tissue. The rate of mtDNA replication might be very important during the process of mtDNA deletion formation and in establishing which deletions clonally expand, but not the rate of clonal expansion once the deletions have become established.

This could also explain the difference between our findings and those of Moraes *et al* in the mito*Pst1* mouse, where smaller mitochondrial genomes were found to accumulate preferentially *in vivo* in the mito*Pst1* mouse model, developed to express a neuronal-specific inducible mitochondrial-targeted restriction endonuclease (*Pst1*) (Fukui and Moraes, 2009). The authors concluded that this was due to a replicative advantage for smaller mitochondrial genomes, but could indicate, or could in fact be a demonstration of a preferential formation of larger mtDNA deletions. In this case, our findings would be in keeping with those of Fukui and Moraes, as we did observe a high prevalence of larger mtDNA deletions in the clonally expanded segments (75% were >5kb and 50% were >6.75kb). This in turn is in keeping with the observation of an mtDNA deletion size distribution in COX-deficient fibre regions where 70% were >5kb and 45% were >6.75kb in aged muscle fibres in human skeletal muscle (Bua *et al.*, 2006).

Of the hypothetical mechanisms which have been proposed to drive the clonal expansion of mtDNA deletions, these results best fit the random genetic drift model (Elson *et al.*, 2001) due to a lack of correlation between the specific genetic defect and the resultant biochemical defect. The evidence that larger mtDNA deletions may either form more commonly or be more prone to clonal expansion initiation – as gathered from this study and that of Bua *et al* (2006) in human skeletal muscle, and from the work of Fukui and Moraes (2009) in the Mito*Pst1* mouse – should be considered for further investigation. If larger mtDNA deletions are found to be most prevalent in

other tissue types, this could highlight a common mechanism for mtDNA deletion formation or for clonal expansion initiation.

7.2.2 Investigating the change in mtDNA deletion load over time in single mtDNA deletion patients.

The progression of single large-scale mtDNA disease has long been attributed to increasing heteroplasmy levels of the mtDNA defect, an assumption based upon the increased numbers of COX-deficient fibres (Chinnery *et al.*, 2003) and decreased wildtype mtDNA copy numbers (Durham *et al.*, 2006) observed over time in this patient group. While evidence has been found to support this in a mouse model of single large-scale mtDNA disease (Sato *et al.*, 2007), conflicting reports have arisen from the study of human mtDNA deletion disease. Early work did suggest that the mtDNA defect continuously accumulated throughout a patient's lifespan (Larsson *et al.*, 1990), but it has more recently been suggested that mtDNA deletions undergo a rapid accumulation early in development, after which the heteroplasmy level of the defect becomes more stable (Pitceathly *et al.*, 2012).

A null hypothesis was put forward that mtDNA deletion levels would increase over time in patient tissue, leading to increased levels of COX-deficiency and therefore driving clinical disease progression. It was also proposed that the observation of mtDNA deletion accumulation throughout the patient's life would support the presence of a replicative advantage for mtDNA deletions over wildtype mtDNA, as selective pressure would dictate that mtDNA deletion levels continue to tend towards homoplasmy. This would be a particularly apt finding given that early evidence of increasing mtDNA deletion levels throughout the patient lifespan (Larsson *et al.*, 1990) led to the initial proposal of a replicative advantage for mtDNA deletions over wildtype mtDNA (Wallace, 1992).

To determine if an increase in mtDNA deletion heteroplasmy is seen in human tissue – specifically in muscle, this being a primary affected tissue in single mtDNA deletion disease - a case study of a single large-scale mtDNA deletion patient was undertaken. Two muscle biopsies – both taken from the *vastus lateralis*, thirteen years apart– were available from this patient, allowing analysis of molecular changes in this patient's

tissue over time. Assessments of mtDNA deletion level and copy number were carried out on homogenate DNA samples (extracted from tissue sections) and on DNA lysates from single isolated COX-positive, intermediate and negative muscle fibres to accurately assess any molecular changes over time. Overall, no molecular progression was found to have occurred over the thirteen years between these two muscle biopsies; mtDNA deletion heteroplasmy levels remained stable, as did mtDNA total and wildtype copy numbers. This was in-keeping with the stable numbers of COX-deficient muscle fibres across the two biopsies, which goes some way to explaining the slow rate of clinical progression for this patient. This suggests that the mtDNA deletion accumulation responsible for disease symptoms may occur early in life before a plateau is reached, as hypothesised by Pitceathly *et al.* (2012). However, a wide patient cohort would have to be investigated to determine whether there are cases where mtDNA deletion level may continue to increase through a patient's lifespan; this is perhaps the case where disease progression is more severe. The lack of apparent mtDNA deletion accumulation over time in this patient opposes the hypothesis that mtDNA deletion levels would increase over time in patient tissue; the outcome of this investigation therefore opposes the presence of a replicative advantage for mtDNA deletions over wildtype mtDNA.

Due to the stable nature of the molecular and biochemical defects over time in this case study, no comment can be made as to the role played by mtDNA deletion heteroplasmy levels in cases of increasing COX-deficiency in tissue. However, the importance of absolute wildtype mtDNA copy number was highlighted in the analysis of isolated muscle fibres – particularly outlying mtDNA deletion heteroplasmy data points in the analysis of COX-deficient and COX-normal fibres. 3 COX-deficient fibres were found to have deletion levels much lower than the norm for biochemically deficient fibres in the patient, while 8 COX-positive fibres contained relatively high deletion levels of more than 60%. All 3 COX-deficient fibres with low deletion levels were found to have low levels of wildtype mtDNA, while COX-positive fibres with unusually high mtDNA deletion levels were found to have similarly high levels of wildtype mtDNA. This highlights the importance of mtDNA maintenance in the muscle, and lends support to the hypothesis that absolute wildtype copy number may be vital for maintaining normal biochemical function, superseding mtDNA deletion heteroplasmy level in determining cellular health (Durham *et al.*, 2005). The results of

the individual fibre studies, if extrapolated to whole tissue level, therefore indicate that decreasing levels of wildtype mtDNA below a threshold level may be the primary cause of patient progression in single mtDNA deletion disease, as hypothesised by Schroder *et al.* (2000). However, it is yet to be determined how significant a role mtDNA deletion heteroplasmy level has in regulating the effect of wildtype mtDNA copy number on cell fate.

7.2.3 Investigating the impact of molecular mtDNA deletion characteristics on disease presentation and progression in single mtDNA deletion patients.

The potential spectrum of disorders caused by single large-scale mtDNA deletions, in terms of both clinical presentation and progression, presents a serious problem for clinicians in that no genetic markers have been found to conclusively identify how severe a patient's symptoms may become, or how quickly they will progress. In order to provide the best possible patient care and support, it is vital that we gain a better understanding of the causes of disease severity and progression. While previous studies have been carried out in this area, these have met with mixed success and many of the research findings have been contradictory. In an attempt to rectify this situation, this study was carried out to identify the relationship between the mtDNA defect and the resultant clinical symptoms in a large cohort of mtDNA deletion patients. While the primary aim of this study was to characterise the mtDNA defects present in this cohort and to determine whether a selective advantage could be observed for larger mtDNA deletions (supporting the presence of a replicative advantage for mtDNA deletion (Wallace, 1992), the availability of high quality data also allowed modelling studies to be carried out by Dr John Grady to assess the impact of molecular mtDNA deletion characteristics on disease presentation and progression.

A large cohort of 113 patients with large-scale mtDNA deletions was investigated as part of this study – details of the specific molecular defect (mtDNA deletion size, heteroplasmy levels and breakpoint location and sequence) were collected specifically for this study, while robust clinical data was available for all patients to allow for evaluations of the impact of molecular factors on clinical presentation and progression. An initial assessment of mtDNA deletion size and level of heteroplasmy

revealed a negative relationship to exist between these two variables – refuting the presence of a replicative advantage for larger mtDNA deletions, and therefore providing evidence against the model of clonal expansion by replicative advantage (Wallace, 1992). Though this negative trend was found to be significant (P = 0.0034), this is likely to be a result of the clinically observed phenotypes of patients from whom samples are available to access; individuals with small deletions at low heteroplasmy levels would not be likely to present clinically with symptoms, and large deletions at high heteroplasmy levels may be so deleterious as to be lethal early in development. An important implication of this is that the heteroplasmy threshold for pathogenicity of a deletion is likely to be dependent on deletion size and location.

Further molecular investigations found unimodal distributions of both 5' and 3' mtDNA deletion breakpoints - similar to the findings of (Samuels *et al.*, 2004) but less centred on the 4977bp common mtDNA deletion breakpoints, suggesting these may not be as important in mtDNA deletion formation as previously proposed – and strong correlations between high mtDNA deletion breakpoint homology, high mtDNA deletion levels, and early symptom onset. However, the results of the breakpoint homology study conflict with the original findings of Sadikovic *et al.* (2010), highlighting a need for further study in this area. The analysis of the impact of molecular mtDNA deletion characteristics upon clinical disease presentation was hampered in this study by a low number of patients presenting with KSS or Pearson syndrome. Expanding the patient cohort to continue this work would increase the statistical strength of any analyses already carried out and could provisionally allow for the investigation of the correlation linking mtDNA deletion breakpoint homology and clinical symptoms.

Following these analyses, the collected molecular data was combined with clinical information and biochemical defect measures to be used in modelling studies by Dr John Grady. Both deletion size and heteroplasmy were found to be predictive of symptom onset age and rate of NMDAS progression, though in both cases the predictive power of these markers was strengthened by co-regression – the implication of this is that each predictor modulates the effect of the other. In addition, deletion size is in all cases the stronger predictor. This positive result led to the initiation of a longitudinal modelling study, using change in NMDAS score over time as a measure of clinical progression. This is being developed as a prognostic tool for

clinicians, with mtDNA deletion size and heteroplasmy having been found to be highly predictive of a patient's rate of clinical progression and deletion location found to play a modulatory role in determining disease course – inclusion of ND6 in an mtDNA deletion is predictive of faster clinical progression, while mtDNA deletions spanning NN4L - COX3 tend to result in a less severe disease course.

7.2.4 Investigating the presence of multiple clonally expanded mtDNA deletions in single muscle fibres.

The presence of multiple clonally expanded mtDNA deletions in single cells has been a point of dispute in this field of research since the initial discovery that mtDNA deletions do not accumulate heterogeneously throughout a given tissue, but rather accumulate to varying degrees of heteroplasmy in individual cells (Brierley *et al.*, 1998). Though a separate study carried out in the same year found a heterogeneous population of mtDNA deletion species to be present in all investigated COX-deficient or COX-intermediate muscle fibres (Kopsidas *et al.*, 1998), the clonal expansion of mtDNA deletions has widely been accepted to refer to the accumulation of a single mtDNA deletion species in a single cell as presented by Brierley *et al.* (1998). Subsequent single cell studies have largely supported the identification of a single clonally expanded mtDNA deletion per cell, though these have been carried out in other tissue types (Bender *et al.*, 2006; Kraytsberg *et al.*, 2006; Markaryan *et al.*, 2010) or animal models (Cao *et al.*, 2001; Gokey *et al.*, 2004).

Evidence that a single mtDNA deletion species is clonally expanded in an individual fibre fits well with a hypothetical selective advantage driving mtDNA deletion accumulation over time; we would expect that, in an mtDNA pool within a single cell where selective pressures are active, the mtDNA species with the greatest selective advantage would tend towards homoplasmy over time. However, the possibility of the clonal expansion of multiple mtDNA deletions was brought to the fore by the investigation of longitudinal spread of mtDNA deletions discussed earlier in this chapter (section *7.2.1*). A number of single fibres isolated from multiple mtDNA deletion patient biopsy sections had to be excluded from this study due to the apparent presence of multiple mtDNA deletions (Section *3.4.2*), warranting further

investigation into the clonal expansion of multiple mtDNA deletions. It was suggested that single molecule PCR – a specialist technique developed by Kraytsberg and Khrapko (2005) to assess a range of mtDNA species within a single sample – could be employed to investigate the presence of multiple mtDNA deletions in single cells, following evidence that this technique is particularly useful for mtDNA analysis in single cells (Kraytsberg *et al.*, 2009).

Single COX-deficient muscle fibres were isolated from tissue sections taken from available biopsy tissue from three patients with multiple mtDNA deletion disease, caused in each case by a different nuclear defect. Two separate species of clonally expanded mtDNA deletion were detected in 40% of all cells assessed; these 'multiple mtDNA deletion fibres' were evenly distributed through the three patient datasets, meaning approximately 40% of COX deficient fibres harboured mtDNA deletion in each of the three patient muscle biopsies. Following this finding, a more in-depth analysis of mtDNA deletion size and heteroplasmy level was undertaken. No significant difference was found to exist in terms of mtDNA deletion size between mtDNA deletion species present in single or multiple mtDNA deletion fibres. This indicates that instances of multiple mtDNA deletion accumulation are not due to an influencing effect of unusually large or small mtDNA deletion sizes. Interestingly, total cellular mtDNA deletion heteroplasmy levels were also found to be consistent between fibres containing single or multiple mtDNA deletions – i.e. where two mtDNA deletion were found to exist in a single cell, the combined mtDNA deletion heteroplasmy for both deletions was, on average, a similar level to that of an mtDNA deletion present in a single mtDNA deletion fibre. It is possible that the consistency of mtDNA deletion levels found between single and multiple mtDNA deletion fibres is indicative of a common method of wildtype mtDNA regulation - i.e. that each cell attempts to regulate the level of wildtype mtDNA rather than each mtDNA deletion species – making the number of mtDNA deletion species present irrelevant to the overall level of mtDNA deletion heteroplasmy. This would be in keeping with the importance of absolute wildtype mtDNA copy number in maintaining normal cellular biochemical function, as described by Durham *et al.* (2006) and Greaves *et al.* (2010), and as highlighted in the work discussed in Section *7.2.2*.

In single fibres containing multiple clonally expanded mtDNA deletions, no apparent relationship was detected between mtDNA deletion size and heteroplasmy levels; mtDNA heteroplasmy levels of smaller or larger mtDNA deletions from each cell were found to be similar, with no significant difference detected in these datasets and no trend for either larger or smaller mtDNA deletions to tend to accumulate to the higher level within a single fibre. Further analyses were carried out to assess whether the difference in size between two mtDNA deletions in a single fibre impacted upon the difference in mtDNA deletion heteroplasmy levels. There was found to be no significant relationship between these two variables – the implication of this finding being that specific mtDNA deletion size does not impact upon the level to which an mtDNA deletion may clonally expand. This is potentially the strongest evidence yet presented in favour of random genetic drift as a mechanism for the clonal expansion of mtDNA deletions; this mechanism would likely result in a random flux of cellular mtDNA content, leading to variable heteroplasmy levels of different mtDNA deletions (Elson *et al.*, 2001). However, future studies must be carried out in other tissue types in order to assess whether a common mechanism for clonal expansion of mtDNA deletions is likely to exist.

The apparent lack of correlation between mtDNA deletion size and heteroplasmy levels prompted a more thorough evaluation of the relationship between these two variables. No correlation between mtDNA deletion size and level was found to exist in the separate datasets for single or multiple mtDNA deletion fibres, while the weak negative trend observed between mtDNA deletion size and heteroplasmy level in the total dataset was found not to be significant. This mirrors the weak negative trend between mtDNA deletion size and heteroplasmy levels observed in single mtDNA deletion patients in the study discussed in Section *7.2.3*, confirming that no replicative advantage exists for larger mtDNA deletions over other mtDNA deletion species.

7.3 Final Conclusions

Over the course of the four studies discussed here, all evidence has suggested that the clonal expansion of mtDNA deletions occurs due to random genetic drift, as first

proposed by Elson (Elson *et al.*, 2001). No evidence has been found to suggest that mtDNA deletions have any selective advantage over wildtype mtDNA, or that a replicative advantage exists to cause larger mtDNA deletions to preferentially accumulate over smaller mtDNA deletions. It is, however, important to note that this body of work was all conducted in human muscle tissue from mtDNA deletion patients, and further studies must therefore be carried out in other tissue types to assess whether a common mechanism is responsible for the clonal expansion of mtDNA deletions here. Similarly, future work must be undertaken in aged tissues to assess whether the same mechanisms are responsible for the accumulation of mtDNA deletions with age and in age-related disease as for the clonal expansion of mtDNA deletions in mitochondrial disease.

While it remains crucial that we fully investigate the mechanism by which clonal expansion occurs, in the hope that understanding how mtDNA deletion accumulation occurs is the first step towards preventing this, the importance of absolute wildtype mtDNA copy number in determining cellular biochemical has also been highlighted over the course of this work (discussed in sections *4.4.6.5* and *6.5*), and warrants further study. Further work is required to determine where the 'functional threshold level' for wildtype mtDNA copy number lies, and how significant a role mtDNA deletion heteroplasmy level has in regulating the effect of wildtype mtDNA copy number on cell fate.

Finally, it is imperative that the longitudinal modelling of clinical disease progression is continued. The current model has identified larger mtDNA deletion size and higher mtDNA deletion heteroplasmy levels to be predictive of more rapid disease progression, with a number of gene loci found to modulate disease progression (specifically, ND6 involvement predicts faster progression while the deletion of genes in the region ND4L to COX3 predict slower progression). This is the first study of its kind and, though further verification of these results is required, is the first step towards providing clinicians with a better set of prognostic tools for patient analysis. Inclusion of a larger patient cohort will increase the accuracy of this disease model, while the inclusion of more data sets (such as breakpoint sequence homology) could potentially also improve this prognostic tool.

Chapter Eight

Chapter 8

Appendices

Appendix A

All available data for the single large-scale mtDNA deletion patient cohort involved in all analyses carried out in Chapter Five. Numerical patient ID's were assigned in order to de-identify clinical data. Clinical phenotypes are listed as described in clinical records; age at clinical symptom onset, age at biopsy and NMDAS assessment details were also obtained from clinical records. COX-deficiency was assessed in all cases in muscle sections, following the application of COX/SDH histochemical activity assays, by Mr Gavin Falkous from the NCG Mitochondrial Diagnostics service. All mtDNA deletion breakpoints were determined by breakpoint sequencing, while mtDNA deletion levels were measured by the quantitative *ND1/ND4* real-time PCR assay.

Appendix B

Full breakpoint sequence details for all patients with identified breakpoint locations. Nucleotide sequences of 49bp (24 bases either side of the breakpoint base, which is enclosed by square parentheses) are provided – these were assessed for the presence of direct repeat sequences of more than one base by clustal alignment, as outlined by Sadikovic *et al.* (2010)

Appendix C

Identification of available data sets for analysis in Chapter Five, as summarised in *Table 5.4*. Appropriate patient data sets marked '**Y**' where data indicated by column heading was all available for data analysis; **NMDAS** where at least one NMDAS test result was available; **W/O NMDAS** where no NMDAS scores were available.

.

Patient ID	Clincal phenotype	AAO	AAB	Sample	COX Def	DelLevel	DelSize	5' bp	3' bp	Deletion size/heteroplasmy level analysis?	Deletion location/heteroplasmy level analysis?	NMDAS assessments
1	Proximal myopathy		43	SKM	5	10						N/A
2	KSS, ptosis, mild proximal myopathy	12	15	SKM	30	76	4978	8482	13460	Yes	Yes	2
3	CPEO	15	39	SKM	12	35	5899	9523	15422	Yes	Yes	7
4	CPEO			SKM		32.2022	7958	6033	13991	Yes	Yes	1
5	Renal disease, retinopathy, short stature, ataxia, tremor and partial hypogonadism	12	21	SKM	20	75	4999	6625	11623	Yes	Yes	N/A
6			28	SKM		53.72529	4978	8482	13460	Yes	Yes	3
7	CPEO and ataxia	45	62	SKM	7	1.1236	4909	8814	13723			4
8	CPEO	20	27	SKM	30	9	5074	6434	11510			5
9	CPEO and myopathy	30	45	SKM	25	39	4241	9498	13739	Yes	Yes	8
10	KSS	11	27	SKM	10	37	9120	6466	15588	Yes	Yes	7
11	CPEO, myopathy and deafness	15	26	SKM	26	82.90922	4641	10946	15587	Yes	Yes	3
12	CPEO and ptosis	48	73	SKM	17	41.3441	2300	12112	14422	Yes	Yes	8
13	CPEO	12	31	Urine	20	2						1
14	CPEO		63	SKM	15	35	4770	9347	14119	Yes	Yes	1
15	CPEO			SKM	16	30.03416	4978	8482	13460	Yes	Yes	N/A
16	CPEO	30		SKM	15	28.0942934	7498	7130	14628	Yes	Yes	N/A
17	CPEO and myopathy	24	44	SKM	10	46.52769184						7
18	CPEO		44	SKM	30	56	4978	8482	13460	Yes	Yes	1
19	CPEO, ptosis and myopathy	18	57	SKM	40	56.58574174	4978	8482	13460	Yes	Yes	N/A
20	CPEO, myopathy and ptosis	24		SKM								1
21	CPEO and proximal myopathy	52	53	Urine	10	37.89777536						N/A
22	Mitochondrial cytopathy		38	SKM	14	42.12949	4978	8482	13460	Yes	Yes	N/A

Patient ID - assigned patient identification number; **Clinical phenotype** – patient phenotype as described in clinical records; **AAO** – age at onset of clinical symptoms; **AAB** – age of patient at time of tissue biopsy; **Sample** – tissue sample type (SKM – skeletal muscle; Urine where SKM was not available; or Blood – from paediatric cases); **COX Def** – recorded percentage of COX-deficient fibres; **DelSize** – recorded mtDNA deletion size in base pairs; **3'bp** – 3' mtDNA deletion breakpoint, **5'bp** – 5' mtDNA deletion breakpoint; **DelLevel** – mtDNA deletion heteroplasmy level (%); **Deletion size/heteroplasmy level analysis** – yes where patient data was used in this set of analysis; **Deletion location/heteroplasmy level analysis** – yes where patient data was used in this set of analysis; **NMDAS assessments** – number of NMDAS assessments undertaken by this patient, N/A where no results were available.

Patient ID	Clincal phenotype	AAO	AAB	Sample	COX Def	DelLevel	DelSize	5' bp	3' bp	Deletion size/heteroplasmy level analysis?	Deletion location/heteroplasmy level analysis?	NMDAS assessments
23	CPEO, ptosis, myopathy and deafness		60	SKM	3	24	7355	7168	14523	Yes	Yes	N/A
24	KSS, hearing loss, visual impairment, retinary pigmentosis, ptosis, short stature, ataxia, tremors and reduced school performance	7	16	SKM	2	40						N/A
25	CPEO	25	40	SKM	48	81	4237	9486	13724	Yes	Yes	6
26	CPEO		30	SKM	15	37	7144	5772	12916	Yes	Yes	4
27	CPEO and Myopathy	28	40	SKM	20	75	4978	8482	13460	Yes	Yes	7
28	Ptosis, CPEO and jaw aching with chewing			SKM	18	76.0483	2300	12112	14422	Yes	Yes	1
29	CPEO and myopathy	15	25	SKM	25	43.59668	6935	7185	14120	Yes	Yes	7
30	CPEO and ataxia	6	46	SKM	15	13	8704	7175	15879			4
31	Unknown (patient sample recieved from Texas)			SKM	11	55	3039	10951	13990	Yes	Yes	N/A
32	CPEO, ptosis and myopathy	15	41	SKM	45	50	6058	8838	14906	Yes	Yes	2
33	CPEO	15	40	SKM	12	50	4752	8287	13041	Yes	Yes	9
34	CPEO	33	41	SKM	70	78	4978	8482	13460	Yes	Yes	1
35	CPEO	14	34	SKM	20	24.559	5813	9754	15567	Yes	Yes	1
36	late-onset CPEO	39	72	SKM	5	10	7500			Yes		N/A
37	CPEO and ptosis		65	SKM	25	44.90469	7977	6537	14514	Yes	Yes	N/A
38	CPEO and abnormal ECG		71	SKM	22	76	4223	9500	13723	Yes	Yes	N/A
39	CPEO	23	51	SKM	32	58	4978	8482	13460	Yes	Yes	7
40	CPEO	35	50	SKM	20	54.76505905	2300	12112	14422	Yes	Yes	10

Patient ID - assigned patient identification number; **Clinical phenotype** – patient phenotype as described in clinical records; **AAO** – age at onset of clinical symptoms; **AAB** – age of patient at time of tissue biopsy; **Sample** – tissue sample type (SKM – skeletal muscle; Urine where SKM was not available; or Blood – from paediatric cases); **COX Def** – recorded percentage of COX-deficient fibres; **DelSize** – recorded mtDNA deletion size in base pairs; **3'bp** – 3' mtDNA deletion breakpoint, **5'bp** – 5' mtDNA deletion breakpoint; **DelLevel** – mtDNA deletion heteroplasmy level (%); **Deletion size/heteroplasmy level analysis** – yes where patient data was used in this set of analysis; **Deletion location/heteroplasmy level analysis** – yes where patient data was used in this set of analysis; **NMDAS assessments** – number of NMDAS assessments undertaken by this patient, N/A where no results were available.

Patient ID	Clincal phenotype	AAO	AAB	Sample	COX Def	DelLevel	DelSize	5' bp	3' bp	Deletion size/heteroplasmy level analysis?	Deletion location/heteroplasmy level analysis?	NMDAS assessments
41	CPEO, bilateral ptosis and glaucoma		63	SKM	13	35	6864	7128	13992	Yes	Yes	2
42	CPEO		46	SKM	30							N/A
43	CPEO and epilepsy	28	41	SKM	80	78	4000			Yes		5
44	CPEO and ataxia	27	58	SKM	30	22	4392	8576	12967	Yes	Yes	3
45	KSS, bilateral ptosis, CPEO, dysarthria, stiffness, ataxia, tremor, deafness and mild myopathy	15	34	SKM	35	78	4978	8482	13460	Yes	Yes	N/A
46	CPEO, ptosis, recurrent eye infection and myopathy	10	34	SKM	15	94.029	6036	8570	14605	Yes	Yes	N/A
47	Unknown (patient sample recieved from Dallas)			SKM		3	4978	8482	13460		Yes	N/A
48	ptosis, CPEO and some fatiguable weakness	14	25	SKM	55	85	4652	10947	15599	Yes	Yes	N/A
49	CPEO and myopathy	45	50	SKM	5	72.428	2803	11637	14440	Yes	Yes	11
50	CPEO and myopathy	10	34	SKM	30	61.22	4977	8482	13460	Yes	Yes	5
51	CPEO			SKM	28	34	4885	7205	12085	Yes	Yes	1
52	KSS, CPEO, ptosis, myopathy and fundal pigmentation		16	SKM	nr	87.5764462	4959	8474	13433	Yes	Yes	N/A
53	CPEO and ptosis		63	SKM	50	55	3527	7729	11268	Yes	Yes	N/A
54	CPEO, muscle atrophy, weakness, retinal pigmentary changes and increased resting lactate		39	SKM	30	87.409	2308	12112	14422	Yes	Yes	N/A
55	KSS			SKM		50	3979	11658	15637	Yes	Yes	N/A
56	CPEO		85	SKM	12	23.087	7671	6741	14422	Yes	Yes	N/A

Patient ID - assigned patient identification number; **Clinical phenotype** – patient phenotype as described in clinical records; **AAO** – age at onset of clinical symptoms; **AAB** – age of patient at time of tissue biopsy; **Sample** – tissue sample type (SKM – skeletal muscle; Urine where SKM was not available; or Blood – from paediatric cases); **COX Def** – recorded percentage of COX-deficient fibres; **DelSize** – recorded mtDNA deletion size in base pairs; **3'bp** – 3' mtDNA deletion breakpoint, **5'bp** – 5' mtDNA deletion breakpoint; **DelLevel** – mtDNA deletion heteroplasmy level (%); **Deletion size/heteroplasmy level analysis** – yes where patient data was used in this set of analysis; **Deletion location/heteroplasmy level analysis** – yes where patient data was used in this set of analysis; **NMDAS assessments** – number of NMDAS assessments undertaken by this patient, N/A where no results were available.

Patient ID	Clincal phenotype	AAO	AAB	Sample	COX Def	DelLevel	DelSize	5' bp	3' bp	Deletion size/heteroplasmy level analysis?	Deletion location/heteroplasmy level analysis?	NMDAS assessments
57	CPEO, mild ptosis and myopathic changes		59	SKM	18	0	5219	5999	11221			1
58	CPEO and dysphagia	16	32	SKM	20	72	4113	11262	15375	Yes	Yes	9
59	CPEO nd myopathy	21	56	SKM	14	34	4978	8482	13460	Yes	Yes	4
60	CPEO	34	39	SKM	34	64.55722187	4604	9057	13661	Yes	Yes	4
61	Ptosis and myopathy			SKM	60	55.982	4770	9347	14119	Yes	Yes	N/A
62	Pearson Syndrome	3		Blood		88	6472	7532	14014	Yes	Yes	N/A
63	CPEO/KSS	10	24	SKM	30	72.706	6472	7532	14014	Yes	Yes	7
64	CPEO and ptosis	14	59	SKM	10	39	7676	6323	13999	Yes	Yes	5
65	CPEO, diplopia, myopathy and fatigue	30	34	SKM	40	35.79268	8039	7637	15676	Yes	Yes	3
66	CPEO and proximal myopathy	15	34	SKM	35	71	5470	6603	12073	Yes	Yes	6
67	CPEO		66	SKM	15	26.09838						N/A
68	KSS	15	29	SKM	50	85	4500			Yes		8
69	CPEO and myopathy	19	38	SKM	9	42						N/A
70	Ptosis, CPEO and facial muscle weakness			SKM	15	45	5958	6002	11960	Yes	Yes	N/A
71	CPEO and ptosis	21	32	SKM	45	69	4382	8586	12968	Yes	Yes	5
72	CPEO, ptosis and myopathy		25	SKM	nr	71.1395812	4978	8482	13460	Yes	Yes	N/A
73	PEO/ptosis/progressive limb muscle weakness and neck flexor, proximal and distal muscle weakness. Echo abnormal (cardiomyopathy); EMG shows myopathic changes.		59	SKM	20	51	7284	6773	14058	Yes	Yes	N/A

Patient ID - assigned patient identification number; **Clinical phenotype** – patient phenotype as described in clinical records; **AAO** – age at onset of clinical symptoms; **AAB** – age of patient at time of tissue biopsy; **Sample** – tissue sample type (SKM – skeletal muscle; Urine where SKM was not available; or Blood – from paediatric cases); **COX Def** – recorded percentage of COX-deficient fibres; **DelSize** – recorded mtDNA deletion size in base pairs; **3'bp** – 3' mtDNA deletion breakpoint, **5'bp** – 5' mtDNA deletion breakpoint; **DelLevel** – mtDNA deletion heteroplasmy level (%); **Deletion size/heteroplasmy level analysis** – yes where patient data was used in this set of analysis; **Deletion location/heteroplasmy level analysis** – yes where patient data was used in this set of analysis; **NMDAS assessments** – number of NMDAS assessments undertaken by this patient, N/A where no results were available.

Patient ID	Clincal phenotype	AAO	AAB	Sample	COX Def	DelLevel	DelSize	5' bp	3' bp	Deletion size/heteroplasmy level analysis?	Deletion location/heteroplasmy level analysis?	NMDAS assessments
74	KSS	0		Blood	nr	86	7714	6377	14093	Yes	Yes	1
75	CPEO and myopathy	12	33	SKM	49	79	5000			Yes		3
76	CPEO and mild myopathy	11	56	SKM	16	42	5000			Yes		1
77	CPEO and proximal myopathy	16	36	SKM	43	67	4978	8482	13460	Yes	Yes	6
78	CPEO		35	SKM	8	25.571	4978	8482	13460	Yes	Yes	N/A
79	CPEO and ptosis	47	60	SKM	13	46	4237	9486	13724	Yes	Yes	6
80	CPEO and ptosis		57	SKM	4	5.737768397	8560	5942	14502			N/A
81	CPEO, ptosis, impaired speech and swallowing, facial and neck weakness	3	43	SKM	60	81	4978	8482	13460	Yes	Yes	1
82	Proximal myopathy	18	49	SKM	20	53	5160	9254	14418	Yes	Yes	11
83	CPEO, MS-like symptoms, dysarthria		40	SKM	20	63.16333	4978	8482	13460	Yes	Yes	N/A
84	CPEO and mild myopathy	5	28	SKM	22	33.27181351	7648	6341	14005	Yes	Yes	4
85	bilateral ptosis and exodeviation	21	25	SKM	40	53	4372	8927	13308	Yes	Yes	N/A
86	Myopathy, and growth hormone deficiency; Leigh's disease on MRI	0	8	SKM		57.90509	8500			Yes		N/A
87	Unknown			SKM		11.84411343						N/A
88	CPEO and mitochondrial myopathy		27	SKM		65.18305	4851	10745	15598	Yes	Yes	N/A
89	CPEO and ptosis	48	70	SKM	2	0						11
90	PEO, ptosis and dysphagia		32	SKM	25	45	5340	6714	12078	Yes	Yes	5
91	CPEO		17	SKM	20	7.004947025	7129	8543	15672	Yes		N/A
92	CPEO	20	38	SKM	0.5	6	7595	7845	15440			4
93	Ptosis, proximal myopathy, short stature and cardiac disease		23	SKM	50	90	6864	7128	13992	Yes	Yes	1
94	Ptosis, CPEO and proximal weakness				80	86.5422						N/A

Patient ID - assigned patient identification number; **Clinical phenotype** – patient phenotype as described in clinical records; **AAO** – age at onset of clinical symptoms; **AAB** – age of patient at time of tissue biopsy; **Sample** – tissue sample type (SKM – skeletal muscle; Urine where SKM was not available; or Blood – from paediatric cases); **COX Def** – recorded percentage of COX-deficient fibres; **DelSize** – recorded mtDNA deletion size in base pairs; **3'bp** – 3' mtDNA deletion breakpoint, **5'bp** – 5' mtDNA deletion breakpoint; **DelLevel** – mtDNA deletion heteroplasmy level (%); **Deletion size/heteroplasmy level analysis** – yes where patient data was used in this set of analysis; **Deletion location/heteroplasmy level analysis** – yes where patient data was used in this set of analysis; **NMDAS assessments** – number of NMDAS assessments undertaken by this patient, N/A where no results were available.

Patient ID	Clincal phenotype	AAO	AAB	Sample	COX Def	DelLevel	DelSize	5' bp	3' bp	Deletion size/heteroplasmy level analysis?	Deletion location/heteroplasmy level analysis?	NMDAS assessments
95	Pearson syndrome			SKM		71.7641	4665	10817	15482	Yes	Yes	N/A
96	CPEO	22	37	SKM	20	39.99085	6549	6006	12555	Yes	Yes	6
97	CPEO and mild myopathy	14	32	SKM	10	62	4978	8482	13460	Yes	Yes	6
98	Ptosis, CPEO and dilated cardiomyopathy			SKM		22.5945	4963	10104	15070	Yes	Yes	1
99	Kearns-Sayre Syndrome	0		skm		86	2549	10310	12859	Yes	Yes	N/A
100	Ptosis, CPEO, thyrotoxicosis, limb and neck flexor weakness, no deep tendon reflexes and respiratory failure			SKM	20	49.7386						N/A
101	Dystonia, bilateral eyelid ptosis, hearing loss and myopathy		67	SKM	nr	56	6978	7821	14797	Yes	Yes	N/A
102	CPEO, myopathy and facial weakness		39	SKM	35	18.62738449	3383	6129	9512	Yes		N/A
103	CPEO and myopathy	58	63	SKM	35	62.586	7886	6641	14532	Yes	Yes	N/A
104	Bilateral ptosis and retinitis pigmentosa		18	SKM	6	47.5894	4978	8482	13460	Yes	Yes	N/A
105	CPEO and ptosis		64	SKM	40	65						N/A
106	Unknown			SKM		? LOW LEVEL	7451	8287	15738			N/A
107	CPEO and ptosis		46	SKM		13	4978	8482	13460			N/A
108	CPEO and ptosis		56	SKM	25	55	2297	12115	14422	Yes	Yes	N/A
109	CPEO and ptosis		42	SKM	15	35	4596	9528	14125	Yes	Yes	N/A
110	CPEO and ptosis		41	SKM		20	5906	8325	14231	Yes	Yes	N/A
111	CPEO and ptosis		39	SKM	5	4						N/A
112	KSS/CPEO		18	SKM	17	60	4599	9752	14351	Yes	Yes	N/A
113	CPEO		39	SKM	60	65	4978	8482	13460	Yes	Yes	N/A

Patient ID - assigned patient identification number; **Clinical phenotype** – patient phenotype as described in clinical records; **AAO** – age at onset of clinical symptoms; **AAB** – age of patient at time of tissue biopsy; **Sample** – tissue sample type (SKM – skeletal muscle; Urine where SKM was not available; or Blood – from paediatric cases); **COX Def** – recorded percentage of COX-deficient fibres; **DelSize** – recorded mtDNA deletion size in base pairs; **3'bp** – 3' mtDNA deletion breakpoint, **5'bp** – 5' mtDNA deletion breakpoint; **DelLevel** – mtDNA deletion heteroplasmy level (%); **Deletion size/heteroplasmy level analysis** – yes where patient data was used in this set of analysis; **Deletion location/heteroplasmy level analysis** – yes where patient data was used in this set of analysis; **NMDAS assessments** – number of NMDAS assessments undertaken by this patient, N/A where no results were available.

Patient ID	DelSize	5' bp	5' bp sequence	3' bp	3' bp sequence	Direct repeat (Y/N)	Repeat sequence
2	4978	8482	aaactaccacctacctccctcacc[a]aagcccataaaaataaaaaattat	13460	cctctcacttcaacctccctcacc[a]ttggcagcctagcattagcaggaa	Y	acctccctcacca
3	5899	9523	tctgagccttttaccactccagcc[t]agcccctacccccaattaggagg	15422	aatcaccttccacccttactacac[a]atcaaagacgccctcggcttactt	N	
4	7958	6033	ccttattcgagccgagctgggcca[g]ccaggcaaccttctaggtaacgac	13991	acgagccaaaacctgcccctactc[c]tcctagacctaacctgactagaaa		
5	4998	6625	cacctattctgatttttcggtcac[c]ctgaagtttatattcttatcctac	11623	agacctaaaatcgctcattgcata[c]tcttcaatcagccacatagccctc	Y	ct
6	4978	8482	aaactaccacctacctccctcacc[a]aagcccataaaaataaaaaattat	13460	cctctcacttcaacctccctcacc[a]ttggcagcctagcattagcaggaa	Y	acctccctcacca
7	4909	8814	tgcctcactcatttacaccaacca[c]ccaactatctataaacctagccat	13723	taaacgcctggcagccggaagcct[a]ttcgcaggatttctcattactaac	N	
8	5076	6434	caatataaaaccccctgccataac[c]caataccaaacgcccctcttcgtc	11510	tataatacgcctcacactcattct[c]aacccccctgacaaaacacatagcc	Y	caa
9	4241	9498	gaagtttttttcttcgcaggatttt[t]tctgagccttttaccactccagcc	13739	ggaagcctattcgcaggatttctc[a]ttactaacaacatttcccccgcat	N	
10	9122	6466	aaacgcccctcttcgtctgatccg[t]cctaatcacagcagtcctacttct	15588	atttcctattcgcctacacaattc[t]ccgatccgtccctaacaaactagg	Y	tcc
11	4641	10946	acctttttcctccgaccccctaaca[a]ccccccctcctaatactaactacct	15587	tatttcctattcgcctacacaatt[c]tccgatccgtccctaacaaactag	N	
12	2310	12112	cattctcctcctatccctcaaccc[c]gacatcattaccgggttttcctct	14422	aaacactcaccaagacctcaaccc[c]tgacccccatgcctcaggatactc	Y	cctcaacccc
14	4772	9347	cataacgctcctcatactaggcct[a]ctaaccaacacactaaccatatac	14119	ttacttcctctctttcttcttccc[a]ctcatcctaaccctactcctaatc	Y	act
15	4978	8482	aaactaccacctacctccctcacc[a]aagcccataaaaataaaaaattat	13460	cctctcacttcaacctccctcacc[a]ttggcagcctagcattagcaggaa	Y	acctccctcacca
16	7498	7130	ggctacaccctagaccaaaccta[c]gccaaaatccatttcactatcata	14628	gaaggcttagaagaaaaccccaca[a]accccattactaaacccacactca	N	
18	4978	8482	aaactaccacctacctccctcacc[a]aagcccataaaaataaaaaattat	13460	cctctcacttcaacctccctcacc[a]ttggcagcctagcattagcaggaa	Y	acctccctcacca
19	4978	8482	aaactaccacctacctccctcacc[a]aagcccataaaaataaaaaattat	13460	cctctcacttcaacctccctcacc[a]ttggcagcctagcattagcaggaa	Y	acctccctcacca
22	4978	8482	aaactaccacctacctccctcacc[a]aagcccataaaaataaaaaattat	13460	cctctcacttcaacctccctcacc[a]ttggcagcctagcattagcaggaa	Y	acctccctcacca
23	7355	7168	tcactatcatattcatcggcgtaa[a]tctaactttcttcccacaacactt	14523	aaattaaaaaaactattaaaccc[a]tataacctcccccaaaattcagaa	Y	at
25	4238	9486	tttattacctcagaagtttttttc[t]tcgcaggatttttctgagcctttt	13724	aaacgcctggcagccggaagccta[t]tcgcaggatttctcattactaaca	Y	ttcgcaggattt
26	7144	5772	aaaaggcgggagaagccccggcag[g]tttgaagctgcttcttcgaatttg	12916	catcctcgccttagcatgatttat[c]ctacactccaactcatgagacccac	N	
27	4978	8482	aaactaccacctacctccctcacc[a]aagcccataaaaataaaaaattat	13460	cctctcacttcaacctccctcacc[a]ttggcagcctagcattagcaggaa	Y	acctccctcacca
28	2310	12112	cattctcctcctatccctcaaccc[c]gacatcattaccgggttttcctct	14422	aaacactcaccaagacctcaaccc[c]tgacccccatgcctcaggatactc	Y	cctcaacccc
29	6935	7185	ggcgtaaatctaactttcttccca[c]aacactttctcggcctatccggaa	14120	tacttcctctctttcttcttccca[c]tcatcctaaccctactcctaatca	Y	ttcttcccac
30	8704	7175	catattcatcggcgtaaatctaac[t]ttcttcccacaacactttctcggc	15879	tccctaattgaaaacaaaatactc[a]aatgggcctgtccttgtagtataa	N	
31	3039	10951	ttcctccgacccccctaacaacccc[c]ctcctaatactaactacctgactc	13990	tacgagccaaaacctgcccctact[c]ctcctagacctaacctgactagaa	Y	cctccta
32	6068	8838	ccaactatctataaacctagccat[g]gccatcccctatgagcgggcaca	14906	caccacaggactattcctagccat[g]cactactcaccagacgcctcaacc	Y	cctagccatg

Patient ID - assigned patient identification number for all patients with identified 5' and 3' mtDNA deletion breakpoints; **DelSize** – recorded mtDNA deletion size in base pairs; **5'bp** – 5' mtDNA deletion breakpoint; **5'bp sequence** – 49 nucleotide sequence surrounding the 5' mtDNA deletion breakpoint nucleotide; **3'bp** – 3' mtDNA deletion breakpoint; **3'bp sequence** – 49 nucleotide sequence surrounding the 3' mtDNA deletion breakpoint nucleotide; **Direct repeat (Y/N)** – Is there a repeat sequence of >1 nucleotides around the mtDNA deletion breakpoints (yes or no); **Repeat sequence** – nucleotide sequence repeated at the 5' and 3' mtDNA deletion breakpoints where a direct repeat has been identified.

Patient ID	DelSize	5' bp	5' bp sequence	3' bp	3' bp sequence	Direct repeat (Y/N)	Repeat sequence
33	4754	8287	cgtatttaccctatagcacccccct[c]taccccctctagagcccactgtaa	13041	taggtctccacccctgactcccct[c]agccatagaaggccccaccccagt	Y	cccctc
34	4978	8482	aaactaccacctacctccctcacc[a]aagcccataaaaataaaaaattat	13460	cctctcacttcaacctccctcacc[a]ttggcagcctagcattagcaggaa	Y	acctccctcacca
35	5813	9754	tcctacaagcctcagagtacttcg[a]gtctcccttcaccatttccgacgg	15567	ccccacatcaagcccgaatgatat[t]tcctattcgcctacacaattctcc	N	
37	7977	6537	gctggcatcactatactactaaca[g]accgcaacctcaacaccaccttct	14514	ccccctaaataaattaaaaaaaacta[t]taaacccatataacctcccccaaa	N	
38	4223	9500	agtttttttcttcgcaggatttttt[c]tgagccttttaccactccagccta	13723	taaacgcctggcagccggaagcct[a]ttcgcaggatttctcattactaac	N	
39	4978	8482	aaactaccacctacctccctcacc[a]aagcccataaaaataaaaaattat	13460	cctctcacttcaacctccctcacc[a]ttggcagcctagcattagcaggaa	Y	acctccctcacca
40	2310	12112	cattctcctcctatccctcaaccc[c]gacatcattaccgggttttcctct	14422	aaacactcaccaagacctcaaccc[c]tgacccccatgcctcaggatactc	Y	cctcaacccc
41	6864	7128	tcaggctacaccctagaccaaacc[t]acgccaaaatccatttcactatca	13992	cgagccaaaacctgcccctactcc[t]cctagacctaacctgactagaaaa	Y	cct
44	4391	8576	tcattgcccccacaatcctaggcc[t]acccgccgcagtactgatcattct	12967	ccttctaaacgctaatccaagcc[t]caccccactactaggcctcctccta	Y	gcct
45	4978	8482	aaactaccacctacctccctcacc[a]aagcccataaaaataaaaaattat	13460	cctctcacttcaacctccctcacc[a]ttggcagcctagcattagcaggaa	Y	acctccctcacca
46	6035	8570	cttcattcattgccccacaatcct[a]ggcctacccgccgcagtactgat	14605	tactaaaccccataaataggaga[a]ggcttagaagaaaaccccacaaac	Y	aggcctt
47	4978	8482	aaactaccacctacctccctcacc[a]aagcccataaaaataaaaaattat	13460	cctctcacttcaacctccctcacc[a]ttggcagcctagcattagcaggaa	Y	acctccctcacca
48	4652	10947	ccttttcctccgacccccctaacaa[c]ccccctcctaatactaactacctg	15599	cgcctacacaattctccgatccgt[c]cctaacaaactaggaggcgtcctt	Y	ccc
49	2803	11637	tcattgcatactcttcaatcagcc[a]catagccctcgtagtaacagccat	14440	caacccctgacccccatgcctcag[g]atactcctcaatagccatcgctgt	N	
50	4978	8482	aaactaccacctacctccctcacc[a]aagcccataaaaataaaaaattat	13460	cctctcacttcaacctccctcacc[a]ttggcagcctagcattagcaggaa	Y	acctccctcacca
51	4880	7205	cccacaacactttctcggcctatc[c]ggaatgccccgacgttactcggac	12085	caccctcatgttcatacacctat[c]ccccattctcctcctatccctcaac	Y	cctatc
52	4959	8474	ttaaacacaaactaccacctacct[c]cctcaccaaagcccataaaaataa	13433	aaaataggaggactactcaaaacc[a]tacctctcacttcaacctccctca	N	
53	3539	7729	tgccctttttcctaacactcacaac[a]aaactaactaatactaacatctca	11268	atcgcactaatttacactcacaac[a]ccctaggctcactaaacattctac	Y	acactcacaaca
54	2310	12112	cattctcctcctatccctcaaccc[c]gacatcattaccgggttttcctct	14422	aaacactcaccaagacctcaaccc[c]tgacccccatgcctcaggatactc	Y	cctcaacccc
55	3979	11658	agccacatagccctcgtagtaacag[c]cattctcatccaaaccccctgaag	15637	gaggcgtccttgccctattactat[c]catcctcatcctagcaataatccc	Y	ccat
56	7681	6741	ggtatggtctgagctatgatatca[a]ttggcttcctagggtttatcgtgt	14422	aaacactcaccaagacctcaaccc[c]tgacccccatgcctcaggatactc	N	
57	5222	5999	atgagctggagtcctaggcacagc[t]ctaagcctccttattcgagccgag	11221	tgaacgcaggcacatacttcctat[t]ctacaccctagtaggctcccttcc	Y	tcta
58	4113	11262	tactcatcgcactaatttacactc[a]caacaccctaggctcactaaacat	15375	gaaacgggatcaaacaacccccta[g]gaatcacctcccattccgataaaa	N	
59	4978	8482	aaactaccacctacctccctcacc[a]aagcccataaaaataaaaaattat	13460	cctctcacttcaacctccctcacc[a]ttggcagcctagcattagcaggaa	Y	acctccctcacca
60	4604	9057	actcatgcacctaattggaagcgc[c]accctagcaatatcaaccattaac	13661	caacctcgcttccccaccctact[a]acattaacgaaaataaccccaccc	N	
61	4772	9347	cataacgctcctcatactaggcct[a]ctaaccaacacactaaccatatac	14119	ttacttcctctctttcttcttccc[a]ctcatcctaaccctactcctaatc	Y	act

Patient ID - assigned patient identification number for all patients with identified 5' and 3' mtDNA deletion breakpoints; **DelSize** – recorded mtDNA deletion size in base pairs; **5'bp** – 5' mtDNA deletion breakpoint; **5'bp sequence** – 49 nucleotide sequence surrounding the 5' mtDNA deletion breakpoint nucleotide; **3'bp** – 3' mtDNA deletion breakpoint; **3'bp sequence** – 49 nucleotide sequence surrounding the 3' mtDNA deletion breakpoint nucleotide; **Direct repeat (Y/N)** – Is there a repeat sequence of >1 nucleotides around the mtDNA deletion breakpoints (yes or no); **Repeat sequence** – nucleotide sequence repeated at the 5' and 3' mtDNA deletion breakpoints where a direct repeat has been identified.

Patient ID	DelSize	5' bp	5' bp sequence	3' bp	3' bp sequence	Direct repeat (Y/N)	Repeat sequence
62	6482	7532	acttttttcaaaaaggtattagaaaaa[a]ccatttcataactttgtcaaagt	14014	cctcctagacctaacctgactagaaa[a]gctattacctaaaacaatttagct	Y	tagaaaa
63	6482	7532	acttttttcaaaaaggtattagaaaaa[a]ccatttcataactttgtcaaagt	14014	cctcctagacctaacctgactagaaa[a]gctattacctaaaacaatttagct	Y	tagaaaa
64	7676	6323	agcagggaactactcccaccctgg[a]gcctccgtagacctaaccatcttc	13999	aaacctgcccctactcctcctaga[c]ctaacctgactagaaaagctatta	N	
65	8039	7637	caagacgctacttcccctatcata[g]aagagcttatcacctttcatgatc	15676	caataatccccatcctccatatat[c]caaacaacaaagcataatatttcg	N	
66	5470	6603	ggagaccccattctataccaacac[c]tattctgatttttcggtcaccctg	12073	tcacacgagaaaacaccctcatgt[t]catacacctatcccccattctcct	N	
70	5958	6002	agctggagtcctaggcacagctct[a]agcctccttattcgagccgagctg	11960	tctcctacttacaggactcaacat[a]ctagtcacagccctatactccctc	Y	ta
71	4382	8586	cacaatcctaggcctacccgccgc[a]gtactgatcattctatttccccct	12968	cttctaaacgctaatccaagcctc[a]ccccactactaggcctcctcctag	Y	ca
72	4978	8482	aaactaccacctacctccctcacc[a]aagcccataaaaataaaaaattat	13460	cctctcacttcaacctccctcacc[a]ttggcagcctagcattagcaggaa	Y	acctccctcacca
73	7285	6773	cctagggtttatcgtgtgagcaca[c]catatatttacagtaggaatagac	14058	tttcacagcaccaaatctccacct[c]catcatcacctcaacccaaaaagg	Y	ccat
74	7716	6377	acacctagcaggtgtctcctctat[c]ttaggggccatcaatttcatcacaac	14093	tcaacccaaaaaggcataattaaa[c]tttacttcctctctttcttcttcc	Y	ctt
77	4978	8482	aaactaccacctacctccctcacc[a]aagcccataaaaataaaaaattat	13460	cctctcacttcaacctccctcacc[a]ttggcagcctagcattagcaggaa	Y	acctccctcacca
78	4978	8482	aaactaccacctacctccctcacc[a]aagcccataaaaataaaaaattat	13460	cctctcacttcaacctccctcacc[a]ttggcagcctagcattagcaggaa	Y	acctccctcacca
79	4238	9486	tttattacctcagaagtttttttc[t]tcgcaggatttttctgagccttt	13724	aaacgcctggcagccggaagccta[t]tcgcaggatttctcattactaaca	Y	ttcgcaggattt
80	8560	5942	ttgactattctctacaaaccacaa[a]gacattggaacactatacctatta	14502	tatccaaagacaaccatcattccc[c]ctaaataaattaaaaaaactatta	N	
81	4978	8482	aaactaccacctacctccctcacc[a]aagcccataaaaataaaaaattat	13460	cctctcacttcaacctccctcacc[a]ttggcagcctagcattagcaggaa	Y	acctccctcacca
82	5164	9254	tcatatagtaaaacccagcccatg[a]cccctaacaggggccctctcagcc	14418	actaaaacactcaccaagacctca[a]cccctgacccccatgcctcaggat	Y	acccct
83	4978	8482	aaactaccacctacctccctcacc[a]aagcccataaaaataaaaaattat	13460	cctctcacttcaacctccctcacc[a]ttggcagcctagcattagcaggaa	Y	acctccctcacca
84	7664	6341	ccctggagcctccgtagacctaac[c]atcttctccttacacctagcaggt	14005	gcccctactcctcctagacctaac[c]tgactagaaaagctattacctaaa	Y	tagaccataacc
85	4381	8927	cacttcttaccacaaggcacacct[a]cacccctttatccccatactagtta	13308	aatcggcatcaaccaaccacacct[a]gcattcctgcacatctgtacccac	Y	cacaccta
88	4853	10745	atatggcctagactacgtacataa[c]ctaaacctactccaatgctaaaac	15598	cgcctacacaattctccgatccgtc[c]ctaacaaactaggaggcgtcctt	Y	cctaa
90	5364	6714	ggaaaaaaagaaccatttggatac[a]taggtatggtctgagctatgatat	12078	gagaaaacaccctcatgttcatac[a]cctatcccccattctcctcctatc	Y	ataca
91	7129	8543	gaaccaaaatgaacgaaaatctgt[t]cgcttcattcattgcccccacaat	15672	ctagcaataatccccatcctccat[a]tatccaaacaacaaagcataatat	N	
92	7595	7845	catccctacgcatcctttacataa[c]agacgaggtcaacgatccctccct	15440	ctacacaatcaaagacgccctcgg[c]ttacttctcttccttctctcctta	N	
93	6864	7128	tcaggctacaccctagaccaaacc[t]acgccaaaatccatttcactatca	13992	cgagccaaaacctgcccctactcc[t]cctagacctaacctgactagaaaa	Y	cct
95	4665	10817	ctaccactgacatgactttccaaa[a]aacacataatttgaatcaacacaa	15482	ctccttaatgacattaacactatt[c]tcaccagacctcctaggcgaccca	N	
96	6549	6006	ggagtcctaggcacagctctaagc[c]tccttattcgagccgagctgggcc	12555	actgacactgagccacaacccaaa[c]aacccagctctccctaagcttcaa	N	

Patient ID - assigned patient identification number for all patients with identified 5' and 3' mtDNA deletion breakpoints; **DelSize** – recorded mtDNA deletion size in base pairs; **5'bp** – 5' mtDNA deletion breakpoint; **5'bp sequence** – 49 nucleotide sequence surrounding the 5' mtDNA deletion breakpoint nucleotide; **3'bp** – 3' mtDNA deletion breakpoint; **3'bp sequence** – 49 nucleotide sequence surrounding the 3' mtDNA deletion breakpoint nucleotide; **Direct repeat (Y/N)** – Is there a repeat sequence of >1 nucleotides around the mtDNA deletion breakpoints (yes or no); **Repeat sequence** – nucleotide sequence repeated at the 5' and 3' mtDNA deletion breakpoints where a direct repeat has been identified.

Patient ID	DelSize	5' bp	5' bp sequence	3' bp	3' bp sequence	Direct repeat (Y/N)	Repeat sequence
97	4978	8482	aaactaccacctacctccctcacc[a]aagcccataaaaataaaaaattat	13460	cctctcacttcaacctccctcacc[a]ttggcagcctagcattagcaggaa	Y	acctccctcacca
98	4966	10104	ataatcaacaccctcctagcctta[c]tactaataattattacattttgac	15070	gaggcctatattacggatcatttct[c]tactcagaaacctgaaacatcgg	Y	ctacta
99	2549	10310	atgagccctacaaacaactaacct[g]ccactaatagttatgtcatccctc	12859	agcagccattcaagcaatcctata[c]aaccgtatcggcgatatcggtttc	N	
101	6976	7821	tcatcctagtcctcatcgccctcc[c]atccctacgcatcctttacataac	14797	aataaaattaattaaccactcatt[c]atcgacctccccaccccatccaac	Y	catc
102	3383	6129	ttcatagtaatacccatcataatc[g]gaggctttggcaactgactagttc	9512	tcgcaggatttttctgagcctttt[a]ccactccagcctagcccctacccc	N	
103	7891	6641	cggtcaccctgaagtttatattct[t]atcctaccaggcttcggaataatc	14532	aaactattaaacccatataacct[c]ccccaaaattcagaataataacaca	N	
104	4978	8482	aaactaccacctacctccctcacc[a]aagcccataaaaataaaaaattat	13460	cctctcacttcaacctccctcacc[a]ttggcagcctagcattagcaggaa	Y	acctccctcacca
106	7451	8287	cctatagcacccccctctacccccct[c]tagagcccactgtaaagctaactt	15738	tcactttattgactcctagccgca[g]acctcctcattctaacctgaatcg	N	
107	4978	8482	aaactaccacctacctccctcacc[a]aagcccataaaaataaaaaattat	13460	cctctcacttcaacctccctcacc[a]ttggcagcctagcattagcaggaa	Y	acctccctcacca
108	2307	12115	tctcctcctatccctcaaccccga[c]atcattaccgggttttcctcttgt	14422	aaacactcaccaagacctcaaccc[c]tgacccccatgcctcaggatactc	N	
109	4597	9528	gccttttaccactccagcctagcc[c]ctacccccccaattaggagggcact	14125	cctctctttcttcttcccactcat[c]ctaaccctactcctaatcacataa	Y	ccta
110	5906	8325	aaagctaacttagcattaaccttt[t]aagttaaagattaagagaaccaac	14231	gtaactactactaatcaacgccca[t]aatcatacaaagcccccgcaccaa	Y	taa
112	4599	9752	cctcctacaagcctcagagtactt[c]gagtctcccttcaccatttccgac	14351	taccacaaccaccaccccatcata[c]tctttcacccacagcaccaatcct	N	
113	4978	8482	aaactaccacctacctccctcacc[a]aagcccataaaaataaaaaattat	13460	cctctcacttcaacctccctcacc[a]ttggcagcctagcattagcaggaa	Y	acctccctcacca

Patient ID - assigned patient identification number for all patients with identified 5' and 3' mtDNA deletion breakpoints; **DelSize** – recorded mtDNA deletion size in base pairs; **5'bp** – 5' mtDNA deletion breakpoint; **5'bp sequence** – 49 nucleotide sequence surrounding the 5' mtDNA deletion breakpoint nucleotide; **3'bp** – 3' mtDNA deletion breakpoint; **3'bp sequence** – 49 nucleotide sequence surrounding the 3' mtDNA deletion breakpoint nucleotide; **Direct repeat (Y/N)** – Is there a repeat sequence of >1 nucleotides around the mtDNA deletion breakpoints (yes or no); **Repeat sequence** – nucleotide sequence repeated at the 5' and 3' mtDNA deletion breakpoints where a direct repeat has been identified.

	NMDAS	W/O NMDAS	NMDAS	W/O NMDAS	NMDAS	W.O NMDAS	NMDAS	W/O NMDAS
Patient ID	**SKM het % and mtDNA del size**		**plus fully sequenced breakpoints**		**plus onset age**		**plus COX deficient fibre %**	
1								
2	Y		Y		Y		Y	
3	Y		Y		Y		Y	
4	Y		Y					
5		Y		Y		Y		Y
6	Y		Y					
7					Y		Y	
8					Y		Y	
9	Y		Y		Y		Y	
10	Y		Y		Y		Y	
11	Y		Y		Y		Y	
12	Y		Y		Y		Y	
13								
14	Y		Y				Y	
15		Y		Y				Y
16		Y		Y		Y		Y
17								
18	Y		Y				Y	
19		Y		Y		Y		Y
20								
21								
22		Y		Y				Y
23		Y		Y				Y
24								
25	Y		Y		Y		Y	
26	Y		Y		Y		Y	
27	Y		Y		Y		Y	
28	Y		Y				Y	
29	Y		Y		Y		Y	
30					Y		Y	
31		Y		Y				Y
32	Y		Y		Y		Y	
33	Y		Y		Y		Y	
34	Y		Y		Y		Y	
35	Y		Y		Y		Y	
36						Y		
37		Y		Y				Y
38		Y		Y				Y
39	Y		Y		Y		Y	
40	Y		Y		Y		Y	
41	Y		Y				Y	
42								

Appropriate patient data sets marked '**Y**' where data indicated by column heading was all available for data analysis; **NMAS** where at least one NMDAS test result was available; **W/O NMDAS** where no NMDAS scores were available.

Patient ID - assigned patient identification number; **SKM het % and mtDNA del size** – where mtDNA deletion heteroplasmy level (%) and deletion size (bp) are both available; **plus fully sequenced breakpoints** – where mtDNA deletion heteroplasmy level (%) and deletion breakpoint location are available; **plus onset age** – mtDNA deletion heteroplasmy level and breakpoint locations plus symptom onset age available; **plus COX-deficient fibre %** - mtDNA deletion heteroplasmy level and breakpoint locations plus COX-deficient fibre level (%) available.

	NMDAS	W/O NMDAS	NMDAS	W/O NMDAS	NMDAS	W.O NMDAS	NMDAS	W/O NMDAS
Patient ID	**SKM het %**		**plus fully**		**plus onset**		**plus COX**	
43	Y				Y		Y	
44	Y		Y		Y		Y	
45		Y		Y		Y		Y
46		Y		Y		Y		Y
47								
48		Y		Y		Y		Y
49	Y		Y		Y		Y	
50	Y		Y		Y		Y	
51	Y		Y				Y	
52		Y		Y				
53		Y		Y				Y
54		Y		Y				Y
55		Y		Y				
56		Y		Y				Y
57							Y	
58	Y		Y		Y		Y	
59	Y		Y		Y		Y	
60	Y		Y		Y		Y	
61		Y		Y				Y
62		Y		Y		Y		
63	Y		Y		Y		Y	
64	Y		Y		Y		Y	
65	Y		Y		Y		Y	
66	Y		Y		Y		Y	
67								
68	Y				Y			
69								
70		Y		Y				Y
71	Y		Y		Y		Y	
72		Y		Y				
73		Y		Y				Y
74	Y		Y		Y			
75	Y				Y			
76	Y				Y			
77	Y		Y		Y		Y	
78		Y		Y				Y
79	Y		Y		Y		Y	
80								Y
81	Y		Y		Y		Y	
82	Y		Y		Y		Y	
83		Y		Y				Y
84	Y		Y		Y		Y	

Appropriate patient data sets marked '**Y**' where data indicated by column heading was all available for data analysis; **NMAS** where at least one NMDAS test result was available; **W/O NMDAS** where no NMDAS scores were available.

Patient ID - assigned patient identification number; **SKM het % and mtDNA del size** – where mtDNA deletion heteroplasmy level (%) and deletion size (bp) are both available; **plus fully sequenced breakpoints** – where mtDNA deletion heteroplasmy level (%) and deletion breakpoint location are available; **plus onset age** – mtDNA deletion heteroplasmy level and breakpoint locations plus symptom onset age available; **plus COX-deficient fibre %** - mtDNA deletion heteroplasmy level and breakpoint locations plus COX-deficient fibre level (%) available.

Patient ID	NMDAS SKM het %	W/O NMDAS	NMDAS plus fully	W/O NMDAS	NMDAS plus onset	W.O NMDAS	NMDAS plus COX	W/O NMDAS
85		Y		Y		Y		Y
86		Y				Y		
87								
88		Y		Y				
89								
90	Y		Y				Y	
91								Y
92					Y		Y	
93	Y		Y				Y	
94								
95		Y		Y				
96	Y		Y		Y		Y	
97	Y		Y		Y		Y	
98	Y		Y					
99		Y		Y		Y		
100								
101		Y		Y				
102								Y
103		Y		Y		Y		Y
104		Y		Y				Y
105								
106		Y						
107								
108		Y		Y				Y
109		Y		Y				Y
110		Y		Y				
111								
112		Y		Y				Y
113		Y		Y				Y
Total	49	37	46	36	42	12	46	30

Appropriate patient data sets marked '**Y**' where data indicated by column heading was all available for data analysis; **NMAS** where at least one NMDAS test result was available; **W/O NMDAS** where no NMDAS scores were available.
Patient ID - assigned patient identification number; **SKM het % and mtDNA del size** – where mtDNA deletion heteroplasmy level (%) and deletion size (bp) are both available; **plus fully sequenced breakpoints** – where mtDNA deletion heteroplasmy level (%) and deletion breakpoint location are available; **plus onset age** – mtDNA deletion heteroplasmy level and breakpoint locations plus symptom onset age available; **plus COX-deficient fibre %** - mtDNA deletion heteroplasmy level and breakpoint locations plus COX-deficient fibre level (%) available.

References

References

Abrahams, J.P., Leslie, A.G.W., Lutter, R. and Walker, J.E. (1994) 'Structure at 2.8 A resolution of F1-ATPase from bovine heart mitochondria', *Nature*, 370(6491), pp. 621-628.

Abu-Amero, K.K. (2011) 'Leber's Hereditary Optic Neuropathy: The Mitochondrial Connection Revisited', *Middle East African journal of ophthalmology*, 18(1), pp. 17-23.

Acehan, D., Jiang, X.J., Morgan, D.G., Heuser, J.E., Wang, X.D. and Akey, C.W. (2002) 'Three-dimensional structure of the apoptosome: Implications for assembly, procaspase-9 binding, and activation', *Molecular Cell*, 9(2), pp. 423-432.

Ahmed, A.U. and Fisher, P.R. (2009) 'IMPORT OF NUCLEAR-ENCODED MITOCHONDRIAL PROTEINS: A COTRANSLATIONAL PERSPECTIVE', in Jeon, K.W. (ed.) *International Review of Cell and Molecular Biology, Vol 273*. San Diego: Elsevier Academic Press Inc, pp. 49-68.

Al Rawi, S., Louvet-Vallée, S., Djeddi, A., Sachse, M., Culetto, E., Hajjar, C., Boyd, L., Legouis, R. and Galy, V. (2011) 'Postfertilization Autophagy of Sperm Organelles Prevents Paternal Mitochondrial DNA Transmission', *Science*, 334(6059), pp. 1144-1147.

Aloni, Y. and Attardi, G. (1971) 'Symmetrical in vivo transcription of mitochondrial DNA in HeLa cells', *Proceedings of the National Academy of Sciences of the United States of America*, 68(8), pp. 1757-1761.

Alonso, A., Martin, P., Albarran, C., Aguilera, B., Garcia, O., Guzman, A., Oliva, H. and Sancho, M. (1997) 'Detection of somatic mutations in the mitochondrial DNA control region of colorectal and gastric tumors by heteroduplex and single-strand conformation analysis', *Electrophoresis*, 18(5), pp. 682-685.

Anderson, S., Bankier, A.T. and Barrell, B.G. (1981a) 'Sequence and organization of the human mitochondrial genome', *Nature*, 290(5806), pp. 457-465.

Anderson, S., Bankier, A.T., Barrell, B.G., de Bruijn, M.H.L., Coulson, A.R., Drouin, J., Eperon, I.C., Nierlich, D.P., Roe, B.A., Sanger, F., Schreier, P.H., Smith, A.J.H., Staden, R. and Young, I.G. (1981b) 'Sequence and organization of the human mitochondrial genome', *Nature*, 290(5806), pp. 457-465.

Andersson, S.G.E., Zomorodipour, A., Andersson, J.O., Sicheritz-Ponten, T., Alsmark, U.C.M., Podowski, R.M., Naslund, A.K., Eriksson, A.-S., Winkler, H.H. and Kurland, C.G. (1998) 'The genome sequence of Rickettsia prowazekii and the origin of mitochondria', *Nature*, 396(6707), pp. 133-140.

Andrews, R.M., Kubacka, I., Chinnery, P.F., Lightowlers, R.N., Turnbull, D.M. and Howell, N. (1999) 'Reanalysis and revision of the Cambridge reference sequence for human mitochondrial DNA', *Nature Genetics*, 23(2), pp. 147-147.

Antonsson, B., Montessuit, S., Sanchez, B. and Martinou, J.C. (2001) 'Bax is present as a high molecular weight oligomer/complex in the mitochondrial membrane of apoptotic cells', *Journal of Biological Chemistry*, 276(15), pp. 11615-11623.

Arii, J. and Tanabe, Y. (2000) 'Leigh syndrome: Serial MR imaging clinical follow-up', *American Journal of Neuroradiology*, 21(8), pp. 1502-1509.

Ashkenazi, A. (2008) 'Targeting the extrinsic apoptosis pathway in cancer', *Cytokine & Growth Factor Reviews*, 19(3–4), pp. 325-331.

Aure, K., Ogier De Baulny, H., Laforet, P., Jardel, C., Eymard, B. and Lombes, A. (2007) 'Chronic progressive ophthalmoplegia with large-scale mtDNA rearrangement: Can we predict progression?', *Brain*, 130(6), pp. 1516-1524.

Bai, R.K., Perng, C.L., Hsu, C.H. and Wong, L.J.C. (2004) 'Quantitative PCR analysis of mitochondrial DNA content in patients with mitochondrial disease', in Lee, H.K., DiMauro, S., Tanaka, M. and Wei, Y.H. (eds.) *Mitochondrial Pathogenesis: From Genes and Apoptosis to Aging and Disease*. New York: New York Acad Sciences, pp. 304-309.

Bao, Q., Riedl, S.J. and Shi, Y.G. (2005) 'Structure of Apaf-1 in the auto-inhibited form - A critical role for ADP', *Cell Cycle*, 4(8), pp. 1001-1003.

Barrell, B.G., Anderson, S. and Bankier, A.T. (1980) 'Different pattern of codon recognition by mammalian mitochondrial tRNAs', *Proceedings of the National Academy of Sciences of the United States of America*, 77(6 I), pp. 3164-3166.

Beinert, H., Holm, R.H. and Münck, E. (1997) 'Iron-Sulfur Clusters: Nature's Modular, Multipurpose Structures', *Science*, 277(5326), pp. 653-659.

Bender, A., Krishnan, K.J., Morris, C.M., Taylor, G.A., Reeve, A.K., Perry, R.H., Jaros, E., Hersheson, J.S., Betts, J., Klopstock, T., Taylor, R.W. and Turnbull, D.M. (2006) 'High levels of mitochondrial DNA deletions in substantia nigra neurons in aging and Parkinson disease', *Nature Genetics*, 38(5), pp. 515-517.

Berg, O.G. and Kurland, C.G. (2000) 'Why mitochondrial genes are most often found in nuclei', *Molecular Biology and Evolution*, 17(6), pp. 951-961.

Bergstrom, C.T. and Pritchard, J. (1998) 'Germline bottlenecks and the evolutionary maintenance of mitochondrial genomes', *Genetics*, 149(4), pp. 2135-2146.

Bernes, S.M., Bacino, C., Prezant, T.R., Pearson, M.A., Wood, T.S., Fournier, P. and Fischelghodsian, N. (1993) 'IDENTICAL MITOCHONDRIAL-DNA DELETION IN MOTHER WITH PROGRESSIVE EXTERNAL OPHTHALMOPLEGIA AND SON WITH PEARSON MARROW-PANCREAS SYNDROME', *Journal of Pediatrics*, 123(4), pp. 598-602.

Berridge, M.J., Lipp, P. and Bootman, M.D. (2000) 'The versatility and universality of calcium signalling', *Nature Reviews Molecular Cell Biology*, 1(1), pp. 11-21.

Berry, E.A., Guergova-Kuras, M., Huang, L.S. and Crofts, A.R. (2000) 'Structure and function of cytochrome bc complexes', *Annual Review of Biochemistry*, 69, pp. 1005-1075.

Bindoff, L.A., Desnuelle, C., Birchmachin, M.A., Pellissier, J.F., Serratrice, G., Dravet, C., Bureau, M., Howell, N. and Turnbull, D.M. (1991) 'MULTIPLE DEFECTS OF THE MITOCHONDRIAL RESPIRATORY-CHAIN IN A MITOCHONDRIAL ENCEPHALOPATHY (MERRF) - A CLINICAL, BIOCHEMICAL AND MOLECULAR STUDY', *Journal of the Neurological Sciences*, 102(1), pp. 17-24.

Birky, C.W. (2001) 'The inheritance of genes in mitochondria and chloroplasts: Laws, mechanisms, and models', *Annual Review of Genetics*, 35, pp. 125-148.

Blackwood, J.K., Whittaker, R.G., Blakely, E.L., Alston, C.L., Turnbull, D.M. and Taylor, R.W. (2010) 'The investigation and diagnosis of pathogenic mitochondrial DNA mutations in human urothelial cells', *Biochemical and Biophysical Research Communications*, 393(4), pp. 740-745.

Bleazard, W., McCaffery, J.M., King, E.J., Bale, S., Mozdy, A., Tieu, Q., Nunnari, J. and Shaw, J.M. (1999) 'The dynamin-related GTPase Dnm1 regulates mitochondrial fission in yeast', *Nature Cell Biology*, 1(5), pp. 298-304.

Bodyak, N.D., Nekhaeva, E., Wei, J.Y. and Khrapko, K. (2001) 'Quantification and sequencing of somatic deleted mtDNA in single cells: Evidence for partially duplicated mtDNA in aged human tissues', *Human Molecular Genetics*, 10(1), pp. 17-24.

Boffoli, D., Scacco, S.C., Vergari, R., Solarino, G., Santacroce, G. and Papa, S. (1994) 'Decline with age of the respiratory chain activity in human skeletal muscle', *Biochimica et Biophysica Acta (BBA)-Molecular Basis of Disease*, 1226(1), pp. 73-82.

Bogenhagen, D. and Clayton, D.A. (1974) 'The number of mitochondrial deoxyribonucleic acid genomes in mouse L and human HeLa cells. Quantitative isolation of mitochondrial deoxyribonucleic acid', *Journal of Biological Chemistry*, 249(24), pp. 7991-7995.

Bogenhagen, D. and Clayton, D.A. (1977) 'Mouse l cell mitochondrial DNA molecules are selected randomly for replication throughout the cell cycle', *Cell*, 11(4), pp. 719-727.

Bogenhagen, D.F. (1999) 'Repair of mtDNA in vertebrates', *American Journal of Human Genetics*, 64(5), pp. 1276-1281.

Bogenhagen, D.F., Rousseau, D. and Burke, S. (2008) 'The layered structure of human mitochondrial DNA nucleoids', *Journal of Biological Chemistry*, 283(6), pp. 3665-3675.

Bohr, V.A. (2002) 'Repair of oxidative DNA damage in nuclear and mitochondrial DNA, and some changes with aging in mammalian cells', *Free Radical Biology and Medicine*, 32(9), pp. 804-812.

Borst, P. (1977) 'Structure and function of mitochondrial DNA', *Trends in Biochemical Sciences*, 2(2), pp. 31-34.

Borst, P. and Ruttenberg, G.J. (1966) 'Renaturation of mitochondrial DNA', *Biochimica Et Biophysica Acta*, 114(3), pp. 645-7.

Box, G.E.P. and Cox, D.R. (1964) 'An Analysis of Transformations', *Journal of the Royal Statistical Society. Series B (Methodological)*, 26(2), pp. 211-252.

Boyer, P.D. (1975) 'MODEL FOR CONFORMATIONAL COUPLING OF MEMBRANE-POTENTIAL AND PROTON TRANSLOCATION TO ATP SYNTHESIS AND TO ACTIVE-TRANSPORT', *FEBS Letters*, 58(1), pp. 1-6.

Boyer, P.D. (1997) 'The ATP synthase - A splendid molecular machine', *Annual Review of Biochemistry*, 66, pp. 717-749.

Bredenoord, A.L., Dondorp, W., Pennings, G., De Die-Smulders, C.E.M. and De Wert, G. (2008) 'PGD to reduce reproductive risk: the case of mitochondrial DNA disorders', *Human Reproduction*, 23(11), pp. 2392-2401.

Brewer, B.J. and Fangman, W.L. (1987) 'The localization of replication origins on ARS plasmids in S. cerevisiae', *Cell*, 51(3), pp. 463-471.

Brewer, B.J. and Fangman, W.L. (1988) 'A replication fork barrier at the 3’ end of yeast ribosomal RNA genes', *Cell*, 55(4), pp. 637-643.

Brierley, E.J., Johnson, M.A., Lightowlers, R.N., James, O.F.W. and Turnbull, D.M. (1998) 'Role of mitochondrial DNA mutations in human aging: Implications for the central nervous system and muscle', *Annals of Neurology*, 43(2), pp. 217-223.

Brown, W.M., George, M. and Wilson, A.C. (1979) 'RAPID EVOLUTION OF ANIMAL MITOCHONDRIAL-DNA', *Proceedings of the National Academy of Sciences of the United States of America*, 76(4), pp. 1967-1971.

Bua, E., Johnson, J., Herbst, A., Delong, B., McKenzie, D., Salamat, S. and Aiken, J.M. (2006) 'Mitochondrial DNA-deletion mutations accumulate intracellularly to detrimental levels in aged human skeletal muscle fibers', *American Journal of Human Genetics*, 79(3), pp. 469-480.

Cao, L., Shitara, H., Horii, T., Nagao, Y., Imai, H., Abe, K., Hara, T., Hayashi, J.-I. and Yonekawa, H. (2007) 'The mitochondrial bottleneck occurs without reduction of mtDNA content in female mouse germ cells', *Nat Genet*, 39(3), pp. 386-390.

Cao, Z.J., Wanagat, J., McKiernan, S.H. and Aiken, J.M. (2001) 'Mitochondrial DNA deletion mutations are concomitant with ragged red regions of individual, aged muscle fibers: analysis by laser-capture microdissection', *Nucleic Acids Research*, 29(21), pp. 4502-4508.

Capaldi, R.A., Aggeler, R., Gilkerson, R., Hanson, G., Knowles, M., Marcus, A., Margineantu, D., Marusich, M., Murray, J., Oglesbee, D., Remington, S.J. and Rossignol, R. (2002) 'A replicating module as the unit of mitochondrial structure and functioning', *Biochimica et Biophysica Acta - Bioenergetics*, 1555(1-3), pp. 192-195.

Carroll, J., Fearnley, I.M., Shannon, R.J., Hirst, J. and Walker, J.E. (2003) 'Analysis of the subunit composition of complex I from bovine heart mitochondria', *Molecular & Cellular Proteomics*, 2(2), pp. 117-126.

Carroll, J., Fearnley, I.M., Skehel, J.M., Shannon, R.J., Hirst, J. and Walker, J.E. (2006) 'Bovine Complex I Is a Complex of 45 Different Subunits', *Journal of Biological Chemistry*, 281(43), pp. 32724-32727.

Chan, D.C. (2006) 'Mitochondrial fusion and fission in mammals', in *Annual Review of Cell and Developmental Biology*. pp. 79-99.

Chan, David C. and Schon, Eric A. (2012) 'Eliminating Mitochondrial DNA from Sperm', *Developmental Cell*, 22(3), pp. 469-470.

Chance, B. (1965) 'THE ENERGY-LINKED REACTION OF CALCIUM WITH MITOCHONDRIA', *The Journal of biological chemistry*, 240, pp. 2729-48.

Chang, D.D. and Clayton, D.A. (1984) 'Precise identification of individual promoters for transcription of each strand of human mitochondrial DNA', *Cell*, 36(3), pp. 635-643.

Chinnery, P.F., DiMauro, S., Shanske, S., Schon, E.A., Zeviani, M., Mariotti, C., Carrara, F., Lombes, A., Laforet, P., Ogier, H., Jaksch, M., Lochmüller, H., Horvath, R., Deschauer, M., Thorburn, D.R., Bindoff, L.A., Poulton, J., Taylor, R.W., Matthews, J.N.S. and Turnbull, D.M. 'Risk of developing a mitochondrial DNA deletion disorder', *The Lancet*, 364(9434), pp. 592-596.

Chinnery, P.F., Howel, D., Turnbull, D.M. and Johnson, M.A. (2003) 'Clinical progression of mitochondrial myopathy is associated with the random accumulation of cytochrome c oxidase negative skeletal muscle fibres', *Journal of the Neurological Sciences*, 211(1–2), pp. 63-66.

Chinnery, P.F., Johnson, M.A., Wardell, T.M., Singh-Kler, R., Hayes, C., Brown, D.T., Taylor, R.W., Bindoff, L.A. and Turnbull, D.M. (2000a) 'The epidemiology of pathogenic mitochondrial DNA mutations', *Annals of Neurology*, 48(2), pp. 188-193.

Chinnery, P.F. and Samuels, D.C. (1999) 'Relaxed replication of mtDNA: A model with implications for the expression of disease', *American Journal of Human Genetics*, 64(4), pp. 1158-1165.

Chinnery, P.F., Taylor, D.J., Manners, D., Styles, P. and Lodi, R. (2001) 'No correlation between muscle A3243G: mutation load and mitochondrial function in vivo', *Neurology*, 56(8), pp. 1101-1104.

Chinnery, P.F., Thorburn, D.R., Samuels, D.C., White, S.L., Dahl, H.-H.M., Turnbull, D.M., Lightowlers, R.N. and Howell, N. (2000b) 'The inheritance of mitochondrial DNA heteroplasmy: random drift, selection or both?', *Trends in Genetics*, 16(11), pp. 500-505.

Chinnery, P.F. and Turnbull, D.M. (1997) 'Clinical features, investigation, and management of patients with defects of mitochondrial DNA', *Journal of Neurology, Neurosurgery & Psychiatry*, 63(5), pp. 559-563.

Christianson, T.W. and Clayton, D.A. (1988) 'A TRIDECAMER DNA-SEQUENCE SUPPORTS HUMAN MITOCHONDRIAL RNA 3'-END FORMATION INVITRO', *Molecular and Cellular Biology*, 8(10), pp. 4502-4509.

Cipolat, S., de Brito, O.M., Dal Zilio, B. and Scorrano, L. (2004) 'OPA1 requires mitofusin 1 to promote mitochondrial fusion', *Proceedings of the National Academy of Sciences of the United States of America*, 101(45), pp. 15927-15932.

Clark, C.G. and Roger, A.J. (1995) 'DIRECT EVIDENCE FOR SECONDARY LOSS OF MITOCHONDRIA IN ENTAMOEBA-HISTOLYTICA', *Proceedings of the National Academy of Sciences of the United States of America*, 92(14), pp. 6518-6521.

Clay Montier, L.L., Deng, J.J. and Bai, Y. (2009) 'Number matters: control of mammalian mitochondrial DNA copy number', *Journal of Genetics and Genomics*, 36(3), pp. 125-131.

Clayton, D.A. (1982) 'Replication of animal mitochondrial DNA', *Cell*, 28(4), pp. 693-705.

Clayton, D.A., Doda, J.N. and Friedber.Ec (1974) 'ABSENCE OF A PYRIMIDINE DIMER REPAIR MECHANISM IN MAMMALIAN MITOCHONDRIA', *Proceedings of the National Academy of Sciences of the United States of America*, 71(7), pp. 2777-2781.

Collins, S. and Meyer, T. (2010) 'CELL BIOLOGY A sensor for calcium uptake', *Nature*, 467(7313), pp. 283-283.

Collinson, I.R., Runswick, M.J., Buchanan, S.K., Fearnley, I.M., Skehel, J.M., Vanraaij, M.J., Griffiths, D.E. and Walker, J.E. (1994) 'F-0 MEMBRANE DOMAIN OF ATP SYNTHASE FROM BOVINE HEART-MITOCHONDRIA - PURIFICATION, SUBUNIT COMPOSITION, AND RECONSTITUTION WITH F1-ATPASE', *Biochemistry*, 33(25), pp. 7971-7978.

Cooper, J.M., Mann, V.M. and Schapira, A.H.V. (1992) 'Analyses of mitochondrial respiratory chain function and mitochondrial DNA deletion in human skeletal muscle: effect of ageing', *Journal of the Neurological Sciences*, 113(1), pp. 91-98.

Cortopassi, G.A. and Arnheim, N. (1990) 'Detection of a specific mitochondrial DNA deletion in tissues of older humans', *Nucleic Acids Research*, 18(23), pp. 6927-6933.

Cote, H.C.F., Brumme, Z.L., Craib, K.J.P., Alexander, C.S., Wynhoven, B., Ting, L.L., Wong, H., Harris, M., Harrigan, P.R., O'Shaughnessy, M.V. and Montaner, J.S.G. (2002) 'Changes in mitochondrial DNA as a marker of nucleoside toxicity in HIV-infected patients', *New England Journal of Medicine*, 346(11), pp. 811-820.

Cox, G.B., Jans, D.A., Fimmel, A.L., Gibson, F. and Hatch, L. (1984) 'HYPOTHESIS - THE MECHANISM OF ATP SYNTHASE - CONFORMATIONAL CHANGE BY ROTATION OF THE B-SUBUNIT', *Biochimica Et Biophysica Acta*, 768(3-4), pp. 201-208.

Craven, L., Tuppen, H.A., Greggains, G.D., Harbottle, S.J., Murphy, J.L., Cree, L.M., Murdoch, A.P., Chinnery, P.F., Taylor, R.W., Lightowlers, R.N., Herbert, M. and Turnbull, D.M. (2010) 'Pronuclear transfer in human embryos to prevent transmission of mitochondrial DNA disease', *Nature*, 465(7294), pp. 82-85.

Cree, L.M., Samuels, D.C., de Sousa Lopes, S.C., Rajasimha, H.K., Wonnapinij, P., Mann, J.R., Dahl, H.-H.M. and Chinnery, P.F. (2008) 'A reduction of mitochondrial DNA molecules during embryogenesis explains the rapid segregation of genotypes', *Nat Genet*, 40(2), pp. 249-254.

D'Aurelio, M., Gajewski, C.D., Lenaz, G. and Manfredi, G. (2006) 'Respiratory chain supercomplexes set the threshold for respiration defects in human mtDNA mutant cybrids', *Human Molecular Genetics*, 15(13), pp. 2157-2169.

Davis, A.F. and Clayton, D.A. (1996) 'In situ localization of mitochondrial DNA replication in intact mammalian cells', *Journal of Cell Biology*, 135(4), pp. 883-893.

De Grey, A.D.N.J. (1997) 'A proposed refinement of the mitochondrial free radical theory of aging', *BioEssays*, 19(2), pp. 161-166.

De Grey, A.D.N.J. (2003) 'Mechanisms underlying the age-related accumulation of mutant mitochondrial DNA: a critical review', *Genetics of Mitochondrial Diseases*.

Degoul, F., Nelson, I., Amselem, S., Romero, N., Obermaier-Kusser, B., Ponsot, G., Marsac, C. and Lestienne, P. (1991) 'Different mechanisms inferred from sequences of

human mitochondrial DNA deletions in ocular myopathies', *Nucleic Acids Research*, 19(3), pp. 493-496.

DeLuca, Steven Z. and O'Farrell, Patrick H. (2012) 'Barriers to Male Transmission of Mitochondrial DNA in Sperm Development', *Developmental Cell*, 22(3), pp. 660-668.

Detmer, S.A. and Chan, D.C. (2007) 'Functions and dysfunctions of mitochondrial dynamics', *Nat Rev Mol Cell Biol*, 8(11), pp. 870-879.

Devenish, R.J., Prescott, M. and Rodgers, A.J.W. (2008) 'The structure and function of mitochondrial F(1)F(0)-ATP synthases', in Jeon, K.W. (ed.) *International Review of Cell and Molecular Biology, Vol 267*. pp. 1-+.

Di Donato, S. (2009) 'Multisystem manifestations of mitochondrial disorders', *Journal of Neurology*, 256(5), pp. 693-710.

Diaz, F., Bayona-Bafaluy, M.P., Rana, M., Mora, M., Hao, H. and Moraes, C.T. (2002) 'Human mitochondrial DNA with large deletions repopulates organelles faster than full-length genomes under relaxed copy number control', *Nucleic Acids Research*, 30(21), pp. 4626-4633.

DiMauro, S., Hirano, M. and Schon, E.A. (2006) 'Approaches to the treatment of mitochondrial diseases', *Muscle & Nerve*, 34(3), pp. 265-283.

Durham, S.E., Bonilla, E., Samuels, D.C., DiMauro, S. and Chinnery, P.F. (2005) 'Mitochondrial DNA copy number threshold in mtDNA depletion myopathy', *Neurology*, 65(3), pp. 453-455.

Durham, S.E., Brown, D.T., Turnbull, D.M. and Chinnery, P.F. (2006) 'Progressive depletion of mtDNA in mitochondrial myopathy', *Neurology*, 67(3), pp. 502-504.

Durham, S.E., Samuels, D.C., Cree, L.M. and Chinnery, P.F. (2007) 'Normal Levels of Wild-Type Mitochondrial DNA Maintain Cytochrome c Oxidase Activity for Two Pathogenic Mitochondrial DNA Mutations but Not for m.3243A'G', *American Journal of Human Genetics*, 81(1), pp. 189-195.

Edmonds, J.L. (2004) 'Surgical and anesthetic management of patients with mitochondrial dysfunction', *Mitochondrion*, 4(5-6), pp. 543-548.

Elliott, H.R., Samuels, D.C., Eden, J.A., Relton, C.L. and Chinnery, P.F. (2008) 'Pathogenic mitochondrial DNA mutations are common in the general population', *American Journal of Human Genetics*, 83(2), pp. 254-260.

Elson, J.L., Samuels, D.C., Johnson, M.A., Turnbull, D.M. and Chinnery, P.F. (2002) 'The length of cytochrome c oxidase-negative segments in muscle fibres in patients with mtDNA myopathy', *Neuromuscular Disorders*, 12(9), pp. 858-864.

Elson, J.L., Samuels, D.C., Turnbull, D.M. and Chinnery, P.F. (2001) 'Random intracellular drift explains the clonal expansion of mitochondrial DNA mutations with age', *American Journal of Human Genetics*, 68(3), pp. 802-806.

Embley, T.M. and Martin, W. (2006) 'Eukaryotic evolution, changes and challenges', *Nature*, 440(7084), pp. 623-630.

Engel, W.K. and Cunningham, G.G. (1963) 'Rapid Examination Of Muscle Tissue. An Improved Trichrome Method For Fresh-Frozen Biopsy Sections', *Neurology*, 13, pp. 919-23.

Escobar-Henriques, M. and Anton, F. (2012) 'Mechanistic perspective of mitochondrial fusion: Tubulation vs. fragmentation', *Biochimica et Biophysica Acta (BBA) - Molecular Cell Research*, (0).

Eskes, R., Desagher, S., Antonsson, B. and Martinou, J.C. (2000) 'Bid induces the oligomerization and insertion of Bax into the outer mitochondrial membrane', *Molecular and Cellular Biology*, 20(3), pp. 929-935.

Evans, W. (1997) 'Functional and metabolic consequences of sarcopenia', *Journal of Nutrition*, 127(5 SUPPL.), pp. 998S-1003S.

Falkenberg, M., Larsson, N.-G. and Gustafsson, C.M. (2007) 'DNA replication and transcription in mammalian mitochondria', in *Annual Review of Biochemistry*. pp. 679-699.

Faxen, K., Gilderson, G., Adelroth, P. and Brzezinski, P. (2005) 'A mechanistic principle for proton pumping by cytochrome c oxidase', *Nature*, 437(7056), pp. 286-289.

Fearnley, J.M. and Lees, A.J. (1991) 'Ageing and Parkinson's disease: Substantia nigra regional selectivity', *Brain*, 114(5), pp. 2283-2301.

Finsterer, J. (2008) 'Leigh and Leigh-Like Syndrome in Children and Adults', *Pediatric Neurology*, 39(4), pp. 223-235.

Fischel-Ghodsian, N. (2000) 'Homoplasmic Mitochondrial DNA Diseases as the Paradigm to Understand the Tissue Specificity and Variable Clinical Severity of Mitochondrial Disorders', *Molecular Genetics and Metabolism*, 71(1–2), pp. 93-99.

Fleming, J.E., Miquel, J., Cottrell, S.F., Yengoyan, L.S. and Economos, A.C. (1982) 'Is cell aging caused by respiration-dependent injury to the mitochondrial genome?', *Gerontology*, 28(1), p. 44.

Fraser, J.A., Biousse, V. and Newman, N.J. (2010) 'The Neuro-ophthalmology of Mitochondrial Disease', *Survey of Ophthalmology*, 55(4), pp. 299-334.

Friedrich, T. and Scheide, D. (2000) 'The respiratory complex I of bacteria, archaea and eukarya and its module common with membrane-bound multisubunit hydrogenases', *FEBS Letters*, 479(1-2), pp. 1-5.

Fukui, H. and Moraes, C.T. (2009) 'Mechanisms of formation and accumulation of mitochondrial DNA deletions in aging neurons', *Human Molecular Genetics*, 18(6), pp. 1028-1036.

Gaballo, A. and Papa, S. (2007) '1.6 The Mitochondrial F1Fo ATP Synthase', in Lajtha, A., Gibson, G. and Dienel, G. (eds.) *Handbook of Neurochemistry and Molecular Neurobiology*. Springer US, pp. 119-134.

Gao, X.G., Wen, X.L., Esser, L., Quinn, B., Yu, L., Yu, C.A. and Xia, D. (2003) 'Structural basis for the quinone reduction in the bc(1) complex: A comparative analysis of crystal structures of mitochondrial cytochrome bc(1) with bound substrate and inhibitors at the Qi site', *Biochemistry*, 42(30), pp. 9067-9080.

Gardner, J., Craven, L., Turnbull, D. and Taylor, R. (2007) 'Experimental Strategies Towards Treating Mitochondrial DNA Disorders', *Bioscience Reports*, 27(1), pp. 139-150.

Gelfand, R. and Attardi, G. (1981) 'Synthesis and turnover of mitochondrial ribonucleic acid in HeLa cells: The mature ribosomal and messenger ribonucleic acid species are metabolically unstable', *Molecular and Cellular Biology*, 1(6), pp. 497-511.

Gerbitz, K.D., Vandenouweland, J.M.W., Maassen, J.A. and Jaksch, M. (1995) 'MITOCHONDRIAL DIABETES-MELLITUS - A REVIEW', *Biochimica Et Biophysica Acta-Molecular Basis of Disease*, 1271(1), pp. 253-260.

Giles, R.E., Blanc, H., Cann, H.M. and Wallace, D.C. (1980) 'MATERNAL INHERITANCE OF HUMAN MITOCHONDRIAL-DNA', *Proceedings of the National Academy of Sciences of the United States of America-Biological Sciences*, 77(11), pp. 6715-6719.

Gilkerson, R.W., Schon, E.A., Hernandez, E. and Davidson, M.M. (2008) 'Mitochondrial nucleoids maintain genetic autonomy but allow for functional complementation', *Journal of Cell Biology*, 181(7), pp. 1117-1128.

Gincel, D., Zaid, H. and Shoshan-Barmatz, V. (2001) 'Calcium binding and translocation by the voltage-dependent anion channel: a possible regulatory mechanism in mitochondrial function', *Biochemical Journal*, 358, pp. 147-155.

Gokey, N.G., Cao, Z.J., Pak, J.W., Lee, D., McKiernan, S.H., McKenzie, D., Weindruch, R. and Aiken, J.M. (2004) 'Molecular analyses of mtDNA deletion mutations in microdissected skeletal muscle fibers from aged rhesus monkeys', *Aging Cell*, 3(5), pp. 319-326.

Goto, Y., Koga, Y., Horai, S. and Nonaka, I. (1990a) 'CHRONIC PROGRESSIVE EXTERNAL OPHTHALMOPLEGIA - A CORRELATIVE STUDY OF MITOCHONDRIAL-DNA DELETIONS AND THEIR PHENOTYPIC-EXPRESSION IN MUSCLE BIOPSIES', *Journal of the Neurological Sciences*, 100(1-2), pp. 63-69.

Goto, Y.I., Nonaka, I. and Horai, S. (1990b) 'A mutation in the tRNA(Leu(UUR)) gene associated with the MELAS subgroup of mitochondrial encephalomyopathies', *Nature*, 348(6302), pp. 651-653.

Gray, H. and Tai Wai, W. (1992) 'Purification and identification of subunit structure of the human mitochondrial DNA polymerase', *Journal of Biological Chemistry*, 267(9), pp. 5835-5841.

Greaves, L.C., Yu-Wai-Man, P., Blakely, E.L., Krishnan, K.J., Beadle, N.E., Kerin, J., Barron, M.J., Griffiths, P.G., Dickinson, A.J., Turnbull, D.M. and Taylor, R.W. (2010) 'Mitochondrial DNA Defects and Selective Extraocular Muscle Involvement in CPEO', *Investigative Ophthalmology & Visual Science*, 51(7), pp. 3340-3346.

Griffiths, G.J., Dubrez, L., Morgan, C.P., Jones, N.A., Whitehouse, J., Corfe, B.M., Dive, C. and Hickman, J.A. (1999) 'Cell damage-induced conformational changes of the pro-apoptotic protein Bak in vivo precede the onset of apoptosis', *J Cell Biol*, 144(5), pp. 903-14.

Grohmann, K., Amalric, F., Crews, S. and Attardi, G. (1978) 'Failure to detect 'cap' structures in mitochondrial DNA-coded poly(A)-containing RNA from HeLa cells', *Nucleic Acids Research*, 5(3), pp. 637-651.

Guja, K.E. and Garcia-Diaz, M. (2012) 'Hitting the brakes: Termination of mitochondrial transcription', *Biochimica et Biophysica Acta (BBA) - Gene Regulatory Mechanisms*, 1819(9–10), pp. 939-947.

Gunter, T.E. and Sheu, S.S. (2009) 'Characteristics and possible functions of mitochondrial Ca2+ transport mechanisms', *Biochimica Et Biophysica Acta-Bioenergetics*, 1787(11), pp. 1291-1308.

Guo, X., Kudryavtseva, E., Bodyak, N., Nicholas, A., Dombrovsky, I., Yang, D., Kraytsberg, Y., Simon, D.K. and Khrapko, K. (2010) 'Mitochondrial DNA deletions in mice in men: Substantia nigra is much less affected in the mouse', *Biochimica et Biophysica Acta (BBA) - Bioenergetics*, 1797(6–7), pp. 1159-1162.

Haber, J.E. (2000) 'Partners and pathways - Repairing a double-strand break', *Trends in Genetics*, 16(6), pp. 259-264.

Hägerhäll, C. (1997) 'Succinate: quinone oxidoreductases: Variations on a conserved theme', *Biochimica et Biophysica Acta (BBA) - Bioenergetics*, 1320(2), pp. 107-141.

Hales, K.G. and Fuller, M.T. (1997) 'Developmentally Regulated Mitochondrial Fusion Mediated by a Conserved, Novel, Predicted GTPase', *Cell*, 90(1), pp. 121-129.

Halestrap, A.P. (2009) 'What is the mitochondrial permeability transition pore?', *Journal of Molecular and Cellular Cardiology*, 46(6), pp. 821-831.

Haque, M.E., Grasso, D. and Spremulli, L.L. (2008) 'The interaction of mammalian mitochondrial translational initiation factor 3 with ribosomes: Evolution of terminal extensions in IF3mt', *Nucleic Acids Research*, 36(2), pp. 589-597.

Harman, D. (1955) *Aging: a theory based on free radical and radiation chemistry*. University of California Radiation Laboratory.

Harman, D. (1972) 'BIOLOGIC CLOCK - MITOCHONDRIA', *Journal of the American Geriatrics Society*, 20(4), pp. 145-&.

Hatefi, Y. (1985) 'THE MITOCHONDRIAL ELECTRON-TRANSPORT AND OXIDATIVE-PHOSPHORYLATION SYSTEM', *Annual Review of Biochemistry*, 54, pp. 1015-1069.

Hatefi, Y., Haavik, A.G. and Griffiths, D.E. (1961) 'Reconstitution of the electron transport system II. Reconstitution of DPNH-cvtochrome c reductase. succinic-cytochrome c reductase and DPNH, succinic-cytochrome c reductase', *Biochemical and Biophysical Research Communications*, 4, pp. 447-53.

Hauswirth, W.W. and Laipis, P.J. (1982) 'MITOCHONDRIAL-DNA POLYMORPHISM IN A MATERNAL LINEAGE OF HOLSTEIN COWS', *Proceedings of the National Academy of Sciences of the United States of America-Biological Sciences*, 79(15), pp. 4686-4690.

Hayashi, J.I., Ohta, S., Kikuchi, A., Takemitsu, M., Goto, Y.I. and Nonaka, I. (1991) 'Introduction of disease-related mitochondrial DNA deletions into HeLa cells lacking mitochondrial DNA results in mitochondrial dysfunction', *Proceedings of the National Academy of Sciences of the United States of America*, 88(23), pp. 10614-10618.

He, L.P., Chinnery, P.F., Durham, S.E., Blakely, E.L., Wardell, T.M., Borthwick, G.M., Taylor, R.W. and Turnbull, D.M. (2002) 'Detection and quantification of mitochondrial DNA deletions in individual cells by real-time PCR', *Nucleic Acids Research*, 30(14).

Helm, M., Florentz, C., Chomyn, A. and Attardi, G. (1999) 'Search for differences in post-transcriptional modification patterns of mitochondrial DNA-encoded wild-type

and mutant human tRNA(Lys) and tRNA(Leu(UUR))', *Nucleic Acids Research*, 27(3), pp. 756-763.

Herbst, A., Pak, J.W., McKenzie, D., Bua, E., Bassiouni, M. and Aiken, J.M. (2007) 'Accumulation of mitochondrial DNA deletion mutations in aged muscle fibers: Evidence for a causal role in muscle fiber loss', *Journals of Gerontology - Series A Biological Sciences and Medical Sciences*, 62(3), pp. 235-245.

Hirst, J. (2013) 'Mitochondrial Complex I', *Annual Review of Biochemistry, Vol 82*, 82, pp. 551-575.

Hirst, J., Carroll, J., Fearnley, I.M., Shannon, R.J. and Walker, J.E. (2003) 'The nuclear encoded subunits of complex I from bovine heart mitochondria', *Biochimica et Biophysica Acta (BBA) - Bioenergetics*, 1604(3), pp. 135-150.

Hixson, J.E. and Clayton, D.A. (1985) 'Initiation of transcription from each of the two human mitochondrial promoters requires unique nucleotides at the transcriptional start sites', *Proceedings of the National Academy of Sciences of the United States of America*, 82(9), pp. 2660-2664.

Holme, E., Larsson, N.G., Oldfors, A., Tulinius, M., Sahlin, P. and Stenman, G. (1993) 'MULTIPLE SYMMETRICAL LIPOMAS WITH HIGH-LEVELS OF MTDNA WITH THE TRNALYSA- G(8344) MUTATION AS THE ONLY MANIFESTATION OF DISEASE IN A CARRIER OF MYOCLONUS EPILEPSY AND RAGGED-RED FIBERS (MERRF) SYNDROME', *American Journal of Human Genetics*, 52(3), pp. 551-556.

Holt, I.J., Harding, A.E., Cooper, J.M., Schapira, A.H.V., Toscano, A., Clark, J.B. and Morgan-Hughes, J.A. (1989) 'Mitochondrial myopathies: Clinical and biochemical features of 30 patients with major deletions of muscle mitochondrial DNA', *Annals of Neurology*, 26(6), pp. 699-708.

Holt, I.J., Harding, A.E. and Morgan-Hughes, J.A. (1988) 'Deletions of muscle mitochondrial DNA in patients with mitochondrial myopathies', *Nature*, 331(6158), pp. 717-719.

Holt, I.J., Harding, A.E., Petty, R.K.H. and Morgan-Hughes, J.A. (1990) 'A new mitochondrial disease associated with mitochondrial DNA heteroplasmy', *American Journal of Human Genetics*, 46(3), pp. 428-433.

Holt, I.J., Lorimer, H.E. and Jacobs, H.T. (2000) 'Coupled Leading- and Lagging-Strand Synthesis of Mammalian Mitochondrial DNA', *Cell*, 100(5), pp. 515-524.

Horton, T.M., Graham, B.H., Corral-Debrinski, M., Shoffner, J.M., Kaufman, A.E., Beal, M.F. and Wallace, D.C. (1995) 'Marked increase in mitochondrial DNA deletion levels in the cerebral cortex of Huntington's disease patients', *Neurology*, 45(10), pp. 1879-1883.

Howell, N., Bindoff, L.A., McCullough, D.A., Kubacka, I., Poulton, J., Mackey, D., Taylor, L. and Turnbull, D.M. (1991) 'LEBER HEREDITARY OPTIC NEUROPATHY - IDENTIFICATION OF THE SAME MITOCHONDRIAL NDI MUTATION IN 6 PEDIGREES', *American Journal of Human Genetics*, 49(5), pp. 939-950.

Howell, N., Huang, P., Kelliher, K. and Ryan, M.L. (1983) 'MITOCHONDRIAL GENETICS OF MAMMALIAN-CELLS - A MOUSE ANTIMYCIN-RESISTANT MUTANT WITH A PROBABLE ALTERATION OF CYTOCHROME-B', *Somatic Cell Genetics*, 9(2), pp. 143-163.

Hudson, G. and Chinnery, P.F. (2006) 'Mitochondrial DNA polymerase-Î³ and human disease', *Human Molecular Genetics*, 15(SUPPL. 2), pp. R244-R252.

Huoponen, K. (2001) 'Leber hereditary optic neuropathy: clinical and molecular genetic findings', *Neurogenetics*, 3(3), pp. 119-125.

James, A.M., Wei, Y.H., Pang, C.Y. and Murphy, M.P. (1996) 'Altered mitochondrial function in fibroblasts containing MELAS or MERRF mitochondrial DNA mutations', *Biochemical Journal*, 318(2), pp. 401-407.

James, D.I., Parone, P.A., Mattenberger, Y. and Martinou, J.C. (2003) 'hFis1, a novel component of the mammalian mitochondrial fission machinery', *Journal of Biological Chemistry*, 278(38), pp. 36373-36379.

Janssen, A.J.M., Smeitink, J.A.M. and Van den Heuvel, L.P. (2003) 'Some practical aspects of providing a diagnostic service for respiratory chain defects', *Annals of Clinical Biochemistry*, 40(1), pp. 3-8.

Janssen, R., Nijtmans, L., Heuvel, L. and Smeitink, J. (2006) 'Mitochondrial complex I: Structure, function and pathology', *Journal of Inherited Metabolic Disease*, 29(4), pp. 499-515.

Jeffreys, A.J., Neumann, R. and Wilson, V. (1990) 'Repeat unit sequence variation in minisatellites: a novel source of DNA polymorphism for studying variation and mutation by single molecule analysis', *Cell*, 60(3), pp. 473-485.

Jeppesen, T.D., Schwartz, M., Frederiksen, A.L., Wibrand, F., Olsen, D.B. and Vissing, J. (2006) 'Muscle phenotype and mutation load in 51 persons with the 3243A > G mitochondrial DNA mutation', *Archives of Neurology*, 63(12), pp. 1701-1706.

Johns, D.R., Neufeld, M.J. and Park, R.D. (1992) 'An ND-6 mitochondrial DNA mutation associated with leber hereditary optic neuropathy', *Biochemical and Biophysical Research Communications*, 187(3), pp. 1551-1557.

Johnson, D.C., Dean, D.R., Smith, A.D. and Johnson, M.K. (2005) 'Structure, function, and formation of biological iron-sulfur clusters', in *Annual Review of Biochemistry*. pp. 247-281.

Jonckheere, A.I., Smeitink, J.A.M. and Rodenburg, R.J.T. (2012) 'Mitochondrial ATP synthase: architecture, function and pathology', *Journal of Inherited Metabolic Disease*, 35(2), pp. 211-225.

Kasamats.H, Robberso.Dl and Vinograd, J. (1971) 'NOVEL CLOSED-CIRCULAR MITOCHONDRIAL DNA WITH PROPERTIES OF A REPLICATING INTERMEDIATE', *Proceedings of the National Academy of Sciences of the United States of America*, 68(9), pp. 2252-&.

Kearns, T.P. and Sayre, G.P. (1958) 'Retinitis pigmentosa, external ophthalmoplegia, and complete heart block: Unusual syndrome with histologic study in one of two cases', *A.M.A. Archives of Ophthalmology*, 60(2), pp. 280-289.

Kerr, J.F.R., Wyllie, A.H. and Currie, A.R. (1972) 'APOPTOSIS - BASIC BIOLOGICAL PHENOMENON WITH WIDE-RANGING IMPLICATIONS IN TISSUE KINETICS', *British Journal of Cancer*, 26(4), pp. 239-&.

Khrapko, K., Bodyak, N., Thilly, W.G., van Orsouw, N.J., Zhang, X.M., Coller, H.A., Perls, T.T., Upton, M., Vijg, J. and Wei, J.Y. (1999) 'Cell-by-cell scanning of whole mitochondrial genomes in aged human heart reveals a significant fraction of myocytes with clonally expanded deletions', *Nucleic Acids Research*, 27(11), pp. 2434-2441.

Kim, I., Rodriguez-Enriquez, S. and Lemasters, J.J. (2007) 'Selective degradation of mitochondria by mitophagy', *Archives of Biochemistry and Biophysics*, 462(2), pp. 245-253.

Kim, S.T., Choi, J.H., Kim, D. and Hwang, O. (2006) 'Increases in TH immunoreactivity, neuromelanin and degeneration in the substantia nigra of middle aged mice', *Neuroscience Letters*, 396(3), pp. 263-268.

Koene, S., Rodenburg, R.J., Knaap, M.S., Willemsen, M.A.A.P., Sperl, W., Laugel, V., Ostergaard, E., Tarnopolsky, M., Martin, M.A., Nesbitt, V., Fletcher, J., Edvardson, S., Procaccio, V., Slama, A., Heuvel, L.P.W.J. and Smeitink, J.A.M. (2012) 'Natural disease course and genotype-phenotype correlations in Complex I deficiency caused by nuclear gene defects: what we learned from 130 cases', *Journal of Inherited Metabolic Disease*, 35(5), pp. 737-747.

Koga, Y., Akita, Y., Takane, N., Sato, Y. and Kato, H. (2000) 'Heterogeneous presentation in A3243G mutation in the mitochondrial tRNA(Leu(UUR)) gene', *Archives of Disease in Childhood*, 82(5), pp. 407-411.

Kopsidas, G., Kovalenko, S.A., Kelso, J.M. and Linnane, A.W. (1998) 'An age-associated correlation between cellular bioenergy decline and mtDNA rearrangements in human skeletal muscle', *Mutation Research/Fundamental and Molecular Mechanisms of Mutagenesis*, 421(1), pp. 27-36.

Korhonen, J.A., Pham, X.H., Pellegrini, M. and Falkenberg, M. (2004) 'Reconstitution of a minimal mtDNA replisome in vitro', *EMBO Journal*, 23(12), pp. 2423-2429.

Kraytsberg, Y., Bodyak, N., Myerow, S., Nicholas, A., Ebralidze, K. and Khrapko, K. (2009) 'Quantitative analysis of somatic mitochondrial DNA mutations by single-cell single-molecule PCR', in *Mitochondrial DNA*. Springer, pp. 329-369.

Kraytsberg, Y. and Khrapko, K. (2005) 'Single-molecule PCR: an artifact-free PCR approach for the analysis of somatic mutations', *Expert review of molecular diagnostics*, 5(5), p. 809.

Kraytsberg, Y., Kudryavtseva, E., McKee, A.C., Geula, C., Kowall, N.W. and Khrapko, K. (2006) 'Mitochondrial DNA deletions are abundant and cause functional impairment in aged human substantia nigra neurons', *Nature Genetics*, 38(5), pp. 518-520.

Krebs, H. (1953) 'The Nobel Prize in Physiology or Medicine', http://www.nobelprize.org/nobel_prizes/medicine/laureates/1953/

Krishnan, K.J., Bender, A., Taylor, R.W. and Turnbull, D.M. (2007) 'A multiplex real-time PCR method to detect and quantify mitochondrial DNA deletions in individual cells', *Analytical Biochemistry*, 370(1), pp. 127-129.

Krishnan, K.J., Reeve, A.K., Samuels, D.C., Chinnery, P.F., Blackwood, J.K., Taylor, R.W., Wanrooij, S., Spelbrink, J.N., Lightowlers, R.N. and Turnbull, D.M. (2008) 'What causes mitochondrial DNA deletions in human cells?', *Nature Genetics*, 40(3), pp. 275-279.

Kunkel, T.A. and Loeb, L.A. (1981) 'FIDELITY OF MAMMALIAN DNA-POLYMERASES', *Science*, 213(4509), pp. 765-767.

Kurland, C.G. and Andersson, S.G.E. (2000) 'Origin and evolution of the mitochondrial proteome', *Microbiology and Molecular Biology Reviews*, 64(4), pp. 786-+.

Kuwana, T., Mackey, M.R., Perkins, G., Ellisman, M.H., Latterich, M., Schneiter, R., Green, D.R. and Newmeyer, D.D. (2002) 'Bid, Bax, and lipids cooperate to form supramolecular openings in the outer mitochondrial membrane', *Cell*, 111(3), pp. 331-342.

Kyriakouli, D.S., Boesch, P., Taylor, R.W. and Lightowlers, R.N. (2008) 'Progress and prospects: gene therapy for mitochondrial DNA disease', *Gene Therapy*, 15(14), pp. 1017-1023.

Labrousse, A.M., Zappaterra, M.D., Rube, D.A. and van der Bliek, A.M. (1999) 'C-elegans dynamin-related protein DRP-1 controls severing of the mitochondrial outer membrane', *Molecular Cell*, 4(5), pp. 815-826.

Laforêt, P., Lombès, A., Eymard, B., Danan, C., Chevallay, M., Rouche, A., Frachon, P. and Fardeau, M. (1995) 'Chronic progressive external ophthalmoplegia with ragged-red fibers: Clinical, morphological and genetic investigations in 43 patients', *Neuromuscular Disorders*, 5(5), pp. 399-413.

Lancaster, C.R.D., Kröger, A., Auer, M. and Michel, H. (1999) 'Structure of fumarate reductase from Wolinella succinogenes at 2.2[thinsp][angst] resolution', *Nature*, 402(6760), pp. 377-385.

Larsson, N. (2010) 'Somatic mitochondrial DNA mutations in mammalian aging.', *Annual Review of Biocheistry*, 79, pp. 683 - 706.

Larsson, N.G., Holme, E., Kristiansson, B., Oldfors, A. and Tulinius, M. (1990) 'PROGRESSIVE INCREASE OF THE MUTATED MITOCHONDRIAL-DNA FRACTION IN KEARNS-SAYRE SYNDROME', *Pediatric Research*, 28(2), pp. 131-136.

Lazarou, M., Smith, S.M., Thorburn, D.R., Ryan, M.T. and McKenzie, M. (2009) 'Assembly of nuclear DNA-encoded subunits into mitochondrial complex IV, and their preferential integration into supercomplex forms in patient mitochondria', *Febs Journal*, 276(22), pp. 6701-6713.

Leber, T. (1871a) 'Ueber hereditäre und congenital-angelegte Sehnervenleiden', *Albrecht von Graefes Archiv für Ophthalmologie*, 17(2), pp. 249-291.

Leber, T. (1871b) 'Ueber hereditäre und congenital-angelegte Sehnervenleiden', *Graefe's Archive for Clinical and Experimental Ophthalmology*, 17(2), pp. 249-291.

LeDoux, S.P., Driggers, W.J., Hollensworth, B.S. and Wilson, G.L. (1999) 'Repair of alkylation and oxidative damage in mitochondrial DNA', *Mutation Research/DNA Repair*, 434(3), pp. 149-159.

LeDoux, S.P., Wilson, G.L., Beecham, E.J., Stevnsner, T., Wassermann, K. and Bohr, V.A. (1992) 'Repair of mitochondrial DNA after various types of DNA damage in Chinese hamster ovary cells', *Carcinogenesis*, 13(11), pp. 1967-1973.

Leigh, D. (1951) 'Subacute necrotizing encephalomyelopathy in an infant', *Journal of neurology, neurosurgery, and psychiatry*, 14(3), pp. 216-221.

Lemos, R.S., Fernandes, A.S., Pereira, M.M., Gomes, C.M. and Teixeira, M. (2002) 'Quinol:fumarate oxidoreductases and succinate:quinone oxidoreductases: Phylogenetic relationships, metal centres and membrane attachment', *Biochimica et Biophysica Acta - Bioenergetics*, 1553(1-2), pp. 158-170.

Letellier, T., Heinrich, R., Malgat, M. and Mazat, J.P. (1994) 'THE KINETIC BASIS OF THRESHOLD EFFECTS OBSERVED IN MITOCHONDRIAL DISEASES - A SYSTEMIC APPROACH', *Biochemical Journal*, 302, pp. 171-174.

Liao, H.X. and Spremulli, L.L. (1989) 'Interaction of bovine mitochondrial ribosomes with messenger RNA', *Journal of Biological Chemistry*, 264(13), pp. 7518-7522.

Lill, R. (2009) 'Function and biogenesis of iron–sulphur proteins', *Nature*, 460(7257), pp. 831-838.

Lill, R., Diekert, K., Kaut, A., Lange, H., Pelzer, W., Prohl, C. and Kispal, G. (1999) 'The essential role of mitochondria in the biogenesis of cellular iron-sulfur proteins', *Biological Chemistry*, 380(10), pp. 1157-1166.

Lim, S.E. and Copeland, W.C. (2001) 'Differential incorporation and removal of antiviral deoxynucleotides by human DNA polymerase gamma', *Journal of Biological Chemistry*, 276(26), pp. 23616-23623.

Linnane, A.W., Marzuki, S., Ozawa, T. and Tanaka, M. (1989) 'Mitochondrial DNA mutations as an important contributor to ageing and degenerative diseases', *Lancet*, 1(8639), pp. 642-645.

López-Gallardo, E., López-Pérez, M.J., Montoya, J. and Ruiz-Pesini, E. (2009) 'CPEO and KSS differ in the percentage and location of the mtDNA deletion', *Mitochondrion*, 9(5), pp. 314-317.

Lopez, M.E., Van Zeeland, N.L., Dahl, D.B., Weindruch, R. and Aiken, J.M. (2000) 'Cellular phenotypes of age-associated skeletal muscle mitochondrial abnormalities in rhesus monkeys', *Mutation Research/Fundamental and Molecular Mechanisms of Mutagenesis*, 452(1), pp. 123-138.

Ma, J. and Spremulli, L.L. (1996) 'Expression, purification, and mechanistic studies of bovine mitochondrial translational initiation factor 2', *Journal of Biological Chemistry*, 271(10), pp. 5805-5811.

Ma, Y.S., Chen, Y.C., Lu, C.Y., Liu, C.Y. and Wei, Y.H. 1042 (2005) 'Upregulation of matrix metalloproteinase 1 and disruption of mitochondrial network in skin fibroblasts of patients with MERRF syndrome' *Annals of the New York Academy of Sciences*. pp. 55-63. Available at: http://www.scopus.com/inward/record.url?eid=2-s2.0-22044452993&partnerID=40&md5=3e943c8ddfabad23670ebc8d39026553.

Maagaard, A., Holberg-Petersen, M., Kollberg, G., Oldfors, A., Sandvik, L. and Bruun, J.N. (2006) 'Mitochondrial (mt)DNA changes in tissue may not be reflected by depletion of mtDNA in peripheral blood mononuclear cells in HIV-infected patients', *Antiviral Therapy*, 11(5), pp. 601-608.

Malkin, R. and Rabinowitz, J.C. (1966) 'The reconstitution of clostridial ferredoxin', *Biochemical and Biophysical Research Communications*, 23(6), pp. 822-827.

Mannella, C.A. (2006) 'Structure and dynamics of the mitochondrial inner membrane cristae', *Biochimica et Biophysica Acta (BBA) - Molecular Cell Research*, 1763(5–6), pp. 542-548.

Mannella, C.A., Marko, M. and Buttle, K. (1997) 'Reconsidering mitochondrial structure: new views of an old organelle', *Trends in Biochemical Sciences*, 22(2), pp. 37-38.

Mannella, C.A., Pfeiffer, D.R., Bradshaw, P.C., Moraru, I.I., Slepchenko, B., Loew, L.M., Hsieh, C.-e., Buttle, K. and Marko, M. (2001) 'Topology of the Mitochondrial Inner Membrane: Dynamics and Bioenergetic Implications', *IUBMB Life*, 52(3-5), pp. 93-100.

Manwaring, N., Jones, M.M., Wang, J.J., Rochtchina, E., Howard, C., Mitchell, P. and Sue, C.M. (2007) 'Population prevalence of the MELAS A3243G mutation', *Mitochondrion*, 7(3), pp. 230-233.

Margulis, L. (1970) *Origin of eukaryotic cells*. Yale University Press, New Haven & London.

Markaryan, A., Nelson, E.G. and Hinojosa, R. (2010) 'Major arc mitochondrial DNA deletions in cytochrome c oxidase-deficient human cochlear spiral ganglion cells', *Acta Oto-Laryngologica*, 130(7), pp. 780-787.

Masukata, H. and Tomizawa, J.-i. (1990) 'A mechanism of formation of a persistent hybrid between elongating RNA and template DNA', *Cell*, 62(2), pp. 331-338.

Mathiesen, C. and Hägerhäll, C. (2002) 'Transmembrane topology of the NuoL, M and N subunits of NADH:quinone oxidoreductase and their homologues among membrane-bound hydrogenases and bona fide antiporters', *Biochimica et Biophysica Acta (BBA) - Bioenergetics*, 1556(2–3), pp. 121-132.

McFarland, R., Taylor, R.W. and Turnbull, D.M. (2002) 'The neurology of mitochondrial DNA disease', *The Lancet Neurology*, 1(6), pp. 343-351.

McShane, M.A., Hammans, S.R., Sweeney, M., Holt, I.J., Beattie, T.J., Brett, E.M. and Harding, A.E. (1991) 'PEARSON SYNDROME AND MITOCHONDRIAL ENCEPHALOMYOPATHY IN A PATIENT WITH A DELETION OF MTDNA', *American Journal of Human Genetics*, 48(1), pp. 39-42.

McVey, M. and Lee, S.E. (2008) 'MMEJ repair of double-strand breaks (director's cut): deleted sequences and alternative endings', *Trends in Genetics*, 24(11), pp. 529-538.

Melov, S., Shoffner, J.M., Kaufman, A. and Wallace, D.C. (1995) 'Marked increase in the number and variety of mitochondrial DNA rearrangements in aging human skeletal muscle', *Nucleic Acids Research*, 23(20), pp. 4122-4126.

Michikawa, Y., Mazzucchelli, F., Bresolin, N., Scarlato, G. and Attardi, G. (1999) 'Aging-dependent large accumulation of point mutations in the human mtDNA control region for replication', *Science*, 286(5440), pp. 774-779.

Mita, S., Rizzuto, R., Moraes, C.T., Shanske, S., Arnaudo, E., Fabrizi, G.M., Koga, Y., Dimauro, S. and Schon, E.A. (1990) 'RECOMBINATION VIA FLANKING DIRECT REPEATS IS A MAJOR CAUSE OF LARGE-SCALE DELETIONS OF HUMAN MITOCHONDRIAL-DNA', *Nucleic Acids Research*, 18(3), pp. 561-567.

Mita, S., Schmidt, B., Schon, E.A., DiMauro, S. and Bonilla, E. (1989) 'Detection of "deleted" mitochondrial genomes in cytochrome-c oxidase-deficient muscle fibers of a patient with Kearns-Sayre syndrome', *Proceedings of the National Academy of Sciences*, 86(23), pp. 9509-9513.

Mitchell, P. (1961) 'Coupling of Phosphorylation to Electron and Hydrogen Transfer by a Chemi-Osmotic type of Mechanism', *Nature*, 191(4784), pp. 144-148.

Mitchell, P. (1976) 'POSSIBLE MOLECULAR MECHANISMS OF PROTONMOTIVE FUNCTION OF CYTOCHROME SYSTEMS', *Journal of Theoretical Biology*, 62(2), pp. 327-367.

Mitra, R.D., Butty, V.L., Shendure, J., Williams, B.R., Housman, D.E. and Church, G.M. (2003) 'Digital genotyping and haplotyping with polymerase colonies', *Proceedings of the National Academy of Sciences*, 100(10), pp. 5926-5931.

Montoya, J., López-Gallardo, E., Díez-Sánchez, C., López-Pérez, M.J. and Ruiz-Pesini, E. (2009) '20 years of human mtDNA pathologic point mutations: Carefully reading the pathogenicity criteria', *Biochimica et Biophysica Acta (BBA) - Bioenergetics*, 1787(5), pp. 476-483.

Montoya, J., Ojala, D. and Attardi, G. (1981) 'Distinctive features of the 5'-terminal sequences of the human mitochondrial mRNAs', *Nature*, 290(5806), pp. 465-470.

Moraes, C.T., DiMauro, S., Zeviani, M., Lombes, A., Shanske, S., Miranda, A.F., Nakase, H., Bonilla, E., Werneck, L.C., Servidei, S., Nonaka, I., Koga, Y., Spiro, A.J., Brownell, A.K.W., Schmidt, B., Schotland, D.L., Zupanc, M. and DeVivo, D.C. (1989) 'Mitochondrial DNA deletions in progressive external ophthalmoplegia and Kearne-Sayre syndrome', *New England Journal of Medicine*, 320(20), pp. 1293-1299.

Moraes, C.T., Sciacco, M., Ricci, E., Tengan, C.H., Hao, H., Bonilla, E., Schon, E.A. and DiMauro, S. (1995) 'Phenotype-genotype correlations in skeletal muscle of patients with mtDNA deletions', *Muscle & Nerve*, 3, pp. S150-3.

Morgan-Hughes, J.A., Sweeney, M.G., Cooper, J.M., Hammans, S.R., Brockington, M., Schapira, A.H.V., Harding, A.E. and Clark, J.B. (1995) 'MITOCHONDRIAL-DNA (MTDNA) DISEASES - CORRELATION OF GENOTYPE TO PHENOTYPE', *Biochimica Et Biophysica Acta-Molecular Basis of Disease*, 1271(1), pp. 135-140.

Moslemi, A.R., Tulinius, M., Holme, E. and Oldfors, A. (1997) 'Threshold expression of the tRNA(Lys) A8344G mutation in single muscle fibers', *Brain Pathology*, 7(4), pp. 1278-1278.

Muchmore, S.W., Sattler, M., Liang, H., Meadows, R.P., Harlan, J.E., Yoon, H.S., Nettesheim, D., Chang, B.S., Thompson, C.B., Wong, S.L., Ng, S.C. and Fesik, S.W. (1996) 'X-ray and NMR structure of human Bcl-x(L), an inhibitor of programmed cell death', *Nature*, 381(6580), pp. 335-341.

Munn, E.A. (1974) 'The Structure of Mitochondria.', *London-New York Academic Press*.

Munnich, A. and Rustin, P. (2001) 'Clinical spectrum and diagnosis of mitochondrial disorders', *American Journal of Medical Genetics*, 106(1), pp. 4-17.

Murphy, J.L., Blakely, E.L., Schaefer, A.M., He, L., Wyrick, P., Haller, R.G., Taylor, R.W., Turnbull, D.M. and Taivassalo, T. (2008) 'Resistance training in patients with single, large-scale deletions of mitochondrial DNA', *Brain*, 131(11), pp. 2832-2840.

Murphy, J.L., Ratnaike, T.E., Shang, E., Falkous, G., Blakely, E.L., Alston, C.L., Taivassalo, T., Haller, R.G., Taylor, R.W. and Turnbull, D.M. (2012) 'Cytochrome c oxidase-intermediate fibres: Importance in understanding the pathogenesis and treatment of mitochondrial myopathy', *Neuromuscular Disorders*, 22(8), pp. 690-698.

Nagao, A. and Suzuki, T. (2007) 'Aminoacyl-tRNA surveillance by EF-Tu in mammalian mitochondria', *Nucleic acids symposium series (2004)*, (51), pp. 41-42.

Nakada, K., Sato, A. and Hayashi, J.-I. (2009) 'Mitochondrial functional complementation in mitochondrial DNA-based diseases', *The International Journal of Biochemistry & Cell Biology*, 41(10), pp. 1907-1913.

Nakamura, M., Yabe, I., Sudo, A., Hosoki, K., Yaguchi, H., Saitoh, S. and Sasaki, H. (2010) 'MERRF/MELAS overlap syndrome: a double pathogenic mutation in mitochondrial tRNA genes', *Journal of Medical Genetics*, 47(10), pp. 659-664.

Nakase, H., Moraes, C.T., Rizzuto, R., Lombes, A., Dimauro, S. and Schon, E.A. (1990a) 'TRANSCRIPTION AND TRANSLATION OF DELETED MITOCHONDRIAL GENOMES IN KEARNS-SAYRE SYNDROME - IMPLICATIONS FOR PATHOGENESIS', *American Journal of Human Genetics*, 46(3), pp. 418-427.

Nakase, H., Moraes, C.T., Rizzuto, R., Lombes, A., DiMauro, S. and Schon, E.A. (1990b) 'Transcription and translation of deleted mitochondrial genomes in Kearns-Sayre syndrome: Implications for pathogenesis', *American Journal of Human Genetics*, 46(3), pp. 418-427.

Nekhaeva, E., Bodyak, N.D., Kraytsberg, Y., McGrath, S.B., Van Orsouw, N.J., Pluzhnikov, A., Wei, J.Y., Vijg, J. and Khrapko, K. (2002) 'Clonally expanded mtDNA point mutations are abundant in individual cells of human tissues', *Proceedings of the National Academy of Sciences of the United States of America*, 99(8), pp. 5521-5526.

Nesbitt, V., Pitceathly, R.D.S., Turnbull, D.M., Taylor, R.W., Sweeney, M.G., Mudanohwo, E.E., Rahman, S., Hanna, M.G. and McFarland, R. (2013) 'The UK MRC Mitochondrial Disease Patient Cohort Study: clinical phenotypes associated with the m.3243A>G mutation—implications for diagnosis and management', *Journal of Neurology, Neurosurgery & Psychiatry*, 84(8), pp. 936-938.

Newman, N.J., Lott, M.T. and Wallace, D.C. (1991) 'THE CLINICAL CHARACTERISTICS OF PEDIGREES OF LEBERS HEREDITARY OPTIC NEUROPATHY WITH THE 11778 MUTATION', *American Journal of Ophthalmology*, 111(6), pp. 750-762.

Nishino, I., Spinazzola, A., Papadimitriou, A., Hammans, S., Steiner, I., Hahn, C.D., Connolly, A.M., Verloes, A., Guimaraes, J., Maillard, I., Hamano, H., Donati, M.A., Semrad, C.E., Russell, J.A., Andreu, A.L., Hadjigeorgiou, G.M., Vu, T.H., Tadesse, S.,

Nygaard, T.G., Nonaka, I., Hirano, I., Bonilla, E., Rowland, L.P., DiMauro, S. and Hirano, M. (2000) 'Mitochondrial neurogastrointestinal encephalomyopathy: An autosomal recessive disorder due to thymidine phosphorylase mutations', *Annals of Neurology*, 47(6), pp. 792-800.

Ojala, D., Montoya, J. and Attardi, G. (1981) 'tRNA punctuation model of RNA processing in human mitochondria', *Nature*, 290(5806), pp. 470-474.

Old, S. and Johnson, M. (1989a) 'Methods of microphotometric assay of succinate dehydrogenase and cytochrome<i>c oxidase activities for use on human skeletal muscle', *The Histochemical Journal*, 21(9), pp. 545-555.

Old, S.L. and Johnson, M.A. (1989b) 'Methods of microphotometric assay of succinate dehydrogenase and cytochrome c oxidase activities for use on human skeletal muscle', *Histochemical Journal*, 21(9-10), pp. 545-555.

Osawa, S., Jukes, T.H., Watanabe, K. and Muto, A. (1992) 'Recent evidence for evolution of the genetic code', *Microbiological Reviews*, 56(1), pp. 229-264.

Ozawa, M., Nishino, I., Horai, S., Nonaka, I. and Goto, Y. (1997) 'Myoclonus epilepsy associated with ragged-red fibers: A G-to-A mutation at nucleotide pair 8363 in mitochondrial tRNA(Lys) in two families', *Muscle & Nerve*, 20(3), pp. 271-278.

Ozawa, T., Tanaka, M., Ikebe, S.-i., Ohno, K., Kondo, T. and Mizuno, Y. (1990) 'Quantitative determination of deleted mitochondrial DNA relative to normal DNA in parkinsonian striatum by a kinetic PCR analysis', *Biochemical and Biophysical Research Communications*, 172(2), pp. 483-489.

Palade, G.E. (1952) 'The fine structure of mitochondria', *Anatomical Record*, 114, pp. 427-461.

Palade, G.E. (1953) 'An electron microscope study of the mitochondrial structure', *J Histochem Cytochem*, 1(4), pp. 188-211.

Palty, R., Silverman, W.F., Hershfinkel, M., Caporale, T., Sensi, S.L., Parnis, J., Nolte, C., Fishman, D., Shoshan-Barmatz, V., Herrmann, S., Khananshvili, D. and Sekler, I. (2010)

'NCLX is an essential component of mitochondrial Na+/Ca2+ exchange', *Proceedings of the National Academy of Sciences of the United States of America*, 107(1), pp. 436-441.

Pankiv, S., Clausen, T.H., Lamark, T., Brech, A., Bruun, J.-A., Outzen, H., Overvatn, A., Bjorkoy, G. and Johansen, T. (2007) 'p62/SQSTM1 binds directly to Atg8/LC3 to facilitate degradation of ubiquitinated protein aggregates by autophagy', *Journal of Biological Chemistry*, 282(33), pp. 24131-24145.

Papa, S., Martino, P.L., Capitanio, G., Gaballo, A., De Rasmo, D., Signorile, A. and Petruzzella, V. (2012) 'The oxidative phosphorylation system in mammalian mitochondria', *Advances in experimental medicine and biology*, 942, pp. 3-37.

Pavlakis, S.G., Phillips, P.C. and DiMauro, S. (1984) 'Mitochondrial myopathy, encephalopathy, lactic acidosis, and strokelike episodes: A distinctive clinical syndrome', *Annals of Neurology*, 16(4), pp. 481-488.

Payne, B.A.I., Wilson, I.J., Hateley, C.A., Horvath, R., Santibanez-Koref, M., Samuels, D.C., Price, D.A. and Chinnery, P.F. (2011) 'Mitochondrial aging is accelerated by anti-retroviral therapy through the clonal expansion of mtDNA mutations', *Nature Genetics*, 43(8), pp. 806-U121.

Pearson, H.A., Lobel, J.S., Kocoshis, S.A., Naiman, J.L., Windmiller, J., Lammi, A.T., Hoffman, R. and Marsh, J.C. (1979) 'A new syndrome of refractory sideroblastic anemia with vacuolization of marrow precursors and exocrine pancreatic dysfunction', *The Journal of Pediatrics*, 95(6), pp. 976-984.

Perkins, G., Renken, C., Martone, M.E., Young, S.J., Ellisman, M. and Frey, T. (1997) 'Electron Tomography of Neuronal Mitochondria: Three-Dimensional Structure and Organization of Cristae and Membrane Contacts', *Journal of Structural Biology*, 119(3), pp. 260-272.

Pettepher, C.C., LeDoux, S.P., Bohr, V.A. and Wilson, G.L. (1991) 'Repair of alkali-labile sites within the mitochondrial DNA of RINr 38 cells after exposure to the nitrosourea streptozotocin', *Journal of Biological Chemistry*, 266(5), pp. 3113-3117.

Pitceathly, R.D.S., Rahman, S. and Hanna, M.G. (2012) 'Single deletions in mitochondrial DNA – Molecular mechanisms and disease phenotypes in clinical practice', *Neuromuscular Disorders*, 22(7), pp. 577-586.

Pohjoismaki, J.L.O., Wanrooij, S., Hyvarinen, A.K., Goffart, S., Holt, I.J., Spelbrink, J.N. and Jacobs, H.T. (2006) 'Alterations to the expression level of mitochondrial transcription factor A, TFAM, modify the mode of mitochondrial DNA replication in cultured human cells', *Nucleic Acids Research*, 34(20), pp. 5815-5828.

Pollack, M. and Leeuwenburgh, C. (2001) 'Apoptosis and aging: Role of the mitochondria', *Journals of Gerontology Series a-Biological Sciences and Medical Sciences*, 56(11), pp. B475-B482.

Porteous, W.K., James, A.M., Sheard, P.W., Porteous, C.M., Packer, M.A., Hyslop, S.J., Melton, J.V., Pang, C.Y., Wei, Y.H. and Murphy, M.P. (1998) 'Bioenergetic consequences of accumulating the common 4977-bp mitochondrial DNA deletion', *European Journal of Biochemistry*, 257(1), pp. 192-201.

Poulton, J., Deadman, M.E., Bindoff, L., Morten, K., Land, J. and Brown, G. (1993) 'FAMILIES OF MTDNA REARRANGEMENTS CAN BE DETECTED IN PATIENTS WITH MTDNA DELETIONS - DUPLICATIONS MAY BE A TRANSIENT INTERMEDIATE FORM', *Human Molecular Genetics*, 2(1), pp. 23-30.

Puskin, J.S., Gunter, T.E., Gunter, K.K. and Russell, P.R. (1976) 'EVIDENCE FOR MORE THAN ONE CA2+ TRANSPORT MECHANISM IN MITOCHONDRIA', *Biochemistry*, 15(17), pp. 3834-3842.

Rabinowi.M and Swift, H. (1970) 'MITOCHONDRIAL NUCLEIC ACIDS AND THEIR RELATION TO BIOGENESIS OF MITOCHONDRIA', *Physiological Reviews*, 50(3), pp. 376-&.

Rapizzi, E., Pinton, P., Szabadkai, G., Wieckowski, M.R., Vandecasteele, G., Baird, G., Tuft, R.A., Fogarty, K.E. and Rizzuto, R. (2002) 'Recombinant expression of the voltage-dependent anion channel enhances the transfer of Ca2+ microdomains to mitochondria', *Journal of Cell Biology*, 159(4), pp. 613-624.

Reenan, R.A.G. and Kolodner, R.D. (1992) 'Characterization of insertion mutations in the Saccharomyces cerevisiae MSH1 and MSH2 genes: Evidence for separate mitochondrial and nuclear functions', *Genetics*, 132(4), pp. 975-985.

Reeve, A.K., Krishnan, K.J., Elson, J.L., Morris, C.M., Bender, A., Lightowlers, R.N. and Turnbull, D.M. (2008a) 'Nature of Mitochondrial DNA Deletions in Substantia Nigra Neurons', *American Journal of Human Genetics*, 82(1), pp. 228-235.

Reeve, A.K., Krishnan, K.J. and Turnbull, D. (2008b) 'Mitochondrial DNA Mutations in Disease, Aging, and Neurodegeneration', in Gibson, G.E., Ratan, R.R. and Beal, M.F. (eds.) *Mitochondria and Oxidative Stress in Neurodegenerative Disorders*. Oxford: Blackwell Publishing, pp. 21-29.

Rizzuto, R. and Pozzan, T. (2006) 'Microdomains of intracellular Ca2+: Molecular determinants and functional consequences', *Physiological Reviews*, 86(1), pp. 369-408.

Robberso.Dl and Clayton, D.A. (1972) 'REPLICATION OF MITOCHONDRIAL-DNA IN MOUSE L CELLS AND THEIR THYMIDINE KINASE-DERIVATIVES - DISPLACEMENT REPLICATION ON A COVALENTLY-CLOSED CIRCULAR TEMPLATE', *Proceedings of the National Academy of Sciences of the United States of America*, 69(12), pp. 3810-3814.

Rodenburg, R. (2011) 'Biochemical diagnosis of mitochondrial disorders', *Journal of Inherited Metabolic Disease*, 34(2), pp. 283-292.

Rodriguez, J. and Lazebnik, Y. (1999) 'Caspase-9 and APAF-1 form an active holoenzyme', *Genes and Development*, 13(24), pp. 3179-3184.

Roger, A.J. (1999) 'Reconstructing early events in eukaryotic evolution', *American Naturalist*, 154, pp. S146-S163.

Rossignol, R., Faustin, B., Rocher, C., Benard, G., Malgat, M. and Letellier, T. (2004) 'Mitochondrial threshold effects', *Biochimica Et Biophysica Acta-Bioenergetics*, 1658, pp. 210-210.

Rotig, A., Bourgeron, T., Chretien, D., Rustin, P. and Munnich, A. (1995) 'SPECTRUM OF MITOCHONDRIAL-DNA REARRANGEMENTS IN THE PEARSON MARROW-PANCREAS SYNDROME', *Human Molecular Genetics*, 4(8), pp. 1327-1330.

Ruiz-Pesini, E., Lott, M.T., Procaccio, V., Poole, J., Brandon, M.C., Mishmar, D., Yi, C., Kreuziger, J., Baldi, P., and Wallace, D.C. (2007) 'An enhanced MITOMAP with a global mtDNA mutational phylogeny.', *Nucleic Acids Research*, 35 (Database issue), pp. D823-D828.

Sadikovic, B., Wang, J., El-Hattab, A., Landsverk, M., Douglas, G., Brundage, E.K., Craigen, W.J., Schmitt, E.S. and Wong, L.-J.C. (2010) 'Sequence homology at the breakpoint and clinical phenotype of mitochondrial DNA deletion syndromes', *PLoS One*, 5(12), p. e15687.

Sagan, L. (1967) 'On the origin of mitosing cells', *Journal of Theoretical Biology*, 14(3), pp. 225-230,IN1-IN4,231-248,IN5-IN6,249-274.

Sallevelt, S.C.E.H., Dreesen, J.C.F.M., Drüsedau, M., Spierts, S., Coonen, E., van Tienen, F.H.J., van Golde, R.J.T., de Coo, I.F.M., Geraedts, J.P.M., de Die-Smulders, C.E.M. and Smeets, H.J.M. (2013) 'Preimplantation genetic diagnosis in mitochondrial DNA disorders: challenge and success', *Journal of Medical Genetics*, 50(2), pp. 125-132.

Salmons, S. and Henriksson, J. (1981) 'THE ADAPTIVE RESPONSE OF SKELETAL-MUSCLE TO INCREASED USE', *Muscle & Nerve*, 4(2), pp. 94-105.

Samuels, D.C., Schon, E.A. and Chinnery, P.F. (2004) 'Two direct repeats cause most human mtDNA deletions', *Trends in Genetics*, 20(9), pp. 393-398.

Sanz, A. and Stefanatos, R.K.A. (2008) 'The mitochondrial free radical theory of aging: a critical view', *Current aging science*, 1(1), pp. 10-21.

Saris, N.E.L. and Carafoli, E. (2005) 'A historical review of cellular calcium handling, with emphasis on mitochondria', *Biochemistry-Moscow*, 70(2), pp. 187-194.

Sato, A., Nakada, K., Shitara, H., Kasahara, A., Yonekawa, H. and Hayashi, J.I. (2007) 'Deletion-mutant mtDNA increases in somatic tissues but decreases in female germ cells with age', *Genetics*, 177(4), pp. 2031-2037.

Sato, M. and Sato, K. (2011) 'Degradation of Paternal Mitochondria by Fertilization-Triggered Autophagy in C. elegans Embryos', *Science*, 334(6059), pp. 1141-1144.

Sazanov, L.A. and Hinchliffe, P. (2006) 'Structure of the hydrophilic domain of respiratory complex I from Thermus thermophilus', *Science*, 311(5766), pp. 1430-1436.

Schaefer, A.M., McFarland, R., Blakely, E.L., He, L., Whittaker, R.G., Taylor, R.W., Chinnery, P.F. and Turnbull, D.M. (2008) 'Prevalence of mitochondrial DNA disease in adults', *Annals of Neurology*, 63(1), pp. 35-39.

Schaefer, A.M., Phoenix, C., Elson, J.L., McFarland, R., Chinnery, P.F. and Turnbull, D.M. (2006) 'Mitochondrial disease in adults: A scale to monitor progression and treatment', *Neurology*, 66(12), pp. 1932-1934.

Schaefer, A.M., Taylor, R.W., Turnbull, D.M. and Chinnery, P.F. (2004) 'The epidemiology of mitochondrial disorders—past, present and future', *Biochimica et Biophysica Acta (BBA) - Bioenergetics*, 1659(2–3), pp. 115-120.

Schapira, A.H.V. (2012) 'Mitochondrial diseases', *The Lancet*, 379(9828), pp. 1825-1834.

Schmiedel, J., Jackson, S., Schäfer, J. and Reichmann, H. (2003) 'Mitochondrial Cytopathies', *Journal of Neurology*, 250(3), pp. 267-277.

Schon, E.A., Bonilla, E. and DiMauro, S. (1997) 'Mitochondrial DNA mutations and pathogenesis', *Journal of Bioenergetics and Biomembranes*, 29(2), pp. 131-149.

Schon, E.A., DiMauro, S. and Hirano, M. (2012) 'Human mitochondrial DNA: roles of inherited and somatic mutations', *Nature Reviews Genetics*, 13(12), pp. 878-890.

Schon, E.A., DiMauro, S., Hirano, M. and Gilkerson, R.W. (2010) 'Therapeutic prospects for mitochondrial disease', *Trends in Molecular Medicine*, 16(6), pp. 268-276.

Schroder, R., Vielhaber, S., Wiedemann, F.R., Kornblum, C., Papassotiropoulos, A., Broich, P., Zierz, S., Elger, C.E., Reichmann, H., Seibel, P., Klockgether, T. and Kunz, W.S. (2000) 'New insights into the metabolic consequences of large-scale mtDNA deletions: A quantitative analysis of biochemical, morphological, and genetic findings in human skeletal muscle', *Journal of Neuropathology and Experimental Neurology*, 59(5), pp. 353-360.

Schwartz, M. and Vissing, J. (2002) 'Paternal Inheritance of Mitochondrial DNA', *New England Journal of Medicine*, 347(8), pp. 576-580.

Sciacco, M., Bonilla, E., Schon, E.A., Dimauro, S. and Moraes, C.T. (1994) 'DISTRIBUTION OF WILD-TYPE AND COMMON DELETION FORMS OF MTDNA IN NORMAL AND RESPIRATION-DEFICIENT MUSCLE-FIBERS FROM PATIENTS WITH MITOCHONDRIAL MYOPATHY (VOL 3, PG 13, 1994)', *Human Molecular Genetics*, 3(4), pp. 687-687.

Shadel, G.S. and Clayton, D.A. 66 (1997) 'Mitochondrial DNA maintenance in vertebrates' *Annual Review of Biochemistry*. pp. 409-436. Available at: http://www.scopus.com/inward/record.url?eid=2-s2.0-0030920779&partnerID=40&md5=45e38098393e6915beb9257face566ed.

Shi, Y. (2006) 'Mechanical aspects of apoptosome assembly', *Current Opinion in Cell Biology*, 18(6), pp. 677-684.

Shmookler Reis, R.J. and Goldstein, S. (1983) 'Mitochondrial DNA in mortal and immortal human cells. Genome number, integrity, and methylation', *Journal of Biological Chemistry*, 258(15), pp. 9078-9085.

Shoffner, J.M., Lott, M.T., Voljavec, A.S., Soueidan, S.A., Costigan, D.A. and Wallace, D.C. (1989) 'Spontaneous Kearns-Sayre/chronic external ophthalmoplegia plus syndrome associated with a mitochondrial DNA deletion: A slip-replication model and metabolic therapy', *Proceedings of the National Academy of Sciences of the United States of America*, 86(20), pp. 7952-7956.

Shoubridge, E.A., Karpati, G. and Hastings, K.E.M. (1990) 'DELETION MUTANTS ARE FUNCTIONALLY DOMINANT OVER WILD-TYPE MITOCHONDRIAL GENOMES IN SKELETAL-MUSCLE FIBER SEGMENTS IN MITOCHONDRIAL DISEASE', *Cell*, 62(1), pp. 43-49.

Shutt, T.E. and Gray, M.W. (2006) 'Bacteriophage origins of mitochondrial replication and transcription proteins', *Trends in Genetics*, 22(2), pp. 90-95.

Sicheritz-Ponten, T., Kurland, C.G. and Andersson, S.G.E. (1998) 'A phylogenetic analysis of the cytochrome b and cytochrome c oxidase I genes supports an origin of

mitochondria from within the Rickettsiaceae', *Biochimica Et Biophysica Acta-Bioenergetics*, 1365(3), pp. 545-551.

Silvestri, G., Moraes, C.T., Shanske, S., Oh, S.J. and Dimauro, S. (1992) 'A new mtDNA mutation in the tRNA(lys) gene associated with myoclonus epilepsy and ragged-red fibers (MERRF)', *American Journal of Human Genetics*, 51(6), pp. 1213-1217.

Simonetti, S., Chen, X., DiMauro, S. and Schon, E.A. (1992) 'Accumulation of deletions in human mitochondrial DNA during normal aging: analysis by quantitative PCR', *Biochimica et Biophysica Acta (BBA)-Molecular Basis of Disease*, 1180(2), pp. 113-122.

Skladal, D., Halliday, J. and Thorburn, D.R. (2003) 'Minimum birth prevalence of mitochondrial respiratory chain disorders in children', *Brain*, 126(8), pp. 1905-1912.

Smeitink, J., van den Heuvel, L. and DiMauro, S. (2001) 'The genetics and pathology of oxidative phosphorylation', *Nat Rev Genet*, 2(5), pp. 342-352.

Smirnova, E., Griparic, L., Shurland, D.L. and van der Bliek, A.M. (2001) 'Dynamin-related protein Drp1 is required for mitochondrial division in mammalian cells', *Molecular Biology of the Cell*, 12(8), pp. 2245-2256.

Smits, P., Smeitink, J. and van den Heuvel, L. (2010) 'Mitochondrial Translation and Beyond: Processes Implicated in Combined Oxidative Phosphorylation Deficiencies', *Journal of Biomedicine and Biotechnology*.

Snyderwine, E.G. and Bohr, V.A. (1992) 'Gene- and strand-specific damage and repair in Chinese hamster ovary cells treated with 4-nitroquinoline 1-oxide', *Cancer Research*, 52(15), pp. 4183-4189.

Sue, C.M., Crimmins, D.S., Soo, Y.S., Pamphlett, R., Presgrave, C.M., Kotsimbos, N., Jean-Francois, M.J.B., Byrne, E. and Morris, J.G.L. (1998) 'Neuroradiological features of six kindreds with MELAS tRNALeu A3243G point mutation: Implications for pathogenesis', *Journal of Neurology Neurosurgery and Psychiatry*, 65(2), pp. 233-240.

Suen, D.-F., Norris, K.L. and Youle, R.J. (2008) 'Mitochondrial dynamics and apoptosis', *Genes & Development*, 22(12), pp. 1577-1590.

Sun, F., Huo, X., Zhai, Y., Wang, A., Xu, J., Su, D., Bartlam, M. and Rao, Z. (2005) 'Crystal Structure of Mitochondrial Respiratory Membrane Protein Complex II', *Cell*, 121(7), pp. 1043-1057.

Sutovsky, P., Moreno, R.D., Ramalho-Santos, J., Dominko, T., Simerly, C. and Schatten, G. (1999) 'Development: Ubiquitin tag for sperm mitochondria', *Nature*, 402(6760), pp. 371-372.

Tang, Y., Schon, E.A., Wilichowski, E., Vazquez-Memije, M.E., Davidson, E. and King, M.P. (2000a) 'Rearrangements of human mitochondrial DNA (mtDNA): New insights into the regulation of mtDNA copy number and gene expression', *Molecular Biology of the Cell*, 11(4), pp. 1471-1485.

Tang, Y.Y., Manfredi, G., Hirano, M. and Schon, E.A. (2000b) 'Maintenance of human rearranged mitochondrial DNAs in long-term cultured transmitochondrial cell lines', *Molecular Biology of the Cell*, 11(7), pp. 2349-2358.

Tatuch, Y., Christodoulou, J., Feigenbaum, A., Clarke, J.T.R., Wherret, J., Smith, C., Rudd, N., Petrova-Benedict, R. and Robinson, B.H. (1992) 'Heteroplasmic mtDNA mutation (T→G) at 8993 can cause Leigh disease when the percentage of abnormal mtDNA is high', *American Journal of Human Genetics*, 50(4), pp. 852-858.

Taylor, R.W., Barron, M.J., Borthwick, G.M., Gospel, A., Chinnery, P.F., Samuels, D.C., Taylor, G.A., Plusa, S.M., Needham, S.J., Greaves, L.C., Kirkwood, T.B.L. and Turnbull, D.M. (2003) 'Mitochondrial DNA mutations in human colonic crypt stem cells', *Journal of Clinical Investigation*, 112(9), pp. 1351-1360.

Taylor, R.W., Schaefer, A.M., Barron, M.J., McFarland, R. and Turnbull, D.M. (2004) 'The diagnosis of mitochondrial muscle disease', *Neuromuscular Disorders*, 14(4), pp. 237-245.

Taylor, R.W. and Turnbull, D.M. (2005) 'Mitochondrial DNA mutations in human disease', *Nature Reviews Genetics*, 6(5), pp. 389-402.

Thauer, R.K. (1988) 'CITRIC-ACID CYCLE, 50 YEARS ON - MODIFICATIONS AND AN ALTERNATIVE PATHWAY IN ANAEROBIC-BACTERIA', *European Journal of Biochemistry*, 176(3), pp. 497-508.

Thompson, J.D., Higgins, D.G. and Gibson, T.J. (1994) 'CLUSTAL W: improving the sensitivity of progressive multiple sequence alignment through sequence weighting, position-specific gap penalties and weight matrix choice', *Nucleic Acids Research*, 22(22), pp. 4673-4680.

Thorburn, D.R. and Dahl, H.-H.M. (2001) 'Mitochondrial disorders: genetics, counseling, prenatal diagnosis and reproductive options', *American Journal of Medical Genetics*, 106(1), pp. 102-114.

Thyagarajan, B., Padua, R.A. and Campbell, C. (1996) 'Mammalian mitochondria possess homologous DNA recombination activity', *Journal of Biological Chemistry*, 271(44), pp. 27536-27543.

Trifunovic, A., Wredenberg, A., Falkenberg, M., Spelbrink, J.N., Rovio, A.T., Bruder, C.E., Bohlooly-Y, M., GldlÃ¶f, S., Oldfors, A., Wibom, R., TÃ¶rnell, J., Jacobs, H.T. and Larsson, N.G. (2004) 'Premature ageing in mice expressing defective mitochondrial DNA polymerase', *Nature*, 429(6990), pp. 417-423.

Trounce, I., Byrne, E. and Marzuki, S. (1989) 'DECLINE IN SKELETAL MUSCLE MITOCHONDRIAL RESPIRATORY CHAIN FUNCTION: POSSIBLE FACTOR IN AGEING', *The Lancet*, 333(8639), pp. 637-639.

Truscott, K.N., Brandner, K. and Pfanner, N. (2003) 'Mechanisms of protein import into mitochondria', *Current Biology*, 13(8), pp. R326-R337.

Tsukihara, T., Aoyama, H., Yamashita, E., Tomizaki, T., Yamaguchi, H., ShinzawaItoh, K., Nakashima, R., Yaono, R. and Yoshikawa, S. (1996) 'The whole structure of the 13-subunit oxidized cytochrome c oxidase at 2.8 angstrom', *Science*, 272(5265), pp. 1136-1144.

Twig, G., Elorza, A., Molina, A.J.A., Mohamed, H., Wikstrom, J.D., Walzer, G., Stiles, L., Haigh, S.E., Katz, S., Las, G., Alroy, J., Wu, M., Py, B.F., Yuan, J., Deeney, J.T., Corkey, B.E. and Shirihai, O.S. (2008) 'Fission and selective fusion govern mitochondrial segregation and elimination by autophagy', *EMBO J*, 27(2), pp. 433-446.

Urata, M., Wada, Y., Kim, S.H., Chumpia, W., Kayamori, Y., Hamasaki, N. and Kang, D. (2004) 'High-sensitivity detection of the A3243G mutation of mitochondrial DNA by a

combination of allele-specific PCR and peptide nucleic acid-directed PCR clamping', *Clinical Chemistry*, 50(11), pp. 2045-2051.

Valsecchi, F., Koopman, W.J.H., Manjeri, G.R., Rodenburg, R.J., Smeitink, J.A.M. and Willems, P.H.G.M. (2010) 'Complex I disorders: Causes, mechanisms, and development of treatment strategies at the cellular level', *Developmental Disabilities Research Reviews*, 16(2), pp. 175-182.

Van Den Heuvel, L., Smits, P. and Smeitink, J. (2010) 'Mitochondrial translation and beyond: Processes implicated in combined oxidative phosphorylation deficiencies', *Journal of Biomedicine and Biotechnology*, 2010.

Vogelstein, B. and Kinzler, K.W. (1999) 'Digital Pcr', *Proceedings of the National Academy of Sciences*, 96(16), pp. 9236-9241.

Wai, T., Teoli, D. and Shoubridge, E.A. (2008) 'The mitochondrial DNA genetic bottleneck results from replication of a subpopulation of genomes', *Nat Genet*, 40(12), pp. 1484-1488.

Wallace, D.C. (1992) 'Mitochondrial genetics: A paradigm for aging and degenerative diseases?', *Science*, 256(5057), pp. 628-632.

Wallace, D.C., Singh, G., Lott, M.T., Hodge, J.A., Schurr, T.G., Lezza, A.M., Elsas, L.J. and Nikoskelainen, E.K. (1988) 'Mitochondrial DNA mutation associated with Leber's hereditary optic neuropathy', *Science*, 242(4884), pp. 1427-1430.

Wanagat, J., Cao, Z., Pathare, P. and Aiken, J.M. (2001) 'Mitochondrial DNA deletion mutations colocalize with segmental electron transport system abnormalities, muscle fiber atrophy, fiber splitting, and oxidative damage in sarcopenia', *FASEB Journal*, 15(2), pp. 322-332.

Wang, C. and Youle, R.J. (2009) 'The Role of Mitochondria in Apoptosis', in *Annual Review of Genetics*. pp. 95-118.

Wang, G.J., Nutter, L.M. and Thayer, S.A. (1997) 'Insensitivity of cultured rat cortical neurons to mitochondrial DNA synthesis inhibitors. Evidence for a slow turnover of mitochondrial DNA', *Biochemical Pharmacology*, 54(1), pp. 181-187.

Wang, Y. and Bogenhagen, D.F. (2006) 'Human mitochondrial DNA nucleoids are linked to protein folding machinery and metabolic enzymes at the mitochondrial inner membrane', *Journal of Biological Chemistry*, 281(35), pp. 25791-25802.

Wanrooij, S. and Falkenberg, M. (2010) 'The human mitochondrial replication fork in health and disease', *Biochimica et Biophysica Acta (BBA) - Bioenergetics*, 1797(8), pp. 1378-1388.

Weber, K., Wilson, J.N., Taylor, L., Brierley, E., Johnson, M.A., Turnbull, D.M. and Bindoff, L.A. (1997) 'A new mtDNA mutation showing accumulation with time and restriction to skeletal muscle', *American Journal of Human Genetics*, 60(2), pp. 373-380.

Westermann, B. (2010) 'Mitochondrial fusion and fission in cell life and death', *Nat Rev Mol Cell Biol*, 11(12), pp. 872-884.

Westermann, B. (2011) 'Organelle Dynamics: ER Embraces Mitochondria for Fission', *Current Biology*, 21(22), pp. R922-R924.

Willems, J.L., Monnens, L.A.H. and Trijbels, J.M.F. (1977) 'Leigh's encephalomyelopathy in a patient with cytochrome c oxidase deficiency in muscle tissue', *Pediatrics*, 60(6), pp. 850-857.

Williams, R.S., Salmons, S., Newsholme, E.A., Kaufman, R.E. and Mellor, J. (1986) 'REGULATION OF NUCLEAR AND MITOCHONDRIAL GENE-EXPRESSION BY CONTRACTILE ACTIVITY IN SKELETAL-MUSCLE', *Journal of Biological Chemistry*, 261(1), pp. 376-380.

Wong, L.C. and Bai, R.K. (2002) 'Real time quantitative PCR analysis of mitochondrial DNA in patients with mitochondrial disease', *American Journal of Human Genetics*, 71(4), pp. 501-501.

Wu, S.B., Ma, Y.S., Wu, Y.T., Chen, Y.C. and Wei, Y.H. (2010) 'Mitochondrial DNA Mutation-Elicited Oxidative Stress, Oxidative Damage, and Altered Gene Expression in Cultured Cells of Patients with MERRF Syndrome', *Molecular Neurobiology*, pp. 1-11.

Xia, D., Yu, C.-A., Kim, H., Xia, J.-Z., Kachurin, A.M., Zhang, L., Yu, L. and Deisenhofer, J. (1997) 'Crystal Structure of the Cytochrome bc1 Complex from Bovine Heart Mitochondria', *Science*, 277(5322), pp. 60-66.

Yagi, T. and Matsuno-Yagi, A. (2003) 'The proton-translocating NADH-quinone oxidoreductase in the respiratory chain: The secret unlocked', *Biochemistry*, 42(8), pp. 2266-2274.

Yamashita, S., Nishino, I., Nonaka, I. and Goto, Y.I. (2008) 'Genotype and phenotype analyses in 136 patients with single large-scale mitochondrial DNA deletions', *Journal of Human Genetics*, 53(7), pp. 598-606.

Yarham, J.W., McFarland, R., Taylor, R.W. and Elson, J.L. (2012) 'A proposed consensus panel of organisms for determining evolutionary conservation of mt-tRNA point mutations', *Mitochondrion*, (0).

Yasukawa, T., Reyes, A., Cluett, T.J., Yang, M.-Y., Bowmaker, M., Jacobs, H.T. and Holt, I.J. (2006) 'Replication of vertebrate mitochondrial DNA entails transient ribonucleotide incorporation throughout the lagging strand', *EMBO Journal*, 25(22), pp. 5358-5371.

Yoneda, M., Chomyn, A., Martinuzzi, A., Hurko, O. and Attardi, G. (1992) 'MARKED REPLICATIVE ADVANTAGE OF HUMAN MTDNA CARRYING A POINT MUTATION THAT CAUSES THE MELAS ENCEPHALOMYOPATHY', *Proceedings of the National Academy of Sciences of the United States of America*, 89(23), pp. 11164-11168.

Youle, R.J. and Narendra, D.P. (2011) 'Mechanisms of mitophagy', *Nat Rev Mol Cell Biol*, 12(1), pp. 9-14.

Youle, R.J. and Strasser, A. (2008) 'The BCL-2 protein family: opposing activities that mediate cell death', *Nature Reviews Molecular Cell Biology*, 9(1), pp. 47-59.

Youle, R.J. and van der Bliek, A.M. (2012) 'Mitochondrial Fission, Fusion, and Stress', *Science*, 337(6098), pp. 1062-1065.

Yu-Wai-Man, P., Griffiths, P.G., Hudson, G. and Chinnery, P.F. (2009) 'Inherited mitochondrial optic neuropathies', *Journal of Medical Genetics*, 46(3), pp. 145-158.

Yu, C.A., Tian, H., Zhang, L., Deng, K.P., Shenoy, S.K., Yu, L., Xia, D., Kim, H. and Deisenhofer, J. (1999) 'Structural basis of multifunctional bovine mitochondrial cytochrome bc(1) complex', *Journal of Bioenergetics and Biomembranes*, 31(3), pp. 191-199.

Zeviani, M. and Di Donato, S. (2004) 'Mitochondrial disorders', *Brain*, 127, pp. 2153-2172.

Zeviani, M., Moraes, C.T., DiMauro, S., Nakase, H., Bonilla, E., Schon, E.A. and Rowland, L.P. (1988) 'Deletions of mitochondrial DNA in Kearns-Sayre syndrome. 1988', *Neurology*, 51(6), pp. following-1525 and 8 pages following.

Zeviani, M., Muntoni, F., Savarese, N., Serra, G., Tiranti, V., Carrara, F., Mariotti, C. and Didonato, S. (1993) 'A MERRF/MELAS overlap syndrome associated with a new point mutation in the mitochondrial DNA tRNA-Lys gene', *European Journal of Human Genetics*, 1(1), pp. 80-87.

Zhang, C., Baumer, A., Maxwell, R.J., Linnane, A.W. and Nagley, P. (1992) 'Multiple mitochondrial DNA deletions in an elderly human individual', *FEBS Letters*, 297(1), pp. 34-38.

Zhu, X., Peng, X., Guan, M.-X. and Yan, Q. (2009) 'Pathogenic mutations of nuclear genes associated with mitochondrial disorders', *Acta Biochimica et Biophysica Sinica*, 41(3), pp. 179-187.